frontiers | Research Topics

The isotypes of α, β and γ tubulin: From evolutionary origins to roles in metazoan development and ligand binding differences

Edited by
Jeffrey Moore, Richard Luduena and Jack Adam Tuszynski

Published in
Frontiers in Cell and Developmental Biology

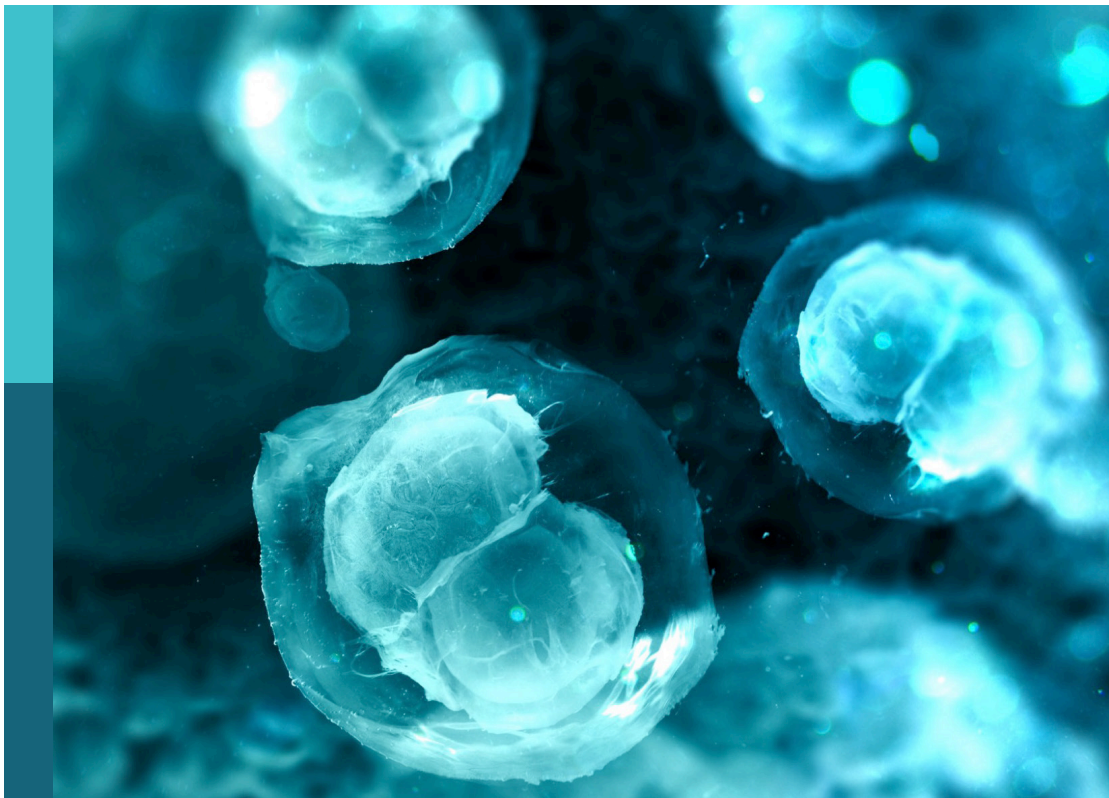

ISSN 1664-8714
ISBN 978-2-83252-145-8
DOI 10.3389/978-2-83252-145-8

About Frontiers

Frontiers is more than just an open access publisher of scholarly articles: it is a pioneering approach to the world of academia, radically improving the way scholarly research is managed. The grand vision of Frontiers is a world where all people have an equal opportunity to seek, share and generate knowledge. Frontiers provides immediate and permanent online open access to all its publications, but this alone is not enough to realize our grand goals.

Frontiers journal series

The Frontiers journal series is a multi-tier and interdisciplinary set of open-access, online journals, promising a paradigm shift from the current review, selection and dissemination processes in academic publishing. All Frontiers journals are driven by researchers for researchers; therefore, they constitute a service to the scholarly community. At the same time, the *Frontiers journal series* operates on a revolutionary invention, the tiered publishing system, initially addressing specific communities of scholars, and gradually climbing up to broader public understanding, thus serving the interests of the lay society, too.

Dedication to quality

Each Frontiers article is a landmark of the highest quality, thanks to genuinely collaborative interactions between authors and review editors, who include some of the world's best academicians. Research must be certified by peers before entering a stream of knowledge that may eventually reach the public - and shape society; therefore, Frontiers only applies the most rigorous and unbiased reviews. Frontiers revolutionizes research publishing by freely delivering the most outstanding research, evaluated with no bias from both the academic and social point of view. By applying the most advanced information technologies, Frontiers is catapulting scholarly publishing into a new generation.

What are Frontiers Research Topics?

Frontiers Research Topics are very popular trademarks of the *Frontiers journals series*: they are collections of at least ten articles, all centered on a particular subject. With their unique mix of varied contributions from Original Research to Review Articles, Frontiers Research Topics unify the most influential researchers, the latest key findings and historical advances in a hot research area.

Find out more on how to host your own Frontiers Research Topic or contribute to one as an author by contacting the Frontiers editorial office: frontiersin.org/about/contact

The isotypes of α, β and γ tubulin: From evolutionary origins to roles in metazoan development and ligand binding differences

Topic editors

Jeffrey Moore — University of Colorado Anschutz Medical Campus, United States

Richard Luduena — The University of Texas Health Science Center at San Antonio, United States

Jack Adam Tuszynski — University of Alberta, Canada

Citation

Moore, J., Luduena, R., Tuszynski, J. A., eds. (2023). *The isotypes of α, β and γ tubulin: From evolutionary origins to roles in metazoan development and ligand binding differences*. Lausanne: Frontiers Media SA.

doi: 10.3389/978-2-83252-145-8

Table of contents

frontiers | Frontiers in Cell and Developmental Biology

TYPE Editorial
PUBLISHED 28 March 2023
DOI 10.3389/fcell.2023.1176739

OPEN ACCESS

EDITED AND REVIEWED BY
Graça Soveral,
University of Lisbon, Portugal

*CORRESPONDENCE
Jack A. Tuszynski,
jackt@ualberta.ca

SPECIALTY SECTION
This article was submitted to Cellular Biochemistry, a section of the journal Frontiers in Cell and Developmental Biology

RECEIVED 28 February 2023
ACCEPTED 13 March 2023
PUBLISHED 28 March 2023

CITATION
Moore J, Luduena R and Tuszynski JA (2023), Editorial: The isotypes of α, β and γ tubulin: From evolutionary origins to roles in metazoan development and ligand binding differences.
Front. Cell Dev. Biol. 11:1176739.
doi: 10.3389/fcell.2023.1176739

Editorial: The isotypes of α, β and γ tubulin: From evolutionary origins to roles in metazoan development and ligand binding differences

Jeffrey Moore[1], Richard Luduena[2] and Jack A. Tuszynski[3,4,5]*

[1]Department of Cell and Developmental Biology, University of Colorado Anschutz Medical Campus, Aurora, CO, United States, [2]Department of Biochemistry and Structural Biology, University of Texas Health Science Center at San Antonio, San Antonio, TX, United States, [3]Department of Physics, University of Alberta, Edmonton, AB, Canada, [4]DIMEAS, Politecnico di Torino, Turin, Italy, [5]Department of Data Science and Engineering, The Silesian University of Technology, Gliwice, Poland

KEYWORDS

microtubules, isotypes, evolution, therapeutic targets, structure-to-function relationship, tubulin

Editorial on the Research Topic
The isotypes of α, β and γ tubulin: From evolutionary origins to roles in metazoan development and ligand binding differences

Tubulin, found in all eukaryotes, exists in many forms: α, β, γ, and others. α and β form a heterodimer, polymerizing into microtubules, often nucleated by γ. Not surprisingly, for a protein that has existed since eukaryotic cells appeared billions of years ago, α, β, and γ diverged into different forms---isotypes---with different amino acid sequences encoded by different genes. This Research Topic explores tubulin isotypes and addresses their evolutionary, functional and medical significance.

Evolutionary significance of tubulin isotypes

For a better perspective we must dive into the origin of tubulin, which is itself a member of a superfamily, including the eubacterial FtsZ as well as other proteins found in many prokaryotes and even viruses. These proteins form filaments and bind to GTP and have similar primary and tertiary structures (reviewed in Ludueña, 2013).

An algorithm based on a model for the evolution of the genetic code, places FtsZ among the oldest 10 proteins, coming in third after ferredoxin and slightly older than proteins involved in nucleic acid metabolism (Davis, 1999; Davis, 2002). FtsZ participates in bacterial cell division and binds to membranes and actin filaments.

Fulton's introductory essay explains the origin of the "multi-tubulin hypothesis," the idea that there have to be distinct types of tubulin performing different functions. In *Naegleria*, a unicellular organism that goes from an amoeboid to a flagellated stage, the former contains microtubules that form the mitotic spindle, while the latter has them forming flagella. The Fulton laboratory showed, using ^{35}S-methionine, that flagellar tubulin formed *de novo*, meaning that the mitotic spindle tubulins were not recycled into flagella, suggesting that there had to be more than one set of α- and β-tubulins. Gene sequencing

revealed two α- and two β-tubulins in *Naegleria*, thus confirming the existence of isotypes. Fulton also suggests that an "engine" pushing the evolution of isotypes may be that duplication of tubulin genes would allow for more tubulin molecules to be produced as needed; later those genes could diverge into isotypes.

Bera and Gupta argue that microorganisms, being easily manipulated, are useful in studying isotypes. They present cases where isotypes have different functions, sometimes forming microtubules differing in dynamic behavior, temporal expression and subcellular localization.

Gasic reviews the eukaryotic realm to show relations among isotypes and to explore the regulation transcription of isotypes, including autoregulation. Gasic argues that isotypes exist to perform different functions and to be expressed in different cell types.

Lu and Zheng focus on *C. elegans*, which has the advantage of easy genetic manipulation and also of being transparent, allowing for microtubule behavior to be visualized in a living cell. Some isotypes are found in every tissue, some in just a few. Some form microtubules with 15 instead of the canonical 13 protofilaments. These authors describe the individual functions of each isotype and point out that tubulin's numerous post-translational modifications add to the complexity and also may not be the same for different isotypes.

Based on these works, we can imagine that gene duplication caused the appearance of tubulin isotypes. When multicellular eukaryotes arose, it is conceivable that they had one isotype for mitosis and another for axonemes, both doing their jobs adequately. Gene duplication would have led to the appearance of more isotypes and gradual refinement as the jobs were distributed among the isotypes, followed by each one evolving to doing its job better. With more gene duplication, new isotypes appeared, each one more specialized, leading to further cell complexity and great variation of cell and tissue function, allowing multicellularity in eukaryotes.

Functional significance of tubulin isotypes

A key prediction of the multi-tubulin hypothesis is that isotypes exhibit distinct functions, presumably imparted by different amino acid sequences and structures.

Montecinos et al. examine the drug-binding properties of chicken erythrocyte tubulin, which is enriched for the βVI isotype and encoded by the TUBB1 gene in humans. They show that tubulin containing βVI is distinct from mammalian brain tubulin in that it binds weakly to most drugs that target the colchicine site, but tighter to several benzimidazole compounds. This indicates a structural divergence of the colchicine site in βVI tubulin, and points to the potential of benzimidazoles, which are commonly used to target parasite tubulins, for further development of drugs that selectively target human isotypes.

Comparing the function and structure of individual isotypes has long been limited by the lack of isotypically pure sources of tubulin. The mini review by Ti recounts the long history of tubulin purification and reconstitution strategies, including recent breakthroughs that have enabled the expression and purification of recombinant, isotypically pure tubulin. These new approaches have opened avenues for comparing isotypes within or across species, and modeling tubulin variants linked to human disease.

The review by Sulimenko et al. extends the isotype comparison to another member of the tubulin family, the γ-tubulins. The human genome encodes two γ-tubulin genes that promote nucleation of αβ-tubulin assembly at centrosomes and other limited sites within cells. The authors describe recent advances in our understanding of the γ-tubulin structure and the mechanism of microtubule nucleation, and emerging functions of γ-tubulin in signaling and DNA repair within the nucleus.

Medical significance of tubulin isotypes

In recent years, many links between tubulin isotypes and human disease have been established. These diseases are either associated with aberrant expression of isotypes or expression of isotypes containing missense mutations that alter function.

Phyo et al. introduce a tubulin code, which becomes rewritten to establish a proliferated, stable microtubule (MT) network that drives cardiac remodeling. They provide evidence of tunable tubulin autoregulation during pathological progression. This "tubulin code" is based on the permutations of tubulin isoforms and their post-translational modifications. A post-translationally-modified MT network is shown to underlie cellular growth in cardiac hypertrophy contributing to contractile dysfunction in heart failure. Using heart failure patient samples and murine models of cardiac remodeling the authors found that autoregulation occurs across tubulin isoforms in the heart concomitantly with rapid transcriptional and autoregulatory activation of specific tubulin isoforms and MT motors.

Buscaglia et al. show that reduced TUBA1A is sufficient to support neuronal migration and cortex development, which provides mechanistic insights into the MT function in support of neurodevelopment. The MT cytoskeleton drives neurite outgrowth, promotes neuronal growth cone responses, and facilitates intracellular cargo transport during neurodevelopment. Since TUBA1A constitutes the majority of α-tubulin in the developing brain, its mutations cause severe brain malformations associated with neurological tubulinopathies. The authors show that a TUBA1A loss-of-function mutation $TUBA1A^{N102D}$ reduces its expression levels and prevents its incorporation into MT polymers. In mice, this leads to grossly normal brain formation except for a major impact on axon extension and impaired formation of forebrain commissures.

Luduena et al. discuss that contrary to normal cells, βII tubulin is present in the cytoplasm and nuclei of many tumor cells. Based on earlier work on nuclear βII, the authors suggest that the presence and location of βII in biopsies could be a useful prognostic indicator and that βII may be involved in cancer progression. They suggest that a signaling pathway in nearby cells causes βII to be synthesized and localized to their nuclei. Hence, the presence of βII in non-cancerous cells could indicate a nearby tumor. A complex which combines αβII with CRISPR-Cas9 could enter the nucleus of a cancer cell and, if guided to the appropriate gene, might destroy the cancer cell or make it less aggressive. These findings offer the possibility that βII localization can aid in cancer diagnosis, prognosis and therapy.

Cushion et al. provide an overview of the α/β-tubulin mutations' involvement in tubulinopathies such as lissencephaly, microcephaly, polymicrogyria, motor neuron disease, and female infertility. The clinical features associated with these diseases have been attributed to the expression patterns of individual tubulin genes and their distinct functional roles. Additional impact of tubulin mutations on microtubule-associated proteins (MAPs) is emphasized by the authors. Depending on their effects on MTs, MAPs can be classified as polymer stabilizers (e.g., tau, MAP2, doublecortin), destabilizers (e.g., spastin, katanin), plus-end binding proteins (e.g., EB1-3, XMAP215, CLASPs) and motor proteins (e.g., dyneins, kinesins). This review analyzes mutation-specific disease mechanisms that influence MAP binding and their phenotypic consequences.

Duly et al. point out that tubulin expression is commonly dysregulated in cancer. This is significantly found to involve βIII-tubulin, which is encoded by the TUBB3 gene. Whereas in normal cells, TUBB3 expression is tightly restricted, and is found almost exclusively in neuronal and testicular tissues, its over-expression has been reported in various epithelial tumours. Importantly, this has been reported to have a strong correlation with drug resistance and aggressiveness of the neoplastic disease. The paper by Duly et al. is focused on the transcriptional and posttranscriptional regulation of TUBB3 in both normal and cancerous tissue. Better understanding of the mechanisms that control TUBB3 expression, especially in cancer is likely to spur the development of improved cancer therapies since tubulin is one of the key targets in a broad spectrum of cancers since various tubulin isotypes exhibit different affinities for microtubule-targeting agents as demonstrated earlier by Huzil et al. (2007).

Author contributions

All authors listed have made a substantial, direct, and intellectual contribution to the work and approved it for publication. All authors contributed equally to the writing of this article.

Conflict of interest

The authors declare that the research was conducted in the absence of any commercial or financial relationships that could be construed as a potential conflict of interest.

Publisher's note

All claims expressed in this article are solely those of the authors and do not necessarily represent those of their affiliated organizations, or those of the publisher, the editors and the reviewers. Any product that may be evaluated in this article, or claim that may be made by its manufacturer, is not guaranteed or endorsed by the publisher.

References

Davis, B. K. (1999). Evolution of the genetic code. *Prog. Biophys. Mol. Biol.* 72, 157–243. doi:10.1016/s0079-6107(99)00006-1

Davis, B. K. (2002). Molecular evolution before the origin of species. *Prog. Biophys. Mol. Biol.* 79, 77–133. doi:10.1016/s0079-6107(02)00012-3

Huzil, J. T., Chen, K., Kurgan, L., and Tuszynski, J. A. (2007). The roles of β-tubulin mutations and isotype expression in acquired drug resistance. *Cancer Inf.* 3, 117693510700300–181. doi:10.1177/117693510700300028

Ludueña, R. F. (2013). A hypothesis on the origin and evolution of tubulin. *Int. Rev. Cell Mol. Biol.* 302, 41–185. doi:10.1016/B978-0-12-407699-0.00002-9

frontiers in Cell and Developmental Biology

ORIGINAL RESEARCH
published: 19 January 2022
doi: 10.3389/fcell.2021.789438

Bridging the Gap: The Importance of TUBA1A α-Tubulin in Forming Midline Commissures

Georgia Buscaglia[1†], *Kyle R. Northington*[1†], *Jayne Aiken*[1,2], *Katelyn J. Hoff*[2] *and Emily A. Bates*[1*]

[1]Department of Pediatrics, University of Colorado Anschutz Medical Campus, Aurora, CO, United States, [2]Department of Cell and Developmental Biology, University of Colorado Anschutz Medical Campus, Aurora, CO, United States

Developing neurons undergo dramatic morphological changes to appropriately migrate and extend axons to make synaptic connections. The microtubule cytoskeleton, made of α/β-tubulin dimers, drives neurite outgrowth, promotes neuronal growth cone responses, and facilitates intracellular transport of critical cargoes during neurodevelopment. *TUBA1A* constitutes the majority of α-tubulin in the developing brain and mutations to *TUBA1A* in humans cause severe brain malformations accompanied by varying neurological defects, collectively termed tubulinopathies. Studies of *TUBA1A* function in mammalian cells have been limited by the presence of multiple genes encoding highly similar tubulin proteins, which leads to α-tubulin antibody promiscuity and makes genetic manipulation challenging. Here, we test mutant tubulin levels and assembly activity and analyze the impact of TUBA1A reduction on growth cone composition, neurite extension, and commissural axon architecture during brain development. We present a novel tagging method for studying and manipulating TUBA1A in cells without impairing tubulin function. Using this tool, we show that a *TUBA1A* loss-of-function mutation *TUBA1A*^{N102D} (*TUBA1A*ND), reduces TUBA1A protein levels and prevents incorporation of TUBA1A into microtubule polymers. Reduced Tuba1a α-tubulin in heterozygous *Tuba1a*$^{ND/+}$ mice leads to grossly normal brain formation except a significant impact on axon extension and impaired formation of forebrain commissures. Neurons with reduced Tuba1a as a result of the *Tuba1a*ND mutation exhibit slower neuron outgrowth compared to controls. Neurons deficient in Tuba1a failed to localize microtubule associated protein-1b (Map1b) to the developing growth cone, likely impacting stabilization of microtubules. Overall, we show that reduced Tuba1a is sufficient to support neuronal migration and cortex development but not commissure formation, and provide mechanistic insight as to how *TUBA1A* tunes microtubule function to support neurodevelopment.

Keywords: TUBA1A protein, microtubule cytoskeleton, MAP1B, commissure defects, tubulinopathy

OPEN ACCESS

Edited by:
Richard Luduena, The University of Texas Health Science Center at San Antonio, United States

Reviewed by:
Monika S. Brill, Technical University of Munich, Germany
Emmanuel Derivery, University of Cambridge, United Kingdom
Pavel Draber, Institute of Molecular Genetics (ASCR), Czechia

***Correspondence:**
Emily A. Bates
Emily.Bates@CUAnschutz.edu

[†]*These authors have contributed equally to this work*

Specialty section:
This article was submitted to Cellular Biochemistry, a section of the journal Frontiers in Cell and Developmental Biology

Received: *04 October 2021*
Accepted: *20 December 2021*
Published: *19 January 2022*

Citation:
Buscaglia G, Northington KR, Aiken J, Hoff KJ and Bates EA (2022) Bridging the Gap: The Importance of TUBA1A α-Tubulin in Forming Midline Commissures. Front. Cell Dev. Biol. 9:789438. doi: 10.3389/fcell.2021.789438

INTRODUCTION

Mammalian brain development is a complex process that requires precise coordination of multiple cell types and extracellular cues to form a fully specified tissue. Despite many advances in understanding the cellular and molecular players involved in brain development, there is still much that remains unknown. Insights into the molecular pathways governing neurodevelopment

can be gained from studying genetic mutations that impair specific aspects of brain development. Severe cortical and neurodevelopmental phenotypes associated with mutations that disrupt tubulin genes, termed tubulinopathies, have recently been described in humans (Poirier et al., 2007; Fallet-Bianco et al., 2008; Cushion et al., 2013; Oegema et al., 2015). Tubulinopathy mutations cause a spectrum of neurodevelopmental phenotypes, but frequently involve cortical malformations such as lissencephaly, agenesis or hypoplasia of the corpus callosum, and cerebellar hypoplasia (Poirier et al., 2007; Tischfield et al., 2011; Cushion et al., 2013; Oegema et al., 2015). Recent studies of human tubulinopathy mutations have revealed that each variant may impact different aspects of microtubule function, such as protein folding, polymerization competency, and microtubule-associated protein (MAP)-binding (Tian et al., 2008; Tian et al., 2010; Aiken et al., 2019a; Aiken et al., 2019b). Tubulin mutations can therefore be used to interrogate the requirement for specific aspects of microtubule function throughout neurodevelopment.

Developing neurons must migrate to the correct location, extend axons to meet sometimes distant synaptic partners, and form functional connections. Throughout this process, neurons undergo dramatic morphological changes that require coordinated interaction between the cytoskeleton and the extracellular environment. In post-mitotic neurons, microtubule polymers made of α/β-tubulin dimers facilitate nucleokinesis and cellular migration, support growth cone navigation, promote axon formation and form the tracks upon which intracellular trafficking occurs (Sakakibara et al., 2013; Liu and Dwyer, 2014; Kapitein and Hoogenraad, 2015; Miller and Suter, 2018). The microtubule network needs to be precisely controlled to fulfill diverse functions in neurons. Microtubule properties can be modulated through post-translational modifications (PTMs) to tubulin subunits, association with MAPs, and through the particular tubulin genes, or isotypes, that a cell expresses (Gadadhar et al., 2017). The human genome contains at least nine unique α- and ten unique β-tubulin genes (Khodiyar et al., 2007; Findeisen et al., 2014). The α-tubulin isotype encoded by the gene *TUBA1A* is abundant in the brain and is the most highly expressed α-tubulin in post-mitotic developing neurons (Miller et al., 1987; Gloster et al., 1994; Gloster et al., 1999). *TUBA1A* mutations are highly represented in cases of human tubulinopathies (Aiken et al., 2017), suggesting that *TUBA1A* plays an important role in neurodevelopment. However, the high degree of sequence conservation between α-tubulin genes has historically made studying *TUBA1A* function in cells challenging, due to the limited availability of tools.

Mouse models harboring mutations to *Tuba1a* can be used as tools to interrogate the function of Tuba1a in the context of the neuronal milieu. As tubulin genes are often required for life and the nucleotide sequence between isotypes is conserved, generation of mutant mouse lines to study *Tuba1a* function *in vivo* has been challenging. To date, only a handful of *Tuba1a* mutant mouse lines have been generated, three by ENU-induced forward genetic screens and one by site-directed CRISPR gene editing (Keays et al., 2007; Gartz Hanson et al., 2016; Bittermann et al., 2019; Leca et al., 2020). We previously revealed that the ENU-induced $Tuba1a^{N102D}$ allele ($Tuba1a^{ND}$) impairs microtubule function in both *S. cerevisiae* and mice through a loss-of-function mechanism by reducing α-tubulin protein (Gartz Hanson et al., 2016; Buscaglia, 2020). Homozygous $Tuba1a^{ND}$ mice exhibit severely impaired brain development and are neonatal lethal, similar to phenotypes seen in the $Tuba1a^{null}$ and *Tuba1a*-R215* mutant mice (Gartz Hanson et al., 2016; Aiken et al., 2017; Bittermann et al., 2019). In homozygous $Tuba1a^{ND}$, $Tuba1a^{Null}$ and *Tuba1a*-R215* mice, as well as many patients with *TUBA1A*-associated tubulinopathies, cortical migration and commissural formation are severely disrupted. This makes it difficult to infer whether axon pathfinding deficits are a direct consequence of altered Tuba1a function or if they are secondary to abnormal cortical layering and migration. $Tuba1a^{ND/+}$ heterozygous mutant mice have reduced Tuba1a function during brain development, which is sufficient to support neuron survival and cortical layer formation (Gartz Hanson et al., 2016; Buscaglia, 2020), but does not support formation of axon commissures. Therefore, $Tuba1a^{ND/+}$ heterozygous animals can provide insight into how Tuba1a contributes specifically to axon pathfinding.

Here, we show that a reduction in developmental Tuba1a protein impairs formation of large brain commissures. Using a novel tubulin visualization technique, we demonstrate that the $TUBA1A^{N102D}$ mutation prevents incorporation of *TUBA1A* into microtubule polymers in cells. In mice, heterozygous $Tuba1a^{ND/+}$ brains fail to form the corpus callosum, anterior and hippocampal commissures. Cultured neurons from $Tuba1a^{ND/+}$ and wild-type cortices reveal that $Tuba1a^{ND/+}$ neurons have shorter neurites than wild-type. Further, we demonstrate that $Tuba1a^{ND/+}$ neurons fail to localize Map1b, a critical developmental MAP, to the developing growth cone. Neither Map1b expression nor binding to microtubules is impaired by reduced Tuba1a function. Trafficking along neurites is perturbed by reduced Tuba1a. Thus failure to localize Map1b is likely due to defects in trafficking. Collectively, our data present evidence that reduction of functional Tuba1a protein allows for normal neuron migration and cortical layering but prevents formation of commissures by impairing axon outgrowth.

MATERIALS AND METHODS

Animals

All animal research was performed in accordance with the Institutional Animal Care and Use Committee at the University of Colorado School of Medicine. All mice used were maintained on a 129S1/C57Bl6 genetic background. Mice were kept on a 12:12 light:dark cycle with *ad libitum* access to food and water. $Tuba1a^{ND/+}$ mice were identified in an ENU mutagenesis screen that was conducted using C57Bl/6J mice and then outcrossed onto 129S1/Svlmj (Gartz Hanson et al., 2016). All of the data for this manuscript were obtained from mice that have been outcrossed over 20 generations to 129S1. $Tuba1a^{ND/+}$ and wild-type littermate mice were maintained on water

supplemented with 0.2 g/L $MgSO_4$ to promote *Tuba1a*$^{ND/+}$ survival and ability to reproduce. Survival rates of *Tuba1a*$^{ND/+}$ with 0.2 g/L $MgSO_4$ are 34/35 total and without $MgSO_4$ supplemented water are three out of nine pups. In contrast, 9/10 wild type litter mates survived without $MgSO_4$ supplemented water and 47/47 wildtype littermates survive with $MgSO_4$ supplemented water. For timed matings, male and female mice (*Tuba1a*$^{ND/+}$ x wild type) were introduced overnight and separated upon confirmation of mating, which was considered embryonic day 0.5. Male and female mice were represented in all studies. All mice were genotyped by PCR amplification of DNA isolated from tail snips followed by Sanger sequencing to differentiate homozygous or heterozygous *Tuba1a*$^{ND/+}$ mice from wild-type. Primers used to amplify mouse DNA for genotyping were: forward:TGGATGGTACGCTTGGTCTT; reverse: CTTTGCAGATGAAGTTCGCA; and sequencing: GTCGAGGTTTCTACGACAGATATC.

Histology

Mice were anesthetized and *trans*-cardially perfused with 0.1 M NaCl and 4% paraformaldehyde (PFA) for histology. Tissues of interest were dissected and post-fixed in 4% PFA. Tissue sectioning was performed on a CM1520 cryostat (Leica, Wetzlar, Germany) and 30 μm cryosections were obtained for all histology. For luxol fast blue staining, sections from brain were stained using a 0.1% luxol fast blue solution. For most immunofluorescence studies PFA-fixed tissues or cells were blocked in phosphate-buffered saline (PBS) containing 5% goat serum or bovine serum albumin (BSA) with 0.3% Triton-X 100. Primary and secondary antibodies were diluted in PBS containing 1% BSA with 0.1% Triton-X 100.

Electron Microscopy

Mice used for electron microscopy were perfused with 0.1 M NaCl and 2.5% glutaraldehyde 4% PFA, after which the brain was dissected and post-fixed in 2.5% glutaraldehyde 4% PFA overnight at 4°C. Following post-fixation, brains were sent for sectioning and imaging by the CU School of Medicine Electron Microscopy Core facility. For analysis, Axons were counted in EM images only if they were captured completely in cross-section (round) and contained either a dark myelin ring surrounding, or had features of an axon (intracellular space had uniform electron density). Structures were only considered as compacted myelin sheaths if they were surrounding a structure resembling a cross-sectional axon and were electron dense.

Plasmids and Reagents

The hexahisitidine (His6) epitope tag was inserted in the α-tubulin internal loop region (Schatz et al., 1987; Heilemann et al., 2008; Hotta et al., 2016). Codon optimization for *rattus norvegicus* (https://www.idtdna.com/codonopt) was used to generate the His6 sequence CATCACCACCATCATCAC, which was inserted into the coding region of human *TUBA1A* from the Mammalian Genome Collection (clone ID: LIFESEQ6302156) between residues I42 and G43. Gibson cloning was used to insert the gBlock of *TUBA1A* internally tagged with His6 (*TUBA1A*-His6) into the pCIG2 plasmid (shared by Dr. Matthew Kennedy, University of Colorado) linearized with NruI and HindIII. *TUBA1A*-His6 incorporation was confirmed by sequencing across the complete *TUBA1A* coding region. The *TUBA1A*^{T349E} (*TUBA1A*^{TE}) polymerization incompetent, and *TUBA1A*^{E255A} (*TUBA1A*^{EA}) highly polymer-stable α-tubulin mutants were identified and described in prior publications (Anders and Botstein, 2001; Johnson et al., 2011; Roostalu et al., 2020). To generate the GFP-TUBA1A vector, the coding region of human TUBA1A from the Mammalian Genome Collection (clone ID: LIFESEQ6302156) was amplified with forward primer TATGGC GGCCGCAGAGTGCTGGTAGTGCTGGTAGTGCTGGTATGC GTGAGTGCATCTCC and reverse primer TATGGCGGCCGCTTA GTATTCCTCTCCTTCTTCCTCACC. The resulting amplicon encompasses the BsrGI cutsite present at the end of GFP, a linker sequence (tripeptide linker SAG), the TUBA1A coding region, and terminates in a NotI site. This amplicon was cloned into the pCIG2 vector at the end of the GFP sequence using sticky-end cloning with BsrGI and NotI. The GFP-MACF43 vector was shared by Dr. Laura Anne Lowery (Boston College) and Dr. Casper Hoogenraad (Utrecht University). Myr-TdTomato plasmid DNA was shared from Dr. Mark Gutierrez and Dr. Santos Franco (University of Colorado).

Cell Culture and Nucleofection

Cos-7 cells (Thermo Fisher Scientific, Waltham, MA; ATCC® CRL-1651™) were cultured in a 37°C humidified incubator with 5% CO_2 in DMEM (Gibco) supplemented with 10% fetal bovine serum (Gibco), 1 mM sodium pyruvate (Thermo), and penicillin/streptomycin (1,000 IU/1,000 μg/ml; Thermo). Cos-7 cells were transfected with 2.5 μg of hexahistidine (His6) tagged *TUBA1A* plasmid DNA using Lipofectamine 3000 (Invitrogen). The Cos-7 cells were fixed and imaged 24 h after the addition of the *TUBA1A* plasmid. Cells were washed with PBS and PHEM buffer (60 mM PIPES, 25 mM HEPES, 10 mM EGTA, 2 mM Mg2Cl), and then fixed in 2% formaldehyde plus 0.05% glutaraldehyde. Immunostaining was performed using primary antibodies directed against: 6X-Histidine (Invitrogen, 4A12E4 37-2900; 1:500), Acetylated Tubulin (Cell Signaling Technology, D20G3; 1:800). Primary antibodies were diluted in blocking buffer (5% BSA with 0.3% Triton-X 100 in PBS) and incubated overnight at 4°C in a humidified chamber. After primary antibody staining, cells were washed three times with PBS. Fluorescently-conjugated secondary antibodies were diluted 1:500 in 1% BSA with 0.1% Triton-X 100 in PBS and incubated for 1 h at room temperature, protected from light. Secondary antibodies were from Life Technologies (Carlsbad, CA) all used at 1:500. For Cos-7 proteasome inhibition assays, 5 μM Lactacystin A (Tomoda and Omura, 2000; Ōmura and Crump, 2019) was added to normal culture medium for 24 h, the day following transfection with *TUBA1A*-His6 constructs. Dissociated neurons were cultured from male and female P0-P2 mouse or rat cortices. Brains were removed and placed into Hanks Balanced Salt Solution (HBSS, Life Technologies) supplemented with 9.9 mM HEPES (Life Technologies) and 1 mM kynurenic acid (Tocris Bioscience, Bristol, United Kingdom). Meninges were removed and cortices were dissected and cut into approximately 1 mm pieces. Cortical pieces

were triturated to a single-cell suspension using glass Pasteur pipettes. Cortical neurons were plated onto 35 mm Poly-D-Lysine coated glass-bottom culture dishes at a density of 350,000 cells (Willco Wells, HBSt-3522). For nucelofected mouse and rat neurons, 4 μg of plasmid DNA was introduced to 4×10^6 neurons using an AMAXA nucleofection kit (VPG-1001, VPG-1003; Lonza). AMAXA-nucleofected cells were plated in 35 mm glass bottom imaging dishes. Neurons were maintained in a 37°C humidified incubator with 5% CO_2 in phenol-free Neurobasal-A medium (Life Technologies) supplemented with B-27 (Thermo Fisher Scientific, Waltham, MA), Penn/strep (Thermo), GlutaMax (Thermo), 5 ng/ml β-FGF (Gibco), and Sodium Pyruvate (Thermo).

RNA Isolation + RTPCR

RNA was isolated from Cos-7 cells, 48 h post-transfection using TRIzol Reagent (Thermo; 15596026). RNA concentration and purity were determined using a spectrophotometer, then cDNA was synthesized using the RT2 First Strand Kit (Qiagen, Hilden, Germany; 330401). qRT-PCR reactions were prepared with SYBR Green RT-PCR Master mix (Thermo; S9194) and run with a CFX Connect Real-Time System (Bio-Rad). Samples were run in triplicate, results were analyzed in Excel. All qPCR data presented in this manuscript was normalized to expression of GFP, which was present on the same plasmid as *TUBA1A*-His6 constructs. Wild-type *TUBA1A* mRNA quantity was set to = 1 and $TUBA1A^{ND}$ relative mRNA quantity was presented relative to wild-type. For all qRT-PCR experiments 3 biological replicates were used per genotype.

Neuron Immunocytochemistry

DIV 2 primary cortical neurons were washed with PBS and fixed with a fixation solution of 4% PFA and 0.2% glutaraldehyde in PBS for 15 min at room temperature. For tubulin extraction, cells were washed with PBS followed by PHEM buffer (60 mM PIPES, 25 mM HEPES, 10 mM EGTA, 2 mM Mg2Cl) then soluble tubulin dimers were extracted using 0.1% triton with 10 μM taxol and 0.1% DMSO in PHEM buffer. Extracted cells were fixed with 2% PFA and 0.05% glutaraldehyde in PBS for 10 min, washed with PBS and then reduced in 0.1% NaBH4 in PBS for 7 min at room temperature. Cells were then washed with PBS and blocked in 3% BSA and 0.2% Triton in PBS for 20 min at room temperature, with agitation. Immunostaining was performed using primary antibodies directed against: 6X-Histidine (Invitrogen, 4A12E4 37-2900; 1:500), total α-tubulin (Sigma, DM1A T6199; 1:5,000), Acetylated Tubulin (Sigma, T7451; 1:1,000), Tyrosinated Tubulin (Chemicon, MAB 1864; 1:1,000), Map1b (Santa Cruz Biotech, sc-135978; 1:500), Map2 (Novus Biologicals, NB300-213; 1:2,000). Primary antibodies were diluted in blocking buffer (5% BSA with 0.3% Triton-X 100 in PBS) and incubated overnight at 4°C in a humidified chamber. After primary antibody staining, cells were washed three times with PBS. Fluorescently-conjugated secondary antibodies were diluted 1:500 in 1% BSA with 0.1% Triton-X 100 in PBS and incubated for 2 h at room temperature, protected from light. Secondary antibodies were from Life Technologies (Carlsbad, CA) all used at 1:500. Alexa Fluor 568-conjugated Phalloidin (Thermo, A12380; 1:20) was added during secondary antibody incubation for labeling of filamentous actin. Tissues or cells of interest were mounted onto glass microscope slides and sealed with glass coverslips and aqueous mounting media containing DAPI (Vector Laboratories, #H-1200) and imaged on a Zeiss 780 or 880 confocal microscope with a ×40 or ×63 oil objective.

Western Blotting

Protein was isolated from brains of P0-P2 mice by dounce homogenization and ultra-centrifugation at 100,000 × g for 45 min at 4°C. Map1b was quantified in three different scenarios. Total Map1b was quantified from the whole brain lysates. For Map1b associated with tubulin, the tubulin-enriched fraction was isolated either with taxol at 37°C according to a previously established protocol (Vallee, 1982) or without taxol at 37°C using centrifugation to separate the tubulin-rich fraction. Cos-7 cell protein was extracted using a Tris-Triton lysis buffer with protease inhibitor cocktail (Sigma). Protein concentrations were assessed using a BCA assay (Thermo), and relative concentration was determined using a Synergy H1 microplate reader (BioTek Instruments, Winooski, VT). 5 μg of either whole brain lysate or tubulin-enriched protein fraction was loaded per lane and run on 4–20% Mini-Protean TGX Stain-Free precast gels (4568093; Bio-Rad Laboratories, Hercules, CA) at 150 mV for 1 h. Prior to protein transfer, Stain-Free gels were activated with UV light for 1 min and imaged for total protein on gel using a ChemiDoc MP imager (Bio-Rad). Proteins were transferred to PVDF blotting membranes (Bio-Rad) in standard 25 mM Tris-base, 192 mM glycine, 15% methanol transfer buffer, or transfer buffer optimized for high molecular-weight proteins (>200 kDa) by the addition of 0.025% SDS. Blots were transferred at 4°C and 75 V for either 1 h for standard molecular-weight proteins, or 3 h for high molecular-weight proteins. Immediately following transfer, PVDF membranes were rinsed in TBST and imaged to quantify the total protein on blot using UV-activated Stain-Free blots. Gels were also imaged post-transfer to assess transfer efficiency for each blot. Membranes were blocked in Tris-buffered Saline containing 0.1% Tween-20 (TBST) with 5% BSA for 1 h and incubated in primary antibody diluted in TBST containing 1% BSA overnight at 4°C. Primary antibodies were: mouse anti 6X-Histidine (Invitrogen, 4A12E4; 1:500), chicken anti-GFP (Invitrogen, A10262; 1:1,000), and mouse anti-Map1b (Santa Cruz, sc-135978; 1:500). Blots were incubated in HRP-conjugated Goat-anti-mouse (1:5,000; Santa Cruz) or goat-anti-chicken (1:5,000; Santa Cruz) secondary antibody diluted in TBST containing 0.5% BSA with streptavidin-HRP (Bio-Rad, 1:10,000) for band visualization for 1 h at room temperature. Blots were developed in ECL solution for 5 min at room temperature (Bio-Rad) and imaged.

Netrin-1 Experiments

Primary wild-type and $Tuba1a^{ND/+}$ neonatal (P0-P3) mouse cortical neurons were nucleofected with 2 μg of Myr-TdTomato plasmid DNA and cultured as described above. Netrin-1 expressing plasmid (OriGene Cat#: MG223704) was transfected into Cos-7 cells using Lipofectamine 3000 (Thermo Fisher Scientific Cat#: L3000015). Cells were washed and media

was replaced with Opti-MEM (Thermo Fisher Scientific Cat#: 31985062). The following day media was removed from cells and placed in an equilibrated Amicon 30 kDa molecular weight cut-off ultracentrifuge tube (Millipore Sigma Cat#: UFC903008). The purified Netrin-1 was collected and quantified using a BCA assay (Thermo Fisher Scientific Cat #:23227). Neurons were measured at DIV1 at 10 min intervals for 60 min, Netrin-1 was added at a final concentration of 500 ng/ml to the media and images were taken for 60 min after the addition of the chemoattractant. Neurons were measured using ImageJ/FIJI software (NIH) and Excel (Microsoft). Statistical analyses were performed, and graphs were created using Prism version 9.0 (GraphPad). For all statistical analyses, $p < 0.05$ was considered statistically significant. Statistical analyses used in each experiment are indicated in their respective figure legends. T-tests were used for any comparisons between two groups and ANOVA was used for any comparison of more than two groups.

dSTORM Super-Resolution Imaging and Analysis

Primary neuronal cultures were generated and immunostained as described in the *Cell Culture and Nucleofection* and *Neuron Immunocytochemistry* sections, excepting the mounting step. Instead, an imaging buffer composed of 50 mM Tris (pH 8), 10 mM NaCl, 10% glucose, 10 mM mercaptoethylamin (MEA, Sigma-Aldrich, M6500), 0.56 mg/ml glucose oxidase (Sigma-Aldrich, G0543), and 34 μg/ml catalase (Sigma-Aldrich, C3155) was sterile filtered onto the sample. The cells were then imaged on a Ziess Elyra P.1 microscope using a Plan-Apochromat 63X 1.4NA objective to achieve high excitation power as previously described (Heilemann et al., 2008; Schüttpelz, 2010). In short, the Alexa 647-labeled sample was excited into a high energy state where the majority of fluorophores enter a long-lived dark state while a small fraction of fluorophores are excited into a bright fluorescent state. Over the imaging period, the cycling of fluorophores from the ground state to either of the excited states, stochastically the dark or bright state, provides fluorophore position information. Super-resolution images were generated by running the raw data through a series of analysis steps. First, the fluorescence background was removed using a previously described temporal median filter in Matlab (Matlab code provided by the University of Colorado School of Medicine Advanced Light Microscopy Core) (Hoogendoorn et al., 2014). Fluorophore positions were then fitted using the ThunderSTORM plugin for ImageJ and Fiji (Schneider et al., 2012; Ovesný, 2014). Sample drift was corrected using redundant cross-correlation algorithm in Matlab as previously described (Wang et al., 2014). Finally, a super-resolution image was created by starting out with all pixels set to zero and incrementing the pixel value by one for every molecule localization that falls into that pixel.

Experimental Design and Statistical Analyses

Band volume of all Western blots was analyzed using Image Lab software (Bio-Rad). Fluorescence intensity measurements, area and morphological assessment, kymograph generation, and quantification of EM images was performed using ImageJ/FIJI software (NIH) and Excel (Microsoft). Statistical analyses were performed, and graphs were created using Prism version 8.0 (GraphPad). Most graphs display all data points to accurately represent the variability in each dataset, except in cases where such presentation obscured visibility. For all statistical analyses, statistical significance was considered to be $p < 0.05$. Statistical analyses used in each experiment are indicated in their respective figure legends. For all graphs mean ± SEM was reported unless otherwise noted. Normality of each dataset was assessed using a Shapiro-Wilk test. In datasets with two groups, parametric data was analyzed using a Student's t-test, while non-parametric data was assessed by Mann-Whitney *U* analysis of medians. Multiple groups were compared by one-way or two-way ANOVA and analyzed *post hoc* by either a Bonferroni or Kruskal-Wallis test for parametric and non-parametric data, respectively.

RESULTS

TUBA1AND α-Tubulin does not Incorporate into Neuronal Microtubules

The high degree of sequence similarity between α-tubulin isotypes has limited study of individual tubulin isotypes at the protein level in cells. As TUBA1A shares 99.5% homology with TUBA1B α-tubulin (only 2 distinct amino acids), commercially available "TUBA1A" specific antibodies are promiscuous and bind more than the intended isotype target. Further, prior attempts to tag TUBA1A neuronal microtubules with N- or C-terminal fluorescent fusion proteins have had detrimental effects on protein function (Gonzalez-Garay and Cabral, 1996; Kimble et al., 2000). These challenges have made the direct visualization of specific tubulin isotypes or mutant tubulin proteins in neurons difficult. Thus, the ways in which TUBA1A specifically contributes to neuronal microtubule protein function have been difficult to ascertain. To address the need for better tools to study TUBA1A protein, we generated a functional hexahistidine (His6)-tagged TUBA1A construct based on a previously identified internal loop in the α-tubulin protein to aid visualization of TUBA1A in mammalian cells (Schatz et al., 1987) (**Figure 1A**). We inserted the His6 tag into an internal loop of TUBA1A between residues I42 and G43, a region of α-tubulin that tolerates addition of amino acids without disrupting tubulin function (Schatz et al., 1987). Addition of the His6 tag in this loop has previously been used to affinity purify tubulin subunits for reconstituted systems (Heilemann et al., 2008; Hotta et al., 2016). However, to our knowledge this internal His6 tag on α-tubulin has never been used for immunohistochemical assays to visualize isotype-specific localization in cells.

Ectopically expressed wild-type TUBA1A-His6 is incorporated into Cos-7 cell microtubules and colocalizes with polymerized acetylated tubulin (Pearson coefficient = 0.31 ± 0.03, **Figures 1B,B′**). Along with wild-type TUBA1A-His6, we ectopically expressed three *TUBA1A* variants in Cos-7 cells. Mutant TUBA1A-His6 ectopic expression in cells facilitates

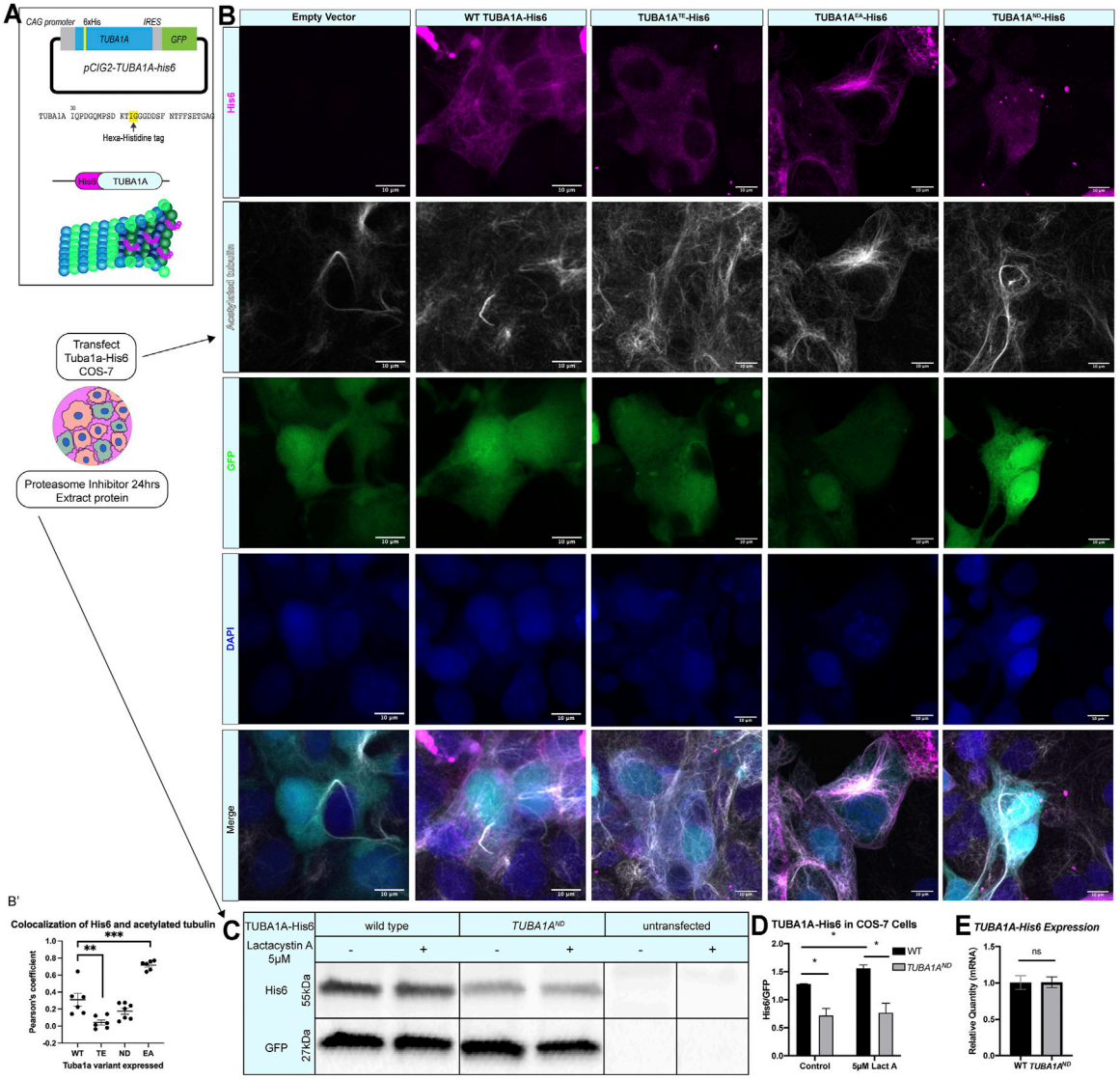

FIGURE 1 | *TUBA1A*ND impairs incorporation into cellular microtubules and reduces α-tubulin protein abundance. **(A)** Schematic of *TUBA1A*-His6 tag and experimental design. His6 epitope tag was added to an internal loop on TUBA1A (top), and TUBA1A-His6 plasmid DNA was transfected into Cos-7 cells to label cellular microtubules in the presence or absence of proteasome inhibitor treatment (bottom). **(B)** Images showing Cos-7 cells transfected with an empty vector control, wild-type *TUBA1A-His6*, *TUBA1A*^{TE}*-His6* (polymerization-incompetent mutant), *TUBA1A*^{EA}*-His6* (highly polymer stable mutant), and *TUBA1A*ND*-His6* plasmid DNA. Cells were immunolabeled with α-His6 antibodies to reveal microtubule incorporation of wild-type and mutant TUBA1A-His6 protein. **(B′)** Scatter plot showing the Pearsons' correlation coefficient to quantify the co-localization of acetylated tubulin with anti-His6 staining $^{**}p < 0.01$ and $^{***}p < 0.001$. **(C)** Western blot for His6 in TUBA1A-His6 transfected Cos-7 cell lysates. A subset of transfected cells were treated with 5 μM Lactacystin A (LactA) for 24 h to block proteasomal degradation. His6 signal was normalized to GFP, which was expressed from the same plasmid. **(D)** Quantification of band density for His6 western blot shown in **(C)**. His6 band density was normalized to GFP-expressing cells in control-treated (left), and cells treated with 5 μM LactA for 24 h (right). Data were analyzed by *t* test. N = 3 transfections; *n* = 3 technical replicates; $p = 0.04$ for all comparisons marked with asterisks; $p = 0.83$ for control vs. LactA-treated *TUBA1A*ND. **(E)** Bar graph representing *TUBA1A* mRNA expression in Cos-7 cells transfected with TUBA1A-His6. *TUBA1A* mRNA expression was normalized to GFP mRNA expression. Data were normalized to *TUBA1A* expression in wild-type (WT) TUBA1A-His6-transfected cells and represent 3 separate transfection experiments and 3 qRT-PCR replicates. Differences between groups were assessed by *t* test ($p = 0.97$). All images were taken at ×40 magnification, scale bars are 10 μm. All graphs show mean of data ± SEM, $^{*}p < 0.05$.

evaluation of the abundance and polymerization capability of mutant TUBA1A proteins. *TUBA1A*^{T349E} (*TUBA1A*^{TE}) is an α-tubulin mutation that prevents tubulin polymerization in yeast (Johnson et al., 2011) and acts as a negative control. The *TUBA1A*^{TE}-His6 shows low levels of punctate His6 staining that does not co-localize with microtubules consistent with previous findings that this mutation prevents TUBA1A^{TE} incorporation into microtubules (Pearson coefficient = 0.042 ± 0.07, **Figures 1B,B′**). However, acetylated tubulin is clearly visible in TUBA1A^{TE} expressing cells indicating that exogenous expression of TUBA1A^{TE} does not interfere with endogenous microtubule networks. In contrast, *TUBA1A*^{E255A}

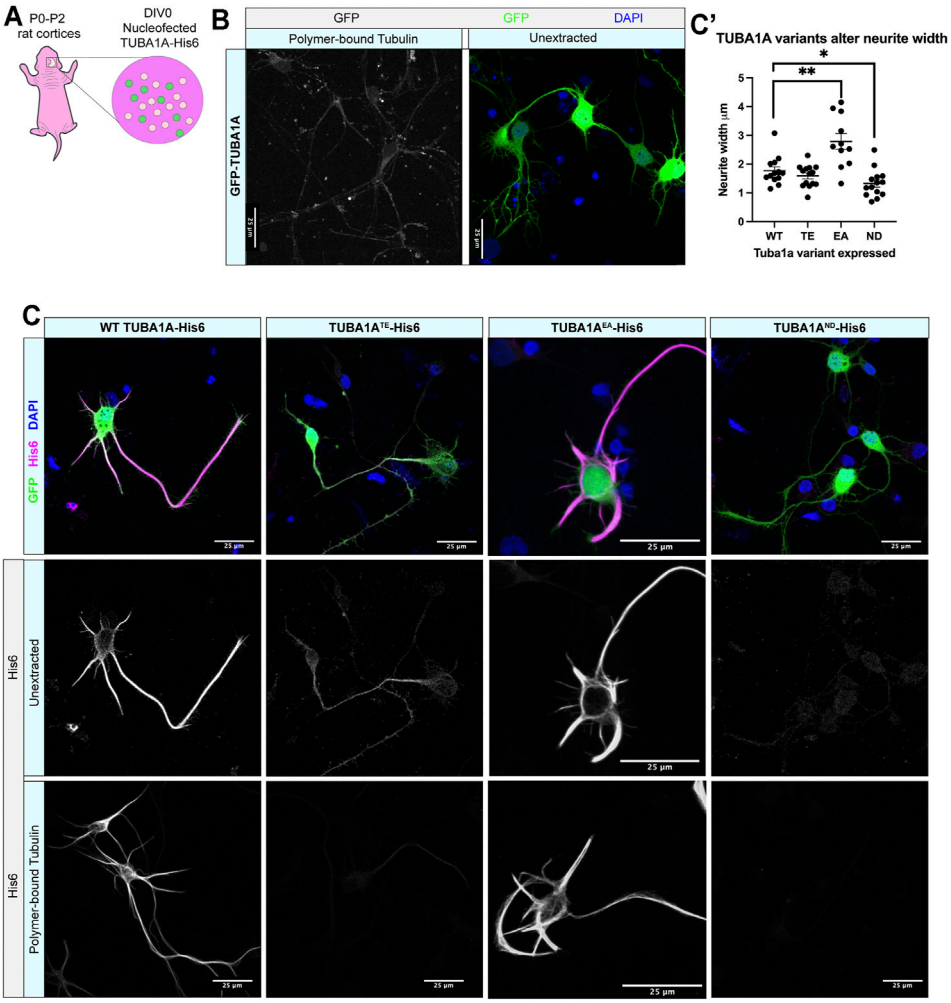

FIGURE 2 | *TUBA1A*ND α-tubulin does not incorporate into neuronal microtubule polymers. **(A)** Schematic of cortical neuron isolation and transfection. **(B)** Cortical rat neurons at DIV 2 transfected with *TUBA1A*-GFP. Left panel shows neurons with soluble tubulin dimers extracted, showing only GFP-labeled TUBA1A that is incorporated into microtubule polymer. Right panel shows neurons with intracellular environment intact (unextracted), containing soluble tubulin dimers and polymerized microtubules transfected to express a TUBA1A-GFP fusion protein. **(C)** Rat cortical neurons at DIV 2 transfected with wild-type (WT) *TUBA1A*-His6 (far left), *TUBA1A*^{TE}-His6 polymerization-incompetent mutant as a negative control (middle left), *TUBA1A*^{EA} stabilizing mutant as a positive control (middle right), *TUBA1A*ND-His6 (far right). Top panels show composite image containing membrane-bound GFP (green) for confirmation of transfection, α-His6 (Magenta) and DAPI (blue) immunolabeling. Middle panels show unextracted and bottom panels show different DIV2 neurons after tubulin has been extracted to reveal only polymer-bound tubulin, labeled with α-His6 antibodies to visualize ectopic *TUBA1A*-His6 proteins. Scale bar is 25 µm. **(C′)** A Scatter plot shows that neurons expressing His6-Tuba1aEA have significantly wider neurites than neurons expressing His6-Tuba1aWT and neurons expressing His6-Tuba1aND have neurites that are significantly thinner than neurons expressing His6-Tuba1aWT $^{*}p < 0.05$, $^{**}p < 0.01$.

(*TUBA1A*^{EA}) is a microtubule stabilizing α-tubulin mutation which inhibits tubulin depolymerization and thus locks microtubules in a polymer-bound state (Anders and Botstein, 2001; Roostalu et al., 2020) (**Figure 1B**). The *TUBA1A*^{EA}-His6 protein is abundantly incorporated into microtubule polymers (Pearson coefficient 0.72 ± 0.02, **Figures 1B,B′**). Acetylated tubulin staining in *TUBA1A*^{EA}-His6 is also increased compared to wild type. Previous reports demonstrate that the *Tuba1a*ND variant causes partial loss of α-tubulin function in yeast and mice (Gartz Hanson et al., 2016; Buscaglia, 2020), but it was unclear whether or not the ND mutant tubulin is capable of polymerization. Our data reveal that TUBA1AND -His6 is not visible in microtubule polymers, but can be detected at low levels in the cytoplasm (Pearson coefficient 0.17 ± 0.03, **Figures 1B,B′**). We conclude that *TUBA1A*ND does not incorporate into microtubules at detectable levels. The acetylated tubulin staining in *TUBA1A*ND-His6 cells is comparable to wild-type; microtubules are present, but TUBA1AND protein is not incorporated.

Western blots of lysates from Cos-7 cells 48 h post-transfection reveal that *TUBA1A*ND-His6 protein is significantly reduced compared to wild-type *TUBA1A*-His6 (**Figures 1C,D**; $p = 0.04$), despite similar *TUBA1A* mRNA levels between wild-type and *TUBA1A*ND transfected Cos-7

cells (**Figure 1E**; $p = 0.97$). To evaluate if *TUBA1A*ND mutant protein is targeted for proteasomal degradation, we treated *TUBA1A*-His6 transfected Cos-7 cells with 5 μM proteasome inhibitor, Lactacystin A [LactA (Tomoda and Omura, 2000; Ōmura and Crump, 2019)], for 24 h and probed for His6 abundance by western blot (**Figure 1C**). Treatment with LactA significantly increased wild-type *TUBA1A*-His6 protein compared to control-treated cells, but had no effect on *TUBA1A*ND-His6 protein abundance (**Figure 1D**; $p = 0.83$). These results indicate that *TUBA1A*ND mutant protein is likely not targeted for degradation by the proteasome. Overall, TUBA1AND mutant protein is not incorporated into microtubules and is less abundant in the cells compared to wild type, despite similar mRNA levels.

We next investigated if *TUBA1A*ND substitution impairs incorporation of TUBA1A protein into neuronal microtubule polymers (**Figure 2**, **Supplementary Figure S1**). Wild-type rat cortical neurons were nucleofected with GFP-*TUBA1A*, wild-type *TUBA1A*-His6, *TUBA1A*^{TE}-His6 (polymerization incompetent mutant), *TUBA1A*^{EA}-His6 (stabilizing mutant), *and* *TUBA1A*ND-His6 DNA at day *in vitro* 0 (DIV 0; **Figure 2A**). Following 2 days in culture (DIV 2), cells were fixed and a subset of neurons were permeabilized to remove soluble tubulin dimers ("tubulin extraction"). Extraction of soluble tubulin leaves behind only polymer-bound tubulin, enabling visualization of ectopic tubulin protein polymerization competence (Zieve and Solomon, 1984). Neurons expressing GFP-*TUBA1A* exhibited abundant GFP signal in intact cells, but tubulin extraction revealed that GFP fusion impaired incorporation of TUBA1A into neuronal microtubule polymers (**Figure 2B**). In contrast, wild-type *TUBA1A*-His6 protein was abundantly visible in both unextracted and extracted neurons, demonstrating that His6-tagging does not impair polymerization ability of TUBA1A in neurons (**Figure 2C**). As predicted, polymerization incompetent *TUBA1A*^{TE}-His6 mutant protein was diffusely visible in intact neurons, but was absent when only polymerized tubulin remained (after extraction) (**Figure 2C**, **Supplementary Figure S1**). The microtubule-stabilizing *TUBA1A*^{EA}*-His6* was retained after extraction and incorporated into polymers more abundantly than wild-type, leading to stubby, microtubule-rich neurites (**Figures 2C,C′**). *TUBA1A*ND-His6 protein was detectable at very low levels in unextracted neurons, but was not visible following tubulin extraction, indicating that *TUBA1A*ND impairs incorporation into neuronal microtubules (**Figures 2C,C′**). These experiments suggest that *TUBA1A*ND reduces abundance of TUBA1A protein and prevents incorporation of mutant TUBA1A into cellular microtubules.

Tuba1a is Required for Formation of Midline Commissures

TUBA1A is a major component of developing neuronal microtubules and is critical for proper brain development (Aiken et al., 2017). Human *TUBA1A* tubulinopathy patients with heterozygous mutations in *TUBA1A* exhibit severe brain malformations including defects in commissure formation and changes to cortical folding patterns (lissencephaly, polymicrogyria, pachygyria). While homozygous *Tuba1a*$^{ND/ND}$ mice have severe brain malformations including defects in cortical layer formation (Gartz Hanson et al., 2016), *Tuba1a*$^{ND/+}$ heterozygous mutant mice undergo normal cortical migration, display comparable brain weight to wild-type littermates at birth, and survive to adulthood (Gartz Hanson et al., 2016; Buscaglia, 2020). However, 93% (14/15 brains) have severe defects in corpus collosum formation including 87% (13/15) with complete agenesis of the corpus callosum and abnormal formation of the anterior and hippocampal commissures (**Figure 3A**). In wild-type mice, 12/12 had well-formed commissures. For a commissure to form properly, nascent callosal "pioneer" axons extend through midline at E15.5, and early "follower" axons begin extending at E17 in mice (Boyer and Gupton, 2018). Evidence of abnormal callosal projections were apparent as early as P0 in *Tuba1a*$^{ND/+}$ brains, as seen by the early formation of aberrant axon bundles adjacent to the callosum, known as Probst bundles (**Figure 3A**) (Probst, 1901). In addition to agenesis of the corpus callosum at midline, lateral regions of adult *Tuba1a*$^{ND/+}$ corpus callosum were found to be significantly thinner than wild-type (**Figure 3B**). Similarly, *Tuba1a*$^{ND/+}$ anterior commissures are smaller than that of wild-type littermates (**Figure 3C**). In wild-type mice, corpus callosum thickness and anterior commissure area both increased significantly between P0 and adulthood; however, normal postnatal expansion of these tracts was not evident in *Tuba1a*$^{ND/+}$ mice (**Figures 3B,C**). The corpus callosum is absent along the rostral-caudal axis in *Tuba1a*$^{ND/+}$ animals. *Tuba1a*$^{ND/+}$ axons fail to organize into typical midline commissural structures, indicating that half of the normal amount of Tuba1a during brain development is not sufficient for commissural formation (Buscaglia, 2020).

Examination of sagittal brain sections taken directly at midline revealed dramatic disorganization of corpus callosum axons in *Tuba1a*$^{ND/+}$ brains (**Figure 4A**). Compared to wild-type, *Tuba1a*$^{ND/+}$ midline commissural axons were largely absent, and the existing axons failed to organize into a tract with uniform orientation (**Figure 4A**). Despite dramatic differences between wild-type and *Tuba1a*$^{ND/+}$ callosal axon organization, *Tuba1a*$^{ND/+}$ axons were highly colocalized with immunolabeled myelin sheaths (**Figure 4A**). To further assess the impact of *Tuba1a*$^{ND/+}$ substitution on callosal axon morphology and myelination, we performed electron microscopy (EM) in both wild-type and *Tuba1a*$^{ND/+}$ corpus callosi. Due to the scarcity of axons present directly at midline in the *Tuba1a*$^{ND/+}$ corpus callosum, we sampled a region of corpus callosum 2 mm lateral to midline for both wild-type and *Tuba1a*$^{ND/+}$ animals (**Figure 4B**). EM images revealed a striking difference in axon density between wild-type and *Tuba1a*$^{ND/+}$ corpus callosi (**Figures 4B,C**; $p = 0.03$). Myelin thickness, measured by G-ratio, was similar between wild-type and *Tuba1a*$^{ND/+}$ brains (**Figure 4D**; $p = 0.34$), as was axon diameter (**Figure 4E**; $p = 0.14$). There was a trend towards decreased myelination in *Tuba1a*$^{ND/+}$ animals ($p = 0.07$), but this difference was not statistically significant (**Figure 4F**). These data provide evidence that *Tuba1a*$^{ND/+}$ callosal axons do not correctly organize to form a commissure. Previously published data indicated that reduced developmental Tuba1a function is tolerable for cortical neuron migration (Gartz Hanson et al., 2016); however,

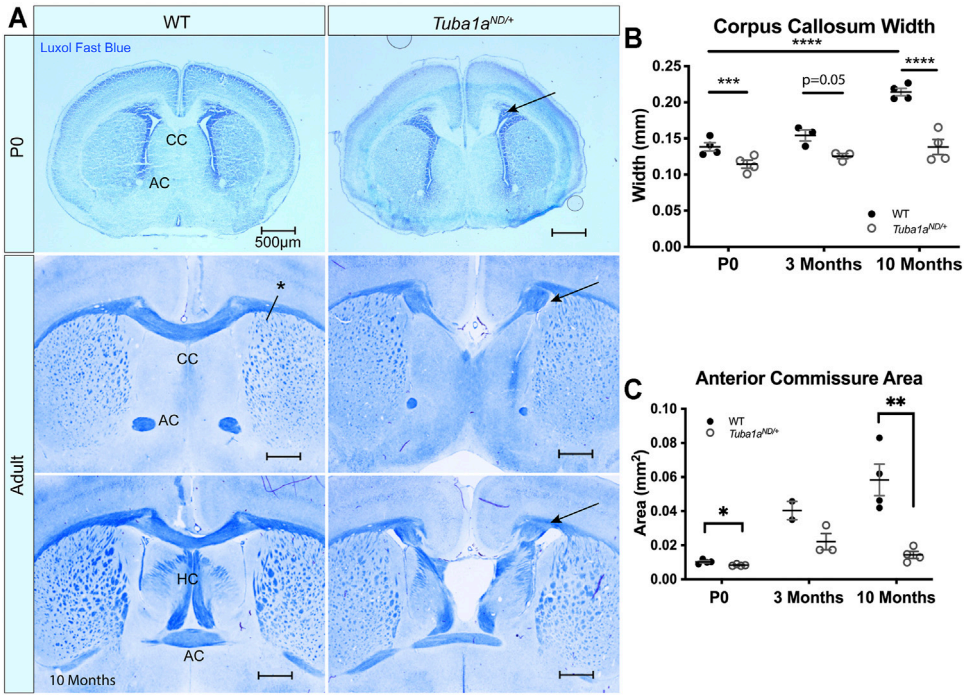

FIGURE 3 | Tuba1a is required for formation of midline commissural structures. **(A)** Luxol fast blue-stained coronal brain sections from postnatal day 0 (P0; top) and Adult (middle-bottom) wild-type and *Tuba1a*$^{ND/+}$ mice. Images portray abnormal midline commissural formation in *Tuba1a*$^{ND/+}$ mouse brains, with labels highlighting the corpus callosum (CC), anterior commissures (AC), and hippocampal commissure (HC). Scale bars are 500 μm. Arrows indicate Probst bundles. Asterisk in A. shows where measurements for B. were obtained. **(B)** Scatter plot representing corpus callosum width at P0, 3 months, and 10 months-old. **(C)** Scatter plot displaying anterior commissure area in P0, 3 months, and 10 months-old wild-type and *Tuba1a*$^{ND/+}$ brains. Wild-type and *Tuba1a*$^{ND/+}$ measurements compared by two-way ANOVA. $^{*}p < 0.05$; $^{**}p < 0.01$; $^{***}p < 0.001$; and $^{****}p < 0.0001$.

our results indicate that reduced Tuba1a is not sufficient to support commissure formation.

Tuba1a is Necessary for Neurite Extension and Cytoskeletal Organization in Growth Cone

To assess potential mechanisms by which reduced Tuba1a prevents commissural axons from crossing the midline, we measured neurite lengths, growth rates, and retraction frequency in cultured primary cortical neurons from P0 wild-type and *Tuba1a*$^{ND/+}$ mice (**Figure 5A**). *Tuba1a*$^{ND/+}$ neurites were significantly shorter than wild-type neurites (32.51 ±1.75 vs. 41.25 ±1.71 μm, $p = 0.0016$ by *t*-test, $n = 157$ WT neurons N = 13 mice and 77 *Tuba1a*$^{ND/+}$ neurons, N = 9 mice) at DIV1 (**Figure 5B**). *Tuba1a*$^{ND/+}$ neurites trended towards slower growth rates (5.828 vs. 4.064 μm/h, $p = 0.1853$ by *t*-test, **Figure 5C**) and increased frequency of retraction (49.25 vs. 53.39%, $p = 0.2247$ by *t*-test, **Figure 5D**) in an hour. Measurements of the longest neurite, the putative "axon", at DIV 3 revealed that *Tuba1a*$^{ND/+}$ neurites remained significantly shorter than those of wild-type neurons (**Figure 5E**; N = 3 mice, $n = 124$ neurons; $p = 0.02$ by *t*-test). Together, these data show that developing neurons with reduced Tuba1a have a diminished capacity for neurite growth compared to wild-type neurons.

To determine if there are differences in the cytoskeleton network that explain shorter *Tuba1a*$^{ND/+}$ neurites, we assessed the abundance of acetylated microtubules and filamentous actin (F-actin) in developing growth cones of wild-type and *Tuba1a*$^{ND/+}$ cortical neurons at DIV 3 (**Figure 5F**). The growth cone is a dynamic developmental structure that uses the coordinated action of the actin and microtubule cytoskeleton to drive neuronal outgrowth in response to internal and external cues (Dent et al., 2011; Craig, 2018). The area of *Tuba1a*$^{ND/+}$ growth cones trended towards reduced area (317.4 ± 31.3 μm^2) compared to wild-type (380.9 ± 30.4 μm^2; **Figure 5G**; $n = 49$ growth cones; $p = 0.15$, by student's t-test). We examined the amount of acetylated tubulin, a post-translational modification associated with stable microtubules (**Figure 5H**) and found there to be no difference in the overall fluorescence intensity of acetylated tubulin in *Tuba1a*$^{ND/+}$ neurons compared to wild-type ($n = 49$ growth cones; $p = 0.89$). In contrast, we observed a significant increase in F-actin fluorescence intensity within the growth cones of *Tuba1a*$^{ND/+}$ neurons compared to wild-type (**Figure 5I**; $n = 49$ growth cones; $p = 0.0014$). Normally, neuronal microtubules splay out in the central, actin-dominated regions of the growth cone, but are bundled towards the peripheral domains of the growth cone (Buck and Zheng, 2002). To assess the degree of growth cone microtubule bundling, we next performed line scans across the widest point of DIV 3 growth cones ≥10 μm (**Figure 5J**), an assay that was modeled after similar experiments in Biswas and Kalil (2018) (Biswas and Kalil, 2018). Line scans of acetylated tubulin through the growth cone revealed differences in microtubule organization between wild-type and *Tuba1a*$^{ND/+}$ neurons (**Figure 5K**; $n = 39$ growth cones; $p < 0.0001$

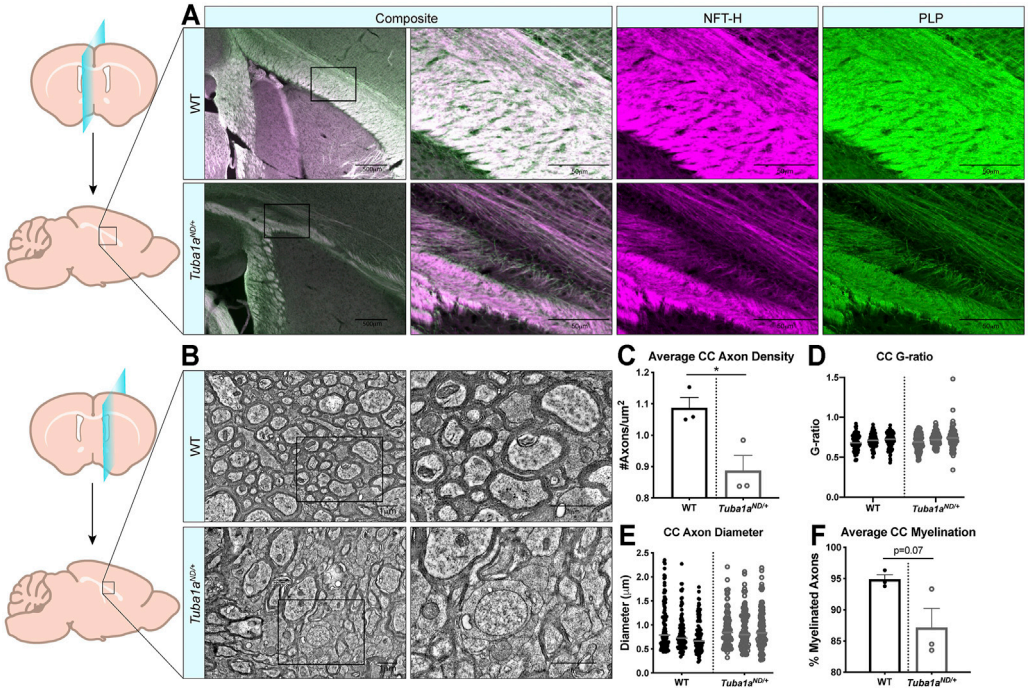

FIGURE 4 | Axon density is reduced by *Tuba1a*$^{ND/+}$ in midline corpus callosum. **(A)** Sagittal brain sections at midline from wild-type (top) and *Tuba1a*$^{ND/+}$ (bottom) brains stained with neurofilament-heavy (NFT-H; magenta) to label axons, and proteolipid protein (PLP; green) to label myelin. Images were taken at ×4 (left) and ×20 (right) magnification with 500 and 50 µm scale bars, respectively. **(B)** Electron microscopy (EM) images of sagittal wild-type (top) and *Tuba1a*$^{ND/+}$ (bottom) sections of corpus callosum 2 mm adjacent to midline. Enlarged regions on right are denoted by boxes, scale bar is 1 µm. **(C)** Scatter plot representing axon density of wild-type and *Tuba1a*$^{ND/+}$ axons in analyzed EM images. Data points represent average values for each animal ($n = 6$ regions containing same total area; $p = 0.03$). **(D)** Scatter plot of G-ratio measurements for wild-type and *Tuba1a*$^{ND/+}$ axons. Data points represent individual myelinated axons and are clustered by animal (N = 3 mice, $n = 100$ axons; $p = 0.34$). **(E)** Scatter plot of axon diameters in wild-type and *Tuba1a*$^{ND/+}$ corpus callosum by EM. Only those axons captured in cross section were assessed for diameter, as skewed axons provide inaccurate measurements. Data points represent individual axons and are clustered by animal ($n = 100$; $p = 0.14$). **(F)** Scatter plot representing the average percent of myelinated axons per animal in wild-type and *Tuba1a*$^{ND/+}$ corpus callosum. Six regions containing the same total area were assessed ($n = 6$; $p = 0.07$). Statistical differences between means of wild-type and *Tuba1a*$^{ND/+}$ datasets were assessed by *t* test, with $^*p < 0.05$.

between genotypes by two-way ANOVA). Specifically, we observed peaks in fluorescence, indicating bundled microtubules, at the edges of the growth cone in wild-type neurons, where acetylated tubulin was more diffuse and lacked obvious organization in *Tuba1a*$^{ND/+}$ growth cones (**Figure 5K**). The ratio of acetylated microtubules to F-actin in the growth cone was significantly reduced in *Tuba1a*$^{ND/+}$ neurons compared to wild-type, indicating changes to the overall growth cone cytoskeletal environment in *Tuba1a*$^{ND/+}$ neurons (**Figure 5L**; $n = 49$ growth cones per genotype; $p = 0.0003$). Together, these data indicate that neurite growth is particularly sensitive to the amount of Tuba1a tubulin available, and that reduction in Tuba1a leads to shorter neurites (a result of subtle changes to growth and retraction rates) with growth cones containing abnormal actin and microtubule architecture.

Tuba1a$^{ND/+}$ Neurites Exhibit Short Term Growth Increase With Global Addition of Netrin-1

Axon extension to form the corpus callosum is directed by guidance cues, including Netrin-1 (Nishikimi et al., 2013). Netrin-1 can act as an attractive guidance cue for developing axons by promoting directional axonal growth (Boyer and Gupton, 2018), and Netrin-1 deficient mice exhibit defects in commissural axon projection (Serafini et al., 1996) similar to that seen in *Tuba1a*$^{ND/+}$ mice (**Figure 3**). To determine if *Tuba1a*$^{ND/+}$ neurons respond to Netrin-1, primary cortical neurons were transfected with a membrane bound tdTomato reporter and cultured for 24 h. At DIV1, time lapse images were taken every 10 min over the course of an hour, then purified Netrin-1 was added to the media. Time lapse images taken after the addition of Netrin-1 revealed that both wild-type and *Tuba1a*$^{ND/+}$ neurons have a slight but significant increased growth rate at 10 min after the addition of Netrin-1 (**Figures 6A,B**). No differences were observed when comparing wild-type and *Tuba1a*$^{ND/+}$ neurons directly at the same time points (**Figure 6C**). These data indicate that both wild-type and *Tuba1a*$^{ND/+}$ neurons exhibit similar short-term responses to global addition of Netrin-1 at DIV1 in culture.

Tuba1aND Neurons Fail to Localize Critical Developmental Protein Map1b to Growth Cone

MAPs play a crucial role in regulating neuronal microtubule function to support proper neurodevelopment. Microtubule-

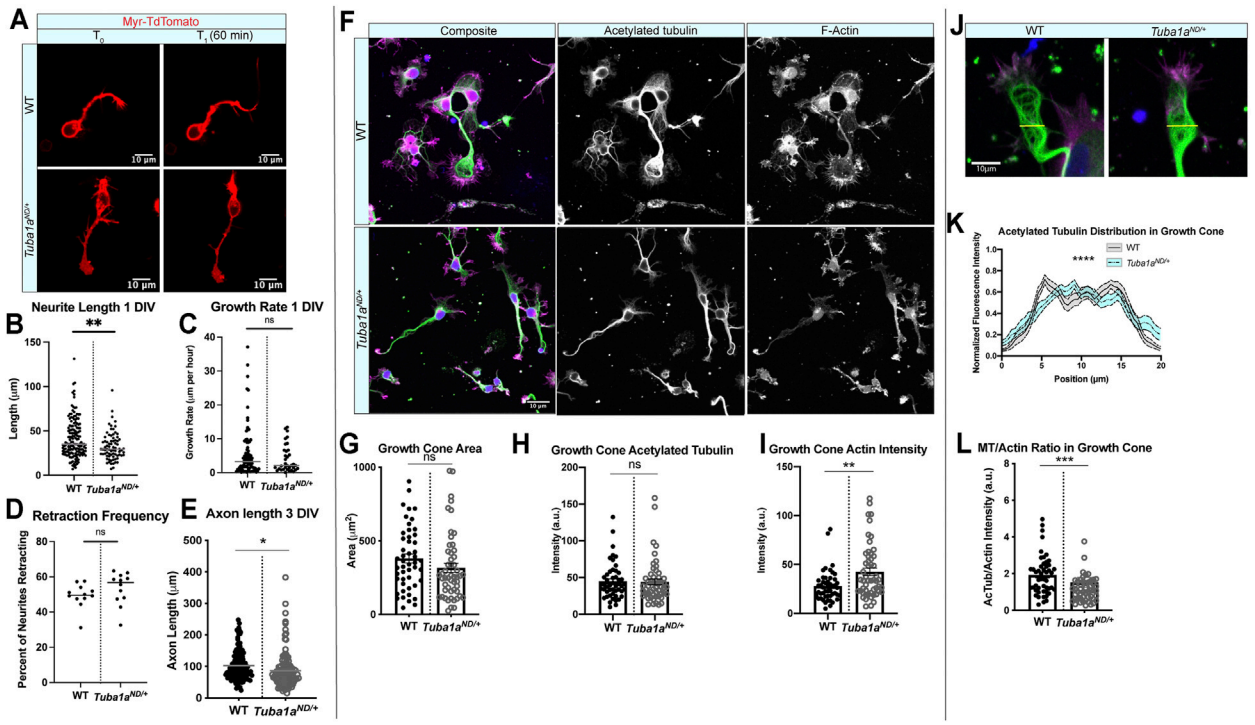

FIGURE 5 | *Tuba1a*ND impairs neurite outgrowth and alters growth cone cytoskeleton in cortical neurons. **(A)** Representative time-lapse images of membrane-labeled Myr-TdTomato neurons at DIV 1. Myr-TdTomato images were acquired 60 min apart to assess neuronal growth rate in wild-type (WT; top) and *Tuba1a*$^{ND/+}$ (bottom) cortical neurons. **(B)** Neurite lengths from WT and *Tuba1a*$^{ND/+}$ mice at DIV 1. Data points represent individual neurons (32.51 ± 1.75 vs. 41.25 ±1.71 µm, p = 0.0016 by t-test, n = 157 WT neurons N = 13 mice and 77 Tuba1aND/+ neurons, N = 9 mice). **(C)** Scatter plot of neurite growth rate in DIV 1 neurons measured over 60 min using Myr-TdTomato tagged primary cortical neurons from WT and *Tuba1a*$^{ND/+}$ mice (5.828 vs. 4.064 µm/h, p = 0.1853). **(D)** Scatter plot of neurite retraction frequency reveals a trend toward more frequent retractions in *Tuba1a*$^{ND/+}$ mice (49.25 vs. 53.39%, p = 0.2247). **(E)** Scatter plot of neurite length at DIV 3 in fixed WT and *Tuba1a*$^{ND/+}$ primary cortical neurons. For each cell, the longest neurite, designated a putative "axon", was measured from the cell soma to the distal neurite tip using an acetylated tubulin marker. Data points represent individual neurons (N = 3 mice, n = 124 neurons; p = 0.02). **(F)** Images of DIV 3 WT (top) and *Tuba1a*$^{ND/+}$ (bottom) cortical neurons stained with antibodies directed against acetylated tubulin (green) and rhodamine phalloidin (F-actin, magenta). Composite images are shown (left) with single channel grayscale images for acetylated tubulin (middle) and F-actin (right). Fluorescent images were post-processed in ImageJ to enhance brightness and contrast, set to a minimum value of 0 and a maximum value of 70. Scale bars are 10 µm. **(G)** Scatter plot of growth cone area at DIV 3 in WT and *Tuba1a*$^{ND/+}$ cortical neurons. Data points represent individual growth cones (N = 3 mice, n = 52 growth cones; p = 0.26). **(H)** Scatter plot of acetylated tubulin intensity within the growth cone of WT and *Tuba1a*$^{ND/+}$ cortical neurons at DIV 3. Acetylated tubulin images were collected using identical microscope imaging settings between samples, fluorescence of quantified images was not adjusted prior to measurement. Acetylated tubulin intensity was normalized to the area of the growth cone. Data points represent individual growth cones (n = 49 growth cones; p = 0.89). **(I)** F-actin intensity within growth cone of WT and *Tuba1a*$^{ND/+}$ cortical neurons at DIV 3. F-actin images were collected using identical microscope imaging settings between samples, fluorescence of quantified images was not adjusted prior to measurement. F-actin intensity was normalized to the area of the growth cone. Data points represent individual growth cones (N = 3 mice, n = 49 growth cones; p = 0.0014). **(J)** Representative images of WT and *Tuba1a*$^{ND/+}$ cortical neuron growth cones showing distribution of acetylated tubulin (green) and F-actin (magenta). The yellow line indicates where microtubule fluorescence intensity measurements were taken. **(K)** Line plot showing the average acetylated tubulin fluorescence intensity across a 20 µm line scan through the central domain of the growth cone, taken perpendicular to the extending neurite shaft or putative axon in DIV 3 WT and *Tuba1a*$^{ND/+}$ neurons. Differences between WT and *Tuba1a*$^{ND/+}$ growth cones were assessed by two-way ANOVA which showed a significant interaction between genotype and fluorescence intensity by position (n = 20 growth cones; p < 0.0001). **(L)**. Scatter plot representing the ratio of acetylated tubulin to F-actin intensity within the growth cones of DIV 3 WT and *Tuba1a*$^{ND/+}$ cortical neurons. Acetylated tubulin and F-actin intensity was measured from a single ROI in each growth cone, fluorescent images were acquired using the same microscope settings between samples and were not post-processed to adjust fluorescence. Data points represent individual growth cones (N = 3 mice, n = 49 growth cones; p = 0.0003 by Mann-Whitney test). For all plots, lines represent mean and error bars report SEM. Differences between WT and *Tuba1a*$^{ND/+}$ datasets were assessed by t test unless otherwise noted. *p < 0.05; **p < 0.01; ***p < 0.001; ****p < 0.0001.

associated protein 1b (Map1b) regulates microtubule dynamics and facilitates actin/microtubule crosstalk to promote axon extension (Del Río et al., 2004). Mice lacking Map1b display an absence of the corpus callosum (Meixner et al., 2000; Gonzalez-Billault et al., 2001), similar to what is seen in *Tuba1a*$^{ND/+}$ mice. To assess whether *Tuba1a*ND might disrupt Map1b function, we performed a series of biochemical and immunocytochemical analyses. Map1b is highly enriched in neurons compared to other cells in the brain, and neuronal expression of Map1b accounts for most of the Map1b in the whole brain (Zhang et al., 2014; Zhang et al., 2016). Western blot analysis of whole brain lysates from wild-type and *Tuba1a*$^{ND/+}$ mouse brains showed no difference in the total amount of Map1b protein (**Figure 7A**; p = 0.98). There was no significant deficit in the association of Map1b with taxol-stabilized microtubules from *Tuba1a*$^{ND/+}$ brain lysates

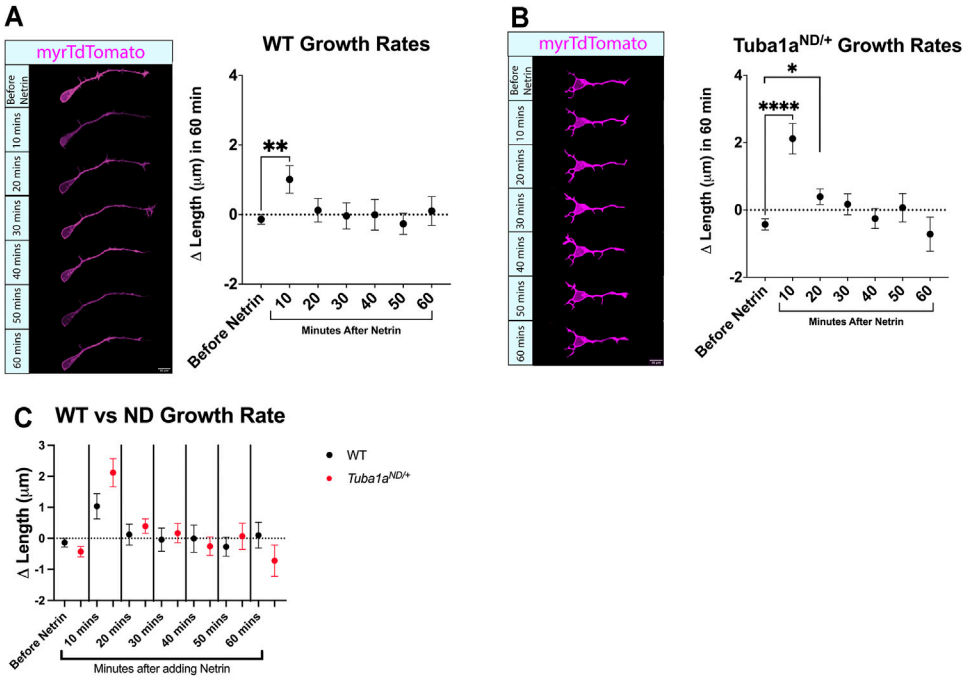

FIGURE 6 | Reduced Tuba1a does not interfere with netrin-1-induced axon growth rates. **(A)** Primary cortical neuron cell cultures were made from *Tuba1a*$^{ND/+}$ mice and wildtype littermates. Cells were plated on glass-bottom dishes and images were collected every 10 min for an hour. Purified Netrin-1 was then added to the dish at 500 ng/ml and images were taken every 10 min for an additional hour. (n = 77 neurons; p = 0.0057, unpaired t-test) **(B)**. Analysis was repeated for *Tuba1a*$^{ND/+}$ mice (n = 91 neurons; p < 0.0001, and n = 83 neurons; p = 0.0488, unpaired t-test) **(C)**. To determine if there was a difference in stimulated growth between the wildtype and *Tuba1a*$^{ND/+}$ mice the growth values were compared at each time point. No differences were found at any time point.

compared to wild-type; in fact, *Tuba1a*$^{ND/+}$ samples contained slightly more Map1b than wild-type (**Figure 7B**; p = 0.03). In addition, we performed a western blot to quantify and compare the amount of Map1b associated with polymerized tubulin in brains from WT and *Tuba1a*$^{ND/+}$ brains without taxol, at 37°C to avoid stimulating tubulin polymerization. We found that there was no difference in Map1b in the polymerized tubulin fraction (**Figure 7C**). These data indicate *Tuba1a*ND does not impair the interaction between Map1b and microtubules. In developing wild-type neurons, Map1b localizes strongly to the growth cone to promote axon growth and facilitate microtubule response to guidance cues (**Figure 7D**) (Black et al., 1994; Mack et al., 2000; Gonzalez-Billault et al., 2001; González-Billault et al., 2002; Tymanskyj et al., 2012). Strikingly, while *Tuba1a*$^{ND/+}$ neurons contained Map1b protein, they exhibited very little Map1b fluorescence in the growth cone compared to wild-type neurons (**Figure 7E**; n = 31 growth cones; p = 0.009). These data provide evidence that while the abundance of Map1b protein is unchanged by *Tuba1a*ND, reduced Tuba1a dramatically impedes the subcellular localization of Map1b to the growth cone. Failure of *Tuba1a*$^{ND/+}$ neurons to localize Map1b to the developing growth cone provides a putative mechanism by which developing axons may fail to correctly organize the growth cone cytoskeleton, leading to the commissural deficits observed in *Tuba1a*$^{ND/+}$ mice.

DISCUSSION

Functions of TUBA1A During Neurodevelopment

Using *TUBA1A*-His6 as a novel imaging tool, we illustrate that the *TUBA1A*ND allele is excluded from microtubule filaments and decreases the abundance of TUBA1A in cells (**Figures 1**, **2**). We further demonstrate that mice with diminished Tuba1a exhibit normal cortical layering but are incapable of forming axon commissures. On a cellular level, decreased Tuba1a impairs neurite outgrowth (**Figures 5**–**7**) and disrupts growth cone localization of Map1b, which acts as a critical regulator of cytoskeletal dynamics during axonal outgrowth (**Figure 8**). The timing of axonal extension is precisely regulated, and growth cones which fail to reach targets at the correct time can miss crucial developmental signaling events. Interactions between MAPs and microtubules play a major role in adapting microtubule function in response to changing intra- and extra-cellular developmental environments (Meixner et al., 2000; Del Río et al., 2004; Tymanskyj et al., 2012). Therefore, it's possible that neurons with reduced Tuba1a may be incapable of maintaining appropriate axonal growth rates or mounting appropriate cytoskeletal responses to extracellular guidance cues due to lack of localization of critical cargos such as MAP1B (**Figure 8B**). Our evidence supports a model in which adequate TUBA1A levels are required for neurite

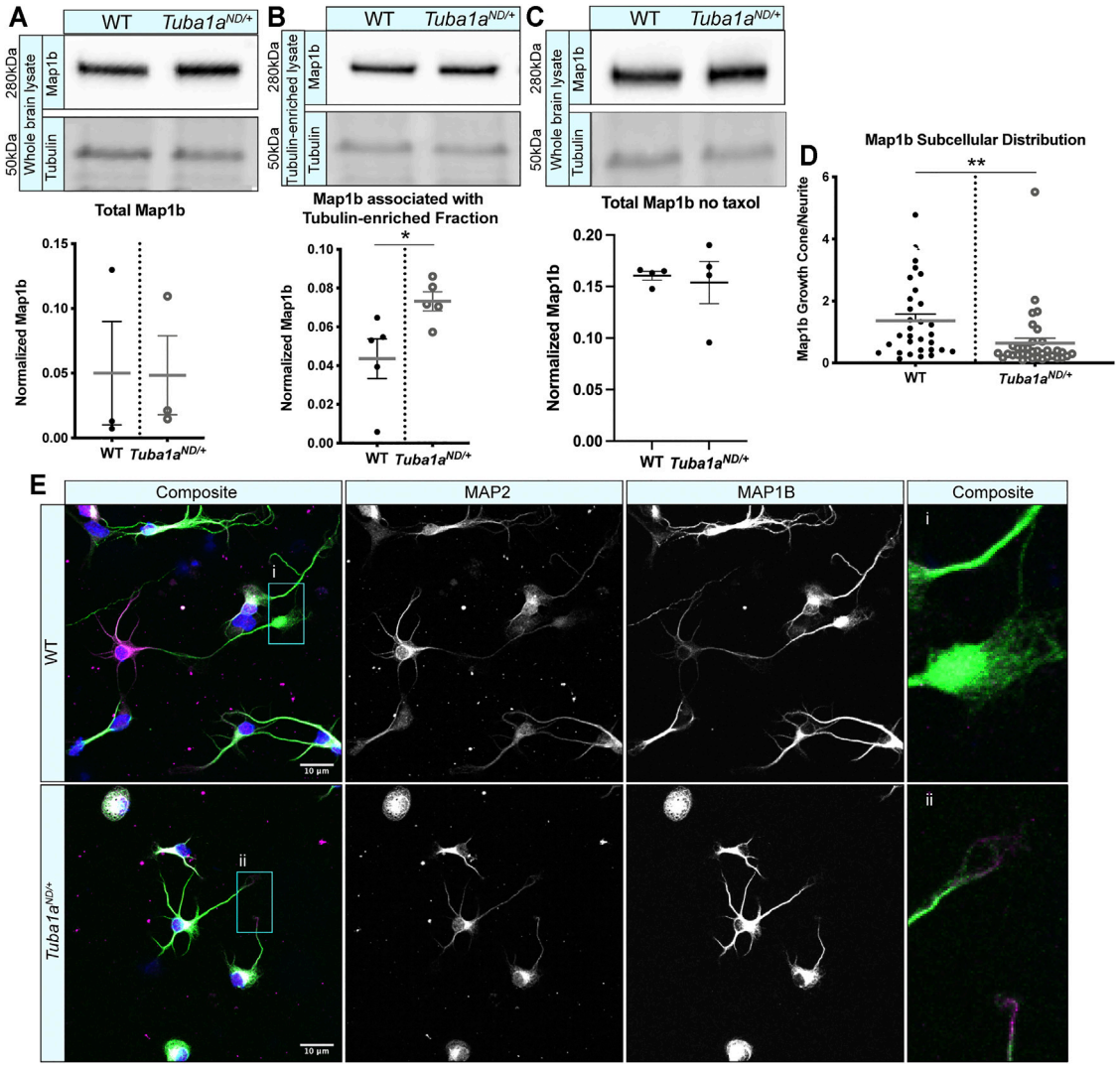

FIGURE 7 | *Tuba1a*ND neurons do not correctly localize Map1b to the developing growth cone. **(A)** Western blot showing total Map1b protein in whole brain lysate from wild-type (WT) and *Tuba1a*$^{ND/+}$ mice. Scatter plot representing total Map1b protein in brain lysate by western blot, normalized to the total protein on a stain-free blot. $p = 0.98$ by *t*-test. **(B)** Western blots showing Map1b protein associated with a taxol stabilized tubulin-enriched fraction from brain (top panel). Due to the amount of protein that was loaded for Map1b western blots, antibody-stained bands for α-tubulin were oversaturated and could not be quantified, thus Map1b was normalized to the 50 kDa band (presumed to be primarily tubulin) on a UV-activated stain-free blot (bottom panel). Scatter plot quantifying Map1b associated with the taxol-stabilized tubulin-enriched brain lysate, normalized to the 50 kDa presumed tubulin band using stain-free western blotting. $p = 0.03$ by *t*-test **(C)**. Western blot showing Map1b from WT and *Tuba1a*$^{ND/+}$ pellet fraction of brain lysates without the addition of taxol. Scatter plot quantifying Map1b associated with tubulin enriched from brain lysates shows no significant difference between the amount of Map1b associated with tubulin when no taxol was added, $p = 0.76$ by *t*-test. Map1b is normalized to the 50 kDa tubulin band using stain-free western blotting. **(D)** Scatter plot showing the subcellular distribution of Map1b protein in WT and *Tuba1a*$^{ND/+}$ cortical neurons at DIV 3. Data are represented as Map1b fluorescent signal in growth cone region divided by a region proximal to the cell body of the same area. Fluorescent images were acquired using identical microscope imaging settings between samples and were not post-processed to adjust fluorescence prior to quantification. $p = 0.009$. **(E)** Representative images showing altered subcellular distribution of Map1b in *Tuba1a*$^{ND/+}$ (bottom) cortical neurons compared to WT (top) at DIV 3. Composite and individual channel grayscale images of MAP2 and Map1b immunocytochemistry are shown, *i* and *ii* indicate enlarged regions shown in insets. Scale bars are 10 m. Differences between groups were evaluated by *t* test. $^*p < 0.05$; $^{**}p < 0.01$.

extension and commissure formation, which is achieved via a dynamic cytoskeleton that can readily respond to external cues through the action of critical factors localized to the growth cone. Without sufficient Tuba1a, axons cannot grow at the appropriate rate or correctly localize important MAP(s), rendering Tuba1a deficient axons incapable of crossing the midline to reach distant targets.

Studying α-Tubulin Isotypes

TUBA1A has long been associated with neurodevelopment due to its spatial and temporal expression as well as its causal role in tubulinopathies (Miller et al., 1987; Gloster et al., 1994; Bamji and Miller, 1996; Gloster et al., 1999; Poirier et al., 2007; Fallet-Bianco et al., 2008; Kumar et al., 2010; Lecourtois et al., 2010; Oegema et al., 2015; Aiken et al., 2017), but cellular visualization of a

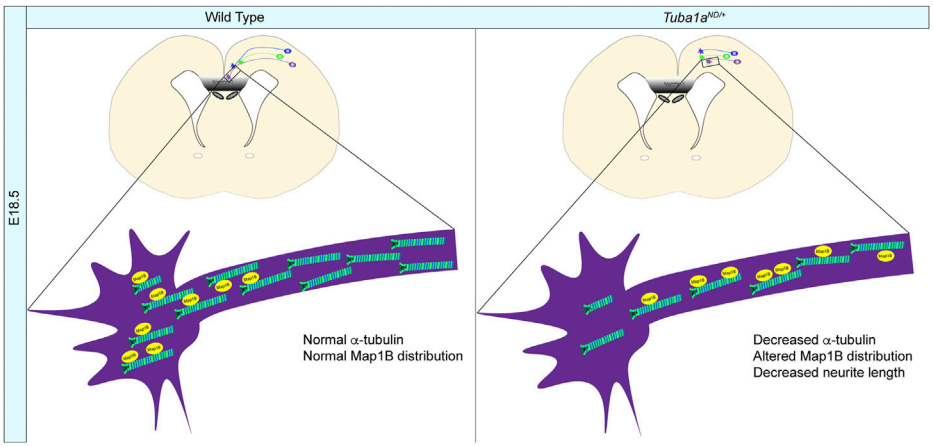

FIGURE 8 | Mechanisms of Tuba1a-induced axonal pathfinding deficits. **(A)** Schematic illustrating how reduced Tuba1a may impair ability of *Tuba1a*$^{ND/+}$ axons to reach key signaling points at the correct developmental time to support proper brain formation. Wild-type axons (WT; left) reaching the midline crossing point of corpus callosum by embryonic day (E) 18.5 are compared to the potentially stunted axonal growth in *Tuba1a*$^{ND/+}$ brains (right). The reduced density of microtubules impair localization of Map1b and potentially other MAPs to contribute to slower growth of developing *Tuba1a*$^{ND/+}$ commissural neurons.

single α-tubulin isotype or mutant has remained elusive due to the limited availability of isotype-specific tools. Studying individual α-tubulin isotypes in neurons has been historically arduous as the high degree of amino acid sequence similarity between α-tubulin isotypes (TUBA1A and TUBA1B proteins are 99.5% identical) leads to antibody promiscuity and has made genetically targeting a single α-tubulin gene challenging. The abundance of clinically identified mutations to *TUBA1A* provide strong evidence that *TUBA1A* is a major player in both tubulinopathy and typical neurodevelopment; however, the lack of available tools to study TUBA1A in cells has prevented researchers from understanding precisely how *TUBA1A* contributes to neurodevelopment. As such, previous studies of tubulinopathy mutations have relied heavily on mRNA analysis and indirect methods of evaluating TUBA1A protein function. Here we harness a previously-identified internal loop within TUBA1A that tolerates addition of small epitope tags without impacting TUBA1A incorporation or dynamics (Schatz et al., 1987; Heilemann et al., 2008; Hotta et al., 2016) to generate an important tool for the study of tubulinopathies and neuronal α-tubulin. Advantages of this tool are many. In Cos-7 cells and neurons, wild-type TUBA1A-His6 was able to incorporate into microtubule polymers, unlike TUBA1A containing a GFP fusion that prohibited incorporation into neuronal microtubules (**Figure 2**). Further, internal tagging does not interfere with C-terminal post translational modifications, which are abundant in neurons and contribute to function. The His6 tag can also be eluted natively so that the same tubulin isotype mutants can be purified for *in vitro* studies to complement localization and functional studies completed in cells. Additionally, the addition of the internal His6 tag did not remove or replace the Lysine 40 acetylation site. In Cos-7 cells and neurons, wild-type *TUBA1A-His6* was able to incorporate into microtubule polymers, unlike *TUBA1A* containing a GFP fusion that prohibited incorporation into neuronal microtubules (**Figure 2**). Importantly, this epitope-tagged TUBA1A can be used to gain insight into how mutant tubulin behaves in cellular microtubule networks (**Figures 1**, **2**). For example, we reveal that *TUBA1A*^{T349E}, a substitution analogous to a previously described mutation that prevents tubulin polymerization in yeast (Johnson et al., 2011), fails to polymerize into neuronal microtubules but does not interfere with endogenous microtubule networks, as revealed by intact acetylated microtubules (**Figure 2C**). In contrast, *TUBA1A*^{E255A}, a lethal α-tubulin stabilizing mutation discovered in yeast which prevents tubulin depolymerization (Anders and Botstein, 2001; Roostalu et al., 2020), is abundantly incorporated into microtubule polymers and increases acetylated tubulin staining compared to wild type (**Figure 2C**). This mutation leads to thickened microtubule-rich protrusions (**Figure 2C**). Overall, this tool enables researchers to gain valuable insight into the cellular function of specific α-tubulin isotypes and determine how mutations impact tubulin function, microtubule networks, and cellular morphology.

When applied to *TUBA1A*^{N102D}, the epitope-tagged TUBA1A visualization revealed that the N102D mutation leads to polymerization-incompetent tubulin similar to the T349E substitution. Ectopic expression of *TUBA1A*-His6 protein in cells revealed that TUBA1AND protein is excluded from microtubule filaments (**Figures 1B**, **2C**) and is approximately half as abundant as wild-type (**Figure 1D**), despite similar amounts of mRNA expression in transfected cells (**Figure 1E**). Based on this evidence, *TUBA1A*ND substitution lowers the total amount of usable α-tubulin in the cell (**Figure 1D**). Newly synthesized α- and β-tubulin proteins enter a complex tubulin folding pathway, where they interact with cytosolic chaperonins and tubulin-binding cofactors to become folded and assembled into tubulin heterodimers (Lewis et al., 1997). We found *TUBA1A*ND protein to be diminished compared to wild-type, and the introduction of the ND substitution into the primary yeast α—tubulin, *Tub1*, (*Tub1*ND) is synthetic lethal when combined with tubulin folding pathway mutants. These data reveal an increased reliance on tubulin assembly cofactors when the ND mutation is present, which may be retained in mammalian systems (Gartz Hanson et al., 2016).

Tuba1a Influences the Microtubule Cytoskeleton in Cells

The microtubule cytoskeleton supports a wide range of different cellular functions in different cell types, ranging from facilitating chromosome segregation during mitosis to forming dynamic and motile structures such as the neuronal growth cone. Understanding how different cells use the same basic building blocks to create vastly different microtubule-based structures is a major question in microtubule biology. Many different mechanisms have been identified by which cells regulate microtubule network properties and overall function. In this study, we provide the first evidence that TUBA1A is essential for regulating neuronal microtubule function to support commissure formation (**Figures 3**, **4**). *Tuba1a*ND neurons exhibit deficits in neurite extension, [**Figures 5**, **6**; (Buscaglia, 2020)], and do not support growth cone localization of at least one critical developmental MAP necessary for commissural axon pathfinding, Map1b (**Figure 6**). Collectively, these data support the conclusion that reduced Tuba1a is sufficient for certain microtubule-dependent neurodevelopmental stages, such as cortical neuron migration (Gartz Hanson et al., 2016), but does not allow for sufficient microtubule function to properly localize proteins to the growth cone or to grow at the rate necessary to form commissures. Thus, axons extending to reach distant targets may be exquisitely sensitive to α-tubulin levels.

We previously showed that while there was an overall reduction in α-tubulin protein in brains of heterozygous *Tuba1a*$^{ND/+}$ mice compared to wild type, there was no significant difference in the overall ratio of post-translational modifications, normalized to total α-tubulin (Buscaglia, 2020). Here, we show that the *Tuba1a*ND mutation changes the distribution of acetylated microtubules subcellularly in the growth cone (**Figure 5**), likely reflecting altered microtubule organization (**Figure 5**). Acetylation is a microtubule PTM that is associated with stable microtubule populations and as such is sparse in dynamic structures like growth cones (Schulze et al., 1987; Robson and Burgoyne, 1989; Mansfield and Gordon-Weeks, 1991; Palazzo et al., 2003; Baas et al., 2016; Eshun-Wilson et al., 2019). However, microtubule acetylation can be induced in growth cones following contact with extracellular matrix proteins and promotes cortical neuron migration *in vivo* and suppresses axon branching *in vitro*, demonstrating a clear role for this PTM in development (Dan et al., 2018; Bergstrom et al., 2007; Creppe et al., 2009). Tubulin PTMs, like acetylation, impact MAP-binding affinity and function, providing a clear mechanism by which changing the PTM landscape of microtubules could alter neuronal microtubule function (Mansfield and Gordon-Weeks, 1991; Bonnet et al., 2001; Reed et al., 2006; Janke and Kneussel, 2010; Lacroix et al., 2010; Sirajuddin et al., 2014; Balabanian et al., 2017). Thus, any changes to the organization or distribution of acetylated microtubules in the growth cone could impact the ability of developing neurons to appropriately navigate their environment and establish correct synaptic targets.

Tuba1a$^{ND/+}$ growth cones showed a significant increase in F-actin fluorescence compared to wild-type, causing an overall shift in the growth cone microtubule-actin balance (**Figure 5**). This may be due to a shift in distribution of F-actin rather than an increase in levels of F-actin. It is well established that interplay between the actin and microtubule cytoskeleton drives growth cone movements in developing neurons (Dent and Kalil, 2001; Dent et al., 2011; Piper et al., 2015; Craig, 2018). Growth cone microtubule polymerization induces F-actin assembly, and coordination of actin and microtubules is regulated by interactions with MAPs to drive appropriate growth cone response (Rochlin et al., 1999; Szikora et al., 2017; Biswas and Kalil, 2018; Slater et al., 2019). As actin and microtubules are tightly regulated within the growth cone, it is reasonable to assume that mutations which disrupt microtubule function, like *Tuba1a*ND, likely also impact the actin cytoskeleton of developing neurons. In *Tuba1a*$^{ND/+}$ neurons, the actin cytoskeleton may occupy increased growth cone territory as the result of microtubule deficiencies, but additional testing of actin-response in developing *Tuba1a*$^{ND/+}$ neurons is needed to assess whether the increase in growth cone actin has any functional consequences.

We show that *Tuba1a*$^{ND/+}$ neurons do not effectively localize at least one developmental MAP, Map1b, to the growth cone (**Figure 7**). We previously demonstrated that axonal transport is impaired in developing *Tuba1a*$^{ND/+}$ neurons (Buscaglia, 2020), thus reduced Tuba1a could lead to altered localization of developmental MAPs due to disrupted trafficking. Our data do not support the conclusion that Map1b expression or binding to microtubules is reduced. Instead, we favor a model in which trafficking is disrupted so that Map1b is not appropriately localized. Intracellular transport is a crucial function of neuronal microtubules throughout life, and microtubule-based transport is essential during neurodevelopment for distributing cellular components into burgeoning neurites (Hoogenraad and Bradke, 2009; Feltrin et al., 2012; Liu et al., 2012; Baraban et al., 2013; Dent and Baas, 2014; Leung et al., 2018; Miller and Suter, 2018). Correct localization of developmental MAPs, mRNAs and organelles are necessary for cytoskeletal response to extracellular guidance cues (Welshhans and Bassell, 2011; Feltrin et al., 2012; Qu et al., 2013; Pilaz et al., 2016; Leung et al., 2018). In particular, Map1b is required for commissure formation (Meixner et al., 2000) and homozygous Map1b knockout animals have similar phenotypes to *Tuba1a*$^{ND/+}$ mice [**Figure 3** and (Meixner et al., 2000)]. Map1b is necessary for neuronal response to the guidance cue, Netrin1, a key player in commissural formation (Serafini et al., 1996; Barallobre et al., 2000; Finger et al., 2002; Lindwall et al., 2007; Fothergill et al., 2014; Arbeille and Bashaw, 2018). While our data show that *Tuba1a*$^{ND/+}$ neurites grow faster in response to global application of Netrin-1 similar to wild type neurons in the time frame we measured, we cannot rule out impairment of turning in response to a localized source of Netrin-1 or response to other guidance cues. With the exception of tubulin and actin, Map1b is the most abundant cytoskeletal protein in the growth cone and localizes asymmetrically to the growth cone (Mack et al., 2000; Igarashi, 2014). Our data suggests that if Map1b is not localized to the growth cone, it cannot perform its function in commissure formation. Map1b acts downstream of several important developmental signaling pathways to regulate function of both actin and microtubules within the growth cone, and dysregulation of this or other MAPs

could therefore impact multiple cytoskeletal components (Mack et al., 2000; Noiges et al., 2002; Tymanskyj et al., 2012).

Reduced Tuba1a Function does not Adequately Support Neurite Growth for Development

The timing of axon growth is crucial for the growth cone to receive and respond to the appropriate guidance cues (Rossi et al., 2017; Krol and Feng, 2018). We showed that neuronal microtubules with reduced Tuba1a do not support axonal growth to the same degree as wild-type microtubules, causing shorter neurite length (**Figure 5**). If neurons lacking appropriate levels of TUBA1A do not reach the correct location at the correct time, it is possible that neurons will fail to receive key developmental signals (**Figure 8**). How does reducing Tuba1a function impair axon extension? One possibility is that there is not enough α-tubulin in the neurite or axon to assemble and extend microtubules. Another, non-exclusive possibility is that the microtubule tracks formed in *Tuba1a*ND axons are not sufficient to support trafficking of microtubule stabilizing factors. Microtubule-based transport is essential during neurodevelopment (Hoogenraad and Bradke, 2009; Feltrin et al., 2012; Liu et al., 2012; Baraban et al., 2013; Dent and Baas, 2014; Leung et al., 2018; Miller and Suter, 2018), and we previously showed that intracellular transport is impaired in developing *Tuba1a*$^{ND/+}$ neurons (Buscaglia, 2020). Map1b is not appropriately localized to the growth cone (**Figures 7**, **8**), suggesting that diminished Tuba1a function in neurons impacts the subcellular localization of Map1b, and potentially other MAPs, to the growth cone through impairments to intracellular trafficking (**Figure 8**).

Human neurodevelopmental disorders that impact microtubule function, such as tubulinopathies, demonstrate that microtubules are critical for neurodevelopment. Tubulinopathy patients exhibit severe, sometimes lethal, brain malformations that frequently impact multiple neurodevelopmental processes, including neuronal survival, migration, and axon extension (Fallet-Bianco et al., 2008; Tian et al., 2008; Keays et al., 2010; Kumar et al., 2010; Tian et al., 2010; Bamba et al., 2016; Belvindrah, 2017; Aiken et al., 2019a; Aiken et al., 2019b). The range of phenotypes exhibited by tubulinopathy patients have made it challenging for scientists to pinpoint specific aspects of neuronal function that are reliant on TUBA1A tubulin. We used *Tuba1a*ND as a tool to interrogate the requirement for Tuba1a in discrete aspects of neurodevelopment. Importantly, commissural abnormalities, such as agenesis of the corpus callosum, are commonly reported features in tubulinopathy patients (Poirier et al., 2007; Fallet-Bianco et al., 2008; Cushion et al., 2013; Oegema et al., 2015; Aiken et al., 2017). Cortical malformations and neuronal migration errors are also common features of *TUBA1A* tubulinopathies; however, it has thus far been unclear whether commissural deficits occur as a primary or secondary consequence of TUBA1A dysfunction. In this study, we provide evidence that axons deficient in Tuba1a fail to properly navigate to meet contralateral binding partners. These data demonstrate that TUBA1A is required for forebrain commissural formation, independent of its role in neuronal survival or migration.

DATA AVAILABILITY STATEMENT

The raw data supporting the conclusion of this article will be made available by the authors, without undue reservation.

ETHICS STATEMENT

The animal study was reviewed and approved by University of Colorado Anschutz Medical Campus IACUC committee.

AUTHOR CONTRIBUTIONS

GB and EB designed experiments. GB and KN performed the majority of the experiments and each wrote first drafts of portions of the manuscript. JA generated the Tuba1a-His6 constructs and together with KH imaged neurons that expressed wild-type or mutant Tuba1a-His6. All authors read, provided feedback and edits to the manuscript. EB directed, and obtained funding for research and edited versions of the manuscript.

ACKNOWLEDGMENTS

We would like to thank Dr. Jeffrey K. Moore for discussions and valuable advice. We thank Matthew Kennedy and Mark del Acqua (University of Colorado School of Medicine) for providing P0-2 rat cortex. We would like to thank funding sources without which our work would not be possible: NIH NIDCR R01DE025311 to EAB, NSF-IOS 1945916 to EAB, University of Colorado Movement Disorder Center to EAB, T32 NS099042 to GB, NSF Graduate Research Fellowship 1553798 to JA, NINDS F32NS117672 to JA, T32GM141742-01 to KN. T32 GM136444 to KH. Emily Bates would like to thank the teachers at her children's schools and Bright Horizons Fitzimons daycare during the Covid-19 pandemic without whom, none of her work could be performed.

SUPPLEMENTARY MATERIAL

The Supplementary Material for this article can be found online at: https://www.frontiersin.org/articles/10.3389/fcell.2021.789438/full#supplementary-material

Supplementary Figure S1 | dSTORM imaging of TUBA1A-His6 signal reveals single microtubules. **(A)** Wide-field (top panels) and dSTORM super-resolution (lower panels and insets) microscopy of DIV7 neurons transfected with TUBA1A-His6 plasmid DNA and immunolabeled with α-His6 antibody. Yellow boxes reveal the location of the magnified insets below. **(B)** dSTORM super-resolution microscopy of DIV4 astrocytes immunolabeled with total α-tubulin antibody (left panels) or transfected with TUBA1A-His6 plasmid DNA and immunolabeled with α-His6 antibody. Yellow boxes reveal the location of the magnified insets below.

REFERENCES

Aiken, J., Buscaglia, G., Bates, E. A., and Moore, J. K. (2017). The α-Tubulin Gene TUBA1A in Brain Development: A Key Ingredient in the Neuronal Isotype Blend. *J. Dev. Biol.* 5 (3). doi:10.3390/jdb5030008

Aiken, J. (2019). *Tubulin Mutations in Brain Development Disorders: Why Haploinsufficiency Does Not Explain TUBA1A Tubulinopathies*. Hoboken): Cytoskeleton.

Aiken, J., Moore, J. K., and Bates, E. A. (2019). TUBA1A Mutations Identified in Lissencephaly Patients Dominantly Disrupt Neuronal Migration and Impair Dynein Activity. *Hum. Mol. Genet.* 28 (8), 1227–1243. doi:10.1093/hmg/ddy416

Anders, K. R., and Botstein, D. (2001). Dominant-Lethal α-Tubulin Mutants Defective in Microtubule Depolymerization in Yeast. *MBoC* 12 (12), 3973–3986. doi:10.1091/mbc.12.12.3973

Arbeille, E., and Bashaw, G. J. (2018). Brain Tumor Promotes Axon Growth across the Midline through Interactions with the Microtubule Stabilizing Protein Apc2. *Plos Genet.* 14 (4), e1007314. doi:10.1371/journal.pgen.1007314

Baas, P. W., Rao, A. N., Matamoros, A. J., and Leo, L. (2016). Stability Properties of Neuronal Microtubules. *Cytoskeleton* 73 (9), 442–460. doi:10.1002/cm.21286

Balabanian, L., Berger, C. L., and Hendricks, A. G. (2017). Acetylated Microtubules Are Preferentially Bundled Leading to Enhanced Kinesin-1 Motility. *Biophysical J.* 113 (7), 1551–1560. doi:10.1016/j.bpj.2017.08.009

Bamba, Y., Shofuda, T., Kato, M., Pooh, R. K., Tateishi, Y., Takanashi, J.-i., et al. (2016). *In Vitro* characterization of Neurite Extension Using Induced Pluripotent Stem Cells Derived from Lissencephaly Patients with TUBA1A Missense Mutations. *Mol. Brain* 9 (1), 70. doi:10.1186/s13041-016-0246-y

Bamji, S. X., and Miller, F. D. (1996). Comparison of the Expression of a T?1:nlacZ Transgene and T?1 ?-tubulin mRNA in the Mature central Nervous System. *J. Comp. Neurol.* 374 (1), 52–69. doi:10.1002/(sici)1096-9861(19961007)374:1<52:aid-cne4>3.0.co;2-m

Baraban, M., Anselme, I., Schneider-Maunoury, S., and Giudicelli, F. (2013). Zebrafish Embryonic Neurons Transport Messenger RNA to Axons and Growth Cones *In Vivo*. *J. Neurosci.* 33 (40), 15726–15734. doi:10.1523/jneurosci.1510-13.2013

Barallobre, M. J., Del Rio, J. A., Alcantara, S., Borrell, V., Aguado, F., Ruiz, M., et al. (2000). Aberrant Development of Hippocampal Circuits and Altered Neural Activity in Netrin 1-deficient Mice. *Development* 127 (22), 4797–4810. doi:10.1242/dev.127.22.4797

Belvindrah, R. (2017). Mutation of the Alpha-Tubulin Tuba1a Leads to Straighter Microtubules and Perturbs Neuronal Migration. *J. Cel Biol.*

Bergstrom, R. A., Sinjoanu, R. C., and Ferreira, A. (2007). Agrin Induced Morphological and Structural Changes in Growth Cones of Cultured Hippocampal Neurons. *Neuroscience* 149 (3), 527–536. doi:10.1016/j.neuroscience.2007.08.017

Biswas, S., and Kalil, K. (2018). The Microtubule-Associated Protein Tau Mediates the Organization of Microtubules and Their Dynamic Exploration of Actin-Rich Lamellipodia and Filopodia of Cortical Growth Cones. *J. Neurosci.* 38 (2), 291–307. doi:10.1523/jneurosci.2281-17.2017

Bittermann, E., Abdelhamed, Z., Liegel, R. P., Menke, C., Timms, A., Beier, D. R., et al. (2019). Differential Requirements of Tubulin Genes in Mammalian Forebrain Development. *Plos Genet.* 15 (8), e1008243. doi:10.1371/journal.pgen.1008243

Black, M., Slaughter, T., and Fischer, I. (1994). Microtubule-associated Protein 1b (MAP1b) Is Concentrated in the Distal Region of Growing Axons. *J. Neurosci.* 14 (2), 857–870. doi:10.1523/jneurosci.14-02-00857.1994

Bonnet, C., Boucher, D., Lazereg, S., Pedrotti, B., Islam, K., Denoulet, P., et al. (2001). Differential Binding Regulation of Microtubule-Associated Proteins MAP1A, MAP1B, and MAP2 by Tubulin Polyglutamylation. *J. Biol. Chem.* 276 (16), 12839–12848. doi:10.1074/jbc.m011380200

Boyer, N. P., and Gupton, S. L. (2018). Revisiting Netrin-1: One Who Guides (Axons). *Front. Cel. Neurosci.* 12, 221. doi:10.3389/fncel.2018.00221

Buck, K. B., and Zheng, J. Q. (2002). Growth Cone Turning Induced by Direct Local Modification of Microtubule Dynamics. *J. Neurosci.* 22 (21), 9358–9367. doi:10.1523/jneurosci.22-21-09358.2002

Buscaglia, G. (2020). *Reduced TUBA1A Tubulin Causes Defects in Trafficking and Impaired Adult Motor Behavior*. Washington, D.C.: eNeuro.

Craig, E. M. (2018). Model for Coordination of Microtubule and Actin Dynamics in Growth Cone Turning. *Front. Cel. Neurosci.* 12, 394. doi:10.3389/fncel.2018.00394

Creppe, C., Malinouskaya, L., Volvert, M.-L., Gillard, M., Close, P., Malaise, O., et al. (2009). Elongator Controls the Migration and Differentiation of Cortical Neurons through Acetylation of α-Tubulin. *Cell* 136 (3), 551–564. doi:10.1016/j.cell.2008.11.043

Cushion, T. D., Dobyns, W. B., Mullins, J. G., Stoodley, N., Chung, S. K., Fry, A. E., et al. (2013). Overlapping Cortical Malformations and Mutations in TUBB2B and TUBA1A. *Brain* 136 (Pt 2), 536–548. doi:10.1093/brain/aws338

Dan, W., Gao, N., Li, L., Zhu, J. X., Diao, L., Huang, J., et al. (2018). α-Tubulin Acetylation Restricts Axon Overbranching by Dampening Microtubule Plus-End Dynamics in Neurons. *Cereb. Cortex* 28 (9), 3332–3346. doi:10.1093/cercor/bhx225

Del Río, J. A., González-Billault, C., Ureña, J. M., Jiménez, E. M., Barallobre, M. J., Pascual, M., et al. (2004). MAP1B Is Required for Netrin 1 Signaling in Neuronal Migration and Axonal Guidance. *Curr. Biol.* 14 (10), 840–850. doi:10.1016/j.cub.2004.04.046

Dent, E. W., Gupton, S. L., and Gertler, F. B. (2011). The Growth Cone Cytoskeleton in Axon Outgrowth and Guidance. *Cold Spring Harb Perspect. Biol.* 3 (3). doi:10.1101/cshperspect.a001800

Dent, E. W., and Baas, P. W. (2014). Microtubules in Neurons as Information Carriers. *J. Neurochem.* 129 (2), 235–239. doi:10.1111/jnc.12621

Dent, E. W., and Kalil, K. (2001). Axon Branching Requires Interactions between Dynamic Microtubules and Actin Filaments. *J. Neurosci.* 21 (24), 9757–9769. doi:10.1523/jneurosci.21-24-09757.2001

Eshun-Wilson, L., Zhang, R., Portran, D., Nachury, M. V., Toso, D. B., Löhr, T., et al. (2019). Effects of α-tubulin Acetylation on Microtubule Structure and Stability. *Proc. Natl. Acad. Sci. USA* 116 (21), 10366–10371. doi:10.1073/pnas.1900441116

Fallet-Bianco, C., Loeuillet, L., Poirier, K., Loget, P., Chapon, F., Pasquier, L., et al. (2008). Neuropathological Phenotype of a Distinct Form of Lissencephaly Associated with Mutations in TUBA1A. *Brain* 131 (Pt 9), 2304–2320. doi:10.1093/brain/awn155

Feltrin, D., Fusco, L., Witte, H., Moretti, F., Martin, K., Letzelter, M., et al. (2012). Growth Cone MKK7 mRNA Targeting Regulates MAP1b-dependent Microtubule Bundling to Control Neurite Elongation. *Plos Biol.* 10 (12), e1001439. doi:10.1371/journal.pbio.1001439

Findeisen, P., Mühlhausen, S., Dempewolf, S., Hertzog, J., Zietlow, A., Carlomagno, T., et al. (2014). Six Subgroups and Extensive Recent Duplications Characterize the Evolution of the Eukaryotic Tubulin Protein Family. *Genome Biol. Evol.* 6 (9), 2274–2288. doi:10.1093/gbe/evu187

Finger, J. H., Bronson, R. T., Harris, B., Johnson, K., Przyborski, S. A., and Ackerman, S. L. (2002). The Netrin 1 ReceptorsUnc5h3andDccAre Necessary at Multiple Choice Points for the Guidance of Corticospinal Tract Axons. *J. Neurosci.* 22 (23), 10346–10356. doi:10.1523/jneurosci.22-23-10346.2002

Fothergill, T., Donahoo, A.-L. S., Douglass, A., Zalucki, O., Yuan, J., Shu, T., et al. (2014). Netrin-DCC Signaling Regulates Corpus Callosum Formation through Attraction of Pioneering Axons and by Modulating Slit2-Mediated Repulsion. *Cereb. Cortex* 24 (5), 1138–1151. doi:10.1093/cercor/bhs395

Gadadhar, S., Bodakuntla, S., Natarajan, K., and Janke, C. (2017). The Tubulin Code at a Glance. *J. Cel Sci* 130 (8), 1347–1353. doi:10.1242/jcs.199471

Gartz Hanson, M., Aiken, J., Sietsema, D. V., Sept, D., Bates, E. A., Niswander, L., et al. (2016). Novel α-tubulin Mutation Disrupts Neural Development and Tubulin Proteostasis. *Dev. Biol.* 409 (2), 406–419. doi:10.1016/j.ydbio.2015.11.022

Gloster, A., El-Bizri, H., Bamji, S. X., Rogers, D., and Miller, F. D. (1999). Early Induction of T?1 ?-tubulin Transcription in Neurons of the Developing Nervous System. *J. Comp. Neurol.* 405 (1), 45–60. doi:10.1002/(sici)1096-9861(19990301)405:1<45:aid-cne4>3.0.co;2-m

Gloster, A., Wu, W., Speelman, A., Weiss, S., Causing, C., Pozniak, C., et al. (1994). The T Alpha 1 Alpha-Tubulin Promoter Specifies Gene Expression as a Function of Neuronal Growth and Regeneration in Transgenic Mice. *J. Neurosci.* 14 (12), 7319–7330. doi:10.1523/jneurosci.14-12-07319.1994

Gonzalez-Billault, C., Avila, J., and Cáceres, A. (2001). Evidence for the Role of MAP1B in Axon Formation. *MBoC* 12 (7), 2087–2098. doi:10.1091/mbc.12.7.2087

González-Billault, C., Engelke, M., Jimȳnez-Mateos, E. M., Wandosell, F., Cáceres, A., and Avila, J. (2002). Participation of Structural Microtubule-Associated Proteins (MAPs) in the Development of Neuronal Polarity. *J. Neurosci. Res.* 67 (6), 713–719.

Gonzalez-Garay, M. L., and Cabral, F. (1996). Alpha-Tubulin Limits its Own Synthesis: Evidence for a Mechanism Involving Translational Repression. *J. Cel Biol* 135 (6 Pt 1), 1525–1534. doi:10.1083/jcb.135.6.1525

Heilemann, M., van de Linde, S., Schüttpelz, M., Kasper, R., Seefeldt, B., Mukherjee, A., et al. (2008). Subdiffraction-resolution Fluorescence Imaging with Conventional Fluorescent Probes. *Angew. Chem. Int. Ed.* 47 (33), 6172–6176. doi:10.1002/anie.200802376

Hoogendoorn, E., Crosby, K. C., Leyton-Puig, D., Breedijk, R. M. P., Jalink, K., Gadella, T. W. J., et al. (2014). The Fidelity of Stochastic Single-Molecule Super-resolution Reconstructions Critically Depends upon Robust Background Estimation. *Sci. Rep.* 4, 3854. doi:10.1038/srep03854

Hoogenraad, C. C., and Bradke, F. (2009). Control of Neuronal Polarity and Plasticity - a Renaissance for Microtubules? *Trends Cel Biol.* 19 (12), 669–676. doi:10.1016/j.tcb.2009.08.006

Hotta, T., Fujita, S., Uchimura, S., Noguchi, M., Demura, T., Muto, E., et al. (2016). Affinity Purification and Characterization of Functional Tubulin from Cell Suspension Cultures of Arabidopsis and Tobacco. *Plant Physiol.* 170 (3), 1189–1205. doi:10.1104/pp.15.01173

Igarashi, M. (2014). Proteomic Identification of the Molecular Basis of Mammalian CNS Growth Cones. *Neurosci. Res.* 88, 1–15. doi:10.1016/j.neures.2014.07.005

Janke, C., and Kneussel, M. (2010). Tubulin post-translational Modifications: Encoding Functions on the Neuronal Microtubule Cytoskeleton. *Trends Neurosciences* 33 (8), 362–372. doi:10.1016/j.tins.2010.05.001

Johnson, V., Ayaz, P., Huddleston, P., and Rice, L. M. (2011). Design, Overexpression, and Purification of Polymerization-Blocked Yeast αβ-Tubulin Mutants. *Biochemistry* 50 (40), 8636–8644. doi:10.1021/bi2005174

Kapitein, L. C., and Hoogenraad, C. C. (2015). Building the Neuronal Microtubule Cytoskeleton. *Neuron* 87 (3), 492–506. doi:10.1016/j.neuron.2015.05.046

Keays, D. A., Cleak, J., Huang, G.-J., Edwards, A., Braun, A., Treiber, C. D., et al. (2010). The Role of Tuba1a in Adult Hippocampal Neurogenesis and the Formation of the Dentate Gyrus. *Dev. Neurosci.* 32 (4), 268–277. doi:10.1159/000319663

Keays, D. A., Tian, G., Poirier, K., Huang, G.-J., Siebold, C., Cleak, J., et al. (2007). Mutations in α-Tubulin Cause Abnormal Neuronal Migration in Mice and Lissencephaly in Humans. *Cell* 128 (1), 45–57. doi:10.1016/j.cell.2006.12.017

Khodiyar, V. K., Maltais, L. J., Sneddon, K. M. B., Smith, J. R., Shimoyama, M., Cabral, F., et al. (2007). A Revised Nomenclature for the Human and Rodent α-tubulin Gene Family. *Genomics* 90 (2), 285–289. doi:10.1016/j.ygeno.2007.04.008

Kimble, M., Kuzmiak, C., McGovern, K. N., and de Hostos, E. L. (2000). Microtubule Organization and the Effects of GFP-Tubulin Expression inDictyostelium Discoideum. *Cell Motil. Cytoskeleton* 47 (1), 48–62. doi:10.1002/1097-0169(200009)47:1<48:aid-cm5>3.0.co;2-q

Krol, A., and Feng, G. (2018). Windows of Opportunity: Timing in Neurodevelopmental Disorders. *Curr. Opin. Neurobiol.* 48, 59–63. doi:10.1016/j.conb.2017.10.014

Kumar, R. A., Pilz, D. T., Babatz, T. D., Cushion, T. D., Harvey, K., Topf, M., et al. (2010). TUBA1A Mutations Cause Wide Spectrum Lissencephaly (Smooth Brain) and Suggest that Multiple Neuronal Migration Pathways Converge on Alpha Tubulins. *Hum. Mol. Genet.* 19 (14), 2817–2827. doi:10.1093/hmg/ddq182

Lacroix, B., van Dijk, J., Gold, N. D., Guizetti, J., Aldrian-Herrada, G., Rogowski, K., et al. (2010). Tubulin Polyglutamylation Stimulates Spastin-Mediated Microtubule Severing. *J. Cel Biol* 189 (6), 945–954. doi:10.1083/jcb.201001024

Leca, I., Phillips, A. W., Hofer, I., Landler, L., Ushakova, L., Cushion, T. D., et al. (2020). A Proteomic Survey of Microtubule-Associated Proteins in a R402H TUBA1A Mutant Mouse. *Plos Genet.* 16 (11), e1009104. doi:10.1371/journal.pgen.1009104

Lecourtois, M., Poirier, K., Friocourt, G., Jaglin, X., Goldenberg, A., Saugier-Veber, P., et al. (2010). Human Lissencephaly with Cerebellar Hypoplasia Due to Mutations in TUBA1A: Expansion of the Foetal Neuropathological Phenotype. *Acta Neuropathol.* 119 (6), 779–789. doi:10.1007/s00401-010-0684-z

Leung, K.-M., Lu, B., Wong, H. H.-W., Lin, J. Q., Turner-Bridger, B., and Holt, C. E. (2018). Cue-Polarized Transport of β-actin mRNA Depends on 3′UTR and Microtubules in Live Growth Cones. *Front. Cel. Neurosci.* 12, 300. doi:10.3389/fncel.2018.00300

Lewis, S., Tian, G., and Cowan, N. (1997). The α- and β-tubulin Folding Pathways. *Trends Cel Biol.* 7 (12), 479–484. doi:10.1016/s0962-8924(97)01168-9

Lindwall, C., Fothergill, T., and Richards, L. J. (2007). Commissure Formation in the Mammalian Forebrain. *Curr. Opin. Neurobiol.* 17 (1), 3–14. doi:10.1016/j.conb.2007.01.008

Liu, G., and Dwyer, T. (2014). Microtubule Dynamics in Axon Guidance. *Neurosci. Bull.* 30 (4), 569–583. doi:10.1007/s12264-014-1444-6

Liu, J. S., Schubert, C. R., Fu, X., Fourniol, F. J., Jaiswal, J. K., Houdusse, A., et al. (2012). Molecular Basis for Specific Regulation of Neuronal Kinesin-3 Motors by Doublecortin Family Proteins. *Mol. Cel* 47 (5), 707–721. doi:10.1016/j.molcel.2012.06.025

Mack, T. G. A., Koester, M. P., and Pollerberg, G. E. (2000). The Microtubule-Associated Protein MAP1B Is Involved in Local Stabilization of Turning Growth Cones. *Mol. Cell Neurosci.* 15 (1), 51–65. doi:10.1006/mcne.1999.0802

Mansfield, S. G., and Gordon-Weeks, P. R. (1991). Dynamic post-translational Modification of Tubulin in Rat Cerebral Cortical Neurons Extending Neurites in Culture: Effects of Taxol. *J. Neurocytol* 20 (8), 654–666. doi:10.1007/bf01187067

Meixner, A., Haverkamp, S., Wässle, H., Führer, S., Thalhammer, J., Kropf, N., et al. (2000). MAP1B Is Required for Axon Guidance and Is Involved in the Development of the central and Peripheral Nervous System. *J. Cel Biol* 151 (6), 1169–1178. doi:10.1083/jcb.151.6.1169

Miller, F. D., Naus, C. C., Durand, M., Bloom, F. E., and Milner, R. J. (1987). Isotypes of Alpha-Tubulin Are Differentially Regulated during Neuronal Maturation. *J. Cel Biol* 105 (6 Pt 2), 3065–3073. doi:10.1083/jcb.105.6.3065

Miller, K. E., and Suter, D. M. (2018). An Integrated Cytoskeletal Model of Neurite Outgrowth. *Front. Cel. Neurosci.* 12, 447. doi:10.3389/fncel.2018.00447

Nishikimi, M., Oishi, K., and Nakajima, K. (2013). Axon Guidance Mechanisms for Establishment of Callosal Connections. *Neural Plast.* 2013, 149060. doi:10.1155/2013/149060

Noiges, R., Eichinger, R., Kutschera, W., Fischer, I., Németh, Z., Wiche, G., et al. (2002). Microtubule-associated Protein 1A (MAP1A) and MAP1B: Light Chains Determine Distinct Functional Properties. *J. Neurosci.* 22 (6), 2106–2114. doi:10.1523/jneurosci.22-06-02106.2002

Oegema, R., Cushion, T. D., Phelps, I. G., Chung, S.-K., Dempsey, J. C., Collins, S., et al. (2015). Recognizable Cerebellar Dysplasia Associated with Mutations in Multiple Tubulin Genes. *Hum. Mol. Genet.* 24 (18), 5313–5325. doi:10.1093/hmg/ddv250

Ōmura, S., and Crump, A. (2019). Lactacystin: First-In-Class Proteasome Inhibitor Still Excelling and an Exemplar for Future Antibiotic Research. *J. Antibiot. (Tokyo)* 72 (4), 189–201. doi:10.1038/s41429-019-0141-8

Ovesný, M. (2014). ThunderSTORM: a Comprehensive ImageJ Plug-In for PALM and STORM Data Analysis and Super-resolution Imaging. *Bioinformatics* 30 (16), 2389–2390.

Palazzo, A., Ackerman, B., and Gundersen, G. G. (2003). Tubulin Acetylation and Cell Motility. *Nature* 421 (6920), 230. doi:10.1038/421230a

Pilaz, L.-J., Lennox, A. L., Rouanet, J. P., and Silver, D. L. (2016). Dynamic mRNA Transport and Local Translation in Radial Glial Progenitors of the Developing Brain. *Curr. Biol.* 26 (24), 3383–3392. doi:10.1016/j.cub.2016.10.040

Piper, M., Lee, A. C., van Horck, F. P., McNeilly, H., Lu, T. B., Harris, W. A., et al. (2015). Differential Requirement of F-Actin and Microtubule Cytoskeleton in Cue-Induced Local Protein Synthesis in Axonal Growth Cones. *Neural Dev.* 10, 3. doi:10.1186/s13064-015-0031-0

Poirier, K., Keays, D. A., Francis, F., Saillour, Y., Bahi, N., Manouvrier, S., et al. (2007). Large Spectrum of Lissencephaly and Pachygyria Phenotypes Resulting from De Novo Missense Mutations in Tubulin Alpha 1A (TUBA1A). *Hum. Mutat.* 28 (11), 1055–1064. doi:10.1002/humu.20572

Probst, M. (1901). Uber den Bau des balkenlosen Grobhirns, sowie uber Mikrogyrie and Heterotypie der grauer Substanz. *Arch. F Psychiatr.* (34), 709–786. doi:10.1007/bf02680175

Qu, C., Dwyer, T., Shao, Q., Yang, T., Huang, H., and Liu, G. (2013). Direct Binding of TUBB3 with DCC Couples Netrin-1 Signaling to Intracellular Microtubule Dynamics in Axon Outgrowth and Guidance. *J. Cel Sci* 126 (Pt 14), 3070–3081. doi:10.1242/jcs.122184

Reed, N. A., Cai, D., Blasius, T. L., Jih, G. T., Meyhofer, E., Gaertig, J., et al. (2006). Microtubule Acetylation Promotes Kinesin-1 Binding and Transport. *Curr. Biol.* 16 (21), 2166–2172. doi:10.1016/j.cub.2006.09.014

Robson, S. J., and Burgoyne, R. D. (1989). Differential Localisation of Tyrosinated, Detyrosinated, and Acetylated ?-tubulins in Neurites and Growth Cones of Dorsal Root Ganglion Neurons. *Cel Motil. Cytoskeleton* 12 (4), 273–282. doi:10.1002/cm.970120408

Rochlin, M. W., Dailey, M. E., and Bridgman, P. C. (1999). Polymerizing Microtubules Activate Site-Directed F-Actin Assembly in Nerve Growth Cones. *MBoC* 10 (7), 2309–2327. doi:10.1091/mbc.10.7.2309

Roostalu, J., Thomas, C., Cade, N. I., Kunzelmann, S., Taylor, I. A., and Surrey, T. (2020). The Speed of GTP Hydrolysis Determines GTP Cap Size and Controls Microtubule Stability. *Elife* 9. doi:10.7554/eLife.51992

Rossi, A. M., Fernandes, V. M., and Desplan, C. (2017). Timing Temporal Transitions during Brain Development. *Curr. Opin. Neurobiol.* 42, 84–92. doi:10.1016/j.conb.2016.11.010

Sakakibara, A., Ando, R., Sapir, T., and Tanaka, T. (2013). Microtubule Dynamics in Neuronal Morphogenesis. *Open Biol.* 3 (7), 130061. doi:10.1098/rsob.130061

Schatz, P. J., Georges, G. E., Solomon, F., and Botstein, D. (1987). Insertions of up to 17 Amino Acids into a Region of Alpha-Tubulin Do Not Disrupt Function *In Vivo*. *Mol. Cel Biol* 7 (10), 3799–3805. doi:10.1128/mcb.7.10.3799-3805.1987

Schneider, C. A., Rasband, W. S., and Eliceiri, K. W. (2012). NIH Image to ImageJ: 25 Years of Image Analysis. *Nat. Methods* 9 (7), 671–675. doi:10.1038/nmeth.2089

Schulze, E., Asai, D. J., Bulinski, J. C., and Kirschner, M. (1987). Posttranslational Modification and Microtubule Stability. *J. Cel Biol* 105 (5), 2167–2177. doi:10.1083/jcb.105.5.2167

Schüttpelz, M. (2010). *dSTORM: Real-Time Subdiffraction-Resolution Fluorescence Imaging with Organic Fluorophores*, 7571. Bellingham, WA: SPIE BiOS.

Serafini, T., Colamarino, S. A., Leonardo, E. D., Wang, H., Beddington, R., Skarnes, W. C., et al. (1996). Netrin-1 Is Required for Commissural Axon Guidance in the Developing Vertebrate Nervous System. *Cell* 87 (6), 1001–1014. doi:10.1016/s0092-8674(00)81795-x

Sirajuddin, M., Rice, L. M., and Vale, R. D. (2014). Regulation of Microtubule Motors by Tubulin Isotypes and post-translational Modifications. *Nat. Cel Biol* 16 (4), 335–344. doi:10.1038/ncb2920

Slater, P. G., Cammarata, G. M., Samuelson, A. G., Magee, A., Hu, Y., and Lowery, L. A. (2019). XMAP215 Promotes Microtubule-F-Actin Interactions to Regulate Growth Cone Microtubules during Axon Guidance in *Xenopus laevis*. *J. Cel Sci* 132 (9), jcs224311. doi:10.1242/jcs.224311

Szikora, S., Földi, I., Tóth, K., Migh, E., Vig, A., Bugyi, B., et al. (2017). The Formin DAAM Is Required for Coordination of the Actin and Microtubule Cytoskeleton in Axonal Growth Cones. *J. Cel Sci* 130 (15), 2506–2519. doi:10.1242/jcs.203455

Tian, G., Jaglin, X. H., Keays, D. A., Francis, F., Chelly, J., and Cowan, N. J. (2010). Disease-associated Mutations in TUBA1A Result in a Spectrum of Defects in the Tubulin Folding and Heterodimer Assembly Pathway. *Hum. Mol. Genet.* 19 (18), 3599–3613. doi:10.1093/hmg/ddq276

Tian, G., Kong, X.-P., Jaglin, X. H., Chelly, J., Keays, D., and Cowan, N. J. (2008). A Pachygyria-Causing α-Tubulin Mutation Results in Inefficient Cycling with CCT and a Deficient Interaction with TBCB. *MBoC* 19 (3), 1152–1161. doi:10.1091/mbc.e07-09-0861

Tischfield, M. A., Cederquist, G. Y., Gupta, M. L., and Engle, E. C. (2011). Phenotypic Spectrum of the Tubulin-Related Disorders and Functional Implications of Disease-Causing Mutations. *Curr. Opin. Genet. Dev.* 21 (3), 286–294. doi:10.1016/j.gde.2011.01.003

Tomoda, H., and Omura, S. (2000). Lactacystin, a Proteasome Inhibitor : Discovery and its Application in Cell Biology. *Yakugaku Zasshi* 120 (10), 935–949. doi:10.1248/yakushi1947.120.10_935

Tymanskyj, S. R., Scales, T. M. E., and Gordon-Weeks, P. R. (2012). MAP1B Enhances Microtubule Assembly Rates and Axon Extension Rates in Developing Neurons. *Mol. Cell Neurosci.* 49 (2), 110–119. doi:10.1016/j.mcn.2011.10.003

Vallee, R. B. (1982). A Taxol-dependent Procedure for the Isolation of Microtubules and Microtubule-Associated Proteins (MAPs). *J. Cel Biol* 92 (2), 435–442. doi:10.1083/jcb.92.2.435

Wang, Y., Schnitzbauer, J., Hu, Z., Li, X., Cheng, Y., Huang, Z.-L., et al. (2014). Localization Events-Based Sample Drift Correction for Localization Microscopy with Redundant Cross-Correlation Algorithm. *Opt. Express* 22 (13), 15982–15991. doi:10.1364/oe.22.015982

Welshhans, K., and Bassell, G. J. (2011). Netrin-1-Induced Local -Actin Synthesis and Growth Cone Guidance Requires Zipcode Binding Protein 1. *J. Neurosci.* 31 (27), 9800–9813. doi:10.1523/jneurosci.0166-11.2011

Zhang, Y., Chen, K., Sloan, S. A., Bennett, M. L., Scholze, A. R., O'Keeffe, S., et al. (2014). An RNA-Sequencing Transcriptome and Splicing Database of Glia, Neurons, and Vascular Cells of the Cerebral Cortex. *J. Neurosci.* 34 (36), 11929–11947. doi:10.1523/jneurosci.1860-14.2014

Zhang, Y., Sloan, S. A., Clarke, L. E., Caneda, C., Plaza, C. A., Blumenthal, P. D., et al. (2016). Purification and Characterization of Progenitor and Mature Human Astrocytes Reveals Transcriptional and Functional Differences with Mouse. *Neuron* 89 (1), 37–53. doi:10.1016/j.neuron.2015.11.013

Zieve, G., and Solomon, F. (1984). Direct Isolation of Neuronal Microtubule Skeletons. *Mol. Cel Biol* 4 (2), 371–374. doi:10.1128/mcb.4.2.371-374.1984

Conflict of Interest: The authors declare that the research was conducted in the absence of any commercial or financial relationships that could be construed as a potential conflict of interest.

frontiers in Cell and Developmental Biology

REVIEW
published: 24 March 2022
doi: 10.3389/fcell.2022.860065

The Expression and Function of Tubulin Isotypes in *Caenorhabditis elegans*

*Yu-Ming Lu and Chaogu Zheng**

School of Biological Sciences, University of Hong Kong, Hong Kong SAR, China

Microtubules, made from the polymerization of the highly conserved α/β-tubulin heterodimers, serve as important components of the cytoskeleton in all eukaryotic cells. The existence of multiple tubulin isotypes in metazoan genomes and a dazzling variety of tubulin posttranslational modifications (PTMs) prompted the "tubulin code" hypothesis, which proposed that microtubule structure and functions are determined by the tubulin composition and PTMs. Evidence for the tubulin code has emerged from studies in several organisms with the characterization of specific tubulins for their expression and functions. The studies of tubulin PTMs are accelerated by the discovery of the enzymes that add or remove the PTMs. In tubulin research, the use of simple organisms, such as *Caenorhabditis elegans*, has been instrumental for understanding the expression and functional specialization of tubulin isotypes and the effects of their PTMs. In this review, we summarize the current understanding of the expression patterns and cellular functions of the nine α-tubulin and six β-tubulin isotypes. Expression studies are greatly facilitated by the CRISPR/Cas9-mediated endogenous GFP knock-in reporters and the organism-wide single cell transcriptomic studies. Meanwhile, functional studies benefit from the ease of genetic manipulation and precise gene replacement in *C. elegans*. These studies identified both ubiquitously expressed tubulin isotypes and tissue-specific isotypes. The isotypes showed functional redundancy, as well as functional specificity, which is likely caused by the subtle differences in their amino acid sequences. Many of these differences concentrate at the C-terminal tails that are subjected to several PTMs. Indeed, tubulin PTM, such as polyglutamylation, is shown to modulate microtubule organization and properties in both ciliated and non-ciliated neurons. Overall, studies from *C. elegans* support the distinct expression and function patterns of tubulin isotypes and the importance of their PTMs and offer the promise of cracking the tubulin code at the whole-genome and the whole-organism level.

Keywords: microtubules, *C. elegans*, scrna-seq, tubulin code, tubulin PTM, tubulin (poly)glutamylation, touch receptor neurons, axonemal microtubules

OPEN ACCESS

Edited by:
Jack Adam Tuszynski,
University of Alberta, Canada

Reviewed by:
Pascale Dupuis-Williams,
ESPCI ParisTech École Supérieure de Physique et de Chimie Industrielles de la Ville de Paris, France
Francesca Bartolini,
Columbia University, United States

***Correspondence:**
Chaogu Zheng
cgzheng@hku.hk

Specialty section:
This article was submitted to Cellular Biochemistry, a section of the journal Frontiers in Cell and Developmental Biology

Received: *22 January 2022*
Accepted: *28 February 2022*
Published: *24 March 2022*

Citation:
Lu Y-M and Zheng C (2022) The Expression and Function of Tubulin Isotypes in Caenorhabditis elegans. Front. Cell Dev. Biol. 10:860065. doi: 10.3389/fcell.2022.860065

INTRODUCTION

Microtubules perform pivotal roles in numerous cellular activities, including cell division, cell shape changes, intracellular trafficking, sperm motility, and neuronal sensation. In dividing cells, kinetochore microtubules attach chromosomes to the spindle pole, allowing the separation of chromosomes into daughter cells, while astral microtubules radiate out from spindle poles toward

the cell cortex to help orient the spindles and control the plane of cell division (Prosser and Pelletier 2017). In the nervous system, microtubules provide mechanical support for axonal outgrowth and serve as transport highways for organelles and vesicles from the cell bodies to axons and dendrites (Matamoros and Baas 2016). Two other specialized organelles, the motile flagella and non-motile cilia, also rely heavily on microtubules, as the microtubule-based axoneme structures control the locomotion of flagellated sperms and how ciliated neurons sense the environment (Guichard et al., 2021; Gadadhar et al., 2022).

Compared to their versatile functions, microtubules have a relatively simple and rigid structure in the shape of 25-nm-wide hollow tubes. They generally harbor 13 linear protofilaments formed from evolutionarily conserved tubulin dimers. After the initiation of *de novo* microtubule assembly ("microtubule nucleation") by the γ-tubulin ring complex of the microtubule-organizing center (Consolati et al., 2020; Liu et al., 2021), tubulin heterodimers composed of one α- and one β-tubulin are recruited to elongate protofilaments at the plus end. Through incorporating and removing tubulin dimers, microtubules switch between the states of polymerization and depolymerization, a process called dynamic instability. Microtubule dynamics is required for spindle assembly and function in dividing cells (Wittmann et al., 2001) and growth cone navigation during axonal pathfinding of growing or regenerating neurons (Gudimchuk and McIntosh 2021; Sanchez-Huertas and Herrera 2021).

The simplicity of microtubule structure and composition makes it intriguing to unravel how the behavior of the multifunctional microtubules are precisely controlled. Previous studies identified microtubule-associated proteins (MAPs) as important regulators of microtubule dynamics and functions. For example, molecular motors walk along microtubules to transport cargoes and generate movement in cilia (Howard 1997; Webb et al., 2020); microtubule-severing enzymes, such as katanin, can rapidly reorganize microtubules by cutting them into shorter fragments during cell division (Sharp and Ross 2012); MAP2 and tau, on the other hand, promote microtubule assembly and protect microtubules from severing in the nervous system (Qiang et al., 2006; Barbier et al., 2019). In addition to MAPs, tubulins themselves are also important determinants of the properties of microtubules.

Eukaryotes contain multiple tubulin genes, called tubulin isotypes. For instance, the human genome has nine α-, ten β-, and two γ-tubulin isotypes (HGCN "tubulins" gene group). These isotypes, as building blocks of microtubule, may possess specific properties that dictate the structure and function of the entire microtubule polymer. One prominent example is the human β1-tubulin (TUBB1) whose mutation leads to disorganized microtubules of blood platelets and thus congenital macrothrombocytopenia (Kunishima et al., 2009), even though six other β-tubulin isotypes are simultaneously abundant in the cells (Cuenca-Zamora et al., 2019). Given that tubulin isotypes generally bear more than 95% identity in amino acid sequences, the distinct functions of the isotypes likely originate from their subtle sequence variations. A region where significant sequence divergence was found is the carboxy-terminal tail, which protrudes from microtubule backbones and remains highly accessible to MAPs. The C-terminal tail is also subjected to a range of tubulin post translational modifications (PTMs) that regulate microtubule dynamics and MAP binding (Magiera and Janke 2014), and tubulin isotypes with varying C-terminal tails may have different susceptibility to PTMs. Therefore, one could hypothesize that the incorporation of specific tubulin isotypes into the microtubules may regulate microtubule properties by controlling the accessibility to certain MAPs.

Altogether, the diversity of tubulin isotypes and the complexity of tubulin PTMs gave rise to the concept of "tubulin code," which proposes that the structural and functional properties of microtubules are precisely controlled by the tubulin isotype composition and their PTMs (Janke and Magiera 2020; Roll-Mecak 2020). Evidence for such code is starting to emerge from recent studies, although more work needs to be done to address the intricate regulatory mechanisms of microtubule behaviors. In this paper, we review the tubulin studies in *Caenorhabditis elegans*, which is a powerful model organism thanks to its relatively simple anatomy with only ~1,000 somatic cells, short (3-days) life cycle, and amenability to genetic manipulations (Brenner 1974; Corsi et al., 2015). *C. elegans* also has transparent embryos and bodies, allowing *in vivo* imaging of microtubule dynamics in living animals. Studies on the expression and function of tubulin isotypes, as well as the effects of their PTMs, provide critical insights into how the isotypes exert specific functions in specific tissues at the whole-organism level.

Expression Patterns of Tubulin Isotypes in *C. elegans*

Tissue Specificity of Tubulin Isotypes

C. elegans genome contains nine α-, six β-, and one γ-tubulin genes (**Figure 1** and **Table 1**). *C. elegans* has no δ- and ε-tubulins associated with the centrioles (Chang and Stearns 2000). When and where tubulin genes are expressed in *C. elegans* had been studied using a range of methods, including the traditional promoter-reporters, immunofluorescence with tubulin-specific antibodies (Fukushige et al., 1995; Lu et al., 2004), transcriptomic approaches (Baugh et al., 2003; Lockhead et al., 2016), and GFP knock-in at the endogenous tubulin loci (Nishida et al., 2021). Recent single-cell RNA-seq data (Taylor et al., 2021) provide opportunities to understand the combinations of tubulin isotypes expressed in each cell and their relative abundance in a quantitative manner. Based on these expression patterns, *C. elegans* tubulin isotypes can be categorized into 1) mitotic and ubiquitous tubulins, 2) ciliary tubulins, 3) mechanosensory tubulins, 4) other tubulins (**Table 1**).

Two α-tubulins (*tba-1* and *tba-2*) and two β-tubulins (*tbb-1* and *tbb-2*) are the four main isotypes expressed in the embryos (Baugh et al., 2003) and virtually all tissues in larva and adults, including *epidermis*, germline, intestine, muscle, and neurons (Nishida et al., 2021). They are incorporated into the mitotic spindle during cell division in the embryos (Honda et al., 2017)

FIGURE 1 | Phylogenetic tree of human and *C. elegans* tubulin isotypes. Neighbor-joining trees were generated by aligning the protein sequences of human and *C. elegans* α-tubulin **(A)** and β-tubulin **(B)** isotypes using ClustalW. *C. elegans* tubulins are in red **(A)** and blue **(B)**, while human tubulins are in black.

TABLE 1 | Summary of the expression and function of *C. elegans* tubulin isotypes.

Isotype Category	a or b	Gene names	Expression Pattern	Function based on knockout phenotypes
Mitotic and ubiquitous tubulins	α-tubulin	*tba-1*	All tissues	Redundant for spindle formation and dynamics in mitosis and meiosis
		tba-2	All tissues	
	β-tubulin	*tbb-1*	All tissues	
		tbb-2	All tissues	
Cilliary tubulins	α-tubulin	*tba-5*	ASG, PHA, ASK, ADF, ASE, ASI, and other ciliated neurons; male CEM and ray neurons	Unknown
		tba-6	IL2; male CEM and ray neurons	Cilary ultrastructure, intraflagellar transport, and extracellular vesicle release in CEM; male sensory function
		tba-9	CEP, ADE, PDE, AWA, AWC, and other ciliated neurons; male CEM and ray neurons	Male sensory function
	β-tubulin	*tbb-4*	Most ciliated neurons	Male sensory function
Mechanosensory tubulins	α-tubulin	*mec-12*	TRNs and most neurons	Mechanosensation
	β-tubulin	*mec-7*	TRNs and a few other neurons	Formation of 15-protofilament microtubule; mechanosensation
Others	α-tubulin	*tba-4*	Epidermis and muscle	Unknown
		tba-7	Intestine	Unknown
		tba-8	Seam cells	Unknown
	β-tubulin	*ben-1*	Many neurons	Benomyl-sensitive
		tbb-6	Pharynx	Unknown

and likely contribute to microtubule formation in every cell of the animal as ubiquitously expressed tubulin isotypes.

Three α-tubulins (*tba-5*, *tba-6*, and *tba-9*) and one β-tubulin (*tbb-4*) are specifically expressed in the ciliated sensory neurons (Hurd et al., 2010; Hao et al., 2011). Among the 302 neurons in *C. elegans* hermaphrodites, 60 of them are ciliated sensory neurons containing axoneme, a microtubule-based structure that forms the core of the cilia. These ciliary isotypes contribute to the formation of axonemal microtubules and cilia functions. Interestingly, among the ciliated sensory

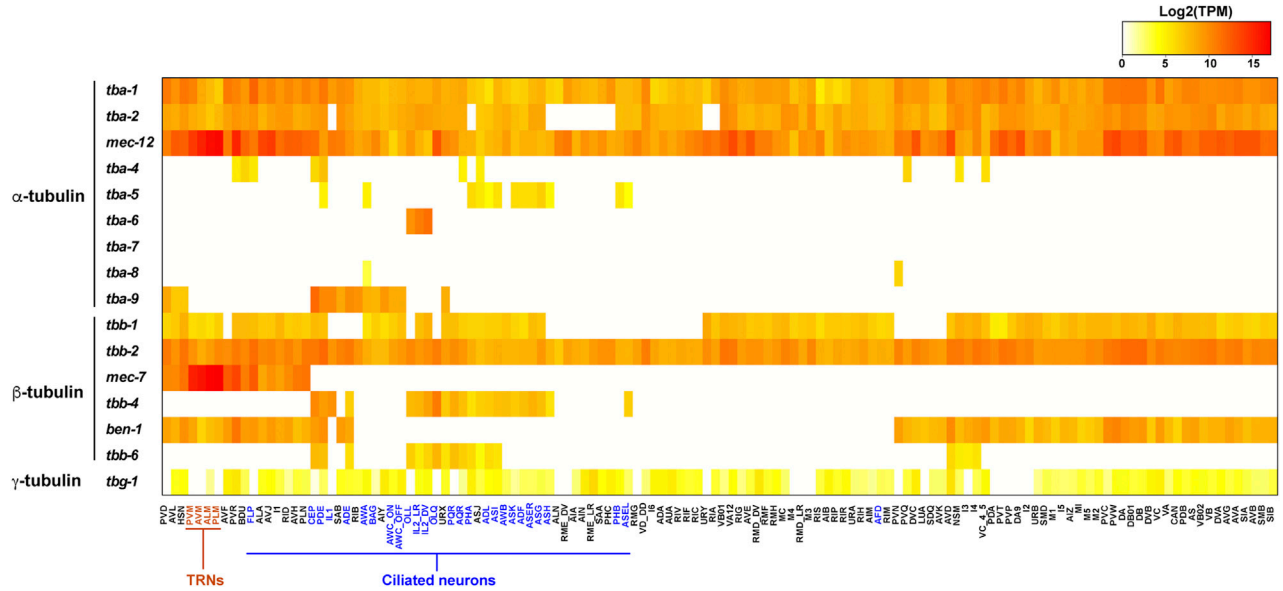

FIGURE 2 | Heatmap for the expression of tubulin isotypes in the *C. elegans* nervous system. Transcript levels (TPM) of tubulin isotypes in each neuron type were extracted from the scRNA-seq data (Taylor et al., 2021) and log2 transformed. TRNs are in red and ciliated neurons are in blue. Raw data can be found in **Supplementary Table S1**.

neurons, the three α-tubulins showed distinct and largely non-overlapping expression in hermaphrodites. Fluorescent reporter studies found that *tba-5* is expressed in the ADF, ADL, AFD, ASE, ASG, ASH, ASI, ASK, AWA, AWB, and PHA neurons, *tba-6* is expressed in IL2, and *tba-9* is expressed in CEP, ADE, PDE, AWA, and AWC neurons (Hurd et al., 2010; Nishida et al., 2021). Information about each neuron type in *C. elegans* can be found at WormAtlas (https://www.wormatlas.org/neurons/Individual%20Neurons/Neuronframeset.html). scRNA-seq identified their expression in more ciliated neurons but their expression patterns remain mostly non-overlapping (**Figure 2**). In contrast, the only ciliary β-tubulin (*tbb-4*) is widely expressed in many ciliated neurons (Hao et al., 2011). The partitioned expression of the three ciliary α-tubulin isotypes leads to the hypothesis that the axonemal microtubules may have different properties in different sets of ciliated neurons, thus requiring the expression of distinct isotypes. Whether *tba-5*, *tba-6* and *tba-9* are functionally interchangeable among different ciliated neurons remains to be tested. These ciliary tubulins are also expressed in the male-specific ciliated sensory neurons (Hurd et al., 2010).

One α-tubulin (*mec-12*) and one β-tubulin (*mec-7*) showed highly enriched expression in the mechanosensory neurons, also known as the touch receptor neurons (TRNs) including ALM, AVM, PLM, and PVM (Hamelin et al., 1992; Fukushige et al., 1999). These neurons contain the special 15-protofilament microtubules, while all other neurons in *C. elegans* have 11-protofilament microtubules (Chalfie and Thomson 1982). Mutations in *mec-7* leads to the loss of the 15-protofilament microtubule structure (Savage et al., 1989), suggesting that tubulin isotype can define the structure and organization of microtubules. Both *mec-12* and *mec-7* are required for the mechanosensory functions of TRNs (Chalfie and Au 1989). It is worth noting that *mec-7* is also expressed in a few other neurons outside of the TRNs, and *mec-12* expression is found in many neurons, including motor neurons and interneurons, although their expression in the six TRNs are much higher compared to other expression (Fukushige et al., 1999; Nishida et al., 2021). This expression pattern is supported by scRNA-seq data (**Figure 2**). Surprisingly, *mec-12* transcripts were found in all neurons at a level comparable to *tba-1* and *tba-2*, suggesting that *mec-12* is potentially a third ubiquitous α-tubulin with specific enrichment in the TRNs.

Other α-tubulin isotypes include *tba-4*, *tba-7*, and *tba-8*, which had very little expression in the nervous system. *tba-4* is expressed in the *epidermis* and muscle, *tba-7* is expressed in the intestine, excretory pore cells, and rectal gland cells, and *tba-8* is expressed specifically in the seam cells of the larva (Hurd 2018; Nishida et al., 2021). Other β-tubulin isotypes include *ben-1* (also known as *tbb-5*), which is the only benomyl-sensitive tubulin whose null mutation renders the animals resistant to the toxic fungicide and is expressed in many neurons (Driscoll et al., 1989; Hurd 2018), and *tbb-6*, which has expression only in the pharynx (Munkacsy et al., 2016). The only *C. elegans* γ-tubulin isotype (*tbg-1*), involved in the initiation of microtubule assembly, is expressed in the germline, embryos, and likely all somatic cells (Strome et al., 2001).

Relative Abundance of Tubulin Isotypes in *C. elegans* Neurons

The combinatorial tubulin code is controlled by the relative abundance of the multiple isotypes in each cell. scRNA-seq data

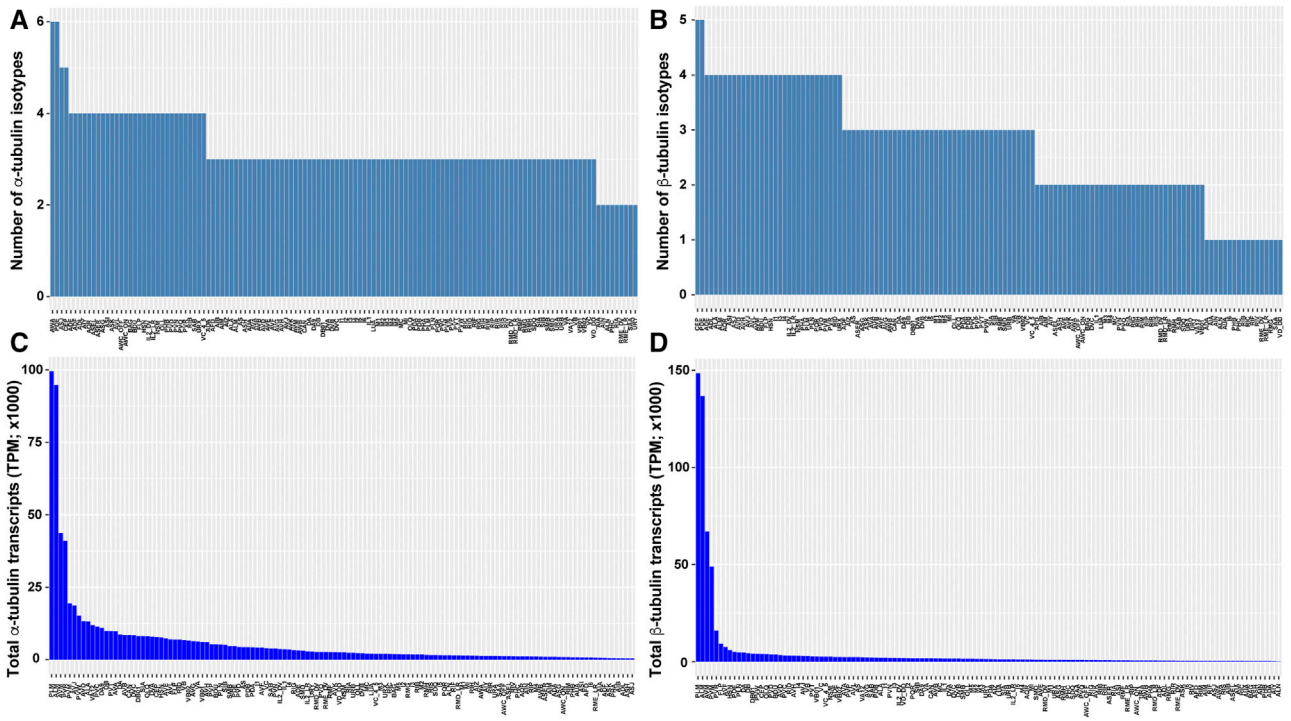

FIGURE 3 | Tubulin isotype numbers and total tubulin transcripts among different neuron types in *C. elegans*. The number of tubulin isotypes expressed (TPM >0) in each neuron type were counted for α-tubulin **(A)** and β-tubulin **(B)** isotypes from the scRNA-seq data. The total number of α-tubulin **(C)** and β-tubulin **(D)** transcripts in each neuron type were calculated by summing the TPM of each isotype.

provides a window to quantitatively assess the isotype composition in a cell at the transcript level (Taylor et al., 2021). In the ciliated neurons, such as the IL2 neurons, the ciliary tubulin *tba-6* showed much higher level of transcription than the ubiquitously expressed *tba-1* and *tba-2*, since *tba-6* counts for 74 and 62% of all α-tubulin transcripts in IL2_DV and IL2_LR neurons, respectively (**Figure 2**). Thus, in the IL2 neurons, the axonemal microtubules may be mostly made of the ciliary isotype TBA-6. In other cases (e.g., *tba-5* and *tbb-4*), the ciliary tubulins are transcribed at a level comparable or lower than the ubiquitous tubulin isotypes, indicating that the cilia-specific isotypes may not be the major isotype in the axonemal microtubules.

Another example is the mechanosensory tubulins, *mec-12* and *mec-7*, which count for over 99% of the total α- and β-tubulin transcripts, respectively, in the TRNs according to the scRNA-seq data (Taylor et al., 2021). Lockhead et al. (2016) also independently quantified the tubulin transcripts in the PLM neurons (the posterior TRN subtype) using single-neuron RNA-seq and found that *mec-12* and *mec-7* count for 95 and 83% of the overall α- and β-tubulin transcripts, respectively. Both transcriptomic studies suggest that *mec-12* and *mec-7* are the dominating tubulin isotypes in the TRNs, while *tba-1*, *tba-2*, *tbb-1*, and *tbb-2* have very low abundance. Thus, it is reasonable to expect that the 15-protofilament microtubules are mostly made of MEC-12/MEC-7 heterodimers, although this idea has yet to be confirmed with *in vivo* evidence.

However, recent studies using N-terminal GFP knock-in at the endogenous tubulin genes found that GFP::TBA-1 and GFP::TBB-2 showed higher levels of fluorescence than GFP::MEC-12 and GFP::MEC-7 in the TRNs, respectively (Nishida et al., 2021). The authors attributed this discrepancy to different translational efficiencies of the isotypes, but it could also be an artefact of the GFP fusion, since the N-terminal GFP may interfere with tubulin autoregulation that relies on the first four residues (MREI) (Lin et al., 2020). Another discrepancy exists between the broad abundance of *mec-12* in all neurons in the scRNA-seq dataset (**Figure 2**) and the weak and restricted fluorescence of GFP::MEC-12 in the animal (Nishida et al., 2021). Further studies combining transcriptomic and proteomic approaches will be needed to address such discrepancies.

scRNA-seq data also revealed divergence in the number of isotypes expressed and the total tubulin transcripts among cell types. For example, *C. elegans* neurons on average express three α-tubulin and three β-tubulin isotypes, but significant inequality in the number of isotypes are found among the neuron types (e.g., PDE neurons express 6 α- and 5 β-tubulin isotypes, whereas ALN neurons express 2 α- and 1 β-tubulin isotypes; **Figures 3A,B**). The total number of tubulin transcripts show even greater variation in the nervous system. Compared to other neurons, the TRNs (especially ALM and PLM neurons) have

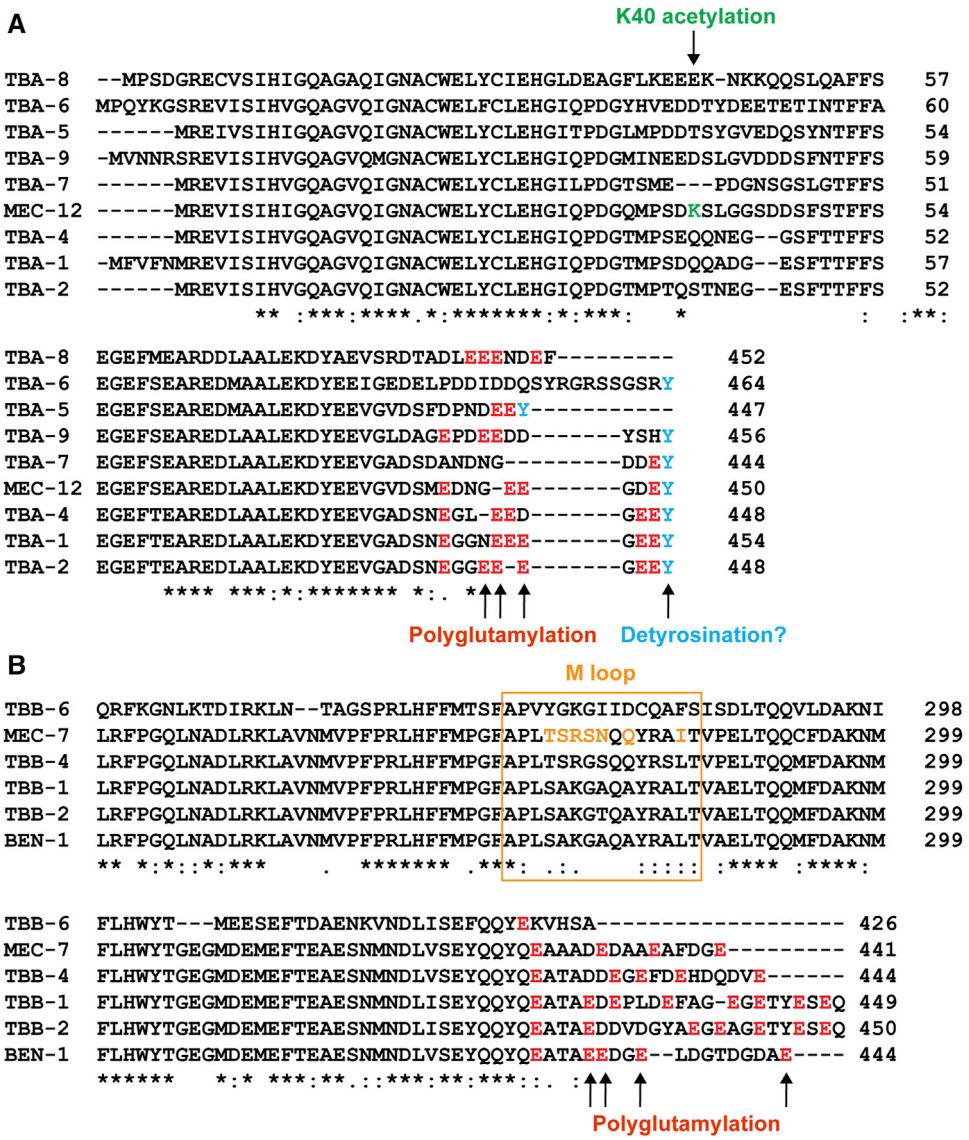

FIGURE 4 | Sequence variation among the tubulin isotypes in *C. elegans*. Alignment of part of the amino acid sequences of α-tubulin **(A)** and β-tubulin **(B)** isotypes. Sites for potential PTMs were color-coded. Green for K40 acetylation, red for polyglutamylation, and blue for potential detyrosination. The sequence for the M loop is labeled by the orange box and the amino acids in the M loop of *MEC-7* that differ from the ubiquitous *TBB-1* and *TBB-2* are in orange as well.

extraordinarily high level of transcripts for both α- and β-tubulin due to the strong expression of the mechanosensory tubulins, *mec-12* and *mec-7* (**Figures 3C,D**). This high abundance of tubulin is correlated with the large number of microtubules found in the TRNs. A cross-section of TRN neurite contains ~31 15-protofilament microtubules which form a bundle, whereas most other neurons have only a few (~5 per cross-section) 11-profilament microtubules (Chalfie and Thomson 1979). Moreover, deletion of either *mec-12* and *mec-7* leads to significant loss of microtubules (Zheng et al., 2017), suggesting that the number of microtubules in a cell may partly depend on the level of tubulin expression. Strikingly, there is a 245- and 1268-fold difference in total α- and β-tubulin transcripts levels, respectively, between the neurons with the highest and lowest tubulin expression levels (**Figures 3C,D**). This finding may reflect different needs for microtubules among distinct cell types.

Functions of Tubulin Isotypes

Functional Redundancy and Specificity of Tubulin Isotypes in Embryogenesis

The expression of multiple tubulin isotypes and their high sequence identity suggest that the isotypes may be functionally redundant, while the distinct expression patterns, relative abundance, and subtle sequence difference indicate that each isotype may carry specific functions. This coexistence of redundancy and specificity have been well supported by experimental data in *C. elegans*.

Cell division in the germline and early embryos of *C. elegans* relies heavily on two pairs of tubulins (*tba-1*, *tba-2*, *tbb-1*, *tbb-2*) that assemble into spindle microtubules during mitosis and meiosis. The two α- and two β-tubulin isotypes are mostly redundant. The loss of either TBA-1 or TBA-2 by gene deletion and RNAi caused little viability defects, while simultaneously depleting both is lethal due to the disruption of spindle formation in embryogenesis (Phillips et al., 2004). Similarly, *tbb-1* and *tbb-2* are partially redundant for embryonic viability (Lu et al., 2004), although the null mutation of *tbb-2* caused partial lethality (Ellis et al., 2004; Lu et al., 2004). Missense mutation in *tbb-2* can also cause severe lethality by acting as gain-of-functions to disrupt spindle microtubule assembly in the embryos (Wright and Hunter 2003; Ellis et al., 2004). As the only γ-tubulin isotype, *tbg-1* is found to be required for the nucleation and organization of centrosomal microtubule asters and the positioning dynamics of the spindle (Strome et al., 2001; Hannak et al., 2002).

In addition to the redundancy, functional difference also exists between the isotypes. For example, microtubule-severing enzyme katanin prefers TBB-2 over TBB-1 during meiosis since the loss of *tbb-2* leads to severe lethality in activity-weakened katanin mutants, but the loss of *tbb-1* does not cause similar synthetic lethality, suggesting that katanin severs microtubules that contain TBB-2 much more efficiently to support the formation of meiotic spindles (Lu et al., 2004). This different susceptibility to katanin activity may be attributed to the significant sequence divergence of the two isotypes at the C-terminal tail, which is an essential site for the interactions between microtubules and MAPs (**Figure 4**). Using similar methods, TBA-2 was later found to be preferred over TBA-1 by katanin (Lu and Mains 2005).

In an elegant gene replacement experiment, Honda et al. (2017) found that when the coding exons of the *tbb-1* locus was endogenously edited to encode TBB-2 (the sequences of TBB-1 and TBB-2 only different in 12 amino acids) or vice versa, the resulted embryos expressing two copies of *tbb-1* or *tbb-2* were viable and had similar levels of total β-tubulin expression as the wild-type. Interestingly, the authors also found that the deletion of *tbb-2* reduced the total level of β-tubulin to 19% of the wild-type level and attributed the partial lethality in *tbb-2(-)* mutants to the paucity of total β-tubulin. These results support that TBB-1 and TBB-2 can functionally replace each other for development. However, the two isotypes can also confer distinct dynamic properties of microtubules. For example, the duration of growth for the astral microtubules is longer in embryos expressing only TBB-2 than the ones expressing only TBB-1, while microtubule disassembly occurs more frequently in the TBB-1-only embryos. Moreover, TBA-1 and TBA-2 also appear to differently affect microtubule dynamics, as microtubules composed of TBA-1/TBB-1 had higher growth rate than microtubules made of TBA-2/TBB-1 (Honda et al., 2017). These results support both the redundancy and functional specificity of tubulin isotypes.

Ciliary Tubulins Affect the Structure and Function of Cilia

Ciliary tubulins (*tba-5*, *tba-6*, *tba-9*, and *tbb-4*) are found to regulate the structure of the axonemal microtubule and the formation of the cilia in ciliated neurons. For example, missense gain-of-function mutations in *tba-5* and *tbb-4* result in the loss of the distal segments of the cilia in many sensory neurons and destabilize singlet microtubules in cilia, but their deletion alleles do not cause any defects (Hao et al., 2011). So, these two ciliary tubulin isotypes are likely functional redundant with the ubiquitous isotypes also expressed in the neurons. Interestingly, TBA-5 and TBB-4 showed different localization patterns within the cilia. TBB-4 localizes along the length of the cilium but is not found at the transition zone or in the dendrites, whereas TBA-5 localizes in dendrites, the transition zone, and the cilia with enrichment in the distal segment of the cilia (Hao et al., 2011).

The loss-of-function mutation in *tba-6* alters the ciliary ultrastructure in male-specific CEM neurons, causing abnormal curvatures of the axoneme and reduced number of B-tubule singlets. The loss of *tba-6* also affects the intraflagellar transport and extracellular vesicle release in the CEM neurons (Silva et al., 2017). *tba-6*, *tba-9*, and *tbb-4* are also expressed in the male tail sensory ray neurons and their deletions all lead to male mating defects likely because the ray neuron function is compromised (Hurd et al., 2010). Interestingly, the loss of *tbb-4* reduces the accumulation of TBA-6 and TBA-9 in the ray neuron cilia, and the loss of *tba-6* reduces the localization of TBB-4, suggesting that these ciliary isotypes may need to work together to form the specialized ciliary microtubules.

Mutations in the Mechanosensory Tubulins Cause Neurite Growth Defects

The α-tubulin *mec-12* and β-tubulin *mec-7* are highly expressed in the mechanosensory TRNs, which contain many (~31 per cross-section) large-diameter, 15-protofilament microtubules (**Figures 5A,B**). In fact, these neurons were originally identified in the electron micrographs by their prominent microtubule structures (e.g., the neuron name "ALM" stands for anterior lateral microtubule) (Chalfie and Thomson 1979). Earlier studies found that missense mutations in either *mec-12* or *mec-7* resulted in the loss of the 15-protofilament microtubules (Savage et al., 1989; Fukushige et al., 1999; Bounoutas et al., 2009). Recent studies using the deletion alleles, however, found that only the *mec-7(-)* mutants but not the *mec-12(-)* mutants lost the 15-protofilament structure (Zheng et al., 2017). *mec-7(-)* mutants instead have the small-diameter 11-protofilament microtubules. Both *mec-7(-)* and *mec-12(-)* mutants have significantly fewer (~6 or 7 per cross-section) microtubules compared to the wild type. This result suggests that the role of MEC-7 in producing the 15-protofilament microtubules cannot be replaced by other β-tubulin isotypes (e.g., TBB-1 and TBB-2) in the TRNs, whereas MEC-12 can be replaced by other α-tubulin isotypes. MEC-7 may possess unique properties that modulate the protofilament number and microtubule organization (e.g., unique sequences in the M loop that affects lateral contact; **Figure 4B**). The reduced number of microtubules in *mec-12(-)* and *mec-7(-)* mutants is likely caused by the decrease in total tubulin levels, since *mec-12* and *mec-7* count for >99% of the total α- and β-tubulin transcripts, respectively, according to the scRNA-seq data. Although the removal of one tubulin isotype

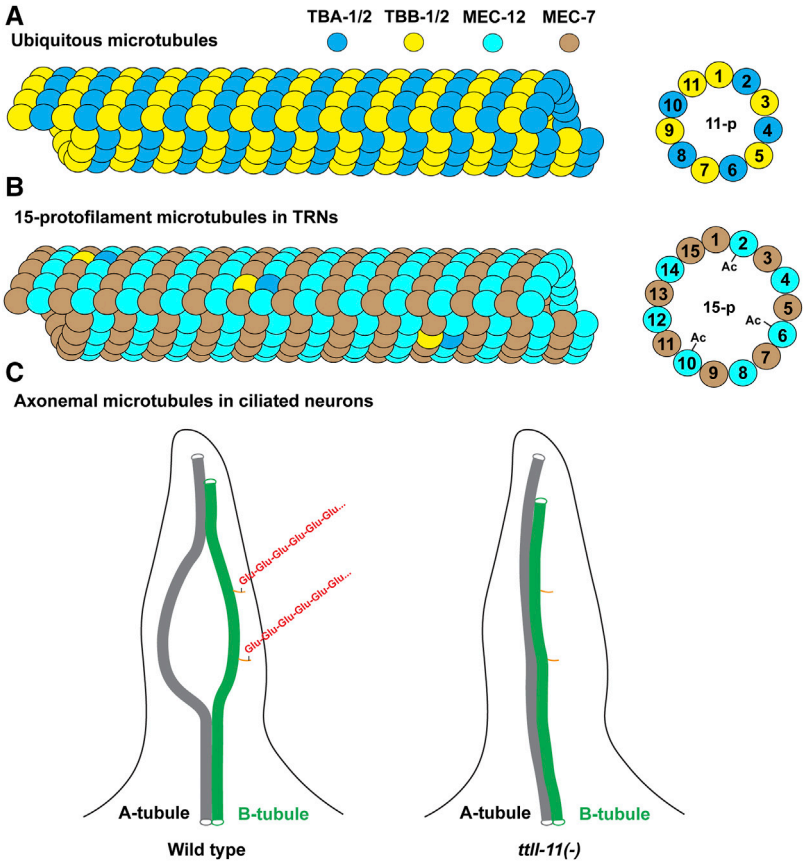

FIGURE 5 | Illustration of microtubule structures in *C. elegans*. **(A)** Most cells in *C. elegans* contain the 11-protofilament microtubules made mostly of the ubiquitous tubulin isotypes TBA-1, TBA-2, TBB-1, and TBB-2. Other expressed isotypes can also be incorporated into the microtubules (not depicted). **(B)** The 15-protofilament microtubules in the TRNs are likely made of MEC-12/MEC-7 heterodimers given their high abundance. The lowly expressed TBA-1/2 and TBB-1/2 may also be incorporated at low levels. Only the microtubules incorporating MEC-12 can be acetylated at the K40 residues. **(C)** The structure of the axonemal microtubules (only one of the nine A-B doublets is depicted). The A-B doublet splay into A-tubule and B-tubule singlets in the middle segment of the cilia. Polyglutmaylation (a chain of "Glu" in red) occurs mostly on the C-terminal tail of the tubulins in the B-tubule. A-B doublet fails to splay into singlets in ttll-11(-) mutants. The orange sticks represent the C-terminal tails of the tubulins on B-tubule. Not all tubulin C-terminal tails on the microtubules are depicted.

may cause the upregulation of other isotypes (e.g., TBB-1 proteins are upregulated ~3-fold in *tbb-2(-)* mutants (Ellis et al., 2004)), it is unclear whether the upregulation of other isotypes can entirely compensate for the loss of the highly transcribed *mec-12* and *mec-7* in the TRNs. Moreover, the abundance of microtubules appeared to be essential for mechanosensation in TRNs, since both *mec-12(-)* and *mec-7(-)* mutants showed significantly reduced touch sensitivity.

TRNs extend long antero-posteriorly running neurites that mediate the sensing of mechanical stimuli along the body. Deletion of *mec-12* or any of the four ubiquitous tubulin isotypes individually did not produce any obvious defects on neurite growth, and the deletion of *mec-7* only caused mild defects (Lockhead et al., 2016; Zheng et al., 2017). These results suggest that the reduced number of microtubules and the 11-protofilament microtubules are sufficient for supporting general neurite growth in the TRNs. Thus, the tubulin isotypes appeared to be generally redundant in regulating neuronal morphogenesis.

Through extensive genetic screens, a large collection of *mec-12* and *mec-7* missense mutations (99 alleles in total) had been isolated and characterized for their effects on neurite growth (Zheng et al., 2017; Lee et al., 2021). In addition to many loss-of-function mutants, two distinct types of gain-of-function alleles were found among the missense alleles, and they had much stronger effects on neurite growth than the deletion alleles. The antimorphic gain-of-function mutations were dominant or semi-dominant and caused severe shortening of all TRN neurites. The mutated residues mostly locate at the GTP binding site and the intradimer and interdimer interfaces, suggesting that the antimorphic mutations may cause the formation of poisonous tubulin dimers, whose incorporation could terminate microtubule polymerization and induce instability, thus blocking neurite growth. On the other hand, the neomorphic gain-of-function mutations resulted in hyperstable microtubules and ectopic neurite growth; these mutations were mostly mapped to the exterior surface of the microtubules and may affect the interaction with MAPs (Zheng

et al., 2017). In genetic terms, antimorphs are dominant-negative mutations that act in opposition to normal gene activity, and neomorphs cause gain of gene function that is different from the normal gene function.

Such structure-function analysis, which were enabled by the phenotypical characterization of a large number of tubulin missense alleles in *C. elegans* TRNs, is valuable in light of the discovery of over 100 tubulin mutations associated with neurodevelopmental disorders in humans (Tischfield et al., 2011; Fourel and Boscheron 2020). In fact, previous work has shown that *C. elegans* TRNs can be used to evaluate the cellular impact of disease-associated human tubulin mutations by engineering these mutations into the endogenous *mec-12* and *mec-7* loci and then examining the phenotype on neurite growth patterns (Zheng et al., 2017). Given the ease of gene editing in *C. elegans*, such phenotypical evaluation can be done in less than two weeks, which provides a tool to understand the nature of the human tubulin mutations.

Lastly, studies of the *mec-12* and *mec-7* alleles also found complex genetic interactions between the tubulin mutations, including epistatic, additive, synthetic, and balancing effects (Lee et al., 2021). For example, the effects of neomorphic gain-of-function mutants can be suppressed by loss-of-function and antimorphic gain-of-function mutations. Neomorphic alleles often show additive effects as expected, but sometimes a weaker neomorphic allele could also mask the effects of a stronger neomorphic allele in inducing ectopic neurite growth. Moreover, the microtubule-stabilizing and -destabilizing effects of neomorphic and antimorphic alleles were found in some cases to neutralize each other to allow normal neurite growth pattern in the double mutants (Lee et al., 2021). These results are in line with earlier molecular genetics studies on tubulins in other organisms (Morris et al., 1979) and can help understand how tubulin isotypes work together.

Other Functional Studies of Tubulins

Since microtubules serve as the tracks for intracellular transport, mutations in tubulins also disrupt the trafficking of organelles and vesicles. For example, mutations in *mec-12* and *mec-7* cause abnormalities in the transport of synaptic vesicles and mechanosensitive channel protein MEC-2 in the TRNs (Huang et al., 1995; Zheng et al., 2017).

Outside of the TRNs, missense mutations are also found to affect neuronal development. For example, a gain-of-function missense mutation in *tba-1* causes defects in axonal extension and neuromuscular synapse formation in the DD motor neurons, which leads to altered locomotion, although *tba-1(-)* null mutants does not show any of these defects (Baran et al., 2010). Interestingly, *tbb-2(-)* null mutants also show axonal growth defects in DD neurons and reduced synapse numbers, suggesting that the missense mutation in *tba-1* may mostly affect microtubules formed by TBA-1 and TBB-2. The same *tba-1* missense mutation delays synapse remodeling in DD neurons, and this delay is exacerbated by the loss of the MAPKKK DLK-1 (Kurup et al., 2015). Further studies found that the *tba-1* gain-of-function mutation and the *dlk-1(-)* null mutation have synergistic effects in reducing microtubule dynamics, which leads to defects in synaptic remodeling.

Both deletion and missense mutations in *ben-1* (or *tbb-5*) confer resistance to the microtubule-depolymerizing drug benomyl in a dominant fashion, suggesting that *ben-1* is haploid insufficient (Driscoll et al., 1989). Except for the resistance to the neurological phenotypes induced by benomyl, *ben-1(-)* mutants had no other obvious defects. Although *ben-1* was thought, for a long time, to be the only tubulin isotype sensitive to benomyl, which may result from specific features in the sequence of BEN-1, a later study isolated a rare *tbb-2* missense mutation that also confers benomyl resistance (Wright and Hunter 2003).

Tubulins were identified in genome-wide RNAi screens for genes required in cell migration. For example, *tba-1*, *tba-2*, *tba-4*, *tbb-1*, *tbb-2*, and *tbg-1* are all found in a gene network that regulates the migration of distal tip cells during the development *C. elegans* gonad (Cram et al., 2006). It is worth noting that both a missense and a nonsense mutation in *tba-7* were previously found to cause ectopic neurite growth and enhanced axonal regeneration in the TRNs (Zheng et al., 2017; Kim et al., 2018). However, follow-up studies found that these defects should be attributed to two independent background mutations in the microtubule-depolymerizing kinesin-13 *klp-7*, which is closely linked to *tba-7* (Lu and Zheng 2021). The function of *tba-7* and other tubulins (including *tbb-6* and *tba-8*) awaits further investigations.

The Effects of Tubulin PTMs in *C. elegans*

Tubulins undergo a variety of posttranslational modifications (PTMs) that regulate the microtubule structure, dynamics, and association with MAPs. Functional PTMs include α-tubulin K40 and K252 acetylation, detyrosination, and Δ2-modification and β-tubulin Q15 polyamination and S172 phosphorylation, as well as polyglutamylation and polyglycylation of the C-terminal tails of both α- and β-tubulin isotypes; their effects in other organisms have been extensively reviewed elsewhere (Magiera and Janke, 2014; Janke and Magiera, 2020). We will focus on the reported function of tubulin PTMs in *C. elegans*.

MEC-12 K40 Acetylation

Among the nine α-tubulin isotypes in *C. elegans*, only MEC-12 possess the lysine 40 residue (**Figure 4A**). So, only MEC-12 is subjected to K40 acetylation, which is catalyzed redundantly by two α-tubulin acetyltransferases—MEC-17 and ATAT-2 (Akella et al., 2010). The loss of either one alone did not reduce MEC-12 acetylation levels, but acetylation is not detectable in the *mec-17(-) atat-2(-)* double mutants (Topalidou et al., 2012). Although K40 acetylation has been found in long-lived microtubules (Schulze et al., 1987), exactly how it contributes to microtubule stability remains unclear. As the only PTM site located inside the lumen of microtubules (**Figure 5B**), acetylated K40 is found by recent studies to reduce inter-protofilament interactions and thus prevent long-lived microtubules from breaking under mechanical stresses (Portran et al., 2017; Eshun-Wilson et al., 2019). However, it remains debatable whether microtubules become

stable after acetylation or whether long-lived microtubules accumulate acetylation (Palazzo et al., 2003).

In *C. elegans*, MEC-17 is specifically expressed in the six TRNs, whereas ATAT-2 is broadly expressed in the nervous system. The deletion of MEC-17 reduces the number and length of microtubules and converts the 15-protofilament organization to 13-protofilament in the TRNs (Cueva et al., 2012; Topalidou et al., 2012). These changes in microtubule structure are not likely caused by the loss of K40 acetylation because MEC-12 K40 acetylation level in *mec-17(-)* mutants is comparable to the wild-type animals due to the existence of ATAT-2. Disorganized microtubules in *mec-17(-)* mutants lead to reduced touch sensitivity and abnormal neurite morphology, as well as early-onset axonal degeneration (Topalidou et al., 2012; Neumann and Hilliard, 2014). Many of these defects, however, can be rescued by the expression of enzymatically inactive MEC-17, which further supports that at least part of MEC-17's function is independent of acetylating MEC-12 K40. Exactly how MEC-17 exerts these functions remains to be understood.

On the other hand, some studies attempted to directly assess the effect of K40 in *mec-12* by transgenic expression of the acetyl-mimic K40Q and the nonacetylatable K40R mutants. Akella et al. (2010) found that expression of either K40Q or K40R could partially rescue touch sensitivity in *mec-12(e1620)* mutants to the same level but neither could rescue as well as the *mec-12(+)* transgene. Cueva et al. (2012) found that *mec-12(K40R)* transgene could not restore the number and length of microtubules and the protofilament number in *mec-12(e1620)* mutants to the same level as the *mec-12(+)* transgene could. These results are difficult to interpret because 1) the *mec-12(e1620)* allele used is in fact not a null allele but an antimorphic gain-of-function (Zheng et al., 2017); 2) transgenes often have variable expression levels and the abundance of tubulins would affect their functions. Better experimental design (e.g., editing the endogenous *mec-12* locus) will be needed to address the role of MEC-12 K40 acetylation.

Tubulin Polyglutamylation

The C-terminal tails of tubulins contain approximately 12 amino acids, which are subjected to at least five PTMs (Janke and Magiera, 2020). One such PTM is polyglutamylation, which adds multiple glutamates to the γ-carboxyl group of any of the glutamic acid residues in the C-terminal tail (Edde et al., 1990). Tubulin polyglutamylation were catalyzed by enzymes of the tubulin tyrosine ligase-like (TTLL) family and the glutamate side chain can also be removed by the cytosolic carboxypeptidases (CCPs) in a process known as deglutamylation (Janke et al., 2005; Rogowski et al., 2010). Mammalian genomes encode multiple TTLL and CCP proteins (e.g., mice have at least nine TTLLs and six CCPs), which showed preferences towards either α- or β-tubulins; some TTLLs are responsible for initiating the glutamylation, and others for elongating the glutamate sidechain (van Dijk et al., 2007; Rogowski et al., 2010). Tubulin polyglutamylation is known to regulate axonemal motility by modulating the activity of dynein motors in the cilia (Kubo et al., 2010; Suryavanshi et al., 2010) and regulate microtubule stabilities in neurons by stimulating spastin-mediated severing of microtubules (Lacroix et al., 2010).

The *C. elegans* genome encodes six TTLLs (TTLL-4, -5, -9, -11, -12, and -15) and two CCPs (CCPP-1 and CCPP-6), although TTLL-12 is the ortholog of mammalian TTLL12, which lacks glutamylase and glycylase activity (Yu et al., 2015). Biochemical studies found that TTLL-4 and CCPP-6 are the major tubulin polyglutamylase and deglutamylase, respectively, in ciliated sensory neurons, because either removing *ttll-4* or overexpressing CCPP-6 abolished the polyglutamylation signal in immunofluorescence (Kimura et al., 2010). In the male-specific ciliated neurons, CCPP-1 regulates axonemal microtubule structures and the ciliary localization of kinesin-3 KLP-6 and its cargo polycystin PKD-2 (O'Hagan et al., 2011). The loss of *ccpp-1* results in B-tubule defects, microtubule disorganization, and ciliary fragmentation, which is consistent with the findings that B-tubules are the main site of polyglutamylation (Kubo et al., 2010). At the behavioral level, in addition to mate-sensing defects, *ccpp-1(-)* mutants showed a progressive, age-dependent defects in dye-filling (uptake of fluorescent dye by sensory cilia) and osmotic avoidance, indicating that hyperpolyglutamylation may disrupt ciliary maintenance (O'Hagan et al., 2011).

Further studies found that TTLL-11 is required for ciliary microtubule polyglutamylation in males (O'Hagan et al., 2017). Intriguingly, *ttll-11(-)* mutants showed some similar defects as *ccpp-1(-)* mutants, including the abnormal enrichment of PKD-2 in the cilia and defects in extracellular vesicle release from the ciliary base, suggesting that an optimal level of glutamylation is needed for ciliary functions. The loss of TTLL-11 alters the axonemal microtubule architecture by preventing the splaying of the A-B doublets into A- and B-tubule singlets (**Figure 5C**); and *ccpp-1(-) ttll-11(-)* double mutants showed similar defects as the *ttll-11(-)* single mutants (O'Hagan et al., 2017). These results suggest that polyglutamylation regulates microtubule organization in the cilia. It is worth noting that *tba-6(-)* mutants also showed similar defects in splaying the A-B tubules (Silva et al., 2017), but the C-terminal tail of TBA-6 does not seem to contain residues for polyglutamylation (**Figure 4A**). One possible explanation is that TBA-6 functions together with other tubulin isotypes, such as TBB-4, which has polyglutamylation sites. The loss of TBA-6 may affect TBB-4 incorporation into the axonemal microtubules and thus reduce the overall glutamylation levels of the microtubules. In fact, Hurd et al. (2010) has previously observed reduced TBB-4 localization in the cilia of *tba-6(-)* mutants, supporting this hypothesis. Whether polyglutamylation of TBB-4 indeed regulates the organization of ciliary microtubules awaits further investigation.

Moreover, mutations in *ttll-11* also suppressed the abnormal localization and increased velocity of kinesin motors KLP-6 and OSM-3 in *ccpp-1(-)* mutants, suggesting that tubulin polyglutamylation serves as an important regulator of kinesin motility in intraflagellar transport (O'Hagan et al., 2017). In a separate study, Chawla et al. (2016) found that although the loss of *ttll* genes individually did not affect male mating efficiency, the *ttll-4(-) ttll-5(-) ttll-11(-)* triple mutants showed defects in the response step of male mating. Thus, it appears both

hyperglutamylation and hypoglutamylation disrupt the function of male-specific cilia. Nevertheless, the triple mutants did not show defects in embryonic viability, brood size, dye-filling, and osmotic avoidance (Chawla et al., 2016).

Excessive amount of polyglutamylation causes neurodegeneration in mammals (Magiera et al., 2018). In *C. elegans* amphid and phasmid neurons, the loss of CCPP-1 leads to progressive ciliary degeneration, which results in dye-filling defects in adults but not at early larval stages. Mutations in *ttll-4*, *ttll-5*, and *ttll-11* individually could all at least partially suppress the age-dependent dye-filling defects of *ccpp-1(-)* mutants (Power et al., 2020), supporting that polyglutamylation regulates ciliary stability and hyperglutamylation promotes ciliary microtubule degeneration.

In the non-ciliated TRNs, hyperglutamylation alters microtubule dynamics and blocks axonal regeneration. Loss of *ccpp-6* reduced the length of PLM regrowth following laser axotomy, whereas the regrowth is enhanced in *ttll-5(-)* mutants (Ghosh-Roy et al., 2012). Microtubules in *ccpp-6(-)* mutants are not able to sustain stabilized growth, while microtubules in *ttll-5(-)* mutants transition into persistent growth faster than the wild-type after axotomy. The same study also suggested that polyglutamylated microtubules may have increased sensitivity to the microtubule-destabilizing kinesin-13 KLP-7, supporting the idea that polyglutamylation may reduce microtubule stability in non-ciliated neurons.

Other Tubulin Posttranslational Modifications

Apart from K40 acetylation and polyglutamylation, the existence and function of other tubulin PTMs in *C. elegans* were unclear. For example, polyglycylation also occurs at the C-terminal tail of tubulins by adding glycine side chains to the same glutamate residues that are subjected to polyglutamylation (Janke and Magiera 2020). Polyglycylation appears to mostly label the axonemal microtubules in motile flagella and cilia. *C. elegans* has neither motile cilia nor orthologs of mammalian polyglycylase, and immunostaining against polyglycylation shows no signal (Kimura et al., 2010).

The C-terminal tail of α-tubulin could also undergo detyrosination, which removes the terminal tyrosine residue. Detyrosination can lead to the removal of the exposed penultimate glutamate residue, generating Δ2-tubulin. Both detyrosination and Δ2-modificatiosn are associated with long-lived stable microtubules and the tyrosination/detyrosination state modulate the interaction with plus end-binding proteins (Peris et al., 2006), the MT-depolymerization activity of kinesin-13 (Peris et al., 2009), and the motility of dynein-dynactin motor (McKenney et al., 2016). Detyrosination is mediated by the tubulin carboxypeptidases, vasohibins (VASH1/VASH2), and their stabilizing chaperone SVBP (Nieuwenhuis et al., 2017). Most *C. elegans* α-tubulin isotypes contain the terminal tyrosine (**Figure 4A**), but *C. elegans* has no ortholog of vasohibins, raising the question whether detyrosination occurs in *C. elegans*. Mutating the terminal tyrosine to alanine in TBA-1 and TBA-2 abolishes tyrosination signal and causes defects in the centration and rotation of centrosome in early embryos, similar to the defects found in dynactin *dnc-1* mutants, which supports that detyrosination may regulate the interaction with dynein-dynactin complex (Barbosa et al., 2017). However, this study only indicates the importance of the terminal tyrosine but could not serve as evidence for detyrosination in *C. elegans*. In addition, detyrosinated tubulins can be retyrosinated by tubulin tyrosine ligase (TTL) (Nieuwenhuis and Brummelkamp 2019). *C. elegans* does not seem to have a direct homolog of mammalian TTL, and whether any of the six TTLL enzymes in *C. elegans* can mediate tubulin retyrosination remains unknown.

Future Directions

The existence of multiple tubulin isotypes with distinct expression patterns and specialized functions, together with the ever-expanding variety of tubulin PTMs, lead to the fascinating concept of "tubulin code". The use of a simple organism such as *C. elegans* can be instrumental for cracking the tubulin code and understanding the regulation of microtubule structure and function by tubulin isotype composition and PTMs. Since CRISPR/Cas9-mediated gene editing is extremely easy and robust in *C. elegans*, we expect genetic studies to continue providing important insights into the functional specificity of tubulin isotypes and the effects of tubulin PTMs. Below, we list some future research directions.

The function of each tubulin isotype can be elucidated by analyzing the phenotype of individual tubulin deletion mutants guided by the tubulin expression map. Specific combination of tubulin mutants could also be constructed based on their expression patterns to overcome the expected genetic redundancies. This systematic analysis will provide a full picture of the expression and functional diversity of tubulin isotypes at the whole-genome and whole-organism level. To assess isotype-specific properties, gene replacement studies can be conducted to convert the endogenous locus of one tubulin isotype to another as done by Honda et al. (2017). This type of gene editing experiments can also be used to address whether the relative abundance of the tubulin isotypes play a role in defining microtubule properties. For example, the *mec-12* and *tba-1* coding regions in the genome can be swapped without changing their promoters and then the microtubule properties can be analyzed to test whether the relative abundance of MEC-12 and TBA-1 is important in TRNs.

The study of the tubulin code will also benefit from the development of the recombinant tubulin technology. Previous *in vitro* studies of tubulins and microtubules mostly rely on the use of tubulin proteins isolated from the bovine brain, which is known to contain tubulins with mixed isotypes and unknown PTMs. Recent studies by Ti et al. (2018) have shown the promise of generating isotypically pure microtubules with define PTMs from a recombinant source. Through cryo-EM reconstructions, the authors found that human TUBA1B/TUBB3 heterodimers form microtubules with 13 protofilaments, while TUBA1B/TUBB2 dimers form microtubules with 14 protofilaments, suggesting that β-tubulin isotype can determine protofilament number. This result echoes the findings that MEC-7 is required for the 15-protofilament microtubule structure in the *C. elegans* TRNs. Structural studies of the microtubules made from recombinant MEC-12/MEC-7 dimers and comparison with the

microtubules made of the ubiquitous tubulins (e.g., TBA-1/TBB-1) can provide the definitive answer for how a specific isotype determines the 15-profilament structure.

The studies of the effects of tubulin PTMs need to include more precise gene editing experiments. Previous studies on tubulin PTMs may be limited in two aspects. First, the effects of the PTMs were studied by mostly deleting the enzymes that add or remove specific PTMs. However, these enzymes may have substrates other than tubulins or have activities independent of its enzymatic functions (e.g., the acetyltransferase MEC-17). So, the effects resulted from losing an enzyme may not be entirely attributed to the change of tubulin PTMs. Second, in some cases, the effects of tubulin PTMs were revealed by the expression of tubulin mutants with PTM-mimicking or unmodifiable amino acid substitutions. Such transgenic expression may create artifacts due to uncontrolled expression levels and potential tubulin mRNA autoregulation (Lin et al., 2020). Therefore, precise engineering of the endogenous tubulin loci to install PTM-mimicking or -inactivating mutations will be better in revealing the role of the PTM. Nonetheless, polymodifications, such as polyglutamylation and polyglycylation, are difficult to mimic genetically. Advances in chemical biology will be needed to create tools for such studies.

In the coming years, we will likely see more and more tubulin PTMs to be identified and their functions to be studied, especially given that proteomic studies have identified 80 residues in tubulins that are subjected to one or multiple types of PTMs (Liu et al., 2015). We expect *C. elegans* to serve as a valuable tool in understanding the role of this network of tubulin PTMs.

AUTHOR CONTRIBUTIONS

Y-ML and CZ wrote the draft and edited it. CZ prepared the figures, secured the funding, and supervised the study. Both authors read and approved the manuscript.

FUNDING

This work is supported by grants from the Food and Health Bureau of Hong Kong (HMRF 07183186 to CZ), the Research Grants Council of Hong Kong (ECS 27104219, GRF 17107021, and CRF C7026-20G to CZ), the University of Hong Kong (seed fund 201910159087 and 202011159053 to CZ), and the National Natural Science Foundation of China (Excellent Young Scientists Fund for Hong Kong and Macau 32122002 to CZ).

ACKNOWLEDGMENTS

We thank Alvin Chu Yin Lau for helping prepare **Figure 2**. We apologize to all authors whose contribution to the topic could not be acknowledged due to space limitation.

SUPPLEMENTARY MATERIAL

The Supplementary Material for this article can be found online at: https://www.frontiersin.org/articles/10.3389/fcell.2022.860065/full#supplementary-material

REFERENCES

Akella, J. S., Wloga, D., Kim, J., Starostina, N. G., Lyons-Abbott, S., Morrissette, N. S., et al. (2010). MEC-17 Is an α-tubulin Acetyltransferase. *Nature* 467, 218–222. doi:10.1038/nature09324

Baran, R., Castelblanco, L., Tang, G., Shapiro, I., Goncharov, A., and Jin, Y. (2010). Motor Neuron Synapse and Axon Defects in a *C. elegans* Alpha-Tubulin Mutant. *PLoS One* 5, e9655. doi:10.1371/journal.pone.0009655

Barbier, P., Zejneli, O., Martinho, M., Lasorsa, A., Belle, V., Smet-Nocca, C., et al. (2019). Role of Tau as a Microtubule-Associated Protein: Structural and Functional Aspects. *Front. Aging Neurosci.* 11, 204. doi:10.3389/fnagi.2019.00204

Barbosa, D. J., Duro, J., Prevo, B., Cheerambathur, D. K., Carvalho, A. X., and Gassmann, R. (2017). Dynactin Binding to Tyrosinated Microtubules Promotes Centrosome Centration in *C. elegans* by Enhancing Dynein-Mediated Organelle Transport. *Plos Genet.* 13, e1006941. doi:10.1371/journal.pgen.1006941

Baugh, L. R., Hill, A. A., Slonim, D. K., Brown, E. L., and Hunter, C. P. (2003). Composition and Dynamics of the *Caenorhabditis elegans* Early Embryonic Transcriptome. *Development* 130, 889–900. doi:10.1242/dev.00302

Bounoutas, A., O'hagan, R., and Chalfie, M. (2009). The Multipurpose 15-protofilament Microtubules in *C. elegans* Have Specific Roles in Mechanosensation. *Curr. Biol.* 19, 1362–1367. doi:10.1016/j.cub.2009.06.036

Brenner, S. (1974). The Genetics of *Caenorhabditis elegans*. *Genetics* 77, 71–94. doi:10.1093/genetics/77.1.71

Chalfie, M., and Au, M. (1989). Genetic Control of Differentiation of the *Caenorhabditis elegans* Touch Receptor Neurons. *Science* 243, 1027–1033. doi:10.1126/science.2646709

Chalfie, M., and Thomson, J. N. (1979). Organization of Neuronal Microtubules in the Nematode *Caenorhabditis elegans*. *J. Cel. Biol.* 82, 278–289. doi:10.1083/jcb.82.1.278

Chalfie, M., and Thomson, J. N. (1982). Structural and Functional Diversity in the Neuronal Microtubules of *Caenorhabditis elegans*. *J. Cel. Biol.* 93, 15–23. doi:10.1083/jcb.93.1.15

Chang, P., and Stearns, T. (2000). δ-Tubulin and ε-Tubulin: Two New Human Centrosomal Tubulins Reveal New Aspects of Centrosome Structure and Function. *Nat. Cel. Biol.* 2, 30–35. doi:10.1038/71350

Chawla, D. G., Shah, R. V., Barth, Z. K., Lee, J. D., Badecker, K. E., Naik, A., et al. (2016). *Caenorhabditis elegans* Glutamylating Enzymes Function Redundantly in Male Mating. *Biol. Open* 5, 1290–1298. doi:10.1242/bio.017442

Consolati, T., Locke, J., Roostalu, J., Chen, Z. A., Gannon, J., Asthana, J., et al. (2020). Microtubule Nucleation Properties of Single Human γTuRCs Explained by Their Cryo-EM Structure. *Dev. Cel.* 53, 603–617.e608. doi:10.1016/j.devcel.2020.04.019

Corsi, A. K., Wightman, B., and Chalfie, M. (2015). A Transparent Window into Biology: A Primer on *Caenorhabditis elegans*. *Genetics* 200, 387–407. doi:10.1534/genetics.115.176099

Cram, E. J., Shang, H., and Schwarzbauer, J. E. (2006). A Systematic RNA Interference Screen Reveals a Cell Migration Gene Network inC. Elegans. *J. Cel. Sci.* 119, 4811–4818. doi:10.1242/jcs.03274

Cuenca-Zamora, E. J., Ferrer-Marín, F., Rivera, J., and Teruel-Montoya, R. (2019). Tubulin in Platelets: When the Shape Matters. *Int. J. Mol. Sci.* 20. doi:10.3390/ijms20143484

Cueva, J. G., Hsin, J., Huang, K. C., and Goodman, M. B. (2012). Posttranslational Acetylation of α-Tubulin Constrains Protofilament Number in Native Microtubules. *Curr. Biol.* 22, 1066–1074. doi:10.1016/j.cub.2012.05.012

Driscoll, M., Dean, E., Reilly, E., Bergholz, E., and Chalfie, M. (1989). Genetic and Molecular Analysis of a *Caenorhabditis elegans* Beta-Tubulin that Conveys Benzimidazole Sensitivity. *J. Cel. Biol.* 109, 2993–3003. doi:10.1083/jcb.109.6.2993

Eddé, B., Rossier, J., Le Caer, J.-P., Desbruyères, E., Gros, F., and Denoulet, P. (1990). Posttranslational Glutamylation of α-tubulin. *Science* 247, 83–85. doi:10.1126/science.1967194

Ellis, G. C., Phillips, J. B., O'rourke, S., Lyczak, R., and Bowerman, B. (2004). Maternally Expressed and Partially Redundant β-tubulins inCaenorhabditis Elegansare Autoregulated. *J. Cel. Sci.* 117, 457–464. doi:10.1242/jcs.00869

Eshun-Wilson, L., Zhang, R., Portran, D., Nachury, M. V., Toso, D. B., Löhr, T., et al. (2019). Effects of α-tubulin Acetylation on Microtubule Structure and Stability. *Proc. Natl. Acad. Sci. USA* 116, 10366–10371. doi:10.1073/pnas.1900441116

Fourel, G., and Boscheron, C. (2020). Tubulin Mutations in Neurodevelopmental Disorders as a Tool to Decipher Microtubule Function. *FEBS Lett.* 594, 3409–3438. doi:10.1002/1873-3468.13958

Fukushige, T., Siddiqui, Z. K., Chou, M., Culotti, J. G., Gogonea, C. B., Siddiqui, S. S., et al. (1999). MEC-12, an Alpha-Tubulin Required for Touch Sensitivity in *C. elegans*. *J. Cel. Sci.* 112 (Pt 3) (Pt 3), 395–403. doi:10.1242/jcs.112.3.395

Fukushige, T., Yasuda, H., and Siddiqui, S. S. (1995). Selective Expression of the Tba-1 α Tubulin Gene in a Set of Mechanosensory and Motor Neurons during the Development of *Caenorhabditis elegans*. *Biochim. Biophys. Acta (Bba) - Gene Struct. Expr.* 1261, 401–416. doi:10.1016/0167-4781(95)00028-f

Gadadhar, S., Hirschmugl, T., and Janke, C. (2022). The Tubulin Code in Mammalian Sperm Development and Function. *Semin. Cel. Dev. Biol.* doi:10.1016/j.semcdb.2021.12.003

Ghosh-Roy, A., Goncharov, A., Jin, Y., and Chisholm, A. D. (2012). Kinesin-13 and Tubulin Posttranslational Modifications Regulate Microtubule Growth in Axon Regeneration. *Dev. Cel.* 23, 716–728. doi:10.1016/j.devcel.2012.08.010

Gudimchuk, N. B., and Mcintosh, J. R. (2021). Regulation of Microtubule Dynamics, Mechanics and Function through the Growing Tip. *Nat. Rev. Mol. Cel. Biol.* 22, 777–795. doi:10.1038/s41580-021-00399-x

Guichard, P., Laporte, M. H., and Hamel, V. (2021). The Centriolar Tubulin Code. *Semin. Cel. Dev. Biol*. doi:10.1016/j.semcdb.2021.12.001

Hamelin, M., Scott, I. M., Way, J. C., and Culotti, J. G. (1992). The Mec-7 Beta-Tubulin Gene of *Caenorhabditis elegans* Is Expressed Primarily in the Touch Receptor Neurons. *EMBO J.* 11, 2885–2893. doi:10.1002/j.1460-2075.1992.tb05357.x

Hannak, E., Oegema, K., Kirkham, M., Gönczy, P., Habermann, B., and Hyman, A. A. (2002). The Kinetically Dominant Assembly Pathway for Centrosomal Asters in *Caenorhabditis elegans* Is γ-tubulin Dependent. *J. Cel. Biol.* 157, 591–602. doi:10.1083/jcb.200202047

Hao, L., Thein, M., Brust-Mascher, I., Civelekoglu-Scholey, G., Lu, Y., Acar, S., et al. (2011). Intraflagellar Transport Delivers Tubulin Isotypes to Sensory Cilium Middle and Distal Segments. *Nat. Cel. Biol.* 13, 790–798. doi:10.1038/ncb2268

Honda, Y., Tsuchiya, K., Sumiyoshi, E., Haruta, N., and Sugimoto, A. (2017). Tubulin Isotype Substitution Revealed that Isotype Combination Modulates Microtubule Dynamics in *C. elegans* Embryos. *J. Cell Sci.* 130, 1652–1661. doi:10.1242/jcs.200923

Howard, J. (1997). Molecular Motors: Structural Adaptations to Cellular Functions. *Nature* 389, 561–567. doi:10.1038/39247

Huang, M., Gu, G., Ferguson, E. L., and Chalfie, M. (1995). A Stomatin-like Protein Necessary for Mechanosensation in *C. elegans*. *Nature* 378, 292–295. doi:10.1038/378292a0

Hurd, D. D., Miller, R. M., Nu´ñez, L., and Portman, D. S. (2010). Specific α- and β-Tubulin Isotypes Optimize the Functions of Sensory Cilia in *Caenorhabditis elegans*. *Genetics* 185, 883–896. doi:10.1534/genetics.110.116996

Hurd, D. D. (20182018). Tubulins in *C. elegans*. *WormBook*, 1–32. doi:10.1895/wormbook.1.182.1

Janke, C., and Magiera, M. M. (2020). The Tubulin Code and its Role in Controlling Microtubule Properties and Functions. *Nat. Rev. Mol. Cel. Biol.* 21, 307–326. doi:10.1038/s41580-020-0214-3

Janke, C., Rogowski, K., Wloga, D., Regnard, C., Kajava, A. V., Strub, J.-M., et al. (2005). Tubulin Polyglutamylase Enzymes Are Members of the TTL Domain Protein Family. *Science* 308, 1758–1762. doi:10.1126/science.1113010

Kim, K. W., Tang, N. H., Piggott, C. A., Andrusiak, M. G., Park, S., Zhu, M., et al. (2018). Expanded Genetic Screening in *Caenorhabditis elegans* Identifies New Regulators and an Inhibitory Role for NAD+ in Axon Regeneration. *Elife* 7. doi:10.7554/eLife.39756

Kimura, Y., Kurabe, N., Ikegami, K., Tsutsumi, K., Konishi, Y., Kaplan, O. I., et al. (2010). Identification of Tubulin Deglutamylase Among *Caenorhabditis elegans* and Mammalian Cytosolic Carboxypeptidases (CCPs). *J. Biol. Chem.* 285, 22936–22941. doi:10.1074/jbc.c110.128280

Kubo, T., Yanagisawa, H.-a., Yagi, T., Hirono, M., and Kamiya, R. (2010). Tubulin Polyglutamylation Regulates Axonemal Motility by Modulating Activities of Inner-Arm Dyneins. *Curr. Biol.* 20, 441–445. doi:10.1016/j.cub.2009.12.058

Kunishima, S., Kobayashi, R., Itoh, T. J., Hamaguchi, M., and Saito, H. (2009). Mutation of the β1-tubulin Gene Associated with Congenital Macrothrombocytopenia Affecting Microtubule Assembly. *Blood* 113, 458–461. doi:10.1182/blood-2008-06-162610

Kurup, N., Yan, D., Goncharov, A., and Jin, Y. (2015). Dynamic Microtubules Drive Circuit Rewiring in the Absence of Neurite Remodeling. *Curr. Biol.* 25, 1594–1605. doi:10.1016/j.cub.2015.04.061

Lacroix, B., Van Dijk, J., Gold, N. D., Guizetti, J., Aldrian-Herrada, G., Rogowski, K., et al. (2010). Tubulin Polyglutamylation Stimulates Spastin-Mediated Microtubule Severing. *J. Cel. Biol.* 189, 945–954. doi:10.1083/jcb.201001024

Lee, H. M. T., Sayegh, N. Y., Gayek, A. S., Jao, S. L. J., Chalfie, M., and Zheng, C. (2021). Epistatic, Synthetic, and Balancing Interactions Among Tubulin Missense Mutations Affecting Neurite Growth in *Caenorhabditis elegans*. *MBoC* 32, 331–347. doi:10.1091/mbc.e20-07-0492

Lin, Z., Gasic, I., Chandrasekaran, V., Peters, N., Shao, S., Mitchison, T. J., et al. (2020). TTC5 Mediates Autoregulation of Tubulin via mRNA Degradation. *Science* 367, 100–104. doi:10.1126/science.aaz4352

Liu, N., Xiong, Y., Ren, Y., Zhang, L., He, X., Wang, X., et al. (2015). Proteomic Profiling and Functional Characterization of Multiple Post-Translational Modifications of Tubulin. *J. Proteome Res.* 14, 3292–3304. doi:10.1021/acs.jproteome.5b00308

Liu, P., Würtz, M., Zupa, E., Pfeffer, S., and Schiebel, E. (2021). Microtubule Nucleation: The Waltz between γ-tubulin Ring Complex and Associated Proteins. *Curr. Opin. Cel. Biol.* 68, 124–131. doi:10.1016/j.ceb.2020.10.004

Lockhead, D., Schwarz, E. M., O'Hagan, R., Bellotti, S., Krieg, M., Barr, M. M., et al. (2016). The Tubulin Repertoire of *Caenorhabditis elegans* Sensory Neurons and its Context-dependent R-ole in P-rocess O-utgrowth. *MBoC* 27, 3717–3728. doi:10.1091/mbc.e16-06-0473

Lu, C., and Mains, P. E. (2005). Mutations of a Redundant α-Tubulin Gene Affect *Caenorhabditis elegans* Early Embryonic Cleavage via MEI-1/Katanin-dependent and -Independent Pathways. *Genetics* 170, 115–126. doi:10.1534/genetics.104.030106

Lu, C., Srayko, M., and Mains, P. E. (2004). TheCaenorhabditis elegansMicrotubule-Severing Complex MEI-1/MEI-2 Katanin Interacts Differently with Two Superficially Redundant β-Tubulin Isotypes. *MBoC* 15, 142–150. doi:10.1091/mbc.e03-06-0418

Lu, Y.-M., and Zheng, C. (2021). TBA-7 Is Not a Microtubule-Destabilizing Tubulin. *MBoC* 32, 1145–1146. doi:10.1091/mbc.e21-04-0157

Magiera, M. M., Bodakuntla, S., Žiak, J., Lacomme, S., Marques Sousa, P., Leboucher, S., et al. (2018). Excessive Tubulin Polyglutamylation Causes Neurodegeneration and Perturbs Neuronal Transport. *EMBO J.* 37. doi:10.15252/embj.2018100440

Magiera, M. M., and Janke, C. (2014). Post-translational Modifications of Tubulin. *Curr. Biol.* 24, R351–R354. doi:10.1016/j.cub.2014.03.032

Matamoros, A. J., and Baas, P. W. (2016). Microtubules in Health and Degenerative Disease of the Nervous System. *Brain Res. Bull.* 126, 217–225. doi:10.1016/j.brainresbull.2016.06.016

Mckenney, R. J., Huynh, W., Vale, R. D., and Sirajuddin, M. (2016). Tyrosination of α-tubulin Controls the Initiation of Processive Dynein-Dynactin Motility. *EMBO J.* 35, 1175–1185. doi:10.15252/embj.201593071

Munkácsy, E., Khan, M. H., Lane, R. K., Borror, M. B., Park, J. H., Bokov, A. F., et al. (2016). DLK-1, SEK-3 and PMK-3 Are Required for the Life Extension Induced by Mitochondrial Bioenergetic Disruption in *C. elegans*. *Plos Genet.* 12, e1006133. doi:10.1371/journal.pgen.1006133

Neumann, B., and Hilliard, M. A. (2014). Loss of MEC-17 Leads to Microtubule Instability and Axonal Degeneration. *Cel. Rep.* 6, 93–103. doi:10.1016/j.celrep.2013.12.004

Nieuwenhuis, J., Adamopoulos, A., Bleijerveld, O. B., Mazouzi, A., Stickel, E., Celie, P., et al. (2017). Vasohibins Encode Tubulin Detyrosinating Activity. *Science* 358, 1453–1456. doi:10.1126/science.aao5676

Nieuwenhuis, J., and Brummelkamp, T. R. (2019). The Tubulin Detyrosination Cycle: Function and Enzymes. *Trends Cel. Biol.* 29, 80–92. doi:10.1016/j.tcb.2018.08.003

Nishida, K., Tsuchiya, K., Obinata, H., Onodera, S., Honda, Y., Lai, Y.-C., et al. (2021). Expression Patterns and Levels of All Tubulin Isotypes Analyzed in GFP Knock-In *C. elegans* Strains. *Cell Struct. Funct.* 46, 51–64. doi:10.1247/csf.21022

O'hagan, R., Silva, M., Nguyen, K. C. Q., Zhang, W., Bellotti, S., Ramadan, Y. H., et al. (2017). Glutamylation Regulates Transport, Specializes Function, and Sculpts the Structure of Cilia. *Curr. Biol.* 27, 3430–e6.e3436. doi:10.1016/j.cub.2017.09.066

O'hagan, R., Piasecki, B. P., Silva, M., Phirke, P., Nguyen, K. C. Q., Hall, D. H., et al. (2011). The Tubulin Deglutamylase CCPP-1 Regulates the Function and Stability of Sensory Cilia in *C. elegans*. *Curr. Biol.* 21, 1685–1694. doi:10.1016/j.cub.2011.08.049

Palazzo, A., Ackerman, B., and Gundersen, G. G. (2003). Tubulin Acetylation and Cell Motility. *Nature* 421, 230. doi:10.1038/421230a

Peris, L., Thery, M., Faure´, J., Saoudi, Y., Lafanechère, L., Chilton, J. K., et al. (2006). Tubulin Tyrosination Is a Major Factor Affecting the Recruitment of CAP-Gly Proteins at Microtubule Plus Ends. *J. Cel. Biol.* 174, 839–849. doi:10.1083/jcb.200512058

Peris, L., Wagenbach, M., Lafanechère, L., Brocard, J., Moore, A. T., Kozielski, F., et al. (2009). Motor-dependent Microtubule Disassembly Driven by Tubulin Tyrosination. *J. Cel. Biol.* 185, 1159–1166. doi:10.1083/jcb.200902142

Phillips, J. B., Lyczak, R., Ellis, G. C., and Bowerman, B. (2004). Roles for Two Partially Redundant α-tubulins during Mitosis in earlyCaenorhabditis Elegansembryos. *Cell Motil. Cytoskeleton* 58, 112–126. doi:10.1002/cm.20003

Portran, D., Schaedel, L., Xu, Z., Théry, M., and Nachury, M. V. (2017). Tubulin Acetylation Protects Long-Lived Microtubules against Mechanical Ageing. *Nat. Cel. Biol.* 19, 391–398. doi:10.1038/ncb3481

Power, K. M., Akella, J. S., Gu, A., Walsh, J. D., Bellotti, S., Morash, M., et al. (2020). Mutation of NEKL-4/NEK10 and TTLL Genes Suppress Neuronal Ciliary Degeneration Caused by Loss of CCPP-1 Deglutamylase Function. *Plos Genet.* 16, e1009052. doi:10.1371/journal.pgen.1009052

Prosser, S. L., and Pelletier, L. (2017). Mitotic Spindle Assembly in Animal Cells: a fine Balancing Act. *Nat. Rev. Mol. Cel. Biol.* 18, 187–201. doi:10.1038/nrm.2016.162

Qiang, L., Yu, W., Andreadis, A., Luo, M., and Baas, P. W. (2006). Tau Protects Microtubules in the Axon from Severing by Katanin. *J. Neurosci.* 26, 3120–3129. doi:10.1523/jneurosci.5392-05.2006

Rogowski, K., Van Dijk, J., Magiera, M. M., Bosc, C., Deloulme, J.-C., Bosson, A., et al. (2010). A Family of Protein-Deglutamylating Enzymes Associated with Neurodegeneration. *Cell* 143, 564–578. doi:10.1016/j.cell.2010.10.014

Roll-Mecak, A. (2020). The Tubulin Code in Microtubule Dynamics and Information Encoding. *Dev. Cel.* 54, 7–20. doi:10.1016/j.devcel.2020.06.008

Ronald Morris, N., Lai, M. H., and Elizabeth Oakley, C. (1979). Identification of a Gene for α-tubulin in Aspergillus nidulans. *Cell* 16, 437–442. doi:10.1016/0092-8674(79)90019-9

Sánchez-Huertas, C., and Herrera, E. (2021). With the Permission of Microtubules: An Updated Overview on Microtubule Function during Axon Pathfinding. *Front. Mol. Neurosci.* 14, 759404. doi:10.3389/fnmol.2021.759404

Savage, C., Hamelin, M., Culotti, J. G., Coulson, A., Albertson, D. G., and Chalfie, M. (1989). mec-7 Is a Beta-Tubulin Gene Required for the Production of 15-protofilament Microtubules in *Caenorhabditis elegans*. *Genes Dev.* 3, 870–881. doi:10.1101/gad.3.6.870

Schulze, E., Asai, D. J., Bulinski, J. C., and Kirschner, M. (1987). Posttranslational Modification and Microtubule Stability. *J. Cel. Biol.* 105, 2167–2177. doi:10.1083/jcb.105.5.2167

Sharp, D. J., and Ross, J. L. (2012). Microtubule-severing Enzymes at the Cutting Edge. *J. Cel. Sci.* 125, 2561–2569. doi:10.1242/jcs.101139

Silva, M., Morsci, N., Nguyen, K. C. Q., Rizvi, A., Rongo, C., Hall, D. H., et al. (2017). Cell-Specific α-Tubulin Isotype Regulates Ciliary Microtubule Ultrastructure, Intraflagellar Transport, and Extracellular Vesicle Biology. *Curr. Biol.* 27, 968–980. doi:10.1016/j.cub.2017.02.039

Strome, S., Powers, J., Dunn, M., Reese, K., Malone, C. J., White, J., et al. (2001). Spindle Dynamics and the Role of γ-Tubulin in EarlyCaenorhabditis elegansEmbryos. *MBoC* 12, 1751–1764. doi:10.1091/mbc.12.6.1751

Suryavanshi, S., Eddé, B., Fox, L. A., Guerrero, S., Hard, R., Hennessey, T., et al. (2010). Tubulin Glutamylation Regulates Ciliary Motility by Altering Inner Dynein Arm Activity. *Curr. Biol.* 20, 435–440. doi:10.1016/j.cub.2009.12.062

Taylor, S. R., Santpere, G., Weinreb, A., Barrett, A., Reilly, M. B., Xu, C., et al. (2021). Molecular Topography of an Entire Nervous System. *Cell* 184, 4329–4347. doi:10.1016/j.cell.2021.06.023

Ti, S.-C., Alushin, G. M., and Kapoor, T. M. (2018). Human β-Tubulin Isotypes Can Regulate Microtubule Protofilament Number and Stability. *Dev. Cel.* 47, 175–190 e175. doi:10.1016/j.devcel.2018.08.014

Tischfield, M. A., Cederquist, G. Y., Gupta, M. L., Jr., and Engle, E. C. (2011). Phenotypic Spectrum of the Tubulin-Related Disorders and Functional Implications of Disease-Causing Mutations. *Curr. Opin. Genet. Dev.* 21, 286–294. doi:10.1016/j.gde.2011.01.003

Topalidou, I., Keller, C., Kalebic, N., Nguyen, K. C. Q., Somhegyi, H., Politi, K. A., et al. (2012). Genetically Separable Functions of the MEC-17 Tubulin Acetyltransferase Affect Microtubule Organization. *Curr. Biol.* 22, 1057–1065. doi:10.1016/j.cub.2012.03.066

Van Dijk, J., Rogowski, K., Miro, J., Lacroix, B., Eddé, B., and Janke, C. (2007). A Targeted Multienzyme Mechanism for Selective Microtubule Polyglutamylation. *Mol. Cel.* 26, 437–448. doi:10.1016/j.molcel.2007.04.012

Webb, S., Mukhopadhyay, A. G., and Roberts, A. J. (2020). Intraflagellar Transport Trains and Motors: Insights from Structure. *Semin. Cel. Dev. Biol.* 107, 82–90. doi:10.1016/j.semcdb.2020.05.021

Wittmann, T., Hyman, A., and Desai, A. (2001). The Spindle: a Dynamic Assembly of Microtubules and Motors. *Nat. Cel. Biol.* 3, E28–E34. doi:10.1038/35050669

Wright, A. J., and Hunter, C. P. (2003). Mutations in a β-Tubulin Disrupt Spindle Orientation and Microtubule Dynamics in the EarlyCaenorhabditis elegansEmbryo. *MBoC* 14, 4512–4525. doi:10.1091/mbc.e03-01-0017

Yu, I., Garnham, C. P., and Roll-Mecak, A. (2015). Writing and Reading the Tubulin Code. *J. Biol. Chem.* 290, 17163–17172. doi:10.1074/jbc.r115.637447

Zheng, C., Diaz-Cuadros, M., Nguyen, K. C. Q., Hall, D. H., and Chalfie, M. (2017). Distinct Effects of Tubulin Isotype Mutations on Neurite Growth in *Caenorhabditis elegans*. *MBoC* 28, 2786–2801. doi:10.1091/mbc.e17-06-0424

Conflict of Interest: The authors declare that the research was conducted in the absence of any commercial or financial relationships that could be construed as a potential conflict of interest.

Publisher's Note: All claims expressed in this article are solely those of the authors and do not necessarily represent those of their affiliated organizations, or those of the publisher, the editors and the reviewers. Any product that may be evaluated in this article, or claim that may be made by its manufacturer, is not guaranteed or endorsed by the publisher.

frontiers | Frontiers in Cell and Developmental Biology

ORIGINAL RESEARCH
published: 01 April 2022
doi: 10.3389/fcell.2022.837486

Transcriptional, Post-Transcriptional, and Post-Translational Mechanisms Rewrite the Tubulin Code During Cardiac Hypertrophy and Failure

*Sai Aung Phyo[1,2], Keita Uchida[2], Christina Yingxian Chen[2], Matthew A. Caporizzo[2], Kenneth Bedi[3], Joanna Griffin[3], Kenneth Margulies[3] and Benjamin L. Prosser[2]**

[1]Department of Genetics and Epigenetics, University of Pennsylvania Perelman School of Medicine, Philadelphia, PA, United States, [2]Department of Physiology, Pennsylvania Muscle Institute, University of Pennsylvania Perelman School of Medicine, Philadelphia, PA, United States, [3]Department of Medicine, Cardiovascular Institute, University of Pennsylvania Perelman School of Medicine, Philadelphia, PA, United States

OPEN ACCESS

Edited by:
Jeffrey Moore,
University of Colorado Anschutz Medical Campus, United States

Reviewed by:
Ryoma Ohi,
University of Michigan, United States
Dan Sackett,
Eunice Kennedy Shriver National Institute of Child Health and Human Development (NICHD), United States

***Correspondence:**
Benjamin L. Prosser
bpros@pennmedicine.upenn.edu

Specialty section:
This article was submitted to Cellular Biochemistry, a section of the journal Frontiers in Cell and Developmental Biology

Received: 16 December 2021
Accepted: 02 February 2022
Published: 01 April 2022

Citation:
Phyo SA, Uchida K, Chen CY, Caporizzo MA, Bedi K, Griffin J, Margulies K and Prosser BL (2022) Transcriptional, Post-Transcriptional, and Post-Translational Mechanisms Rewrite the Tubulin Code During Cardiac Hypertrophy and Failure. Front. Cell Dev. Biol. 10:837486. doi: 10.3389/fcell.2022.837486

A proliferated and post-translationally modified microtubule network underlies cellular growth in cardiac hypertrophy and contributes to contractile dysfunction in heart failure. Yet how the heart achieves this modified network is poorly understood. Determining how the "tubulin code"—the permutations of tubulin isoforms and post-translational modifications—is rewritten upon cardiac stress may provide new targets to modulate cardiac remodeling. Further, while tubulin can autoregulate its own expression, it is unknown if autoregulation is operant in the heart or tuned in response to stress. Here we use heart failure patient samples and murine models of cardiac remodeling to interrogate transcriptional, autoregulatory, and post-translational mechanisms that contribute to microtubule network remodeling at different stages of heart disease. We find that autoregulation is operant across tubulin isoforms in the heart and leads to an apparent disconnect in tubulin mRNA and protein levels in heart failure. We also find that within 4 h of a hypertrophic stimulus and prior to cardiac growth, microtubule detyrosination is rapidly induced to help stabilize the network. This occurs concomitant with rapid transcriptional and autoregulatory activation of specific tubulin isoforms and microtubule motors. Upon continued hypertrophic stimulation, there is an increase in post-translationally modified microtubule tracks and anterograde motors to support cardiac growth, while total tubulin content increases through progressive transcriptional and autoregulatory induction of tubulin isoforms. Our work provides a new model for how the tubulin code is rapidly rewritten to establish a proliferated, stable microtubule network that drives cardiac remodeling, and provides the first evidence of tunable tubulin autoregulation during pathological progression.

Keywords: hypertrophy, heart failure, tubulin isoforms, transcription, autoregulation

Abbreviations: DEG, differentially expressed gene; HF, heart failure; HW, heart weight; Iso, isoproterenol; IEG, immediate early gene; PTM, post-translational modification; MAP, microtubule-associated proteins; αTAT1, α-tubulin acetyltransferase 1; VASH1/2, vasohibins 1 and 2; TL, tibia length; LV, left-ventricle; Ctrl, vehicle control; PE, phenylephrine.

INTRODUCTION

Heart Failure (HF) is a complex pathological condition in which cardiac performance fails to match systemic demand. HF is commonly preceded by an enlargement of the heart known as cardiac hypertrophy, which serves as a major risk factor for progression to HF. As such, understanding the molecular determinants of hypertrophy may reveal novel targets for HF prevention.

Microtubules are hollow tubes formed from the polymerization of α- and β- tubulin dimers that play essential roles in the structural support of cells, intracellular transport, and cell division. They exhibit stochastic growth and shrinkage and maintain a dynamic equilibrium between free and polymerized tubulin (**Supplementary Figure S1A**). Through their trafficking role, microtubules regulate cardiomyocyte electrical activity, mitochondrial dynamics, protein degradation and local translation, while also forming load-bearing structures that influence myocyte mechanics and mechano-signaling (Caporizzo et al., 2019).

During cardiac hypertrophy and heart failure, the microtubule network is significantly remodeled and acts as a double-edged sword. On one hand, a proliferated, stable microtubule network is essential for the development of cardiac hypertrophy in response to stressors such as adrenergic stimulation and hemodynamic overload (Sato et al., 1997; Fassett et al., 2009; Fassett et al., 2019; Scarborough et al., 2021). Upon such hypertrophic stimuli, a dense microtubule network and the anterograde motor protein kinesin-1 coordinates the trafficking of mRNA and the translational machinery to control local synthesis and integration of nascent proteins (Scarborough et al., 2021). In the absence of microtubules, increased protein translation is decoupled from protein integration and the heart fails to grow (Scarborough et al., 2021), identifying an essential role of microtubule-based transport in adaptive cardiac growth.

Yet upon chronic stress, the densified microtubule network can also contribute to contractile dysfunction in HF(Tsutsui et al., 1999; Caporizzo et al., 2018; Chen et al., 2018). A collective body of research has established a causal link between aberrant microtubule network remodeling and impaired cardiac mechanics in HF. Tubulin mass, and consequently microtubule network density, is consistently increased in the myocardium of HF patients (Chen et al., 2018; Schuldt et al., 2021) and pressure-overloaded animals (Sato et al., 1997; Fassett et al., 2019), and its destabilization can improve dysfunctional cardiac mechanics (Tsutsui et al., 1993; Cheng et al., 2008; Chen et al., 2018; Caporizzo et al., 2020).

While the state of the microtubule network in advanced HF has been well-defined by recent studies (Chen et al., 2018; Schuldt et al., 2020), we know little about the drivers and temporal progression of changes to the microtubule network that occur during cardiac remodeling. A seemingly obvious mechanism to increase tubulin mass is transcriptional upregulation; yet when we examine published transcriptomic and proteomic data from HF samples, we observe a surprising but consistent inverse correlation between tubulin mRNA and protein levels across different causes of HF in multiple studies (**Figures 1A,B**). This motivates a deeper examination between transcriptional and translation coupling of tubulin isoforms and other factors that could contribute to microtubule proliferation.

There are a multitude of α and β tubulin isoforms that arise from alternative tubulin genes; in humans, there are nine α and nine β -tubulin isoforms, and in mice, seven α and eight β isoforms (**Supplementary Figure S1B**). The abundance of tubulin transcripts can be controlled through autoregulation, a tubulin-specific mRNA rheostat in which an excess of free tubulin can activate a ribosomal RNase to degrade nascent tubulin transcripts (autoinhibition); conversely, if free tubulin levels are reduced, autoregulation is released (autoactivation) to promote tubulin synthesis and restore free tubulin content (Gasic and Mitchison 2019) (**Figure 1C**). The extent to which tubulin isoforms are controlled through transcriptional or autoregulatory mechanisms has not been characterized, and autoregulation has not been examined in any capacity in the heart. Finally, any pathological relevance of autoregulation in cardiac or other tissues is largely unexplored.

The stabilization (i.e., protection from breakdown) of polymerized microtubules is another potentially important driver of the dense microtubule network observed in hypertrophy and HF. Microtubules are stabilized through association with microtubule-associated proteins (MAPs) and motors as well as through post-translational modifications (PTMs) of tubulin (**Supplementary Figure S1**). Acetylation of polymerized α-tubulin produces long-lived and resilient microtubules that are resistant against repeated mechanical stresses (Kalebic et al., 2013; Portran et al., 2017), while detyrosination - the removal of a tyrosine residue on the C-terminal tail of α-tubulin by vasohibins 1 and 2 (VASH1/2) (Aillaud et al., 2017; Nieuwenhuis et al., 2017)—stabilizes microtubules by modulating their interactions with depolymerizing effector proteins (Peris et al., 2009; Chen et al., 2021). The permutations of PTMs and tubulin isoforms is known as the "tubulin code" (**Supplementary Figure S1**), which creates microtubule networks with distinct biochemical and mechanical properties. Altered detyrosination (Chen et al., 2018; Yu et al., 2021), acetylation (Swiatlowska et al., 2020), and MAP (Cheng et al., 2010; Li et al., 2018; Yu et al., 2021) binding are each implicated in pathological cardiac remodeling; yet how the tubulin code is rewritten during cardiac hypertrophy and HF remains largely unclear.

In this study, we interrogate changes to the tubulin code, MAPs, and motors at discrete stages of pathological cardiac remodeling. We find that surprisingly rapid and isoform-specific transcriptional induction and autoactivation of tubulin mRNA combine with post-translational detyrosination to drive microtubule stabilization and proliferation during early cardiac growth. We also find that in progressed heart failure, there is a switch to autoinhibition that reduces tubulin mRNA expression in the face of elevated tubulin protein content. This work identifies roles for autoregulation in rewriting the tubulin code during cardiac remodeling and may inform on approaches intended to modulate the course of hypertrophy and its progression to HF.

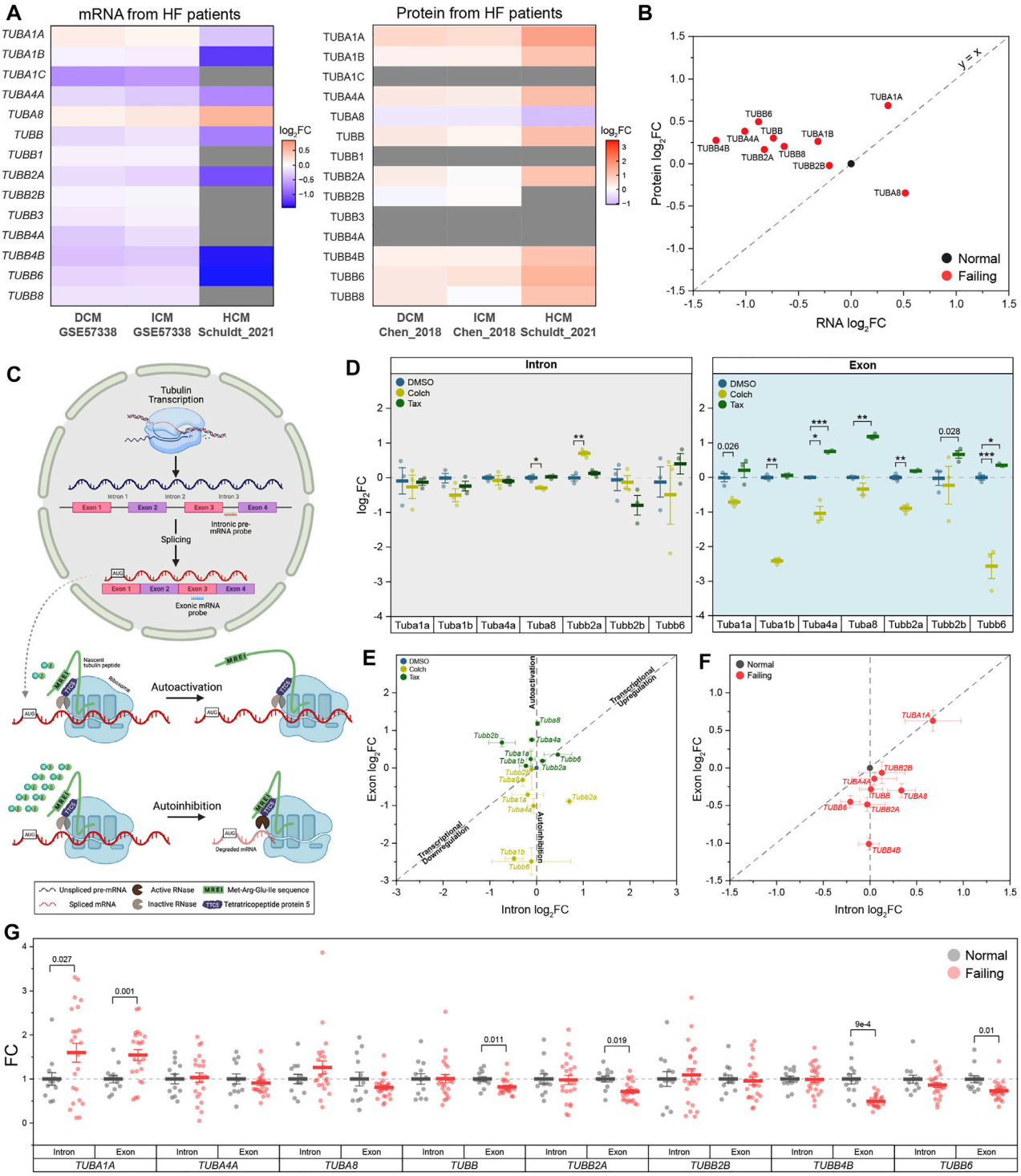

FIGURE 1 | Tubulin autoregulation is operant in the heart and activated in heart failure. **(A)** Heatmaps of previously published mRNA (left) & protein (right) data of human αβ-tubulin isoforms during dilated (DCM) (Liu et al., 2015, Chen et al., 2018), ischemic (ICM) (Liu et al., 2015, Chen et al., 2018), & hypertrophic (HCM) (Schuldt et al., 2021) cardiomyopathies. **(B)** Scatter-plot of log_2fold-change of mRNA on x-axis and log_2fold-change of protein on y-axis in heart failure; each data point represents an average log_2fold-change value from DCM and ICM groups from **(A)**, and y = x represents a proportionate change between mRNA and peptide. **(C)** Schematic of tubulin autoregulation: The introns of tubulin pre-mRNA are spliced out and the mRNA is fully translated in the absence of excess free tubulin; in the presence of excess free tubulin, the mRNA, but not the pre-mRNA, is degraded. **(D)** Relative log_2fold-change of mRNA counts of intronic (left) and exonic (right) αβ-tubulin isoforms in isolated adult mouse cardiomyocytes after treatment with either depolymerizing (Colch) or polymerizing (Tax) agents (n = 3); whiskers represent ± 1SEM, bolded line represents mean, * represents p-value from Welch-corrected two-tailed two-sample t-test on non-log data <0.025 (Bonferroni-corrected for two comparisons), ** represents

(*Continued*)

FIGURE 1 | p < 0.01, and *** represents p < 0.001. ***(E)*** *Scatter-plot of relative log_2fold-change of intron on x-axis and exon on y-axis after Colch or Tax treatment in adult mouse cardiomyocytes; whiskers represent ± 1SEM.* ***(F)*** *Scatter-plot of relative log_2fold-change of intron on x-axis and exon on y-axis in near-normal and failing patient heart samples; whiskers represent ± 1SEM.* ***(G)*** *Relative fold-change of mRNA counts of intronic and exonic αβ-tubulin isoforms in near-normal and failing patient heart samples; whiskers represent ± 1SEM, bolded line represents mean, and p-values are from Welch-corrected two-tailed two-sample t-test.*

METHODS

Human Myocardial Tissue

Procurement of human myocardial tissue was performed under protocols and ethical regulations approved by Institutional Review Boards at the University of Pennsylvania and the Gift-of-Life Donor Program (Pennsylvania, United States) and as described (Chen et al., 2018). In summary, failing human hearts were procured at the time of orthotropic heart transplantation at the Hospital of the University of Pennsylvania following informed consent from all participants. Non-failing hearts were obtained at the time of organ donation from cadaveric donors. In all cases, hearts were arrested *in situ* using ice-cold cardioplegia solution and transported on wet ice. Transmural myocardial samples were dissected from the mid left ventricular free wall below the papillary muscle and the samples were kept frozen at 80°C. Contractile parameters, including left ventricle ejection fraction, were determined by echocardiography in subjects. In this study, a total of 35 donor hearts were used. 12 donors were classified as near-normal non-failing (NF) without left-ventricular hypertrophy, and 23 donors were classified as heart failure with 12 hearts from hypertrophic cardiomyopathy patients and 11 hearts from dilated cardiomyopathy patients.

Animal Care

Animal care and procedures were approved and performed in accordance with the standards set forth by the University of Pennsylvania Institutional Animal Care and Use Committee (IACUC) and the Guide for the Care and Use of Laboratory Animals published by the US National Institutes of Health (NIH).

Drug Injection

Eight to 12 weeks old male C57/Bl6 mice were used throughout the study. On days 0 and 2, based on their body weights, mice were subcutaneously injected with either ascorbic acid (Ctrl, Sigma-Aldrich: A92902), 10 mg/kg phenylephrine (PE, Sigma-Aldrich: P6126) prepared in Ctrl, or 5 mg/kg isoproterenol (Iso, Sigma-Aldrich: I6504) prepared in Ctrl.

Cardiac Tissue Harvest

Mice were put under general anesthesia using isoflurane and the hearts were surgically removed. Excised hearts were thoroughly washed in ice-cooled PBS and extra-cardiac tissues were removed. To properly measure heart weight (HW), residual blood from the chambers was removed by sandwiching the heart between Kimwipes and gently squeezing it. After HW measurement, atrial and right ventricular tissues were removed, the remaining septal and left-ventricular tissues were cut into five pieces of similar size and from similar locations of the heart. The weights of the individual pieces were recorded, frozen in liquid nitrogen, and stored at -80°C until further processing. Concurrent with tissue harvest, the tibia length (TL) of respective mouse was measured to calculate HW-over-TL (HW/TL).

Exclusion Criteria

During the study: for the 4-h time point, there were six mice per treatment group for a total of 18 mice, and for the 4-days time point, there were eight mice per treatment group for a total of 24 mice. As we aimed to study mice who underwent consistent cardiac hypertrophy, for the 4-days time point, we set exclusion criteria as the followings: (1) hearts whose HW/TL were beyond 2 SD of the population mean, and (2) experimental hearts whose classical hypertrophy response genes were not changed relative to that of the control hearts. After the removal of outliers, in the final study: for the 4-h time point, there are six mice per treatment group for a total of 18 mice, and for the 4-days time point, there are seven mice in Ctrl, seven mice in PE, and six mice in Iso, for a total of 20 mice.

Mouse Cardiomyocyte Isolation, Culture, and Drug Treatment

Primary adult ventricular myocytes were isolated from eight- to 12-week-old C57/Bl6 mice using the protocol previously described (Prosser et al., 2011). Briefly, mice were put under general anesthesia using isoflurane and were injected peritoneally with heparin (~1,000 units/kg). The heart was excised and cannulated to a Langendorff apparatus for retrograde perfusion with enzymatic digestion solution at 37°C. Once digested, the heart was minced and triturated with glass pipettes. The isolated cardiomyocytes were centrifuged at 300 revolution per minute for 2 min. The supernatant containing debris was discarded and the isolated cells were resuspended in cardiomyocyte media containing Medium 199 (GIBCO: 11150-59) supplemented with 1x insulin-transferrin-selenium-X (GIBCO: 51500-56), 20 mM HEPES pH 7.4, 0.1 mg/ml Primocin, and 25 μmol/L of cytochalasin D. Immediately following cell isolation, the cardiomyocytes were treated with either DMSO, 10 μM colchicine, or 10 μM taxol, and incubated at 37°C and 5% CO_2 for 6 h.

Echocardiography

On day 4, transthoracic echocardiography was performed on mice, which were anesthetized using intraperitoneal injection of 0.01 ml/G body-weight of 2.5% Avertin, using Vevo2100 Ultrasound System (VisualSonics Inc., Toronto, Ontario, Canada). Fractional shortening, chamber dimensions, and ventricular wall-thickness were measured

from short axis M-mode images at the mid-level view of the papillary muscle.

Total Protein Lysate Preparation

Frozen aliquoted cardiac tissue obtained from similar locations of the heart was pulverized finely using a liquid nitrogen-cooled mortar and pestle. 1x Radioimmunoprecipitation assay (RIPA) buffer (Cayman Chemical Company: 10010263) supplemented with 1x protease inhibitor cocktail (Cell Signaling Technology: 5872S) and 1:200 diluted endonuclease (Lucigen: OC7850K) was immediately added to the pulverized tissue at a constant ratio of 15 µL/mg of tissue. The sample was then mechanically homogenized using a handheld homogenizer until visible chunks of tissues were dissociated. The sample was incubated for 10 min on ice to allow endonuclease to cleave DNA. After processing of all samples, the samples underwent two freeze-thaw cycles, after which, equal-volume of 5% SDS-10% glycerol boiling (SGB) buffer was added to each sample. The samples were vortexed thoroughly then heated to 100°C for 8 min. Residual undissolved cell debris were removed from the resulting samples by centrifugation at 8000 g for 5 min at room temperature (22°C). The concentrations of the total protein were determined using Bicinchoninic acid (BCA) assay; all samples were diluted to 4 µg/µL using RIPA:SGB buffer. The diluted total protein lysates were aliquoted and stored at −80°C until further processing.

Microtubule Fractionation

100 mM PIPES-KOH pH 6.8, 1 mM $MgCl_2$, 1 mM EGTA-KOH pH 7.7 (PME) buffer was prepared fresh and was supplemented with 1 mM DTT, 1 mM GTP (Sigma-Aldrich: G8877), and 1x protease inhibitor cocktail. Seven parts supplemented PME buffer was mixed with three parts glycerol; the final PME-30G buffer was kept incubated in a 37°C water bath. Frozen aliquoted cardiac tissue obtained from similar locations of the heart was pulverized crudely using a liquid nitrogen-cooled mortar and pestle. Immediately following pulverization, warmed PME-30G buffer was added at a constant ratio of 20 µL/mg of tissue. The sample was then mechanically homogenized using the handheld homogenizer until visible chunks of tissues were dissociated and was set aside at 22°C until all samples were processed. All processed samples were then centrifuged at 16000 g for 15 min at 30°C; the supernatants were transferred into fresh tubes and were saved as free tubulin (Free) fractions. 10 µL of 1 part RIPA and 1 part SGB (RIPA:SGB) buffer was added to the pellet obtained from 1 mg of tissue and the sample was homogenized using the handheld homogenizer. After processing of all samples, the samples were heated to 100°C for 8 min, cooled on ice, and centrifuged at 8000 g for 5 min at 22°C; the supernatants were transferred into fresh tubes and were saved as polymerized tubulin (Poly) fractions. The concentrations of the Poly fractions were determined using BCA assay. The Poly fractions were diluted to 4 µg/µL using RIPA:SGB buffer; the respective Free fraction was diluted with PME-30G buffer using twice the volume needed to dilute the Poly fraction. The final diluted Free and Poly fractions were aliquoted and stored at −80°C until further processing.

Sample Preparations and Western Blot Analysis

To quantify the relative abundance of specific proteins of interest in the total protein lysate, aliquoted diluted total protein lysate samples were thawed at 22°C. One part 4x loading buffer (125 mM Tris-HCl pH 6.8, 35% v/v glycerol, 0.2% w/v Orange G) freshly supplemented with 10% v/v β-mercepthoethanol (BME) was mixed with three parts total protein lysate to get final concentrations of 1x loading buffer with 2.5% BME, and 3 µg/µL of total protein. The final samples were heated to 100°C for 8 min. The heated samples were cooled to 22°C, centrifuged briefly, vortexed thoroughly, and loaded 5µL/sample onto precast protein gels (Bio-Rad: 5671085).

To quantify the relative abundances of the Free and Poly fractions, aliquoted diluted Free and Poly fractions were thawed at 22°C. For the Free fractions, 2x loading buffer (62.5 mM Tris-HCL pH 6.8, 5% v/v SDS, 0% glycerol, 0.1% w/v Orange G) freshly supplemented with 5% v/v BME was used, whereas, for the Poly fractions, 4x loading buffer freshly supplemented with 10% v/v BME was used; to prepare the final samples, the respective loading buffers were diluted to 1x using the Free and Poly fractions. The final samples were heated to 100°C for 8 min. The heated samples were cooled to 22°C, centrifuged briefly, vortexed thoroughly, and loaded 5 µL/Poly fraction and 10 µL/Free fraction onto precast protein gels.

Protein gel electrophoresis was carried out under constant voltage of 135 V for the Midi gels for 1 h. The resolved proteins were transferred onto a nitrocellulose membrane using the Turbo Transfer System (Bio-Rad) under recommended conditions. The post-transferred membrane was blocked in blocking buffer (LI-COR Biosciences: 927-60003) for at least 1 h at 22°C (or overnight at 4°C). The blocked membrane was incubated overnight at 4°C with primary antibodies diluted in 1x Tris buffered saline with Tween-20 (TBST, Cell Signaling Technology: 9997S). The membrane was washed twice using TBST, and incubated for 1 h at 22°C with secondary antibodies diluted in blocking buffer. The final immunoblotted membrane was washed twice using TBST and was imaged using the Odyssey Western Blot Imaging System (LI-COR Biosciences).

WB Data Analysis

The WB data was analyzed using Image Studio Lite (LI-COR Biosciences). The signal intensity of an individual band was obtained by drawing a rectangular block encompassing the entire band. The background was thresholded using the parameters: median, border width = 3, Top/Bottom. Two technical replicates (n) per sample, and six biological replicates (N) per treatment for 4-h time point and eight biological replicates per treatment for 5-days time point were used in the analysis. GAPDH intensity was used as a loading control. A mean value of the Ctrls that were run on the same blot was used to normalize the data and to calculate the relative fold-changes over the Ctrl. Statistical analyses were performed as described below.

Primary and Secondary Antibodies

(see table below)

Target	Vendor	Host species	Clonal	Product no	Concentration used in WB
Total α-tubulin	Abcam	Mouse	Mono	ab7291	1:3000
Total α-tubulin	Abcam	Rabbit	Poly	ab4074	1:2000
Total β-tubulin	Abcam	Rabbit	Poly	ab6046	1:1500
Acetylated α-tubulin	Abcam	Mouse	Mono	ab24610	1:1000
Detyrosinated α-tubulin	Abcam	Rabbit	Poly	ab48389	1:1000
Polyglutamylated α-tubulin	Adipogen	Mouse	Mono	50-436-394	1:500
Δ2 α-tubulin	Moutin Lab	Rabbit	Poly		1:5000
Polyglycylated tubulin	EMD Millipore	Mouse	Mono	MABS276	1:700
Kif15	Proteintech	Rabbit	Poly	55407-1-AP	1:500
Vash1	Abcam	Rabbit	Mono	ab199732	1:1000
Mapre1 (EB1)	Sigma-Aldrich	Rabbit	Poly	E3406	1:500
GAPDH	GenScript	Mouse	Mono	A01622-40	1:2000
H3	Abcam	Mouse	Mono	ab24834	1:3000
Anti-mouse	LI-COR	Donkey	Poly	925-32212	1:10000
Anti-rabbit	LI-COR	Donkey	Poly	925-68073	1:10000

Mass Spectrometry (MS) Sample Preparation

To quantify the relative changes of multiple proteins of interest in the total protein lysate, aliquoted diluted total protein lysate samples were thawed at 22°C. One part 4x loading buffer freshly supplemented with 10% v/v BME was mixed with three parts total protein lysate. The final samples were heated to 100°C for 8 min. The heated samples were cooled to 22°C, centrifuged briefly, vortexed thoroughly, and loaded 50 µL/sample onto precast protein gels (Bio-Rad: 4561034). Protein gel electrophoresis was carried out under constant voltage of 110 V for the Mini gels for 1.5 h. The resolved protein gel was stained with Coomassie blue (Bio-Rad: 1610435) using the provided protocol. After the destaining of the gel, the 50 kDa bands were carefully excised and stored in deionized water at 4°C until further processing.

The gel bands were destained with 100 mM ammonium bicarbonate/acetonitrile (50:50). The bands were reduced in 10 mM dithiothreitol/100 mM Ammonium bicarbonate for over 60 min at 52°C; the bands were then alkylated with 50 mM iodoacetamide/100 mM ammonium bicarbonate at 22°C for 1 h in the dark. The proteins in the gel bands were digested with enzymes while incubating overnight at 37°C; different enzymes such as trypsin, Chymotrypsin, and Glu-C were used according to protein sequences. The supernatants were transferred and kept in fresh tubes. Additional peptides were extracted from the gel by adding 50% acetonitrile/1% TFA and incubated for 10 min on a shaker. The supernatants were combined and dried. The dried samples were reconstituted using 0.1% formic acid for MS analysis.

MS Analysis Using Nano-LC-MS/MS

Peptides were analyzed on a Q-Exactive HF (Thermo Fisher Scientific) attached to an Ultimate 3000 rslcnano system (Thermo Fisher Scientific) at 400 nL/min. Peptides were eluted with a 55 min gradient from 5% to 32% ACN (25 min) and 90% ACN over 5 min in 0.1% formic acid. Data-dependent acquisition mode with a dynamic exclusion of 45 s was enabled. One full MS scan was collected with a scan range of 350–1,200 *m/z*, resolution of 70 K, maximum injection time of 50 milliseconds, and AGC of 1×10^6. Then, a series of MS2 scans were acquired for the most abundant ions from the MS1 scan (top 12). Ions were filtered with charges 2–4. An isolation window of 2 m/*z* was used with quadruple isolation mode. Ions were fragmented using higher-energy collisional dissociation (HCD) with a collision energy of 27%. Orbitrap detection was used with a scan range of 140–2000 m/*z*, resolution of 30 K, maximum injection time of 54millisecondsmilliseconds, and AGC of 50,000.

MS Data Analysis

Proteome Discoverer (Thermo Fisher Scientific, version 2.4) was used to process the raw spectra. Default search parameters were used, including precursor mass tolerance of 10 ppm, fragment mass tolerance of 0.02 Da, enzymes specific cleavage, and up to 2 mis-cleavage. Carbamidomethyl [C] was set as a fixed modification, while Oxidation [M] and Acetylation [N-terminal and K] were set as variable modifications. The target-decoy approach was used to filter the search results, in which the false discovery rate was less than 1% at the peptide and protein levels. For measuring the relative protein abundances, all the chromatographic data were aligned and normalized to peptide groups and protein abundances, missing values were imputed and scaled. The normalized protein abundance values from four Ctrls, 5 PE, and four Iso 4-days mice were used in the subsequent analysis. Since the different tubulin isoforms share multiple homologous regions, only unique peptides that are unambiguous to each isoform were used to calculate protein abundance. The unique peptides acquired for the analyzed isoforms ranged from 1–13 peptides and the full suite of peptide and protein groups used in the analysis can be found in the public proteomic repository as outlined in the data availability statement. Statistical analyses were performed on the calculated protein abundances as described below.

Total RNA Extraction

Frozen aliquoted cardiac tissue obtained from similar locations of the heart was pulverized finely using a liquid nitrogen-cooled mortar and pestle. 500 µL of ice-cooled RNAzol (Molecular Research Center: RN 190) was added to the pulverized tissue

and immediately homogenized using the handheld homogenizer until visible chunks of tissues were dissociated. 200 µL of molecular grade water was added to the sample; the sample was vortexed and incubated for 15 min at 22°C. After processing of all samples, the samples were then centrifuged at 12000 g for 15 min at 22°C. 550 µL of the clear supernatant was carefully removed and transferred into a fresh tube. 550 µL of isopropanol was then added to the supernatant, vortexed, and incubated for 10 min at 22°C. The samples were centrifuged at 16000 g for 10 min at 22°C, and the resulting supernatants were discarded. The visible RNA pellets were washed in 75% ethanol in molecular grade water three times. The undried RNA pellets were resuspended in 30 µL of RNase free water. The total RNA concentrations, and 260/230 and 260/280 ratios were determined using NanoDrop ND-1000 Spectrophotometer (NanoDrop Technologies). The RNA samples were stored at -80°C until further analysis.

NanoString nCounter Analysis

Total RNAs from 37 samples were analyzed. The concentration of the total RNA was reassessed using NanoDrop spectrophotometer. The quality of the total RNA was assessed using the Agilent 4200 TapeStation (Agilent Technologies). Only samples that were pure as defined by OD 260/280 and 260/230 ratios >1.8, and integrity RIN value >8.0 were used in the study. 100 ng of total RNA per sample for tubulin and hypertrophy panels or 200 ng of total RNA per sample for tubulin autoregulation panel was used for the subsequent step. Hybridization between the target mRNA and reporter-capture probe pairs was performed for 18 h at 65°C using Mastercycler Pro S Thermal Cycler (Eppendorf) according to the manufacturer's protocol. Post-hybridization processing was carried out on a fully automated nCounter Prep Station (NanoString Technologies) liquid-handling robotic device using the High Sensitivity setting. For image acquisition and data processing, the probe/target complexes were immobilized on the nCounter cartridge that was then placed in the nCounter Digital Analyzer (NanoString Technologies) as per the manufacturer's protocol with FOV set to 555. The expression level of a gene was measured by counting the number of times the probe with a unique barcode, which was targeted against that gene, was detected. The barcode counts were then tabulated in a comma-separated value (.csv) format.

NanoString nCounter Data and Statistical Analysis

The raw digital counts of expressions were exported into nSolver Analysis software (NanoString, version 4.0) for downstream analysis. The data was analyzed in nSolver using the Nanostring Analysis and Advanced Analysis software packages. The background of the data was thresholded using the geometric means after removing negative control values that are three-times higher than the rest. The data was then normalized using the geometric means of the positive controls, after removing "F" if the value is too close to background, and the three housekeeping genes (Gapdh, Rpl4, Tbp). Without removing low count values, the Bonferroni-corrected differentially expressed gene (DEG) analysis of the normalized data was computed using Treatment as covariates. For tubulin autoregulation panel, raw counts were exported, and statistical analyses were carried as outlined below.

Statistical Analysis

Graphing and statistical analyses were performed using OrginPro 2019 software (OriginLabs). First, the normality of the data was determined using the Shapiro-Wilk test. For comparison of data distributions whose normality cannot be rejected at 0.05 level, the calculated probability of the means (p) between the control and the experimental group was calculated using the two-tailed two-sample Welch-corrected student's t-test. For comparison of data distributions whose normality is rejected at 0.05 level, the p-value between the control and the experimental group was calculated using the two-tailed two-sample Kolmogorov-Smirnov test. For significance level, we used the Bonferroni-corrected significance cut-off of $p < 0.025$ denoted by *; ** represents $p < 0.01$ and *** represents $p < 0.001$. p-values to two significant figures were reported for $0.05 < p < 0.025$. For all bar graphs, the bar represents mean and the whisker represents +1 SEM. For all box plots, the bolded line represents mean, and the whiskers represent ±1 standard error of mean (SEM).

RESULTS

Tubulin Autoregulation is Operant in the Heart and Induced in Heart Failure

Despite the importance of microtubule proliferation in cardiac pathology, any role of tubulin autoregulation has not been examined. We utilized a previously established strategy to test for autoregulation by measuring the relative abundances of pre-spliced (i.e. intron-containing) and spliced (i.e. those without introns) tubulin mRNAs (Gasic et al., 2019). Using this approach, one can detect transcriptional regulation of a target through correlated changes in intronic and exonic mRNA levels (y = x in **Figure 1E**, for example), whereas post-transcriptional autoregulation would only affect exonic mRNA (shift along the y-axis of **Figure 1E**). To study autoregulation in an isoform-specific fashion, we designed NanoString nCounter probes for direct and unique detection of either intronic or exonic regions of individual tubulin isoforms. To determine if autoregulation is operant in heart muscle cells, we treated isolated mouse cardiomyocytes for 6 h with colchicine, a microtubule depolymerizing agent predicted to trigger autoinhibition (decrease in only exonic species) by increasing free tubulin, or taxol, a microtubule polymerizing agent predicted to trigger autoactivation (increase in only exonic species) by shifting free tubulin into the polymerized pool. Consistently, depolymerization significantly reduced the amount of exonic but not intronic mRNA across most tubulin isoforms, while polymerization increased the amount of exonic tubulin mRNA (**Figures 1D,E**). This data serves as the first demonstration that autoregulation is operant in the cardiomyocyte and that it regulates the majority of tubulin isoforms.

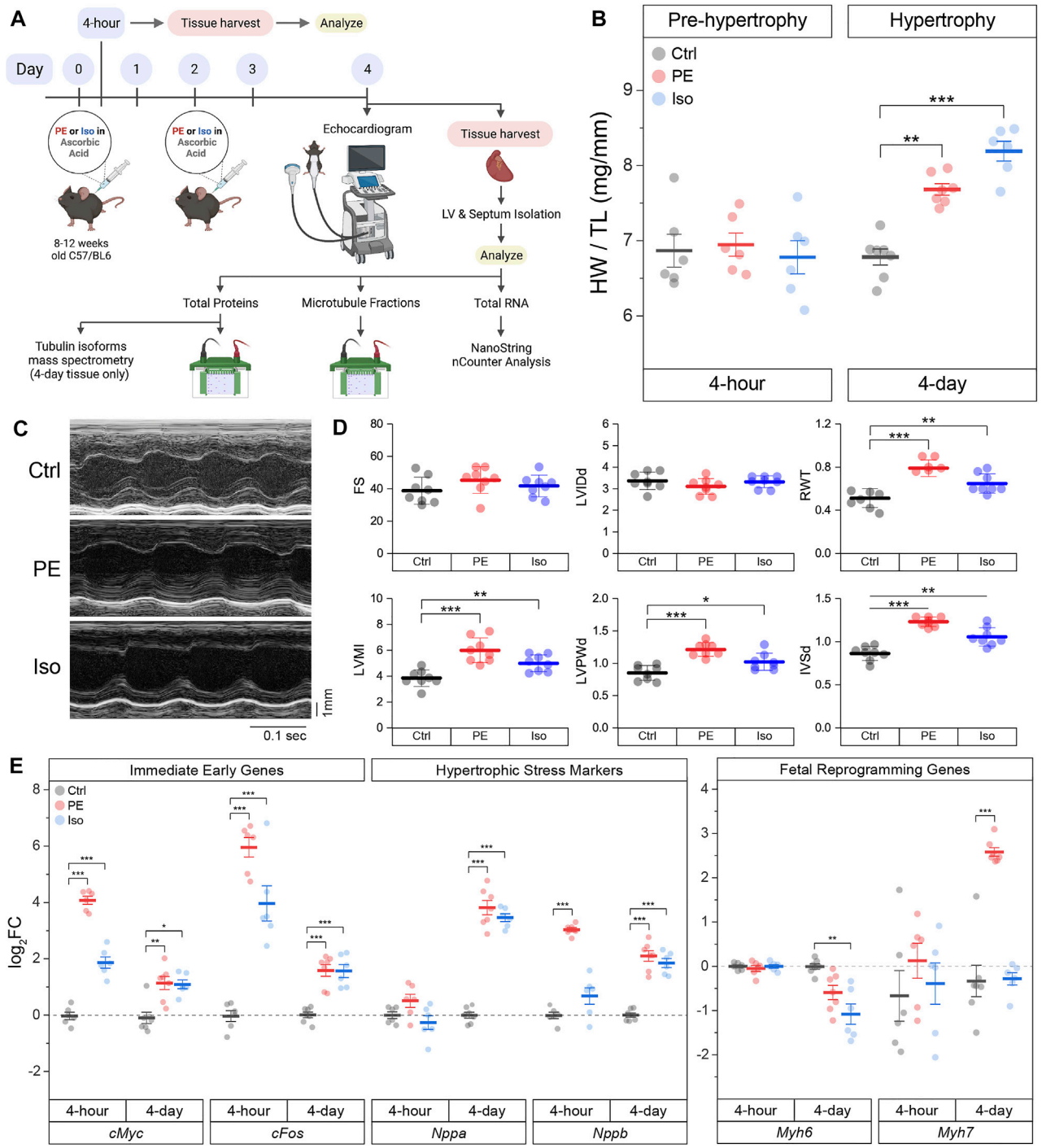

FIGURE 2 | Acute α- or β- adrenergic stimulation induces cardiac hypertrophy. **(A)** Graphical scheme of the experimental plan. **(B)** Heart-weight/Tibia length (HW/TL) data of mice 4-h (n = 6) or 4-days (n = Ctrl:7, PE:7, Iso:6) following 10 mg/kg/injection of phenylephrine (PE) or 5 mg/kg/injection of isoproterenol (Iso). **(C)** Representative echocardiographic M-mode images of 4-days mice hearts. **(D)** Quantification of relevant echocardiographic parameters: FS = Fractional Shortening, LVIDd = Left-Ventricular Internal Diameter at end diastole, RWT = Relative Wall Thickness, LVMI = Left-Ventricular Mass Index, LVPWd = Left-Ventricular Posterior Wall thickness at end diastole, IVSd = InterVentricular Septal thickness at end diastole (n = 8). **(E)** Relative $\log_2$fold-change of nCounter mRNA counts of Immediate Early Genes (IEGs), hypertrophic stress markers, and genes of fetal reprogramming (n = 4 h: 6, 4 days: Ctrl:7, PE:7, Iso:6). For all box plots, whiskers represent ± 1SEM and bolded-lines represent mean. For **(B, D)**, * represents p-value from Welch-corrected two-tailed two-sample student's t-test < 0.025, ** represents $p < 0.01$, and *** represents $p < 0.001$. For **(E)**, * represents Bonferroni adjusted (for 45 genes) p-value < 0.025 (Bonferroni-corrected for two comparisons), ** represents adj_$p < 0.01$, and *** represents adj_$p < 0.001$ (see Methods for more statistical details).

Next, we tested whether tubulin autoregulation can partially explain the discrepancy in mRNA and protein levels observed in HF. To this end, we designed a separate Nanostring probe set against introns and exons of human tubulin isoforms and probed RNA extracted from 35 cardiac samples from 12 non-failing donors and 23 patients with advanced heart failure. **Figures 1F,G** shows the relative intron and exon abundances for all tubulin isoforms that could be readily detected at the intron, exon and protein level (Chen et al., 2018) (**Figures 1A,B**). In failing hearts, the majority of tubulin isoforms showed reduced exonic relative to intronic levels, indicative of active autoinhibition across most isoforms. An exception is *TUBA1A*, the only isoform that demonstrated significant transcriptional induction; consistently *TUBA1A* is also being the only isoform to show both increased and correlated mRNA and protein levels in this HF population (**Figures 1A,B**). Of additional note, *TUBB4B* is by far the most abundant β-tubulin isoform expressed in the heart, and it exhibits robust autoinhibition in HF, yet maintains increased protein abundance. Taken together this data indicates that in HF, elevated tubulin protein triggers persistent autoinhibition of tubulin mRNA. The maintained elevation in tubulin protein may be explained by significantly increased tubulin stability/lifetime.

However, there remains no explanation as to how the heart achieved the increased tubulin protein in the first place or whether autoregulation plays any role in the establishment of the increased tubulin mass observed in pathological cardiac remodeling. To better understand this, we employed mice models of cardiac hypertrophy that allows us to explore the early roles of tubulin transcription, autoregulation, and stability.

Acute Adrenergic Agonism Induces Anatomic and Transcriptional Cardiac Remodeling

To determine how the microtubule network remodels during the development of cardiac hypertrophy, we characterized the myocardial cytoskeleton at two time points in two mouse models of adrenergic agonist-induced hypertrophy (Scarborough et al., 2021) (**Figure 2A**). A 4-h post-injection time point was chosen to capture a stage when hearts were exposed to hypertrophic stimuli but have not yet hypertrophied, and a 4-days post-injection time point was chosen to capture a stage when hearts had demonstrably hypertrophied. As expected, no change in heart-weight-to-tibia-length (HW/TL) was observed 4 h after injection of either phenylephrine (PE) or isoproterenol (Iso) compared to vehicle control (Ctrl) (**Figure 2B**, left). When mice were given a second injection on day 2 and hearts were collected on day 4, we observed a consistent cardiac hypertrophy with both PE and Iso (**Figure 2B**, right). To assess left-ventricular remodeling and function, we performed echocardiography on the 4-days hypertrophy animals. We observed consistent evidence of concentric hypertrophy upon both PE and Iso treatment, with elevated left-ventricular (LV) mass and increased wall and septal thickness (**Figures 2C,D**). Neither group exhibited evidence of decompensation toward HF, with no evidence of ventricular dilation or depressed contractility, indicating a compensated, concentric hypertrophy in response to acute adrenergic agonism.

We further validated our models using NanoString nCounter to assess transcriptional markers of cardiac remodeling in the hearts of PE and Iso treated mice. Using direct RNA counting of 42 transcripts sorted into immediate early genes (IEGs), hypertrophy-related genes, and fibrosis-related genes, we analyzed differentially expressed genes (DEGs) in the septa and LV of our time-matched control and experimental groups. We hypothesized that IEGs would be upregulated after 4-h of adrenergic stimulation, followed by upregulation of canonical markers of hypertrophic remodeling after 4 days. Consistent with this hypothesis, we observed robust upregulation of the canonical IEGs—*cMyc* and *cFos*—in both PE and Iso treated mice at 4-h (**Figure 2E** and **Supplementary Figure S2**), followed by induction of stress markers—*Nppa* and *Nppb*—at 4-days, along with markers of fetal reprogramming including myosin isoform switching (reduced *Myh6:Myh7* ratio).

The full complement of DEGs in each experimental group at the 4-h and 4-days time points are depicted in **Supplementary Figure S2**. At both 4-h and 4-days after adrenergic agonism, we observed upregulation of hypertrophy-related gene *Fhl1* (Friedrich et al., 2012), and fibrosis-related genes *Ctgf* (Hayata et al., 2008) & *Vcan* (Vistnes et al., 2014). Additional potentially relevant DEGs included the upregulation of *Col4a1* (Steffensen and Rasmussen 2018) and *Timp1* (Barton et al., 2003), and the downregulation of *Agrn*(Bassat et al., 2017; Baehr et al., 2020), among others.

The Microtubule Network Is Rapidly Detyrosinated Upon Hypertrophic Stimulation

Having validated the 4-h and 4-days models, we examined microtubule network remodeling in these contexts. We first determined whether the total αβ-tubulin content and free vs. polymerized tubulin pools are altered in the pre-hypertrophic (4-h) state. We observed no significant differences in these metrics of total tubulin content or fractionation at this early time point (**Figures 3A–C**).

We next determined whether tubulin is rapidly post-translationally modified upon hypertrophic stimulation. We immunoblotted for the five best-studied PTMs using validated antibodies: acetylation, detyrosination, polyglutamylation, polyglycylation, and Δ2 tubulin. Polyglutamylation, polyglycylation, and Δ2 are well characterized in cilia, flagella, and the brain (Paturle-Lafanechère et al., 1994; Aillaud et al., 2016), but they have not been studied in the heart. Detyrosination and acetylation, which occur predominantly on polymerized microtubules, are common markers of stable, long-lived microtubules, and of microtubule damage and repair-stabilization processes (Portran et al., 2017; Xu et al., 2017) respectively.

At the 4-h time point, we did not observe any significant differences in either the absolute (PTM/GAPDH) or the relative

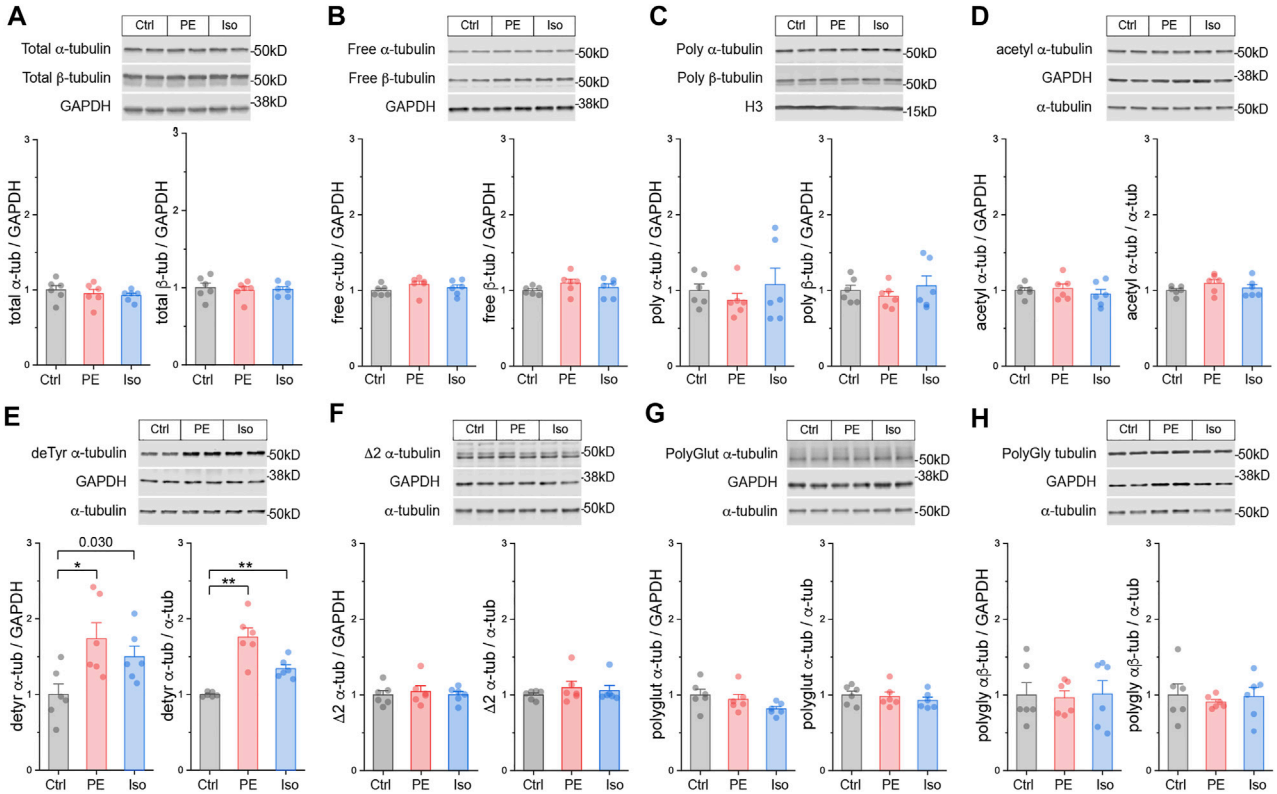

FIGURE 3 | The microtubule network is rapidly detyrosinated upon hypertrophic stimulation. Representative immunblots and relative fold-change of α-tubulin (left) and β-tubulin (right) in **(A)** total proteins, **(B)** free or **(C)** polymerized -tubulin fractions ($n = 6$). Representative immunoblots with technical duplicate lanes and relative fold-change using GAPDH (left) or α-tubulin (right) as loading controls for **(D)** acetylated α-tubulin, **(E)** detyrosinated α-tubulin, **(F)** Δ2 α-tubulin, **(G)** polyglutamylated α-tubulin, & **(H)** polyglycylated pan-tubulin ($n = 6$). For all bar plots, whiskers represent + 1SEM and bar represents mean. For all graphs, * represents p-value from Welch-corrected two-tailed two-sample t-test < 0.025 (Bonferroni-corrected for two comparisons), ** represents $p < 0.01$, and *** represents $p < 0.001$.

(PTM/α-tubulin) amounts of acetylation, polyglutamylation, polyglycylation, or Δ2 tubulin (**Figures 3D,F–H**). Surprisingly, we did observe robust induction of the absolute and relative amounts of detyrosination in both PE and Iso treated groups (**Figure 3E**). These data suggest that within 4 h of hypertrophic stimulation, prior to other overt changes in tubulin mass, microtubules are rapidly detyrosinated, which may serve as an early driver of microtubule stabilization.

Post-Translationally Modified Microtubules Proliferate During the Establishment of Cardiac Hypertrophy

We next characterized microtubule network remodeling at day 4, concurrent with cardiac hypertrophy. We probed the three tubulin pools and immunoblotted for α-tubulin, β-tubulin, acetylation, detyrosination, polyglutamylation, polyglycylation, Δ2 as described above.

At this stage we observed increased free, polymerized, and total αβ-tubulin protein in the hearts of PE and Iso-treated mice (**Figures 4A–C**). In the PE group, the ratio of free:polymerized α-tubulin decreased (**Supplementary Figure S3A**), consistent with enhanced microtubule stability. In PE-treated mice, we observed increases in the absolute amounts of acetylation, polyglutamylation, and polyglycylation, and in the absolute and relative amounts of detyrosination. Iso treated mice showed a similar trend for each PTM, but of reduced magnitude and greater variability (**Figures 4C–H**). Taken together, these data indicate that during cardiac hypertrophy tubulin content increases, the polymerized network densifies, and there is a proportionally increased abundance of post-translationally modified microtubules with a modest enrichment of detyrosination.

We next sought to determine how specific tubulin isoforms contribute to the increase in tubulin content observed at 4-days. To this end, we utilized mass spectrometric (MS) analysis of the total tubulin pool. We observed that the predominant α- and β-tubulin isoforms of murine LV were Tuba1a and Tubb4b, respectively (**Figure 5A**). Each of these predominant isoforms were modestly increased upon PE and Iso treatment. We also determined the relative changes of all detectable tubulin isoforms and observed significant increases in Tuba1a, Tuba1c, Tubb2a, Tubb2b, Tubb3, Tubb5, and Tubb6 (**Figures 5A,B**). Of note, Tuba4a—the only tubulin isoform that is synthesized in its detyrosinated form—was clearly not increased upon hypertrophic stimulation. This indicates that the early

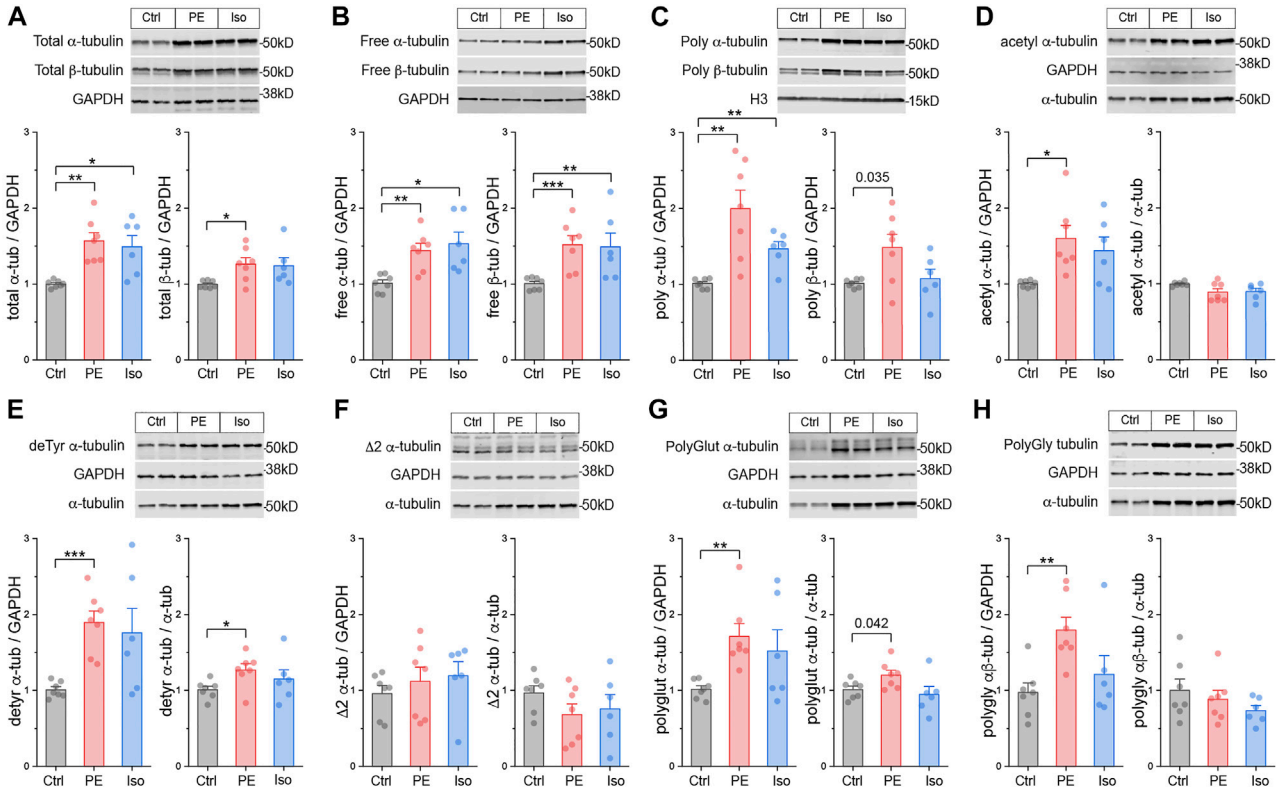

FIGURE 4 | Total tubulin content increases and the microtubule network densifies during hypertrophy. Representative immunoblots and relative fold-change of α-tubulin **(left)** and β-tubulin (right) in the **(A)** total proteins, **(B)** free, or **(C)** polymerized -tubulin fractions (n = Ctrl:7, PE:7, Iso:6). Representative immuno- blots with technical duplicate lanes and relative fold-change using GAPDH (left) or α-tubulin (right) as loading controls for **(D)** acetylated α-tubulin, **(E)** detyrosinated α-tubulin, **(F)** Δ2 α-tubulin, **(G)** polyglutamylated α-tubulin, & **(H)** polyglycylated pan-tubulin (n = Ctrl:7, PE:7, Iso:6). For all bar plots, whiskers represent + 1SEM and bar represents mean; * represents p-value from Welch-corrected two-tailed two-sample t-test < 0.025 (Bonferroni-corrected for two comparisons), ** represents $p < 0.01$, and *** represents $p < 0.001$.

increases in detyrosination are not due to increased synthesis of Tuba4a, and instead likely due to altered activity of the enzymes of the tyrosination cycle. Tubb6 exhibited the highest degree of upregulation with a ~4-fold increase upon PE treatment; this is notable as Tubb6 induction has been causally implicated in microtubule network reorganization in Duchenne Muscular Dystrophy (Randazzo et al., 2019). Despite significant upregulation of multiple low abundance isoforms, the overall composition of the total tubulin pool is largely conserved at this stage of hypertrophic remodeling (**Figure 5A**).

Transcriptional Analysis of αβ-Tubulin Isoforms, Tubulin Modifying Enzymes, and MAPs During the Induction and Establishment of Hypertrophy

We next examined the contribution of transcriptional changes to the protein and network level microtubule remodeling at the 4-h and 4-days timepoints. To this end, we utilized NanoString analysis of total RNA using another set of 47 genes that includes tubulin isoforms, tubulin modifying enzymes, and MAPs.

While tubulin protein content was unchanged 4-h after adrenergic stimulation, we noted significant upregulation of several tubulin transcripts with both PE and Iso treatment at this stage, including *Tuba1c, Tubb2a and Tubb6*, with additional and more robust upregulation of *Tubb2b and Tubb3* by day 4 (**Figure 5C**). Consistent with proteomics assessments, *Tuba4a* and *Tuba8* were either unchanged or even downregulated upon PE and Iso treatment.

Regardless of the directionality of response, specific tubulin isoforms generally responded similarly to either adrenergic stimulus (**Figure 5C**). Further, in contrast to what was observed in advanced HF, transcript levels were also well-correlated with protein abundance across most isoforms at the 4-days time point (R^2 = 0.38, slope = 0.20, p = 1.4e-4) (**Figure 5D**). Consistent with protein expression lagging transcriptional regulation, the four isoforms (Tuba4a, Tuba8, Tubb2b, Tubb3) that displayed the greatest deviation in the change in the mRNA relative to the change in the protein levels (i.e., located furthest away from the y = x line when plotting $\log_2$FC of mRNA vs protein levels) were transcripts that showed delayed regulation; these isoforms were unchanged after 4-h but differentially expressed by 4-days. Consistent upregulation at the transcript and protein level was

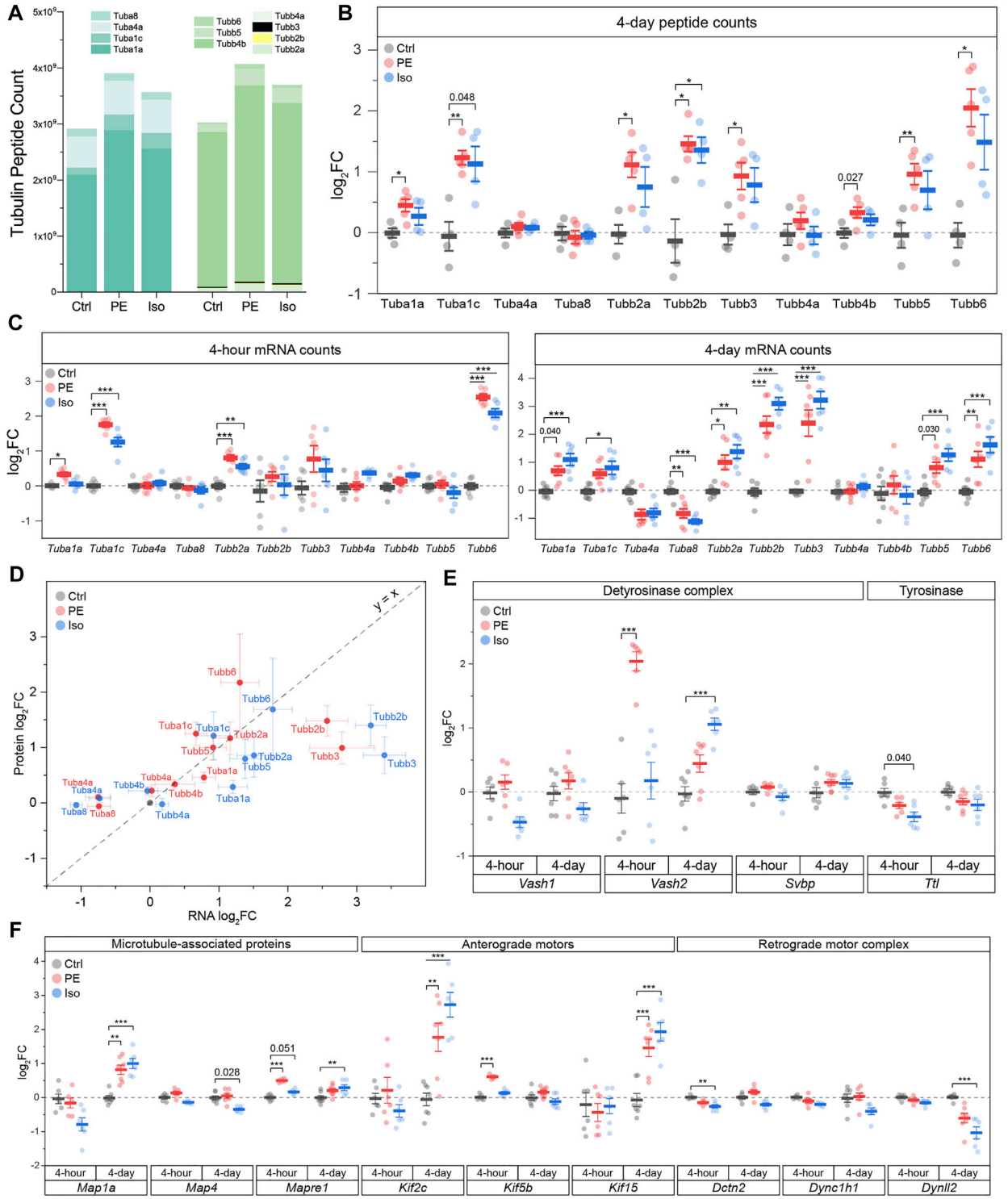

FIGURE 5 | Differential expression of tubulin isoforms, modifying enzymes and MAPs during the onset and establishment of hypertrophy. **(A)** MS counts of unique peptides of detectable αβ-tubulin isoforms at 4-days timepoint. For all following box plots, whiskers represent ± 1SEM and bolded line represents mean. **(B)** Relative log_2fold-change of αβ-tubulin isoforms peptide counts at 4-days (n = Ctrl: 4, PE: 5, Iso: 4); * represents p-value from Welch-corrected two-tailed two-sample t-test on non-log data <0.025 (Bonferroni-corrected for two comparisons), ** represents $p < 0.01$, and *** represents $p < 0.001$. **(C)** relative log_2fold-change of nCounter

(*Continued*)

FIGURE 5 | mRNA counts of detectable tubulin isoforms at 4-h (left) (n = 6) and 4-days timepoints (right) (n = Ctrl:7, PE:7, Iso:6); * represents Bonferroni adjusted (for 50 genes) p-value < 0.025, ** represents adj_p < 0.01, and *** represents adj_p < 0.001 (see Methods and Materials for more statistical details). **(D)** Scatter-plot of log_2fold-change of mRNA on x-axis and log_2fold-change of protein on y-axis at 4-days timepoint; whiskers represent ± 1SEM and y = x represents a proportionate change between mRNA and peptide. Relative log_2fold-change of nCounter mRNA counts of **(E)** detyrosinase complex and tyrosinase, & **(F)** MAPs, anterograde, & retrograde motors at 4-h (n = 6) and 4-days timepoints (n = Ctrl:7, PE:7, Iso:6); * represents Bonferroni adjusted (for 50 genes) p-value < 0.025, ** represents adj_p < 0.01, and *** represents adj_p < 0.001 (see Methods for more statistical details).

seen for Tuba1c, Tubb2a, Tubb2b, Tubb3, and Tubb6. Combined with the early upregulation of tubulin transcripts, this data indicates that increased tubulin mRNA at least partly underlies the isoform-specific increase in tubulin protein, and therefore tubulin mass, that is necessary for hypertrophic remodeling (Sato et al., 1997; Tsutsui et al., 1999; Scarborough et al., 2021).

We noted several additional transcriptional changes of tubulin modifying enzymes and MAPs that may bear relevance to cardiac remodeling and warrant further investigation (**Figures 5E,F**; **Supplementary Figure S4**). These include: (1) *Vash2,* which encodes a tubulin detyrosinase, exhibited the greatest differential expression among the 47 assessed transcripts at the 4-h PE time point; this may contribute to the robust early induction of detyrosination in this group (2) Early upregulation of *Kif5b* after 4-h in PE (Tigchelaar et al., 2016), which encodes the primary transport kinesin heavy chain 1 implicated in mRNA transport during myocyte growth (Scarborough et al., 2021); (3) upregulation of *Mapre1* in both PE and Iso at 4-h, which encodes a member of microtubule associated protein RP/EB family of +TIP tracking protein that guides microtubule growth; (4) Robust upregulation of *Kif15* in both PE and Iso by 4-days, which encodes a kinesin family member implicated in stabilizing parallel growing microtubules; (5) induction of *Map1a* in both PE and Iso at 4-days, which encodes a stabilizing structural MAP.

We next sought to determine whether these mRNA changes were reflected at the protein level for targets for which we could obtain robust signal via western blot from validated antibodies. Generally, transcripts that were upregulated early at the 4-h time point such as *Kif5b* and *Mapre1* also appeared to be upregulated at the protein level by day 4, whereas transcripts that were unchanged or only upregulated later at 4-days (such as *Vash1* and *Kif15*), did not show protein level changes at day 4 (**Supplementary Figures S3B,C**).

All tubulin-associated transcript volcano plots (**Supplementary Figure S4**) were asymmetric, tending to show a greater degree of upregulated than downregulated genes, implying a generalized induction of a tubulin-associated program at 4-days. This was particularly evident in the PE groups, and with progressive upregulation from the 4-h to 4-days time point. There were, however, notable down-regulated transcripts. While kinesin isoforms, which encode plus-end directed anterograde motors, were generally upregulated in treated groups, transcripts encoding subunits of the dynein/dynactin minus-end directed motor (*Dynll2, Dync1h1, Dctn2*) were either downregulated or unchanged (**Figure 5F**). This preferential induction of anterograde motors would bias trafficking toward the microtubule plus-end and away from the minus-end, which has implications for directed cardiac growth and for autophagic flux, which requires minus-end directed transport (McLendon et al., 2014). We also noted the early downregulation of enzymes involved in the polyglutamylation cycle, such as cytosolic carboxypeptidase 5 (*Ccp5*) and TTL-like family members 1 and 5 (*Ttll1/5*), which were all reduced in PE and Iso at the 4-h time point (**Supplementary Figure S4**).

To determine the conservation of these tubulin-associated transcriptional responses across varied hypertrophic stimuli, we compared our data with publicly available RNA sequencing datasets from two separate studies that examined early time-points following pressure-overload and angiotensin II induced hypertrophy. While data is not available for all transcripts, transcripts that were consistently reported across studies demonstrate well-conserved transcriptional signatures at both early (hours) and later (days) timepoints (**Supplementary Figure S5**), including the consistent upregulation of most αβ-tubulin isoforms but with the notable downregulation of *Tuba4a* and *Tuba8*.

Transcriptional and Autoregulatory Mechanisms Underlie Isoform-specific Increases in αβ-Tubulin mRNA

The above transcriptional and proteomic profiling indicates that the upregulation of tubulin mRNAs is an early driver of microtubule proliferation during the development of hypertrophy. This may arise from two non-exclusive mechanisms—(1) increased transcription or (2) decreased autoregulation (i.e., autoactivation). To differentiate between the two, we utilized the tubulin isoform and location -specific approach outlined above to interrogate the mechanism of tubulin upregulation during cardiac hypertrophy. Overall, we observed that by day 4 the exonic levels of almost all tubulin isoforms increased more than intronic levels, suggesting a generalized autoactivation of tubulin isoforms driven by microtubule stabilization (**Figure 6**). The most prominent cases of autoactivation are that of *Tubb2b*, whose increase in transcript level is solely through an increase in exonic species at both 4-h and 4-days, and *Tuba1a*, whose immediate response at 4-h was through an increase in exonic level with no change in intronic level (**Figure 6A**). Additionally, in a subset of the tubulin isoforms—*Tuba1b*, *Tubb2a*, *Tubb5*, and *Tubb6*—we observed robust increases in intronic levels that indicate direct transcriptional activation by the hypertrophic stimuli (**Figures 6B** and **Supplementary Figure S6**). Interestingly, despite a generalized upregulation and autoactivation of tubulin isoforms in the early stages of hypertrophy, *Tuba4a* and *Tuba8* are downregulated and autoinhibited, respectively.

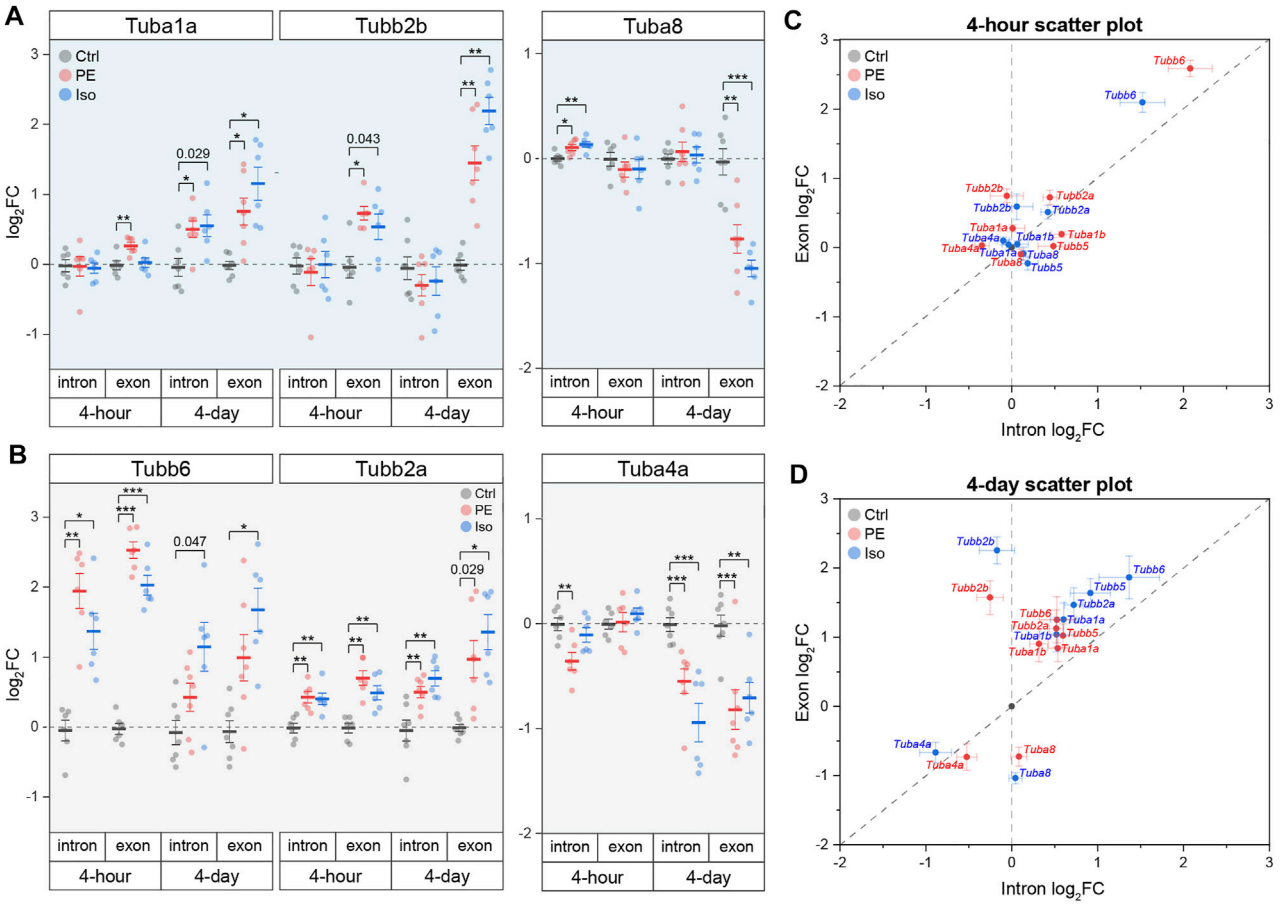

FIGURE 6 | Tubulin isoforms are differentially regulated at the mRNA level through isoform-specific transcription and/or autoregulation during cardiac hypertrophy. Relative log_2fold-change of mRNA counts of αβ-tubulin isoforms that are predominantly regulated through **(A)** autoregulation, or **(B)** transcription (n = 4 h: 6, 4 days: Ctrl: 7, PE:7, Iso:6); * represents p-value from Welch-corrected two-tailed two-sample t-test on non-log data <0.025 (Bonferroni-corrected for two comparisons), ** represents $p < 0.01$, and *** represents $p < 0.001$. Scatter-plots of relative log_2fold-change of intron on x-axis and exon on y-axis at **(C)** 4-h and **(D)** 4-days timepoints; whiskers represent ± 1SEM.

These data collectively show that αβ-tubulin mRNA is controlled in an isoform-specific and time-dependent fashion through both transcriptional and autoregulatory mechanisms to rewrite the tubulin code during cardiac remodeling.

DISCUSSION

In this work we combined transcriptomic and proteomic assessments of advanced heart failure samples and temporally well-defined murine models of cardiac remodeling to understand how a dense and modified microtubule network is achieved. Among other observations expanded upon below, we arrive at four primary conclusions: 1) tubulin autoregulation is operant in the heart and represses mRNA levels of tubulin isoforms in HF, contributing to the observed discrepancy between tubulin RNA and protein in HF; 2) the microtubule network is rapidly post-translationally detyrosinated within 4 h of a hypertrophic stimuli; 3) concomitantly, the abundance of tubulin mRNA is rapidly altered in an isoform-specific fashion through both transcriptional and autoregulatory mechanisms; 4) the time-dependent upregulation of discrete αβ-tubulin transcripts drives an increase in microtubule mass during cardiac hypertrophy.

Combining our work with past literature, we arrive at a sequential model for the formation of a proliferated and stabilized microtubule network in the remodeled heart (**Supplementary Figure S7**). Within hours of a hypertrophic stimuli and prior to detectable growth, the microtubule network is detyrosinated (**Figure 3E**). Our data indicate that this increase in detyrosination is likely due to transcriptional (**Figure 5E**) or post-translational (Yu et al., 2021) upregulation of the recently identified detyrosinating enzyme complex, as our data argues against alternative mechanisms such as increased Tuba4a expression (**Figure 5C**), increased polymerized or long-lasting microtubule substrate (**Figures 3C,D**), or decreased TTL expression (**Supplementary Figures S3B,C**). Detyrosination serves as a network stabilizer to protect microtubules from breaking down by regulating their interaction with effector proteins (Peris et al., 2009; Chen et al., 2021). Microtubule stabilization, in turn, shuttles free tubulin into the polymerized microtubule pool, triggering autoactivation that increases tubulin

mRNA stability and translation. How autoregulation may achieve isoform-specificity is not understood, although indicated by our data (see *Tubb2b* vs. *Tuba8*, **Figure 6**). In concert with post-transcriptional upregulation of tubulin mRNA, increased transcription of several isoforms concomitantly increases tubulin mRNA. Independent of the mode of upregulation, tubulin mRNAs appear to be efficiently translated, as mRNA levels are well correlated with peptide abundance across tubulin isoforms (**Figure 5D**). As the stimuli persists and the heart enlarges, the newly translated tubulin is integrated into the microtubule network, resulting in increased microtubule mass and additional substrate for post-translational modifications (**Figure 4**).

Insights into tubulin isoforms in muscle biology have pointed towards the potential detrimental effects of specific isoforms in muscle pathologies; for example, TUBB6 is upregulated in dystrophic skeletal muscles, and it contributes to microtubule disorganization and altered muscle regeneration in muscular dystrophy (Randazzo et al., 2019). Elevated TUBA4A in human cardiomyopathy contributes to the increased detyrosination that impedes myocyte function (Chen et al., 2018; Schuldt et al., 2021). Strikingly, when we examine publicly available transcriptomic and proteomic data from chronically hypertrophied or failing human hearts (**Figure 1A**), we observe an inverse relationship between the transcript and protein levels of almost all αβ-tubulin isoforms. It is worth noting that TUBA8 is the lone tubulin transcript that is consistently *increased* in HF while the protein level is consistently *decreased*. Intriguingly, *Tuba8* was also the sole isoform to clearly escape autoactivation (and appear seemingly autoinhibited) during early hypertrophic remodeling (**Figure 6A**). We have no current explanation for how or why Tuba8 shows unique regulation in both settings. In contrast to this inverse relationship in HF, we observed that during the establishment of hypertrophy, transcript and protein levels are highly correlated, suggesting an uncoupling of transcript and protein levels that occurs later in the course of cardiac remodeling. Chronic, robust microtubule stabilization and increased tubulin lifetime could account for the stably elevated tubulin protein content despite persistent autoinhibition that we observe in HF.

Our analysis permits the temporal evaluation of several cytoskeletal- or hypertrophy- associated factors at distinct stages representing the onset and establishment of cardiac hypertrophy. Beyond the key conclusions listed above, several additional observations on cytoskeletal remodeling are of note. The association of the microtubule network with motor proteins such as kinesins alters its mechano-biochemical properties as well as its density. As an example, Kif15 (kinesin-12) has been shown to cross-link nearby parallel microtubules, causing them to bundle, and subsequently decreases the catastrophic events of dynamic microtubules (Drechsler and McAinsh 2016). Interestingly, during both PE and Iso -induced hypertrophy, *Kif15* is upregulated, suggesting that *Kif15* could contribute to microtubule network densification. Kif5b (Kinesin-1), the predominant anterograde motor in the heart, was previously reported to be increased in PE induced-hypertrophy of neonatal rat ventricular cardiomyocytes (Tigchelaar et al., 2016). We observed similar and rapid increase in Kif5b transcript and protein levels in our hypertrophy models (**Figure 5F**, **Supplementary Figure S3C**). Kinesin-1 was recently identified to be required for the distribution of mRNA and ribosomes that enables cardiomyocyte hypertrophy (Scarborough et al., 2021), and past work indicates that kinesin-1 prefers to transport cargo along detyrosinated microtubule tracks (Kaul et al., 2014). Meanwhile, the dynein/dynactin retrograde motor protein complex (transcriptionally downregulated, **Figure 5F**), prefers tyrosinated microtubule tracks (Nirschl et al., 2016). Taking together, these observations suggest that the heart both rapidly induces its primary anterograde transport motor and remodels its preferred tracks in response to a hypertrophic stimulus.

Our findings indicate that rapid transcriptional, autoregulatory, and post-translational mechanisms remodel the microtubule network following a hypertrophic stimulus. Contextualized with past literature, these changes will support the ability of the microtubule network to bear increased mechanical load, facilitate mechanotransduction, and enhance transport of the translational machinery that is required for growth. In summary, the data points towards a concerted and adaptive response to establish hypertrophy, and we provide a resource for further investigation into the diverse roles of microtubules in cardiac remodeling.

DATA AVAILABILITY STATEMENT

The Nanostring data presented in the study have been deposited to the GEO Omnibus repository with the accession number GSE194397. The mass spectrometry proteomics data have been deposited to the ProteomeXchange Consortium via the PRIDE partner repository with the dataset identifier PXD031797.

ETHICS STATEMENT

The studies involving human participants were reviewed and approved by Institutional Review Boards at the University of Pennsylvania and the Gift-of-Life Donor Program (Pennsylvania, United States). The patients/participants provided their written informed consent to participate in this study. The animal study was reviewed and approved by University of Pennsylvania Institutional Animal Care and Use Committee (IACUC) and the Guide for the Care and Use of Laboratory Animals published by the US National Institutes of Health (NIH).

AUTHOR CONTRIBUTIONS

SP and BP designed the study. SP, KU, CC, MC, JG and KB performed data acquisition and analysis. SP and BP wrote the manuscript, and all authors assisted in editing.

FUNDING

Funding for this work came was provided by the National Institute of Health (NIH) R01s-HL133080 and HL149891 to BP, T32 HL007843 to KU, by the Fondation Leducq Research

Grant no. 20CVD01 to BP, and by the Center for Engineering Mechanobiology to BP through a grant from the National Science Foundation's Science and Technology program: 15-48571.

ACKNOWLEDGMENTS

We thank the Mouse Cardiovascular Phenotyping Core of the Cardiovascular Institute at the University of Pennsylvania for the echocardiography, the Quantitative Proteomics Resource Core of School of Medicine at the University of Pennsylvania for the mass spectrometry, the Penn Center for Musculoskeletal Disorders Histology Core (P30-AR069619) and the Genomics Core at the Wistar Institute for the NanoString analyses. We would also like to thank Dr. Marie-Jo Moutin for providing us with the Δ2 antibody. Some of the figures were created by BioRender.com.

SUPPLEMENTARY MATERIAL

The Supplementary Material for this article can be found online at: https://www.frontiersin.org/articles/10.3389/fcell.2022.837486/full#supplementary-material

REFERENCES

Aillaud, C., Bosc, C., Saoudi, Y., Denarier, E., Peris, L., Sago, L., et al. (2016). Evidence for New C-Terminally Truncated Variants of α- and β-Tubulins. *Mol. Biol. Cel.* 27 (4), 640–653. doi:10.1091/mbc.e15-03-0137

Aillaud, C., Bosc, C., Peris, L., Bosson, A., Heemeryck, P., Van Dijk, J., et al. (2017). Vasohibins/SVBP Are Tubulin Carboxypeptidases (TCPs) that Regulate Neuron Differentiation. *Science* 358 (6369), 1448–1453. doi:10.1126/science.aao4165

Baehr, A., Umansky, K. B., Bassat, E., Jurisch, V., Klett, K., Bozoglu, T., et al. (2020). Agrin Promotes Coordinated Therapeutic Processes Leading to Improved Cardiac Repair in Pigs. *Circulation* 142 (9), 868–881. doi:10.1161/circulationaha.119.045116

Barton, P. J. R., Birks, E. J., Felkin, L. E., Cullen, M. E., Koban, M. U., and Yacoub, M. H. (2003). Increased Expression of Extracellular Matrix Regulators TIMP1 and MMP1 in Deteriorating Heart Failure. *J. Heart Lung Transplant.* 22 (7), 738–744. doi:10.1016/s1053-2498(02)00557-0

Bassat, E., Mutlak, Y. E., Genzelinakh, A., Shadrin, I. Y., Baruch Umansky, K., Yifa, O., et al. (2017). The Extracellular Matrix Protein Agrin Promotes Heart Regeneration in Mice. *Nature* 547 (7662), 179–184. doi:10.1038/nature22978

Bottermann, K., Leitner, L., Pfeffer, M., Nemmer, J., Deenen, R., Köhrer, K., et al. (2018). *Effect of Cardiomyocyte and Vascular Smooth Muscle Cell Specific KO of P38 MAPKα on Gene Expression Profile of the Heart*. Germany: University of Duesseldorf. Gene Expression Omnibus. ID: GSE86074.

Caporizzo, M. A., Chen, C. Y., Salomon, A. K., Margulies, K. B., and Prosser, B. L. (2018). Microtubules Provide a Viscoelastic Resistance to Myocyte Motion. *Biophysical J.* 115 (9), 1796–1807. doi:10.1016/j.bpj.2018.09.019

Caporizzo, M. A., Chen, C. Y., and Prosser, B. L. (2019). Cardiac Microtubules in Health and Heart Disease. *Exp. Biol. Med. (Maywood)* 244 (15), 1255–1272. doi:10.1177/1535370219868960

Caporizzo, M. A., Chen, C. Y., Bedi, K., Margulies, K. B., and Prosser, B. L. (2020). Microtubules Increase Diastolic Stiffness in Failing Human Cardiomyocytes and Myocardium. *Circulation* 141 (11), 902–915. doi:10.1161/circulationaha.119.043930

Chen, C. Y., Caporizzo, M. A., Bedi, K., Vite, A., Bogush, A. I., Robison, P., et al. (2018). Suppression of Detyrosinated Microtubules Improves Cardiomyocyte Function in Human Heart Failure. *Nat. Med.* 24 (8), 1225–1233. doi:10.1038/s41591-018-0046-2

Chen, J., Kholina, E., Szyk, A., Fedorov, V. A., Kovalenko, I., Gudimchuk, N., et al. (2021). α-Tubulin Tail Modifications Regulate Microtubule Stability through Selective Effector Recruitment, Not Changes in Intrinsic Polymer Dynamics. *Dev. Cel* 56 (14), 2016–2028.e4. doi:10.1016/j.devcel.2021.05.005

Cheng, G., Zile, M. R., Takahashi, M., Baicu, C. F., Bonnema, D. D., Cabral, F., et al. (2008). A Direct Test of the Hypothesis that Increased Microtubule Network Density Contributes to Contractile Dysfunction of the Hypertrophied Heart. *Am. J. Physiology-Heart Circulatory Physiol.* 294 (5), H2231–H2241. doi:10.1152/ajpheart.91515.2007

Cheng, G., Takahashi, M., Shunmugavel, A., Wallenborn, J. G., DePaoli-Roach, A. A., Gergs, U., et al. (2010). Basis for MAP4 Dephosphorylation-Related Microtubule Network Densification in Pressure Overload Cardiac Hypertrophy. *J. Biol. Chem.* 285 (49), 38125–38140. doi:10.1074/jbc.m110.148650

Doroudgar, S., Hofmann, C., Boileau, E., Malone, B., Riechert, E., Gorska, A. A., et al. (2019). Monitoring Cell-type-specific Gene Expression Using Ribosome Profiling *In Vivo* during Cardiac Hemodynamic Stress. *Circ. Res.* 125, 431–448. doi:10.1161/CIRCRESAHA.119.314817

Drechsler, H., and McAinsh, A. D. (2016). Kinesin-12 Motors Cooperate to Suppress Microtubule Catastrophes and Drive the Formation of Parallel Microtubule Bundles. *Proc. Natl. Acad. Sci. USA* 113 (12), E1635–E1644. doi:10.1073/pnas.1516370113

Fassett, J. T., Xu, X., Hu, X., Zhu, G., French, J., Chen, Y., et al. (2009). Adenosine Regulation of Microtubule Dynamics in Cardiac Hypertrophy. *Am. J. Physiol-Heart Circ. Physiol.* 297 (2), H523–H532. doi:10.1152/ajpheart.00462.2009

Fassett, J., Xu, X., Kwak, D., Zhu, G., Fassett, E. K., Zhang, P., et al. (2019). Adenosine Kinase Attenuates Cardiomyocyte Microtubule Stabilization and Protects against Pressure Overload-Induced Hypertrophy and LV Dysfunction. *J. Mol. Cell Cardiol.* 130, 49–58. doi:10.1016/j.yjmcc.2019.03.015

Friedrich, F. W., Wilding, B. R., Reischmann, S., Crocini, C., Lang, P., Charron, P., et al. (2012). Evidence for FHL1 as a Novel Disease Gene for Isolated Hypertrophic Cardiomyopathy. *Hum. Mol. Genet.* 21 (14), 3237–3254. doi:10.1093/hmg/dds157

Gasic, I., and Mitchison, T. J. (2019). Autoregulation and Repair in Microtubule Homeostasis. *Curr. Opin. Cel Biol.* 56, 80–87. doi:10.1016/j.ceb.2018.10.003

Gasic, I., Boswell, S. A., and Mitchison, T. J. (2019). Tubulin mRNA Stability Is Sensitive to Change in Microtubule Dynamics Caused by Multiple Physiological and Toxic Cues. *Plos Biol.* 17 (4), e3000225. doi:10.1371/journal.pbio.3000225

Hayata, N., Fujio, Y., Yamamoto, Y., Iwakura, T., Obana, M., Takai, M., et al. (2008). Connective Tissue Growth Factor Induces Cardiac Hypertrophy through Akt Signaling. *Biochem. Biophys. Res. Commun.* 370 (2), 274–278. doi:10.1016/j.bbrc.2008.03.100

Kalebic, N., Sorrentino, S., Perlas, E., Bolasco, G., Martinez, C., and Heppenstall, P. A. (2013). αTAT1 Is the Major α-tubulin Acetyltransferase in Mice. *Nat. Commun.* 4 (1), 1962. doi:10.1038/ncomms2962

Kaul, N., Soppina, V., and Verhey, K. J. (2014). Effects of α-Tubulin K40 Acetylation and Detyrosination on Kinesin-1 Motility in a Purified System. *Biophys. J.* 106 (12), 2636–2643. doi:10.1016/j.bpj.2014.05.008

Li, L., Zhang, Q., Zhang, X., Zhang, J., Wang, X., Ren, J., et al. (2018). Microtubule Associated Protein 4 Phosphorylation Leads to Pathological Cardiac Remodeling in Mice. *Ebiomedicine* 37, 221–235. doi:10.1016/j.ebiom.2018.10.017

Liu, Y., Morley, M., Brandimarto, J., Hannenhalli, S., Hu, Y., Ashley, E. A., et al. (2015). RNA-seq Identifies Novel Myocardial Gene Expression Signatures of Heart Failure. *Genomics* 105 (2), 83–89. doi:10.1016/j.ygeno.2014.12.002

McLendon, P. M., Ferguson, B. S., Osinska, H., Bhuiyan, M. S., James, J., McKinsey, T. A., et al. (2014). Tubulin Hyperacetylation Is Adaptive in Cardiac Proteotoxicity by Promoting Autophagy. *Proc. Natl. Acad. Sci. USA* 111 (48), E5178–E5186. doi:10.1073/pnas.1415589111

Nieuwenhuis, J., Adamopoulos, A., Bleijerveld, O. B., Mazouzi, A., Stickel, E., Celie, P., et al. (2017). Vasohibins Encode Tubulin Detyrosinating Activity. *Science* 358 (6369), 1453–1456. doi:10.1126/science.aao5676

Nirschl, J. J., Magiera, M. M., Lazarus, J. E., Janke, C., and Holzbaur, E. L. F. (2016). α-Tubulin Tyrosination and CLIP-170 Phosphorylation Regulate the Initiation of Dynein-Driven Transport in Neurons. *Cel Rep.* 14 (11), 2637–2652. doi:10.1016/j.celrep.2016.02.046

Paturle-Lafanechère, L., Manier, M., Trigault, N., Pirollet, F., Mazarguil, H., and Job, D. (1994). Accumulation of delta 2-tubulin, a Major Tubulin Variant that Cannot Be Tyrosinated, in Neuronal Tissues and in Stable Microtubule Assemblies. *J. Cel. Sci.* 107 (Pt 6), 1529–1543.

Peris, L., Wagenbach, M., Lafanechère, L., Brocard, J., Moore, A. T., Kozielski, F., et al. (2009). Motor-dependent Microtubule Disassembly Driven by Tubulin Tyrosination. *J. Cel. Biol.* 185 (7), 1159–1166. doi:10.1083/jcb.200902142

Portran, D., Schaedel, L., Xu, Z., Théry, M., and Nachury, M. V. (2017). Tubulin Acetylation Protects Long-Lived Microtubules against Mechanical Ageing. *Nat. Cel Biol.* 19 (4), 391–398. doi:10.1038/ncb3481

Prosser, B. L., Ward, C. W., and Lederer, W. J. (2011). X-ROS Signaling: Rapid Mechano-Chemo Transduction in Heart. *Science* 333 (6048), 1440–1445. doi:10.1126/science.1202768

Randazzo, D., Khalique, U., Belanto, J. J., Kenea, A., Talsness, D. M., Olthoff, J. T., et al. (2019). Persistent Upregulation of the β-tubulin Tubb6, Linked to Muscle Regeneration, Is a Source of Microtubule Disorganization in Dystrophic Muscle. *Hum. Mol. Genet.* 28 (7), 1117–1135. doi:10.1093/hmg/ddy418

Sato, H., Nagai, T., Kuppuswamy, D., Narishige, T., Koide, M., Menick, D. R., et al. (1997). Microtubule Stabilization in Pressure Overload Cardiac Hypertrophy. *J. Cel Biol.* 139 (4), 963–973. doi:10.1083/jcb.139.4.963

Scarborough, E. A., Uchida, K., Vogel, M., Erlitzki, N., Iyer, M., Phyo, S. A., et al. (2021). Microtubules Orchestrate Local Translation to Enable Cardiac Growth. *Nat. Commun.* 12 (1), 1547. doi:10.1038/s41467-021-21685-4

Schuldt, M., Pei, J., Harakalova, M., Dorsch, L. M., Schlossarek, S., Mokry, M., et al. (2021). Proteomic and Functional Studies Reveal Detyrosinated Tubulin as Treatment Target in Sarcomere Mutation-Induced Hypertrophic Cardiomyopathy. *Circ. Hear Fail* 14 (1), e007022. doi:10.1161/CIRCHEARTFAILURE.120.007022

Steffensen, L. B., and Rasmussen, L. M. (2018). A Role for Collagen Type IV in Cardiovascular Disease. *Am. J. Physiol.-Heart Circ. Physiol.* 315 (3), H610–H625. doi:10.1152/ajpheart.00070.2018

Swiatlowska, P., Sanchez-Alonso, J. L., Mansfield, C., Scaini, D., Korchev, Y., Novak, P., et al. (2020). Short-term Angiotensin II Treatment Regulates Cardiac Nanomechanics via Microtubule Modifications. *Nanoscale* 12 (30), 16315–16329. doi:10.1039/d0nr02474k

Tigchelaar, W., de Jong, A. M., Bloks, V. W., van Gilst, W. H., de Boer, R. A., and Silljé, H. H. W. (2016). Hypertrophy Induced KIF5B Controls Mitochondrial Localization and Function in Neonatal Rat Cardiomyocytes. *J. Mol. Cell Cardiol.* 97, 70–81. doi:10.1016/j.yjmcc.2016.04.005

Tsutsui, H., Ishihara, K., and Cooper, G. (1993). Cytoskeletal Role in the Contractile Dysfunction of Hypertrophied Myocardium. *Science* 260 (5108), 682–687. doi:10.1126/science.8097594

Tsutsui, H., Tagawa, H., Cooper, IV, G., and Takeshita, A. (1999). Role of Microtubules in the Transition from Compensated Cardiac Hypertrophy to Failure. *Heart Fail. Rev.* 4 (4), 311–318. doi:10.1023/a:1009847418264

Vistnes, M., Aronsen, J. M., Lunde, I. G., Sjaastad, I., Carlson, C. R., and Christensen, G. (2014). Pentosan Polysulfate Decreases Myocardial Expression of the Extracellular Matrix Enzyme ADAMTS4 and Improves Cardiac Function *In Vivo* in Rats Subjected to Pressure Overload by Aortic Banding. *Plos One* 9 (3), e89621. doi:10.1371/journal.pone.0089621

Xu, Z., Schaedel, L., Portran, D., Aguilar, A., Gaillard, J., Marinkovich, M. P., et al. (2017). Microtubules Acquire Resistance from Mechanical Breakage through Intralumenal Acetylation. *Science* 356 (6335), 328–332. doi:10.1126/science.aai8764

Yu, X., Chen, X., Amrute-Nayak, M., Allgeyer, E., Zhao, A., Chenoweth, H., et al. (2021). MARK4 Controls Ischaemic Heart Failure through Microtubule Detyrosination. *Nature* 594, 560–565. doi:10.1038/s41586-021-03573-5

Conflict of Interest: The authors declare that the research was conducted in the absence of any commercial or financial relationships that could be construed as a potential conflict of interest.

Publisher's Note: All claims expressed in this article are solely those of the authors and do not necessarily represent those of their affiliated organizations, or those of the publisher, the editors, and the reviewers. Any product that may be evaluated in this article, or claim that may be made by its manufacturer, is not guaranteed or endorsed by the publisher.

frontiers | Frontiers in Cell and Developmental Biology

PERSPECTIVE
published: 25 April 2022
doi: 10.3389/fcell.2022.867374

The Amazing Evolutionary Complexity of Eukaryotic Tubulins: Lessons from *Naegleria* and the Multi-tubulin Hypothesis

Chandler Fulton *

Department of Biology, Brandeis University, Waltham, MA, United States

The multi-tubulin hypothesis proposed in 1976 was motivated by finding that the tubulin to build the flagellar apparatus was synthesized *de novo* during the optional differentiation of *Naegleria* from walking amoebae to swimming flagellates. In the next decade, with the tools of cloning and sequencing, we were able to establish that the rate of flagellar tubulin synthesis in *Naegleria* is determined by the abundance of flagellar α- and β-tubulin mRNAs. These experiments also established that the tubulins for *Naegleria* mitosis were encoded by separate, divergent genes, candidates for which remain incompletely characterized. Meanwhile an unanticipated abundance of tubulin isotypes has been discovered by other researchers. Together with the surprises of genome complexity, these tubulin isotypes require us to rethink how we might utilize the opportunities and challenges offered by the evolutionary diversity of eukaryotes.

Keywords: tubulin isotypes, multi-tubulin, microtubules, *naegleria*, evolution, protists, heterolobosea

OPEN ACCESS

Edited by:
Jeffrey Moore,
University of Colorado Anschutz Medical Campus, United States

Reviewed by:
Richard Luduena,
The University of Texas Health Science Center at San Antonio, United States

***Correspondence:**
Chandler Fulton
fulton@brandeis.edu

Specialty section:
This article was submitted to Cellular Biochemistry, a section of the journal Frontiers in Cell and Developmental Biology

Received: *01 February 2022*
Accepted: *22 February 2022*
Published: *25 April 2022*

Citation:
Fulton C (2022) The Amazing Evolutionary Complexity of Eukaryotic Tubulins: Lessons from Naegleria and the Multi-tubulin Hypothesis. Front. Cell Dev. Biol. 10:867374. doi: 10.3389/fcell.2022.867374

INTRODUCTION

The multi-tubulin hypothesis (Fulton and Simpson, 1976) was presented in a fully subscribed 5-day meeting on Cell Motility at Cold Spring Harbor Laboratory, which included 92 papers and was published in three volumes (Goldman et al., 1976). I presented our paper late one evening in the old Lecture Hall; the auditorium remained crowded despite the late hour. Talks were allowed 15 min. The audience was respectful, but our hypothesis was counter to the widely accepted, sensible hypothesis that tubulin was tubulin, and a pool of tubulin subunits were drawn upon to assemble microtubules for different uses, such as for mitosis and for assembling flagellar axonemes (references in Fulton and Simpson, 1976). After the talk I fielded some tough questions. One of my colleagues felt strongly enough to state that our hypothesis could not be true, we must be missing something. Her comment reflected the opinion of many. Such reactions certainly made me realize how strongly we were swimming against the current.

Here I summarize the results that led us to this hypothesis 45 years ago, based on our study of cell differentiation in the free-living, single-celled amoeboflagellate *Naegleria*, followed by what we have learned from our studies since then about multiple tubulin isotypes in this organism. This is followed by a discussion of what *Naegleria* and the multi-tubulins have taught us about the incredible diversity of eukaryotes, about how evolution has tinkered with basic building blocks of eukaryotes, and about what "far-out" organisms like *Naegleria* can contribute to biology.

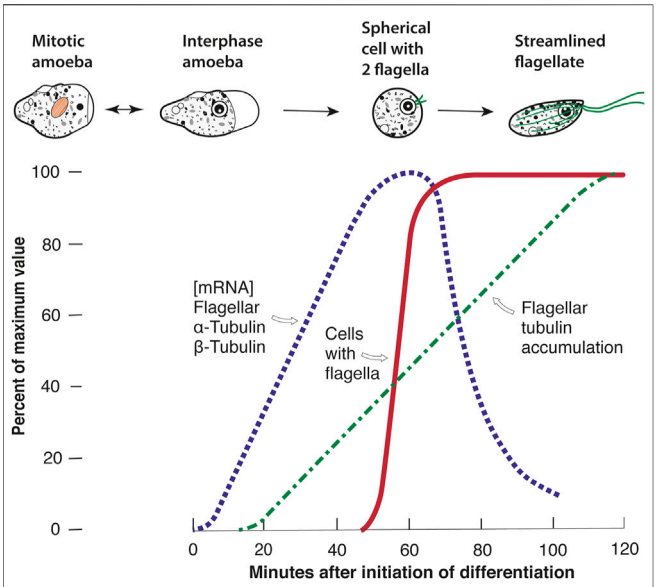

FIGURE 1 | The tubulin repertoire of *Naegleria gruberi* NEG. Interphase amoebae lack any cytoplasmic (or nuclear) microtubules. Dividing amoebae assemble mitotic tubulins (shown in orange) during their intranuclear mitosis. During the optional differentiation from amoebae to flagellates, induced by transfer from growth environment to nutrient-free buffer, the cells undergo a dramatic phenotypic change to rapidly swimming flagellates. The cells lose their capacity for amoeboid movement and round up. Basal bodies form and move to the cell surface, where they nucleate the growth of flagella. As the flagella elongate so do the cells, forming a streamlined shape with a cytoplasmic cytoskeleton of microtubules (shown in green). The differentiation can be made synchronous and temporarily reproducible. The graph shows the one-step differentiation experiment, measured as a quantal change (the appearance of flagella on fixed cell samples), and quantitative changes in flagellar tubulin mRNA and protein. See text for references.

HOW *NAEGLERIA* LED US TO THE MULTI-TUBULIN HYPOTHESIS

I started my career as a faculty member in 1960. As a graduate student I had led two lives. I was fortunate to have been mentored in microbial genetics as the first student of Norton Zinder, who had recently discovered genetic transduction and "infective heredity" (Zinder, 1992). This was a time when microbial genetics was becoming molecular biology. I was particularly impressed by Jacob and Monod's awesome achievement of discovering the pathways by which gene expression in *E. coli* and in temperate bacteriophage λ were regulated, something about which virtually nothing was previously known, entirely by using classical genetics of mutants and crosses (Jacob and Monod, 1961).

Simultaneously, I had become fascinated by the mystery of eukaryotic cell differentiation. My undergraduate education was rich in classical biology, including invertebrate biology, where I learned about how all eukaryotes had similar cells but used them to build different body plans (e.g., Buchsbaum, 1948). While a graduate student, I took and then for three summers taught in the Embryology Course at the Marine Biological Laboratory, under the direction of Mac V. Edds. When I started independent research, I wanted to combine these two interests: to induce eukaryotic cells to rapidly differentiate from one major phenotype (A) to another (B), and then use genetics to dissect the mechanism. I explored organisms from vertebrate cells to single-celled algae, and ultimately chose the amoeboflagellate *Naegleria*. I was familiar with this little-studied protist because I had encountered it as a contaminant in 1958 when I attempted to grow hydra cells in culture, in hopes of regenerating hydra from a cloned cell. The hydra cells never grew, but I was initially misled by what proved to be a contaminant that looked "just like" hydra cells, amoebae representing ectoderm, and flagellates endodermal cells. From protozoology books I learned the contaminant was a free-living protozoan called *Naegleria*. It taught me how easily one could imagine hydra as a multicellular amoeboflagellate.

When I had my own lab and we began searching for a single-celled eukaryote that underwent a dramatic phenotypic change (A to B), the change of *Naegleria* from amoebae to flagellates (A–F) came to mind. We obtained some *Naegleria*, domesticated the organism, and trained it to undergo a rapid, synchronous, and temporally reproducible differentiation on command (**Figure 1**, red line) (Fulton and Dingle, 1967; Fulton, 1977a). The differentiation can be induced under the experimenter's control simply by transfer of amoebae from a growth environment to a nutrient-free environment. It is completely optional, as the amoebae can grow for many hundreds of generations without ever differentiating. In the laboratory, the flagellates are transient, and eventually revert to amoebae. To this day this one-step differentiation remains one of the most controllable phenotypic changes available. Under the conditions used for the experiments in **Figure 1**, half the cells of *N. gruberi* NEG have visible flagella at 60 min (the T_{50}). Anticipating genetics, we began to isolate an array of mutants (Fulton, 1970), but to this day there is no laboratory genetics for *Naegleria* [even though we know from more recent work that the cloned strain we mostly utilize, *N. gruberi* NEG, is a diploid that almost certainly arose from a mating before it was collected from nature 60 years ago (Fritz-Laylin et al., 2010)].

One dramatic feature of the quick-change act is the formation of flagella and of a streamlined flagellate body shape. Overall, *Naegleria* has a remarkable microtubule wardrobe. The amoebae have microtubules only in their mitotic spindle. Interphase amoebae have no microtubules in their cytoplasm or nucleus [many references, including (Walsh, 1984)]. The only commonly studied eukaryote I know that displays such an extreme absence of cytoplasmic microtubules is interphase amoebae of *Entamoeba* (Meza et al., 2006), which is a member of the Amoebozoa supergroup that diverged at the base of the animal cell lineage (Eichinger et al., 2005), and thus is much more closely related to animals than to the much earlier diverging Excavates, the diverse group to which *Naegleria* belongs (as described later).

Naegleria amoebae appear to utilize actin-based motility machines almost entirely, and shut down the synthesis of actin and other components promptly during differentiation. As far as I am aware, *Naegleria* (and a few very close relatives) are unique in this combination: a primarily actin-based motility machine

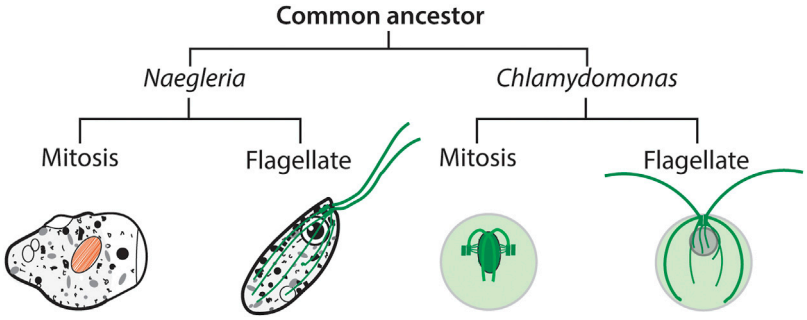

FIGURE 2 | The last eukaryotic common ancestor (LECA) of *Naegleria* and *Chlamydomonas* separated about 2,000 million years ago (Hedges et al., 2004), by which time LECA used microtubules for eukaryotic mitosis and for 9 + 2 flagellar axonemes with 9-triplet basal bodies. In *Chlamydomonas*, a single α-tubulin and single β-tubulin suffice for the mitotic spindle, the basal bodies, the flagella, and various accessory cytoplasmic microtubules in both dividing and swimming cells. In *Naegleria*, the flagellates synthesize very conserved α- and β-tubulin subunits to build the flagellar apparatus (shown in green), and some highly divergent protein(s) to assemble the mitotic spindle (shown in orange). The *Chlamydomonas* schematic diagrams are based on (Cross and Umen, 2015).

switching to a primarily tubulin-based motility machine—a dramatic switch which justifies its being referred to as a "yin-yang organism" (Lai et al., 1984). During mitosis the cells assemble a "closed mitosis," which means the nuclear envelope does not disassemble. Mitosis is also "acentriolar," meaning the microtubules do not focus to cell centers. The mitosis is relatively barrel shape. This pattern of closed acentriolar mitosis seems unusual to those who focus on vertebrate cells, but is quite common among eukaryotes. Examples of organisms that use either closed or open mitoses are found in every major eukaryotic group except for the Excavates, in which only organisms with closed mitoses have been observed so far (Boettcher and Barral, 2013). An example of a closed mitosis is seen in a green alga in which the cell centers do not form the cell poles, as shown in **Figure 2**. Among the Myxomycetes in the Amoebozoa group, some individual species like *Physarum polycephalum* employ open mitosis with centrioles as cell centers in their single-celled amoeboid phase, but closed mitoses without centrioles in their syncytial "slime mold" phase (Fulton, 1970, p. 388; Solnica-Krezel et al., 1991). Thus even a single organism can alternate between these fundamental forms of mitosis.

In mitotic *Naegleria*, the microtubules appear quite normal at electron microscope resolution (Fulton, 1970, Figure 11; Schuster, 1975). Walsh has published a magisterial study of mitosis (Walsh, 2012), to which (Velle et al., 2022) offer some helpful additions. Nothing known about mitosis suggests that its tubulin would be "abnormal." Unusually in *Naegleria* the nucleolus does not disassemble during mitosis, but divides with the chromosomes (Walsh, 2012). The mitosis is also efficient; remarkably these 15 µm diameter eukaryotic cells are able to divide as frequently as every 1.7 h (Fulton and Dingle, 1967). Mitosis, from prophase to cytokinesis, has been estimated to take 15–20 min (Fulton, 1970, p. 386).

The individual chromosomes are difficult to resolve in electron micrographs (Fulton, 1970; Schuster, 1975). The chromosomes are tiny, and too small to count, but a normal mitotic chromosome cycle can be visualized using Feulgen stain (Rafalko, 1947; Fulton, 1970), orcein stain (Fulton and Guerrini, 1969), or DAPI fluorescence (Walsh, 2012).

When these amoebae are induced to differentiate to flagellates, the cells turn their attention to tubulins. As differentiation progresses, these tubulins are assembled, successively, into the centriole-like basal bodies, which occurs about 10 min before flagella are visible. This feature of *Naegleria*, the *de novo* formation of centriole structures, also came as an unexpected surprise to the paradigm of the essential continuity of centrioles when it was described (Fulton and Dingle, 1971). Subsequently, as the flagella are assembled and elongate from the cell surface, the flagellar axonemes are assembled (Dingle and Fulton, 1966), and then an array of cytoskeletal microtubules is assembled as the flagellates elongate and become streamlined (Fulton, 1977b; Walsh, 1984). The structures of the 9-triplet centrioles, the 9 + 2 axonemes, and the microtubule cytoskeleton are all canonical. Once the whole array is assembled, flagellates can swim about a hundred times faster than the amoebae can walk (Fulton, 1977b). The flagellates ultimately revert to amoebae.

Our first look at microtubules came with a series of surprises: no microtubules in non-mitotic amoebae, no centrioles, no detection of chromosomes in electron microscopy of dividing cells, *de novo* assembly of centrioles. It was becoming clear that *Naegleria* was not a single-celled representative of a "typical" eukaryotic cell. Yet in its microtubules, and their behavior, there was no indication of any structural or functional abnormalities. *Naegleria* was asserting, loudly and clearly: "I am not a single-celled animal. I have different lessons to teach." Because of our proto-zoa ("first-animals") bias, it took us a while to hear her message.

We assumed, based on prevailing knowledge, that the tubulin involved in assembling mitotic microtubules would provide a pool to be used in the assembly of the flagellar apparatus. For example, Inoué's idea of the dynamic equilibrium between a tubulin pool and the reversible assembly of mitotic apparatus (Inoué and Sato, 1967) was widely accepted. The flagella offered a promising place to begin seeking to understand the molecular biology and regulatory events of differentiation, and microtubules

were their dominant feature, so we began to look at tubulins. This led us inexorably toward the multi-tubulin hypothesis.

In our first study of tubulins, Joel Kowit and I purified flagellar outer doublets, and from batches of 4.5×10^{10} cells (containing 4.2 g of total cell protein) we obtained a yield of 1.5 mg of tubulin that was 93% pure (Kowit and Fulton, 1974b). This tubulin showed similarity to other tubulins in molecular weight, the electrophoretic mobility of α- and β-subunits, and amino acid composition. It was injected into a rabbit, which yielded an antiserum with antibodies specific to the tubulin of *Naegleria* flagellates. We measured the amount of antigen in amoebae and flagellates, and found to our surprise that at least 97–98% of the "flagellar tubulin antigen" arises during differentiation. The simplest explanation of the dramatic rise is that this specific tubulin is synthesized *de novo* during differentiation, although a model involving post-translational modification could account for the results.

In extensive subsequent use, our polyclonal antibodies to flagellar outer doublet tubulin have reacted, *via* immunostaining, with *Naegleria* basal bodies, flagella and cytoskeletal microtubules, but not with *Naegleria* mitotic spindles, and not with tubulins of other tested species, including sea urchin tubulins and ciliate cilia. Subsequently Charles Walsh developed monoclonal antibodies to *Naegleria* flagellar α- and β-tubulins that also recognize both *Naegleria* mitotic and flagellar microtubules as well as the tubulins of other species (Walsh, 1984). These monoclonal antibodies have been widely used.

To determine whether flagellar tubulin was truly synthesized *de novo*, we subsequently labeled amoebae with ^{35}S-methionine, and then during differentiation "chased" this radioactivity with as much unlabeled methionine as did not affect differentiation. These pulse-chase experiments showed that at least 70% of the flagellar tubulin was assembled *de novo* during differentiation, which is a minimum estimate since during growth some of the radioactive methionine was converted to cysteine and this ^{35}S could not be chased during differentiation. Using both the pulse-chase experiments and our anti-flagellar tubulin antibody we were able to reveal the timetable of synthesis of flagellar tubulin as shown in **Figure 1**, green dashed line (Kowit and Fulton, 1974a). We also showed that more flagellar tubulin was synthesized than was needed for assembly of flagella. For example, if we arrested all protein synthesis when 40% of the antigen had accumulated, the flagella still grew to full length (Fulton and Walsh, 1980).

The multi-tubulin hypothesis (Fulton and Simpson, 1976) confronted the puzzle presented by the *de novo* synthesis of flagellar tubulin during differentiation, which was also supported by additional data. An examination of the literature showed no examples where interconversion of a tubulin pool between more than one microtubule structure had been established, e.g., mitotic ↔ flagellar microtubules, although it seemed reasonable that this sometimes happened. The literature also provided examples, especially from studies of sea urchin tubulins by Ray Stephens and others (e.g., Fulton et al., 1971; Stephens, 1975), that could be more simply explained if more than one tubulin isotype were utilized.

The multi-tubulin hypothesis paper also discussed "tubulin pools" which were in vogue at the time, but subsequently we found that the estimated pool sizes were excessively large due to contamination of the samples with non-tubulin proteins (Fulton and Simpson, 1979). Fortunately, these estimates did not alter our argument.

At the time of this paper, the cloning and sequencing of genes had not been achieved, and we knew little about tubulin sequences in any organism, although with considerable effort some segments of sequence had been obtained (e.g., Luduena and Woodward, 1973). It was possible to explain away all the antibody results as due to changes like post-translational modifications, and even the *de novo* synthesis of *Naegleria* flagellar tubulin could be explained *in extremis* as the way this organism made sufficient tubulin during differentiation. A colleague could offer an interesting argument, as one did in a phone call to me, that our work "was not ready for prime time because we had not shown the precursor of flagellar tubulin," something that would be impossible to do if the tubulin was, in fact, synthesized *de novo*. At the same time, we found no direct evidence in the literature that tubulin utilized to form one structure formed a pool that remained available to form another structure. Thus we were left with a conjecture that argued some microtubules used specific tubulin subunits made by specific genes. While tubulins within an organism did not appear to be entirely equal, it also seemed likely that common tubulin pools were repeatedly reutilized in a dynamic equilibrium with assembled microtubules, as in the successive mitoses during embryonic cleavages. The multi-tubulin hypothesis provided a stimulus for us and others to seek definite answers as soon as it became feasible.

WHAT WE HAVE LEARNED ABOUT *NAEGLERIA*'S TUBULINS SINCE 1976

It was only a few years before biologists were able to clone and sequence genes, and to measure messenger RNA. Then the complexities of tubulins quickly became clear, and the multi-tubulin concept rapidly "evolved" to specific cases, which led to the ongoing excitement about tubulin isotypes.

First I focus on what we and others learned about *Naegleria*.

We were eager to measure the flagellar tubulin mRNA, but cloning and sequencing were not quite ready. The first major breakthrough came when Elaine Lai developed a procedure to measure flagellar tubulin mRNA by cell-free translation (Lai et al., 1979). The protocol involved three crucial steps: purify polyA-mRNA from successive time-points in synchronous differentiation, translate that mRNA in a cell-free system from wheat germ that was limited only by the amount of mRNA, and then measure the amount of translated flagellar tubulin produced using our antibody. The measurements produced the results shown in **Figure 1**, blue dotted line. Beginning early in differentiation, flagellar tubulin mRNA can first be detected, rises to a peak at about 60 min, and then declines with a half-life of 8 min. When these results were utilized to determine the rate of flagellar tubulin synthesis, the cumulative rate produced the curve of **Figure 1**, green dashed line, matching the previously

measured accumulation of flagellar tubulin antigen. This revealed that the amount of flagellar tubulin antigen gave a true reflection of the synthesis and that the rate of synthesis was directly proportional to the amount of flagellar tubulin mRNA. This experiment also showed that there was no post-translational modification of flagellar tubulin specific to differentiating *Naegleria* that led to the reactivity of the flagellar tubulin with the antibody. Since we were interested in studying what induced flagellar tubulin gene expression during differentiation, we were very excited by these results. In separate experiments, we showed that both transcription and translation were essential for the differentiation and the synthesis of flagellar components, including tubulins (Fulton and Walsh, 1980).

Very shortly thereafter the cloning and sequencing of tubulin genes became possible, beginning with chicken tubulin genes (Cleveland et al., 1980). Soon there were families of tubulin genes. As new information became available, it quickly became clear that α- and β-tubulin subunits had diverged from a common ancestor, and that they had evolved to many similar but distinct isotypes that formed various heterodimers. The first description of a tissue-specific isotype came from Raff's laboratory, the testis-specific β-2 tubulin isotype in *Drosophila* that is required for spermatogenesis (Kemphues et al., 1982).

Naegleria genes proved unexpectedly divergent, and in most cases it was challenging to clone their genes using heterologous probes from other organisms (e.g., chicken tubulin genes)—the highly efficient "cloning by phone" approach. Cloning the *Naegleria* genes took us several years—both because of the extensive separate evolution of these DNAs (see below) and because *Naegleria* genes are AT-rich (averaging 65% AT). We eventually cloned and sequenced flagellar α-tubulin genes (Lai et al., 1988) and β-tubulin genes (Lai et al., 1994). By focusing on differentiation-specific mRNAs, others cloned these genes in the related *N. pringsheimi* NB-1 (Mar et al., 1986; Shea and Walsh, 1987; Lee and Walsh, 1988). Our colleagues' results and ours are fully concordant. The encoded tubulin sequences proved to be conserved, and the *Naegleria* flagellar tubulin monomers showed ≥90% similarity to those of many other organisms, from vertebrates to *Chlamydomonas*. Even though the encoded amino acid sequences were conserved, the DNA sequences had evolved so much as to make these invisible to heterologous probes (see discussion in Lai et al., 1988).

We cloned three α-tubulin and three β-tubulin genes, each representing three distinct genes but with only silent substitutions so they encoded identical subunits. We estimated the abundance of the genes by Southern blot analysis at about eight α-tubulins and eight to ten β-tubulins. In a separate study, an electrophoretic karyotype led us to estimate ~23 chromosomes in *Naegleria*, and found most of the α-tubulin genes on one chromosome and the β-tubulin genes scattered on three or four chromosomes (Clark et al., 1990). In the genome project, a similar karyotype using the same strain led to an estimate of about 12 chromosomes (Fritz-Laylin et al., 2010). It is hoped someday that this information can be refined with genetic studies.

The cloning and sequencing of these genes revealed another unexpected result: in most organisms the α-tubulin encodes a C-terminal tyrosine, whereas in *Naegleria* and a few other species the C-terminal tyrosine is encoded on the β-tubulin subunit (Lai et al., 1994). These C-terminal tyrosines participate in a cycle of tyrosination and detyrosination, and it is of interest that this function can be served by a tyrosine at the terminus of either subunit. Other cases of exceptional tubulins have been described, such as a testis-specific chicken α-tubulin that lacks a terminal tyrosine (Pratt et al., 1987), and the tyrosination cycle has been extensively studied (Nieuwenhuis and Brummelkamp, 2019).

Using these *Naegleria* flagellar tubulin DNA clones, we could directly estimate the mRNA levels in amoebae and during differentiation. The results were striking: the abundance of both tubulin subunits rose and fell on exactly the timetable previously measured using translatable mRNA (**Figure 1**, blue-dotted line). The tubulin mRNAs become detectable quickly, within 10 min of differentiation (Lai et al., 1988). The abundance of translatable mRNA matched the abundance of physical, transcribed mRNA. In addition, no homologous mRNA could be detected prior to the onset of differentiation. This is shown by the absence of homologous α-tubulin mRNA even in heavily overloaded Northern blots, using RNA taken from exponentially growing amoebae (Figure 9 in Lai et al., 1988), as well as by seeking measurable α-tubulin mRNA in mitotically synchronized amoebae (synchronized as in Fulton and Guerrini, 1969). No trace of flagellar tubulin mRNA has been found except in differentiating cells. These experiments established that some other, divergent tubulin genes had to be responsible for the mitotic spindle, but the identity of these mitotic tubulin genes eluded us.

An exciting advance was made by Lee's laboratory when they found an α-tubulin clone in a *Naegleria* closely related to strain *N. gruberi* NEG, now called *N. pringsheimi* strain NB-1 (Chung et al., 2002). This gene, which they called α6, encodes an α-tubulin of 452 amino acids that shows only 62% identity with *Naegleria* flagellar α-tubulin. They also found a partial clone of a similar but not identical gene, which was not further characterized. The encoded products of both genes were among the most exceptionally divergent of tubulin genes known. For example, the yeast *Saccharomyces cerevisiae* α-tubulin shows ≥70% identity to *Naegleria* or *Chlamydomonas* flagellar tubulin. The authors found that the *Naegleria* α6 gene was expressed in growing amoebae, but the expression was promptly shut down when differentiation was initiated. Finally, they prepared antibody to a peptide of the α6 sequence, and obtained faint staining of the nucleus of mitotic amoebae. Thus, to use their own words: "this report definitely proves the multi-tubulin hypothesis in *N. gruberi*." Their excellent report left open one important question. The staining of the mitotic nucleus is light and not clearly localized to the microtubules. Again, to quote the authors: "it is not clear whether α6-tubulin is the only (or major) α-tubulin for mitotic spindle fiber microtubules or is a specialized α-tubulin that accounts for a minor percentage of the microtubules." Determining whether such divergent tubulin as α6 is able, on its own, to build *Naegleria*'s mitotic spindle, remains an important question that needs to be answered using protein- and immuno-chemistry.

In 2010 the draft genome of *Naegleria gruberi* NEG-M (the axenic derivative of strain NEG) was completed (Fritz-Laylin

et al., 2010). Among many surprises of *Naegleria*'s genome, which will be discussed shortly, this analysis permitted a survey of all the curated tubulins of this strain (presented as Supplementary Figure S4B in Fritz-Laylin et al., 2010). Redundant protein sequences were not counted, so the multiple α- and β-tubulin genes characterized previously—and estimated at eight to ten copies—are listed singly. They also reported a single α-tubulin gene with a sequence slightly divergent from the cloned sequence ("Naegrub 53,284"). They found strain NEG's putative mitotic tubulin genes, a non-identical pair of α-tubulin genes similar to the α6 of strain NB-1, and in addition a pair of β-tubulin genes of similarly divergent nature which they deduced might be the mitotic β-tubulin genes. In addition, they reported a set of tubulins that I consider a "bonus," highly divergent members of both families, with seven different α-tubulins and five β-tubulins. These are divergent not only in sequence, sharing at best about 60% encoded sequence with the flagellar tubulin genes, but also with gaps and additions which suggest they are unlikely to encode tubulins that would themselves assemble into microtubules. Finally, the genome was found to contain conserved, single, encoded gamma, epsilon and delta tubulins.

A preliminary paper extends the result of the Lee laboratory on strain NB-1 α6 tubulin (Velle et al., 2022). Both putative mitotic α-tubulin genes of strain *N. gruberi* NEG-M are shown to be expressed in growing amoebae, and this finding is extended to both putative mitotic β-tubulin genes of NEG-M, with none of the four genes expressed during differentiation. This finding supports the hypothesis that these divergent tubulin subunits, both α and β, play some role in growing amoebae, but still leaves open the question of whether they are either necessary or sufficient to build the mitotic microtubules. We need more direct evidence. These putative mitotic tubulin subunits are among the most divergent sequences found. I estimated a 61–64% identity of the two mitotic α to *Naegleria* flagellar α-tubulin subunits and 62–66% identity of the two mitotic β to *Naegleria* flagellar β-tubulin subunits, while most tubulins are conserved in the vicinity of ≥90% identity. None of these four putative mitotic α- or β-subunits encode a C-terminal tyrosine. It would almost be surprising if they can assemble into microtubules on their own. So while it remains clear that the mitotic spindles are built of something other than flagellar tubulin, we cannot conclude that these divergent tubulins are sufficient to build the mitotic microtubules until this question is answered by experiment. I suspect this investigation is likely to yield results of interest. Walsh has even raised the intriguing suggestion that perhaps a protein of the nucleolus, which co-divides with the chromosomes in *Naegleria*, may be involved in the spindle fibers (Walsh, 2012). Until biochemistry defines the structural components, we remain forced to the conclusion that the mitotic spindle is made of some tubulin(s) or proteins different from flagellar tubulin.

While this research with *Naegleria* was ongoing, many were obtaining fascinating results with tubulin isotypes in diverse organisms, from ciliates to *Drosophila*, yeast to mammals, including some protists [including a recent review focused on post-translational modifications in protists (Joachimiak and Wloga, 2021)]. Some results in other eukaryotic microorganisms make it clear that *Naegleria*'s use of very different tubulins for mitosis versus flagella is by no means the only evolutionary solution. Budding yeast, *Saccharomyces cerevisiae*, encode a single β-tubulin gene and they can be engineered to produce only one of two α-tubulin isotypes (Schatz et al., 1988; Luchniak et al., 2013). These yeast, with single α- and β-tubulin genes, appear to perform their microtubule functions, i.e., division, "normally." But yeast do not make flagella.

Lest we allow the ability of some organisms, such as the exampled yeast, to manage with single tubulin genes, to dull our sensitivity to tubulin isotypes, an elegant new paper shows a surprise: that while budding yeast can be engineered to grow with single α- and β-tubulin genes, both α-tubulin genes in a wildtype yeast are functional in spindle positioning (Nsamba et al., 2021). As those studying tubulin isotypes have demonstrated repeatedly, there are subtleties in multiple tubulins. More await discovery.

The closely choreographed life cycle of the green alga *Chlamydomonas reinhardtii* uses microtubules for multiple functions (Johnson and Porter, 1968; Cross and Umen, 2015). Vegetative cells are flagellates that swim using two flagella, have classic 9-triplet basal bodies, and a complex array of microtubules forming a microtubular cytoskeleton. In anticipation of cell division, the basal bodies detach from the flagella, the latter then degenerate. The basal bodies each form a duplicate. Mitosis is closed, with an intact nuclear envelope, although some microtubules go through fenestrae in the envelope into the cytoplasm. Although the duplicated basal bodies are present through mitosis, the mitotic cells do not form apical poles focused on the centrioles, as in mammalian cells, but instead the two pairs of basal bodies associate with the cleavage furrow. Microtubules form the spindle and a complex of nuclear and cytoplasmic structures during division. As division into two cells is completed, the centrioles move to the cell membrane, and there new flagella are formed on each daughter cell. *Chlamydomonas* is haploid, with few excess genes (Merchant et al., 2007). It achieves its complex series of microtubule functions using duplicate α-tubulin and two β-tubulin genes (Youngblom et al., 1984; Silflow et al., 1985), which have been shown each to encode one identical heterodimer (Youngblom et al., 1984; James et al., 1993). Thus, as far as is known, this alga can accomplish its full repertoire of microtubular arrays using a single tubulin heterodimer, with whatever posttranslational modification and accessory proteins are involved in building the diverse structures. These four genes are turned on in tandem when regeneration of flagella is induced by excision (Silflow and Rosenbaum, 1981). Recently the *Chlamydomonas* tubulin genes have been disrupted using insertions that create null alleles (Kato-Minoura et al., 2020). This allowed the authors to engineer a *Chlamydomonas* mutant that had only one α-tubulin and one β-tubulin gene. This mutant grew at almost a normal rate and regenerated flagella normally after excision, revealing that "a single gene for each type is enough to supply the tubulin necessary for its cellular functions." Thus it appears clear that *Chlamydomonas* can make a diversity of microtubules—singlets, doublets, and triplets—comparable to

those found in *Naegleria* mitosis and flagellates, using a single α-β-tubulin heterodimer.

This presents us with a conundrum, illustrated in **Figure 2**. *Chlamydomonas* uses the same tubulin heterodimer for mitosis and flagella, whereas *Naegleria* goes to the trouble of having a separate set of flagellar tubulin genes and some sort of mitotic tubulin genes, whether or not these are the postulated putative mitotic tubulin genes. Aside from the conundrum of how this situation arose, the distinct mitotic and flagellar tubulins in *Naegleria* could provide modules for meeting the cells' needs. In particular, when "time to differentiate" is signaled perhaps an army of about eight α- and eight β-tubulin genes need to be expressed simultaneously to produce sufficient flagellar tubulin on schedule (**Figure 1**). *Naegleria* amoebae respond to the command to differentiate promptly whether they are in early stationary phase—healthy but no longer preparing for another mitosis—or in log culture, or even if they are in the midst of preparing for synchronous cell division (Fulton and Guerrini, 1969). It seems clear that whatever amoebae are doing, if they have biosynthetic capacity when they receive the "differentiate" signal they drop everything and respond immediately (Fulton, 1977a, p. 614). This rapid response must have an important selective advantage, but despite more than a half-century of laboratory study we still do not know the role of the temporary flagellates in *Naegleria*'s worldwide success, so the advantage remains a mystery today. Yet, possessing a separate complementary set of tubulin genes might allow quick responses to "grow" vs. "differentiate" signals. What Moore and Wethekam have called "expression-control modules" may be a significant part of the advantages of multiple tubulins (Moore and Wethekam, 2021).

WHAT WE CURRENTLY KNOW, AND DON'T KNOW, ABOUT *NAEGLERIA* TUBULINS

Although we have learned a lot, important unanswered questions about *Naegleria* tubulins remain that merit investigation:

- While it is a reasonable inference that the highly divergent tubulin genes found in the *Naegleria* genome may be responsible in part or in full for the mitotic microtubules, this needs to be established by showing that the products of these genes are in fact assembled into the mitotic microtubules. Until then we may still have "surprises" ahead.
- If *Chlamydomonas*, for example, can use one set of tubulin genes for both tasks, and *Naegleria* and its relatives are virtually unique in possessing a divergent set of mitotic tubulin genes, how did this arise in evolution? As will be discussed further below, understanding the origin of *Naegleria*'s mitotic tubulins could be crucial to understanding early tubulin evolution.
- As to issues of multiple isotypes of tubulin, the finding of two sets of tubulin genes—flagellar and putative mitotic—in *Naegleria* does not give full understanding of the pattern of tubulin isotypes in *Naegleria*. There are multiple α- and β-tubulin genes in the flagellar sets, including some "bonus" subunits so divergent that while they are clearly tubulin subunits, they are not likely to assemble typical microtubules. Are these isotypes specific to basal bodies and their triplet fibers, or to specific components of the flagellar axoneme, or to the flagellate's cytoskeleton?

Some of these experiments would require a gene editing method for knocking out individual genes, such as by using CRISPR-Cas. Up to this point *Naegleria* has successfully resisted any efforts to alter its genes by external manipulation. The efforts continue!

WHAT WE HAVE LEARNED ABOUT THE UNANTICIPATED DIVERSITY OF EUKARYOTES, AND HOW THIS DIVERSITY CAN CONTRIBUTE TO BIOLOGY

Evolution!

No discovery in biology has produced so extended an argument as Darwin's recognition of biological evolution. Everything about tubulins and their isotypes needs to be considered in the context of this ongoing excitement.

All eukaryotes depend on spindle microtubules for mitosis—loss of this function would apparently be a lethal mutation—and so great a diversity of eukaryotes possess canonical flagella and centrioles such that we can confidently assert that LECA, the Last Eucaryotic Common Ancestor, had both capabilities. It is clear that tubulin arose from prokaryotic proteins and developed as heterodimers of α- and β-subunits. All this was accomplished by LECA.

The growing ease of cloning and sequencing genes in the 1980's, culminating with the first draft of the human genome by 2001, produced new data that led to a cataclysmic change in our understanding of eukaryotic diversity. This change rapidly altered the thinking of everyone concerned with eukaryotes and their genes (e.g., Lynch, 2007). These issues bring into focus several major aspects of our understanding of eukaryotes, and these in turn affect all of us interested in tubulin isotypes. One could explore each of these topics at length, but here I hope to raise a few of the most important considerations.

As Sydney Brenner so aptly put it: "We are all conscious today that we are drowning in a sea of data and starving for knowledge" (Brenner, 2002). As these data have accumulated, they have brought several realizations that undermined the precepts on which many based their approach to research in the 1960's and 1970's. The idea that eukaryotes were similar cells built on a basic plan that formed a diversity of cell types—from two or three types in a "first animal" like *Naegleria* to 200 or more in a mammal. This idea is expressed in a quotation attributed to Jacques Monod that "what's true for *E. coli* is true for the elephant" (Monod and Jacob, 1961). [The origin of this famous statement is thought-provoking (Friedmann, 2004)]. In the 1960's, the successes of genetics and biochemistry had lulled us into a sense that the

unity of biology was such that we could define principles—like the *lac* operon or the Krebs cycle—and these would govern all eukaryotes. Ideas like these guided my early research career. Then came the tsunami of data. We were suddenly immersed in a total unanticipated diversity, of genes and of eukaryotes. We learned decisively that *Naegleria* is not a unicellular elephant!

Some might call "arrogant" the 1960's attitude that using our brains we should be able to make sense of everything. Certainly evolution has nothing in its guiding forces that necessarily encourage it to build as an engineer would, or even to build in a manner that would make it easy for the human mind to grasp. Great messy complexities involving hundreds or thousands of interacting components can be selected for if they are functional, even if the contraption does not conform to a simple engineering diagram for us to understand. There is not any known mechanism guiding the forces driving evolution that specifies "if it ain't broke don't fix it" (an idea attributed to the 1970's but one that presumably also guided stone age "engineers"). Even if something works, evolution has no hesitation to break it, and it is then left to selection to determine what happens next. If evolution destroys a mitotic apparatus, for example, that clearly is the end for that cell's ability to reproduce.

When vertebrates and their cells, even human cells, became accessible to cloning and sequencing, the emphasis shifted from an interest in "all" eukaryotes as models to a narrow focus on our closer relations, and especially on mammals. This has been encouraged by the support mechanisms for science. Simultaneously, we are learning that the complexity of eukaryotes is far greater than anyone imagined in the 1960's, or even a decade ago. And lest we become inclined to think that all we need to know will come from mammals and their ills, we should remind ourselves that about half the Nobel Prizes in Physiology and Medicine which have involved research that utilized organisms have gotten their insights based on research using non-vertebrate organisms, from bacteria (e.g., CRISPR) to yeasts (autophagy), from ciliates (telomeres) to flies (e.g., circadian rhythms).

It was early, and correctly, recognized that all known eukaryotes arose from a single ancestral cell, a last eukaryotic common ancestor (LECA), beginning perhaps as long ago as 2,200 mya (million years ago) or more (Parfrey et al., 2011), when oxygen was rising in the atmosphere.

There have been many attempts to reconstruct the phylogeny of eukaryotes from the LECA. At first ribosomal DNA sequences were used to build trees, and for a moment these trees looked like normal trees with a single main trunk (the common ancestor) branching off. *Naegleria* appeared to be an early-branching eukaryote (Hinkle and Sogin, 1993), but such trees between distant organisms were plagued by "long-branch attraction." This method using ribosomal DNA sequences did lead correctly to the recognition that two groups previously considered very far apart, the animals and fungi, were in fact close relatives (Wainright et al., 1993).

By the time the *Naegleria* draft genome was completed (Fritz-Laylin et al., 2010), it had become clear that *Naegleria* was an early diverging eukaryote. By that time the immense diversity of eukaryotes had been loosely organized into five to eight "supergroups."

An example of such a tree using supergroups is shown in the genome paper. The draft genome of the Heterolobosean amoeboflagellate *N. gruberi* NEG-M, the first of a free-living "excavate," surprised us in many ways, including a large and complex gene repertoire, with over 15,727 curated genes that included abilities for anaerobic and aerobic respiration, and a surprising number of eukaryotic regulatory inventions for signaling, sexual, cytoskeletal, and metabolic modules (Fritz-Laylin et al., 2010).

After 2010, widespread sequencing of protist genomes has led to an explosion of new insights, results which make "the supergroup level even more arbitrary than before" and has reorganized dozens of early branches forming the eukaryotic tree (Burki et al., 2020). Such efforts are resolving the tree of life, and carry much new information, but the trees also are volatile and changing rapidly.

We focus here on a single group, the Heterolobosea, a part of the "excavate" subgroup (currently usually known as Discoba). As of 2014, and still today, the excavates—a world of little-known beasts with many fascinating properties—were the least studied of all supergroups in terms of genome sequences and of publications (Lynch et al., 2014). The Heterolobosea subgroup are a diverse group of mostly single-celled protists, of which *Naegleria* is the only "well known" member. The pioneering Heterolobosea separated from LECA very early, perhaps about 2000–2,100 mya (Hedges et al., 2004). At around the same time, their distant living relatives including *Euglena* and the trypanosomes (*Trypanosoma* and *Leishmania*) had begun their separate evolutionary journeys. When such generalizations are applied to all the groups of eukaryotic protists, the diversity is immense, as is our ignorance about them. Later separations from LECA include some of the best-known branches, including the one that led to plants and the one that led to the fungi-metazoa lineage.

Even within the genus *Naegleria*, there are roughly 40 species, and these include organisms that appear to be themselves quite diverse (De Jonckheere, 2004). For example, *N. gruberi* and the opportunistic human pathogen *N. fowleri* were long ago argued to be evolutionarily as distant from one another as are frogs and people (Baverstock et al., 1989), a striking conclusion about two members of a single genus. Remarkably this great evolutionary distance within the genus is supported by comparing large sets of their chromosomal genes using as an outgroup the distant trypanosomes, which lie outside the Heterolobosea (Liechti et al., 2019; their Figure 3)—although the authors of this exceptional tree make no comment about the extreme difference. Such evolutionary distances within a genus makes the diversity of protists even more exceptional.

So far the divergent putative mitotic tubulins have only been found within the few sequenced Heterolobosea (Velle et al., 2022). Now that the *N. fowleri* genome has been expanded (Liechti et al., 2019), when one searches databases using the putative mitotic tubulins from *N. gruberi*, one finds similar, but somewhat divergent, homologous pairs in the *N. fowleri* genome, as well as homologs to both flagellar tubulin subunits.

LECA had to assemble tubulins for a mitotic spindle and for a flagellar apparatus. Some organisms, such as *Chlamydomonas*, appear to utilize a common set α- and β-tubulins to assemble microtubules for these two functions. In a world of logic, this would imply that the common ancestor might have used its tubulin genes in this manner. The key question for *Naegleria* is: were separate tubulin isotypes originally used for mitosis and flagellar apparatus, or was an integrated set of specialized isotypes the "original" arrangement? If the original was a single set, then what event occurred that led to *Naegleria*'s having a set of flagellar tubulins and a set of very divergent mitotic tubulins? *Naegleria*'s system now works very well, allowing an amoeba to grow and divide rapidly. Indeed, for *Naegleria*, with only one cell type that reproduces, the fastest growing amoebae will "win" the evolutionary race at every generation, and the genus is common globally wherever there is fresh water. But how, from an engineer's viewpoint, could this situation arise? At some point evolution had to switch over either from a single tubulin set that did both or from two specific sets. Tinkering with events as complex as the separation of a cell's genes and the assembly of its flagellar apparatus is dangerous. Somehow we must invoke gene duplication and divergence, but this does not explain what happened. I think that when we understand how this occurred in the midst of early evolution, we will have grasped something important both about tubulins and the evolution of organisms that use it. In a broader sense, this single example makes it clear that continuing study of diverse eukaryotes is going to enhance our understanding in ways that focusing simply on mammals never will.

One conjecture is that Heterolobosea evolved at a time when oxygen was very limiting, and having a specialized tubulin allowed them to manage division under anoxic conditions. We know from the *Naegleria* genome that the organism has a capacity for both aerobic respiration and anaerobic metabolism (Fritz-Laylin et al., 2010). Green algae, and others separating from LECA later, could utilize mitotic machinery that depended on a higher oxygen atmosphere. Another possibility, already mentioned, is that having separate tubulins for mitosis and flagella allowed *Naegleria* to switch modules quickly. Whatever the reason, changing one's mitotic machinery seems like a very dangerous activity, even for an investigator as bold as evolution.

The vastness of this 2200-million-year global experiment takes one's breath away. Genomics are just beginning to reveal the complexity and subtleties of eukaryotes, as more species and groups are analyzed. The day when what's good for the elephant is good for *Naegleria* is gone. We can expect to learn much in the coming decades. But we have certainly learned not to think of eukaryotes as a uniform group, but instead as a group whose diversity has much to teach us that our own small group, the mammals, cannot. The "far-out organism" *Naegleria* showed us multi-tubulins, as it demonstrated the capacity of centrioles to assemble *de novo*; these surprises subsequently have been extended to mammals and changed our ways of thinking. *Naegleria* has more to contribute, as do numerous other neglected protists.

In the meantime, the more we know about tubulins, the more it seems true that, paraphrasing George Orwell about the pigs in *Animal Farm*: "all tubulins are equal, but some tubulins are more equal than others" (Fulton and Simpson, 1976). Tubulins are certainly not all equal, as was generally believed in 1976, nor does each function of tubulin require a separate isotype. As we understand tubulin isotypes better, we will have a richer understanding of evolution's playground and the diversity of eukaryotes. This is an exciting time for converting our growing data on tubulin isotypes into understanding.

DATA AVAILABILITY STATEMENT

The original contributions presented in the study are included in the article/Supplementary Materials, further inquiries can be directed to the corresponding author.

AUTHOR CONTRIBUTIONS

The author confirms being the sole contributor of this work and has approved it for publication.

ACKNOWLEDGMENTS

I thank Elaine Y. Lai, who has been an equal partner in this research since the multi-tubulin hypothesis. So much we have learned has depended on her contributions and wisdom, including helpful critical suggestions on this manuscript, that our contributions have become inseparable. Words are insufficient to express my appreciation.

REFERENCES

Baverstock, P. R., Illana, S., Christy, P. E., Robinson, B. S., and Johnson, A. M. (1989). srRNA Evolution and Phylogenetic Relationships of the Genus *Naegleria* (Protista: Rhizopoda). *Mol. Biol. Evol.* 6, 243–257. doi:10.1093/oxfordjournals.molbev.a040549

Boettcher, B., and Barral, Y. (2013). The Cell Biology of Open and Closed Mitosis. *Nucleus* 4 (3), 160–165. doi:10.4161/nucl.24676

Brenner, S. (2002). *Nature's Gift to Science. Nobel Prize Lecture*. Available at: https://www.nobelprize.org/uploads/2018/06/brenner-lecture.pdf.

Buchsbaum, R. M. (1948). *Animals Without Backbones: An Introduction to the Invertebrates*. Revised Edition. Chicago: University of Chicago Press.

Burki, F., Roger, A. J., Brown, M. W., and Simpson, A. G. B. (2020). The New Tree of Eukaryotes. *Trends Ecol. Evol.* 35 (1), 43–55. doi:10.1016/j.tree.2019.08.008

Chung, S., Cho, J., Cheon, H., Paik, S., and Lee, J. (2002). Cloning and Characterization of a Divergent α-Tubulin that Is Expressed Specifically in Dividing Amebae of *Naegleria gruberi*. *Gene* 293 (1-2), 77–86. doi:10.1016/s0378-1119(02)00509-7

Clark, C. G., Lai, E. Y., Fulton, C., and Cross, G. A. M. (1990). Electrophoretic Karyotype and Linkage Groups of the Amoeboflagellate *Naegleria gruberi*. *J. Protozool.* 37 (5), 400–408. doi:10.1111/j.1550-7408.1990.tb01164.x

Cleveland, D. W., Lopata, M. A., MacDonald, R. J., Cowan, N. J., Rutter, W. J., and Kirschner, M. W. (1980). Number and Evolutionary Conservation of Alpha- and Beta-Tubulin and Cytoplasmic Beta- and Gamma-Actin Genes Using

Specific Cloned cDNA Probes. *Cell* 20 (1), 95–105. doi:10.1016/0092-8674(80)90238-x

Cross, F. R., and Umen, J. G. (2015). The *Chlamydomonas* Cell Cycle. *Plant J.* 82 (3), 370–392. doi:10.1111/tpj.12795

De Jonckheere, J. (2004). Molecular Definition and the Ubiquity of Species in the Genus *Naegleria*. *Protist.* 155 (1), 89–103. doi:10.1078/1434461000167

Dingle, A. D., and Fulton, C. (1966). Development of the Flagellar Apparatus of *Naegleria*. *J. Cell Biol.* 31, 43–54. doi:10.1083/jcb.31.1.43

Eichinger, L., Pachebat, J. A., Glöckner, G., Rajandream, M. A., Sucgang, R., Berriman, M., et al. (2005). The Genome of the Social Amoeba *Dictyostelium discoideum*. *Nature* 435 (7038), 43–57. doi:10.1038/nature03481

Friedmann, H. C. (2004). From "Butyribacterium" to "*E. coli*": An Essay on Unity in Biochemistry. *Perspect. Biol. Med.* 47 (1), 47–66. doi:10.1353/pbm.2004.0007

Fritz-Laylin, L. K., Prochnik, S. E., Ginger, M. L., Dacks, J. B., Carpenter, M. L., Field, M. C., et al. (2010). The Genome of *Naegleria gruberi* Illuminates Early Eukaryotic Versatility. *Cell* 140 (5), 631–642. doi:10.1016/j.cell.2010.01.032

Fulton, C. (1970). Amebo-Flagellates as Research Partners: The Laboratory Biology of *Naegleria* and *Tetramitus*. *Methods Cell Physiol (D. M. Prescott, ed.)* 4, 341–476. doi:10.1016/S0091-679X(08)61759-8

Fulton, C. (1977a). Cell Differentiation in *Naegleria gruberi*. *Annu. Rev. Microbiol.* 31, 597–629. doi:10.1146/annurev.mi.31.100177.003121

Fulton, C. (1977b). Intracellular Regulation of Cell Shape and Motility in *Naegleria*. First Insights and a Working Hypothesis. *J. Supramol. Struct.* 6, 13–43. doi:10.1002/jss.400060103

Fulton, C., and Dingle, A. D. (1967). Appearance of the Flagellate Phenotype in Populations of *Naegleria* Amebae. *Dev. Biol.* 15, 165–191. doi:10.1016/0012-1606(67)90012-7

Fulton, C., and Dingle, A. D. (1971). Basal Bodies, but Not Centrioles, in *Naegleria*. *J. Cell Biol.* 51, 826–836. doi:10.1083/jcb.51.3.826

Fulton, C., and Guerrini, A. M. (1969). Mitotic Synchrony in *Naegleria* Amebae. *Exp. Cell Res.* 56, 194–200. doi:10.1016/0014-4827(69)90002-0

Fulton, C., Kane, R. E., and Stephens, R. E. (1971). Serological Similarity of Flagellar and Mitotic Microtubules. *J. Cell Biol.* 50, 762–773. doi:10.1083/jcb.50.3.762

Fulton, C., and Simpson, P. A. (1976). "Selective Synthesis and Utilization of Flagellar Tubulin. The Multi-tubulin Hypothesis," in *Cell Motility*. Editors R. Goldman, T. Pollard, and J. Rosenbaum (Cold Spring Harbor, NY: Cold Spring Harbor Laboratory), 987–1005.

Fulton, C., and Simpson, P. A. (1979). "Tubulin Pools, Synthesis and Utilization," in *Microtubules*. Editors K. Roberts and J. S. Hyams (London: Academic Press), 117–174.

Fulton, C., and Walsh, C. (1980). Cell Differentiation and Flagellar Elongation in *Naegleria gruberi*. Dependence on Transcription and Translation. *J. Cell Biol.* 85, 346–360. doi:10.1083/jcb.85.2.346

Goldman, R. D., Pollard, T. D., and Rosenbaum, J. (Editors) (1976). *Cell Motility*. Cold Spring Harbor, NY: Cold Spring Harbor Laboratory.

Hedges, S. B., Blair, J. E., Venturi, M. L., and Shoe, J. L. (2004). A Molecular Timescale of Eukaryote Evolution and the Rise of Complex Multicellular Life. *BMC Evol. Biol.* 4, 2. doi:10.1186/1471-2148-4-2

Hinkle, G., and Sogin, M. L. (1993). The Evolution of the Vahlkampfiidae as Deduced from 16S-like Ribosomal RNA Analysis. *J. Eukaryot. Microbiol.* 40, 599–603. doi:10.1111/j.1550-7408.1993.tb06114.x

Inoué, S., and Sato, H. (1967). Cell Motility by Labile Association of Molecules. The Nature of Mitotic Spindle Fibers and Their Role in Chromosome Movement. *J. Gen. Physiol.* 50 (6 Suppl), 259–292.

Jacob, F., and Monod, J. (1961). Genetic Regulatory Mechanisms in the Synthesis of Proteins. *J. Mol. Biol.* 3, 318–356. doi:10.1016/s0022-2836(61)80072-7

James, S. W., Silflow, C. D., Stroom, P., and Lefebvre, P. A. (1993). A Mutation in the α1-Tubulin Gene of *Chlamydomonas reinhardtii* Confers Resistance to Anti-Microtubule Herbicides. *J. Cell Sci.* 106 (Pt 1), 209–218. doi:10.1242/jcs.106.1.209

Joachimiak, E., and Wloga, D. (2021). Tubulin Post-Translational Modifications in Protists - Tiny Models for Solving Big Questions. *Semin. Cell Dev. Biol.* S1084-9521 (1021), 00312–00318. doi:10.1016/j.semcdb.2021.12.004

Johnson, U. G., and Porter, K. R. (1968). Fine Structure of Cell Division in *Chlamydomonas reinhardi*. Basal Bodies and Microtubules. *J. Cell Biol.* 38 (2), 403–425. doi:10.1083/jcb.38.2.403

Kato-Minoura, T., Ogiwara, Y., Yamano, T., Fukuzawa, H., and Kamiya, R. (2020). *Chlamydomonas reinhardtii* Tubulin-Gene Disruptants for Efficient Isolation of Strains Bearing Tubulin Mutations. *PLoS One* 15 (11), e0242694. doi:10.1371/journal.pone.0242694

Kemphues, K. J., Kaufman, T. C., Raff, R. A., and Raff, E. C. (1982). The Testis-specific Beta-Tubulin Subunit in *Drosophila melanogaster* Has Multiple Functions in Spermatogenesis. *Cell* 31 (3 Pt 2), 655–670. doi:10.1016/0092-8674(82)90321-x

Kowit, J. D., and Fulton, C. (1974a). Programmed Synthesis of Tubulin for the Flagella that Develop during Cell Differentiation in *Naegleria gruberi*. *Proc. Natl. Acad. Sci. USA* 71, 2877–2881. doi:10.1073/pnas.71.7.2877

Kowit, J. D., and Fulton, C. (1974b). Purification and Properties of Flagellar Outer Doublet Tubulin from *Naegleria gruberi* and a Radioimmune Assay for Tubulin. *J. Biol. Chem.* 249, 3638–3646. doi:10.1016/s0021-9258(19)42621-5

Lai, E. Y., Remillard, S. P., and Fulton, C. (1984). "Tubulin and Actin: Yin-Yang Gene Expression during *Naegleria* Differentiation," in *Molecular Biology of the Cytoskeleton*. Editors G. Borisy, D. Cleveland, and D. Murphy (New York: Cold Spring Harbor Laboratory Press), 257–266.

Lai, E. Y., Remillard, S. P., and Fulton, C. (1988). The α-Tubulin Gene Family Expressed during Cell Differentiation in *Naegleria gruberi*. *J. Cell Biol.* 106, 2035–2046. doi:10.1083/jcb.106.6.2035

Lai, E. Y., Remillard, S. P., and Fulton, C. (1994). A β-Tubulin Gene of *Naegleria* Encodes a Carboxy-Terminal Tyrosine. Aromatic Amino Acids are Conserved at Carboxy Termini. *J. Mol. Biol.* 235, 377–388. doi:10.1016/s0022-2836(05)80045-2

Lai, E. Y., Walsh, C., Wardell, D., and Fulton, C. (1979). Programmed Appearance of Translatable Flagellar Tubulin mRNA during Cell Differentiation in Naegleria. *Cell* 17, 867–878. doi:10.1016/0092-8674(79)90327-1

Lee, J. H., and Walsh, C. J. (1988). Transcriptional Regulation of Coordinate Changes in Flagellar mRNAs during Differentiation of *Naegleria gruberi* Amebae into Flagellates. *Mol. Cell. Biol.* 8 (6), 2280–2287. doi:10.1128/mcb.8.6.2280-2287.1988

Liechti, N., Schürch, N., Bruggmann, R., and Wittwer, M. (2019). Nanopore Sequencing Improves the Draft Genome of the Human Pathogenic Amoeba *Naegleria fowleri*. *Sci. Rep.* 9 (1), 16040. doi:10.1038/s41598-019-52572-0

Luchniak, A., Fukuda, Y., and Gupta, M. L. J. (2013). Structure-Function Analysis of Yeast Tubulin. *Methods Cell Biol.* 115, 355–374. doi:10.1016/B978-0-12-407757-7.00022-0

Luduena, R. F., and Woodward, D. O. (1973). Isolation and Partial Characterization of Alpha- and Beta-Tubulin from Outer Doublets of Sea-Urchin Sperm and Microtubules of Chick-Embryo Brain. *Proc. Natl. Acad. Sci. USA* 70 (12), 3594–3598. doi:10.1073/pnas.70.12.3594

Lynch, M. (2007). *The Origins of Genome Architecture*. Sunderland, MA: Sinauer Associates.

Lynch, M., Field, M. C., Goodson, H. V., Malik, H. S., Pereira-Leal, J. B., Roos, D. S., et al. (2014). Evolutionary Cell Biology: Two Origins, One Objective. *Proc. Natl. Acad. Sci. USA* 111 (48), 16990–16994. doi:10.1073/pnas.1415861111

Mar, J., Lee, J. H., Shea, D., and Walsh, C. J. (1986). New Poly(A)+RNAs Appear Coordinately during the Differentiation of *Naegleria gruberi* Amebae into Flagellates. *J. Cell Biol.* 102 (2), 353–361. doi:10.1083/jcb.102.2.353

Merchant, S. S., Prochnik, S. E., Vallon, O., Harris, E. H., Karpowicz, S. J., Witman, G. B., et al. (2007). The *Chlamydomonas* Genome Reveals the Evolution of Key Animal and Plant Functions. *Science* 318 (5848), 245–250. doi:10.1126/science.1143609

Meza, I., Talamás-Rohana, P., and Vargas, M. A. (2006). The Cytoskeleton of *Entamoeba histolytica*: Structure, Function, and Regulation by Signaling Pathways. *Arch. Med. Res.* 37 (2), 234–243. doi:10.1016/j.arcmed.2005.09.008

Monod, J., and Jacob, F. (1961). Teleonomic Mechanisms in Cellular Metabolism, Growth, and Differentiation. *Cold Spring Harb. Symp. Quant. Biol.* 26, 389–401. doi:10.1101/sqb.1961.026.01.048

Moore, J. K., and Wethekam, L. (2021). Specialist α-Tubulins for Pluralist Microtubules. *J. Cell Biol.* 220 (12), e202110038. doi:10.1083/jcb.202110038

Nieuwenhuis, J., and Brummelkamp, T. R. (2019). The Tubulin Detyrosination Cycle: Function and Enzymes. *Trends Cell Biol.* 29 (1), 80–92. doi:10.1016/j.tcb.2018.08.003

Nsamba, E. T., Bera, A., Costanzo, M., Boone, C., and Gupta, M. L. (2021). Tubulin Isotypes Optimize Distinct Spindle Positioning Mechanisms During Yeast Mitosis. *J. Cell Biol.* 220 (12), e202110038. doi:10.1083/jcb.202010155

Parfrey, L. W., Lahr, D. J. G., Knoll, A. H., and Katz, L. A. (2011). Estimating the Timing of Early Eukaryotic Diversification with Multigene Molecular Clocks.

Proc. Natl. Acad. Sci. USA 108 (33), 13624–13629. doi:10.1073/pnas.1110633108

Pratt, L. F., Okamura, S., and Cleveland, D. W. (1987). A Divergent Testis-Specific Alpha-Tubulin Isotype that Does Not Contain a Coded C-Terminal Tyrosine. *Mol. Cell. Biol.* 7 (1), 552–555. doi:10.1128/mcb.7.1.552-555.1987

Rafalko, J. S. (1947). Cytological Observations on the Amoeboflagellate, *Naegleria gruberi* (Protozoa). *J. Morphol.* 81 (1), 1–44. doi:10.1002/jmor.1050810102

Schatz, P. J., Solomon, F., and Botstein, D. (1988). Isolation and Characterization of Conditional-Lethal Mutations in the TUB1 Alpha-Tubulin Gene of the Yeast *Saccharomyces cerevisiae*. *Genetics* 120 (3), 681–695. doi:10.1093/genetics/120.3.681

Schuster, F. L. (1975). Ultrastructure of Mitosis in the Amoeboflagellate *Naegleria gruberi*. *Tissue Cell* 7, 1–12. doi:10.1016/s0040-8166(75)80003-6

Shea, D. K., and Walsh, C. J. (1987). mRNAs for Alpha- and Beta-Tubulin and Flagellar Calmodulin Are Among Those Coordinately Regulated when *Naegleria gruberi* Amebae Differentiate into Flagellates. *J. Cell Biol.* 105 (3), 1303–1309. doi:10.1083/jcb.105.3.1303

Silflow, C. D., Chisholm, R. L., Conner, T. W., and Ranum, L. P. (1985). The Two Alpha-Tubulin Genes of *Chlamydomonas reinhardi* Code for Slightly Different Proteins. *Mol. Cell. Biol.* 5 (9), 2389–2398. doi:10.1128/mcb.5.9.2389-2398.1985

Silflow, C. D., and Rosenbaum, J. L. (1981). Multiple Alpha- and Beta-Tubulin Genes in Chlamydomonas and Regulation of Tubulin mRNA Levels after Deflagellation. *Cell* 24 (1), 81–88. doi:10.1016/0092-8674(81)90503-1

Solnica-Krezel, L., Burland, T. G., and Dove, W. F. (1991). Variable Pathways for Developmental Changes of Mitosis and Cytokinesis in *Physarum polycephalum*. *J. Cell Biol.* 113 (3), 591–604. doi:10.1083/jcb.113.3.591

Stephens, R. E. (1975). Structural Chemistry of the Axoneme: Evidence for Chemically and Functionally Unique Tubulin Dimers in Outer Fibers. *Soc. Gen. Physiol. Ser.* 30, 181–206.

Velle, K. B., Trupinić, M., Ivec, A., Swafford, A., Nolton, E., Rice, L., et al. (2022). *Naegleria*'s Mitotic Spindles Are Built from Unique Tubulins and Highlight Core Spindle Features. *Curr. Biol.* [Epub ahead of print]. doi:10.1016/j.cub.2022.01.034

Wainright, P. O., Hinkle, G., Sogin, M. L., and Stickel, S. K. (1993). Monophyletic Origins of the Metazoa: an Evolutionary Link with Fungi. *Science* 260, 340–342. doi:10.1126/science.8469985

Walsh, C. (1984). Synthesis and Assembly of the Cytoskeleton of *Naegleria gruberi* Flagellates. *J. Cell Biol.* 98, 449–456. doi:10.1083/jcb.98.2.449

Walsh, C. J. (2012). The Structure of the Mitotic Spindle and Nucleolus during Mitosis in the Amebo-Flagellate *Naegleria*. *PLoS One* 7 (4), e34763. doi:10.1371/journal.pone.0034763

Youngblom, J., Schloss, J. A., and Silflow, C. D. (1984). The Two Beta-Tubulin Genes of *Chlamydomonas reinhardtii* Code for Identical Proteins. *Mol. Cell. Biol.* 4 (12), 2686–2696. doi:10.1128/mcb.4.12.2686-2696.1984

Zinder, N. D. (1992). Forty Years Ago: the Discovery of Bacterial Transduction. *Genetics* 132 (2), 291–294. doi:10.1093/genetics/132.2.291

Conflict of Interest: The author declares that the research was conducted in the absence of any commercial or financial relationships that could be construed as a potential conflict of interest.

Publisher's Note: All claims expressed in this article are solely those of the authors and do not necessarily represent those of their affiliated organizations, or those of the publisher, the editors and the reviewers. Any product that may be evaluated in this article, or claim that may be made by its manufacturer, is not guaranteed or endorsed by the publisher.

frontiers | Frontiers in Cell and Developmental Biology

MINI REVIEW
published: 28 April 2022
doi: 10.3389/fcell.2022.861648

Reconstituting Microtubules: A Decades-Long Effort From Building Block Identification to the Generation of Recombinant α/β-Tubulin

*Shih-Chieh Ti**

School of Biomedical Sciences, Faculty of Medicine, The University of Hong Kong, Pokfulam, Hong Kong SAR, China

Microtubules are cytoskeletal filaments underlying the morphology and functions of all eukaryotic cells. In higher eukaryotes, the basic building blocks of these non-covalent polymers, α- and β-tubulins, are encoded by expanded tubulin family genes (i.e., isotypes) at distinct loci in the genome. While α/β-tubulin heterodimers have been isolated and examined for more than 50 years, how tubulin isotypes contribute to the microtubule organization and functions that support diverse cellular architectures remains a fundamental question. To address this knowledge gap, *in vitro* reconstitution of microtubules with purified α/β-tubulin proteins has been employed for biochemical and biophysical characterization. These *in vitro* assays have provided mechanistic insights into the regulation of microtubule dynamics, stability, and interactions with other associated proteins. Here we survey the evolving strategies of generating purified α/β-tubulin heterodimers and highlight the advances in tubulin protein biochemistry that shed light on the roles of tubulin isotypes in determining microtubule structures and properties.

Keywords: tubulin, microtubules, tubulin isotypes, tubulin protein biochemistry, recombinant tubulin

OPEN ACCESS

Edited by:
Jeffrey Moore,
University of Colorado Anschutz Medical Campus, United States

Reviewed by:
Luke Rice,
University of Texas Southwestern Medical Center, United States
Jawdat Al-Bassam,
University of California, Davis, United States
Mohan Gupta,
Iowa State University, United States

***Correspondence:**
Shih-Chieh Ti
jeffti@hku.hk

Specialty section:
This article was submitted to Cellular Biochemistry, a section of the journal Frontiers in Cell and Developmental Biology

Received: *24 January 2022*
Accepted: *18 April 2022*
Published: *28 April 2022*

Citation:
Ti S-C (2022) Reconstituting Microtubules: A Decades-Long Effort From Building Block Identification to the Generation of Recombinant α/β-Tubulin. Front. Cell Dev. Biol. 10:861648. doi: 10.3389/fcell.2022.861648

INTRODUCTION

α/β-tubulin heterodimers polymerize into microtubules that are fundamental to various cellular processes, including cell division, migration, and organelle transport [reviewed in (Nogales, 2000)]. However, not all cells form microtubules with the same composition. Cells can express multiple tubulin isotypes that are different from each other in amino acid sequences (Ludueña and Banerjee, 2008). Humans have at least nine α- and ten β-tubulin isotypes (Findeisen et al., 2014), and most of them can acquire a variety of post-translational modifications, including acetylation, polyglutamylation, and de-tyrosination (Janke and Bulinski, 2011). This diversity in tubulin is important; specialized cells, such as neurons, often express specific tubulin isotypes (Ludueña and Banerjee, 2008), and accumulation of α-tubulin acetylation is a marker for long-lived, stable microtubules (Janke and Bulinski, 2011). Exactly how heterogeneous microtubule composition is established and used by cells to facilitate functional outputs is still an open question.

In vivo genetics and cell biology studies have revealed the critical roles of tubulin isotypes and tubulin post-translational modifications in forming functional cellular microtubule architectures (i.e., the tubulin code) (Sullivan, 1988; Wilson and Borisy, 1997; Verhey and Gaertig, 2007; Janke and Bulinski, 2011). In particular, among tubulin variants that cause phenotypes in a wide variety of eukaryotes, mutations in specific tubulin isotypes have been associated with human diseases such as neurological disorders, impaired oocyte maturation, and defective platelet formation (Gadadhar

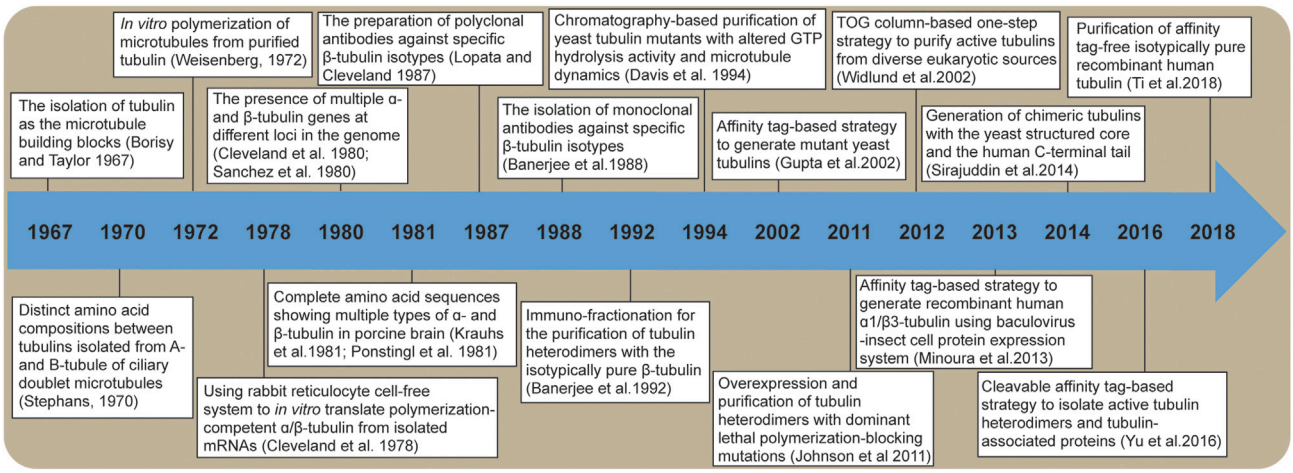

FIGURE 1 | A timeline of major breakthroughs that have advanced our understanding of tubulin isotypes.

et al., 2017; Pham and Morrissette, 2019). However, the challenge of generating biochemically pure tubulin has limited our ability to reconstitute microtubules with a defined tubulin composition for quantitative *in vitro* biochemical and biophysical characterization. How tubulin isotypes determine microtubule properties (e.g., dynamics and post-translational modifications) remains unclear. This review focuses on the milestones in protein biochemistry that have advanced our understanding of microtubule biology (**Figure 1**). From the initial isolation of α/β-tubulin protein heterodimers as the building block of microtubules, the characterization of purified tubulin variants, to the recent breakthrough in generating recombinant tubulin, the decades-long effort is now ready to decipher the molecular mechanisms underlying the biological functions of tubulin isotypes.

The Isolation of "Tubulin" as the Building Blocks of Microtubules

In the early 1960s, negative stain electron microscopy images observed the ubiquitous tubular filaments (i.e., microtubules) in diverse cell types across species (Ledbetter and Porter, 1963; Slautterback, 1963). Further examinations, with improved fixing reagents and negative staining strategies, described microtubules as thirteen beaded profibrils surrounding the long axis of the filaments (Pease, 1963; Ledbetter and Porter, 1964; Gall, 1966; Phillips, 1966) (**Figure 2**). While these fine features are coherent to the modern structural model of microtubules, identifying the building blocks was challenging, mainly due to the lack of effective assays for tracing a microtubule-associated property during biochemical fractionation of the cell lysate.

Colchicine disrupts diverse cellular functions without inhibiting DNA, RNA, and protein synthesis (Taylor, 1965). To reveal the mechanism of action, Borisy and Taylor tracked the radioactivity of tritium-labeled colchicine in fractionated cell homogenates. They found that colchicine targeted a 6S protein enriched in cells or tissues with abundant microtubules, suggesting the colchicine-binding protein to be a subunit of the filaments (Borisy and Taylor, 1967). The following early characterization of the microtubule subunit proteins depended on studies using cilia and flagella, which have the unique 9 + 2 arrangement of microtubules that can be solubilized and fractionated in mild conditions (Gibbons and Grimstone, 1960; Gibbons, 1963). Guided by colchicine-binding activity as well as the electron micrographs of cilia and flagella, the microtubule building blocks were isolated as a dimeric protein of two 55 kDa components, and each protein dimer bound two molecules of guanine nucleotide and one molecule of colchicine (Shelanski and Taylor, 1967, 1968; Stephens et al., 1967; Renaud et al., 1968). Further analyses identified the microtubule subunits as heterodimers of two different kinds of proteins, α- and β-tubulin (Bryan and Wilson, 1971; Feit et al., 1971; Olmsted et al., 1971). With the name 'tubulin' (Mohri, 1968), the purified microtubule subunit proteins have led to *in vitro* biochemical and biophysical studies providing mechanistic insights into diverse cellular processes, such as cell division, cell migration, and intracellular cargo transport.

The Formulation of the "Multi-Tubulin Hypothesis"

Compared to the colchicine-binding protein isolated from the mammalian brain, the purified cilia and flagella tubulin showed the similarity of microtubule subunits in molecular weight, amino acid composition, and guanine nucleotide-binding activity (Weisenberg et al., 1968). This study not only revealed the conservation of microtubule building blocks but also established the critical knowledge (e.g., time sensitivity, the necessity of Mg-GTP, and limited exposure to high salt) for employing brain tissues as the source to purify a large quantity of active tubulin. In particular, the rapid exchange of one tubulin-bound guanine nucleotide with free nucleotides confers the necessity of including GTP during the purification process to maintain the native conformation of tubulin (Weisenberg et al., 1968).

The initial characterization indicated the biochemical similarity in tubulin isolated from different sources. However,

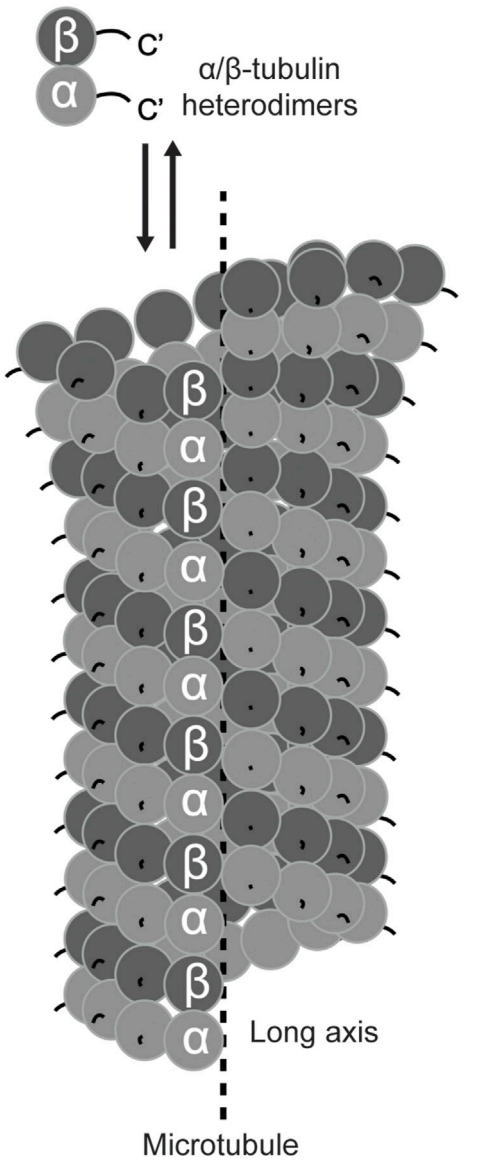

FIGURE 2 | Schematic of α/β-tubulin heterodimers and a microtubule. The structured cores of α- (light grey) and β- (dark grey) tubulin are shown in circles. The unstructured C-terminal tails are exposed on the surface of the microtubule.

the variations in the stability of cellular architectures when subjected to chemical (e.g., colchicine) and physical (e.g., exposure to non-physiological temperature) treatment suggested microtubules with different tubulin compositions. The evidence supporting this hypothesis originated from ciliary and flagellar cold-resistant doublet microtubules, where A-tubules had higher thermostability than B-tubules and remained intact when treated with the elevated temperature (Behnke and Forer, 1967). Temperature-dependent fractionation (i.e., thermal fractionation) of flagellar doublet microtubules revealed the distinct amino acid compositions between tubulins isolated from A- and B-tubules (Stephens, 1970). Further study demonstrated the presence of different types of tubulin in cilia and neuronal cells (Olmsted et al., 1971). These early biochemical studies formulated the 'multi-tubulin hypothesis' that the diversity of tubulin proteins underlies the formation of microtubule networks for various biological functions in cells (Fulton and Simpson, 1976).

The Discovery of Tubulin Variants With Distinct Amino Acid Sequences

For several years after the success in tubulin isolation, it had been challenging to reconstitute and characterize the mechanisms of microtubule assembly and disassembly, which play a fundamental role in the cellular functions of the cytoskeletal filaments. To address this limitation, a critical study with detailed biochemical characterization recognized the key factors [magnesium ions (Mg^{2+}), EGTA, and warm temperature (35°C)] stimulating *in vitro* microtubule assembly from purified tubulin proteins (Weisenberg, 1972). In contrast, elements like calcium ions (Ca^{2+}), EDTA, and cold temperature (0°C) inhibited the formation of the filaments (Weisenberg, 1972). Further characterization identified a high concentration of glycerol [4 M, or about 37% (w/v)] as a reagent that conferred rapid nucleation and superior stability of the tubulin polymers, allowing the development of a strategy to purify tubulin proteins by reversible microtubule polymerization (Shelanski et al., 1973). With phosphocellulose chromatography removing the tubulin-associated proteins, the temperature-dependent microtubule polymerization and depolymerization provided a robust methodology for isolating a large quantity of brain tubulin (Borisy et al., 1975; Weingarten et al., 1975). Since then, purified mammalian brain tubulin (usually from porcine or bovine) has served as a popular material for *in vitro* assays to dissect the molecular basis of microtubule structure, polymerization dynamics, and interaction with microtubule-associated proteins. By improving the efficiency of *in vitro* microtubule polymerization, a recent protocol can generate tubulin with controlled post-translational modifications from cell lines or brain tissues of genetically engineered mice (Souphron et al., 2019).

Cycles of microtubule assembly and disassembly have been the core of protocols for obtaining tubulin from non-neuronal cell lines (Doenges et al., 1977; Nagle et al., 1977; Weber et al., 1977; Weatherbee et al., 1978; Doenges et al., 1979; Newton et al., 2002) as well as from different tissues of a variety of species, such as sea urchin (Binder and Rosenbaum, 1978; Farrell and Wilson, 1978; Keller et al., 1982; Detrich and Wilson, 1983), fungi (Kilmartin, 1981; Yoon and Oakley, 1995; Braun et al., 2009; Drummond et al., 2011), nematodes (Dawson et al., 1983), surf clam (Suprenant and Rebhun, 1984), and cold-water fish (Langford, 1978; Williams et al., 1985; Detrich and Overton, 1986; Detrich et al., 1989; Detrich et al., 2000). These pioneering studies revealed the source-dependent variation in the intrinsic properties of the filaments (e.g., stability, critical concentration, and protofilament numbers), the optimal temperature for polymer assembly, and the responses to microtubule-destabilizing small molecules. *In vitro* polymerization of microtubules started showing the various properties of tubulin purified from different biological contexts.

Advances in the purification strategy provided high quality and enough material for analyzing tubulin polymorphism. Electrofocusing analysis of brain tubulin showed a heterogeneous mixture of a dozen polypeptides with distinct isoelectric points, suggesting the presence of subspecies of tubulin (Feit et al., 1971; George et al., 1981). Tryptic peptide mapping revealed the significant diversity of the primary sequences among tubulin subspecies (George et al., 1981). Peptide sequencing by Edman degradation further supported the heterogeneity in the primary sequences of brain tubulin, which contained at least four types of α- and two types of β-tubulin polypeptides with aspartic and glutamic residues enriched at the carboxy-terminus (i.e., the C-terminal tail) (Krauhs et al., 1981; Ponstingl et al., 1981). These studies proposed that the acidic C-terminal tails could interact with positively charged domains of microtubule-associated proteins (Krauhs et al., 1981; Ponstingl et al., 1981). Meanwhile, the cloning of mRNAs and genomic DNA analysis disclosed multiple α- and β-tubulin genes (i.e., isotypes) at different loci in the genome (Cleveland et al., 1978; Cleveland et al., 1980; Sanchez et al., 1980; Cleveland et al., 1981a). Together, the polymorphism in the tubulin primary sequences likely regulates the properties of microtubule-based cellular architectures.

Immunofractionation of Tubulin Heterodimers With Specific β-Tubulin Isotypes

According to the molecular genetic analyses of the tubulin genes, the most divergent region between tubulin isotypes is the ~15-residue polypeptide chain at the C-terminal tail (Sullivan and Cleveland, 1986; Villasante et al., 1986; Wang et al., 1986; Pratt et al., 1987). In particular, the amino acid sequence of the C-terminal tail is not only evolutionarily conserved across different vertebrate species but also characteristic to each β-tubulin isotype (Sullivan and Cleveland, 1986; Wang et al., 1986). While genetics and cell biology studies suggested the distinct biological functions of tubulin isotypes, the regulatory roles of tubulin isotype compositions on intrinsic microtubule properties (e.g., polymerization dynamics) was unknown due to the significant challenge of generating isotypically pure tubulin for *in vitro* biochemical and biophysical assays (Cleveland, 1987).

As the C-terminal tail has the characteristic amino acid sequence of each tubulin isotype, synthetic peptides corresponding to the tail domain can be the antigen for acquiring isotype-specific antibodies (Lopata and Cleveland, 1987). By using peptide-derived polyclonal antibodies against each of the six vertebrate β-tubulin isotypes, immunofluorescence mapped the spatial distribution of β-tubulin isotypes in cultured cells (Lopata and Cleveland, 1987). The success of this antibody-mediated approach further motivated the isolation of monoclonal antibodies for *in vitro* protein biochemistry studies of tubulin isotypes, establishing that bovine brain β-tubulin is a mixture of four subspecies: type I (β_I, 3%), type II (β_{II}, 58%), type III (β_{III}, 25%) and type IV (β_{IV}, 13%) (Banerjee et al., 1988). The immunodepletion of β_{III}-tubulin conferred the fractionated brain tubulin an increased rate and a greater extent of microtubule assembly, suggesting the regulatory roles of tubulin isotype compositions in the microtubule polymerization properties (Banerjee et al., 1990). By employing monoclonal antibodies against β_{II}-, β_{III}- and β_{IV}-tubulin, carefully designed immunoaffinity chromatography of bovine brain tubulin allowed the purification of tubulin heterodimers with isotypically pure β-tubulin, $\alpha\beta_{II}$-, $\alpha\beta_{III}$- and $\alpha\beta_{IV}$-tubulin (Banerjee et al., 1992).

The immunofractionation of bovine brain tubulin led the way for tubulin isotypes' functional studies. Thermodynamic characterization revealed the effects of β-tubulin isotypes on the binding affinity of antimitotic alkaloid colchicine for tubulin heterodimers (Banerjee and Luduena, 1992). Compared to the affinity for $\alpha\beta_{III}$-tubulin, colchicine bound to $\alpha\beta_{II}$- and $\alpha\beta_{IV}$-tubulin about 2-fold and 30-fold tighter, respectively, (Banerjee and Luduena, 1992). In addition, the characterization of microtubule assembly showed that β-tubulin isotype compositions determined the critical concentration for polymer nucleation and the elongation behavior of the filaments (Banerjee et al., 1992; Lu and Luduena, 1994). By using differential interference contrast (DIC) video microscopy to observe single dynamic microtubules, the detailed quantification established that, in comparison to $\alpha\beta_{II}$- and $\alpha\beta_{IV}$-tubulin, $\alpha\beta_{III}$-tubulin assembled into filaments with higher dynamicity (Panda et al., 1994). The compositions of β-tubulin isotypes can modulate the dynamic instability parameters (e.g., growth rate, shortening rate, and catastrophe frequency) of microtubules (Panda et al., 1994).

In vitro reconstitution using immunofractionated brain tubulin allowed the generation of microtubules with a defined tubulin isotype composition and opened a new avenue toward dissecting the multi-tubulin hypothesis. However, three limitations prevented the general adoption of this immunoaffinity approach for studying tubulin isotypes. First, the low variance in the C-terminal tails limits the availability of antibodies targeting specific α-tubulin isotypes. This restriction makes it challenging to understand how the crosstalk between isotypes of α- and β-tubulin determines the microtubule properties. Second, the purification of brain tubulin usually requires microtubule polymerization cycles, which are selective for tubulin isotypes that favor this process. Third, tubulin is not abundant in most non-neuronal cells. It has been challenging to achieve the critical concentration for microtubule polymerization in tubulin purification procedures. The low tubulin recovery efficiency of polymerization cycles further hinders the generation of enough tubulin from other cell or tissue types for immunofractionation. Tubulin purification strategies with higher efficiency and flexibility would be essential for dissecting the underlying molecular mechanisms by which tubulin isotypes regulate microtubule functions and structures.

Tubulin-Affinity Chromatography For Efficient Isolation of α/β-Tubulin Heterodimers

One approach exploits tubulin-binding ligands that can be immobilized on the stationary phase as an affinity

chromatography column to isolate α/β-tubulin heterodimers from complex cell extracts. In cells, conserved XMAP215/Dis1 family proteins are processive microtubule polymerases that employ the tumor overexpressed gene (TOG) domains to specifically recruit α/β-tubulin from the cytoplasm onto the growing filament ends (Al-Bassam et al., 2006; Al-Bassam et al., 2007; Brouhard et al., 2008; Widlund et al., 2011). Due to the selective and reversible binding to tubulin, the immobilized TOG domains serve as an optimal purification matrix (i.e., TOG-column) to sequester native tubulin from cell lines or tissues of various species (Widlund et al., 2012). This one-step affinity chromatography strategy allows the rapid and efficient isolation of α/β-tubulin heterodimers from extracts of cells with low tubulin expression levels, for example, *S. cerevisiae* (about 0.05% of the total protein) (Kilmartin, 1981; Widlund et al., 2012).

The success of tubulin purification using a TOG-column overcomes the following two significant drawbacks of *in vitro* biochemical reconstitution assays using mammalian brain tubulin. First, while tubulin is conserved in eukaryotes (*S. cerevisiae* and human α-tubulin protein primary sequences are about 75% identical), microtubule-associated proteins behave differently in assays with mammalian brain tubulin or with tubulin purified from homologous species (Alonso et al., 2007; Kollman et al., 2015). The TOG-column-mediated affinity chromatography strategy is revolutionary as the purified native tubulin from corresponding biological contexts is handy for homologous *in vitro* reconstitution assays. In particular, current studies have reconstituted flagellar sliding using axonemal tubulin and dynein (Alper J. et al., 2013; Alper J. D. et al., 2013; Alper et al., 2014), dissected the length regulation mechanisms of *S. cerevisiae, D. melanogaster*, or *A. thaliana* microtubules (Fujita et al., 2013; Podolski et al., 2014; Hibbel et al., 2015; Hotta et al., 2016; Moriwaki and Goshima, 2016; Otani et al., 2018; Edzuka and Goshima, 2019), elucidated the structural insight into the binding of motors and microtubule-associated proteins to *S. pombe* or human filaments (Atherton et al., 2019; von Loeffelholz et al., 2019; von Loeffelholz et al., 2017), revealed the molecular basis of the unique polymerization dynamics of *C. elegans* microtubules (Chaaban et al., 2018), identified parasite-specific small molecules targeting microtubule polymerization (Hirst et al., 2022), as well as established the roles of microtubule dynamics in the control of spindle morphology of Xenopus species (Hirst et al., 2020; Biswas et al., 2021).

Second, tubulin purified from mammalian brain tissues has various post-translational modifications (Janke and Bulinski, 2011). It has been difficult to use brain tubulin for studying the molecular mechanisms by which individual tubulin modifications regulate microtubule properties and functions. TOG-affinity chromatography allows the purification of tubulin from sources that have a clean profile of tubulin post-translational modifications, such as a human embryonic kidney cell line (tsA201) (Vemu et al., 2014; Vemu et al., 2017). The mass spectrometric analysis showed that the purified tsA201 tubulin contained α1B-, βI-, βII- and βIVB-tubulin with no detectable post-translational modification (i.e., naïve tubulin) (Vemu et al., 2014). This 'naïve' tsA201 tubulin can then be selectively modified by recombinant tubulin-modifying enzymes (Vemu et al., 2014). This enzymatic approach to generating filaments with a defined composition of post-translational modifications has led to mechanistic insights into the roles of tubulin's chemical adducts in the regulation of microtubule structures and functions (Garnham et al., 2015; Valenstein and Roll-Mecak, 2016; Garnham et al., 2017; Mahalingan et al., 2020; Zheng et al., 2022).

While the TOG affinity-based approach can effectively isolate soluble tubulin from any cell lysate with no preference to specific tubulin isotypes (Widlund et al., 2012), limitations remained on characterizing how the variance in tubulin primary sequences (i.e., isotypes or mutations) could impact microtubule properties (e.g., structure, polymerization dynamics, as well as interactions with motors and microtubule-associated proteins). A recombinant protein strategy of expressing and purifying tubulin variants is essential. However, the generation of recombinant tubulin has been somewhat challenging.

Significant Barriers to Achieving Recombinant Tubulin Stem From Its Complex Biosynthesis

In vitro transcription and translation system using a rabbit reticulocyte lysate system allows the purification of a small quantity of recombinant tubulin (Cleveland et al., 1978). However, achieving a yield at the milligram scale of recombinant tubulin is not trivial, likely due to the following two cellular mechanisms regulating tubulin biosynthesis and homeostasis.

First, the formation of native α/β-tubulin heterodimers requires the newly synthesized tubulin polypeptides to go through the tubulin-folding pathway that employs a complex chaperone system including prefoldin, cytosolic chaperonin, and tubulin-specific folding cofactors (Gao et al., 1992; Yaffe et al., 1992; Tian et al., 1996; Lewis et al., 1997; Tian et al., 1997; Vainberg et al., 1998; Bhamidipati et al., 2000). As common prokaryotic organisms for producing recombinant proteins (e.g., *E. coli*) lack these chaperone components, the overexpressed tubulin polypeptides of interest form non-functional aggregates in these organisms. Second, the tubulin biosynthesis is under a tight regulation that employs a negative feedback loop to self-regulate the stability of tubulin mRNAs in response to the concentration of soluble α/β-tubulin heterodimers (Ben-Ze'ev et al., 1979; Cleveland, 1989; Cleveland et al., 1981b; Gasic et al., 2019). This negative correlation, also known as tubulin autoregulation, involves a ribosome-associating factor, TTC5, that binds to the N-terminus of nascent tubulin polypeptides and stimulates co-translational degradation of tubulin mRNA following increased soluble tubulin concentration (Yen et al., 1988; Theodorakis and Cleveland, 1992; Lin et al., 2020).

Together, due to the complex eukaryotic machinery that controls the folding and the concentration of soluble tubulin in the cytoplasm, the yield of recombinant tubulin is irrelevant to the ectopic overexpression level of the tubulin genes of interest. It has been challenging to generate recombinant tubulin in the

native state for dissecting how variation in the primary protein sequences affects the structures and functions of microtubules.

Exploiting Yeast Cells to Express and Purify Recombinant Tubulin

The genomes of budding yeast *S. cerevisiae* and fission yeast *S. pombe* encode two α- and one β-tubulin isotypes, which the yeast genetic tools can engineer to construct strains harboring modified tubulin genes. With the established methodology to purify milligram quantities of wild-type yeast tubulin proteins (Barnes et al., 1992; Davis et al., 1993), the relatively simple tubulin isotype composition has made these unicellular fungi a powerful platform to access mutant tubulin proteins. In particular, the stable haploid and diploid states of yeast cells provide an opportunity to characterize tubulin harboring lethal mutations (Davis et al., 1994). Furthermore, the genetically modified strains with only one α-tubulin isotype have been the source for generating isotypically pure yeast α/β-tubulin heterodimers, which allows the assembly of microtubules with a defined tubulin isotype composition (Bode et al., 2003; Braun et al., 2009; des Georges et al., 2008; Uchimura et al., 2010; Uchimura et al., 2006).

To isolate the mutant tubulin from yeast cells for *in vitro* assays, researchers engineered the yeast β-tubulin C-terminus to include a hexahistidine tag for affinity purification or to alter the quantities of negatively charged glutamic acid residues for ion-exchange chromatography (Davis et al., 1994; Gupta et al., 2002). These yeast strains expressed α- and β-tubulin proteins from the endogenous gene loci or extra copies of the α- and β-tubulin genes controlled by a galactose-induced overexpression promoter. The chromatography-based strategy and affinity purification allowed the isolation of mutant tubulin without cycles of polymerization and depolymerization (Davis et al., 1994; Gupta et al., 2002). The mutagenesis analyses of yeast tubulin have provided mechanistic insights into the roles of GTP hydrolysis activity in microtubule dynamics (Davis et al., 1994; Dougherty et al., 2001), investigated the structure-activity relationship of tubulin-targeting small molecules (Gupta et al., 2002; Gupta et al., 2003), and examined the microtubule-binding site regulating the kinesin motor activity (Uchimura et al., 2006; Uchimura et al., 2010). However, the excess amounts of β-tubulin (alone or together with α-tubulin) causes cell cycle arrest, chromosome losses, and depolymerization of cellular microtubules (Burke et al., 1989). The lethality limited the yield of recombinant yeast tubulin and restricted access to dominant loss-of-function mutant tubulin for *in vitro* biochemical and biophysical characterization. The full capacity of the yeast protein expression system remained unexplored.

A robust strategy has unleashed the power of using *S. cerevisiae* to express and purify recombinant mutant tubulin (Johnson et al., 2011). The success of this chromatography-based approach depends on a transient (three to five hours) but strong protein overexpression from galactose-inducible promoters in high-copy-number plasmids. By significantly improving the final yield while bypassing the lethality due to excess α- and β-tubulin, this strategy opens a new avenue to characterizing tubulin constructs harboring dominant polymerization-blocking mutations, which have explicated the principles of protein machinery that regulates microtubule growth and stability (Ayaz et al., 2012; Ayaz et al., 2014; Geyer et al., 2018; Majumdar et al., 2018). Further mutagenesis analyses of recombinant yeast tubulin revealed the long-overdue molecular bases of microtubule dynamics, such as the allosteric effects of nucleotide states and the regulatory roles of nucleotide exchange on growing filament ends (Geyer et al., 2015; Piedra et al., 2016), demonstrated the effects of disease-related tubulin mutations on microtubule properties (Denarier et al., 2021; Park et al., 2021), and elucidated the mechanism of kinesin-8 family depolymerase activity (Arellano-Santoyo et al., 2017).

This established recombinant yeast tubulin system also has stimulated the development of new methodologies to label tubulin for revealing molecular features of microtubules. For example, site- and topology-specifically labeled yeast tubulin with probes or tags can facilitate studies of how proteins, small molecules, and post-translation modifications interact and regulate microtubules (Kleiner et al., 2013). Furthermore, strategies tagging the C-terminus of yeast β-tubulin with a microbead or a gold nanoparticle have significantly improved the resolution of light microscopy for characterizing *in vitro* reconstituted microtubules (Driver et al., 2017; Mickolajczyk et al., 2019). Direct measurements by laser tweezers determined the strain energy stored in microtubule protofilaments (Driver et al., 2017), while direct observation of tubulin subunits association and dissociation at growing filament ends provided quantitative insights into microtubule dynamics (Mickolajczyk et al., 2019).

Using this yeast-based strategy to generate recombinant human tubulin was unsuccessful (Sirajuddin et al., 2014). Instead, an alternative approach employed chimeric proteins consisting of the folded yeast tubulin core and the human tubulin unstructured C-terminal tail that contains sites for several post-translational modifications and interacts with most microtubule-associated proteins (Sirajuddin et al., 2014; Janke and Magiera, 2020). These chimeric tubulin proteins were purified by affinity chromatography using a hexahistidine-tag in the acetylation loop of the α-tubulin subunit. These tubulin chimeras have been a powerful tool to characterize the regulatory roles of tubulin isotypes and post-translational modifications in protein activities such as the processivity and velocity of microtubule motors (Sirajuddin et al., 2014) and the permeability of voltage-dependent anion channels (Rostovtseva et al., 2018).

The Recent Breakthrough in Making Recombinant Higher Eukaryotic Tubulin

The genome of higher eukaryotes encodes a substantially expanded number of α- and β-tubulin isotypes. For example, the human genome encodes at least nine α- and ten β-tubulin isotypes that show cell-type-specific expression profiles (Ludueña and Banerjee, 2008; Findeisen et al., 2014). While genetics and cell biology studies suggested that each tubulin gene could have unique cellular functions (Janke and Magiera, 2020), it remains unclear how tubulin isotypes modulate microtubule

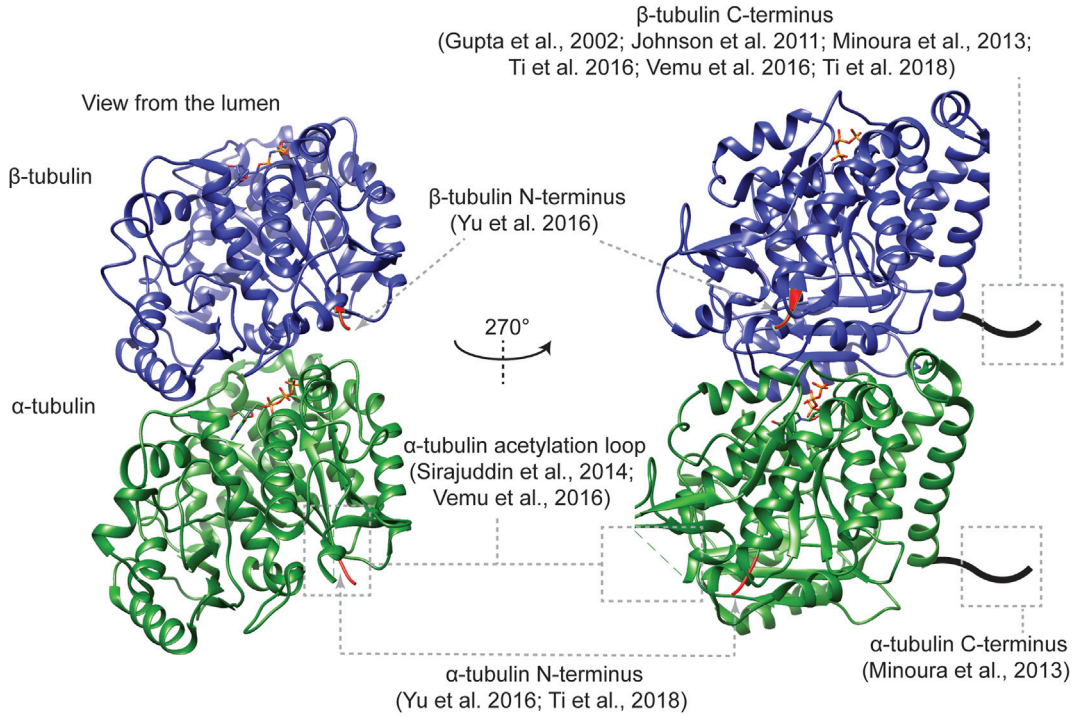

FIGURE 3 | The location of affinity tags for the purification of recombinant tubulin. The ribbon diagrams show the structure of an α/β-tubulin heterodimer (PDB ID: 6e7b). The first three residues at the N-termini of each tubulin are in red, while the rest of α- and β-tubulin are in green and blue, respectively. The stick model represents the tubulin-bound nucleotides.

structures and functions. Due to the complex cellular machinery that regulates tubulin biosynthesis and homeostasis, it has been challenging to purify active human tubulin in the recombinant form.

In 2013, a pioneering strategy used the baculovirus-insect cell protein expression system to generate polymerization competent recombinant human tubulin (Minoura et al., 2013). By employing a hexahistidine-tag fused to the C-terminus of α-tubulin and a FLAG-tag at the C-terminus of β-tubulin, this affinity chromatography-based workflow allowed co-expressing both tubulin and generating high purity of active human α1/β3-tubulin, mouse α1/β2-tubulin and Drosophila α1/β1-tubulin (Minoura et al., 2013; Ayukawa et al., 2021; Diao et al., 2021). Later, another approach used an internal hexahistidine-tag at α-tubulin (Sirajuddin et al., 2014) together with a protease-cleavable FLAG-tag at the C-terminus of β-tubulin also successfully produced isotypically pure human α1/β3-tubulin (Vemu et al., 2016). The success in generating active α/β-tubulin isotypes of higher eukaryotes has offered the opportunities to dissect the molecular mechanisms by which high eukaryotic tubulins regulate microtubule properties. In particular, recombinant human α1/β3-tubulin has become a popular material for characterizing the impacts of disease-related tubulin mutations on the behaviors of kinesin motors (Minoura et al., 2016), the modulation of microtubule dynamics by tubulin isotype composition (Vemu et al., 2017), the incorporation of soluble GTP-tubulin into damaged sites along the microtubule shaft (Vemu et al., 2018), and the effects of GTP hydrolysis on microtubule structures and dynamics (Roostalu et al., 2020; LaFrance et al., 2022). However, these recombinant proteins contain uncleavable charged affinity tags fused to the tubulin domains that interact with microtubule-associated proteins (e.g., the C-terminal tail) or inter-tubulin contacts within the microtubule lattice (e.g., the acetylation loop). It will be favorable to access recombinant tubulin with cleavable affinity tags.

Tubulin with a cleavable affinity tag can be a powerful tool for identifying tubulin-associated proteins (Yu et al., 2016; Yu and Galjart, 2018). A SUMO protease cleavable biotinylation tag at the N-terminus of human α1-or β3-tubulin mediated the isolation of tubulin and the associated tubulin-binding proteins from the cell lysate (Yu et al., 2016; Yu and Galjart, 2018). The expression of the tubulin constructs together with bacterial biotin ligase (BirA) in HEK293T cells led to the generation of biotinylated human tubulin. After streptavidin-coupled matrix-based enrichment, SUMO protease treatment facilitated the release of biotin-tagged tubulin and the tubulin-associated proteins for further mass spectrometry analyses. While this approach provides an opportunity to reveal the interaction proteome of human tubulin isotypes or disease-related mutant tubulins (Yu and Galjart, 2018), the relatively low yield has limited the application of this strategy to generate recombinant human tubulin for *in vitro* reconstitution of microtubules.

To obtain affinity tag-free recombinant tubulin, we reasoned that the cleavable affinity tag must be at the N- or C-terminus of tubulin

for enzymatic removal of the peptide tag after affinity chromatography. While it is promising to fuse the affinity peptide ligand to the C-terminus of β-tubulin, the initial attempts to tag either end of α-tubulin significantly reduced the amount of recombinant human tubulin obtained. By employing the baculovirus-insect cell system, we expressed untagged human α1B-tubulin together with human β2-or β3-tubulin fused at the C-terminus with a tobacco etch virus (TEV) protease cleavable hexahistidine-tag (Ti et al., 2016). Our three-step tubulin purification strategy involved nickel-affinity chromatography followed by tag removal and the final TOG-column affinity chromatography. This approach yielded isotypically pure human β-tubulin dimerized with either recombinant human α1B-tubulin or endogenous insect α-tubulin, indicating that the C-terminal hexahistidine tag is sufficient to isolate specifically human β-tubulin from the complex cell lysate. The characterization of the isotypically pure recombinant human β-tubulin revealed how disease-related β-tubulin mutations, human β-tubulin isotypes, and tubulin allosteric conformational changes affect microtubule dynamics (Pamula et al., 2016; Ti et al., 2016; Ye et al., 2020).

Our systematic evaluation indicated that both the composition and position (N- or C-terminus) of the fused polypeptide are critical for the yield of functional human tubulin. To achieve optimal cleavage efficiency of the affinity tags, we incorporated a TEV-cleavable decahistidine tag with an Ala-Pro dipeptide linker to the N-terminus of human α1B-tubulin and a TEV-cleavable strep tag with a Gly-Gly-Ser-Gly-Gly pentapeptide linker to the C-terminus of human β2-and β3-tubulin (Ti et al., 2018; Ti et al., 2020). We note that the enzymatic digestion gets rid of the affinity tags but leaves residual 'scars' at the N-terminus of the α-tubulin (Gly-Ala-Pro) and the C-terminus of the β-tubulin (Glu-Asn-Leu-Tyr-Phe-Gln). We speculate that combining our approach with other protein engineering tools (e.g., protein ligation) will generate recombinant human tubulin with native sequence.

With these constructs, we recently developed an affinity chromatography-based purification strategy that allows the routine preparation of affinity tag-free recombinant human tubulin. As the sequential isolation of human α- and β-tubulin depends solely on the affinity tags, this approach applies to studies of tubulin variants (e.g., isotypes and mutants) that could impact the binding to TOG domains or the microtubule polymerization properties. By employing this strategy, current studies have revealed the effects of human β-tubulin isotypes on the microtubule stability and protofilament numbers (Ti et al., 2018) as well as dissected the molecular mechanisms by which methyltransferases modify human α-tubulin (Kearns et al., 2021). Together, the ability to obtain biochemically pure higher eukaryotic tubulin has paved the way to deciphering the functions of tubulin diversity and a clearer understanding of microtubule biology.

CONCLUSION AND PERSPECTIVES

Tubulin protein biochemistry has been evolving since more than 50 years ago, when the colchicine-binding activity led to the isolation of the building blocks of endogenous microtubules (Borisy and Taylor, 1967; Shelanski and Taylor, 1967). With recently established affinity tag-based strategies of generating recombinant α/β-tubulin with defined primary sequences (**Figure 3**), it becomes feasible to correlate *in vivo* tubulin mutagenesis analyses with *in vitro* biochemical and biophysical characterization of mutant tubulin. This integrative approach is potentially applicable to the mutagenesis analysis of any tubulin isotype of interest for a mechanistic understanding of how tubulin diversity regulates cellular microtubule structures and functions.

The advances in tubulin protein biochemistry also provide opportunities to address some fundamental questions in microtubule biology by developing the needed tools such as 1) isotype-specific antibodies/nanobodies to characterize the spatial distribution of tubulin isotypes in cellular microtubules, 2) recombinant tubulin incorporated with a probe at a specific site for the identification of small molecules or protein binders targeting explicit tubulin isotypes, 3) engineered tubulin harboring defined modifications to investigate the crosstalk between tubulin isotypes and post-translation modifications (i.e., the tubulin code), and 4) small molecules targeting tubulin isotypes of interest not only for dissecting the biological functions but also for novel chemotherapeutic agents. By combining recombinant tubulin with a chemical biology toolbox for protein engineering (e.g., amber suppression and protein ligation), these technology breakthroughs will expand our ability to tackle the challenges in the field. We speculate that decades of research have set the stage to unveil the molecular basis of how cells establish and use the heterogeneous microtubule composition to facilitate the functional outputs.

AUTHOR CONTRIBUTIONS

S-CT prepared the manuscript and secured the funding that supported this research.

ACKNOWLEDGMENTS

We are grateful for the support from the Research Grants Council of Hong Kong (ECS 27124120 and GRF 17118421) and the University of Hong Kong (Seed Fund 201909185025, 202010160017, and 202011159046).

REFERENCES

Al-Bassam, J., Larsen, N. A., Hyman, A. A., and Harrison, S. C. (2007). Crystal Structure of a TOG Domain: Conserved Features of XMAP215/Dis1-Family TOG Domains and Implications for Tubulin Binding. *Structure* 15, 355–362. doi:10.1016/j.str.2007.01.012

Al-Bassam, J., van Breugel, M., Harrison, S. C., and Hyman, A. (2006). Stu2p Binds Tubulin and Undergoes an Open-To-Closed Conformational Change. *J. Cel Biol* 172, 1009–1022. doi:10.1083/jcb.200511010

Alonso, M. C., Drummond, D. R., Kain, S., Hoeng, J., Amos, L., and Cross, R. A. (2007). An ATP Gate Controls Tubulin Binding by the Tethered Head of Kinesin-1. *Science* 316, 120–123. doi:10.1126/science.1136985

Alper, J. D., Decker, F., Agana, B., and Howard, J. (2014). The Motility of Axonemal Dynein Is Regulated by the Tubulin Code. *Biophysical J.* 107, 2872–2880. doi:10.1016/j.bpj.2014.10.061

Alper, J. D., Tovar, M., and Howard, J. (2013b). Displacement-weighted Velocity Analysis of Gliding Assays Reveals that Chlamydomonas Axonemal Dynein Preferentially Moves Conspecific Microtubules. *Biophysical J.* 104, 1989–1998. doi:10.1016/j.bpj.2013.03.041

Alper, J., Geyer, V., Mukundan, V., and Howard, J. (2013a). Reconstitution of Flagellar Sliding. *Methods Enzymol.* 524, 343–369. doi:10.1016/b978-0-12-397945-2.00019-6

Arellano-Santoyo, H., Geyer, E. A., Stokasimov, E., Chen, G.-Y., Su, X., Hancock, W., et al. (2017). A Tubulin Binding Switch Underlies Kip3/Kinesin-8 Depolymerase Activity. *Develop. Cel* 42, 37–51. doi:10.1016/j.devcel.2017.06.011

Atherton, J., Luo, Y., Xiang, S., Yang, C., Rai, A., Jiang, K., et al. (2019). Structural Determinants of Microtubule Minus End Preference in CAMSAP CKK Domains. *Nat. Commun.* 10, 5236. doi:10.1038/s41467-019-13247-6

Ayaz, P., Munyoki, S., Geyer, E. A., Piedra, F. A., Vu, E. S., Bromberg, R., et al. (2014). A Tethered Delivery Mechanism Explains the Catalytic Action of a Microtubule Polymerase. *Elife* 3, e03069. doi:10.7554/eLife.03069

Ayaz, P., Ye, X., Huddleston, P., Brautigam, C. A., and Rice, L. M. (2012). A TOG: αβ-tubulin Complex Structure Reveals Conformation-Based Mechanisms for a Microtubule Polymerase. *Science* 337, 857–860. doi:10.1126/science.1221698

Ayukawa, R., Iwata, S., Imai, H., Kamimura, S., Hayashi, M., Ngo, K. X., et al. (2021). GTP-dependent Formation of Straight Tubulin Oligomers Leads to Microtubule Nucleation. *J. Cel Biol* 220. doi:10.1083/jcb.202007033

Banerjee, A., and Luduena, R. F. (1992). Kinetics of Colchicine Binding to Purified Beta-Tubulin Isotypes from Bovine Brain. *J. Biol. Chem.* 267, 13335–13339. doi:10.1016/s0021-9258(18)42215-6

Banerjee, A., Roach, M. C., Trcka, P., and Ludueña, R. F. (1990). Increased Microtubule Assembly in Bovine Brain Tubulin Lacking the Type III Isotype of Beta-Tubulin. *J. Biol. Chem.* 265, 1794–1799. doi:10.1016/s0021-9258(19)40087-2

Banerjee, A., Roach, M. C., Trcka, P., and Luduena, R. F. (1992). Preparation of a Monoclonal Antibody Specific for the Class IV Isotype of Beta-Tubulin. Purification and Assembly of Alpha Beta II, Alpha Beta III, and Alpha Beta IV Tubulin Dimers from Bovine Brain. *J. Biol. Chem.* 267, 5625–5630. doi:10.1016/s0021-9258(18)42811-6

Banerjee, A., Roach, M. C., Wall, K. A., Lopata, M. A., Cleveland, D. W., and Ludueña, R. F. (1988). A Monoclonal Antibody against the Type II Isotype of Beta-Tubulin. Preparation of Isotypically Altered Tubulin. *J. Biol. Chem.* 263, 3029–3034. doi:10.1016/s0021-9258(18)69171-9

Barnes, G., Louie, K. A., and Botstein, D. (1992). Yeast Proteins Associated with Microtubules *In Vitro* and *In Vivo*. *MBoC* 3, 29–47. doi:10.1091/mbc.3.1.29

Behnke, O., and Forer, A. (1967). Evidence for Four Classes of Microtubules in Individual Cells. *J. Cel Sci* 2, 169–192. doi:10.1242/jcs.2.2.169

Ben-Ze'ev, A., Farmer, S. R., and Penman, S. (1979). Mechanisms of Regulating Tubulin Synthesis in Cultured Mammalian Cells. *Cell* 17, 319–325. doi:10.1016/0092-8674(79)90157-0

Bhamidipati, A., Lewis, S. A., and Cowan, N. J. (2000). ADP Ribosylation Factor-like Protein 2 (Arl2) Regulates the Interaction of Tubulin-Folding Cofactor D with Native Tubulin. *J. Cel Biol* 149, 1087–1096. doi:10.1083/jcb.149.5.1087

Binder, L. I., and Rosenbaum, J. L. (1978). The *In Vitro* Assembly of Flagellar Outer Doublet Tubulin. *J. Cel Biol* 79, 500–515. doi:10.1083/jcb.79.2.500

Biswas, A., Kim, K., Cojoc, G., Guck, J., and Reber, S. (2021). The Xenopus Spindle Is as Dense as the Surrounding Cytoplasm. *Develop. Cel* 56, 967–975. doi:10.1016/j.devcel.2021.03.013

Bode, C. J., Gupta, M. L., Suprenant, K. A., and Himes, R. H. (2003). The Two α-tubulin Isotypes in Budding Yeast Have Opposing Effects on Microtubule Dynamics *In Vitro*. *EMBO Rep.* 4, 94–99. doi:10.1038/sj.embor.embor716

Borisy, G. G., Marcum, J. M., Olmsted, J. B., Murphy, D. B., and Johnson, K. A. (1975). Purification of Tubulin and Associated High Molecular Weight Proteins from Porcine Brain and Characterization of Microtubule Assembly *In Vitro*. *Ann. NY Acad. Sci.* 253, 107–132. doi:10.1111/j.1749-6632.1975.tb19196.x

Borisy, G. G., and Taylor, E. W. (1967). The Mechanism of Action of Colchicine. *J. Cel Biol* 34, 525–533. doi:10.1083/jcb.34.2.525

Braun, M., Drummond, D. R., Cross, R. A., and McAinsh, A. D. (2009). The Kinesin-14 Klp2 Organizes Microtubules into Parallel Bundles by an ATP-dependent Sorting Mechanism. *Nat. Cel Biol* 11, 724–730. doi:10.1038/ncb1878

Brouhard, G. J., Stear, J. H., Noetzel, T. L., Al-Bassam, J., Kinoshita, K., Harrison, S. C., et al. (2008). XMAP215 Is a Processive Microtubule Polymerase. *Cell* 132, 79–88. doi:10.1016/j.cell.2007.11.043

Bryan, J., and Wilson, L. (1971). Are Cytoplasmic Microtubules Heteropolymers? *Proc. Natl. Acad. Sci. U.S.A.* 68, 1762–1766. doi:10.1073/pnas.68.8.1762

Burke, D., Gasdaska, P., and Hartwell, L. (1989). Dominant Effects of Tubulin Overexpression in *Saccharomyces cerevisiae*. *Mol. Cel Biol* 9, 1049–1059. doi:10.1128/mcb.9.3.1049-1059.1989

Chaaban, S., Jariwala, S., Hsu, C.-T., Redemann, S., Kollman, J. M., Müller-Reichert, T., et al. (2018). The Structure and Dynamics of *C. elegans* Tubulin Reveals the Mechanistic Basis of Microtubule Growth. *Develop. Cel* 47, 191–204. doi:10.1016/j.devcel.2018.08.023

Cleveland, D. W. (1989). Autoregulated Control of Tubilin Synthesis in Animal Cells. *Curr. Opin. Cel Biol.* 1, 10–14. doi:10.1016/s0955-0674(89)80030-4

Cleveland, D. W., Hughes, S. H., Stubblefield, E., Kirschner, M. W., and Varmus, H. E. (1981a). Multiple Alpha and Beta Tubulin Genes Represent Unlinked and Dispersed Gene Families. *J. Biol. Chem.* 256, 3130–3134. doi:10.1016/s0021-9258(19)69734-6

Cleveland, D. W., Kirschner, M. W., and Cowan, N. J. (1978). Isolation of Separate mRNAs for α- and β-Tubulin and Characterization of the Corresponding *In Vitro* Translation Products. *Cell* 15, 1021–1031. doi:10.1016/0092-8674(78)90286-6

Cleveland, D. W., Lopata, M. A., MacDonald, R. J., Cowan, N. J., Rutter, W. J., and Kirschner, M. W. (1980). Number and Evolutionary Conservation of α- and β-tubulin and Cytoplasmic β- and γ-actin Genes Using Specific Cloned cDNA Probes. *Cell* 20, 95–105. doi:10.1016/0092-8674(80)90238-x

Cleveland, D. W., Lopata, M. A., Sherline, P., and Kirschner, M. W. (1981b). Unpolymerized Tubulin Modulates the Level of Tubulin mRNAs. *Cell* 25, 537–546. doi:10.1016/0092-8674(81)90072-6

Cleveland, D. W. (1987). The Multitubulin Hypothesis Revisited: what Have We Learned? *J. Cel Biol* 104, 381–383. doi:10.1083/jcb.104.3.381

Davis, A., Sage, C. R., Dougherty, C. A., and Farrell, K. W. (1994). Microtubule Dynamics Modulated by Guanosine Triphosphate Hydrolysis Activity of β-Tubulin. *Science* 264, 839–842. doi:10.1126/science.8171338

Davis, A., Sage, C. R., Wilson, L., and Farrell, K. W. (1993). Purification and Biochemical Characterization of Tubulin from the Budding Yeast *Saccharomyces cerevisiae*. *Biochemistry* 32, 8823–8835. doi:10.1021/bi00085a013

Dawson, P. J., Gutteridge, W. E., and Gull, K. (1983). Purification and Characterisation of Tubulin from the Parasitic Nematode, Ascaridia Galli. *Mol. Biochem. Parasitol.* 7, 267–277. doi:10.1016/0166-6851(83)90026-9

Denarier, E., Ecklund, K. H., Berthier, G., Favier, A., O'Toole, E. T., Gory-Fauré, S., et al. (2021). Modeling a Disease-Correlated Tubulin Mutation in Budding Yeast Reveals Insight into MAP-Mediated Dynein Function. *MBoC* 32, ar10. doi:10.1091/mbc.e21-05-0237

des Georges, A., Katsuki, M., Drummond, D. R., Osei, M., Cross, R. A., and Amos, L. A. (2008). Mal3, the *Schizosaccharomyces pombe* Homolog of EB1, Changes the Microtubule Lattice. *Nat. Struct. Mol. Biol.* 15, 1102–1108. doi:10.1038/nsmb.1482

Detrich, H. W., 3rd, Johnson, K. A., and Marchese-Ragona, S. P. (1989). Polymerization of Antarctic Fish Tubulins at Low Temperatures: Energetic Aspects. *Biochemistry* 28, 10085–10093. doi:10.1021/bi00452a031

Detrich, H. W., 3rd, and Overton, S. A. (1986). Heterogeneity and Structure of Brain Tubulins from Cold-Adapted Antarctic Fishes. Comparison to Brain Tubulins from a Temperate Fish and a Mammal. *J. Biol. Chem.* 261, 10922–10930. doi:10.1016/s0021-9258(18)67475-7

Detrich, H. W., 3rd, Parker, S. K., Williams, R. C., Jr., Nogales, E., and Downing, K. H. (2000). Cold Adaptation of Microtubule Assembly and Dynamics. *J. Biol. Chem.* 275, 37038–37047. doi:10.1074/jbc.m005699200

Detrich, H. W., 3rd, and Wilson, L. (1983). Purification, Characterization, and Assembly Properties of Tubulin from Unfertilized Eggs of the Sea Urchin *Strongylocentrotus purpuratus*. *Biochemistry* 22, 2453–2462. doi:10.1021/bi00279a023

Diao, L., Liu, M. Y., Song, Y. L., Zhang, X., Liang, X., and Bao, L. (2021). alpha1A and alpha1C Form Microtubules to Display Distinct Properties Mainly

Mediated by Their C-Terminal Tails. *J. Mol. Cel Biol* 13, 864. doi:10.1093/jmcb/mjab062

Doenges, K. H., Nagle, B. W., Uhlmann, A., and Bryan, J. (1977). *In Vitro* assembly of Tubulin from Nonneural Cells (Ehrlich Ascites Tumor Cells). *Biochemistry* 16, 3455–3459. doi:10.1021/bi00634a025

Doenges, K. H., Weissinger, M., Fritzsche, R., and Schroeter, D. (1979). Assembly of Nonneural Microtubules in the Absence of Glycerol and Microtubule-Associated Proteins. *Biochemistry* 18, 1698–1702. doi:10.1021/bi00576a010

Dougherty, C. A., Sage, C. R., Davis, A., and Farrell, K. W. (2001). Mutation in the β-Tubulin Signature Motif Suppresses Microtubule GTPase Activity and Dynamics, and Slows Mitosis. *Biochemistry* 40, 15725–15732. doi:10.1021/bi010070y

Driver, J. W., Geyer, E. A., Bailey, M. E., Rice, L. M., and Asbury, C. L. (2017). Direct Measurement of Conformational Strain Energy in Protofilaments Curling Outward from Disassembling Microtubule Tips. *Elife* 6. doi:10.7554/eLife.28433

Drummond, D. R., Kain, S., Newcombe, A., Hoey, C., Katsuki, M., and Cross, R. A. (2011). Purification of Tubulin from the Fission Yeast *Schizosaccharomyces pombe*. *Methods Mol. Biol.* 777, 29–55. doi:10.1007/978-1-61779-252-6_3

Edzuka, T., and Goshima, G. (2019). Drosophila Kinesin-8 Stabilizes the Kinetochore-Microtubule Interaction. *J. Cel Biol* 218, 474–488. doi:10.1083/jcb.201807077

Farrell, K. W., and Wilson, L. (1978). Microtubule Reassembly *In Vitro* of Strongylocentrotus, Purpuratus Sperm Tail Outer Doublet Tubulin. *J. Mol. Biol.* 121, 393–410. doi:10.1016/0022-2836(78)90371-6

Feit, H., Slusarek, L., and Shelanski, M. L. (1971). Heterogeneity of Tubulin Subunits. *Proc. Natl. Acad. Sci. U.S.A.* 68, 2028–2031. doi:10.1073/pnas.68.9.2028

Findeisen, P., Mühlhausen, S., Dempewolf, S., Hertzog, J., Zietlow, A., Carlomagno, T., et al. (2014). Six Subgroups and Extensive Recent Duplications Characterize the Evolution of the Eukaryotic Tubulin Protein Family. *Genome Biol. Evol.* 6, 2274–2288. doi:10.1093/gbe/evu187

Fujita, S., Pytela, J., Hotta, T., Kato, T., Hamada, T., Akamatsu, R., et al. (2013). An Atypical Tubulin Kinase Mediates Stress-Induced Microtubule Depolymerization in Arabidopsis. *Curr. Biol.* 23, 1969–1978. doi:10.1016/j.cub.2013.08.006

Fulton, C., and Simpson, P. A. (1976). Selective Synthesis and Utilization of Flagellar Tubulin. The Multi-Tubulin Hypothesis. *Cel Motil.* 3, 987–1005.

Gadadhar, S., Bodakuntla, S., Natarajan, K., and Janke, C. (2017). The Tubulin Code at a Glance. *J. Cel Sci* 130, 1347–1353. doi:10.1242/jcs.199471

Gall, J. G. (1966). Microtubule fine Structure. *J. Cel Biol* 31, 639–643. doi:10.1083/jcb.31.3.639

Gao, Y., Thomas, J. O., Chow, R. L., Lee, G.-H., and Cowan, N. J. (1992). A Cytoplasmic Chaperonin that Catalyzes β-actin Folding. *Cell* 69, 1043–1050. doi:10.1016/0092-8674(92)90622-j

Garnham, C. P., Vemu, A., Wilson-Kubalek, E. M., Yu, I., Szyk, A., Lander, G. C., et al. (2015). Multivalent Microtubule Recognition by Tubulin Tyrosine Ligase-like Family Glutamylases. *Cell* 161, 1112–1123. doi:10.1016/j.cell.2015.04.003

Garnham, C. P., Yu, I., Li, Y., and Roll-Mecak, A. (2017). Crystal Structure of Tubulin Tyrosine Ligase-like 3 Reveals Essential Architectural Elements Unique to Tubulin Monoglycylases. *Proc. Natl. Acad. Sci. U.S.A.* 114, 6545–6550. doi:10.1073/pnas.1617286114

Gasic, I., Boswell, S. A., and Mitchison, T. J. (2019). Tubulin mRNA Stability Is Sensitive to Change in Microtubule Dynamics Caused by Multiple Physiological and Toxic Cues. *Plos Biol.* 17, e3000225. doi:10.1371/journal.pbio.3000225

George, H. J., Misra, L., Field, D. J., and Lee, J. C. (1981). Polymorphism of Brain Tubulin. *Biochemistry* 20, 2402–2409. doi:10.1021/bi00512a006

Geyer, E. A., Burns, A., Lalonde, B. A., Ye, X., Piedra, F. A., Huffaker, T. C., et al. (2015). A Mutation Uncouples the Tubulin Conformational and GTPase Cycles, Revealing Allosteric Control of Microtubule Dynamics. *Elife* 4, e10113. doi:10.7554/eLife.10113

Geyer, E. A., Miller, M. P., Brautigam, C. A., Biggins, S., and Rice, L. M. (2018). Design Principles of a Microtubule Polymerase. *Elife* 7, e34574. doi:10.7554/eLife.34574

Gibbons, I. R., and Grimstone, A. V. (1960). On Flagellar Structure in Certain Flagellates. *J. Biophys. Biochem. Cytol.* 7, 697–716. doi:10.1083/jcb.7.4.697

Gibbons, I. R. (1963). Studies on the Protein Components of Cilia from Tetrahymena Pyriformis. *Proc. Natl. Acad. Sci. U.S.A.* 50, 1002–1010. doi:10.1073/pnas.50.5.1002

Gupta, M. L., Jr., Bode, C. J., Georg, G. I., and Himes, R. H. (2003). Understanding Tubulin-Taxol Interactions: Mutations that Impart Taxol Binding to Yeast Tubulin. *Proc. Natl. Acad. Sci. U.S.A.* 100, 6394–6397. doi:10.1073/pnas.1131967100

Gupta, M. L., Jr., Bode, C. J., Thrower, D. A., Pearson, C. G., Suprenant, K. A., Bloom, K. S., et al. (2002). β-Tubulin C354 Mutations that Severely Decrease Microtubule Dynamics Do Not Prevent Nuclear Migration in Yeast. *MBoC* 13, 2919–2932. doi:10.1091/mbc.e02-01-0003

Hibbel, A., Bogdanova, A., Mahamdeh, M., Jannasch, A., Storch, M., Schäffer, E., et al. (2015). Kinesin Kip2 Enhances Microtubule Growth *In Vitro* through Length-dependent Feedback on Polymerization and Catastrophe. *Elife* 4, e10542. doi:10.7554/eLife.10542

Hirst, W. G., Biswas, A., Mahalingan, K. K., and Reber, S. (2020). Differences in Intrinsic Tubulin Dynamic Properties Contribute to Spindle Length Control in Xenopus Species. *Curr. Biol.* 30, 2184–2190. e2185. doi:10.1016/j.cub.2020.03.067

Hirst, W. G., Fachet, D., Kuropka, B., Weise, C., Saliba, K. J., and Reber, S. (2022). Purification of Functional Plasmodium Falciparum Tubulin Allows for the Identification of Parasite-specific Microtubule Inhibitors. *Curr. Biol.* 32, 919. doi:10.1016/j.cub.2021.12.049

Hotta, T., Fujita, S., Uchimura, S., Noguchi, M., Demura, T., Muto, E., et al. (2016). Affinity Purification and Characterization of Functional Tubulin from Cell Suspension Cultures of Arabidopsis and Tobacco. *Plant Physiol.* 170, 1189–1205. doi:10.1104/pp.15.01173

Janke, C., and Chloë Bulinski, J. (2011). Post-translational Regulation of the Microtubule Cytoskeleton: Mechanisms and Functions. *Nat. Rev. Mol. Cel Biol* 12, 773–786. doi:10.1038/nrm3227

Janke, C., and Magiera, M. M. (2020). The Tubulin Code and its Role in Controlling Microtubule Properties and Functions. *Nat. Rev. Mol. Cel Biol* 21, 307–326. doi:10.1038/s41580-020-0214-3

Johnson, V., Ayaz, P., Huddleston, P., and Rice, L. M. (2011). Design, Overexpression, and Purification of Polymerization-Blocked Yeast αβ-Tubulin Mutants. *Biochemistry* 50, 8636–8644. doi:10.1021/bi2005174

Kearns, S., Mason, F. M., Rathmell, W. K., Park, I. Y., Walker, C., Verhey, K. J., et al. (2021). Molecular Determinants for α-tubulin Methylation by SETD2. *J. Biol. Chem.* 297, 100898. doi:10.1016/j.jbc.2021.100898

Keller, T. C., 3rd, Jemiolo, D. K., Burgess, W. H., and Rebhun, L. I. (1982). *Strongylocentrotus purpuratus* Spindle Tubulin. II. Characteristics of its Sensitivity to Ca++ and the Effects of Calmodulin Isolated from Bovine Brain and *S. purpuratus* Eggs. *J. Cel Biol* 93, 797–803. doi:10.1083/jcb.93.3.797

Kilmartin, J. V. (1981). Purification of Yeast Tubulin by Self-Assembly *In Vitro*. *Biochemistry* 20, 3629–3633. doi:10.1021/bi00515a050

Kleiner, R. E., Ti, S.-C., and Kapoor, T. M. (2013). Site-specific Chemistry on the Microtubule Polymer. *J. Am. Chem. Soc.* 135, 12520–12523. doi:10.1021/ja405199h

Kollman, J. M., Greenberg, C. H., Li, S., Moritz, M., Zelter, A., Fong, K. K., et al. (2015). Ring Closure Activates Yeast γTuRC for Species-specific Microtubule Nucleation. *Nat. Struct. Mol. Biol.* 22, 132–137. doi:10.1038/nsmb.2953

Krauhs, E., Little, M., Kempf, T., Hofer-Warbinek, R., Ade, W., and Ponstingl, H. (1981). Complete Amino Acid Sequence of Beta-Tubulin from Porcine Brain. *Proc. Natl. Acad. Sci. U.S.A.* 78, 4156–4160. doi:10.1073/pnas.78.7.4156

LaFrance, B. J., Roostalu, J., Henkin, G., Greber, B. J., Zhang, R., Normanno, D., et al. (2022). Structural Transitions in the GTP Cap Visualized by Cryo-Electron Microscopy of Catalytically Inactive Microtubules. *Proc. Natl. Acad. Sci. U S A.* 119, e2114994119. doi:10.1073/pnas.2114994119

Langford, G. M. (1978). *In Vitro* assembly of Dogfish Brain Tubulin and the Induction of Coiled Ribbon Polymers by Calcium. *Exp. Cel Res.* 111, 139–151. doi:10.1016/0014-4827(78)90244-6

Ledbetter, M. C., and Porter, K. R. (1963). A "Microtubule" in Plant Cell Fine Structure. *J. Cel Biol* 19, 239–250. doi:10.1083/jcb.19.1.239

Ledbetter, M. C., and Porter, K. R. (1964). Morphology of Microtubules of Plant Cell. *Science* 144, 872–874. doi:10.1126/science.144.3620.872

Lewis, S. A., Tian, G., and Cowan, N. J. (1997). The α- and β-tubulin Folding Pathways. *Trends Cell Biology* 7, 479–484. doi:10.1016/s0962-8924(97)01168-9

Lin, Z., Gasic, I., Chandrasekaran, V., Peters, N., Shao, S., Mitchison, T. J., et al. (2020). TTC5 Mediates Autoregulation of Tubulin via mRNA Degradation. *Science* 367, 100–104. doi:10.1126/science.aaz4352

Lopata, M. A., and Cleveland, D. W. (1987). *In Vivo* microtubules Are Copolymers of Available Beta-Tubulin Isotypes: Localization of Each of Six Vertebrate Beta-Tubulin Isotypes Using Polyclonal Antibodies Elicited by Synthetic Peptide Antigens. *J. Cel Biol* 105, 1707–1720. doi:10.1083/jcb.105.4.1707

Lu, Q., and Luduena, R. F. (1994). *In Vitro* analysis of Microtubule Assembly of Isotypically Pure Tubulin Dimers. Intrinsic Differences in the Assembly Properties of Alpha Beta II, Alpha Beta III, and Alpha Beta IV Tubulin Dimers in the Absence of Microtubule-Associated Proteins. *J. Biol. Chem.* 269, 2041–2047. doi:10.1016/s0021-9258(17)42132-6

Ludueña, R. F., and Banerjee, A. (2008). "The Isotypes of Tubulin," in *The Role of Microtubules in Cell Biology, Neurobiology, and Oncology*. Editor T. Fojo (Totowa, NJ, USA: Humana Press), 123–175.

Mahalingan, K. K., Keith Keenan, E., Strickland, M., Li, Y., Liu, Y., Ball, H. L., et al. (2020). Structural Basis for Polyglutamate Chain Initiation and Elongation by TTLL Family Enzymes. *Nat. Struct. Mol. Biol.* 27, 802–813. doi:10.1038/s41594-020-0462-0

Majumdar, S., Kim, T., Chen, Z., Munyoki, S., Tso, S.-C., Brautigam, C. A., et al. (2018). An Isolated CLASP TOG Domain Suppresses Microtubule Catastrophe and Promotes rescue. *MBoC* 29, 1359–1375. doi:10.1091/mbc.e17-12-0748

Mickolajczyk, K. J., Geyer, E. A., Kim, T., Rice, L. M., and Hancock, W. O. (2019). Direct Observation of Individual Tubulin Dimers Binding to Growing Microtubules. *Proc. Natl. Acad. Sci. U.S.A.* 116, 7314–7322. doi:10.1073/pnas.1815823116

Minoura, I., Hachikubo, Y., Yamakita, Y., Takazaki, H., Ayukawa, R., Uchimura, S., et al. (2013). Overexpression, Purification, and Functional Analysis of Recombinant Human Tubulin Dimer. *FEBS Lett.* 587, 3450–3455. doi:10.1016/j.febslet.2013.08.032

Minoura, I., Takazaki, H., Ayukawa, R., Saruta, C., Hachikubo, Y., Uchimura, S., et al. (2016). Reversal of Axonal Growth Defects in an Extraocular Fibrosis Model by Engineering the Kinesin-Microtubule Interface. *Nat. Commun.* 7, 10058. doi:10.1038/ncomms10058

Mohri, H. (1968). Amino-acid Composition of "Tubulin" Constituting Microtubules of Sperm Flagella. *Nature* 217, 1053–1054. doi:10.1038/2171053a0

Moriwaki, T., and Goshima, G. (2016). Five Factors Can Reconstitute All Three Phases of Microtubule Polymerization Dynamics. *J. Cel Biol* 215, 357–368. doi:10.1083/jcb.201604118

Nagle, B. W., Doenges, K. H., and Bryan, J. (1977). Assembly of Tubulin from Cultured Cells and Comparison with the Neurotubulin Model. *Cell* 12, 573–586. doi:10.1016/0092-8674(77)90258-6

Newton, C. N., DeLuca, J. G., Himes, R. H., Miller, H. P., Jordan, M. A., and Wilson, L. (2002). Intrinsically Slow Dynamic Instability of HeLa Cell Microtubules *In Vitro*. *J. Biol. Chem.* 277, 42456–42462. doi:10.1074/jbc.m207134200

Nogales, E. (2000). Structural Insights into Microtubule Function. *Annu. Rev. Biochem.* 69, 277–302. doi:10.1146/annurev.biochem.69.1.277

Olmsted, J. B., Witman, G. B., Carlson, K., and Rosenbaum, J. L. (1971). Comparison of the Microtubule Proteins of Neuroblastoma Cells, Brain, and Chlamydomonas Flagella. *Proc. Natl. Acad. Sci. U.S.A.* 68, 2273–2277. doi:10.1073/pnas.68.9.2273

Otani, K., Ishizaki, K., Nishihama, R., Takatani, S., Kohchi, T., Takahashi, T., et al. (2018). An Evolutionarily Conserved NIMA-Related Kinase Directs Rhizoid Tip Growth in the Basal Land Plant Marchantia Polymorpha. *Development* 145, 154617. doi:10.1242/dev.154617

Pamula, M. C., Ti, S.-C., and Kapoor, T. M. (2016). The Structured Core of Human β Tubulin Confers Isotype-specific Polymerization Properties. *J. Cel Biol* 213, 425–433. doi:10.1083/jcb.201603050

Panda, D., Miller, H. P., Banerjee, A., Ludueña, R. F., and Wilson, L. (1994). Microtubule Dynamics *In Vitro* Are Regulated by the Tubulin Isotype Composition. *Proc. Natl. Acad. Sci. U.S.A.* 91, 11358–11362. doi:10.1073/pnas.91.24.11358

Park, K., Hoff, K. J., Wethekam, L., Stence, N., Saenz, M., and Moore, J. K. (2021). Kinetically Stabilizing Mutations in Beta Tubulins Create Isotype-specific Brain Malformations. *Front. Cel Dev. Biol.* 9, 765992. doi:10.3389/fcell.2021.765992

Pease, D. C. (1963). The Ultrastructure of Flagellar Fibrils. *J. Cel Biol* 18, 313–326. doi:10.1083/jcb.18.2.313

Pham, C. L., and Morrissette, N. S. (2019). The Tubulin Mutation Database: A Resource for the Cytoskeleton Community. *Cytoskeleton* 76, 186–191. doi:10.1002/cm.21514

Phillips, D. M. (1966). Substructure of Flagellar Tubules. *J. Cel Biol* 31, 635–638. doi:10.1083/jcb.31.3.635

Piedra, F.-A., Kim, T., Garza, E. S., Geyer, E. A., Burns, A., Ye, X., et al. (2016). GDP-to-GTP Exchange on the Microtubule End Can Contribute to the Frequency of Catastrophe. *MBoC* 27, 3515–3525. doi:10.1091/mbc.e16-03-0199

Podolski, M., Mahamdeh, M., and Howard, J. (2014). Stu2, the Budding Yeast XMAP215/Dis1 Homolog, Promotes Assembly of Yeast Microtubules by Increasing Growth Rate and Decreasing Catastrophe Frequency. *J. Biol. Chem.* 289, 28087–28093. doi:10.1074/jbc.m114.584300

Ponstingl, H., Krauhs, E., Little, M., and Kempf, T. (1981). Complete Amino Acid Sequence of Alpha-Tubulin from Porcine Brain. *Proc. Natl. Acad. Sci. U.S.A.* 78, 2757–2761. doi:10.1073/pnas.78.5.2757

Pratt, L. F., Okamura, S., and Cleveland, D. W. (1987). A Divergent Testis-specific Alpha-Tubulin Isotype that Does Not Contain a Coded C-Terminal Tyrosine. *Mol. Cel. Biol.* 7, 552–555. doi:10.1128/mcb.7.1.552

Renaud, F. L., Rowe, A. J., and Gibbons, I. R. (1968). Some Properties of the Protein Forming the Outer Fibers of Cilia. *J. Cel Biol* 36, 79–90. doi:10.1083/jcb.36.1.79

Roostalu, J., Thomas, C., Cade, N. I., Kunzelmann, S., Taylor, I. A., and Surrey, T. (2020). The Speed of GTP Hydrolysis Determines GTP Cap Size and Controls Microtubule Stability. *Elife* 9, e51992. doi:10.7554/eLife.51992

Rostovtseva, T. K., Gurnev, P. A., Hoogerheide, D. P., Rovini, A., Sirajuddin, M., and Bezrukov, S. M. (2018). Sequence Diversity of Tubulin Isotypes in Regulation of the Mitochondrial Voltage-dependent Anion Channel. *J. Biol. Chem.* 293, 10949–10962. doi:10.1074/jbc.ra117.001569

Sánchez, F., Natzle, J. E., Cleveland, D. W., Kirschner, M. W., and McCarthy, B. J. (1980). A Dispersed Multigene Family Encoding Tubulin in *Drosophila melanogaster*. *Cell* 22, 845–854. doi:10.1016/0092-8674(80)90561-9

Shelanski, M. L., Gaskin, F., and Cantor, C. R. (1973). Microtubule Assembly in the Absence of Added Nucleotides. *Proc. Natl. Acad. Sci. U.S.A.* 70, 765–768. doi:10.1073/pnas.70.3.765

Shelanski, M. L., and Taylor, E. W. (1967). Isolation of a Protein Subunit from Microtubules. *J. Cel Biol* 34, 549–554. doi:10.1083/jcb.34.2.549

Shelanski, M. L., and Taylor, E. W. (1968). Properties of the Protein Subunit of central-pair and Outer-Doublet Microtubules of Sea Urchin Flagella. *J. Cel Biol* 38, 304–315. doi:10.1083/jcb.38.2.304

Sirajuddin, M., Rice, L. M., and Vale, R. D. (2014). Regulation of Microtubule Motors by Tubulin Isotypes and post-translational Modifications. *Nat. Cel Biol* 16, 335–344. doi:10.1038/ncb2920

Slautterback, D. B. (1963). Cytoplasmic Microtubules. *J. Cel Biol* 18, 367–388. doi:10.1083/jcb.18.2.367

Souphron, J., Bodakuntla, S., Jijumon, A. S., Lakisic, G., Gautreau, A. M., Janke, C., et al. (2019). Purification of Tubulin with Controlled post-translational Modifications by Polymerization-Depolymerization Cycles. *Nat. Protoc.* 14, 1634–1660. doi:10.1038/s41596-019-0153-7

Stephens, R. E., Renaud, F. L., Gibbons, I. R., and Stevens, R. E. (1967). Guanine Nucleotide Associated with the Protein of the Outer Fibers of Flagella and Cilia. *Science* 156, 1606–1608. doi:10.1126/science.156.3782.1606

Stephens, R. E. (1970). Thermal Fractionation of Outer Fiber Doublet Microtubules into A- and B-Subfiber Components: A- and B-Tubulin. *J. Mol. Biol.* 47, 353–363. doi:10.1016/0022-2836(70)90307-4

Sullivan, K. F., and Cleveland, D. W. (1986). Identification of Conserved Isotype-Defining Variable Region Sequences for Four Vertebrate Beta Tubulin Polypeptide Classes. *Proc. Natl. Acad. Sci. U.S.A.* 83, 4327–4331. doi:10.1073/pnas.83.12.4327

Sullivan, K. F. (1988). Structure and Utilization of Tubulin Isotypes. *Annu. Rev. Cel. Biol.* 4, 687–716. doi:10.1146/annurev.cb.04.110188.003351

Suprenant, K. A., and Rebhun, L. I. (1984). Purification and Characterization of Oocyte Cytoplasmic Tubulin and Meiotic Spindle Tubulin of the Surf Clam *Spisula solidissima*. *J. Cel Biol* 98, 253–266. doi:10.1083/jcb.98.1.253

Taylor, E. W. (1965). The Mechanism of Colchicine Inhibition of Mitosis. I. Kinetics of Inhibition and the Binding of H3-Colchicine. *J. Cel Biol* 25 (Suppl. l), 145–160. doi:10.1083/jcb.25.1.145

Theodorakis, N. G., and Cleveland, D. W. (1992). Physical Evidence for Cotranslational Regulation of Beta-Tubulin mRNA Degradation. *Mol. Cel. Biol.* 12, 791–799. doi:10.1128/mcb.12.2.791

Ti, S.-C., Alushin, G. M., and Kapoor, T. M. (2018). Human β-Tubulin Isotypes Can Regulate Microtubule Protofilament Number and Stability. *Develop. Cel* 47, 175–190. e175. doi:10.1016/j.devcel.2018.08.014

Ti, S.-C., Pamula, M. C., Howes, S. C., Duellberg, C., Cade, N. I., Kleiner, R. E., et al. (2016). Mutations in Human Tubulin Proximal to the Kinesin-Binding Site Alter Dynamic Instability at Microtubule Plus- and Minus-Ends. *Develop. Cel* 37, 72–84. doi:10.1016/j.devcel.2016.03.003

Ti, S. C., Wieczorek, M., and Kapoor, T. M. (2020). Purification of Affinity Tag-free Recombinant Tubulin from Insect Cells. *STAR Protoc.* 1, 100011. doi:10.1016/j.xpro.2019.100011

Tian, G., Huang, Y., Rommelaere, H., Vandekerckhove, J., Ampe, C., and Cowan, N. J. (1996). Pathway Leading to Correctly Folded β-Tubulin. *Cell* 86, 287–296. doi:10.1016/s0092-8674(00)80100-2

Tian, G., Lewis, S. A., Feierbach, B., Stearns, T., Rommelaere, H., Ampe, C., et al. (1997). Tubulin Subunits Exist in an Activated Conformational State Generated and Maintained by Protein Cofactors. *J. Cel Biol* 138, 821–832. doi:10.1083/jcb.138.4.821

Uchimura, S., Oguchi, Y., Hachikubo, Y., Ishiwata, S. i., and Muto, E. (2010). Key Residues on Microtubule Responsible for Activation of Kinesin ATPase. *EMBO J.* 29, 1167–1175. doi:10.1038/emboj.2010.25

Uchimura, S., Oguchi, Y., Katsuki, M., Usui, T., Osada, H., Nikawa, J.-i., et al. (2006). Identification of a strong Binding Site for Kinesin on the Microtubule Using Mutant Analysis of Tubulin. *EMBO J.* 25, 5932–5941. doi:10.1038/sj.emboj.7601442

Vainberg, I. E., Lewis, S. A., Rommelaere, H., Ampe, C., Vandekerckhove, J., Klein, H. L., et al. (1998). Prefoldin, a Chaperone that Delivers Unfolded Proteins to Cytosolic Chaperonin. *Cell* 93, 863–873. doi:10.1016/s0092-8674(00)81446-4

Valenstein, M. L., and Roll-Mecak, A. (2016). Graded Control of Microtubule Severing by Tubulin Glutamylation. *Cell* 164, 911–921. doi:10.1016/j.cell.2016.01.019

Vemu, A., Szczesna, E., Zehr, E. A., Spector, J. O., Grigorieff, N., Deaconescu, A. M., et al. (2018). Severing Enzymes Amplify Microtubule Arrays through Lattice GTP-Tubulin Incorporation. *Science* 361, 1504. doi:10.1126/science.aau1504

Vemu, A., Atherton, J., Spector, J. O., Moores, C. A., and Roll-Mecak, A. (2017). Tubulin Isoform Composition Tunes Microtubule Dynamics. *MBoC* 28, 3564–3572. doi:10.1091/mbc.e17-02-0124

Vemu, A., Atherton, J., Spector, J. O., Szyk, A., Moores, C. A., and Roll-Mecak, A. (2016). Structure and Dynamics of Single-Isoform Recombinant Neuronal Human Tubulin. *J. Biol. Chem.* 291, 12907–12915. doi:10.1074/jbc.c116.731133

Vemu, A., Garnham, C. P., Lee, D.-Y., and Roll-Mecak, A. (2014). Generation of Differentially Modified Microtubules Using *In Vitro* Enzymatic Approaches. *Methods Enzymol.* 540, 149–166. doi:10.1016/b978-0-12-397924-7.00009-1

Verhey, K. J., and Gaertig, J. (2007). The Tubulin Code. *Cell Cycle* 6, 2152–2160. doi:10.4161/cc.6.17.4633

Villasante, A., Wang, D., Dobner, P., Dolph, P., Lewis, S. A., and Cowan, N. J. (1986). Six Mouse Alpha-Tubulin mRNAs Encode Five Distinct Isotypes: Testis-specific Expression of Two Sister Genes. *Mol. Cel. Biol.* 6, 2409–2419. doi:10.1128/mcb.6.7.2409

von Loeffelholz, O., Peña, A., Drummond, D. R., Cross, R., and Moores, C. A. (2019). Cryo-EM Structure (4.5-Å) of Yeast Kinesin-5-Microtubule Complex Reveals a Distinct Binding Footprint and Mechanism of Drug Resistance. *J. Mol. Biol.* 431, 864–872. doi:10.1016/j.jmb.2019.01.011

von Loeffelholz, O., Venables, N. A., Drummond, D. R., Katsuki, M., Cross, R., and Moores, C. A. (2017). Nucleotide- and Mal3-dependent Changes in Fission Yeast Microtubules Suggest a Structural Plasticity View of Dynamics. *Nat. Commun.* 8, 2110. doi:10.1038/s41467-017-02241-5

Wang, D., Villasante, A., Lewis, S. A., and Cowan, N. J. (1986). The Mammalian Beta-Tubulin Repertoire: Hematopoietic Expression of a Novel, Heterologous Beta-Tubulin Isotype. *J. Cel Biol* 103, 1903–1910. doi:10.1083/jcb.103.5.1903

Weatherbee, J. A., Luftig, R. B., and Weihing, R. R. (1978). *In Vitro* polymerization of Microtubules from HeLa Cells. *J. Cel Biol* 78, 47–57. doi:10.1083/jcb.78.1.47

Weber, K., Koch, R., Herzog, W., and Vandekerckhove, J. (1977). The Isolation of Tubulin and Actin from Mouse 3T3 Cells Transformed by Simian Virus 40 (SV3T3 Cells), an Established Cell Line Growing in Culture. *Eur. J. Biochem.* 78, 27–32. doi:10.1111/j.1432-1033.1977.tb11710.x

Weingarten, M. D., Lockwood, A. H., Hwo, S. Y., and Kirschner, M. W. (1975). A Protein Factor Essential for Microtubule Assembly. *Proc. Natl. Acad. Sci. U.S.A.* 72, 1858–1862. doi:10.1073/pnas.72.5.1858

Weisenberg, R. C., Broisy, G. G., and Taylor, E. W. (1968). Colchicine-binding Protein of Mammalian Brain and its Relation to Microtubules. *Biochemistry* 7, 4466–4479. doi:10.1021/bi00852a043

Weisenberg, R. C. (1972). Microtubule Formation *In Vitro* in Solutions Containing Low Calcium Concentrations. *Science* 177, 1104–1105. doi:10.1126/science.177.4054.1104

Widlund, P. O., Podolski, M., Reber, S., Alper, J., Storch, M., Hyman, A. A., et al. (2012). One-step Purification of Assembly-Competent Tubulin from Diverse Eukaryotic Sources. *MBoC* 23, 4393–4401. doi:10.1091/mbc.e12-06-0444

Widlund, P. O., Stear, J. H., Pozniakovsky, A., Zanic, M., Reber, S., Brouhard, G. J., et al. (2011). XMAP215 Polymerase Activity Is Built by Combining Multiple Tubulin-Binding TOG Domains and a Basic Lattice-Binding Region. *Proc. Natl. Acad. Sci. U.S.A.* 108, 2741–2746. doi:10.1073/pnas.1016498108

Williams, R. C., Jr., Correia, J. J., and De Vries, A. L. (1985). Formation of Microtubules at Low Temperature by Tubulin from Antarctic Fish. *Biochemistry* 24, 2790–2798. doi:10.1021/bi00332a029

Wilson, P. G., and Borisy, G. G. (1997). Evolution of the Multi-Tubulin Hypothesis. *Bioessays* 19, 451–454. doi:10.1002/bies.950190603

Yaffe, M. B., Farr, G. W., Miklos, D., Horwich, A. L., Sternlicht, M. L., and Sternlicht, H. (1992). TCP1 Complex Is a Molecular Chaperone in Tubulin Biogenesis. *Nature* 358, 245–248. doi:10.1038/358245a0

Ye, X., Kim, T., Geyer, E. A., and Rice, L. M. (2020). Insights into Allosteric Control of Microtubule Dynamics from a Buried β-tubulin Mutation that Causes Faster Growth and Slower Shrinkage. *Protein Sci.* 29, 1429–1439. doi:10.1002/pro.3842

Yen, T. J., Machlin, P. S., and Cleveland, D. W. (1988). Autoregulated Instability of β-tubulin mRNAs by Recognition of the Nascent Amino Terminus of βtubulin. *Nature* 334, 580–585. doi:10.1038/334580a0

Yoon, Y., and Oakley, B. R. (1995). Purification and Characterization of Assembly-Competent Tubulin from Aspergillus nidulans. *Biochemistry* 34, 6373–6381. doi:10.1021/bi00019a016

Yu, N., and Galjart, N. (2018). TAPping into the Treasures of Tubulin Using Novel Protein Production Methods. *Essays Biochem.* 62, 781–792. doi:10.1042/ebc20180033

Yu, N., Signorile, L., Basu, S., Ottema, S., Lebbink, J. H. G., Leslie, K., et al. (2016). Isolation of Functional Tubulin Dimers and of Tubulin-Associated Proteins from Mammalian Cells. *Curr. Biol.* 26, 1728–1736. doi:10.1016/j.cub.2016.04.069

Zheng, P., Obara, C. J., Szczesna, E., Nixon-Abell, J., Mahalingan, K. K., Roll-Mecak, A., et al. (2022). ER Proteins Decipher the Tubulin Code to Regulate Organelle Distribution. *Nature* 601, 132–138. doi:10.1038/s41586-021-04204-9

Conflict of Interest: The authors declare that the research was conducted in the absence of any commercial or financial relationships that could be construed as a potential conflict of interest.

frontiers | Frontiers in Cell and Developmental Biology

REVIEW
published: 28 April 2022
doi: 10.3389/fcell.2022.851542

βIII-Tubulin Gene Regulation in Health and Disease

Alastair M. P. Duly[1†], *Felicity C. L. Kao*[1,2,3†], *Wee Siang Teo*[1,2] *and Maria Kavallaris*[1,2,3,4*]

[1]*Children's Cancer Institute, Lowy Cancer Research Center, UNSW Sydney, Randwick, NSW, Australia,* [2]*Australian Center for NanoMedicine, UNSW Sydney, Sydney, NSW, Australia,* [3]*School of Women and Children's Health, Faculty of Medicine and Health, UNSW Sydney, Sydney, NSW, Australia,* [4]*UNSW RNA Institute, UNSW Sydney, Sydney, NSW, Australia*

Microtubule proteins form a dynamic component of the cytoskeleton, and play key roles in cellular processes, such as vesicular transport, cell motility and mitosis. Expression of microtubule proteins are often dysregulated in cancer. In particular, the microtubule protein βIII-tubulin, encoded by the *TUBB3* gene, is aberrantly expressed in a range of epithelial tumours and is associated with drug resistance and aggressive disease. In normal cells, *TUBB3* expression is tightly restricted, and is found almost exclusively in neuronal and testicular tissues. Understanding the mechanisms that control *TUBB3* expression, both in cancer, mature and developing tissues will help to unravel the basic biology of the protein, its role in cancer, and may ultimately lead to the development of new therapeutic approaches to target this protein. This review is devoted to the transcriptional and posttranscriptional regulation of *TUBB3* in normal and cancerous tissue.

Keywords: *TUBB3*, βIII-tubulin, microtubule, gene regulation, cancer, neuronal tubulin, tubulin, human

OPEN ACCESS

Edited by:
Jack Adam Tuszynski,
University of Alberta, Canada

Reviewed by:
Pavel Draber,
Institute of Molecular Genetics (ASCR), Czechia
Paraskevi Giannakakou,
Weill Cornell Medicine, United States

***Correspondence:**
Maria Kavallaris
m.kavallaris@ccia.unsw.edu.au

†These authors have contributed equally to this work

Specialty section:
This article was submitted to Cellular Biochemistry, a section of the journal Frontiers in Cell and Developmental Biology

Received: *10 January 2022*
Accepted: *07 April 2022*
Published: *28 April 2022*

Citation:
Duly AMP, Kao FCL, Teo WS and Kavallaris M (2022) βIII-Tubulin Gene Regulation in Health and Disease. Front. Cell Dev. Biol. 10:851542. doi: 10.3389/fcell.2022.851542

1 INTRODUCTION

Microtubules are one of the major constituents of the cell cytoskeleton and are made up of α- and β-tubulin heterodimers. Microtubules are highly dynamic filament structures that play critical roles in cellular processes, including vesicular transport, cell motility and mitosis. The α/β-tubulin heterodimers are made up of combinations of the different α- and β-tubulin isotypes (reviewed in Nogales 2000), of which in humans there are currently eight and seven different α- and β-tubulin isotypes, respectively (reviewed in Ludueña 2013). Each of the isotypes are encoded by a different gene and display different tissue and developmental stage expression (reviewed in Ludueña 1993; Verdier-Pinard et al., 2009). While each isotype shares high degrees of structural homology with each other, they have some differences at the peptide sequence level, specifically at their carboxy-terminal tails (Sullivan and Cleveland 1986). Sequence variations within the carboxy-terminal tails of various tubulin isotypes, have been demonstrated to regulate the dynamic assembly and disassembly of microtubule structures (Parker et al., 2018).

A strong interest exists for studying microtubules due to their importance as a target for anticancer therapies. Drugs targeting microtubules and microtubule dynamics are widely used in many cancer therapeutic regimens (reviewed in Jordan and Wilson 2004; La Regina et al., 2019). Clinically relevant Tubulin-Binding Agents (TBAs) such as the taxanes, vinca alkaloids, epothilones, and Eribulin, all bind to the β-tubulin subunits of the αβ-heterodimers (reviewed in Jordan and Wilson 2004; La Regina et al., 2019). These agents disrupt normal mitotic spindle function, block the metaphase to anaphase transition of the cell cycle, and induce mitotic arrest and cell death (reviewed in Jordan and Wilson 2004; La Regina et al., 2019). Despite the clinical success of TBAs and advances in chemotherapies, the persistent emergence of drug resistance largely hinders their clinical utility and is the primary cause of treatment failure for many cancers. Mechanisms mediating TBA

resistance can occur at multiple levels (reviewed in Kavallaris, 2010; Katsetos and Draber, 2012; Parker et al., 2017). Previous studies have reported that altered expression of specific β-tubulin isotypes is strongly associated with resistance to TBAs (Kavallaris et al., 1997; Ranganathan et al., 1998a; Kavallaris et al., 1999). Of note, one particular isotype, βIII-tubulin, encoded by the *TUBB3* gene, has demonstrated aberrant expression in the clinical setting, and has been identified as a marker of drug resistance and tumour aggressiveness in a sub-set of epithelial cancers (reviewed in Kavallaris, 2010; Karki et al., 2013; Mariani et al., 2015). In addition, there is clinical evidence in lung, ovarian, glioblastoma, and breast cancer, that patients with aberrant βIII-tubulin expression exhibit poorly differentiated tumour tissue, high grade malignancy, shorter disease progression, unfavourable prognosis and worse overall survival (reviewed in Seve and Dumontet 2008; Kavallaris 2010; Katsetos et al., 2011; Katsetos et al., 2015; Mariani et al., 2015; Kanakkanthara and Miller 2021). Post-translational modifications to tubulin proteins, including βIII-tubulin, are found in normal tissue and cancer cells, and have been well described elsewhere (Ludueña 1998; Wattanathamsan and Pongrakhananon 2021; Bär et al., 2022).

Interest in βIII-tubulin is not limited to its expression in cancer. Expression of βIII-tubulin is also observed in the early stages of neurogenesis of fetal development (Caccamo et al., 1989; Lee et al., 1990b; Jiang and Oblinger 1992; Linhartová et al., 1992; Easter et al., 1993; Hausrat et al., 2021). βIII-tubulin itself is primarily thought of as a neuronal protein, observed in neurons and involved with neurogenesis and axonal growth (Caccamo et al., 1989; Jiang and Oblinger 1992; Easter et al., 1993; Tischfield et al., 2010; Latremoliere et al., 2018; Hausrat et al., 2021). This notion has been strengthened by the identification of mutations in *TUBB3*, the gene that encodes for βIII-tubulin, resulting in nervous system disorders such as Congenital Fibrosis of the Extraocular Muscles type 3 (CFEOM3), which combines the weakening of the extraocular muscles with intellectual disability, as well as axonal abnormalities and disorganisation of cortical neurons (Poirier et al., 2010; Tischfield et al., 2010). Evidence also suggests βIII-tubulin has roles outside of neurogenesis, such as the formation of neural crest cell formation (Haendel et al., 1996; Chacon and Rogers 2019) and recently, in the mineralisation stages of tooth development (Oshima and Yawaka 2020). As such, despite the original neuronal findings, βIII-tubulin expression is increasingly observed outside of neuronal tissue, with reports of adult stem cells expressing βIII-tubulin, such as melanocytes (Locher et al., 2013) and spermatogenic cells (Person et al., 2017). Additionally, the expression of βIII-tubulin in induced pluripotent stem cells has also been observed (Daily et al., 2017; Kuang et al., 2019). However, the role of βIII-tubulin in these cells remains unclear.

Despite the relevance of βIII-tubulin protein in development and cancer, there is limited information on the precise elements that regulate the gene expression of *TUBB3* in normal and cancerous human cells. This review will focus on the normal regulation of *TUBB3* transcription, the role of this gene in neurogenesis and development, and on factors contributing to the dysregulation of *TUBB3* expression in cancer and drivers of its aberrant expression. The review will present what is known and critically discuss gene regulatory elements including the drivers, or repressors, of *TUBB3* gene expression.

2 The Human *TUBB3* Gene Loci

Originally referred to as class III isotype β4, human βIII-tubulin was first identified in 1986 after being previously discovered in chickens a few years beforehand (Lopata et al., 1983; Sullivan and Cleveland 1986). At the time, the protein sequence of βIII-tubulin was found to be conserved across mammals, however, it was observed to be highly divergent from other β-tubulin isotypes in its carboxyl terminal region (Sullivan and Cleveland 1986). The sequence of the human βIII-tubulin gene *TUBB3* was not identified until much later, with the sequence of the more common mRNA variant being determined in 1998 (Ranganathan et al., 1998b), and its genomic location confirmed in 2010 (Tischfield et al., 2010). The *TUBB3* loci is present within the telomeric region of the long arm of chromosome 16 (Katsetos et al., 2002). Furthermore, up until 2010, *TUBB3* was also referred to as CFEOM3 when Doherty et al. (1999) first described the gene in Extraocular Congenital Fibrosis Syndrome and identified the chromosomal location of the gene through linkage analysis of DNA microsatellite markers. It was Tischfield et al. (2010) who then identified that CFEOM3 and *TUBB3* were one and the same after mapping eight different CFEOM3 causing mutations to *TUBB3*. *TUBB3* mutations are also seen and have been reported in tumours, however the impact of these mutations are unknown (reviewed in Kanakkanthara and Miller 2021).

The human *TUBB3* gene (NG_027810.1) is 21,089 bp in length and in a genomic context, the cytogenetic location of the gene is 16q24.3 on the plus strand (**Figure 1**). Within this locus, the Ensembl database reports that there are 15 unique *TUBB3* transcripts (**Table 1**), however only 2, referred to as variants 1 and 2, have been studied. This could be due to these two having a higher abundance of mRNA than the other transcripts, with several transcripts being predicted to undergo nonsense mediated decay (Cunningham et al., 2018), or the other transcripts exist as mere sequencing artifacts. Given that *TUBB3* is primarily expressed in neuronal tissue, it is possible that these alternative transcripts of *TUBB3* represent further specialised neuronal forms of the transcript, as neuronal tissue is known to have an expanded repertoire of gene expression and alternative splicing (The GTEx Consortium, 2015; Melé et al., 2015). *TUBB3* also has two pseudogenes, *TUBB3P1* and *TUBB3P2*. *TUBB3P1* the larger of the two is located on chromosome 6, while *TUBB3P2* is located on chromosome 7. It is unknown if these pseudogenes possess any functional capacity.

From the transcripts identified for *TUBB3*, there are two main points of commonality between all of them. Firstly, the majority of the identified *TUBB3* transcripts consist of four exons, and secondly, there are two exons that are present in the majority of transcripts (**Table 1**; **Figure 2**). In transcript variants 1 and 2, these two common exons are exons 2 and 3. These two particular exons also appear in the unusual read-through product of the upstream gene encoding for the G-coupled protein receptor melanocortin 1 receptor (MC1R), which results in the formation of an unusual chimeric MC1R protein featuring the βIII-tubulin carboxyl terminus that appears to attenuate MC1R

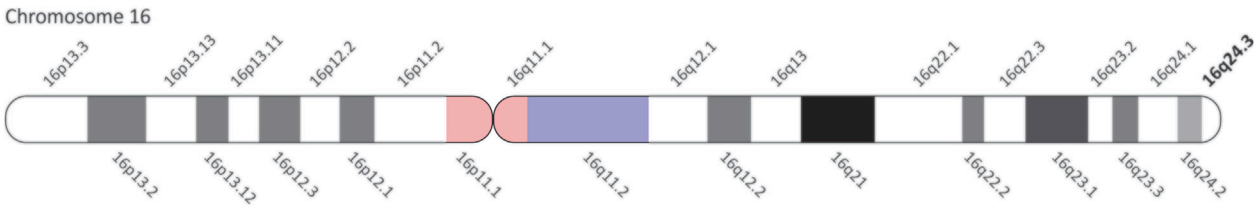

FIGURE 1 | Location of the human *TUBB3* loci. Cytogenetic map of chromosome 16 showing all regions. *TUBB3* is located within 16q24.3, located at the bottom of chromosome 16 (bolded).

TABLE 1 | All identified human *TUBB3* transcripts.

Transcript ID	Size (bp)	Biotype	Variant (NCBI)	RefSeq	Protein	UniProt
ENST00000315491.12	1,706	Protein coding	1	NM_006,086	450aa	Q13509
ENST00000553656.5	550	Nonsense mediated decay			51aa	G3V4U2
ENST00000553967.1	736	Protein coding			164aa	G3V2N6
ENST00000554116.5	542	Processed transcript			No protein	—
ENST00000554336.5	903	Protein coding			118aa	G3V2R8
ENST00000554444.5	1,978	Protein coding	2	NM_001,197,181	378aa	Q13509
ENST00000554927.1	561	Retained intron			No protein	—
ENST00000555576.5	572	Protein coding			97aa	G3V5W4
ENST00000555609.5	1,855	Nonsense mediated decay			55aa	G3V3J6
ENST00000555810.5	767	Protein coding			189aa	G3V2A3
ENST00000556536.5	925	Nonsense mediated decay			148aa	G3V3R4
ENST00000556565.5	566	Protein coding			46aa	G3V542
ENST00000557262.5	888	Nonsense mediated decay			51aa	G3V4U2
ENST00000557490.5	806	Nonsense mediated decay			87aa	G3V3W7
ENST00000625617.2	570	Protein coding			148aa	G3V3R4

Information sourced from Ensembl database (Cunningham et al., 2018).

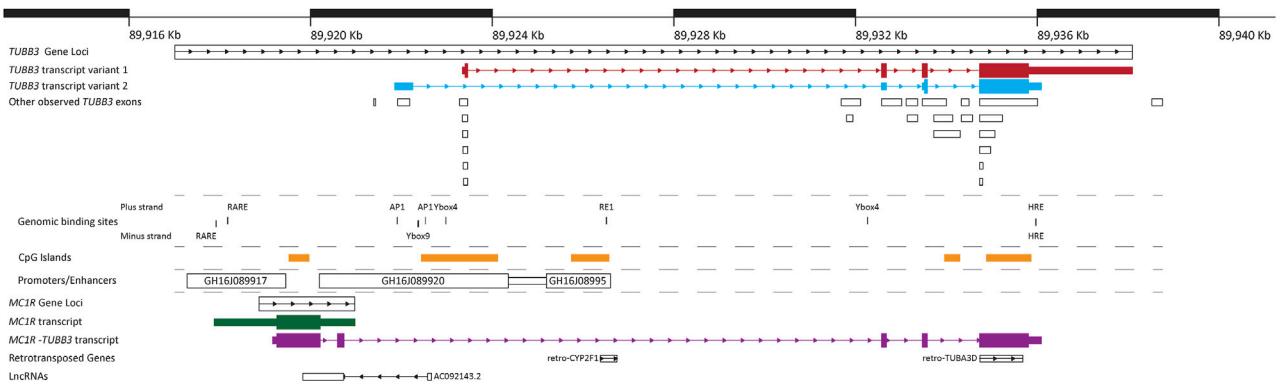

FIGURE 2 | Structure of the human *TUBB3* loci. A map of the human *TUBB3* loci showing the main two transcripts of *TUBB3* as well as several other genomic structures and DNA binding sites in the region. Gene loci's (*TUBB3*, *MC1R*, retro-CYP2F1 and retro-TUBA3D) are represented by boxes with internal arrows showing sequence direction. Individual RNA transcripts are represented by a combination of thin and thick boxes for exons, and arrows for introns; thin boxes represent untranslated regions (5′ and 3′ UTRs), while thick boxes represent translated regions. *TUBB3* transcript variants 1 and 2 are show in red and blue respectively, with addition observed *TUBB3* exons presented in white boxes; additional information of *TUBB3* transcripts is shown in **Table 1**. *MC1R* transcript is shown in green, the *MC1R-TUBB3* chimera transcript is shown in purple, and the lncRNA AC092143.2 is shown in white. Known genomic binding sites are represented with black lines, with thickness corresponding to size; additional information on known genomic binding sites is shown in **Table 2.** CpG islands presented within the *TUBB3* loci are represented by orange rectangles. Promoters/Enhancers are shown as white boxes with their name. Locations of *TUBB3*, *MC1R* and *MC1R-TUBB3* transcripts, and CpG islands was extracted from the Ensembl database (Cunningham et al., 2018). Promoters/Enhancers sourced from Genehancer (Fishilevich et al., 2017). Location of retro-transposed genes and lncRNAs sourced from the UCSC genome browser (Haeussler et al., 2019). Positions based on human genome GCRh38/hg38 assembly.

TABLE 2 | Validated genomic binding sites within the human *TUBB3* loci.

Element type	Genomic Location (chr 16)	Role	Identified observed in	References
Binding sites				
RARE 1[a]	89,917,926–89,917,910	Promotes expression	Cancer stem-like cells derived from patient Bladder cancer cells	Namekawa et al. (2020)
RARE 2	89,918,166–89,918,182			
AP1 binding Site 1	89,921,904–89,921,910	Promotes expression	MCF-7 breast carcinoma cells	Saussede-Aim et al. (2009b)
AP1 binding Site 2	89,921,924–89,921,930			
Ybox-9 element[a]	89,922,380–89,922,356	Promotes expression	A2780, OVCAR-3, SKOV6 and Ov2774 ovarian carcinoma cells	Raspaglio et al. (2014)
YBOX-4 element 1	89,922,975–89,922,982	Promotes expression	H522 non-small cell lung cancer cells	Castillo et al. (2012)
YBOX-4 element 2	89,932,859–89,932,866			
Rest1 binding site	89,926,504–89,926,524	Represses expression	HEK293 embryonic kidney cells; HeLa cervical cancer cells	Shibazaki et al. (2012)
Hypoxia response element[b]	89,935,970–89,935,974	Promotes expression	A2780 ovarian carcinoma cells; GL15 and U87 glioblastoma cells	(Raspaglio et al., 2008; Bordji et al., 2014)
CPG islands				
38 CPGS	89,919,506–89,919,948	Role unknown		
132 CPGS	89,922,423–89,924,099	Role unclear	OVCAR-3, JHOC-5 and JHOC-8 ovarian carcinoma cells;	Izutsu et al. (2008)
86 CPGS	89,925,728–89,926,552	Potential repressor	OVCAR-3, JHOC-5 and JHOC-8 ovarian carcinoma cells; HMV-I, HMV-II, MM-RU, SK-MEL-28, PM-WK, CRL1579, and G361 melanoma cells; NHEM-M and NHEM-D primary neonatal epidermal melanocytes	(Izutsu et al., 2008; Akasaka et al., 2009)
30 CPGS	89,933,944–89,934,279	Role unknown		
80 CPGS	89,934,864–89,935,848	Role unknown		
Promoter regions				
GH16J089917	89,917,279–89,919,454	*MC1R* and *MC1R-TUBB3* promoter		Fishilevich et al. (2017)
GH16J089920/GH16J08995	89,920,191–89,924,356 & 89,925,193–89,926,602	*TUBB3* promoter		Fishilevich et al. (2017)

[a]*Elements are on the minus strand.*
[b]*HRE, is present on both the plus and minus strand.*

signaling (**Table 1**; **Figure 2**) (Dalziel et al., 2011; Herraiz et al., 2015) (reviewed in Herraiz et al., 2017). Further investigation into the *TUBB3* locus using alternative sequencing techniques may need to be performed to further validate these *TUBB3* transcripts, and to better understand the prevalence of this *MC1R-TUBB3* chimera. Because of this, only the two validated transcripts of *TUBB3* will be referred to herein.

Within the *TUBB3* loci, there are several elements. The main *TUBB3* promoter is the largest promoter found within the loci (consisting of the promoter GH16J089920 and the promoter/enhancer GH16J08995) (Fishilevich et al., 2017). Several CpG islands or regions of DNA methylation, are also observed within the loci. However, only one, which is located within the first intron of *TUBB3*, has been linked to modulating the expression of *TUBB3* (Izutsu et al., 2008; Akasaka et al., 2009; Gao et al., 2012). Binding sites for several DNA binding proteins have also been identified in the human *TUBB3* loci, the majority of which are observed on the plus strand. These include Retinoic Acid Response Elements, binding sites for AP1, a Ybox9 element and two Ybox4 elements, an RE1 site and overlapping Hypoxia Response Element (HRE) located in the 3′ region of the loci present on both the plus and minus strands (**Figure 2**; **Table 2**) (Saussede-Aim et al., 2009b; Shibazaki et al., 2012; Bordji et al., 2014; Raspaglio et al., 2014; Namekawa et al., 2020). The HRE element on the plus strand is also a canonical E-box motif, though it remains to be determined if other E-box binding proteins can bind to it. Studies performed in other animals also suggest that within the *TUBB3* loci there is an Androgen Receptor Element (ARE), an additional E-box motif, and other elements listed in **Table 3** (Dennis et al., 2002; De Gendt et al., 2011). The gene *MC1R*, whose loci is observed to be wholly within the *TUBB3* loci, has a transcription region 2.5 kb upstream of the *TUBB3* transcription start site (**Figure 2**). The *MC1R* promotor, GH16J089917, is also found within the 5' region of the *TUBB3* loci (Fishilevich et al., 2017).

Outside of the above elements associated with the expression of *TUBB3*, two retro-transposed genes are located within the loci on the plus strand (**Figure 2**). The first retro-transposed gene is that of *CYP2F1*, located within the first intron of *TUBB3*, and the second are elements of several exons of *TUBA3D* (Baertsch et al., 2008). Finally, on the minus strand, a single lncRNA, known as AC092143.2 or lnc-CENPBD1-3:7 exists within the *TUBB3* loci. Functionally, the potential role of these retro-transposed genes and lncRNA has yet to be investigated. In summary, the *TUBB3* loci is complex, and contains many unexplored elements that may be involved with influencing its expression, and several elements associated with *TUBB3* expression need to be mapped.

TABLE 3 | Transcription factors and Genomic elements associated with *Tubb3* expression in Mice and Rats.

Element type	Species Identified in	Role	Binding site validated	References
Transcription factors				
Sp1	Rat	Promotes expression	*in silico* only	(Dennis et al., 2002; Sleiman et al., 2011)
Ap2	Rat	Unknown	*in silico* only	Dennis et al. (2002)
Pea3[a]	Rat	Unknown	*in silico* only	Dennis et al. (2002)
Pit1[a]	Rat	Unknown	*in silico* only	Dennis et al. (2002)
C/EBP family	Rat	Unknown	*in silico* only	Dennis et al. (2002)
Rest1	Rat & Mouse	Inhibits expression	*in silico* only	(Dennis et al., 2002; Shibazaki et al., 2012)
Scrt1	Mouse	Promotes expression	No, potentially E-Box motifs	Nakakura et al. (2001b)
Math2	Mouse	Promotes expression	No, potentially E-Box motifs	Uittenbogaard and Chiaramello (2002)
pRB	Mouse	Promotes expression	No, potentially E-Box motifs	Toma et al. (2000)
Id2	Mouse	Inhibits expression	N/A, impairs other transcription factors binding	Le Dréau et al. (2018)
Pax3	Rat & Mouse	Inhibits expression	Yes (Rat)	(Cao et al., 2017; Wei et al., 2018)
SoxC family (Sox4, Sox11, Sox12)	Mouse	Promotes expression	Yes	(Bergsland et al., 2006; Hoser et al., 2008)
Binding elements				
E-box motifs	Rat	Unknown	*in silico* only	Dennis et al. (2002)
Central nervous system enhancer motifs	Rat	Unknown	*in silico* only	Dennis et al. (2002)
Tata box	Rat	Unknown	*in silico* only	Dennis et al. (2002)
Androgen response elements	Mouse & Rat	Promotes expression	Yes (Mice)	De Gendt et al. (2011)

[a]*Pit1 and Pea3 sites not observed in mice (Liu et al., 2007).*

3 Regulation and Expression of the *TUBB3* Gene

Traditionally, βIII-tubulin has been considered a neuronal specific protein, and has been primarily used as a marker for neurons (Caccamo et al., 1989). With the advancement of sequencing approaches, it has become evident that the gene encoding for βIII-tubulin, *TUBB3,* is expressed in a wide range of tissues across the body. *TUBB3* expression is enriched in both the central and peripheral nervous systems, however, expression is also high in the testis (The GTEx Consortium, 2015). Recently, a large scale immuno-histological study was performed by Person et al. (2017) to gain a better understanding of βIII-tubulin expression across the human body in normal and cancerous tissues. Much like what was observed from sequencing studies, their work identified βIII-tubulin expression at varying amounts in the majority of human tissues, however, no comparison between expression in cancerous and normal tissues was performed (Person et al., 2017). Within the individual normal tissues, βIII-tubulin expression appeared predominantly in neurons, endothelial cells, fibroblasts and localized stem-like cells (Person et al., 2017).

As βIII-tubulin/*TUBB3* displays differential expression across different cell types across the human body (The GTEx Consortium, 2015; Person et al., 2017), it suggests that there may be unique or tissue-specific transcriptional regulatory mechanisms for *TUBB3* in different tissues. And indeed, several different mechanisms have been identified suggesting a complex nature to the regulation of *TUBB3* in normal tissue. The presence of multiple different regulatory mechanisms does suggest however, that there are multiple routes that can lead to perturbed *TUBB3* expression such as that observed in cancerous tissue. This section will focus on these mechanisms, by discussing what has been learnt about the normal regulation of *TUBB3* in healthy tissues, after which the focus will shift to what has been uncovered from studies into dysregulated *TUBB3* expression in cancer. Transcription factors with a mechanical link to the regulation of *TUBB3* have been summarised in **Table 4**.

3.1 Drivers of *TUBB3* Expression in Normal Tissue

As mentioned, *TUBB3* displays differential expression across the body, and factors driving its expression in different cell types in normal tissue have been proposed. To date, the primary focus into what drives *TUBB3* expression in normal tissue has focused on its expression in both the central and peripheral nervous systems (CNS and PNS, respectively), and recently has been expanded to the roles *TUBB3* may be playing in neural crest cell formation during development. Additionally, the field has made some headway in understanding why *TUBB3* expression is predominantly repressed outside of neuronal tissues, and what mechanisms appear to be driving the observed *TUBB3* enrichment in the testis.

TABLE 4 | Transcription factors with known impact on *TUBB3* expression.

Transcription factor	Species	Role	References
Androgen receptor	Mouse, Human	Promotes	(Denolet et al., 2006; De Gendt et al., 2011) Butler et al. (2001)
Estrogen receptor	Human	Promotes	Saussede-Aim et al. (2009a)
HIF1α	Human	Promotes Inhibits	Raspaglio et al. (2014), Bordji et al. (2014)
HIF2a	Human	Promotes	Raspaglio et al. (2008)
ID2	Human, Mouse	Inhibits	(Le Dréau et al., 2018), Azzarelli et al. (2022)
Math2	Mouse	Promotes	Uittenbogaard and Chiaramello (2002)
MZF1	Human	Promotes	Kanojia et al. (2020)
Pax3	Rat, Mouse	Inhibits	Cao et al. (2017), Wei et al. (2018)
RARa	Human	Promotes	Namekawa et al. (2020)
RE1	Human	Inhibits	Shibazaki et al. (2012)
Scrt1	Mouse	Promotes	Nakakura et al. (2001b)
SOXC family (4, 11, 12)	Mouse, Human[a]	Promotes	(Bergsland et al., 2006; Hoser et al., 2008) (Castillo et al., 2012; Fu et al., 2019)
SOX9	Human	Promotes	Raspaglio et al. (2014)
ZEB1	Human	Promotes[b]	(Lobert et al., 2013; Kanojia et al., 2020)
ZIC1	Human	Promotes	(Fu et al. 2019)

[a]*Only SOX4 and SOX11 have been confirmed in humans.*
[b]*ZEB1 is only implied as binding site, while identified, was not reported.*

3.1.1 Neurogenesis and Neural Crest Cell Formation

βIII-tubulin has been considered as one of the earliest markers of neuronal differentiation of both the CNS and PNS where it is expressed either during, or prior to, terminal mitosis of the progenitor cells. This being either neuroepithelial cells for the CNS (Caccamo et al., 1989; Lee et al., 1990b; Linhartová et al., 1992; Easter et al., 1993), or neural crest cells for the PNS (Moody et al., 1989; Haendel et al., 1996). Indeed, cloning and *in silico* characterization of the 5' flanking region of rat *Tubb3* gene has revealed its minimal promoter region and several potential neuronal regulatory motifs (Dennis et al., 2002). This included putative binding sites for transcription factors Sp1, Ap2, Pea3, Pit1, and the C/EBP family, several E-box motifs, and a CNS enhancer motif (**Table 3**) (Dennis et al., 2002). There are differences in the expression of *Tubb3* between the CNS and PNS. As shown in rats and mice, *Tubb3* expression peaks during periods of axonal guidance and neuronal maturation, and then declines in the CNS with maturity while in the PNS continues to maintain high expression (Jiang and Oblinger 1992; Hausrat et al., 2021). This suggests that there may be specific regulatory mechanisms even within neuronal tissues. Indeed, several transcription factors have been identified in mouse and rat models that are involved with the expression of *Tubb3* in neurogenesis in either the CNS or the PNS (**Table 3**).

A regulatory candidate in the CNS is Scratch1 (*Scrt1*), a Snail family zinc finger transcription factor that is specifically expressed in post-mitotic and newly differentiating neurons (Nakakura et al., 2001a). After initially identifying the co-expression of Scratch with βIII-tubulin by treating mouse P19 embryonal carcinoma cells with retinoic acid, Nakakura et al. (2001b) discovered that overexpressing Scratch1 by itself was sufficient to induce βIII-tubulin (Nakakura et al., 2001b). Two Retinoic Acid Response Elements have been recently identified within the human *TUBB3* gene, and retinoic acid alone can induce *TUBB3* expression (Namekawa et al., 2020). Another CNS transcription factor shown to stimulate βIII-tubulin expression during neuronal differentiation is the basic helix-loop-helix differentiation transcription factor Math2 (Uittenbogaard and Chiaramello 2002; Uittenbogaard and Chiaramello 2004). Although the binding sites of Scratch1 and Math2 in the *Tubb3* loci have not been elucidated, both are known to bind to E-box motifs (Nakakura et al., 2001a; Uittenbogaard et al., 2003) and are potentially binding previously predicted sites (Dennis et al., 2002).

In addition to promoting gene expression, inhibitors of βIII-tubulin expression have also been identified in neuronal tissues. One of these inhibitors is ID2, which was originally speculated to be able to represses *TUBB3* transcription (Katsetos et al., 2003). This was because elevated Id2 was shown to interfere with retinoblastoma tumour suppressor protein's (pRb) capacity to bind to basic helix-loop-helix transcription factors, like the *Tubb3* regulator Math2 (Uittenbogaard and Chiaramello 2002), and prevented the expression of neuronal specific genes in primary murine cortical progenitor cells (Toma et al., 2000). While alterations to *Tubb3*/βIII-tubulin expression were not examined by Toma et al. (2000), Id2 has since been demonstrated to indirectly impair *Tubb3* transcription (Le Dréau et al., 2018). More recently, ID2 levels have been shown to influence neuronal differentiation of human glioblastoma stem cells, with elevated ID2 reducing the number of βIII-tubulin positive cells (Azzarelli et al., 2022). Another inhibitor of *Tubb3* transcription is Pax3, which in rat neuronal stem cells was able to bind to the *Tubb3* promoter regions and inhibit both transcription and translation (Cao et al., 2017). Subsequent work in mouse neuronal stem cells identified that during neurogenesis, Pax3 expression was reduced through elevated levels of miR-124, which resulted in increased *Tubb3* expression and the development of neuronal phenotypes (Wei et al., 2018). In the same study, low levels of βIII-tubulin were present in these neuronal stem cells, suggesting that Pax3 partially suppresses *Tubb3* expression (Wei et al., 2018).

Specific protein 1 (Sp1) is a transcription factor predicted to have many putative binding sites in the rat *Tubb3* promoter region, suggesting it may have a potential role in the regulation of

Tubb3 expression (Dennis et al., 2002). Sp1 is also predicted to have binding sites within the human *TUBB3* promoter GH16J089920 (Fishilevich et al., 2017) (**Figure 2**). Sp1, a protein that is considered to be ubiquitously expressed in mammalian tissue, is known to function by binding GC-rich sequences and recruiting essential machineries to TATA boxes (one of which was also identified by Dennis et al., 2002) to initiate transcription of its target genes (Naar et al., 1998). The targeted inhibition of Sp1 activity in primary rat cortical neurons has been demonstrated to reduce the expression of *Tubb3*, alongside several other genes (Sleiman et al., 2011), suggesting that Sp1 is involved in *Tubb3* transcription activation. Although Sp1 expression decreases after neuronal differentiation and is not detected in differentiated neurons (Mao et al., 2007; Mao et al., 2009). *Tubb3* expression also declines in the CNS with neuronal maturity (Jiang and Oblinger 1992; Hausrat et al., 2021). Like Pax3, Sp1, is also a target of miR-124 (Mondanizadeh et al., 2015), although a link between Sp1, miR-124 and *Tubb3* expression has not been reported.

While the factors involving *Tubb3* expression described in the preceding section are associated with neuronal differentiation of the CNS, it is uncertain whether these shared by differentiating neurons of the PNS. During fetal development, however, βIII-tubulin has been shown to be expressed by neural crest cell progenitors (Pax7 positive cells), and by pre-migratory neural crest cells (Sox9 and Slug positive cells) prior to neurogenesis in the CNS (Chacon and Rogers 2019). Neural crest cells are considered to be multipotent progenitor cells able to give rise to various cells including neurons and melanocytes, and form the majority of the PNS (Acloque et al., 2008). This identification of βIII-tubulin expression in pre-migratory neural crest cells suggests that along with being involved with neurogenesis that βIII-tubulin has a separate role involved with neural crest cell development (Acloque et al., 2008). In this context, several factors linked with βIII-tubulin have been identified. For example, Ap2 has been linked to neural crest cell development (Mitchell et al., 1991) and identified to have several binding sites in the rat *Tubb3* promoter (Dennis et al., 2002), however whether Ap2 can promote *Tubb3* expression is yet to be determined.

The SRY-related HMG-box transcription factors of the SoxC gene family, Sox4, Sox11 and Sox12, are associated with the formation of neural crest cells (Uy et al., 2015). These transcription factors, which have been primarily linked with neuronal differentiation (Bergsland et al., 2006), are known to induce *Tubb3* expression. Bergsland et al. (2006) first identified that the 5' Untranslated Region (UTR) of the mouse *Tubb3* gene contains three binding sites for either Sox4 or Sox11. Through increasing the expression of either Sox4 or Sox11 in developing murine embryos, Bergsland et al. (2006) observed an increase of *Tubb3* and βIII-tubulin expression, and a reduction of both *Tubb3* and βIII-tubulin when Sox4 or Sox11 was silenced through the use of siRNA. Subsequently Sox12 was also demonstrated to bind to the mouse *Tubb3* promoter, and modulate βIII-tubulin as well (Hoser et al., 2008). Sox11 had the greatest impact on βIII-tubulin expression in neurogenesis (Bergsland et al., 2006; Hoser et al., 2008), and is required for binding to NeuroG1 in order to promote *Tubb3* in early-born neurons, a process that can be inhibited through Bm2 (Chen et al., 2015). Since these three genes have been linked to neural crest formation (Uy et al., 2015), it is therefore plausible to think that the expression of *Tubb3* observed by the neural crest progenitors (Chacon and Rogers 2019) could be driven by members of the SoxC family.

The animal studies discussed in the preceding section have been invaluable in deciphering the regulatory factors during neuronal development of βIII-tubulin. Equivalent studies examining *TUBB3* expression in neuronal tissues and neural crest cells have yet to be validated in human cells, although genomic mapping has identified transcription factors that interact with the human and rat/mouse promotors. The validated human transcription factors involved with promoting *TUBB3* expression in a neuronal setting are SOX11 and ZIC1 (Fu et al., 2019). While either SOX11 or ZIC1 promotes the expression of *TUBB3*/βIII-tubulin and induces a neuronal phenotype in U87 glioblastoma cells, the expression of ZIC1 greatly enhances the impact SOX11 has on *TUBB3* expression and neuronal differentiation (Fu et al., 2019). SOX4 has also been shown to regulate *TUBB3* expression cancer (Castillo et al., 2012), and this will be discussed in a subsequent section.

3.1.2 Non-Neuronal Expression Repression or Cell Cycle Dependent Expression?

One potential reason the expression of *TUBB3* is limited outside of neuronal tissue is due to the REST binding site (RE1) present within the first intronic region of *TUBB3*, which is located after the first exon of the first *TUBB3* transcript variant (**Figure 2**; **Table 2**) (Shibazaki et al., 2012). An RE1 site is also present in the 5' UTR of rat *Tubb3* (Dennis et al., 2002). REST is a global transcriptional silencer that represses neuron-specific gene expression in non-neuronal cells (reviewed in Ooi and Wood 2007). Typically, REST forms complexes with chromatin-modifying enzymes, such as HDACs, coREST, mSin3a, MeCP2, and suppresses neuronal gene expression by epigenetic mechanisms (reviewed in Ooi and Wood 2007). Given the binding partners of REST, it is unsurprising that the human REST site located within the CpG island is found within the GH16J08995 "enhancer" (**Figure 2**). It is possible that in normal healthy tissue, as a result of REST binding, that this CpG island displays increased methylation, limiting the transcription of *TUBB3* and potentially accounting for the reduced expression of *TUBB3* observed in non-neuronal tissue. This needs to be further investigated as both *TUBB3* and βIII-tubulin expression is observed in several non-neuronal tissues and cells including human fetal astrocytes, melanocytes, and spermatogenic cells (Dráberová et al., 2008; Leandro-García et al., 2010; Lehmann et al., 2017; Person et al., 2017).

Prior to identifying the REST binding site in *TUBB3*, Shibazaki et al. (2012) identified that *TUBB3* expression in HEK293 and HeLa cells fluctuated with the cell cycle. *TUBB3* expression increased throughout the S phase and βIII-tubulin expression peaked in the G2/M phase, where it appeared enriched around mitotic spindles (Shibazaki et al., 2012). Immunoprecipitation studies showed that REST was no longer bound to its RE1 site in *TUBB3* during the G2/M phase, but rather rebound during the G1

phase, where *TUBB3* expression was observed to decrease (Shibazaki et al., 2012). Knockdown studies also indicated that cell-cycle dependent *TUBB3* expression is required for mitosis and normal cell growth in their cells (Shibazaki et al., 2012). This was further supported by studies that found that silencing *TUBB3* expression sensitized cancer cell lines to epothilones, a TBA that causes cells to accumulate in G2M phase of the cell cycle (Gan et al., 2011; Narvi et al., 2013). This finding suggests that *TUBB3* is not as neuronally specific as traditionally thought. Future studies are needed to better understand the role of REST in *TUBB3* regulation.

3.1.3 Testis and Other Non-Neuronal Tissues

An unexpected finding from a Lewis and Cowan 1988 study was the identification of βIII-tubulin expression in mouse testis (Lewis and Cowan 1988). This finding was initially dismissed, as the βIII-tubulin antibody that was used was also known to bind to βIVb-tubulin, which at the time was considered the only β-tubulin isotype to be expressed in the testis (Lewis and Cowan 1988). Lee et al., 1990a went on to validate βIII-tubulin expression in testis using a newly developed βIII-tubulin monoclonal antibody (TUJ1). Denolet et al. (2006) later identified the altered expression of *Tubb3* in mouse Sertoli cells, "nurse" cells in the testes involved with spermatogenesis, in response to the loss of the androgen receptor. This work was then followed up by De Gendt et al. (2011) who identified several Androgen Response Elements (ARE) present in both mouse and rat *Tubb3*, and suggested that *Tubb3* plays a critical role in spermatogenesis. The location of AREs in the human *TUBB3* gene have not been reported and we cannot exclude the possibility that the association with the AR is indirect. Nevertheless, βIII-tubulin is expressed in human Sertoli cells (Person et al., 2017). Furthermore, testosterone has been shown to induce *TUBB3*/βIII-tubulin expression in human cell lines (Butler et al., 2001), suggesting that these elements potentially exist in the human *TUBB3* gene. Person et al., 2017 also observed the strongest βIII-tubulin staining in testicular tissue in the spermatogenic cells, stem cells that give rise to sperm cells (Person et al., 2017), supporting the notion of *TUBB3* being involved with spermatogenesis (De Gendt et al., 2011). In contrast, treating rat primary cortical neurons with supra-physiological doses of testosterone failed to elevate *Tubb3* expression, despite the strong expression of the androgen receptor in the same cells (Zelleroth et al., 2021).

TUBB3 and βIII-tubulin expression has also been demonstrated to be controlled by the estrogen receptor (Saussede-Aim et al., 2009a), which could account for the observed expression in ovary tissue (Person et al., 2017). Though it is currently unclear if *TUBB3* is expressed in oogonial stem cells *in vivo*, the female equivalent of spermatogenic cells, cultured murine oogonial stem cells have been shown to express βIII-tubulin (Cao et al., 2017). The location of the estrogen response element in the human *TUBB3* loci is unknown, as it is not present in either the 5' or 3' UTR of *TUBB3* (Saussede-Aim et al., 2009a).

3.1.4 Translational Regulation of *TUBB3* in Normal Tissues

In additional to studying the transcriptional regulation of *TUBB3*, there has also been investigations into the regulatory factors involved with the translation of, and the stability of the *TUBB3* mRNA transcript. Work performed by Theodorakis and Cleveland (1992) demonstrated that increased cytosolic levels of β-tubulins results in a reduction to β-tubulin mRNA transcripts without impacting the level of α-tubulin transcripts. Their work suggested that there is an RNA binding agent that recognizes the first 13 coding nucleotides of the various β-tubulin transcripts that is involved with RNA stabilization, however as levels of β-tubulin protein increased, this unknown binding agent loses its affinity for the RNA resulting in destabilization of the mRNA (Theodorakis and Cleveland 1992). This was demonstrated by blocking the suspected binding site, which resulted in a loss in β-tubulin RNA (Theodorakis and Cleveland 1992). As this seminal work did not address the individual β-tubulin transcripts, how this relates to individual tubulin isotypes such as *TUBB3*/βIII-tubulin remains to be investigated.

In neurogenesis, translation of *TUBB3* is also regulated in a neuronal specific manner. In mouse P19 and Neuro2a cells, RNA binding protein Tristetraprolin was shown to bind to *Tubb3* and impair its translation (Dai et al., 2015). The authors identified many neuronal mRNAs to contain binding sites for Tristetraprolin (Dai et al., 2015). By initiating neuronal differentiation in these cells, they observed a reduction in Tristetraprolin levels followed by an increase in *Tubb3* translation, a result they were able to mimic through Tristetraprolin knockdown studies as well (Dai et al., 2015). Human *TUBB3* itself does contain a potential Tristetraprolin binding site, which appears to overlap with the binding site for the members of the miR-200 family, suggesting this mechanism of regulating *TUBB3* transcription is likely to be active in the human developing nervous system as well.

3.2 Expression of *TUBB3* in Cancer—A Loss in Regulation

Despite the well-established link between βIII-tubulin overexpression, drug resistance and poor clinical outcomes in patients, the regulation of *TUBB3* expression in cancer cells remains poorly understood. It is becoming apparent that mechanisms driving aberrant *TUBB3* expression in tumours are complex and may vary depending on cell type and gender. Indeed, the impact of aberrant *TUBB3* expression impacts drug resistance in different types of cancer, as in ovarian and non-small cell lung cancer where elevated *TUBB3* expression is associated with drug resistance (Kavallaris et al., 1997; Kavallaris et al., 1999), while increased *TUBB3* expression in breast cancer and melanoma cells has been identified as a sign of increased drug sensitivity (Akasaka et al., 2009; Wang et al., 2013). Due to this perturbation of *TUBB3* expression in cancer, several studies have investigated whether the altered expression of *TUBB3* is a response to chemotherapeutic agents or as a result of gene dysregulation.

In cancers where *TUBB3* is overexpressed, change in gene expression is often compared to the expression of total β-tubulin. For example, in neuronal tissues βIII-tubulin expression makes up approximately 25% of the β-tubulin pool, *TUBB3* however

only accounts for 4% of the total *TUBB* expression, with *TUBB4* and *TUBB2A* making up at least 90% of the total *TUBB* expression (Cleveland et al., 1990; Leandro-García et al., 2010). This trend is seen in patient tumours, where *TUBB3* only makes up a low to moderate proportion of the *TUBB* mRNA pool in ovarian, breast and lung cancer (with proportions ranging up to 7.5, 18, and 16% respectively) (Leandro-García et al., 2010). What makes this change aberrant though is that between normal and cancerous tissue, this change in *TUBB3* expression accounts for a 71- and 43-fold increase in expression in lung and breast cancer respectively (Leandro-García et al., 2010).

3.2.1 Impact of Chemotherapy on *TUBB3* Expression

Induction of *TUBB3* expression has been widely reported in numerous cancer cell lines by both short term (Ranganathan et al., 1998b) and long term (Ranganathan et al., 1996; Kavallaris et al., 1997; Ranganathan et al., 1998a; Ranganathan et al., 1998b; Shalli et al., 2005) exposure to TBAs, a class of chemotherapeutics that target tubulin and microtubule dynamics (reviewed in Jordan and Wilson, 2004; La Regina et al., 2019). The factors responsible for this response may not be unique to βIII-tubulin as the levels of several other β-tubulin isotypes were also significantly increased (Ranganathan et al., 1996; Ranganathan et al., 1998a; Shalli et al., 2005). These results should be interpreted with caution though as very high doses of TBAs were used in some of the short-term studies. For example, in MCF7 cells, *TUBB3* gene expression has been shown to be inducible following acute exposure to extremely high concentrations of vinorelbine, vinblastine or colchicine (1 μm), or paclitaxel (400 nm) (Saussede-Aim et al., 2009b; Lobert et al., 2011). Concentrations of vinblastine at 1 μm are known to completely depolymerise microtubules and increase microtubule polymer mass *in vitro* (Jordan et al., 1991; Toso et al., 1993). The concentration used is not clinically relevant and the Vinca alkaloid-induced *TUBB3* expression is likely to be a compensatory response to microtubule depolymerisation, or an "off- target" effect on the transcriptional machinery or signalling pathways. Using this extreme dose of vinorelbine or vinblastine (1 μm) in mutagenesis studies, Saussede-Aim et al. (2009b) reported that Vinca alkaloid treatments were enhancing *TUBB3* promoter activity *via* two AP1 binding sites located within the GH16J089920 promoter of the *TUBB3* loci (**Figure 2**; **Table 2**) (Saussede-Aim et al., 2009b). However, using chromatin immunoprecipitation (ChIP) for canonical AP1 binding transcription factors failed to identify what was binding to the AP1 site in response to vinorelbine exposure, suggesting that there was a non-canonical AP1 binding protein inducing *TUBB3* expression in response to vinorelbine (Saussede-Aim et al., 2009b). Future investigation using ChIP is required to identify transcription factors responsible for Vinca alkaloid-induced *TUBB3* expression at clinically relevant doses.

Like Vinca alkaloids, Taxol has been reported to alter the level of *TUBB3* expression in tumours. For example, Kavallaris et al. (1997) reported that, while the level of individual β-tubulin isotypes remained the same in normal ovary and primary untreated ovarian tumours, analysis of ovarian carcinoma specimens from the same patient before and after chemotherapy revealed that *TUBB3* and *TUBB2C* gene expression increased significantly in Taxol-resistant tumours post-treatment (Kavallaris et al., 1997). As patients develop Taxol resistance after several cycles of Taxol/platinum combination therapy, it is difficult to differentiate whether the increased *TUBB3* expression observed was a direct consequence of chemotherapy-induced changes, or as a result of selection of resistant cell populations where altered tubulin expression provided a survival advantage. Kavallaris et al. (1999) went on to show that Taxol resistant non-small cell lung cancer cells were overexpressing *TUBB3* and βIII-tubulin, and that partial suppression of *TUBB3* using antisense oligonucleotides sensitized cells to Taxol (Kavallaris et al., 1999), linking *TUBB3*/βIII-tubulin expression with Taxol sensitivity. Later, potent knockdown of *TUBB3* using siRNA and shRNA confirmed a direct functional role for βIII-tubulin in mediating *in vitro* and *in vivo* sensitivity to broad classes of chemotherapy in non-small cell lung cancer, identifying βIII-tubulin as a survival factor in cancer cells (Gan et al., 2007; Gan et al., 2010b; McCarroll et al., 2010; Gan et al., 2011).

3.2.2 The 5' Region of *TUBB3* in Cancer

Several regulatory elements in addition to AP1 binding sites mentioned earlier, have been identified within the 5' UTR of the *TUBB3* loci, which includes two CpG islands. The shorter of the two (consisting of 38 CpGs) is located just upstream of the GH16J089920 promoter, while the second CpG island, and also the largest in the *TUBB3* loci (132 CpGs), is located within the promoter and covering the first exon of the first *TUBB3* transcript variant (**Figure 2**; **Table 2**). The larger CpG island has been identified as hypomethylated in several ovarian cancer cell lines, but not in non-cancerous ovarian tissues (Izutsu et al., 2008). Given the identification of multiple SP1 and AP2 binding sites within the rat genome around the first exon of *Tubb3* (Dennis et al., 2002), Izutsu et al. (2008) suggested that these sites may be present at similar locations of the human *TUBB3* loci too. Since SP1 and its DNA-binding activities are inducible under oxidative stress and DNA-damage (Ryu et al., 2003), and assuming there are SP1/AP2 binding sites within this region as suggested by Izutsu et al. (2008), it is possible that under chemotherapeutic insults, hypomethylated *TUBB3* promoter regions with enhanced SP1 signalling may contribute to aberrant *TUBB3* expression in ovarian cancer. Further studies are required to clarify whether SP1 and AP2 can directly bind to those hypomethylated regions and drive aberrant *TUBB3* expression. Moreover, it will be important to determine if hypomethylation of *TUBB3* occurs in patient samples with upregulated βIII-tubulin expression.

There are two Retinoic Acid Response Elements (RARE) upstream of the smaller CpG island, towards the extreme 5′ end of the *TUBB3* loci and within the *MC1R* promoter region (**Figure 2**; **Table 2**). RAREs are bound to by the transcription factor Retinoic Acid Receptor α (RARα) in response to elevated levels of retinoic acid, resulting in gene expression. The two RAREs within the *TUBB3* loci were recently discovered by Namekawa et al. while trying to improve the generation of long-term cultures of Patient Derived Cancer cells (PDCs) that were enriched for Cancer Stem-like Cells

(CSCs) from surgically removed bladder tumours (Namekawa et al., 2020). CSCs are renewable cells that constitute a small population within a cancerous cell population, and are implicated in tumour drug resistance, as well as tumour recurrence and metastasis (reviewed in Clevers 2011; Diaz and Leon 2011). These PDCs were grown in a 3D spheroid culture to aid in CSC enrichment, and were observed to have elevated expression of *ALDH1A1*, a marker for CSCs and whose protein product RALDH1 oxidises retinaldehyde into retinoic acid (Namekawa et al., 2020). Knockdown studies of *ALDH1A1* showed that its expression was required for the *in vitro* maintenance of the PDCs, and prevented spheroid formation, leading the authors to speculate that spheroid formation was occurring due to elevated levels of retinoic acid caused by elevated *ALDH1A1* (Namekawa et al., 2020). After demonstrating that spheroid formation was reliant on retinoic acid levels independently of *ALDH1A1* expression, Namekawa et al. (2020) proceeded to search for genes that were being upregulated by the retinoic acid response pathway. By performing ChIP for RARα, they identified two RAREs in the 5' UTR of the *TUBB3* loci, which were then confirmed to be able to promote the expression of *TUBB3*, and that *TUBB3* expression was elevated by the PDCs too (Namekawa et al., 2020). Subsequent knockdown studies of *TUBB3* in PDCs confirmed it as downstream to the elevation of *ALDH1A1* expression, as *TUBB3* expression was required for *in vitro* spheroid formation (Namekawa et al., 2020). This prompted the suggestion that *TUBB3* expression may contribute to the maintenance of CSCs in bladder cancer (Namekawa et al., 2020), which could account for why elevated *TUBB3* is observed with more aggressive subtypes of bladder cancer (Hinsch et al., 2017).

Recent work has identified that MZF1 is able to bind to the *TUBB3* loci, with three potential sites predicted up to 600 base pairs upstream of the first exon of *TUBB3* transcript variant 2 (Kanojia et al., 2020). The ability of MZF1 to bind to the *TUBB3* loci was identified while looking for means to upregulate βIII-tubulin expression in HER2 positive breast cancer in an effort to induce sensitivity to the TBA, vinorelbine (Kanojia et al., 2020). Building on previous work that identified *TUBB3* expression to be modulated by the members of the Bromdodmain and Extraterminal (BET) protein family (Piunti et al., 2017), Kanojia et al. (2020) identified increased *TUBB3*/βIII-tubulin expression in response to BET inhibition which led to increased sensitivity to Vinorelbine both *in vitro* and *in vivo* (Kanojia et al., 2020). Seeking a mechanism to account for why BET inhibition was promoting *TUBB3* expression, the *TUBB3* promoter (GH6J089920) was scanned and led to the identification of several potential binding sites for transcription factors (Kanojia et al., 2020). As MZF1 was associated with better survival in breast cancer patients, and because *MZF1* expression decreased upon treatment with BET inhibitors, Kanojia et al. (2020) performed knockdown/overexpression studies and ChIP-qPCR, confirming that MZF1 could bind to the *TUBB3* loci and repress *TUBB3*/βIII-tubulin expression.

Near the AP1 sites, exist two more transcription factor binding sites within the 5′ UTR of the first *TUBB3* transcript variant, both of which are Ybox elements (**Figure 2**; **Table 2**). Ybox elements are canonically bound to by *SRY*-related HMG-box transcription factors, and as mentioned earlier several of these transcription factors have been linked to modulating *TUBB3* expression in a neuronal setting. Two of these transcription factors have been linked to modulating *TUBB3* expression in cancer, SOX4 and SOX9 (Castillo et al., 2012; Raspaglio et al., 2014). While both are linked to neurogenesis and neuronal crest cell formation (Bergsland et al., 2006; Martini et al., 2013; Uy et al., 2015), increased SOX4 expression is also commonly linked with several forms of cancer, in particular lung cancer, and has been suggested as a driver oncogene (Liu et al., 2006; Castillo et al., 2012). Despite its increase in expression, the impact of increased SOX4 expression on the genes it was upregulating was unknown. To address this issue, Castillo et al. (2012) investigated genes that were positively regulated by SOX4 expression in small cell lung cancer through knockdown studies. After identifying several potential genes downregulated upon knockdown of *SOX4* expression, Castillo et al. (2012) screened these genes for potential SOX4 binding sites (Scharer et al., 2009), and subsequently confirmed SOX4 binding through ChIP and qPCR of the SOX4 bound sequences (Castillo et al., 2012). As Sox4 had been previously linked to regulating *Tubb3*/βIII-tubulin expression in neurogenesis (Bergsland et al., 2006), the authors used *TUBB3* as a positive control for their assays as it was downregulated in the initial *SOX4* knockdown microarray, and they went on to validate two SOX4 binding sites in the *TUBB3* loci (**Figure 2**; **Table 2**) (Castillo et al., 2012). Of note, the Ybox4 element identified in the 5' region was determined to be the more dominant (**Figure 2**) (Castillo et al., 2012). Thus Castillo et al. (2012) reported that the dysregulation of a direct factor associated with neurogenesis in cancer may be involved with promoting the aberrant expression of *TUBB3* in some cancers. Due to its association with hypoxic stress response, the Ybox9 element and SOX9 will be discussed in a subsequent section.

3.2.3 The First Intron of *TUBB3*—Epigenetic Dysregulation or Loss of REST1 Expression?

Epigenetic dysregulation is a common feature of cancers (Hanahan 2022). Like many genes, *TUBB3* can be epigenetically regulated. REST-mediated mechanisms and chromatin remodelling have been demonstrated to play an important role in *TUBB3* regulation in several epithelial cancer cells (Izutsu et al., 2008; Akasaka et al., 2009; Gao et al., 2012; Shibazaki et al., 2012). For example, in ovarian cancer cells, DNA demethylation CpG island (containing 86 CpGs) within *TUBB3* intron 1 has been shown to result in βIII-tubulin overexpression, with chromatin acetylation accelerating the process and increasing *TUBB3* expression as well (Izutsu et al., 2008; Akasaka et al., 2009). Subsequently, Izutsu et al. (2008) performed *in silico* analysis' within this region and identified the RE1 site, later validated by others (Shibazaki et al., 2012), suggesting REST may also be involved with the observed increase in *TUBB3* expression. Follow-up investigations of this predicted RE1 site by Akasaka et al. (2009) identified that histone deacetylation of this RE1

motif partially contributes to *TUBB3*/βIII-tubulin overexpression in melanoma.

The loss of REST in a range of cancers has also been linked to the aberrant expression of neuronal genes in the clinic, including *TUBB3*. A negative correlation between REST and *TUBB3* expression has been reported in skin, ovarian, and small cell lung cancer biopsy samples (Akasaka et al., 2009; Kreisler et al., 2010; Hatano et al., 2011; Gao et al., 2012), while in normal non-neoplastic tissues *TUBB3* is barely detectable. Additionally, *REST* gene deletion and frame-shift mutations are frequently observed in colon and small cell lung cancers (Coulson et al., 2000; Westbrook et al., 2005). In mouse colonic crypts, targeted *Rest* genetic ablation has resulted in upregulation of *Tubb3* expression (Hatano et al., 2011; Gao et al., 2012). Furthermore, *TUBB3*/βIII-tubulin expression can be independently induced upon *REST* siRNA treatment in cancer cells (Akasaka et al., 2009; Gao et al., 2012). Together, these findings suggest REST as a transcriptional silencer of *TUBB3* and that dysfunctional REST, in conjunction with epigenetic modifications in *TUBB3* intron 1, may be important mechanisms underlying aberrant *TUBB3* expression in tumours of non-neuronal origin. Since other neuronal differentiation factors mentioned previously are also linked to this altered *TUBB3* expression (Castillo et al., 2012; Raspaglio et al., 2014; Namekawa et al., 2020), it poses the question—are dysregulated processes associated with neuronal gene regulation the primary causes of aberrant *TUBB3* expression in tumours of non-neuronal origin? Further research is required in order to better understand the role that these neuronal factors are playing in *TUBB3* expression in cancer.

3.2.4 The 3' UTR of *TUBB3*—Stress Response

From the observed increases in *TUBB3* expression in response to exposure to TBAs, (Ranganathan et al., 1996; Kavallaris et al., 1997; Ranganathan et al., 1998a; Ranganathan et al., 1998b; Shalli et al., 2005), one can speculate that the induction of βIII-tubulin could enable tumour cells to adapt and survive in a stressful microenvironment. Gan et al. (2007) provided the first evidence that expression of *TUBB3*/βIII-tubulin was a survival factor that when suppressed using gene silencing not only sensitized tumour cells to TBAs but also to broad classes of drugs including DNA-damaging agents and antimetabolites. A notion that is strengthened by the observation that the levels of *TUBB3* were able to modulate the PTEN/AKT signaling axis (McCarroll et al., 2015a), a prosurvival pathway commonly perturbed in a range of tumours (reviewed in Song et al., 2012; Taddei et al., 2012). Indeed, growing evidence suggests that βIII-tubulin expression is a key adaptive response that is activated on cellular exposure to a stressful microenvironment, such as hypoxic conditions (Raspaglio et al., 2008; Forde et al., 2010; Danza et al., 2012; Bordji et al., 2014; Raspaglio et al., 2014) or glucose deprivation in cancers cells (Parker et al., 2016). In solid tumours, cells often grow within a hypoxic microenvironment, and cells with a highly efficient hypoxia-inducing factor orchestrated survival program possess an advantage to offset its selective pressure.

In tumours, the hypoxia-inducing factor HIF1α has been implicated in the transcriptional regulation of βIII-tubulin via the 3′UTR of the *TUBB3* gene and is thought to protect tumours against hypoxic injury (Raspaglio et al., 2008; Forde et al., 2010; Danza et al., 2012; Bordji et al., 2014; Raspaglio et al., 2014). In A2780 ovarian cancer cells, hypoxia has been shown to strongly induce *TUBB3* gene and βIII-tubulin protein expression and this phenotype was directly linked to cisplatin and paclitaxel resistance (Raspaglio et al., 2008; Raspaglio et al., 2014). This process was shown to be transcriptionally regulated through the binding of HIF1α to a hypoxia response element (HRE) within the 3′ UTR of *TUBB3* (Raspaglio et al., 2008) (**Figure 2**; **Table 2**). An alternative transcriptional mechanism regulating *TUBB3*, involving HIF2α and the SoxC gene SOX9, has also been described (Raspaglio et al., 2014). In ovarian cancer specimens, high levels of *TUBB3* mRNA and βIII-tubulin protein were significantly associated with increasing levels of SOX9 and HIF2α (Raspaglio et al., 2014). Silencing both SOX9 and HIF2α abrogated this hypoxia-activated *TUBB3* expression, suggesting roles for SOX9 and HIF2α as positive *TUBB3* regulators under hypoxic conditions. Subsequent *in silico* analysis and ChIP studies demonstrated the binding of SOX9 to a specific binding site (the Ybox9 element mentioned earlier) within the 5′ region of *TUBB3* (**Figure 2**; **Table 2**), with gene-reporter and site-directed mutagenesis studies all supporting the involvement of SOX9 in *TUBB3* regulation in hypoxia (Raspaglio et al., 2014).

HIF1α and HIF2α may potentially regulate *TUBB3* expression in hypoxic conditions by mechanisms that differ in diverse cancer types. While both appear to have a positive impact on expression in ovarian cancer (Raspaglio et al., 2008; Raspaglio et al., 2014), HIF1α appears to play an inhibitory role on *TUBB3*/βIII-tubulin expression in glioblastoma cells (Bordji et al., 2014). In glioblastoma hypoxia reduced HIF1α expression, leading to HIF2α binding to the two overlapping HREs located in the 3′UTR of the gene (Bordji et al., 2014). Additionally, epigenetic regulation could account for this regulation in specific cancer cell lines, as hypomethylation of the HRE is required for *TUBB3* expression in ovarian cancer cells, prostate cancer cells and prostate tumours (Raspaglio et al., 2008; Forde et al., 2010). This suggests that both HIF1α and HIF2α/SOX9 mediated *TUBB3* regulation could be a cell-specific response, as it is not inducible upon hypoxia in some cell lines expressing high basal levels of βIII-tubulin (Raspaglio et al., 2008; Shen and Yu 2008; Danza et al., 2012; Levallet et al., 2012; Bordji et al., 2014; Raspaglio et al., 2014).

3.2.5 miR-200c and HuR—Partners in Crime

Another common mechanism used by cells as a means of translational regulation are microRNAs (miRNAs), small non-coding RNAs that can modulate the post-transcriptional regulation of gene expression through modulation of mRNA stability and translational efficiency through complementary base pair binding (Goodall et al., 2013; Maciotta et al., 2013). One particular family of miRNAs, the miR-200 family, has been linked to modulating the translation of *TUBB3* in the context of cancer. The miR-200 family, consisting of miR-141, −200a, −200b, −200c, and −429, have an established role in cancer, with their downregulation being linked to angiogenesis, drug resistance and the epithelial-mesenchymal transition of cancer cells (Mongroo

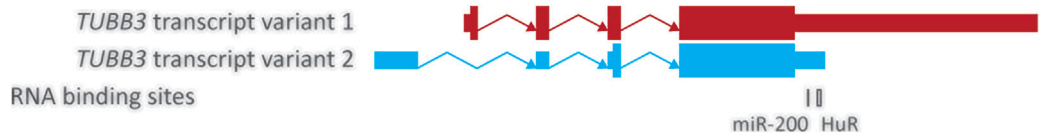

FIGURE 3 | Structure of the common *TUBB3* mRNA transcripts. Structure of the two common *TUBB3* transcripts showing the validated binding sites of the HuR protein and the miR-200 family. Transcripts are represented by a combination of thin and thick boxes for exons, and arrows for introns; thin boxes represent untranslated regions (5′ and 3' UTRs), while thick boxes represent translated regions. *TUBB3* transcript variants 1 and 2 are show in red and blue respectively and have been aligned to show common regions. RNA binding sites represented by boxes under their approximate location, with thickness corresponding to size. HuR binding site validated by (Prislei et al., 2013); miR-200c binding confirmed by (Cochrane et al., 2009); miR-200b binding confirmed by (Wu et al., 2020); miR-429 binding predicted by (Susanna et al., 2011); miR-200c binding confirmed by (Cochrane et al., 2009); miR-200b binding confirmed by (Wu et al., 2020); miR-429 binding predicted by (Susanna et al., 2011).

and Rustgi 2010; Pecot et al., 2013; Brozovic et al., 2015; Sulaiman et al., 2016). The expression of all five members of this miRNA family have been shown to inversely correlate with the levels of *TUBB3* in ovarian cancer patients (Susanna et al., 2011), however only two of them, miR-200b and −200c, have been demonstrated to directly bind to *TUBB3*, while miR-429 is predicted to do so (Cochrane et al., 2009; Susanna et al., 2011; Wu et al., 2020). Given these miRNAs are from the same family, they all share a similar seed sequence and are able to bind to *TUBB3* at the same location (**Figure 3**).

The most well studied member of the miR-200 family in regards to *TUBB3,* is miR-200c, which has also been shown to have an interesting relationship with the RNA binding protein HuR in its modulation of *TUBB3* translation (Cochrane et al., 2009; Cochrane et al., 2010; Raspaglio et al., 2010). Cochrane et al. (2009) and Cochrane et al. (2010) found that miR-200c binds to the *TUBB3* 3' UTR (**Figure 3**) which results in a reduction of βIII-tubulin without impacting the expression of *TUBB3* (Cochrane et al., 2009; Cochrane et al., 2010). In the context of cancer, identification of miR-200c regulating *TUBB3* expression came from *in vitro* work examining reduced miR-200c in model breast, ovarian and endometrial cancer cell lines (Cochrane et al., 2009; Cochrane et al., 2010). Changes in miR-200c have also been reported in a number of cancer cell lines and clinical specimens. Specifically, several separate studies reported that low miR-200c expression is significantly associated with high βIII-tubulin protein levels, resistance to TBAs, high incidence of recurrence and poor survival in ovarian cancer patients (Susanna et al., 2011; Brozovic et al., 2015; Sulaiman et al., 2016). These findings suggest miR-200c negatively regulates *TUBB3* expression and loss of miR-200c may result in βIII-tubulin overexpression in ovarian, breast and endometrial cancer. Additionally, recent work has demonstrated that intratumour delivery of miR-200c overexpressing exosomes can target *TUBB3* in *in vivo* models of tongue squamous cell carcinoma and restore tumour chemosensitivity (Cui et al., 2020), suggesting miR-200c has potential as a therapeutic strategy to treat individuals with βIII-tubulin overexpressing tumours.

In contrast, another study examined miR-200c expression in patients with ovarian cancer and found no relation between elevated miR-200c, βIII-tubulin levels, or chemotherapy sensitivity, leading them to examine additional elements involved with βIII-tubulin translation (Prislei et al., 2013). One element Prislei et al. (2013) chose to focus on was the expression of the RNA binding protein HuR, that had been associated with promoting the translation of *TUBB3* (Raspaglio et al., 2010). In ovarian cancer, Raspaglio et al. (2010) identified that while hypoglycaemic conditions caused an increase in *TUBB3* expression, the expression of βIII-tubulin in these conditions was reliant on the stabilization of the *TUBB3* transcript by cytosolic HuR binding to its 3' UTR (**Figure 3**) (Raspaglio et al., 2010). The authors additionally identified that high cytosolic levels of HuR in tumours was associated with high βIII-tubulin expression and poor survival in ovarian cancer patients (Raspaglio et al., 2010). Building on this work, Prislei et al. (2013) divided up their patient cohort into those with high cytosolic or high nuclear HuR expression. They found that those with high cytosolic HuR expression with elevated miR-200c levels unexpectedly had elevated βIII-tubulin levels, exhibited chemotherapy resistance and poor patient outcomes (Prislei et al., 2013). *In vitro* work then identified that miR-200c was capable of recruiting cytosolic HuR to its binding site on the *TUBB3* transcript (**Figure 3**), resulting in further stabilization of the *TUBB3* transcript which potentially accounts for the higher expression of βIII-tubulin observed in patients (Prislei et al., 2013). How miR-200c impacts the recruitment of HuR to the *TUBB3* transcript is unclear and understanding this relationship would be beneficial to unravelling how *TUBB3* expression is modulated by miRNAs.

3.2.6 Un-mapped Regulatory Elements of *TUBB3*

While the previous section highlighted elements that have been mapped to the *TUBB3* loci, there are several elements that have been demonstrated to regulate *TUBB3* expression but have no clear binding to the *TUBB3* loci. Mentioned earlier, the gonadal steroids estrogen and testosterone have both been shown to induce *TUBB3* expression and have emerged as potential drivers of *TUBB3*/βIII-tubulin expression in cancer (Butler et al., 2001; Saussede-Aim et al., 2009a; Mariani et al., 2012), however estrogen and androgen receptor elements (ERE and ARE respectively) in the *TUBB3* loci not been identified. In breast cancer cells, Saussede-Aim et al. (2009a) described an estrogen-dependent *TUBB3* regulatory pathway, where *TUBB3*/βIII-tubulin expression was inducible upon oestradiol exposure. While *in silico* analysis of the 5′ and 3' UTRs of the *TUBB3* loci failed to identify where the location of any EREs were, several binding sites for transcription factors known to be

implicated in indirect estrogen-regulation such as AP1, NF-κB, and SP1 were identified in the first intron of *TUBB3* (Saussede-Aim et al., 2009a). In the same study, oestradiol-induced *TUBB3* expression could not be reproduced in estrogen receptor (ER) negative breast cancer cell lines, and was abrogated after exposure to the ER antagonists tamoxifen and fulvestrant in several ER-expressing breast cancer cell lines. These findings suggest that oestradiol-induced *TUBB3* expression is ER-dependent. The authors proposed that ERs may regulate *TUBB3* in an indirect manner, facilitating transcription factor binding to nearby corresponding sites in intron 1 and subsequent *TUBB3* transcription activation. Conflicting results were reported in invasive breast cancer specimens, where high *TUBB3* expression was identified in both ER positive and ER negative breast tumour specimens (Wang et al., 2013), raising the question as to whether ER is relevant to *TUBB3* regulation in the clinic. This disparity could be explained by the different biology in cell models and clinical specimens. In the study by Wang et al. (2013), specimens were collected from patients with different pathological stages, with or without neoadjuvant chemotherapy, all of which could potentially contribute to high *TUBB3* expression. In addition, patients in this study were not treated with estrogen and therefore further studies are required to assess the clinical value of ER in *TUBB3* regulation in breast cancer.

In colorectal cancer, elevated *TUBB3* expression is associated with invasive phenotypes in both genders (Portyanko et al., 2009; Zhao et al., 2016). *In vitro* analysis of 23 colorectal cancer cell lines suggested that *TUBB3*/βIII-tubulin is activated after exposure to androgens in males (Mariani et al., 2012), as seen with estrogens in breast cancer cells (Saussede-Aim et al., 2009a). In both male and female colorectal cancer cell lines, stable silencing of androgen receptors (AR) yielded significant downregulation of *TUBB3*/βIII-tubulin, raising the possibility that ARs play a significant role in driving *TUBB3* expression. Importantly, in male colorectal cancer cells, the AR-dependent *TUBB3* regulatory pathway is constitutively activated via testicular androgen, while in colorectal cancer cell lines derived from women *TUBB3* is only inducible upon serum starvation (Mariani et al., 2012). This finding suggests that for males and females, there are differences in how the AR regulatory regions are impacted and are able to induce *TUBB3* expression in response to external stimuli. While mapped in mice and rats (De Gendt et al., 2011), future mutagenesis and ChIP studies are required to identify AR binding regions within the human *TUBB3* gene to understand this sex based expression pattern of *TUBB3*.

Other factors have also been proposed to play a role in *TUBB3* regulation. For example, overexpression of Semaphorin-6A (*SEMA6A*) is correlated with *TUBB3*/βIII-tubulin upregulation in ovarian cancer cells, while the reverse is observed in *SEMA6A* knockdown cells (Prislei et al., 2008). Likewise, levels of the transcription factor ZEB1 have also been shown to influence *TUBB3* expression in ovarian cancer in the same manner as Semaphorin-6A (Lobert et al., 2013). Additionally, Kanojia et al. (2020) identified a potential ZEB1 binding site within the *TUBB3* 5' UTR, and their data supports that ZEB1 promotes *TUBB3* expression, as increasing *ZEB1* expression led to an elevation of *TUBB3* expression. In contrast to Semaphorin-6A and ZEB1, the overexpression of the Snail family zinc finger transcription factor SLUG in non-small cell lung cancer cells suppressed expression of *TUBB3*/βIII-tubulin, as well as the β-tubulin isotype, *TUBB4A*/βIVa-tubulin (Tamura et al., 2013). This study then focused on the relationship between Slug and *TUBB4A*, and did not investigate the SLUG induced suppression of *TUBB3* further (Tamura et al., 2013).

Slug is co-expressed with βIII-tubulin and Sox9 in pre-migratory avian neural crest cells (Chacon and Rogers 2019). Additionally, SLUG has been shown to directly interact with SOX9 to promote the formation of cancer stem-like cells in lung cancer (Luanpitpong et al., 2016), and there is the recent speculation that *TUBB3* may be playing a role in the maintenance of cancer stem like cells (Namekawa et al., 2020). Though it does present as an oddity, these studies suggest that Slug may only be a *TUBB3* repressor under certain conditions. Two other family members, Snail and Scratch1, are also involved in *TUBB3* regulation. As previously mentioned, Scratch1 expression results in increased βIII-tubulin in a neuronal setting (Nakakura et al., 2001b). In contrast, Scratch1 may not be involved with *TUBB3* regulation in a cancer setting due to its lack of expression in a wide range of patient samples obtained from different tumours (Bastid et al., 2010). The expression of the third family member, Snail/*SNAI1* itself, has also been shown to correlate with the expression of *TUBB3*/βIII-tubulin in colon cancer cells (Sobierajska et al., 2016), however other than expression, no mechanistic study has been reported. Snail and Slug both present as interesting regulators of *TUBB3*, as they are both expressed in a large range of cancers (Bastid et al., 2010), and also because of their roles in the epithelial–mesenchymal transition in tumour cells, the process linked with metastasis (Thiery and Sleeman 2006). Additional studies are required to assess whether Snail or Slug can directly bind to the *TUBB3* loci and regulate its expression, especially given βIII-tubulin's roles in drug resistance and tumor aggressiveness.

Finally, K-Ras signalling has been associated with the regulation of βIII-tubulin translation in cancer (Levallet et al., 2012). While investigating K-Ras signalling in non-small cell lung cancer, Levallet et al. (2012) identified K-Ras mutations in clinical samples were strongly and frequently associated with positive βIII-tubulin expression. In immortalised human bronchial cells, expression of a K-Ras mutant protein was shown to significantly increase βIII-tubulin protein levels, while *TUBB3* mRNA remained unchanged (Levallet et al., 2012). This observation raises the possibility that βIII-tubulin translation or turnover may be controlled by K-Ras-induced signalling cascades. In further support of this notion, siRNA knockdown of K-Ras and pharmacologic inhibition of K-Ras downstream effectors resulted in βIII-tubulin protein downregulation (Levallet et al., 2012). Additionally, overexpression of EGFR enhanced βIII-tubulin translation in both K-Ras wild type and mutant expressing cell lines, however non-small cell lung cancer associated EGFR mutations appeared to have no impact on βIII-tubulin translation (Levallet et al., 2012). Understanding, what is driving the increased translation of

TUBB3 in this circumstance would greatly enhance our knowledge on βIII-tubulin translation and stability.

3.2.7 Targeting the *TUBB3* Transcript

Due to the high degree of homology of βIII-tubulin with other β-tubulin isotypes, small molecule inhibitors against this protein are difficult to develop. Given the high expression of *TUBB3*/βIII-tubulin in epithelial cancers, strategies to silence *TUBB3* have been explored. Cui et al. (2020) demonstrated that targeting the *TUBB3* transcript directly was sufficient to restore tumour chemosensitivity. There is strong preclinical evidence that targeting the *TUBB3* transcript through the use of transient or stable gene silencing can increase drug sensitivity, reduce tumour growth, and suppress metastasis in non-small cell lung cancer and pancreatic cancer (Kavallaris et al., 1999; Gan et al., 2007; Gan et al., 2010a; McCarroll et al., 2010; McCarroll et al., 2015b). Along with our colleagues, we have been exploring the development of therapeutic strategies to silence *TUBB3,* and hence βIII-tubulin, in tumors that overexpress this isotype. In pancreatic cancer, we developed polymeric star nanoparticles capable of delivering and potently silencing *TUBB3* siRNA in a clinically relevant orthotopic model of pancreatic cancer and showed that this increased drug sensitivity and reduced metastasis (Teo et al., 2016; McCarroll et al., 2019; Conte et al., 2021). Recently we described the developed of nanoparticles loaded with docetaxel (DTX) and an siRNA against *TUBB3*, in order to have a synergistic effect in the treatment of lung cancer (Conte et al., 2021). In this study we showed that combining DTX/*TUBB3*-siRNA into nanoparticles led to a significant decrease in *TUBB3* and cell viability of tumour cell spheroids compared to nanoparticles loaded with DTX alone—demonstrating the combined anticancer effects of βIII-tubulin reduction and increased drug sensitivity (Conte et al., 2021). Collectively, these studies highlight the potential of developing therapeutic strategies to target *TUBB3* in cancer cells.

4 CONCLUSION

In both normal and cancerous tissue, it is clear the regulation of both *TUBB3* expression and translation is controlled by a complex and multifaced system. This review highlights that a combination of transcriptional controls and altered epigenetic modifications, in conjunction with disrupted signalling pathways may all contribute to disrupted *TUBB3* expression in cancers and subsequent response to therapy. Genomic advances such as single cell analysis and spatial transcriptomics may lead to improved identification of differences between cell-types, and the regulation of *TUBB3* within the tumour microenvironment. Progressing our understanding of βIII-tubulin regulation is not only important in identifying how the nervous system develops but also in cancer, where it will aid in the identification of potential therapeutic targets and treatment strategies.

AUTHOR CONTRIBUTIONS

AD, FK and WT wrote the original draft. MK supervised and edited this work. All authors have read and agreed to the submitted version of this manuscript.

FUNDING

MK is supported by grants from the National Health and Medical Research (Program Grant APP1091261 and Principal Research Fellowship APP1119152), Cancer Institute New South Wales Program Grant (TPG 2037) and Cancer Australia grant (1141485). FK was supported by an Australian Postgraduate Award, Lung Foundation Australia Lung Cancer National Program Postgraduate Grant-in-Aid, and The LH Ainsworth Cancer Research Scholarship FK. This work was supported by the Children's Cancer Institute, which is affiliated with the University of New South Wales (UNSW Sydney), and the Sydney Children's Hospital Network.

REFERENCES

Acloque, H., Wilkinson, D. G., and Nieto, M. A. (2008). Chapter 9 *In Situ* Hybridization Analysis of Chick Embryos in Whole-Mount and Tissue Sections. *Methods Cel Biol.* 87, 169–185. doi:10.1016/s0091-679x(08)00209-4

Akasaka, K., Maesawa, C., Shibazaki, M., Maeda, F., Takahashi, K., Akasaka, T., et al. (2009). Loss of Class III β-Tubulin Induced by Histone Deacetylation Is Associated with Chemosensitivity to Paclitaxel in Malignant Melanoma Cells. *J. Invest. Dermatol.* 129 (6), 1516–1526. doi:10.1038/jid.2008.406

Azzarelli, R., McNally, A., Dell'Amico, C., Onorati, M., Simons, B., and Philpott, A. (2022). ASCL1 Phosphorylation and ID2 Upregulation Are Roadblocks to Glioblastoma Stem Cell Differentiation. *Sci. Rep.* 12 (1), 2341. doi:10.1038/s41598-022-06248-x

Baertsch, R., Diekhans, M., Kent, W. J., Haussler, D., and Brosius, J. (2008). Retrocopy Contributions to the Evolution of the Human Genome. *BMC Genomics* 9 (1), 466. doi:10.1186/1471-2164-9-466

Bär, J., Popp, Y., Bucher, M., and Mikhaylova, M. (2022). Direct and Indirect Effects of Tubulin post-translational Modifications on Microtubule Stability: Insights and Regulations. *Biochim. Biophys. Acta (Bba) - Mol. Cel Res.* 1869 (6), 119241.

Bastid, J., Bouchet, B. P., Ciancia, C., Pourchet, J., Audoynaud, C., Grelier, G., et al. (2010). The SNAIL Family Member SCRATCH1 Is Not Expressed in Human Tumors. *Oncol. Rep.* 23 (2), 523–529.

Bergsland, M., Werme, M., Malewicz, M., Perlmann, T., and Muhr, J. (2006). The Establishment of Neuronal Properties Is Controlled by Sox4 and Sox11. *Genes Dev.* 20 (24), 3475–3486. doi:10.1101/gad.403406

Bordji, K., Grandval, A., Cuhna-Alves, L., Lechapt-Zalcman, E., and Bernaudin, M. (2014). Hypoxia-inducible Factor-2α (HIF-2α), but Not HIF-1α, Is Essential for Hypoxic Induction of Class III β-tubulin Expression in Human Glioblastoma Cells. *FEBS J.* 281 (23), 5220–5236. doi:10.1111/febs.13062

Brozovic, A., Duran, G. E., Wang, Y. C., Francisco, E. B., and Sikic, B. I. (2015). The miR-200 Family Differentially Regulates Sensitivity to Paclitaxel and Carboplatin in Human Ovarian Carcinoma OVCAR-3 and MES-OV Cells. *Mol. Oncol.* 9 (8), 1678–1693. doi:10.1016/j.molonc.2015.04.015

Butler, R., Leigh, P. N., and Gallo, J.-M. (2001). Androgen-induced Up-Regulation of Tubulin Isoforms in Neuroblastoma Cells. *J. Neurochem.* 78 (4), 854–861. doi:10.1046/j.1471-4159.2001.00475.x

Caccamo, D., Katsetos, C. D., Herman, M. M., Frankfurter, A., Collins, V. P., and Rubinstein, L. J. (1989). Immunohistochemistry of a Spontaneous Murine Ovarian Teratoma with Neuroepithelial Differentiation. Neuron-Associated β-Tubulin as a Marker for Primitive Neuroepithelium. *Lab. Invest.* 60 (3), 390–398.

Cao, S., Du, J., Lv, Y., Lin, H., Mao, Z., Xu, M., et al. (2017). PAX3 Inhibits β-Tubulin-III Expression and Neuronal Differentiation of Neural Stem Cell. *Biochem. Biophysical Res. Commun.* 485 (2), 307–311. doi:10.1016/j.bbrc.2017.02.086

Castillo, S. D., Matheu, A., Mariani, N., Carretero, J., Lopez-Rios, F., Lovell-Badge, R., et al. (2012). Novel Transcriptional Targets of the SRY-HMG Box Transcription Factor SOX4 Link its Expression to the Development of Small Cell Lung Cancer. *Cancer Res.* 72 (1), 176–186. doi:10.1158/0008-5472.can-11-3506

Chacon, J., and Rogers, C. D. (2019). Early Expression of Tubulin β-III in Avian Cranial Neural Crest Cells. *Gene Expr. Patterns* 34, 119067. doi:10.1016/j.gep.2019.119067

Chen, C., Lee, G. A., Pourmorady, A., Sock, E., and Donoghue, M. J. (2015). Orchestration of Neuronal Differentiation and Progenitor Pool Expansion in the Developing Cortex by SoxC Genes. *J. Neurosci.* 35 (29), 10629–10642. doi:10.1523/jneurosci.1663-15.2015

Cleveland, D. W., Joshi, H. C., and Murphy, D. B. (1990). Tubulin Site Interpretation. *Nature* 344 (6265), 389. doi:10.1038/344389a0

Clevers, H. (2011). The Cancer Stem Cell: Premises, Promises and Challenges. *Nat. Med.* 17 (3), 313–319. doi:10.1038/nm.2304

Cochrane, D. R., Howe, E. N., Spoelstra, N. S., and Richer, J. K. (2010). Loss of miR-200c: A Marker of Aggressiveness and Chemoresistance in Female Reproductive Cancers. *J. Oncol.* 2010, 821717. doi:10.1155/2010/821717

Cochrane, D. R., Spoelstra, N. S., Howe, E. N., Nordeen, S. K., and Richer, J. K. (2009). MicroRNA-200c Mitigates Invasiveness and Restores Sensitivity to Microtubule-Targeting Chemotherapeutic Agents. *Mol. Cancer Ther.* 8 (5), 1055–1066. doi:10.1158/1535-7163.mct-08-1046

Conte, C., Monteiro, P. F., Gurnani, P., Stolnik, S., Ungaro, F., Quaglia, F., et al. (2021). Multi-component Bioresponsive Nanoparticles for Synchronous Delivery of Docetaxel and TUBB3 siRNA to Lung Cancer Cells. *Nanoscale* 13 (26), 11414–11426. doi:10.1039/d1nr02179f

Coulson, J. M., Edgson, J. L., Woll, P. J., and Quinn, J. P. (2000). A Splice Variant of the Neuron-Restrictive Silencer Factor Repressor Is Expressed in Small Cell Lung Cancer: A Potential Role in Derepression of Neuroendocrine Genes and a Useful Clinical Marker. *Cancer Res.* 60 (7), 1840–1844.

Cui, J., Wang, H., Zhang, X., Sun, X., Zhang, J., and Ma, J. (2020). Exosomal miR-200c Suppresses Chemoresistance of Docetaxel in Tongue Squamous Cell Carcinoma by Suppressing TUBB3 and PPP2R1B. *Aging* 12 (8), 6756–6773. doi:10.18632/aging.103036

Cunningham, F., Achuthan, P., Akanni, W., Allen, J., Amode, M. R., Armean, I. M., et al. (2018). Ensembl 2019. *Nucleic Acids Res.* 47 (D1), D745–D751. doi:10.1093/nar/gky1113

Dai, W., Li, W., Hoque, M., Li, Z., Tian, B., and Makeyev, E. V. (2015). A post-transcriptional Mechanism Pacing Expression of Neural Genes with Precursor Cell Differentiation Status. *Nat. Commun.* 6 (1), 7576. doi:10.1038/ncomms8576

Daily, K., Ho Sui, S. J., Schriml, L. M., Dexheimer, P. J., Salomonis, N., Schroll, R., et al. (2017). Molecular, Phenotypic, and Sample-Associated Data to Describe Pluripotent Stem Cell Lines and Derivatives. *Sci. Data* 4, 170030. doi:10.1038/sdata.2017.30

Dalziel, M., Kolesnichenko, M., das Neves, R. P., Iborra, F., Goding, C., and Furger, A. (2011). α-MSH Regulates Intergenic Splicing of MC1R and TUBB3 in Human Melanocytes. *Nucleic Acids Res.* 39 (6), 2378–2392. doi:10.1093/nar/gkq1125

Danza, G., Di Serio, C., Rosati, F., Lonetto, G., Sturli, N., Kacer, D., et al. (2012). Notch Signaling Modulates Hypoxia-Induced Neuroendocrine Differentiation of Human Prostate Cancer Cells. *Mol. Cancer Res.* 10 (2), 230–238. doi:10.1158/1541-7786.mcr-11-0296

De Gendt, K., Denolet, E., Willems, A., Daniels, V. W., Clinckemalie, L., Denayer, S., et al. (2011). Expression of Tubb3, a β-Tubulin Isotype, Is Regulated by Androgens in Mouse and Rat Sertoli Cells1. *Biol. Reprod.* 85 (5), 934–945. doi:10.1095/biolreprod.110.090704

Dennis, K., Uittenbogaard, M., Chiaramello, A., and Moody, S. A. (2002). Cloning and Characterization of the 5'-flanking Region of the Rat Neuron-specific Class III β-Tubulin Gene. *Gene* 294 (1-2), 269–277. doi:10.1016/s0378-1119(02)00801-6

Denolet, E., De Gendt, K., Allemeersch, J., Engelen, K., Marchal, K., Van Hummelen, P., et al. (2006). The Effect of a Sertoli Cell-Selective Knockout of the Androgen Receptor on Testicular Gene Expression in Prepubertal Mice. *Mol. Endocrinol.* 20 (2), 321–334. doi:10.1210/me.2005-0113

Diaz, A., and Leon, K. (2011). Therapeutic Approaches to Target Cancer Stem Cells. *Cancers* 3 (3), 3331–3352. doi:10.3390/cancers3033331

D. Katsetos, C., Draber, P., and Kavallaris, M. (2011). Targeting βIII-Tubulin in Glioblastoma Multiforme: From Cell Biology and Histopathology to Cancer Therapeutics. *Acamc* 11 (8), 719–728. doi:10.2174/187152011797378760

D. Katsetos, C., and Draber, P. (2012). Tubulins as Therapeutic Targets in Cancer: from Bench to Bedside. *Cpd* 18 (19), 2778–2792. doi:10.2174/138161212800626193

Doherty, E. J., Macy, M. E., Wang, S. M., Dykeman, C. P., Melanson, M. T., and Engle, E. C. (1999). CFEOM3: a New Extraocular Congenital Fibrosis Syndrome that Maps to 16q24.2-q24.3. *Invest. Ophthalmol. Vis. Sci.* 40 (8), 1687–1694.

Dráberová, E., Del Valle, L., Gordon, J., Marková, V., Smejkalová, B., Bertrand, L., et al. (2008). Class III β-Tubulin Is Constitutively Coexpressed with Glial Fibrillary Acidic Protein and Nestin in Midgestational Human Fetal Astrocytes: Implications for Phenotypic Identity. *J. Neuropathol. Exp. Neurol.* 67 (4), 341–354.

Easter, S., Jr., Ross, L., and Frankfurter, A. (1993). Initial Tract Formation in the Mouse Brain. *J. Neurosci.* 13 (1), 285–299. doi:10.1523/jneurosci.13-01-00285.1993

Fishilevich, S., Nudel, R., Rappaport, N., Hadar, R., Plaschkes, I., Iny Stein, T., et al. (2017). GeneHancer: Genome-wide Integration of Enhancers and Target Genes in GeneCards. *Database (Oxford)* 2017, bax028. doi:10.1093/database/bax028

Forde, J. C., Perry, A. S., Brennan, K., Martin, L. M., Lawler, M. P., Lynch, T. H., et al. (2010). Docetaxel Maintains its Cytotoxic Activity under Hypoxic Conditions in Prostate Cancer Cells. *Urol. Oncol.* 30 (6), 912–919. doi:10.1016/j.urolonc.2010.08.015

Fu, J. Q., Chen, Z., Hu, Y. J., Fan, Z. H., Guo, Z. X., Liang, J. Y., et al. (2019). A Single Factor Induces Neuronal Differentiation to Suppress Glioma Cell Growth. *CNS Neurosci. Ther.* 25 (4), 486–495. doi:10.1111/cns.13066

Gan, P. P., McCarroll, J. A., Byrne, F. L., Garner, J., and Kavallaris, M. (2011). Specific β-Tubulin Isotypes Can Functionally Enhance or Diminish Epothilone B Sensitivity in Non-small Cell Lung Cancer Cells. *PLoS ONE* 6 (6), e21717. doi:10.1371/journal.pone.0021717

Gan, P. P., McCarroll, J. A., Po'uha, S. T., Kamath, K., Jordan, M. A., and Kavallaris, M. (2010a). Microtubule Dynamics, Mitotic Arrest, and Apoptosis: Drug-Induced Differential Effects of βIII-Tubulin. *Mol. Cancer Ther.* 9 (5), 1339–1348. doi:10.1158/1535-7163.mct-09-0679

Gan, P. P., McCarroll, J. A., Po'uha, S. T., Kamath, K., Jordan, M. A., and Kavallaris, M. (2010b). Microtubule Dynamics, Mitotic Arrest, and Apoptosis: Drug-Induced Differential Effects of βIII-Tubulin. *Mol. Cancer Ther.* 9 (5), 1339–1348. doi:10.1158/1535-7163.mct-09-0679

Gan, P. P., Pasquier, E., and Kavallaris, M. (2007). Class III β-Tubulin Mediates Sensitivity to Chemotherapeutic Drugs in Non-small Cell Lung Cancer. *Cancer Res.* 67 (19), 9356–9363. doi:10.1158/0008-5472.can-07-0509

Gao, S., Zhao, X., Lin, B., Hu, Z., Yan, L., and Gao, J. (2012). Clinical Implications of REST and TUBB3 in Ovarian Cancer and its Relationship to Paclitaxel Resistance. *Tumor Biol.* 33 (5), 1759–1765. doi:10.1007/s13277-012-0435-y

Goodall, E. F., Heath, P. R., Bandmann, O., Kirby, J., and Shaw, P. J. (2013). Neuronal Dark Matter: the Emerging Role of microRNAs in Neurodegeneration. *Front. Cel. Neurosci.* 7, 178. doi:10.3389/fncel.2013.00178

GTEx Consortium (2015). Human Genomics. The Genotype-Tissue Expression (GTEx) Pilot Analysis: Multitissue Gene Regulation in Humans. *Science* 348 (6235), 648–660. doi:10.1126/science.1262110

Haendel, M. A., Bollinger, K. E., and Baas, P. W. (1996). Cytoskeletal Changes during Neurogenesis in Cultures of Avain Neural Crest Cells. *J. Neurocytol* 25 (4), 289–301. doi:10.1007/BF02284803

Haeussler, M., Zweig, A. S., Tyner, C., Speir, M. L., Rosenbloom, K. R., Raney, B. J., et al. (2019). The UCSC Genome Browser Database: 2019 Update. *Nucleic Acids Res.* 47 (D1), D853–d858. doi:10.1093/nar/gky1095

Hanahan, D. (2022). Hallmarks of Cancer: New Dimensions. *Cancer Discov.* 12 (1), 31–46. doi:10.1158/2159-8290.cd-21-1059

Hatano, Y., Yamada, Y., Hata, K., Phutthaphadoong, S., Aoki, H., and Hara, A. (2011). Genetic Ablation of a Candidate Tumor Suppressor Gene, Rest, Does Not Promote Mouse colon Carcinogenesis. *Cancer Sci.* 102 (9), 1659–1664. doi:10.1111/j.1349-7006.2011.02006.x

Hausrat, T. J., Radwitz, J., Lombino, F. L., Breiden, P., and Kneussel, M. (2021). Alpha- and β-tubulin Isotypes Are Differentially Expressed during Brain Development. *Develop. Neurobiol.* 81 (3), 333–350. doi:10.1002/dneu.22745

Herraiz, C., Garcia-Borron, J. C., Jiménez-Cervantes, C., and Olivares, C. (2017). MC1R Signaling. Intracellular Partners and Pathophysiological Implications. *Biochim. Biophys. Acta (Bba) - Mol. Basis Dis.* 1863 (10), 2448–2461. doi:10.1016/j.bbadis.2017.02.027

Herraiz, C., Olivares, C., Castejón-Griñán, M., Abrisqueta, M., Jiménez-Cervantes, C., and García-Borrón, J. C. (2015). Functional Characterization of MC1R-TUBB3 Intergenic Splice Variants of the Human Melanocortin 1 Receptor. *PloS one* 10 (12), e0144757. doi:10.1371/journal.pone.0144757

Hinsch, A., Chaker, A., Burdelski, C., Koop, C., Tsourlakis, M. C., Steurer, S., et al. (2017). β III-Tubulin Overexpression Is Linked to Aggressive Tumor Features and Genetic Instability in Urinary Bladder Cancer. *Hum. Pathol.* 61, 210–220. doi:10.1016/j.humpath.2016.11.005

Hoser, M., Potzner, M. R., Koch, J. M. C., Bösl, M. R., Wegner, M., and Sock, E. (2008). Sox12 Deletion in the Mouse Reveals Nonreciprocal Redundancy with the Related Sox4 and Sox11 Transcription Factors. *Mol. Cel Biol* 28 (15), 4675–4687. doi:10.1128/mcb.00338-08

Izutsu, N., Maesawa, C., Shibazaki, M., Oikawa, H., Shoji, T., Sugiyama, T., et al. (2008). Epigenetic Modification Is Involved in Aberrant Expression of Class III β-tubulin, TUBB3, in Ovarian Cancer Cells. *Int. J. Oncol.* 32 (6), 1227–1235. doi:10.3892/ijo.32.6.1227

Jiang, Y. Q., and Oblinger, M. M. (1992). Differential Regulation of β III and Other Tubulin Genes during Peripheral and central Neuron Development. *J. Cel Sci* 103 (Pt 3) (Pt 3), 643–651. doi:10.1242/jcs.103.3.643

Jordan, M. A., Thrower, D., and Wilson, L. (1991). Mechanism of Inhibition of Cell Proliferation by Vinca Alkaloids. *Cancer Res.* 51 (8), 2212–2222.

Jordan, M. A., and Wilson, L. (2004). Microtubules as a Target for Anticancer Drugs. *Nat. Rev. Cancer* 4 (4), 253–265. doi:10.1038/nrc1317

Kanakkanthara, A., and Miller, J. H. (2021). Biii-Tubulin Overexpression in Cancer: Causes, Consequences, and Potential Therapies. *Biochim. Biophys. Acta (Bba) - Rev. Cancer* 1876 (2), 188607. doi:10.1016/j.bbcan.2021.188607

Kanojia, D., Panek, W. K., Cordero, A., Fares, J., Xiao, A., Savchuk, S., et al. (2020). BET Inhibition Increases βIII-tubulin Expression and Sensitizes Metastatic Breast Cancer in the Brain to Vinorelbine. *Sci. Transl Med.* 12 (558). doi:10.1126/scitranslmed.aax2879

Karki, R., Mariani, M., Andreoli, M., He, S., Scambia, G., Shahabi, S., et al. (2013). Biii-Tubulin: Biomarker of Taxane Resistance or Drug Target? *Expert Opin. Ther. Targets* 17 (4), 461–472. doi:10.1517/14728222.2013.766170

Katsetos, C. D., Del Valle, L., Geddes, J. F., Aldape, K., Boyd, J. C., Legido, A., et al. (2002). Localization of the Neuronal Class III β-Tubulin in Oligodendrogliomas: Comparison with Ki-67 Proliferative Index and 1p/19q Status. *J. Neuropathol. Exp. Neurol.* 61 (4), 307–320. doi:10.1093/jnen/61.4.307

Katsetos, C. D., Herman, M. M., and Mörk, S. J. (2003). Class III β-tubulin in Human Development and Cancer. *Cell Motil. Cytoskeleton* 55 (2), 77–96. doi:10.1002/cm.10116

Katsetos, C. D., Reginato, M. J., Baas, P. W., D'Agostino, L., Legido, A., Tuszyn´ski, J. A., et al. (2015). Emerging Microtubule Targets in Glioma Therapy. *Semin. Pediatr. Neurol.* 22 (1), 49–72. doi:10.1016/j.spen.2015.03.009

Kavallaris, M., Burkhart, C. A., and Horwitz, S. B. (1999). Antisense Oligonucleotides to Class III β-tubulin Sensitize Drug-Resistant Cells to Taxol. *Br. J. Cancer* 80 (7), 1020–1025. doi:10.1038/sj.bjc.6690507

Kavallaris, M., Kuo, D. Y., Burkhart, C. A., Regl, D. L., Norris, M. D., Haber, M., et al. (1997). Taxol-resistant Epithelial Ovarian Tumors Are Associated with Altered Expression of Specific β-Tubulin Isotypes. *J. Clin. Invest.* 100 (5), 1282–1293. doi:10.1172/jci119642

Kavallaris, M. (2010). Microtubules and Resistance to Tubulin-Binding Agents. *Nat. Rev. Cancer* 10 (3), 194–204. doi:10.1038/nrc2803

Kreisler, A., Strissel, P. L., Strick, R., Neumann, S. B., Schumacher, U., and Becker, C.-M. (2010). Regulation of the NRSF/REST Gene by Methylation and CREB Affects the Cellular Phenotype of Small-Cell Lung Cancer. *Oncogene* 29 (43), 5828–5838. doi:10.1038/onc.2010.321

Kuang, Y.-L., Munoz, A., Nalula, G., Santostefano, K. E., Sanghez, V., Sanchez, G., et al. (2019). Evaluation of Commonly Used Ectoderm Markers in iPSC Trilineage Differentiation. *Stem Cel. Res.* 37, 101434. doi:10.1016/j.scr.2019.101434

La Regina, G., Coluccia, A., Naccarato, V., and Silvestri, R. (2019). Towards Modern Anticancer Agents that Interact with Tubulin. *Eur. J. Pharm. Sci.* 131, 58–68. doi:10.1016/j.ejps.2019.01.028

Latremoliere, A., Cheng, L., DeLisle, M., Wu, C., Chew, S., Hutchinson, E. B., et al. (2018). Neuronal-Specific TUBB3 Is Not Required for Normal Neuronal Function but Is Essential for Timely Axon Regeneration. *Cel Rep.* 24 (7), 1865–1879. e1869. doi:10.1016/j.celrep.2018.07.029

Le Dréau, G., Escalona, R., Fueyo, R., Herrera, A., Martínez, J. D., Usieto, S., et al. (2018). E Proteins Sharpen Neurogenesis by Modulating Proneural bHLH Transcription Factors' Activity in an E-box-dependent Manner. *Elife* 7.

Leandro-García, L. J., Leskelä, S., Landa, I., Montero-Conde, C., López-Jiménez, E., Letón, R., et al. (2010). Tumoral and Tissue-specific Expression of the Major Human β-tubulin Isotypes. *Cytoskeleton* 67 (4), 214–223.

Lee, M. K., Rebhun, L. I., and Frankfurter, A. (1990a). Posttranslational Modification of Class III Beta-Tubulin. *Proc. Natl. Acad. Sci. U.S.A.* 87 (18), 7195–7199. doi:10.1073/pnas.87.18.7195

Lee, M. K., Tuttle, J. B., Rebhun, L. I., Cleveland, D. W., and Frankfurter, A. (1990b). The Expression and Posttranslational Modification of a Neuron-specific ?-tubulin Isotype during Chick Embryogenesis. *Cel Motil. Cytoskeleton* 17 (2), 118–132. doi:10.1002/cm.970170207

Lehmann, S. G., Bourgoin-Voillard, S., Seve, M., and Rachidi, W. (2017). Tubulin Beta-3 Chain as a New Candidate Protein Biomarker of Human Skin Aging: A Preliminary Study. *Oxid Med. Cel Longev* 2017, 5140360. doi:10.1155/2017/5140360

Levallet, G., Bergot, E., Antoine, M., Creveuil, C., Santos, A. O., Beau-Faller, M., et al. (2012). High TUBB3 Expression, an Independent Prognostic Marker in Patients with Early Non-small Cell Lung Cancer Treated by Preoperative Chemotherapy, Is Regulated by K-Ras Signaling Pathway. *Mol. Cancer Ther.* 11 (5), 1203–1213. doi:10.1158/1535-7163.mct-11-0899

Lewis, S. A., and Cowan, N. J. (1988). Complex Regulation and Functional Versatility of Mammalian Alpha- and Beta-Tubulin Isotypes during the Differentiation of Testis and Muscle Cells. *J. Cel Biol* 106 (6), 2023–2033. doi:10.1083/jcb.106.6.2023

Linhartová, I., Dráber, P., Dráberová, E., and Viklický, V. (1992). Immunological Discrimination of Beta-Tubulin Isoforms in Developing Mouse Brain. Post-translational Modification of Non-class-III Beta-Tubulins. *Biochem. J.* 288 (Pt 3Pt 3), 919–924.

Liu, L., Geisert, E. E., Frankfurter, A., Spano, A. J., Jiang, C. X., Yue, J., et al. (2007). A Transgenic Mouse Class-III β Tubulin Reporter Using Yellow Fluorescent Protein. *genesis* 45 (9), 560–569. doi:10.1002/dvg.20325

Liu, P., Ramachandran, S., Ali Seyed, M., Scharer, C. D., Laycock, N., Dalton, W. B., et al. (2006). Sex-Determining Region Y Box 4 Is a Transforming Oncogene in Human Prostate Cancer Cells. *Cancer Res.* 66 (8), 4011–4019. doi:10.1158/0008-5472.can-05-3055

Lobert, S., Graichen, M. E., and Morris, K. (2013). Coordinated Regulation of β-Tubulin Isotypes and Epithelial-To-Mesenchymal Transition Protein ZEB1 in Breast Cancer Cells. *Biochemistry* 52 (32), 5482–5490. doi:10.1021/bi400340g

Lobert, S., Jefferson, B., and Morris, K. (2011). Regulation of β-tubulin Isotypes by Micro-RNA 100 in MCF7 Breast Cancer Cells. *Cytoskeleton* 68 (6), 355–362. doi:10.1002/cm.20517

Locher, H., de Rooij, K. E., de Groot, J. C., van Doorn, R., Gruis, N. A., Löwik, C. W., et al. (2013). Class III β-tubulin, a Novel Biomarker in the Human Melanocyte Lineage. *Differentiation* 85 (4-5), 173–181. doi:10.1016/j.diff.2013.05.003

Lopata, M. A., Havercroft, J. C., Chow, L. T., and Cleveland, D. W. (1983). Four Unique Genes Required for β Tubulin Expression in Vertebrates. *Cell* 32 (3), 713–724. doi:10.1016/0092-8674(83)90057-0

Luanpitpong, S., Li, J., Manke, A., Brundage, K., Ellis, E., McLaughlin, S. L., et al. (2016). SLUG Is Required for SOX9 Stabilization and Functions to Promote Cancer Stem Cells and Metastasis in Human Lung Carcinoma. *Oncogene* 35 (22), 2824–2833. doi:10.1038/onc.2015.351

Ludueña, R. F. (2013). A Hypothesis on the Origin and Evolution of Tubulin. *Int. Rev. Cel Mol Biol* 302, 41–185.

Ludueña, R. F. (1993). Are Tubulin Isotypes Functionally Significant. *Mol. Biol. Cel* 4 (5), 445–457.

Ludueña, R. F. (1998). Multiple Forms of Tubulin: Different Gene Products and Covalent Modifications. *Int. Rev. Cytol.* 178, 207–275.

Maciotta, S., Meregalli, M., and Torrente, Y. (2013). The Involvement of microRNAs in Neurodegenerative Diseases. *Front. Cel. Neurosci.* 7, 265. doi:10.3389/fncel.2013.00265

Mao, X. R., Moerman-Herzog, A. M., Chen, Y., and Barger, S. W. (2009). Unique Aspects of Transcriptional Regulation in Neurons - Nuances in NFkappaB and Sp1-Related Factors. *J. Neuroinflammation* 6 (1), 16. doi:10.1186/1742-2094-6-16

Mao, X., Yang, S.-H., Simpkins, J. W., and Barger, S. W. (2007). Glutamate Receptor Activation Evokes Calpain-Mediated Degradation of Sp3 and Sp4, the Prominent Sp-Family Transcription Factors in Neurons. *J. Neurochem.* 100 (5), 1300–1314. doi:10.1111/j.1471-4159.2006.04297.x

Mariani, M., Karki, R., Spennato, M., Pandya, D., He, S., Andreoli, M., et al. (2015). Class III β-tubulin in normal and Cancer Tissues. *Gene* 563 (2), 109–114. doi:10.1016/j.gene.2015.03.061

Mariani, M., Zannoni, G. F., Sioletic, S., Sieber, S., Martino, C., Martinelli, E., et al. (2012). Gender Influences the Class III and V β-Tubulin Ability to Predict Poor Outcome in Colorectal Cancer. *Clin. Cancer Res.* 18 (10), 2964–2975. doi:10.1158/1078-0432.ccr-11-2318

Martini, S., Bernoth, K., Main, H., Ortega, G. D. C., Lendahl, U., Just, U., et al. (2013). A Critical Role for Sox9 in Notch-Induced Astrogliogenesis and Stem Cell Maintenance. *STEM CELLS* 31 (4), 741–751. doi:10.1002/stem.1320

McCarroll, J. A., Gan, P. P., Erlich, R. B., Liu, M., Dwarte, T., Sagnella, S. S., et al. (2015a). TUBB3/βIII-Tubulin Acts through the PTEN/AKT Signaling Axis to Promote Tumorigenesis and Anoikis Resistance in Non-small Cell Lung Cancer. *Cancer Res.* 75 (2), 415–425. doi:10.1158/0008-5472.can-14-2740

McCarroll, J. A., Gan, P. P., Liu, M., and Kavallaris, M. (2010). Biii-Tubulin Is a Multifunctional Protein Involved in Drug Sensitivity and Tumorigenesis in Non-small Cell Lung Cancer. *Cancer Res.* 70 (12), 4995–5003. doi:10.1158/0008-5472.can-09-4487

McCarroll, J. A., Sharbeen, G., Kavallaris, M., and Phillips, P. A. (2019). The Use of Star Polymer Nanoparticles for the Delivery of siRNA to Mouse Orthotopic Pancreatic Tumor Models. *Methods Mol. Biol.*, 329–353. doi:10.1007/978-1-4939-9220-1_23

McCarroll, J. A., Sharbeen, G., Liu, J., Youkhana, J., Goldstein, D., McCarthy, N., et al. (2015b). Biii-Tubulin: A Novel Mediator of Chemoresistance and Metastases in Pancreatic Cancer. *Oncotarget* 6 (4), 2235–2249. doi:10.18632/oncotarget.2946

Melé, M., Ferreira, P. G., Reverter, F., DeLuca, D. S., Monlong, J., Sammeth, M., et al. (2015). The Human Transcriptome across Tissues and Individuals. *Science* 348 (6235), 660–665.

Mitchell, P. J., Timmons, P. M., Hébert, J. M., Rigby, P. W., and Tjian, R. (1991). Transcription Factor AP-2 Is Expressed in Neural Crest Cell Lineages during Mouse Embryogenesis. *Genes Dev.* 5 (1), 105–119. doi:10.1101/gad.5.1.105

Mondanizadeh, M., Arefian, E., Mosayebi, G., Saidijam, M., Khansarinejad, B., and Hashemi, S. M. (2015). MicroRNA-124 Regulates Neuronal Differentiation of Mesenchymal Stem Cells by Targeting Sp1 mRNA. *J. Cel. Biochem.* 116 (6), 943–953. doi:10.1002/jcb.25045

Mongroo, P. S., and Rustgi, A. K. (2010). The Role of the miR-200 Family in Epithelial-Mesenchymal Transition. *Cancer Biol. Ther.* 10 (3), 219–222. doi:10.4161/cbt.10.3.12548

Moody, S. A., Quigg, M. S., and Frankfurter, A. (1989). Development of the Peripheral Trigeminal System in the Chick Revealed by an Isotype-specific Anti-beta-tubulin Monoclonal Antibody. *J. Comp. Neurol.* 279 (4), 567–580. doi:10.1002/cne.902790406

Näär, A. M., Beaurang, P. A., Robinson, K. M., Oliner, J. D., Avizonis, D., Scheek, S., et al. (1998). Chromatin, TAFs, and a Novel Multiprotein Coactivator Are Required for Synergistic Activation by Sp1 and SREBP-1a *In Vitro*. *Genes Dev.* 12 (19), 3020–3031. doi:10.1101/gad.12.19.3020

Nakakura, E. K., Watkins, D. N., Sriuranpong, V., Borges, M. W., Nelkin, B. D., and Ball, D. W. (2001b). Mammalian Scratch Participates in Neuronal Differentiation in P19 Embryonal Carcinoma Cells. *Brain Res. Mol. Brain Res.* 95 (1-2), 162–166. doi:10.1016/s0169-328x(01)00246-7

Nakakura, E. K., Watkins, D. N., Schuebel, K. E., Sriuranpong, V., Borges, M. W., Nelkin, B. D., et al. (2001a). Mammalian Scratch: a Neural-specific Snail Family Transcriptional Repressor. *Proc. Natl. Acad. Sci. U.S.A.* 98 (7), 4010–4015. doi:10.1073/pnas.051014098

Namekawa, T., Ikeda, K., Horie-Inoue, K., Suzuki, T., Okamoto, K., Ichikawa, T., et al. (2020). ALDH1A1 in Patient-derived Bladder Cancer Spheroids Activates Retinoic Acid Signaling Leading to TUBB3 Overexpression and Tumor Progression. *Int. J. Cancer* 146 (4), 1099–1113. doi:10.1002/ijc.32505

Narvi, E., Jaakkola, K., Winsel, S., Oetken-Lindholm, C., Halonen, P., Kallio, L., et al. (2013). Altered TUBB3 Expression Contributes to the Epothilone Response of Mitotic Cells. *Br. J. Cancer* 108 (1), 82–90. doi:10.1038/bjc.2012.553

Nogales, E. (2000). Structural Insights into Microtubule Function. *Annu. Rev. Biochem.* 69, 277–302. doi:10.1146/annurev.biochem.69.1.277

Ooi, L., and Wood, I. C. (2007). Chromatin Crosstalk in Development and Disease: Lessons from REST. *Nat. Rev. Genet.* 8 (7), 544–554. doi:10.1038/nrg2100

Oshima, S., and Yawaka, Y. (2020). Class III β-tubulin Expression during Hard Tissue Formation in Developing Mouse Teeth. *Pediatr. Dental J.* 30 (1), 9–16. doi:10.1016/j.pdj.2019.12.002

Parker, A. L., Teo, W. S., McCarroll, J. A., and Kavallaris, M. (2017). An Emerging Role for Tubulin Isotypes in Modulating Cancer Biology and Chemotherapy Resistance. *Int. J. Mol. Sci.* 18 (7). doi:10.3390/ijms18071434

Parker, A. L., Teo, W. S., Pandzic, E., Vicente, J. J., McCarroll, J. A., Wordeman, L., et al. (2018). β-Tubulin Carboxy-Terminal Tails Exhibit Isotype-specific Effects on Microtubule Dynamics in Human Gene-Edited Cells. *Life Sci. Alliance* 1 (2). doi:10.26508/lsa.201800059

Parker, A. L., Turner, N., McCarroll, J. A., and Kavallaris, M. (2016). Biii-Tubulin Alters Glucose Metabolism and Stress Response Signaling to Promote Cell Survival and Proliferation in Glucose-Starved Non-small Cell Lung Cancer Cells. *Carcin* 37 (8), 787–798. doi:10.1093/carcin/bgw058

Pecot, C. V., Rupaimoole, R., Yang, D., Akbani, R., Ivan, C., Lu, C., et al. (2013). Tumour Angiogenesis Regulation by the miR-200 Family. *Nat. Commun.* 4 (1), 2427. doi:10.1038/ncomms3427

Person, F., Wilczak, W., Hube-Magg, C., Burdelski, C., Möller-Koop, C., Simon, R., et al. (2017). Prevalence of βIII-tubulin (TUBB3) Expression in Human normal Tissues and Cancers. *Tumour Biol.* 39 (10), 1010428317712166. doi:10.1177/1010428317712166

Piunti, A., Hashizume, R., Morgan, M. A., Bartom, E. T., Horbinski, C. M., Marshall, S. A., et al. (2017). Therapeutic Targeting of Polycomb and BET Bromodomain Proteins in Diffuse Intrinsic Pontine Gliomas. *Nat. Med.* 23 (4), 493–500. doi:10.1038/nm.4296

Poirier, K., Saillour, Y., Bahi-Buisson, N., Jaglin, X. H., Fallet-Bianco, C., Nabbout, R., et al. (2010). Mutations in the Neuronal β-tubulin Subunit TUBB3 Result in Malformation of Cortical Development and Neuronal Migration Defects. *Hum. Mol. Genet.* 19 (22), 4462–4473. doi:10.1093/hmg/ddq377

Portyanko, A., Kovalev, P., Gorgun, J., and Cherstvoy, E. (2009). Biii-Tubulin at the Invasive Margin of Colorectal Cancer: Possible Link to Invasion. *Virchows Arch.* 454 (5), 541–548. doi:10.1007/s00428-009-0764-4

Prislei, S., Martinelli, E., Mariani, M., Raspaglio, G., Sieber, S., Ferrandina, G., et al. (2013). MiR-200c and HuR in Ovarian Cancer. *BMC Cancer* 13, 72. doi:10.1186/1471-2407-13-72

Prislei, S., Mozzetti, S., Filippetti, F., De Donato, M., Raspaglio, G., Cicchillitti, L., et al. (2008). From Plasma Membrane to Cytoskeleton: a Novel Function for Semaphorin 6A. *Mol. Cancer Ther.* 7 (1), 233–241. doi:10.1158/1535-7163.mct-07-0390

Ranganathan, S., Dexter, D. W., Benetatos, C. A., Chapman, A. E., Tew, K. D., and Hudes, G. R. (1996). Increase of Beta(III)- and beta(IVa)-tubulin Isotopes in Human Prostate Carcinoma Cells as a Result of Estramustine Resistance. *Cancer Res.* 56 (11), 2584–2589.

Ranganathan, S., Benetatos, C., Colarusso, P., Dexter, D., and Hudes, G. (1998a). Altered β-tubulin Isotype Expression in Paclitaxel-Resistant Human Prostate Carcinoma Cells. *Br. J. Cancer* 77 (4), 562–566. doi:10.1038/bjc.1998.91

Ranganathan, S., Dexter, D. W., Benetatos, C. A., and Hudes, G. R. (1998b). Cloning and Sequencing of Human βIII-tubulin cDNA: Induction of βIII Isotype in Human Prostate Carcinoma Cells by Acute Exposure to Antimicrotubule Agents. *Biochim. Biophys. Acta (Bba) - Gene Struct. Expr.* 1395 (2), 237–245. doi:10.1016/s0167-4781(97)00168-1

Raspaglio, G., Filippetti, F., Prislei, S., Penci, R., De Maria, I., Cicchillitti, L., et al. (2008). Hypoxia Induces Class III Beta-Tubulin Gene Expression by HIF-1alpha Binding to its 3' Flanking Region. *Gene* 409 (1-2), 100–108. doi:10.1016/j.gene.2007.11.015

Raspaglio, G., De Maria, I., Filippetti, F., Martinelli, E., Zannoni, G. F., Prislei, S., et al. (2010). HuR Regulates β-Tubulin Isotype Expression in Ovarian Cancer. *Cancer Res.* 70 (14), 5891–5900. doi:10.1158/0008-5472.can-09-4656

Raspaglio, G., Petrillo, M., Martinelli, E., Li Puma, D. D., Mariani, M., De Donato, M., et al. (2014). Sox9 and Hif-2α Regulate TUBB3 Gene Expression and Affect Ovarian Cancer Aggressiveness. *Gene* 542 (2), 173–181. doi:10.1016/j.gene.2014.03.037

Ryu, H., Lee, J., Zaman, K., Kubilis, J., Ferrante, R. J., Ross, B. D., et al. (2003). Sp1 and Sp3 Are Oxidative Stress-Inducible, Antideath Transcription Factors in Cortical Neurons. *J. Neurosci.* 23 (9), 3597–3606. doi:10.1523/jneurosci.23-09-03597.2003

Saussede-Aim, J., Matera, E. L., Herveau, S., Rouault, J. P., Ferlini, C., and Dumontet, C. (2009b). Vinorelbine Induces Beta3-Tubulin Gene Expression through an AP-1 Site. *Anticancer Res.* 29 (8), 3003–3009.

Saussede-Aim, J., Matera, E.-L., Ferlini, C., and Dumontet, C. (2009a). β3-Tubulin Is Induced by Estradiol in Human Breast Carcinoma Cells through an Estrogen-Receptor Dependent Pathway. *Cel Motil. Cytoskeleton* 66 (7), 378–388. doi:10.1002/cm.20377

Scharer, C. D., McCabe, C. D., Ali-Seyed, M., Berger, M. F., Bulyk, M. L., and Moreno, C. S. (2009). Genome-wide Promoter Analysis of the SOX4 Transcriptional Network in Prostate Cancer Cells. *Cancer Res.* 69 (2), 709–717. doi:10.1158/0008-5472.can-08-3415

Sève, P., and Dumontet, C. (2008). Is Class III β-tubulin a Predictive Factor in Patients Receiving Tubulin-Binding Agents? *Lancet Oncol.* 9 (2), 168–175. doi:10.1016/s1470-2045(08)70029-9

Shalli, K., Brown, I., Heys, S. D., and Schofield, C. A. (2005). Alterations of β-tubulin Isotypes in Breast Cancer Cells Resistant to Docetaxel. *FASEB j.* 19 (10), 1299–1301. doi:10.1096/fj.04-3178fje

Shen, Y., and Yu, L.-C. (2008). Potential protection of Curcumin against Hypoxia-Induced Decreases in Beta-III Tubulin Content in Rat Prefrontal Cortical Neurons. *Neurochem. Res.* 33 (10), 2112–2117. doi:10.1007/s11064-008-9720-y

Shibazaki, M., Maesawa, C., Akasaka, K., Kasai, S., Yasuhira, S., Kanno, K., et al. (2012). Transcriptional and post-transcriptional Regulation of βIII-tubulin Protein Expression in Relation with Cell Cycle-dependent Regulation of Tumor Cells. *Int. J. Oncol.* 40 (3), 695–702. doi:10.3892/ijo.2011.1291

Sleiman, S. F., Langley, B. C., Basso, M., Berlin, J., Xia, L., Payappilly, J. B., et al. (2011). Mithramycin Is a Gene-Selective Sp1 Inhibitor that Identifies a Biological Intersection between Cancer and Neurodegeneration. *J. Neurosci.* 31 (18), 6858–6870. doi:10.1523/jneurosci.0710-11.2011

Sobierajska, K., Wieczorek, K., Ciszewski, W. M., Sacewicz-Hofman, I., Wawro, M. E., Wiktorska, M., et al. (2016). β-III Tubulin Modulates the Behavior of Snail Overexpressed during the Epithelial-To-Mesenchymal Transition in colon Cancer Cells. *Biochim. Biophys. Acta (Bba) - Mol. Cel Res.* 1863 (9), 2221–2233. doi:10.1016/j.bbamcr.2016.05.008

Song, M. S., Salmena, L., and Pandolfi, P. P. (2012). The Functions and Regulation of the PTEN Tumour Suppressor. *Nat. Rev. Mol. Cel Biol* 13 (5), 283–296. doi:10.1038/nrm3330

Sulaiman, S. A., Ab Mutalib, N. S., and Jamal, R. (2016). miR-200c Regulation of Metastases in Ovarian Cancer: Potential Role in Epithelial and Mesenchymal Transition. *Front. Pharmacol.* 7 (271), 271. doi:10.3389/fphar.2016.00271

Sullivan, K. F., and Cleveland, D. W. (1986). Identification of Conserved Isotype-Defining Variable Region Sequences for Four Vertebrate Beta Tubulin Polypeptide Classes. *Proc. Natl. Acad. Sci. U.S.A.* 83 (12), 4327–4331. doi:10.1073/pnas.83.12.4327

Susanna, L., Luis, J. L.-G., Marta, M., Jorge, B., Lucía, I.-P., Iván, M., et al. (2011). The miR-200 Family Controls β-tubulin III Expression and Is Associated with Paclitaxel-Based Treatment Response and Progression-free Survival in Ovarian Cancer Patients. *Endocrine-Related Cancer* 18 (1), 85–95.

Taddei, M., Giannoni, E., Fiaschi, T., and Chiarugi, P. (2012). Anoikis: an Emerging Hallmark in Health and Diseases. *J. Pathol.* 226 (2), 380–393. doi:10.1002/path.3000

Tamura, D., Arao, T., Nagai, T., Kaneda, H., Aomatsu, K., Fujita, Y., et al. (2013). Slug Increases Sensitivity to Tubulin-binding Agents via the Downregulation of βIII and βIVa-tubulin in Lung Cancer Cells. *Cancer Med.* 2 (2), 144–154. doi:10.1002/cam4.68

Teo, J., McCarroll, J. A., Boyer, C., Youkhana, J., Sagnella, S. M., Duong, H. T. T., et al. (2016). A Rationally Optimized Nanoparticle System for the Delivery of RNA Interference Therapeutics into Pancreatic Tumors *In Vivo*. *Biomacromolecules* 17 (7), 2337–2351. doi:10.1021/acs.biomac.6b00185

Theodorakis, N. G., and Cleveland, D. W. (1992). Physical Evidence for Cotranslational Regulation of Beta-Tubulin mRNA Degradation. *Mol. Cel. Biol.* 12 (2), 791–799. doi:10.1128/mcb.12.2.791

Thiery, J. P., and Sleeman, J. P. (2006). Complex Networks Orchestrate Epithelial-Mesenchymal Transitions. *Nat. Rev. Mol. Cel Biol* 7 (2), 131–142. doi:10.1038/nrm1835

Tischfield, M. A., Baris, H. N., Wu, C., Rudolph, G., Van Maldergem, L., He, W., et al. (2010). Human TUBB3 Mutations Perturb Microtubule Dynamics, Kinesin Interactions, and Axon Guidance. *Cell* 140 (1), 74–87. doi:10.1016/j.cell.2009.12.011

Toma, J. G., El-Bizri, H., Barnabé-Heider, F., Aloyz, R., and Miller, F. D. (2000). Evidence that helix-loop-helix Proteins Collaborate with Retinoblastoma Tumor Suppressor Protein to Regulate Cortical Neurogenesis. *J. Neurosci.* 20 (20), 7648–7656. doi:10.1523/jneurosci.20-20-07648.2000

Toso, R. J., Jordan, M. A., Farrell, K. W., Matsumoto, B., and Wilson, L. (1993). Kinetic Stabilization of Microtubule Dynamic Instability *In Vitro* by Vinblastine. *Biochemistry* 32 (5), 1285–1293. doi:10.1021/bi00056a013

Uittenbogaard, M., and Chiaramello, A. (2002). Constitutive Overexpression of the Basic helix-loop-helix Nex1/MATH-2 Transcription Factor Promotes Neuronal Differentiation of PC12 Cells and Neurite Regeneration. *J. Neurosci. Res.* 67 (2), 235–245. doi:10.1002/jnr.10119

Uittenbogaard, M., and Chiaramello, A. (2004). Expression Profiling upon Nex1/MATH-2-Mediated Neuritogenesis in PC12 Cells and its Implication in Regeneration. *J. Neurochem.* 91 (6), 1332–1343. doi:10.1111/j.1471-4159.2004.02814.x

Uittenbogaard, M., Martinka, D. L., and Chiaramello, A. (2003). The Basic helix-loop-helix Differentiation Factor Nex1/MATH-2 Functions as a Key Activator of the GAP-43 Gene. *J. Neurochem.* 84 (4), 678–688. doi:10.1046/j.1471-4159.2003.01572.x

Uy, B. R., Simoes-Costa, M., Koo, D. E. S., Sauka-Spengler, T., and Bronner, M. E. (2015). Evolutionarily Conserved Role for SoxC Genes in Neural Crest Specification and Neuronal Differentiation. *Developmental Biol.* 397 (2), 282–292. doi:10.1016/j.ydbio.2014.09.022

Verdier-Pinard, P., Pasquier, E., Xiao, H., Burd, B., Villard, C., Lafitte, D., et al. (2009). Tubulin Proteomics: towards Breaking the Code. *Anal. Biochem.* 384 (2), 197–206. doi:10.1016/j.ab.2008.09.020

Wang, Y., Sparano, J. A., Fineberg, S., Stead, L., Sunkara, J., Horwitz, S. B., et al. (2013). High Expression of Class III β-Tubulin Predicts Good Response to Neoadjuvant Taxane and Doxorubicin/Cyclophosphamide-Based Chemotherapy in Estrogen Receptor-Negative Breast Cancer. *Clin. Breast Cancer* 13 (2), 103–108. doi:10.1016/j.clbc.2012.11.003

Wattanathamsan, O., and Pongrakhananon, V. (2021). Post-translational Modifications of Tubulin: Their Role in Cancers and the Regulation of Signaling Molecules. *Cancer Gene Ther.* doi:10.1038/s41417-021-00396-4

Wei, C., Ren, L., Li, K., and Lu, Z. (2018). The Regulation of Survival and Differentiation of Neural Stem Cells by miR-124 via Modulating PAX3. *Neurosci. Lett.* 683, 19–26. doi:10.1016/j.neulet.2018.05.051

Westbrook, T. F., Martin, E. S., Schlabach, M. R., Leng, Y., Liang, A. C., Feng, B., et al. (2005). A Genetic Screen for Candidate Tumor Suppressors Identifies REST. *Cell* 121 (6), 837–848. doi:10.1016/j.cell.2005.03.033

Wu, Y. Z., Lin, H. Y., Zhang, Y., and Chen, W. F. (2020). miR-200b-3p Mitigates Oxaliplatin Resistance via Targeting TUBB3 in Colorectal Cancer. *J. Gene Med.*, e3178.

Zelleroth, S., Nylander, E., Örtenblad, A., Stam, F., Nyberg, F., Grönbladh, A., et al. (2021). Structurally Different Anabolic Androgenic Steroids Reduce Neurite Outgrowth and Neuronal Viability in Primary Rat Cortical Cell Cultures. *J. Steroid Biochem. Mol. Biol.* 210, 105863. doi:10.1016/j.jsbmb.2021.105863

Zhao, X., Yue, C., Chen, J., Tian, C., Yang, D., Xing, L., et al. (2016). Class III β-Tubulin in Colorectal Cancer: Tissue Distribution and Clinical Analysis of Chinese Patients. *Med. Sci. Monit.* 22, 3915–3924. doi:10.12659/msm.901252

Conflict of Interest: The authors declare that the research was conducted in the absence of any commercial or financial relationships that could be construed as a potential conflict of interest.

Publisher's Note: All claims expressed in this article are solely those of the authors and do not necessarily represent those of their affiliated organizations, or those of the publisher, the editors and the reviewers. Any product that may be evaluated in this article, or claim that may be made by its manufacturer, is not guaranteed or endorsed by the publisher.

frontiers | Frontiers in Cell and Developmental Biology

MINI REVIEW
published: 26 May 2022
doi: 10.3389/fcell.2022.898076

Regulation of Tubulin Gene Expression: From Isotype Identity to Functional Specialization

Ivana Gasic *

Department of Molecular and Cellular Biology, University of Geneva, Geneva, Switzerland

Genomes of higher eukaryotes encode a large tubulin gene superfamily consisting of at least six α and six β-tubulin isotypes. While some α and β-tubulin isotypes are ubiquitously expressed, others are cell-type specific. The subset of α and β-tubulins that is expressed in a given cell type is defined transcriptionally. But the precise mechanisms of how cells choose which α and β isotypes to express and at what level remain poorly understood. Differential expression of tubulin isotypes is particularly prominent during development and in specialized cells, suggesting that some isotypes are better suited for certain cell type-specific functions. Recent studies begin to rationalize this phenomenon, uncovering important differences in tubulin isotype behavior and their impact on the biomechanical properties of the microtubule cytoskeleton. I summarize our understanding of the regulation of tubulin isotype expression, focusing on the role of these complex regulatory pathways in building a customized microtubule network best suited for cellular needs.

Keywords: tubulin, isotype, microtubule, transcription, autoregulation

OPEN ACCESS

Edited by:
Jeffrey Moore,
University of Colorado Anschutz Medical Campus, United States

Reviewed by:
Carsten Janke,
Institut Curie, France
Naomi Morrissette,
University of California, Irvine, United States

***Correspondence:**
Ivana Gasic
ivana.gasic@unige.ch

Specialty section:
This article was submitted to Cellular Biochemistry, a section of the journal Frontiers in Cell and Developmental Biology

Received: *16 March 2022*
Accepted: *11 May 2022*
Published: *26 May 2022*

Citation:
Gasic I (2022) Regulation of Tubulin Gene Expression: From Isotype Identity to Functional Specialization. Front. Cell Dev. Biol. 10:898076. doi: 10.3389/fcell.2022.898076

INTRODUCTION

A vast diversity of subcellular architectures exists in nature. One prominent example is the cytoskeleton found in various arrays not only across the different cell types but also within the same cell type and over the course of the cell cycle. The morphological diversity tangoes with functional specialization. This is acutely evident for one group of cytoskeletal elements—the microtubules. Microtubules are dynamic polymers of α and β-tubulin isotypes, which carry out a number of diverse functions in cells, including flagellar motility, intracellular transport, chromosome segregation, and the establishment and maintenance of cellular morphology (Muroyama and Lechler, 2017). How do eukaryotic cells create such a spectacular diversity in form and function with a set of presumably uniform building blocks? It is well established that a plethora of tubulin and microtubule associated proteins (MAPs) are able to shape the biomechanical properties of microtubules, thus introducing a sophisticated layer of regulation and functional specialization (Goodson and Jonasson, 2018; Cuveillier et al., 2020). But in principle, alterations in the properties of tubulins themselves could both directly and indirectly (through MAPs) affect the assembly and biomechanical properties of microtubules. This idea, first articulated as the multitubulin hypothesis, is based on biochemical differences observed among tubulins isolated from single species and the discovery that most eukaryotic cells express multiple isotypes of α and β-tubulin proteins (Fulton and Simpson, 1976; Stephens, 1978; Cleveland et al., 1980). While the influence of MAPs on microtubule network morphology and function has been reviewed elsewhere (Goodson and Jonasson, 2018), I focus on the role of the regulation of α and β-tubulin gene

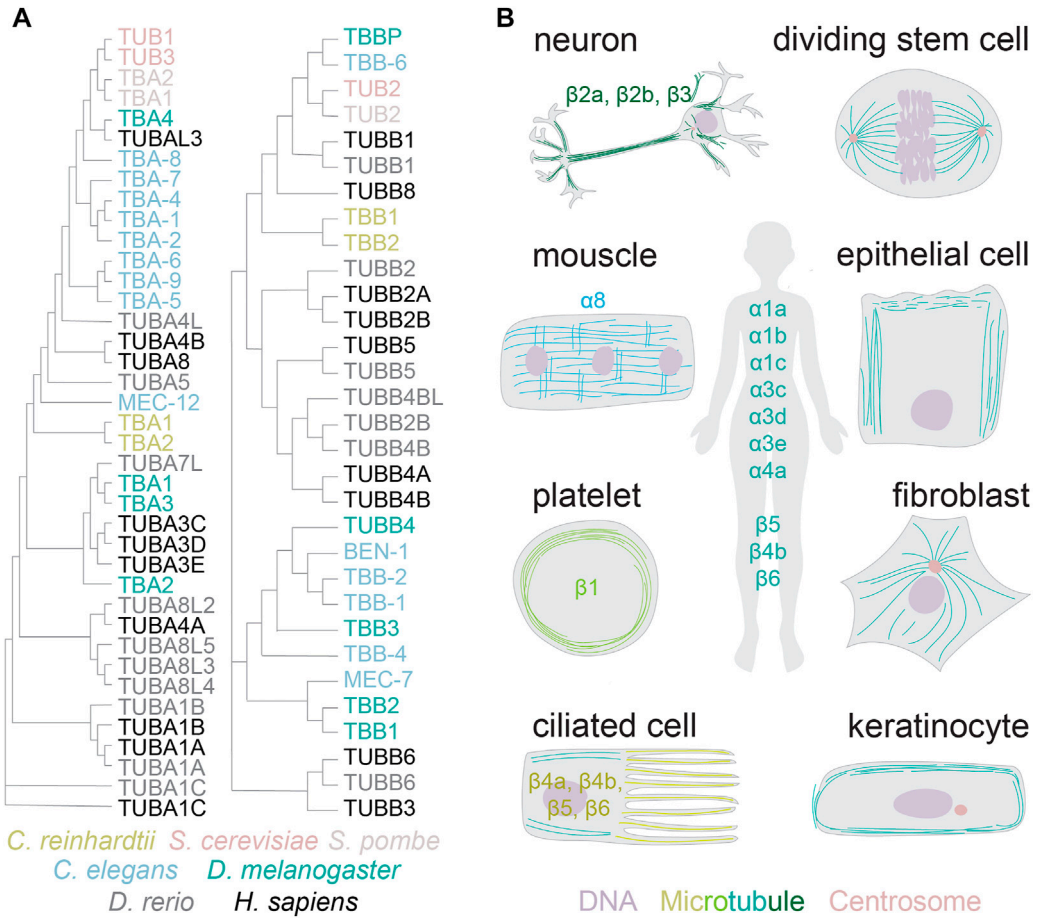

FIGURE 1 | Tubulin gene networks and protein distribution. **(A)** Phylogenetic neighbour-joining tree without distance corrections (with cladogram branch length, created with Clustal Omega). Color coded are tubulins from the species referenced in this review article. **(B)** The distribution of tubulin isotypes and diversity of microtubule architectures across specialized cells in higher eukaryotes.

expression in eukaryotic cells. I refer to isotypes as tubulin species arising from multiple genes and refrain from addressing their posttranslational modifications, which others have thoroughly discussed (Magiera and Janke, 2014; Yu et al., 2015; Gadadhar et al., 2017; Roll-Mecak, 2020; Guichard et al., 2021). Finally, I review some examples of the functional specializations of isotypes and raise the question of why cells evolved such a high complexity of tubulin gene networks.

TUBULIN ISOTYPE EXPRESSION AND FUNCTIONAL SPECIALIZATION

Tubulin Superfamily and Transcriptional Regulation of Gene Expression

Genomes of higher land plants and metazoans encode the core microtubule proteins, α and β-tubulins, in large multi-gene families (**Figure 1A**) (Gasic and Mitchison, 2019). Unicellular eukaryotes, such as yeast and green algae, encode one to two different α and β-tubulin subunits. The complexity of tubulin gene networks increases with multicellularity: higher eukaryotes encode six to nine tubulin isotypes of each subunit (MacRae and Langdon, 1989). The isotypes share up to 99% identity, with most differences residing in the carboxy-terminal tails (Sullivan, 1988). Most isotypes are constitutively expressed, such as α1a and β5 (Ludueña, 1997). Others are restricted to specific tissues and cell types (**Figure 1B**). Prominent examples include platelet-specific β1 or neuron-specific β3-tubulin (Ludueña, 1997; Breuss et al., 2017). It is generally assumed that transcriptional regulation defines the expressed tubulins for both the constitutive and specialized forms.

In most cell types, tubulin gene transcription is considered a part of a general "housekeeping" program. But the mechanisms behind it remain poorly understood. For instance, transcriptional factors that may drive such constitutive expression remain largely elusive. Numerous regulatory regions in tubulin genes have been found (**Figure 2A**), but the precise mechanisms of how they orchestrate tubulin gene transcription have been investigated only in some specific contexts. Four main complications challenge studies of tubulin gene transcription. First, most cells express multiple tubulin genes, subsets of which differ from one cell type to another. Hence, lessons learned from one cell

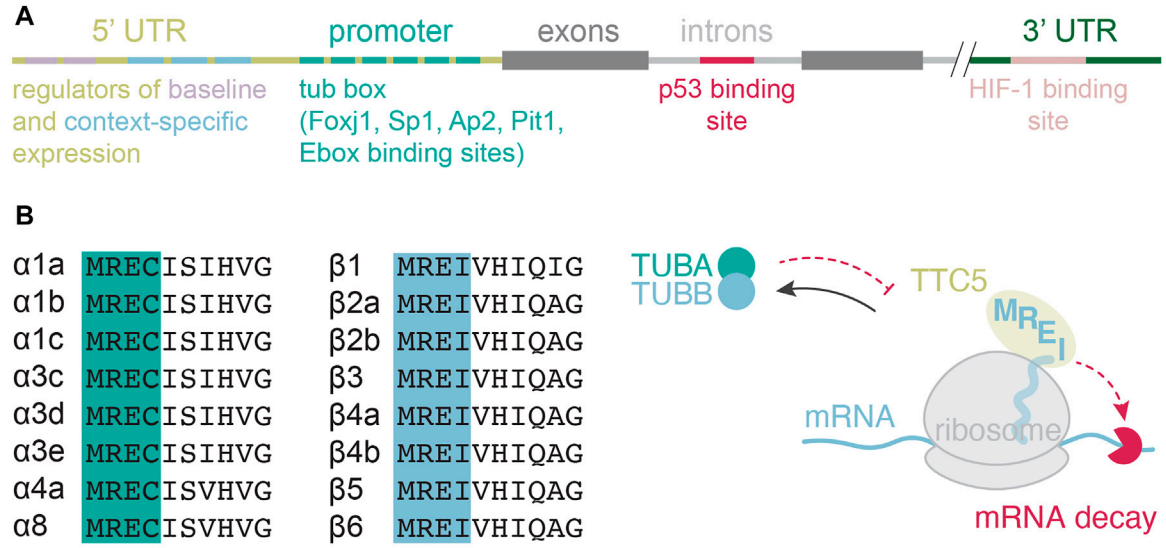

FIGURE 2 | Transcriptional and posttranscriptional regulation of tubulin gene expression. **(A)** Transcriptional regulatory elements mapped in various isotubulin genes and across species. **(B)** Amino-terminal protein sequence alignment of isotubulins and the current model for tubulin autoregulation.

type or one subset of tubulin isotypes do not apply to another one. Second, this intricacy is further exacerbated by the complexity of interacting partners and functions that tubulins perform (Muroyama and Lechler, 2017). Third, the encoded gene products are highly similar making them difficult to distinguish in downstream applications. And fourth, most of the field has historically been focused on using immortalized, fibroblast-like two-dimensional cell cultures to study tubulin biology. Such cells are not only taken out of their natural context, but also largely simplified systems that have hence lost their "identity" when it comes to tubulin gene expression regulation and microtubule function. The availability of complex model systems that better represent nature, such as organoid cultures, as well as sophisticated genetic engineering, immunolabeling, and genome-wide transcriptomic analyses should facilitate progress in identification and characterization of the transcriptional networks that govern constitutive tubulin gene expression.

Transcriptional regulation of tubulin genes is much better understood in conditions where tubulin is required to build specialized assemblies. One prominent example is a burst in tubulin gene transcription during flagellar regrowth following deflagellation in unicellular green algae *Chlamydomonas reinhardtii*. *C. reinhardtii* possesses four tubulins called α1, α2, β1, and β2-tubulin, encoded by four distinct genes. Rapid flagellar excision induced by mechanical stress or an acid shock triggers a coordinated transcription of a set of flagellar genes including tubulins. This robust response has been used to study the principles governing transcriptional control of the activated tubulin genes, leading to the discovery of the first tubulin gene promoter—the β2 (Davies et al., 1992; Davies and Grossman, 1994). The identified promoter contains seven repeats of a 10-base pair (bp) motif, named tub box, between the TATA box and the transcription initiation site (**Figure 2A**). The tub box motifs are required for β2-tubulin gene transcription following deflagellation. Similar investigations aimed at identifying the regulatory elements in the α1-tubulin gene revealed yet higher complexity with two promoter regions that act as regulatory elements (**Figure 2A**). The upmost region (-176 to -122 bp) emerged as a regulator of baseline transcription, keeping the expression levels low. The second region (-85 to -16 bp) encodes an activator for deflagellation-induced gene expression (Periz and Keller, 1997). Recent genetic studies identified two paralogous Foxj1a and Foxj1b transcription factors as core drivers of the motile ciliogenic program in the zebrafish embryo (Yu et al., 2008). Foxj1a turns on a set of genes required for the formation and function of motile cilia. The paralogous foxj1b appears to regulate motile cilia formation in the otic vesicle. Curiously, foxj1a is not required for the formation of primary cilia, which are immotile and involved in signaling (Yu et al., 2008). This finding further supports the idea that transcriptional programs that control the expression of tubulins and related genes are highly function-and context-dependent.

In the fruit fly *Drosophila melanogaster,* β2-tubulin isotype is expressed exclusively during spermatogenesis. The β2-tubulin promoter element responsible for the tissue specific gene expression is spread over a region of 80 bp and is sufficient to drive germline-specific expression in the testis (Michiels et al., 1989). An additional 14 bp activator element called β2UE1 confers promoter specificity to spermatogenesis (Santel et al., 2000). Equally complex regulatory elements are likely to be present and govern the expression of other tissue-specific tubulins. For instance, the neuron-specific α1-tubulin gene promoter contains a conserved repetitive homeodomain consensus sequence core (TAAT) with a flanking basic helix—loop–helix binding enhancer box (E-box) (Hieber et al., 1998; Goldman and Ding, 2000). While these elements are not essential for α1-tubulin gene transcription in the zebrafish

retinal ganglion cells during development or in regenerating retina after neuronal damage, they are necessary for induced gene transcription in response to optic nerve crush (Senut et al., 2004). The neuron-specific β countertype is β3-tubulin, whose start site and the TATA box at position -28 bp are similar to other tubulin genes. The promoter region of β3-tubulin gene encodes numerous putative binding sites for specificity protein 1 (Sp1), Activating Enhancer Binding Protein 2 (AP2), pituitary-specific transcription factor 1 (Pit1), or Ebox (**Figure 2A**) (Dennis et al., 2002). But how these binding sites are engaged to drive neuron-specific expression of β3-tubulin remains to be elucidated.

In addition to the elements upstream of transcription initiation site, some regulatory sequences are also found in introns of tubulin genes (**Figure 2A**). For instance, the first intron of mouse β2-tubulin gene contains a p53 binding site, which acts as a silencer for β2-tubulin transcription. Antagonizing the binding of p53 induces gene expression (Arai et al., 2006). The discovery of this mechanism rationalized resistance of a mouse melanoma cell line B16F10 to vinca alkaloids: vinca alkaloids prevent p53 binding to the intronic regulatory element thus driving overproduction of β2-tubulin (Arai et al., 2006). In the case of the *Drosophila* β3-tubulin gene, constitutive expression is achieved through at least two cis-acting elements, upstream and downstream of the transcription initiation site (Gasch et al., 1989), but regulatory elements in the intron mediate transcription in a tissue-specific manner (Gasch et al., 1989). Two opposing factors recognize the intronic regulatory elements to balance gene transcription: the ultrabithorax (Ubx) driving transcription of β3-tubulin gene, and the engrailed (En) repressing it (Serrano et al., 1997).

Finally, additional transcriptional regulatory sequences have been found in the 3′ untranslated regions of tubulin genes (UTR, **Figure 2A**). One such example is the hypoxia inducible factor 1 (HIF-1) binding site present in the 3′-flanking region of human β3-tubulin gene, which is thought to drive ectopic β3-tubulin expression in tumors (Raspaglio et al., 2008). In healthy tissues, β3-tubulin is restricted to neuronal and Sertoli cells (Easter et al., 1993), and during defined periods of development (Katsetos et al., 2003), indicating the existence of spatio-temporal clues governing its expression. But tumor cells are frequently found to abnormally express β3-tubulin and in significantly larger quantities (reviewed in (Drukman and Kavallaris, 2002)). In tumors, the expression levels of β3-tubulin correlate with poor prognosis, indicating that not only the isotype composition but also protein levels are relevant. How tumor cells lose the breaks and enter β3-tubulin overproduction remains unknown. In general, transcriptional networks and regulated proteolysis together set protein abundances. But for tubulins in higher eukaryotes, a posttranslational mechanism called tubulin autoregulation is thought to act as an additional tailor of protein levels.

Tubulin Autoregulation

Tubulin autoregulation is a general mechanism that operates on all α and β-tubulin isotypes (**Figure 2B**) and in all higher eukaryotic cells tested so far (Gasic and Mitchison, 2019; Fellous et al., 1982; Pittenger and Cleveland, 1985; Caron et al., 1985; Lau et al., 1986; Cleveland, 1989). When in excess of cellular needs, tubulin proteins negatively regulate the stability of their encoding mRNAs (Ben-Ze'ev et al., 1979; Cleveland et al., 1981). This negative feedback mechanism requires an ongoing translation (Gay et al., 1989), as cells use tubulin nascent proteins to recognize tubulin mRNAs and target them for degradation. The recognition motif resides in the first four amino-acids of nascent α and β-tubulins (Theodorakis and Cleveland, 1992; Yen et al., 1988; Bachurski et al., 1994), and is recognized by tetratricopeptide protein 5 (TTC5), which acts as the specificity factor in tubulin autoregulation (**Figure 2B**) (Lin et al., 2020).

Pioneering studies of tubulin autoregulation failed to resolve the regulation of individual tubulin subunits due to technical limitations, such as lack of tubulin isotype specificity probes. Recent efforts deployed reverse transcription-based quantitative polymerase chain reaction and transcriptomics, offering a much higher resolution of individual isotype regulation. These studies reveal that all the expressed α and β-tubulins are subject to autoregulation in higher eukaryotes (Gasic et al., 2019). This is perhaps not surprising, given the mechanistic dependence of tubulin autoregulation on the nascent tubulin tetrapeptide sequences and their high conservation (**Figure 2B**).

While all the tubulin isotypes are subject to posttranscriptional regulation in higher eukaryotes, the extent to which they are autoregulated varies within the same cell type and across the different tissues (Gasic et al., 2019). The most likely explanation is that these differences stem from varying rates of isotubulin translation—the more a certain mRNA species is translated, the higher the rate of mRNA decay in tubulin autoregulation. For instance, β3-tubulin mRNA appears to be less regulated even though reasonably abundant in human cultured cells. It is possible that β3-tubulin mRNA is little or not translated in cultured cells, especially given that β3-tubulin isotype is neuron specific. Further studies are required to evaluate the level of β3-tubulin mRNA autoregulation in neurons and cancer tissues where its expression is elevated. Likewise, whether cells translate tubulin isotypes at different rates remains unknown. The availability of ribosome footprint profiling technologies should facilitate progress in this direction. An alternative explanation is that the observed differences in autoregulation between tubulin isotypes are not real, but rather a technical artifact, where transcripts present in very small amounts may falsely show large fold changes in abundances across samples. For instance, β2b-tubulin mRNA is present at very low levels and may not be regulated at all in cultured cells (Gasic et al., 2019). Remarkably, in neurons, β2b-tubulin mRNA appears to be chaperoned by the microtubule plus-end-tracking protein adenomatous polyposis coli (APC). APC associates with the 3' UTR of β2b-tubulin bringing it into the growth cone, where it is translated and the protein incorporated into microtubules (Preitner et al., 2014). Whether APC or other mRNA binding proteins may act to protect specific tubulin mRNAs from autoregulation or modulate their rate of decay remains to be elucidated. More generally, it remains to be seen whether tubulin autoregulation can further exacerbate the differences in tubulin isotype levels in cells and to what extent.

Collectively, transcriptional regulation and autoregulation paint a picture in which the different tubulin isotypes are

specifically expressed at different levels. Why do cells recruit such complex cellular machineries to provide differential expression of tubulin isotypes? A growing body of evidence points toward functional diversification and specialization of tubulin isotypes, some examples of which I discuss further.

Functional Specialization of Tubulin Isotypes

Initial analyses of tubulin mutations, gene disruption, introduction of chimeric genes, and immunolabeling of endogenous tubulins to visualize the distribution in cells revealed that tubulin isotypes are largely interchangeable (Bond et al., 1986; Joshi et al., 1987; Lewis et al., 1987; Lopata and Cleveland, 1987). These studies, however, used exclusively the divergent carboxy-termini but no other regions to differentiate between the tubulin isotypes. Results of a deeper look at tubulin isotype properties and functions have not borne up to the original findings. A growing body of evidence suggests that tubulin isotypes carry inherent differences, conferring distinct architectures and biomechanical properties to microtubules (Lu and Luduena, 1994; Panda et al., 1994; Vemu et al., 2017). Such functional specialization is present already in yeast, where two α-tubulin isotypes show opposing effects on microtubule dynamics *in vitro*, and a biased affinity towards the spindle positioning machinery during yeast mitosis (Bode et al., 2003; Nsamba et al., 2021).

Perhaps the most peculiar tubulin assemblies are axonemes. Localized at the center of cilia and flagella, axonemes provide these subcellular compartments structural integrity, mobility, and mediate transport and signaling. Axonemes emanate from centrioles—a pair of cylindrical structures composed of nine triplet microtubules organized in a radially symmetrical array (Guichard et al., 2021). This 9-fold radial symmetry carries over into the axoneme, albeit not as triplet but as doublet microtubules. An additional central pair of parallel microtubules is seen in motile cilia. The central pair and transition from triple to doublet organization are not sole differences between centrioles and axonemes: while the fruit fly β1-tubulin isotype dominates centriolar microtubules, the β2 isotype dominates the axonemal ones (Nielsen et al., 2001). This specificity in tubulin isotype composition has been studied mainly in *Drosophila melanogaster* and appears to be critical for centriole and axoneme formation and function. In fruit fly male germ line, the β1-tubulin alone cannot function in axonemes (Raff et al., 2000). These males form significantly shorter axonemes without the central pair of microtubules. Similarly, when β1-tubulin exceeds β2, the axonemes contain 10 instead of nine doublets in addition to promiscuous axoneme formation in the cytoplasm. An abnormal expression of β3-tubulin disrupts the assembly of microtubule doublets (Hoyle and Raff, 1990). In addition to β2, mammalian cilia also contain substantial proportion of the β4-tubulin isotypes a and b, both of which contain axoneme-specific carboxy-terminal motifs (Jensen - Smith et al., 2003). It remains to be elucidated how the tubulin isotype composition impacts the axoneme architecture and function. One tempting explanation lies in the interaction with the other structural and functional components of the axonemes. For instance, the motor proteins responsible for cargo transport inside the axoneme may have a preference for walking on certain tubulin isotypes (Jordan et al., 2018).

Another example of highly specialized microtubule network is seen in platelets, where microtubules are organized as a circumferential ring known as the marginal band (**Figure 1**). Marginal bands provide structural integrity and the typical discoidal shape to platelets. Several studies estimate β1-tubulin to comprise the majority of total β-tubulin in these cells (Lewis et al., 1987; Burkhart et al., 2012). This highly divergent tubulin isotype confers curvature to the microtubules of the marginal band. It remains unknown whether this is a direct effect of tubulin conformation or an indirect effect through microtubule binding proteins. Ectopically expressed β1-tubulin drives the formation of curved cytoplasmic microtubules in other cell types, and confers resistance to microtubule destabilizing poisons (Yang et al., 2011). Curiously, marginal bands in avian red blood cells contain also β3-tubulin thought to facilitate microtubule assembly and resistance to cold-induced depolymerization (Murphy and Wallis, 1985; Murphy and Wallis, 1986; Joshi et al., 1987). The β3 isotype is, however, not required for the formation of the marginal band in these cells (Swan and Solomon, 1984). The molecular-level details of how these different isotubulins contribute to the organization of the marginal band remain to be uncovered. The availability of sophisticated tools for structural analyses should facilitate progress in understanding the microtubule cytoskeleton in these highly specialized structures, and promises to reveal interesting mechanisms that cells utilize to create pattern architectures.

Molecular studies in the worm *Caenorhabditis elegans*, also indicate that particular tubulin isotypes can influence the supramolecular organization of microtubule lattices. For instance, the β-tubulin isotype MEC-7 from *C. elegans* is expressed primarily in microtubules within the axons of touch receptor neurons (Hamelin et al., 1992). Although worm microtubules normally consist of 11 protofilaments, the touch receptor axonal microtubules are structurally distinct and consist of 15 protofilaments. The MEC-7-null mutants, however, form axonal microtubules based on 11 protofilaments, indicating that the MEC-7 isotype specifically influences the architecture of axonal microtubules (Savage et al., 1994). The α-tubulin MEC-12 is also required for 15-protofilamtent microtubule assembly (Fukushige et al., 1999). Loss of either MEC-7 or 12 leads to touch insensitivity (Savage et al., 1994).

In addition to structural changes in the microtubule network, tubulin isotype composition has been found to influence microtubule biomechanical properties. One such example are microtubules in neurites. During neurite extension, cells quadruple the expression of β2 and β3 isotubulins and double the expression of β1-tubulin isotype. The expressed tubulins are incorporated into neurite microtubules in different proportions: while β2-tubulin dominates the neurite microtubules, β1, β3, and β4-tubulin isotypes are present in smaller quantities, and β5-tubulin is partially excluded (Joshi and Cleveland, 1989). Neurite microtubules are known to be substantially more stable than

those found in cell bodies. The specific neurite isotubulin composition may provide structural stabilization within the microtubule lattice. *In vitro* studies with purified tubulins and in the absence of MAPs show that microtubules assembled from β2 or β4 isotypes are considerably less dynamic than those assembled of the neuron-specific β3-tubulin (Lu and Luduena, 1994; Panda et al., 1994; Pamula et al., 2016; Vemu et al., 2017). This finding is somewhat counterintuitive and suggests that potential other factors are deployed to stabilize neurite microtubules. During neurite outgrowth and concomitantly with the change in tubulin expression, cells begin to express the neuron-specific microtubule associated protein 2 (MAP2) and increase the expression of microtubule associated protein tau (MAPT) (Joshi and Cleveland, 1989). It is possible that MAP2 and MAPT bind the neurite microtubules with higher affinity, thus stabilizing them.

Protein regions that confer differences in the biochemical properties of tubulin isotypes remain elusive. Even though the most divergent and thus top candidates, the role of carboxy-terminal tails of tubulins in their dynamic behavior *in vitro* remains controversial (Pamula et al., 2016; Fees and Moore, 2018). Systematic studies *in vitro* and in cells are necessary to unambiguously elucidate the role of carboxy-terminal tails in regulating tubulin biochemical properties. In addition to carboxy-terminal tails, lateral contact interfaces also harbor large sequence variability between tubulin isotypes and are thus potential regulation sites for tubulins' intrinsic biomechanical properties. High-resolution structures of isotypically pure microtubules may bring answers to how tubulin composition fine-tunes microtubule dynamics in cells. Recent structural analyses of *C. elegans* microtubules provide a proof of concept and reveal distinct features at lateral contact sites of tubulins likely responsible for the exceptionally high dynamic behavior of these microtubules (Chaaban et al., 2018).

DISCUSSION

Multi-gene families encode numerous important proteins, such as the histones, actins, various metabolic enzymes, or components of the immune system. Why does nature maintain multiple copies of genes that encode closely related proteins? For tubulins, the answer seems to reside in three independent but related aspects of gene function. First, the existence of multiple genes provides the opportunity for their differential expression throughout development and in specialized tissues. Various insults as well as physiological inputs trigger changes in tubulin gene expression. While some act purely via modulation of tubulin autoregulation, such as nutrient withdrawal, others such as amino-acid deficiency trigger transcriptional responses. In some instances, both regulatory mechanisms are engaged simultaneously (Gasic et al., 2019). We know very little about how all these pathways converge to provide cells with sufficient but not surplus tubulin. Is tubulin gene expression ever constitutive and as such at steady state? Or is it rather a dynamic result of a complex matrix of inputs that cells receive? If at any time a large number of inputs can modify tubulin gene expression, how do cells orchestrate their responses? It is tempting to speculate that the complexity in the number and nature of signals that shape tubulin gene expression may have been the primary drive for tubulin multiplication. Further investigations into how cells engage the elements in tubulin promoter regions to respond to various stimuli may provide some answers to these long-standing questions.

Second, the existence of multi-gene families allows diversification in the structures and functions of the encoded gene products. While we begin to unravel the differences amongst tubulin isotypes, a lot more work is warranted to provide a comprehensive view of their biochemical properties. Our understanding of how the different isotubulins are paired in heterodimers or how they are distributed in microtubule networks is rudimentary. Are some combinations of α and β isotypes favorable? How do their different combinations contribute to the biomechanical properties of microtubules? These questions are rather complex to study as there is a large number of possible combinations between the α and β isotypes further complicated by their spatial distribution in cells. Are some isotypes segregated in specific areas of the microtubule network? What would be the role of such an isotype code? In dynamic, short lived microtubules any information stored in this type of code would be quickly scrambled. But in long-lived microtubules, like those in neurons, spatial distribution of tubulin isotypes could encode information. To solve this puzzle, we need experimental systems that better represent nature and the diversity of microtubule architectures, as well as advanced tools to visualize individual tubulin isotypes.

Third, and much less discussed possible explanation is backup compensation, given that all tubulins can build microtubule networks capable of carrying out their most fundamental functions, such as cell division. In this concept, tubulin isotypes need not be discretely specialized. Rather, the focus is on conserved parts of the proteins. Differential expression of tubulin isotypes is then purely a consequence of the engagement of upstream transcriptional regulatory mechanisms that work to supply cells with tubulins of generalized function.

Most of the documented differences in isotype distribution across the different cell types and microtubule structures, as well as their functional specializations are related to β subunits. Are α-tubulins inherently more redundant? Do they harbor fewer differences and hence contribute less to the specialization of the microtubule cytoskeleton? Given fewer studies of α-tubulins it is difficult to answer these questions. Further studies may reveal new biology of α-tubulins or may reveal that they remain conserved. What would be further physiological implications of such different evolution of two proteins that form obligate heterodimers? And what can we learn about protein evolution from tubulins? These promise to be interesting areas of further exploration.

Careful analyses of tubulin gene expression at both transcriptional and posttranscriptional level are required and necessary to understand how cells define which

tubulins to produce and in what quantities. Similarly, detailed studies of tubulin biomechanical properties are warranted to understand how the isotype composition fine-tunes microtubule dynamics. But more integrated approaches may be required to gain a comprehensive view of how this complex gene network is organized and deployed in various cell types.

AUTHOR CONTRIBUTIONS

IG reviewed the literature, conceived and wrote the manuscript, and prepared the figures.

FUNDING

IG is supported by the Swiss National Science Foundation Eccellenza Fellowship (PCEFP3_194312) and is the Dale F. Frey Breakthrough Scientist of the Damon Runyon Cancer Research Foundation (DFS:39-20).

ACKNOWLEDGMENTS

IG wishes to thank Alina Batiuk for fruitful discussions and inputs on the manuscript.

REFERENCES

Arai, K., Matsumoto, Y., Nagashima, Y., and Yagasaki, K. (2006). Regulation of Class II β-Tubulin Expression by Tumor Suppressor P53 Protein in Mouse Melanoma Cells in Response toVincaAlkaloid. *Mol. Cancer Res.* 4 (4), 247–255. doi:10.1158/1541-7786.mcr-05-0183

Bachurski, C. J., Theodorakis, N. G., Coulson, R. M., and Cleveland, D. W. (1994). An Amino-Terminal Tetrapeptide Specifies Cotranslational Degradation of Beta-Tubulin but Not Alpha-Tubulin mRNAs. *Mol. Cell Biol. [Internet]* 14 (6), 4076–4086. doi:10.1128/mcb.14.6.4076-4086.1994

Ben-Ze'ev, A., Farmer, S. R., and Penman, S. (1979). Mechanisms of Regulating Tubulin Synthesis in Cultured Mammalian Cells. *Cell [Internet]* 17 (2), 319–325. Available from http://www.sciencedirect.com/science/article/pii/0092867479901570.

Bode, C. J., Gupta, M. L., Suprenant, K. A., and Himes, R. H. (2003). The Two α-tubulin Isotypes in Budding Yeast Have Opposing Effects on Microtubule Dynamics *In Vitro*. *Embo Rep.* 4 (1), 94–99. doi:10.1038/sj.embor.embor716

Bond, J., Fridovich-Keil, J. L., Pillus, L., Mulligan, R. C., and Solomon, F. (1986). A Chicken-Yeast Chimeric ?-tubulin Protein Is Incorporated into Mouse Microtubules *In Vivo*. *Cell* 44 (3), 461–468. doi:10.1016/0092-8674(86)90467-8

Breuss, M. W., Leca, I., Gstrein, T., Hansen, A. H., and Keays, D. A. (2017). Tubulins and Brain Development - the Origins of Functional Specification. *Mol. Cell. Neurosci.* 84, 58–67. doi:10.1016/j.mcn.2017.03.002

Burkhart, J. M., Vaudel, M., Gambaryan, S., Radau, S., Walter, U., Martens, L., et al. (2012). The First Comprehensive and Quantitative Analysis of Human Platelet Protein Composition Allows the Comparative Analysis of Structural and Functional Pathways. *Blood* 120 (15), e73–e82. doi:10.1182/blood-2012-04-416594

Caron, J. M., Jones, A. L., and Kirschner, M. W. (1985). Autoregulation of Tubulin Synthesis in Hepatocytes and Fibroblasts. *J. Cell Biol. [Internet]* 101 (5 Pt 1), 1763–1772. doi:10.1083/jcb.101.5.1763

Chaaban, S., Jariwala, S., Hsu, C.-T., Redemann, S., Kollman, J. M., Müller-Reichert, T., et al. (2018). The Structure and Dynamics of *C. elegans* Tubulin Reveals the Mechanistic Basis of Microtubule Growth. *Dev. Cell* 47 (2), 191–204. e8. doi:10.1016/j.devcel.2018.08.023

Cleveland, D. W. (1989). Autoregulated Control of Tubilin Synthesis in Animal Cells. *Curr. Opin. Cell Biol. [Internet]* 1 (1), 10–14. doi:10.1016/s0955-0674(89)80030-4

Cleveland, D. W., Lopata, M. A., MacDonald, R. J., Cowan, N. J., Rutter, W. J., and Kirschner, M. W. (1980). Number and Evolutionary Conservation of α- and β-tubulin and Cytoplasmic β- and γ-actin Genes Using Specific Cloned cDNA Probes. *Cell* 20 (1), 95–105. doi:10.1016/0092-8674(80)90238-x

Cleveland, D. W., Lopata, M. A., Sherline, P., and Kirschner, M. W. (1981). Unpolymerized Tubulin Modulates the Level of Tubulin mRNAs. *Cell [Internet]* 25 (2), 537–546. doi:10.1016/0092-8674(81)90072-6

Cuveillier, C., Delaroche, J., Seggio, M., Gory-Fauré, S., Bosc, C., Denarier, E., et al. (2020). MAP6 Is an Intraluminal Protein that Induces Neuronal Microtubules to Coil. *Sci. Adv. [Internet]* 6 (14), eaaz4344. doi:10.1126/sciadv.aaz4344

Davies, J. P., and Grossman, A. R. (1994). Sequences Controlling Transcription of the Chlamydomonas Reinhardtii Beta 2-tubulin Gene after Deflagellation and during the Cell Cycle. *Mol. Cell Biol.* 14 (8), 5165–5174. doi:10.1128/mcb.14.8.5165-5174.1994

Davies, J. P., Weeks, D. P., and Grossman, A. R. (1992). Expression of the Arylsulfatase Gene from Theβ2-Tubulin Promoter inChlamydomonas Reinhardtii. *Nucl. Acids Res.* 20 (12), 2959–2965. doi:10.1093/nar/20.12.2959

Dennis, K., Uittenbogaard, M., Chiaramello, A., and Moody, S. A. (2002). Cloning and Characterization of the 5'-flanking Region of the Rat Neuron-specific Class III Beta-Tubulin Gene. *Gene* 294 (1–2), 269–277. doi:10.1016/s0378-1119(02)00801-6

Drukman, S., and Kavallaris, M. (2002). Microtubule Alterations and Resistance to Tubulin-Binding Agents (Review). *Int. J. Oncol.* 21 (3), 621–628. doi:10.3892/ijo.21.3.621

Easter, S., Ross, L., and Frankfurter, A. (1993). Initial Tract Formation in the Mouse Brain. *J. Neurosci.* 13 (1), 285–299. doi:10.1523/jneurosci.13-01-00285.1993

Fees, C. P., and Moore, J. K. (2018). *Life Sci. Alliance [Internet]* 1 (2), e201800054. doi:10.26508/lsa.201800054

Fellous, A., Ginzburg, I., and Littauer, U. Z. (1982). Modulation of Tubulin mRNA Levels by Interferon in Human Lymphoblastoid Cells. *EMBO J. [Internet]* 1 (7), 835–839. doi:10.1002/j.1460-2075.1982.tb01256.x

Fukushige, T., Siddiqui, Z. K., Chou, M., Culotti, J. G., Gogonea, C. B., Siddiqui, S. S., et al. (1999). MEC-12, an Alpha-Tubulin Required for Touch Sensitivity in *C. elegans*. *J. Cell Sci.* 112 (3), 395–403. doi:10.1242/jcs.112.3.395

Fulton, C., and Simpson, P. (1976). Selective Synthesis and Utilisation of Flagellar Tubulin. The Multi-Tubulin Hypothesis. *Cell Motil.* 3, 987–1005.

Gadadhar, S., Bodakuntla, S., Natarajan, K., and Janke, C. (2017). The Tubulin Code at a Glance. *J. Cell Sci. [Internet]* 130 (8), 1347–1353. doi:10.1242/jcs.199471

Gasch, A., Hinz, U., and Renkawitz-Pohl, R. (1989). Intron and Upstream Sequences Regulate Expression of the Drosophila Beta 3-tubulin Gene in the Visceral and Somatic Musculature, Respectively. *Proc. Natl. Acad. Sci. U.S.A.* 86 (9), 3215–3218. doi:10.1073/pnas.86.9.3215

Gasic, I., Boswell, S. A., and Mitchison, T. J. (2019). Tubulin mRNA Stability Is Sensitive to Change in Microtubule Dynamics Caused by Multiple Physiological and Toxic Cues. *PLoS Biol. [Internet]* 17 (4), e3000225. doi:10.1371/journal.pbio.3000225

Gasic, I., and Mitchison, T. J. (2019). Autoregulation and Repair in Microtubule Homeostasis. *Curr. Opin. Cell Biol. [Internet]* 56, 80–87. doi:10.1016/j.ceb.2018.10.003

Gay, D. A., Sisodia, S. S., and Cleveland, D. W. (1989). Autoregulatory Control of Beta-Tubulin mRNA Stability Is Linked to Translation Elongation. *Proc. Natl. Acad. Sci. U. S. A. [Internet]* 86 (15), 5763–5767. doi:10.1073/pnas.86.15.5763

Goldman, D., and Ding, J. (2000). Different Regulatory Elements Are Necessary for αI Tubulin Induction during CNS Development and Regeneration. *Neuroreport* 11 (17), 3859–3863. doi:10.1097/00001756-200011270-00051

Goodson, H. V., and Jonasson, E. M. (2018). Microtubules and Microtubule-Associated Proteins. *Cold Spring Harb. Perspect. Biol.* 10 (6), a022608. doi:10.1101/cshperspect.a022608

Guichard, P., Laporte, M. H., and Hamel, V. (2021). The Centriolar Tubulin Code. *Semin. Cell Dev. Biol.* doi:10.1016/j.semcdb.2021.12.001

Hamelin, M., Scott, I. M., Way, J. C., and Culotti, J. G. (1992). The Mec-7 Beta-Tubulin Gene of *Caenorhabditis elegans* Is Expressed Primarily in the Touch Receptor Neurons. *Embo J. [Internet]* 11 (8), 2885–2893. doi:10.1002/j.1460-2075.1992.tb05357.x

Hieber, V., Dai, X., Foreman, M., and Goldman, D. (1998). Induction of ?1-tubulin Gene Expression during Development and Regeneration of the Fish Central Nervous System. *J. Neurobiol.* 37 (3), 429–440. doi:10.1002/(sici)1097-4695(19981115)37:3<429:aid-neu8>3.0.co;2-n

Hoyle, H. D., and Raff, E. C. (1990). Two Drosophila Beta Tubulin Isoforms Are Not Functionally Equivalent. *J. Cell Biol.* 111 (3), 1009–1026. doi:10.1083/jcb.111.3.1009

Jensen-Smith, H. C., Ludueña, R. F., and Hallworth, R. (2003). Requirement for the βI and βIV Tubulin Isotypes in Mammalian Cilia. *Cell Motil. Cytoskel* 55 (3), 213–220.

Jordan, M. A., Diener, D. R., Stepanek, L., and Pigino, G. (2018). The Cryo-EM Structure of Intraflagellar Transport Trains Reveals How Dynein Is Inactivated to Ensure Unidirectional Anterograde Movement in Cilia. *Nat. Cell Biol.* 20 (11), 1250–1255. doi:10.1038/s41556-018-0213-1

Joshi, H. C., and Cleveland, D. W. (1989). Differential Utilization of Beta-Tubulin Isotypes in Differentiating Neurites. *J. Cell Biol.* 109 (2), 663–673. doi:10.1083/jcb.109.2.663

Joshi, H. C., Yen, T. J., and Cleveland, D. W. (1987). *In Vivo* coassembly of a Divergent Beta-Tubulin Subunit (C Beta 6) into Microtubules of Different Function. *J. Cell Biol.* 105 (5), 2179–2190. doi:10.1083/jcb.105.5.2179

Katsetos, C. D., Legido, A., Perentes, E., and Mörk, S. J. (2003). Class III β-Tubulin Isotype: A Key Cytoskeletal Protein at the Crossroads of Developmental Neurobiology and Tumor Neuropathology. *J. Child. Neurol.* 18 (12), 851–866. doi:10.1177/088307380301801205

Lau, J. T., Pittenger, M. F., Havercroft, J. C., and Cleveland, D. W. (1986). Reconstruction of Tubulin Gene Regulation in Cultured Mammalian Cells. *Ann. N. Y. Acad. Sci. [Internet]* 466 (1), 75–88. doi:10.1111/j.1749-6632.1986.tb38385.x

Lewis, S. A., Gu, W., and Cowan, N. J. (1987). Free Intermingling of Mammalian β-tubulin Isotypes Among Functionally Distinct Microtubules. *Cell* 49 (4), 539–548. doi:10.1016/0092-8674(87)90456-9

Lin, Z., Gasic, I., Chandrasekaran, V., Peters, N., Shao, S., Mitchison, T. J., et al. (2020). TTC5 Mediates Autoregulation of Tubulin via mRNA Degradation. *Sci. [Internet]* 367 (6473), 100–104. doi:10.1126/science.aaz4352

Lopata, M. A., and Cleveland, D. W. (1987). *In Vivo* microtubules Are Copolymers of Available Beta-Tubulin Isotypes: Localization of Each of Six Vertebrate Beta-Tubulin Isotypes Using Polyclonal Antibodies Elicited by Synthetic Peptide Antigens. *J. Cell Biol.* 105 (4), 1707–1720. doi:10.1083/jcb.105.4.1707

Lu, Q., and Luduena, R. F. (1994). *In Vitro* analysis of Microtubule Assembly of Isotypically Pure Tubulin Dimers. Intrinsic Differences in the Assembly Properties of Alpha Beta II, Alpha Beta III, and Alpha Beta IV Tubulin Dimers in the Absence of Microtubule-Associated Proteins. *J. Biol. Chem.* 269 (3), 2041–2047. doi:10.1016/s0021-9258(17)42132-6

Ludueña, R. F. (1997). Multiple Forms of Tubulin: Different Gene Products and Covalent Modifications. *Int. Rev. Cytol.* 178, 207–275.

MacRae, T. H., and Langdon, C. M. (1989). Tubulin Synthesis, Structure, and Function: what Are the Relationships? *Biochem. Cell Biol. [Internet]* 67 (11–12), 770–790. doi:10.1139/o89-116

Magiera, M. M., and Janke, C. (2014). Post-translational Modifications of Tubulin. *Curr. Biol. [Internet]* 24 (9), R351–R354. doi:10.1016/j.cub.2014.03.032

Michiels, F., Gasch, A., Kaltschmidt, B., and Renkawitz-Pohl, R. (1989). A 14 Bp Promoter Element Directs the Testis Specificity of the Drosophila Beta 2 Tubulin Gene. *EMBO J.* 8 (5), 1559–1565. doi:10.1002/j.1460-2075.1989.tb03540.x

Muroyama, A., and Lechler, T. (2017). Microtubule Organization, Dynamics and Functions in Differentiated Cells. *Dev. [Internet]* 144 (17), 3012–3021. doi:10.1242/dev.153171

Murphy, D. B., and Wallis, K. T. (1985). Erythrocyte Microtubule Assembly *In Vitro*. Determination of the Effects of Erythrocyte Tau, Tubulin Isoforms, and Tubulin Oligomers on Erythrocyte Tubulin Assembly, and Comparison with Brain Microtubule Assembly. *J. Biol. Chem.* 260 (22), 12293–12301. doi:10.1016/s0021-9258(17)39024-5

Murphy, D. B., and Wallis, K. T. (1986). Erythrocyte Microtubule Assembly *In Vitro*. Tubulin Oligomers Limit the Rate of Microtubule Self-Assembly. *J. Biol. Chem.* 261 (5), 2319–2324. doi:10.1016/s0021-9258(17)35938-0

Nielsen, M. G., Turner, F. R., Hutchens, J. A., and Raff, E. C. (2001). Axoneme-specific β-tubulin Specialization. *Curr. Biol.* 11 (7), 529–533. doi:10.1016/s0960-9822(01)00150-6

Nsamba, E. T., Bera, A., Costanzo, M., Boone, C., and Gupta, M. L. (2021). Tubulin Isotypes Optimize Distinct Spindle Positioning Mechanisms during Yeast Mitosis. *J. Cell Biol.* 220 (12), e202010155. doi:10.1083/jcb.202010155

Pamula, M. C., Ti, S.-C., and Kapoor, T. M. (2016). The Structured Core of Human β Tubulin Confers Isotype-specific Polymerization Properties. *J. Cell Biol.* 213 (4), 425–433. doi:10.1083/jcb.201603050

Panda, D., Miller, H. P., Banerjee, A., Ludueña, R. F., and Wilson, L. (1994). Microtubule Dynamics *In Vitro* Are Regulated by the Tubulin Isotype Composition. *Proc. Natl. Acad. Sci. U.S.A.* 91 (24), 11358–11362. doi:10.1073/pnas.91.24.11358

Periz, G., and Keller, L. R. (1997). DNA Elements Regulating Alpha1-Tubulin Gene Induction during Regeneration of Eukaryotic Flagella. *Mol. Cell Biol.* 17 (7), 3858–3866. doi:10.1128/mcb.17.7.3858

Pittenger, M. F., and Cleveland, D. W. (1985). Retention of Autoregulatory Control of Tubulin Synthesis in Cytoplasts: Demonstration of a Cytoplasmic Mechanism that Regulates the Level of Tubulin Expression. *J. Cell Biol.* 101 (5 Pt 1), 1941–1952. doi:10.1083/jcb.101.5.1941

Preitner, N., Quan, J., Nowakowski, D. W., Hancock, M. L., Shi, J., Tcherkezian, J., et al. (2014). APC Is an RNA-Binding Protein, and its Interactome Provides a Link to Neural Development and Microtubule Assembly. *Cell* 158 (2), 368–382. doi:10.1016/j.cell.2014.05.042

Raff, E. C., Hutchens, J. A., Hoyle, H. D., Nielsen, M. G., and Turner, F. R. (2000). Conserved Axoneme Symmetry Altered by a Component β-tubulin. *Curr. Biol.* 10 (21), 1391–1394. doi:10.1016/s0960-9822(00)00784-3

Raspaglio, G., Filippetti, F., Prislei, S., Penci, R., De Maria, I., Cicchillitti, L., et al. (2008). *Gene [Internet]* 409 (1–2), 100–108. doi:10.1016/j.gene.2007.11.015

Roll-Mecak, A. (2020). The Tubulin Code in Microtubule Dynamics and Information Encoding. *Dev. Cell* 54 (1), 7–20. doi:10.1016/j.devcel.2020.06.008

Santel, A., Kaufmann, J., Hyland, R., and Renkawitz-Pohl, R. (2000). The Initiator Element of the Drosophila Beta2 Tubulin Gene Core Promoter Contributes to Gene Expression *In Vivo* but Is Not Required for Male Germ-Cell Specific Expression. *Nucleic Acids Res.* 28 (6), 1439–1446. doi:10.1093/nar/28.6.1439

Savage, C., Xue, Y., Mitani, S., Hall, D., Zakhary, R., and Chalfie, M. (1994). Mutations in the *Caenorhabditis elegans* Beta-Tubulin Gene Mec-7: Effects on Microtubule Assembly and Stability and on Tubulin Autoregulation. *J. Cell Sci. [Internet]* 107 (Pt 8), 2165–2175. doi:10.1242/jcs.107.8.2165

Senut, M.-C., Gulati-Leekha, A., and Goldman, D. (2004). An Element in the 1-Tubulin Promoter Is Necessary for Retinal Expression during Optic Nerve Regeneration but Not after Eye Injury in the Adult Zebrafish. *J. Neurosci. [Internet]* 24 (35), 7663–7673. doi:10.1523/jneurosci.2281-04.2004

Serrano, N., Brock, H. W., and Maschat, F. (1997). beta3-tubulin Is Directly Repressed by the Engrailed Protein in Drosophila. *Development* 124 (13), 2527–2536. doi:10.1242/dev.124.13.2527

Stephens, R. E. (1978). Primary Structural Differences Among Tubulin Subunits from Flagella, Cilia, and the Cytoplasm. *Biochemistry* 17 (14), 2882–2891. doi:10.1021/bi00607a029

Sullivan, K. F. (1988). Structure and Utilization of Tubulin Isotypes. *Annu. Rev. Cell. Biol.* 4 (1), 687–716. doi:10.1146/annurev.cb.04.110188.003351

Swan, J. A., and Solomon, F. (1984). Reformation of the Marginal Band of Avian Erythrocytes *In Vitro* Using Calf-Brain Tubulin: Peripheral Determinants of Microtubule Form. *J. Cell Biol.* 99 (6), 2108–2113. doi:10.1083/jcb.99.6.2108

Theodorakis, N. G., and Cleveland, D. W. (1992). Physical Evidence for Cotranslational Regulation of Beta-Tubulin mRNA Degradation. *Mol. Cell Biol. [Internet]* 12 (2), 791–799. doi:10.1128/mcb.12.2.791-799.1992

Vemu, A., Atherton, J., Spector, J. O., Moores, C. A., and Roll-Mecak, A. (2017). "Tubulin Isoform Composition Tunes Microtubule Dynamics," in *MBoC.* Molecular Biology of the Cell. Editor L Blanchoin, 28, 3564–3572. doi:10.1091/mbc.e17-02-0124

Yang, H., Ganguly, A., Yin, S., and Cabral, F. (2011). Megakaryocyte Lineage-specific Class VI β-tubulin Suppresses Microtubule Dynamics, Fragments Microtubules, and Blocks Cell Division. *Cytoskeleton* 68 (3), 175–187. doi:10.1002/cm.20503

Yen, T. J., Machlin, P. S., and Cleveland, D. W. (1988). Autoregulated Instability of Beta-Tubulin mRNAs by Recognition of the Nascent Amino Terminus of Beta-Tubulin. *Nat. [Internet]* 334 (6183), 580–585. doi:10.1038/334580a0

Yu, I., Garnham, C. P., and Roll-Mecak, A. (2015). Writing and Reading the Tubulin Code. *J. Biol. Chem.* 290 (28), 17163–17172. doi:10.1074/jbc.r115.637447

Yu, X., Ng, C. P., Habacher, H., and Roy, S. (2008). Foxj1 Transcription Factors Are Master Regulators of the Motile Ciliogenic Program. *Nat. Genet. [Internet]* 40 (12), 1445–1453. doi:10.1038/ng.263

Conflict of Interest: The authors declare that the research was conducted in the absence of any commercial or financial relationships that could be construed as a potential conflict of interest.

frontiers | Frontiers in Cell and Developmental Biology

HYPOTHESIS AND THEORY
published: 30 May 2022
doi: 10.3389/fcell.2022.870088

Nuclear βII-Tubulin and its Possible Utility in Cancer Diagnosis, Prognosis and Treatment

Richard F. Ludueña[1], Consuelo Walss-Bass[2], Anna Portyanko[3], Jiayan Guo[4] and I-Tien Yeh[5]*

[1]Department of Biochemistry and Structural Biology, University of Texas Health Science Center at San Antonio, San Antonio, TX, United States, [2]Department of Psychiatry and Behavioral Sciences, University of Texas Health Science Center at Houston, Houston, TX, United States, [3]Belarussian State Medical University, Minsk, Belarus, [4]Fosun Pharma, Shanghai, China, [5]Department of Pathology, University of Texas Health Science Center at San Antonio, San Antonio, TX, United States

Microtubules are organelles that usually occur only in the cytosol. Walss et al. (1999) discovered the βII isotype of tubulin, complexed with α, in the nuclei of certain cultured cells, in non-microtubule form. When fluorescently labeled tubulins were microinjected into the cells, only $\alpha\beta$II appeared in the nucleus, and only after one cycle of nuclear disassembly and reassembly. It appeared as if $\alpha\beta$II does not cross the nuclear envelope but is trapped in the nucleus by the re-forming nuclear envelope in whose reassembly βII may be involved. βII is present in the cytoplasm and nuclei of many tumor cells. With some exceptions, normal tissues that expressed βII rarely had βII in their nuclei. It is possible that βII is involved in nuclear reassembly and then disappears from the nucleus. Ruksha et al. (2019) observed that patients whose colon cancer cells in the invasive front showed no βII had a median survival of about 5.5 years, which was more than halved if they had cytosolic βII and further lessened if they had nuclear βII, suggesting that the presence and location of βII in biopsies could be a useful prognostic indicator and also that βII may be involved in cancer progression. Yeh and Ludueña. (2004) observed that many tumors were surrounded by non-cancerous cells exhibiting cytosolic and nuclear βII, suggesting a signaling pathway that causes βII to be synthesized in nearby cells and localized to their nuclei. βII could be useful in cancer diagnosis, since the presence of βII in non-cancerous cells could indicate a nearby tumor. Investigation of this pathway might reveal novel targets for chemotherapy. Another possibility would be to combine $\alpha\beta$II with CRISPR-Cas9. This complex would likely enter the nucleus of a cancer cell and, if guided to the appropriate gene, might destroy the cancer cell or make it less aggressive; possible targets will be discussed here. The possibilities raised here about the utility of βII in cancer diagnosis, prognosis, biology and therapy may repay further investigation.

Keywords: Beta-II-Tubulin, nucleus, cancer diagnosis, Cancer prognosis, cancer treatment, CRISPR-Cas9

OPEN ACCESS

Edited by:
Allen Liu,
University of Michigan, United States

Reviewed by:
Pavla Binarova,
Academy of Sciences of the Czech Republic (ASCR), Czechia
Dan Sackett,
Eunice Kennedy Shriver National Institute of Child Health and Human Development (NIH), United States

****Correspondence:***
Richard F. Ludueña
luduena@uthscsa.edu

Specialty section:
This article was submitted to Cellular Biochemistry, a section of the journal Frontiers in Cell and Developmental Biology

Received: *05 February 2022*
Accepted: *02 May 2022*
Published: *30 May 2022*

Citation:
Ludueña RF, Walss-Bass C, Portyanko A, Guo J and Yeh I-T (2022) Nuclear βII-Tubulin and its Possible Utility in Cancer Diagnosis, Prognosis and Treatment. Front. Cell Dev. Biol. 10:870088. doi: 10.3389/fcell.2022.870088

INTRODUCTION

Microtubules are composed of the protein tubulin, which is a heterodimer of two subunits, designated *a* and *ß* (Ludueña et al., 1977). Both *a* and *ß* consist of multiple isotypes, each of which is encoded by different genes; the amino acid sequence differences among the vertebrate isotypes have been highly conserved in evolution, suggesting that they may be functionally significant (Ludueña, 2013). In this study

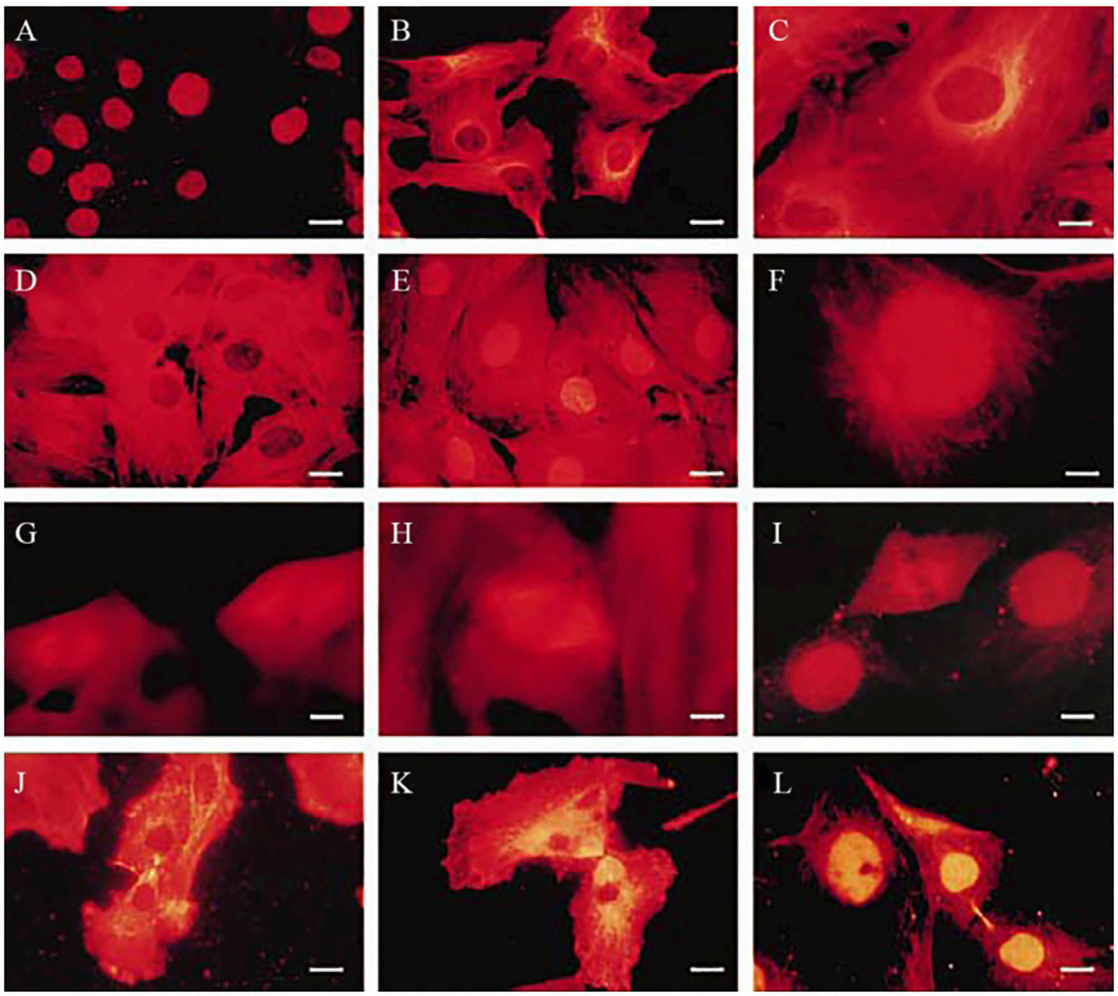

FIGURE 1 | Detection of *ß*-tubulin isotypes during the cell cycle of cultured rat kidney mesangial cells by indirect immunofluorescence. **(A)** Interphase cells treated with anti- *ß*II (0.03 mg/ml). Note that only the nuclei are stained. **(B)** Interphase cells treated with anti- *ß*I (0.1 mg/ml). Note very little staining in the nuclei. **(C)** Interphase cells treated with anti-βIV (0.17 mg/ml). Note very little staining in the nuclei. **(D)** Cells treated with 30 µg/ml nocodazole, stained with anti-βI (0.1 mg/ml). Note widespread staining except in the nuclei. **(E)** Cells treated with 30 µg/ml nocodazole, stained with anti-*ß*II (0.1 mg/ml). Note staining in the nuclei. **(F)** Cell during prophase, treated with anti-*ß*II (0.05 mg/ml). Note that asters are beginning to form and that they contain *ß*II. **(G)** Cells during metaphase, treated with anti-*ß*I (0.1 mg/ml). *ß*I is in the spindle. **(H)** Cell during metaphase, treated with anti-*ß*IV (0.17 mg/ml). *ß*IV is in the spindle. **(I)** Cell during metaphase, treated with anti-*ß*II (0.05 mg/ml). *ß*II is in the spindle. **(J)** Cell during late telophase, treated with anti-*ß*I (0.05 mg/ml). *ß*I is not in the re-forming nuclei. **(K)** Cell during late telophase, treated with anti-*ß*IV (0.08 mg/ml). *ß*IV is not in the re-forming nuclei. **(L)** Cell during late telophase, treated with anti-*ß*II (0.05 mg/ml). Note that the nuclei, staining brightly for *ß*II, have now re-formed. Bar = 28 µm (From. Walss et al., 1999).

we have focused on the *ß* isotypes. These isotypes exhibit major differences in their tissue distributions. Under normal circumstances, the βI and βIV isotypes are widely distributed among cells and tissues (Roach et al., 1998). In contrast, βII is highly expressed in nerves, both in neurons and supporting cells such as glia, and also in muscle cells, while βIII is particularly common in neurons (not in glia) and also in the testes (Burgoyne et al., 1988; Lewis and Cowan, 1988). The *ß*V isotype is widespread but not predominant, being slightly higher in a few cell types (Nakamura et al., 2004; Chao et al., 2012). The *ß*VI isotype is restricted to hematopoietic tissues, such as bone marrow, platelets and non-mammalian erythrocytes (Murphy and Wallis, 1983; Wang et al., 1986). Although every *ß* isotype can participate in some of the main microtubule functions, such as forming the mitotic spindle and mediating intracellular transport (Lopata and Cleveland, 1987), our results and those of others have indicated that there is some specialization. *ß*II appears to be associated with membrane rearrangements, such as neurite outgrowth (Guo et al., 2010; Guo et al., 2011), while *ß*III, when mixed with small amounts of other *ß* isotypes, forms very dynamic microtubules (Panda et al., 1994; Vemu et al., 2016) and also protects cells from various stresses (Gan et al., 2007; Guo et al., 2010; Guo et al., 2018). In addition, studies on purified *αß*II, αβIII and αβIV dimers have shown that the anti-tumor drugs vinblastine and taxol interact most strongly with *αß*II and most weakly with *αß*III (Derry et al., 1997; Khan and Ludueña, 2003).

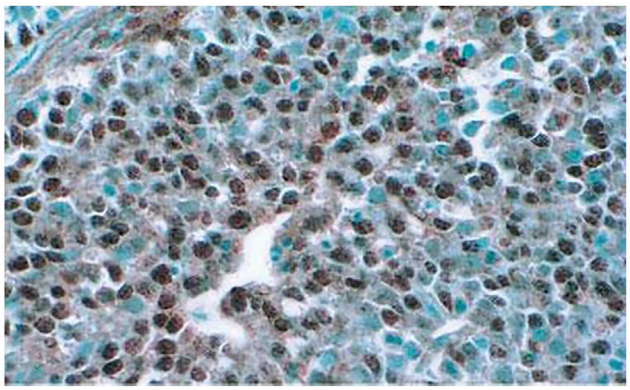

FIGURE 2 | Carcinoma of the Ovary stained for βII. A monoclonal antibody to βII was the primary antibody followed by a rabbit anti-mouse antibody and then Streptavidin horseradish peroxidase, followed by diaminobenzidine and OsO_2. Brown color indicates the location of βII. Note that most of the cell nuclei stain for βII. Methyl green, which binds to DNA, was used as the counter-stain. Note that a few nuclei do not have βII (From Yeh and Ludueña, 2004).

In cancer cells, the expression of the ß isotypes changes dramatically. Many cancer cells express βII and the most aggressive cancers express βIII, regardless of the extent to which either of these is expressed in the non-transformed cells from which these cancers originated (Katsetos et al., 2003; Yeh and Ludueña, 2004).

NUCLEAR *B*II

The nuclear βII isotype was first observed in rat kidney mesangial cells (Walss et al., 1999). Nuclear βII was bound to *a* and was normal in that it bound to drugs such as taxol, vinblastine and colchicine (Walss et al., 1999; Xu and Ludueña, 2002; Walss-Bass et al., 2003). Nuclear βII was not in the form of microtubules but rather appeared to be in small bodies, whose internal organization was unclear (Walss et al., 1999). During mitosis, βII participated in forming the mitotic spindle and then was back in the nucleus by interphase (Walss et al., 1999) (**Figure 1**). **Figure 1** also shows that, although βI and βIV are also present in these cells, only βII ends up in the nucleus. Microinjection of fluorescently labeled αβII, αβIII, and αβIV indicated that only αβII entered the nucleus and only after one cycle of nuclear assembly and disassembly (Walss-Bass et al., 2001), suggesting that, rather than penetrating the nuclear envelope, αβII was in the nucleus while the envelope re-formed around it, consistent with the finding that βII-tubulin appears to have a specific connection to heterochromatin protein 1 and to the nuclear envelope (Kourmouli et al., 2001). In general, microtubules are restricted to the cytosol, so it is unusual to see apparently viable tubulin in the nucleoplasm.

NUCLEAR BII IN CANCER PROGNOSIS

A study of a large number of cancers from multiple patients showed that many of them expressed βII in the cytosol and most also had βII in the nuclei (Yeh and Ludueña, 2004; Ruksha et al., 2019) (**Figure 2**). This may partially explain why drugs such as vinblastine and taxol, which interact more strongly with βII (Derry et al., 1997; Khan and Ludueña, 2003), are useful agents in cancer chemotherapy, and also why they cause substantial neuropathy (Markman, 2003; Mukhtar et al., 2014). A study of colon cancer patients (Ruksha et al., 2019) indicated that patients whose cancer cells in the invasive front showed no βII had a median survival rate of about 5.5 years, while those whose cells had only cytosolic βII had a median survival of just under 2 years. Those with nuclear βII had a 5-year survival rate of zero and a medial survival of 13 months (**Figure 3**). It would appear that the presence of βII and its localization in the nuclei, as seen in a tumor biopsy or in an excised tumor, would be useful prognostic indicators of the survival of the patient. These results also raise the possibility that βII expression in the nuclei may be necessary for cancer progression. On the other hand, Yeh and Ludueña (2004) also found that some normal tissues also contained cells with nuclear βII, although the frequency of occurrence was generally fairly low. This raises the possibility that nuclear βII may play a role in re-formation of the nuclear envelope after mitosis, even in normal cells, after which it disappears; this would be consistent with the observations of,Kourmouli et al. (2001) about βII being associated with proteins that bind to the nuclear envelope, although their results do not rule out the possibility of the βI and βIV isotypes having equally tight binding to the nuclear envelope.

NUCLEAR BII IN CANCER DIAGNOSIS

We observed that many tumors were surrounded by zones of non-transformed cells that contained substantial amounts of cytosolic βII and also of nuclear βII (Yeh and Ludueña, 2004; Ruksha et al., 2019) (**Figure 4**). These often included lymphocytes as well (Yeh and Ludueña, 2004). These results raise the possibility that, by some as yet unknown mechanism, tumor cells cause nearby cells to express βII-tubulin and localize it to their nuclei. This also suggests a potential role in cancer diagnosis. If a biopsy probe misses the tumor itself, resulting in an apparent false negative, then it might pull out cells close to the tumor that contain cytosolic and perhaps nuclear βII. This would not only enhance the power of the biopsy, but perhaps even give an indication of the grade of the tumor. The outcome would be the possibility of earlier diagnosis of the tumor and an increased chance of treating the patient successfully.

NUCLEAR BII IN CANCER THERAPY

The results described above strongly suggest that expression of βII in cancer cells and its localization in their nuclei serve a function required by the cancer cell. This function would probably involve some kind of signaling pathway. A microarray experiment may be able to identify the components of this pathway. Drugs could then be developed

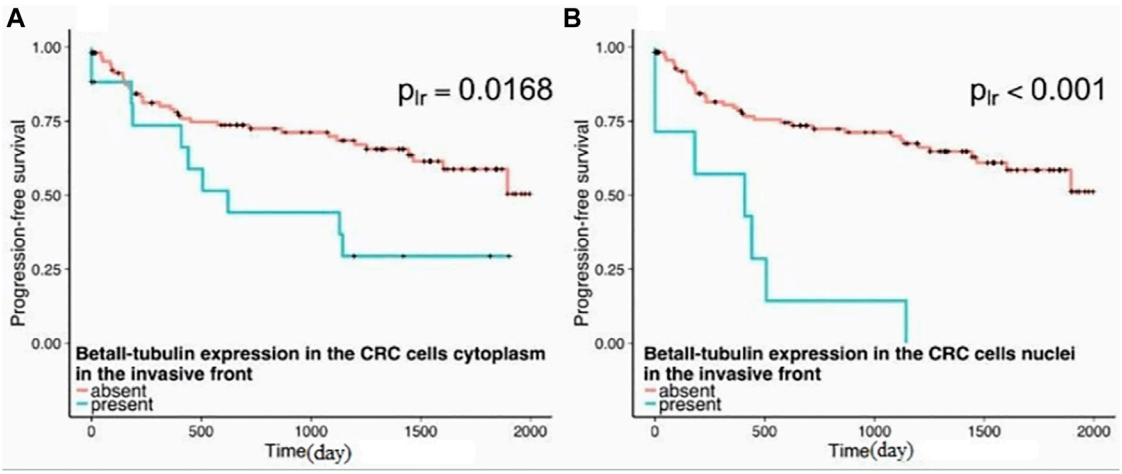

FIGURE 3 | Progression-free survival in patients as a function of the presence of βII-positive staining in the invasive front of colorectal cancer tumors. **(A)** The progression-free survival is decreased in patients with the presence of cytoplasmic βII-tubulin in the invasive front (plr = 0.0168). **(B)** Patients with the presence of nuclear βII tubulin staining in the invasive front demonstrate worse prognosis in comparison with patients without positive staining in the nuclei (plr< 0.001) (From Ruksha et al., 2019).

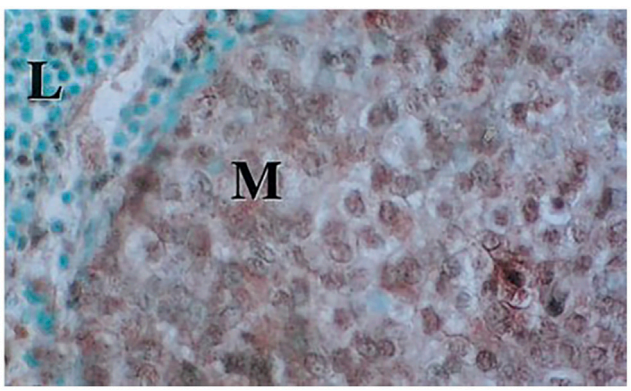

FIGURE 4 | Lymph node with metastatic breast carcinoma. Sample was processed as in **Figure 2**. Note both cytoplasmic and nuclear staining for βII in the metastatic tumor cells (M) and some weak nuclear staining for βII in the adjacent lymphocytes (L). (From Yeh and Ludueña, 2004).

to inhibit a key pathway component and thus slow or block the progression of the cancer.

COULD NUCLEAR βII BE COMBINED WITH CRISPR-CAS9 TO CREATE A NOVEL ANTI-TUMOR THERAPY?

CRISPR-Cas9 is an agent that, when combined with a guideRNA (gRNA), can inactivate targeted genes, as determined by the gRNA; the strategy is to "correct" mutations that cause hereditary diseases (Naso et al., 2017). Some recent attempts to treat cancer involve using CRISPR-Cas9 to "correct" mutations in oncogenes (Li et al., 2020).

The approach we are suggesting here does not involve "correcting" any mutations, but rather targeting specific genes only in the cancer cell. One might imagine that combining CRISPR-Cas9 with *β*II-tubulin could create an agent that could enter the nuclei of cancer cells. For any agent involving CRISPR-Cas9, there would be three questions that need to be answered:

First, how could a *β*II-CRISPR-Cas9 complex enter the target cell? If there is a receptor on the tumor cell membrane then it may be possible to add to the complex a factor that would bind to the receptor, for example, a lipid nanoparticle directed at the liver; this has been used with CRISPR-Cas9 to treat transthyretin amyloidosis (Finn et al., 2018; Gillmore et al., 2021). Otherwise, it may be necessary to encapsulate the complex in something that would bind to many types of cells, such as an adeno-associated virus (Naso et al., 2017). In addition to potential immunological issues, this could pose potential dangers that will be discussed below.

Second, how could a *β*II-CRISPR-Cas9 complex enter the nucleus? It is likely that this would require that the *β*II in the complex be bound to *a*-tubulin, so that the *β*II is in its normal functional conformation. If this is feasible, entry of the complex into the nuclei could be the easiest of the steps. Just as is the case with αβII, the nucleus would re-assemble around it (Walss et al., 1999). No nuclear recognition signal would be required. This is likely to happen in many cancer cells, but not in many normal cells. However, the fact that we found some normal cells with nuclear *β*II (Yeh and Ludueña, 2004) suggests that the *α*β*β*II-CRISPR-Cas9 complex could end up in the nuclei of some normal cells as well. We do not as yet know the precise function that nuclear *β*II serves in the normal cells where it occurs but it may play a role in reassembly of the nuclear envelope as suggested by Kourmouli et al. (2001) after which it could be degraded. If this is so, this process could occur in some normal tissues, at least in the ones where we have observed nuclear *β*II, such as bone marrow

(Yeh and Ludueña, 2004). Cells such as neurons would virtually never reproduce and that may explain why we have not seen nuclear βII in these cells. In short, it is possible that some normal cells may contain nuclear βII for a very brief time and that the αβII-tubulin-CRISPR-Cas9 complex could enter the nuclei of these cells, and possibly cause some damage.

The issue of targeting the αβII-tubulin-CRISPR-Cas9 complex to enter the nucleus is complicated by the fact that we do not know the precise role of nuclear βII and that the results at this point are not consistent with an absolute requirement for nuclear βII in cell division. One the one hand, Yeh and Ludueña (2004), looking at excisions of tumors from human patients, found that nuclear βII was present in every sample (although not every tumor cell) of tumors of the stomach, colon, bone, and prostate and in at least half of the tumors of the pancreas, lung, lymphocytes, ovary and breast. On the other hand, nuclear βII was rarer in melanomas, squamous cell carcinomas, and brain tumors. This is consistent with the observation that mitosis-specific drugs are less effective in cancer chemotherapy than are those that target microtubules, which have numerous functions in cells (Komlodi-Pasztor et al., 2011; Mitchison, 2012). Similarly, normal bone marrow cells, which reproduce more rapidly than some cancer cells (Mitchison, 2012) showed some nuclear βII (Yeh and Ludueña, 2004); however, other normal tissues, such as small bowel and colon, which one would expect to have high rates of reproduction, showed none (Yeh and Ludueña, 2004; Ruksha et al., 2019). In short, if nuclear βII plays an important role in reproduction in some cells, one cannot conclude that this role is universal, and if a tubulin is required for this role, it is possible that in certain cells, including some tumor cells, some other tubulin isotype may serve. In other words, it is possible that there are tumors into whose nuclei an αβII-CRISPR-Cas9 complex might not enter. It is possible, however, that a biopsy or other assay might determine if a given tumor contains nuclear βII, in which case the likelihood of the complex entering the nucleus would probably be higher.

Third, what would the gRNA target? There are several possibilities:

A)The gRNA could target the genes for housekeeping proteins, such as aldolase or any component in the glycolytic pathway or Krebs cycle. This would virtually ensure the death of the cell, which would be unable to metabolise. For normal cells, this could be catastrophic, so toxicity could be a serious problem.
B)The gRNA could target genes encoding proteins involved in cell reproduction, such as DNA polymerase. This would prevent the cancer from growing. However, many normal cells need to reproduce and hence this could cause long-term problems such as loss of bone marrow or intestinal epithelia.
C)The gRNA could target the βIII-tubulin isotype. This could be the most beneficial outcome. First, it would be the least likely to have disadvantageous side effects, since only two normal tissues express substantial amounts of βIII. Neurons do not have nuclear βII and hence the synthesis of βIII would not be affected. The other tissue is the testis, which could be a problem, but not for women. One of the great advantages of a gRNA targeting βIII is that it could prevent cancer progression. As described above, many cancers express both βII and βIII. The expression of βII makes them susceptible to treatment with anti-tumor drugs such as taxol and vinblastine (Derry et al., 1997; Khan and Ludueña, 2003), but cancers can often escape that by making more βIII (Mozzetti et al., 2005). If βIII synthesis is blocked then it is possible that lower doses of taxol and vinblastine, causing less neuropathy, may be sufficient to treat the tumor successfully.

POTENTIAL PROBLEMS AND THEIR POTENTIAL SOLUTIONS

The first potential problem to be faced would be technical: the construction of the αβII-CRISPR-Cas9 complex in such a way that the αβII is linked to the rest of the complex without being denatured. One might begin by making recombinant human αβII tubulin. This has already been accomplished for human αβIII tubulin (Vemu et al., 2016), so making recombinant human αβII should not be too difficult. The linking of the dimer to the CRISPR-Cas9 complex could perhaps be accomplished using one of many available chemical cross-linkers. Many of these target sulfhydryl groups, but this could be a problem since the sulfhydryl group of C239 in β-tubulin is very reactive and its reaction inhibits microtubule assembly and probably makes the tubulin molecule non-functional (Palanivelu and Ludueña, 1982; Little and Ludueña, 1985; Bai et al., 1989). Reaction of the sulfhydryl group is inhibited by any drug binding to the colchicine site (Ludueña and Roach, 1991). It would probably be better to use a cross-linker targeting amino groups. One such reagent, dimethyl-3,3'-(tetramethylenedioxy) dipropionimidate dihydrochloride (DTDI), was used to covalently link α to β and the reaction was actually enhanced by either colchicine or vinblastine, suggesting that the DTDI reaction was not blocking access to important sites on the tubulin molecule as well as raising the possibility that it could stabilize the conformation of the tubulin (Ludueña et al., 1977). Perhaps that reagent could also be used to link αβII to the CRISPR-Cas9 complex. Obviously, a good deal of experimentation to optimize the reaction would be required.

The tubulin molecule has long been known to have an unstable conformation (Wilson, 1970); it spontaneously denatures when it is in solution (Schwarz et al., 1998) and this needs to be considered in the methodology proposed here. However, the different isotypes have different stabilities. Using a variety of approaches, it appears safe to say that the conformation of the αβII dimer, although not as stable as that of the αβIII dimer, is more stable than that of the αβIV dimer (Banerjee et al., 1994; Sharma and Ludueña, 1994; Banerjee et al., 1997; Schwarz et al., 1998). Also, the observations of Walss et al. (1999) indicate that the αβII dimer can go from its nuclear state, forming a small body, possibly a filament, to forming the microtubules of the mitotic spindle and then returning to whatever state it was in when it reappears in the nucleus; presumably, the conformation of the αβII dimer survives intact through all of these changes, thereby speaking to some degree of stability. That the nuclear αβII dimer is in a normal conformation is supported by the observation that

it can bind to colchicine, vinblastine and taxol (Walss et al., 1999; Xu and Luduena, 2002.; Walss-Bass et al., 2003). Second, the *αβ*II dimer has to be able to survive being linked to the CRISPR-Cas9 complex. At the moment, we can safely say that the *αβ*II dimer retains its conformation after being linked to the fluorescent marker 5-(4,6-dichlorotriazin-2-yl)aminofluorescein (DTAF) (Walss et al., 1999). At any stage during this process, the intactness of the tubulin conformation can be assayed by test of its ability to bind to colchicine (Borisy, 1972).

It may be difficult to find a way to ensure that the *αβ*II-CRISPR-Cas9 complex enters the target cell. It would depend on how the complex is packaged. If it is something that would allow the complex to enter any cell type, then there may be too many side effects, even if the cancer is neutralized, although these could perhaps be controllable, as will be described below. Also, it is not possible *a priori* to estimate how many of the cancer target cells would be penetrated by the complex. A narrower approach would be to target the tumor to a cell-type-specific receptor. An example would be the CD20 protein on the surface of B-cell lymphocytes (Pavlasova and Mraz, 2019). If the αβII-CRISPR-Cas9 complex could be targeted to CD20 and then somehow internalized into the B-cell, the mechanism of action of the complex would be more lethal to cancerous B-cells than to normal B-cells and thus, the immune system of the patient is more likely to remain functional. This is analogous to the mechanism of action of CD20-binding monoclonal antibodies, such as rituximab, useful in treating many hematologic tumors (Saini et al., 2011), although its action against the target cell is external rather than internal. Other tumors may be in tissues that express analogous surface antigens and the same logic could apply.

Another problem is that the *αβ*II-CRISPR-Cas9 complex may enter the nuclei of normal cells, some of which clearly have nuclear *β*II (Yeh and Ludueña, 2004), and may thus be toxic. This could perhaps be prevented by having the αβII-CRISPR-Cas9 complex self-destruct. Since the *αβ*II only appears to enter the nucleus during mitosis, and if in a given cell type, the interval between divisions is longer, then it may be advantageous to have the complex disappear. If the *αβ*II-CRISPR-Cas9 complex were modified in some way so that the ubiquitin system could degrade it after an interval of time, the probability of the complex lasting long enough to do serious damage to a slow-dividing cell will be greatly diminished. The modification could be as simple as engineering an arginine onto the N-terminus, since this residue allows for rapid degradation (Varshavsky, 1996). Perhaps even better, since most tubulins begin with a Met-Arg sequence, once could simply remove the N-terminal methionine, leaving the arginine as the new N-terminus. Slower degradation could be mediated by putting in a glutamate instead (Varshavsky, 1996). Similarly, the C-terminal end could be modified in any of a number of ways to favor degradation (Chatr-Aryamontri et al., 2018)). In short, it may be possible to "fine-tune" the rate at which degradation occurs so as to have the *αβ*II-CRISPR-Cas9 complex remain in the cytosol long enough to enter the nucleus of a rapidly dividing tumor cell, but not so long that it might do the same in a normal cell. Since some tumor cells could divide slowly and some normal cells divide quickly, this would have to be carefully addressed. It may be advisable to do the modifications on the *a*-tubulin subunit, since the *β*II subunit should arguably remain intact to be able to remain in the nucleus. This fine-tuning approach could also address another possible drawback, namely that the Cas9 endonuclease component of the *αβ*II-CRISPR-Cas9 complex, even with the appropriate gRNA, may cause nonspecific damage to more than just the target genes, a process called chromothripsis (Leibowitz et al., 2021) and thus could be too toxic.

Of the various potential targets for the gRNA described above, the most intriguing one, as mentioned above, is *β*III, because very few normal cells, except for neurons and the testis, appear to express it, and because it is produced by so many aggressive cancers. However, there are reports of *β*III being expressed in non-neuronal cells at low levels and participating in forming the mitotic spindle (Jouhilahti et al., 2008). Again, just as described above, designing the *αβ*II-CRISPR-Cas9 complex to have a limited lifetime could cope with this issue as well. Finally, if the complex only lowers *β*III expression levels rather than eliminating *β*III altogether, treatment could consist of the complex combined with a drug favoring binding to *β*III. Several such drugs have been designed to bind to the colchicine site on *β*III (Pallante et al., 2020); one of these is more effective than paclitaxel on a *β*III-overexpressing human breast cancer cell line in a transgenic mouse model (Yeh et al., 2016). Similarly, the taxane cabazitaxel is more effective than docetaxel at inhibiting dynamics *in vitro* of microtubules that contain *β*III-tubulin than of microtubules that lack *β*III (Smiyun et al., 2017) and appears to be a useful treatment in advanced prostate cancer (Wallis et al., 2021). These or similar drugs might be therapeutically useful in combination with the *αβ*II-CRISPR-Cas9 complex proposed here.

A potentially more serious problem, however, arises from the *β*V isotype, which is fairly closely related to *β*III. Although the αβV dimer has never been purified and its specific properties determined, the fact that *β*V shares two unusual features with *β*III: a cysteine cluster (C124, C127, C129), and the lack of the easily oxidized C239 (Bai et al., 1989), together with its ability to make microtubules disassemble rapidly *in vivo* (Bhattacharya and Cabral, 2004, 2009) raise the possibility that *β*V may be able to protect cells from oxidative stress and also form dynamic microtubules. In short, *β*V may easily substitute for *β*III in a cancer cell and keep the cell viable despite treatment with an *αβ*II-CRISPR-Cas9 complex with a gRNA directed against *β*III. In other words, it is possible that silencing of *β*III by the complex could result in over-expression of *β*V by the cancer cell and the cancer would continue to grow and spread; in fact, some observations suggest that cancers can over-express either *β*III or *β*V (Hiser et al., 2006; Cucchiarelli et al., 2008; Leandro-García et al., 2010; Chao et al., 2012). One mitigating circumstance is that over-expression of *β*V does not seem to be so strongly associated with aggressiveness as is the case with *β*III (Christoph et al., 2012). On the other hand, over-expression of *β*V may be associated with increased resistance to taxanes (Işeri et al., 2010). A possible solution to this would be to have a second *αβ*II-CRISPR-Cas9 complex with a gRNA directed against *β*V. Alternatively, if more were understood about the drug-binding properties of *β*V, perhaps a *β*V-specific drug could be designed as a backup chemotherapeutic agent.

SUMMARY AND PROSPECTUS

The data presented here suggests very strongly that nuclear βII expression in and near cancer cells could be useful in the diagnosis and prognosis of cancer. It is also potentially possible that elucidating the pathway leading to over-expression of βII in cancer cells and its localization to the nuclei could lead to development of novel cancer treatments. It cannot be emphasized enough, however, that the concept of using an $\alpha\beta$II-CRISPR-Cas9 complex to treat cancer is entirely hypothetical. In addition to the potential problems outlined above, it is possible that an $\alpha\beta$II-CRISPR-Cas9 complex may be too large and unwieldy to enter a cancer cell, let alone do the job we hope for in the nucleus of that cell. However, it could not hurt to try and, if the arguments made above are borne out, such a complex could become a novel and useful treatment for cancer.

DATA AVAILABILITY STATEMENT

The original contributions presented in the study are included in the article/Supplementary Material, further inquiries can be directed to the corresponding author.

ETHICS STATEMENT

This study reviews data collected from previously published studies that were reviewed and approved by human subjects review boards at the University of Texas Health Science Center at San Antonio and the Belarusian Medical University. The patients/participants provided their written informed consent to participate in this study. This paper only reviews previously published work that was approved.

AUTHOR CONTRIBUTIONS

RL wrote the first draft of the manuscript, supervised many of the experiments, and proposed the connection with CRISPR. CW-B made the initial discovery of βII-tubulin in the nuclei of cultured cells. AP discovered the connection between cytosolic βII, nuclear βII and cancer survival, JG discovered he connection between βII and membrane rearrangements, and I-TY revealed the widespread presence of βII and nuclear βII in cancers. All authors contributed to manuscript revision, read, and approved the submitted version.

FUNDING

The research on which these findings were based was supported by NIH grants GM23476 and CA26376, Welch Foundation grant AQ-0726, US Army BCRP grant DAMD17-01-1-0411 and US Army PCRP grant DAMD17-01-1-0411 to RL, by NIH grant P30 CA54174 to I-TY, and by grant B-1636 from the International Science and Technology Center and grant 1.2.42 from the State Program of Scientific Investigation of Belarus to AP.

ACKNOWLEDGMENTS

The research on which these findings were based was supported by NIH grants GM23476 and CA26376, Welch Foundation grant AQ-0726, US Army BCRP grant DAMD17-01-1-0411 and US Army PCRP grant DAMD17-01-1-0411 to R.F.L., by NIH grant P30 CA54174 to I.T.Y., and by grant B-1636 from the International Science and Technology Center and grant 1.2.42 from the State Program of Scientific Investigation of Belarus to A.P. We thank Drs. Philip Serwer, John C. Lee and Borries Demeler for helpful discussions. RFL thanks Ken and Clara Korte for information about B-cell lymphoma.

REFERENCES

Bai, R. L., Lin, C. M., Nguyen Nga Yen, N. N., Liu, T. Y., and Hamel, E. (1989). Identification of the Cysteine Residue of .beta.-tubulin Alkylated by the Antimitotic Agent 2,4-dichlorobenzyl Thiocyanate, Facilitated by Separatio of the Protein Subunits of Tubulin by Hydrophobic Column Chromatography. *Biochemistry* 28, 5606–5612. doi:10.1021/bi00439a040

Banerjee, A., D'Hoore, A., and Engelborghs, Y. (1994). Interaction of Desacetamidocolchicine, a Fast Binding Analogue of Colchicine with Isotypically Pure Tubulin Dimers Alpha Beta II, Alpha Beta III, and Alpha Beta IV. *J. Biol. Chem.* 269, 10324–10329. doi:10.1016/s0021-9258(17)34064-4

Banerjee, A., Engelborghs, Y., D'hoore, A., and Fitzgerald, T. J. (1997). Interactions of a Bicyclic Analog of Colchicine with Beta-Tubulin Isoforms alphabetaII, alphabetaIII and alphabetaIV. *Eur. J. Biochem.* 246, 420–424. doi:10.1111/j.1432-1033.1997.00420.x

Bhattacharya, R., and Cabral, F. (2004). A Ubiquitous β-tubulin Disrupts Microtubule Assembly and Inhibits Cell Proliferation. *MBoC* 15, 3123–3131. doi:10.1091/mbc.e04-01-0060

Bhattacharya, R., and Cabral, F. (2009). Molecular Basis for Class V β-Tubulin Effects on Microtubule Assembly and Paclitaxel Resistance. *J. Biol. Chem.* 284, 13023–13032. doi:10.1074/jbc.M900167200

Borisy, G. G. (1972). A Rapid Method for Quantitative Determination of Microtubule Protein Using DEAE-Cellulose Filters. *Anal. Biochem.* 50, 373–385. doi:10.1016/0003-2697(72)90046-2

Burgoyne, R. D., Cambray-Deakin, M. A., Lewis, S. A., Sarkar, S., and Cowan, N. J. (1988). Differential Distribution of Beta-Tubulin Isotypes in Cerebellum. *EMBO J.* 7, 2311–2319. doi:10.1002/j.1460-2075.1988.tb03074.x

Chao, S. K., Wang, Y., Verdier-Pinard, P., Yang, C. P., Liu, L., Rodriguez-Gabin, A., et al. (2012). Characterization of a Human βV-tubulin Antibody and Expression of This Isotype in Normal and Malignant Human Tissue. *Cytoskelet. Hob.* 69, 566–576. doi:10.1002/cm.21043

Chatr-Aryamontri, A., Van der Sloot, A., and Tyers, M. (2018). At Long Last, a C-Terminal Bookend for the Ubiquitin Code. *Mol. Cell* 70, 568–571. doi:10.1016/j.molcel.2018.05.006

Christoph, D. C., Kasper, S., Gauler, T. C., Loesch, C., Engelhard, M., Theegarten, D., et al. (2012). Bv-Tubulin Expression Is Associated with Outcome Following Taxane-Based Chemotherapy in Non-small Cell Lung Cancer. *Br. J. Cancer* 107, 823–830. doi:10.1038/bjc.2012.324

Cucchiarelli, V., Hiser, L., Smith, H., Frankfurter, A., Spano, A., Correia, J. J., et al. (2008). β-tubulin Isotype Classes II and V Expression Patterns in Nonsmall Cell Lung Carcinomas. *Cell Motil. Cytoskelet.* 65, 675–685. doi:10.1002/cm.20297

Derry, W. B., Wilson, L., Khan, I. A., Ludueña, R. F., and Jordan, M. A. (1997). Taxol Differentially Modulates the Dynamics of Microtubules Assembled from

Unfractionated and Purified β-Tubulin Isotypes. *Biochemistry* 36, 3554–3562. doi:10.1021/bi962724m

Finn, J. D., Smith, A. R., Patel, M. C., Shaw, L., Youniss, M. R., Van Heteren, J., et al. (2018). A Single Administration of CRISPR/Cas9 Lipid Nanoparticles Achieves Robust and Persistent *In Vivo* Genome Editing. *Cell Rep.* 22, 2227–2235. doi:10.1016/j.celrep.2018.02.014

Gan, P. P., Pasquier, E., and Kavallaris, M. (2007). Class III β-Tubulin Mediates Sensitivity to Chemotherapeutic Drugs in Non-small Cell Lung Cancer. *Cancer Res.* 67, 9356–9363. doi:10.1158/0008-5472.CAN-07-0509

Gillmore, J. D., Gane, E., Taubel, J., Kao, J., Fontana, M., Maitland, M. L., et al. (2021). CRISPR-Cas9 *In Vivo* Gene Editing for Transthyretin Amyloidosis. *N. Engl. J. Med.* 385, 493–502. doi:10.1056/NEJMoa2107454

Guo, J., Kim, H. S., Asmis, R., and Ludueña, R. F. (2018). Interactions of β Tubulin Isotypes with Glutathione in Differentiated Neuroblastoma Cells Subject to Oxidative Stress. *Cytoskeleton* 75, 283–289. doi:10.1002/cm.21447

Guo, J., Qiang, M., and Ludueña, R. F. (2011). The Distribution of β-tubulin Isotypes in Cultured Neurons from Embryonic, Newborn, and Adult Mouse Brains. *Brain Res.* 1420, 8–18. doi:10.1016/j.brainres.2011.08.066

Guo, J., Walss-Bass, C., and Ludueña, R. F. (2010). The β Isotypes of Tubulin in Neuronal Differentiation. *Cytoskeleton* 67, 431–441. doi:10.1002/cm.20455

Hiser, L., Aggarwal, A., Young, R., Frankfurter, A., Spano, A., Correia, J. J., et al. (2006). Comparison of β-tubulin mRNA and Protein Levels in 12 Human Cancer Cell Lines. *Cell Motil. Cytoskelet.* 63, 41–52. doi:10.1002/cm.20109

Işeri, Ö. D., Kars, M. D., and Gunduz, U. (2010). Drug-resistant MCF-7 Cells Have Altered Expression Levels of β- Tubulin Isotypes and Mutations in TUBB Gene. *Int. J. Hematol. Oncol.* 20, 75–83. https://hdl.handle.net/11511/54102.

Jouhilahti, E.-M., Peltonen, S., and Peltonen, J. (2008). Class III β-Tubulin Is a Component of the Mitotic Spindle in Multiple Cell Types. *J. Histochem Cytochem.* 56, 1113–1119. doi:10.1369/jhc.2008.952002

Katsetos, C. D., Herman, M. M., and Mörk, S. J. (2003). Class III β-tubulin in Human Development and Cancer. *Cell Motil. Cytoskelet.* 55, 77–96. doi:10.1002/cm.10116

Khan, I. A., and Ludueña, R. F. (2003). Different Effects of Vinblastine on the Polymerization of Isotypically Purified Tubulins from Bovine Brain. *Investig. New Drugs* 21, 3–13. doi:10.1023/a:1022946305242

Komlodi-Pasztor, E., Sackett, D., Wilkerson, J., and Fojo, T. (2011). Mitosis Is Not a Key Target of Microtubule Agents in Patient Tumors. *Nat. Rev. Clin. Oncol.* 8, 244–250. doi:10.1038/nrclinonc.2010.228

Kourmouli, N., Dialynas, G., Petraki, C., Pyrpasopoulou, A., Singh, P. B., Georgatos, S. D., et al. (2001). Binding of Heterochromatin Protein 1 to the Nuclear Envelope Is Regulated by a Soluble Form of Tubulin. *J. Biol. Chem.* 276, 13007–13014. doi:10.1074/jbc.m007135200

Leandro-García, L. J., Leskelä, S., Landa, I., Montero-Conde, C., López-Jiménez, E., Letón, R., et al. (2010). Tumoral and Tissue-specific Expression of the Major Human β-tubulin Isotypes. *Cytoskeleton* 67, 214–223. doi:10.1002/cm.20436

Leibowitz, M. L., Papathanasiou, S., Doerfler, P. A., Blaine, L. J., Sun, L., Yao, Y., et al. (2021). Chromothripsis as an On-Target Consequence of CRISPR-Cas9 Genome Editing. *Nat. Genet.* 53, 895–905. doi:10.1038/s41588-021-00838-7

Lewis, S. A., and Cowan, N. J. (1988). Complex Regulation and Functional Versatility of Mammalian Alpha- and Beta-Tubulin Isotypes during the Differentiation of Testis and Muscle Cells. *J. Cell Biol.* 106, 2023–2033. doi:10.1083/jcb.106.6.2023

Li, L., Mi, D., Pei, H., Duan, Q., Wang, X., Zhou, W., et al. (2020). *In Vivo* target Protein Degradation Induced by PROTACs Based on E3 Ligase DCAF15. *Signal Transduct. Target Ther.* 5, 129. doi:10.1038/s41392-020-00245-0

Little, M., and Ludueña, R. F. (1985). Structural Differences between Brain Beta 1- and Beta 2-tubulins: Implications for Microtubule Assembly and Colchicine Binding. *EMBO J.* 4, 51–56. doi:10.1002/j.1460-2075.1985.tb02316.x

Lopata, M. A., and Cleveland, D. W. (1987). *In Vivo* microtubules Are Copolymers of Available Beta-Tubulin Isotypes: Localization of Each of Six Vertebrate Beta-Tubulin Isotypes Using Polyclonal Antibodies Elicited by Synthetic Peptide Antigens. *J. Cell Biol.* 105, 1707–1720. doi:10.1083/jcb.105.4.1707

Ludueña, R. F. (2013). A Hypothesis on the Origin and Evolution of Tubulin. *Int. Rev. Cell Mol. Biol.* 302, 41–185. doi:10.1016/B978-0-12-407699-0.00002-9

Ludueña, R. F., and Roach, M. C. (1991). Tubulin Sulfhydryl Groups as Probes and Targets for Antimitotic and Antimicrotubule Agents. *Pharmacol. Ther.* 49, 133–152. doi:10.1016/0163-7258(91)90027-j

Ludueña, R. F., Shooter, E. M., and Wilson, L. (1977). Structure of the Tubulin Dimer. *J. Biol. Chem.* 252, 7006–7014. doi:10.1016/S0021-9258(19)66927-9

Markman, M. (2003). Managing Taxane Toxicities. *Support Care Cancer* 11, 144–147. doi:10.1007/s00520-002-0405-9

Mitchison, T. J. (2012). The Proliferation Rate Paradox in Antimitotic Chemotherapy. *MBoC* 23, 1–6. doi:10.1091/mbc.E10-04-0335

Mozzetti, S., Ferlini, C., Concolino, P., Filippetti, F., Raspaglio, G., Prislei, S., et al. (2005). Class III Beta-Tubulin Overexpression Is a Prominent Mechanism of Paclitaxel Resistance in Ovarian Cancer Patients. *Clin. Cancer Res.* 11, 298–305.

Mukhtar, E., Adhami, V. M., and Mukhtar, H. (2014). Targeting Microtubules by Natural Agents for Cancer Therapy. *Mol. Cancer Ther.* 13, 275–284. doi:10.1158/1535-7163.MCT-13-0791

Murphy, D. B., and Wallis, K. T. (1983). Brain and Erythrocyte Microtubules from Chicken Contain Different Beta-Tubulin Polypeptides. *J. Biol. Chem.* 258, 7870–7875. doi:10.1016/s0021-9258(18)32259-2

Nakamura, M., Tsutsumi, K., Ooka, S., Sekine, T., Koizuka, I., Nishioka, K., et al. (2004). Identification of β-Tubulin Isoform V as an Autoantigen in Allergic Rhinitis by a Proteomic Approach. *Microbiol. Immunol.* 48, 427–434. doi:10.1111/j.1348-0421.2004.tb03532.x

Naso, M. F., Tomkowicz, B., Perry, W. L., and Strohl, W. R. (2017). Adeno-associated Virus (AAV) as a Vector for Gene Therapy. *BioDrugs* 31, 317–334. doi:10.1007/s40259-017-0234-5

Palanivelu, P., and Ludueña, R. F. (1982). Interactions of the Tau-Tubulin-Vinblastine Complex with Colchicine, Podophyllotoxin, and N,N'-ethylenebis(iodoacetamide). *J. Biol. Chem.* 257, 6311–6315. doi:10.1016/s0021-9258(20)65141-9

Pallante, L., Rocca, A., Klejborowska, G., Huczynski, A., Grasso, G., Tuszynski, J. A., et al. (2020). In Silico Investigations of the Mode of Action of Novel Colchicine Derivatives Targeting β-Tubulin Isotypes: A Search for a Selective and Specific β-III Tubulin Ligand. *Front. Chem.* 8, 108. doi:10.3389/fchem.2020.00108

Panda, D., Miller, H. P., Banerjee, A., Ludueña, R. F., and Wilson, L. (1994). Microtubule Dynamics *In Vitro* Are Regulated by the Tubulin Isotype Composition. *Proc. Natl. Acad. Sci. U.S.A.* 91, 11358–11362. doi:10.1073/pnas.91.24.11358

Pavlasova, G., and Mraz, M. (2020). The Regulation and Function of CD20: an "enigma" of B-Cell Biology and Targeted Therapy. *Haematologica* 105, 1494–1506. doi:10.3324/haematol.2019.243543

Roach, M. C., Boucher, V. L., Walss, C., Ravdin, P. M., and Ludueña, R. F. (1998). Preparation of a Monoclonal Antibody Specific for the Class I Isotype of β-tubulin: The β Isotypes of Tubulin Differ in Their Cellular Distributions within Human Tissues. *Cell Motil. Cytoskelet.* 39, 273–285. doi:10.1002/(sici)1097-0169(1998)39:4<273::aid-cm3>3.0.co;2-4

Ruksha, K., Mezheyeuski, A., Nerovnya, A., Bich, T., Tur, G., Gorgun, J., et al. (2019). Over-Expression of βII-Tubulin and Especially its Localization in Cell Nuclei Correlates with Poorer Outcomes in Colorectal Cancer. *Cells* 8 (1), 25. doi:10.3390/cells8010025

Saini, K. S., Azim, H. A., Cocorocchio, E., Vanazzi, A., Saini, M. L., Raviele, P. R., et al. (2011). Rituximab in Hodgkin Lymphoma: Is the Target Always a Hit? *Cancer Treat. Rev.* 37, 385–390. doi:10.1016/j.ctrv.2010.11.005

Schwarz, P. M., Liggins, J. R., and Ludueña, R. F. (1998). β-Tubulin Isotypes Purified from Bovine Brain Have Different Relative Stabilities. *Biochemistry* 37, 4687–4692. doi:10.1021/bi972763d

Sharma, J., and Ludueña, R. F. (1994). Use ofN,N′-polymethylenebis(iodoacetamide) Derivatives as Probes for the Detection of Conformational Differences in Tubulin Isotypes. *J. Protein Chem.* 13, 165–176. doi:10.1007/BF01891975

Smiyun, G., Azarenko, O., Miller, H., Rifkind, A., Lapointe, N. E., Wilson, L., et al. (2017). βIII-Tubulin Enhances Efficacy of Cabazitaxel as Compared with Docetaxel. *Cancer Chemother. Pharmacol.* 80, 151–164. doi:10.1007/s00280-017-3345-2

Varshavsky, A. (1996). The N-End Rule: Functions, Mysteries, Uses. *Proc. Natl. Acad. Sci. U.S.A.* 93, 12142–12149. doi:10.1073/pnas.93.22.12142

Vemu, A., Atherton, J., Spector, J. O., Szyk, A., Moores, C. A., and Roll-Mecak, A. (2016). Structure and Dynamics of Single-Isoform Recombinant Neuronal Human Tubulin. *J. Biol. Chem.* 291, 12907–12915. doi:10.1074/jbc.C116.731133

Wallis, C. J. D., Klaassen, Z., Jackson, W. C., Dess, R. T., Reichert, Z. R., Sun, Y., et al. (2021). Olaparib vs Cabazitaxel in Metastatic Castration-Resistant Prostate Cancer. *JAMA Netw. Open* 4 (5), e2110950. doi:10.1001/jamanetworkopen.2021.10950

Walss, C., Kreisberg, J. I., and Luduena, R. F. (1999). Presence of the ?II Isotype of Tubulin in the Nuclei of Cultured Mesangial Cells from Rat Kidney. *Cell Motil. Cytoskelet.* 42, 274–284. doi:10.1002/(sici)1097-0169(1999)42:4<274::aid-cm2>3.0.co;2-5

Walss-Bass, C., Kreisberg, J. I., and Ludueña, R. F. (2003). Effect of the Antitumor Drug Vinblastine on Nuclear betaII-Tubulin in Cultured Rat Kidney Mesangial Cells. *Invest. New Drugs* 21, 15–20. doi:10.1023/a:1022947706151

Walss-Bass, C., Kreisberg, J. I., and Ludueña, R. F. (2001). Mechanism of Localization of βII-tubulin in the Nuclei of Cultured Rat Kidney Mesangial Cells. *Cell Motil. Cytoskelet.* 49, 208–217. doi:10.1002/cm.1034

Wang, D., Villasante, A., Lewis, S. A., and Cowan, N. J. (1986). The Mammalian Beta-Tubulin Repertoire: Hematopoietic Expression of a Novel, Heterologous Beta-Tubulin Isotype. *J. Cell Biol.* 103, 1903–1910. doi:10.1083/jcb.103.5.1903

Wilson, L. (1970). Properties of Colchicine Binding Protein from Chick Embryo Brain. Interactions with Vinca Alkaloids and Podophyllotoxin. *Biochemistry* 9, 4999–5007. doi:10.1021/bi00827a026

Xu, K., and Ludueña, R. F. (2002). Characterization of Nuclear βII-tubulin in Tumor Cells: A Possible Novel Target for Taxol. *Cell Motil. Cytoskelet.* 53, 39–52. doi:10.1002/cm.10060

Yeh, I.-T., and Ludueña, R. F. (2004). The βIIisotype of Tubulin Is Present in the Cell Nuclei of a Variety of Cancers. *Cell Motil. Cytoskelet.* 57, 96–106. doi:10.1002/cm.10157

Yeh, L.-C. C., Banerjee, A., Prasad, V., Tuszynski, J. A., Weis, A. L., Bakos, T., et al. (2016). Effect of CH-35, a Novel Anti-tumor Colchicine Analogue, on Breast Cancer Cells Overexpressing the βIII Isotype of Tubulin. *Invest New Drugs* 34, 129–137. doi:10.1007/s10637-015-0315-6

Conflict of Interest: JG was employed by the company Fosun Pharma.

The remaining authors declare that the research was conducted in the absence of any commercial or financial relationships that could be construed as a potential conflict of interest.

Publisher's Note: All claims expressed in this article are solely those of the authors and do not necessarily represent those of their affiliated organizations, or those of the publisher, the editors and the reviewers. Any product that may be evaluated in this article, or claim that may be made by its manufacturer, is not guaranteed or endorsed by the publisher.

frontiers | Frontiers in Cell and Developmental Biology

ORIGINAL RESEARCH
published: 31 May 2022
doi: 10.3389/fcell.2022.884287

Interaction of Colchicine-Site Ligands With the Blood Cell-Specific Isotype of β-Tubulin—Notable Affinity for Benzimidazoles

Felipe Montecinos[1‡], *Maura Loew*[2†‡], *Tak I. Chio*[2†], *Susan L. Bane*[2*] *and Dan L. Sackett*[1*]

[1]Division of Basic and Translational Biophysics, Eunice Kennedy Shriver National Institute of Child Health and Human Development, National Institutes of Health, Bethesda, MD, United States, [2]Department of Chemistry, Binghamton University, State University of New York, Binghamton, NY, United States

OPEN ACCESS

Edited by:
Jeffrey Moore,
University of Colorado Anschutz Medical Campus, United States

Reviewed by:
Jack Adam Tuszynski,
University of Alberta, Canada
Stanley Nithianantham,
St. Jude Children's Research Hospital, United States

***Correspondence:**
Susan L. Bane
sbane@binghamton.edu
Dan L. Sackett
sackettd@mail.nih.gov

†Present addresses:
Maura Loew,
Agilift LLC, Havertown, PA, United States
Tak I. Chio,
Department of Pathology and Laboratory Medicine, Center for Neurodegenerative Disease Research, University of Pennsylvania School of Medicine, Philadelphia, PA, United States

‡These authors have contributed equally to his work

Specialty section:
This article was submitted to Cellular Biochemistry, a section of the journal Frontiers in Cell and Developmental Biology

Received: 26 February 2022
Accepted: 02 May 2022
Published: 31 May 2022

Citation:
Montecinos F, Loew M, Chio TI, Bane SL and Sackett DL (2022) Interaction of Colchicine-Site Ligands With the Blood Cell-Specific Isotype of β-Tubulin—Notable Affinity for Benzimidazoles. Front. Cell Dev. Biol. 10:884287. doi: 10.3389/fcell.2022.884287

Tubulin, the main component of microtubules, is an α-β heterodimer that contains one of multiple isotypes of each monomer. Although the isotypes of each monomer are very similar, the beta tubulin isotype found in blood cells is significantly divergent in amino acid sequence compared to other beta tubulins. This isotype, beta class VI, coded by human gene TUBB1, is found in hematologic cells and is recognized as playing a role in platelet biogenesis and function. Tubulin from the erythrocytes of the chicken *Gallus gallus* contains almost exclusively βVI tubulin. This form of tubulin has been reported to differ from brain tubulin in binding of colchicine-site ligands, previously thought to be a ubiquitous characteristic of tubulin from higher eukaryotes. In this study, we sought to gain a better understanding of the structure-activity relationship of the colchicine site of this divergent isotype, using chicken erythrocyte tubulin (CeTb) as the model. We developed a fluorescence-based assay to detect binding of drugs to the colchicine site and used it to study the interaction of 53 colchicine-site ligands with CeTb. Among the ligands known to bind at this site, most colchicine derivatives had lower affinity for CeTb compared to brain tubulin. Remarkably, many of the benzimidazole class of ligands shows increased affinity for CeTb compared to brain tubulin. Because the colchicine site of human βVI tubulin is very similar to that of chicken βVI tubulin, these results may have relevance to the effect of anti-cancer agents on hematologic tissues in humans.

Keywords: tubulin isotypes, beta tubulin, erythrocytes, colchicine, benzimidazoles, repurposing drugs

1 INTRODUCTION

Microtubules (MT) are subcellular structures whose arrays provide cells with structural rigidity, polarity, and mechanisms of intracellular transport. As such, they are central players in cell division, shape maintenance and changes, differentiation, and motility. Because of these multiple roles, MT have been targets of a large variety of therapeutic agents, binding to a number of known binding sites on the MT subunit protein, tubulin (Steinmetz and Prota, 2018).

Tubulin is a heterodimer composed of a non-covalent association of one alpha- and one beta-monomer. Multiple forms of each monomer exist in many species (such as humans), coded by multiple genes that produce very similar but non-identical proteins (isotypes) that are expressed in different levels in different tissues, and at different stages in development. Most MT-targeting ligands

bind to sites on beta-tubulin, which have been considered to be largely the same in different isotypes. Therefore, measurements of protein drug binding (of colchicine, for example) has long been taken to be equivalent to measurements of active tubulin. However, some differences in the drug-binding properties of the β isotypes have been noted (Banerjee and Luduena, 1992).

The most divergent β tubulin isotype is known as β1, class VI (human protein is Q9H4B7), coded by the gene TUBB1, and has been studied less than other isotypes. We will refer to this as βVI tubulin, and is found in erythrocytes (Leandro-García et al., 2012), platelets (Feierbach et al., 1999), megakaryocytes (Lecine et al., 2000), as well as other sites such as brain and nasal epithelium (Palasca et al., 2018; Hausrat et al., 2021). Mice deficient in βVI have reduced levels of platelets, and the platelets they do have lack the characteristic discoid shape (Schwer et al., 2001; Italiano et al., 2003). Humans with mutations or deficits in TUBB1 reveal clotting disturbances and other disorders (Stoupa et al., 2018).

Nonmammalian red blood cells (RBCs), as well as immature mammalian RBCs such as human erythroblasts (Dmitrieff et al., 2017) contain a peripheral ring of MT that acts to maintain the ellipsoidal shape of the cells. Chicken (*Gallus gallus*) RBCs represent a readily available source of these MT, assembled from tubulin heterodimers that contain almost exclusively chicken βVI tubulin (P09207), coded by gene TUBB1 (NM_205445.2). We will refer to this (Chicken erythrocyte

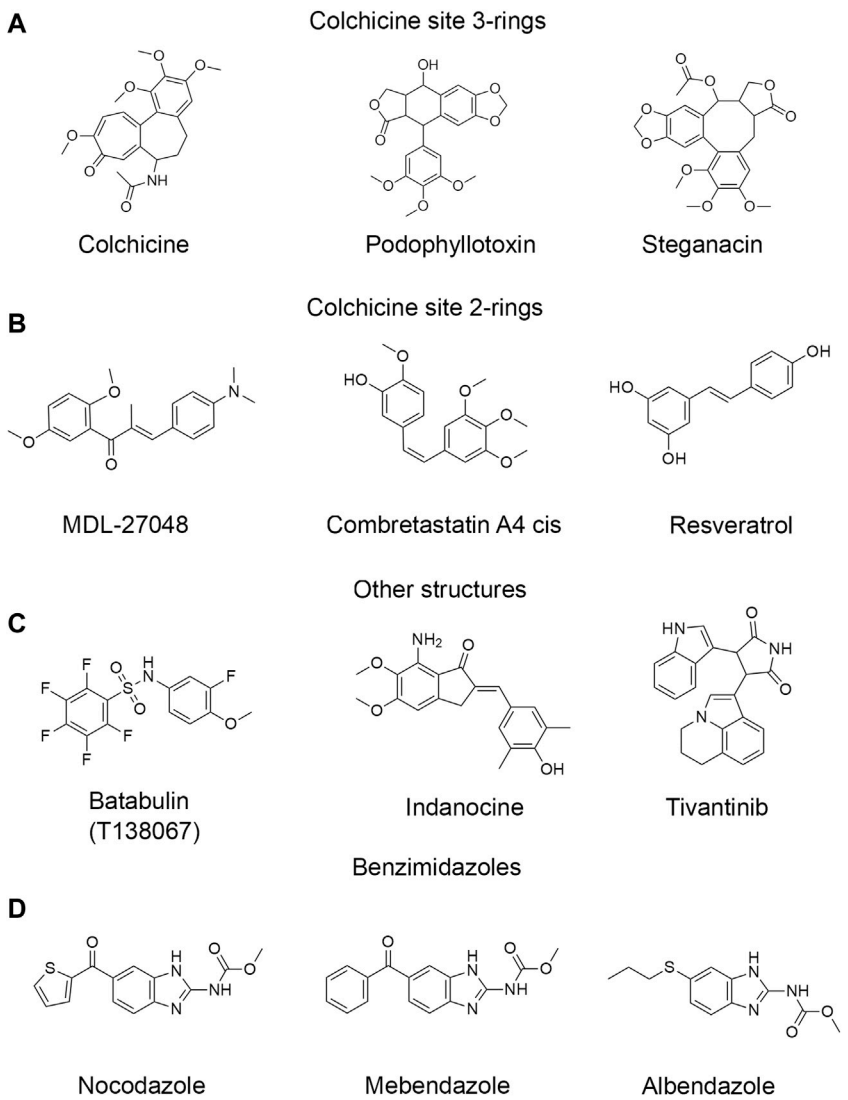

FIGURE 1 | Structures of representative colchicine site drugs used in this work. **(A)** colchicine site 3-ring drugs: colchicine, podophyllotoxin and steganacin. **(B)** colchicine site 2-ring drugs: MDL, combretastatin A4 cis, resveratrol. **(C)** drugs with other non-colchicine structures: tubulazole C, indanocine, tivantinib. **(D)** benzimidazole drugs: nocodazole, carbendazim, oxibendazole. Full list of drugs structures is found in **Supplementary Figures S1–S4**.

Tubulin) as CeTb. Previous studies with this tubulin have reported some differences from brain tubulin in binding of ligands, for example to the colchicine site (Sharma et al., 2010).

In this work, we compared binding affinities of mammalian brain tubulins (BTb) and CeTb for 53 different ligands reported to bind at the colchicine site of tubulin, using a fluorescence-based competition assay. We use the term "BTb" for mammalian brain tubulins, typically from bovine or rat brain. When we specifically compare different brain tubulins we will specify the organism: rat brain tubulin—RBTb, or bovine brain tubulin—BBTb, or chicken brain tubulin—CBTb. The compounds selected for this survey (**Figure 1** and **Supplementary Figures S1–S4**) include close colchicine analogs, as well as compounds whose structures bear no obvious relation to that of colchicine, but have been reported to bind to the colchicine site. Notable in this group are the benzimidazoles, whose extensive history as antihelmintic drugs in veterinary and human contexts have led to recent studies of repurposing for treatment of human cancers (Son et al., 2020).

2 MATERIALS AND METHODS

2.1 Protein Purification

Rat brain tubulin was purified from microtubule protein previously extracted from frozen rat brains, as described previously (Sackett et al., 1991; Montecinos-Franjola et al., 2019). Tubulin from chicken brain and from chicken red blood cells was purified from frozen whole brains and from washed red blood cells (#33131-1, Pel-Freez Biologicals, Rogers, AZ) (https://www.pelfreez-bio.com/products/animal-serum-plasma-complement-and-ancillary-products/whole-blood-and-red-blood-cells/), respectively, as described previously (Sackett, 1995; Montecinos-Franjola et al., 2019). Bovine brain tubulin protein was from Cytoskeleton, Inc., Boulder, CO (#HTS02-A) or from Sigma-Aldrich, St. Louis, MO (#T4925). Purified proteins were stored in PM buffer (0.1M Pipes-KOH, pH 7.0, 1 mM $MgCl_2$) at −80°C. The estimation of protein concentration was made using the Bradford assay (Bio-Rad) with BSA as the calibration standard (#23209, ThermoFisher Scientific, Waltham, MA).

2.2 Chemicals

MDL-(E)-1-(2,5-dimethoxyphenyl)-3-[4-(dimethylamino) phenyl]-2-methylprop-2-en-1-one (MDL) was not commercially available and therefore was synthesized according to the literature (Ducki et al., 1998) with the following minor modifications. In the second step, the oxidation of 1-(2,5-dimethoxyphenyl)-1-propanol using pyridinium dichromate, one equivalent of acetic anhydride was used per equivalent of starting material. The product from this reaction was stirred in diethyl ether with 2 g of Florisil per mmol of starting material and then filtered to remove excess pyridinium dichromate. The structure of the product was confirmed by 1H NMR. An extinction coefficient was measured in DMSO ($\varepsilon_{385\ nm} = 2.69 \times 10^4\ M^{-1}cm^{-1}$).

Drugs and test compounds were obtained from multiple sources listed in **Supplementary Table S1**. Concentrated stock solutions were prepared in water, in PM buffer or in DMSO as indicated in the same table, and stored at −20°C. The concentration was determined spectrophotometrically for those compounds with known extinction coefficients.

2.3 Polymerization Kinetics

Tubulin was polymerized at a concentration of 2 μM in PM buffer (0.1 M Pipes pH 7, 1 mM $MgCl_2$) + 0.1 mM GTP in a volume of 60 μL. The reaction mixture was transferred to a 10-mm pathlength microcuvette (Hellma United States Inc., Plainview, NY) and placed in the cuvette holder of a SpectraMax M2 Multimode Microplate Reader (Molecular Devices, San Jose, CA) equipped with temperature control set at 37°C for these experiments. Drugs at 20 μM were added directly to the polymerization mixture and incubated for 15 min previous to starting the recordings. Tubulin polymerization kinetics was followed by recording the absorbance at 350 nm. After recording the baseline, tubulin polymerization was induced by the addition of 2 μM paclitaxel (taxol). The final concentration of DMSO in the mixtures was 4%–5% v/v.

2.4 Fluorescence Measurements

The fluorescence emission of MDL was recorded at 550 nm in the SpectraMax M2 Multimode Microplate Reader with excitation at 400 nm. Tubulin samples at 1 μM were prepared in PM buffer in 60 μL volume, incubated for 30 min, and then transferred to a 10-mm pathlength microcuvette which later was placed in the cuvette holder of the SpectraMax M2 set at 25°C. The kinetics of MDL binding and its displacement by competitor drugs was detected by recording the fluorescence emission at 550 nm every 5 s. MDL was used at 10 μM and podophyllotoxin at 100 μM. For fluorescence spectra recordings, the drugs were added at 50 μM final prior to addition of MDL and the DMSO was adjusted to 5% v/v.

2.5 Determination of Dissociation Constants and Competition Experiments

The equilibrium dissociation constants for the binding of MDL to tubulin were determined from the concentration-dependent changes in the fluorescence emission at 550 nm upon serial dilution of the MDL. The starting mix contained 1 μM tubulin and 10 μM MDL all in PM buffer (starting mix). The dilution mix contained 1 μM tubulin in PM buffer and was prepared in a larger volume (dilution mix). The concentration of DMSO was adjusted to 5% v/v in both cases. The dilution series was prepared by mixing the "starting mix" and the "dilution mix" at a 1:3 ratio resulting in a decrease of the MDL concentration to 1/3 of the original, or 3.3 μM, while keeping the tubulin concentration constant at 1 μM. This new sample was then mixed at 1:3 ratio with the "dilution mix" for obtaining the next sample in the dilution series at 1.1 μM MDL. Subsequent samples in the dilution series were prepared in the same fashion until reaching a low concentration <1 nM MDL. Next, 60 μL of the dilution series were transferred to a 96-well black half-area flat bottom fluorescence microplates (#3642 Corning, NY) including the blanks. The loaded plates were incubated for at least 30 min

and then placed in the SpectraMax M2 Multimode Microplate Reader for recording the fluorescence signals with temperature control set at 25°C.

For competition experiments with colchicine-site drugs, the samples were prepared in a similar fashion with some changes. For full dilution series experiments (e.g., podophyllotoxin and benzimidazoles), the starting mix contained 1 μM tubulin and 5 μM MDL all in PM buffer (starting mix). The dilution mix contained 1 μM tubulin, 5 μM MDL and 100 μM drugs, all in PM buffer, and was prepared in a larger volume (dilution mix). The concentration of DMSO was adjusted to 8% v/v in both cases to promote the solubility of the ligands. The dilution series was prepared by mixing equal amounts (1:1) of each mix resulting in a 50% decrease of the initial drug concentration at each step of the dilutions series, while keeping constant the concentrations of tubulin at 1 μM and of MDL at 5 μM. For the single concentration drug screening experiments, the samples contained 1 μM tubulin (unless otherwise specified), 5 μM MDL and the drugs were added at a final concentration of 50 μM directly to the mixtures. Next, 60 μL of the samples were transferred to 96-well microplates. For competition experiments, the loaded plates were incubated for at least 1 h due to the slower kinetics observed for MDL release from the colchicine binding site after addition of the competing drugs. The MDL fluorescence was recorded in the SpectraMax M2 Mulitmode Microplate Reader with temperature control set at 25°C.

2.6 Data Analysis

The dissociation constant for the MDL-tubulin interaction was determined by fluorescence intensity measurements as previously described for MDL and other colchicine binding-site drugs (Peyrot et al., 1992; Sharma et al., 2010). The raw fluorescence signal was blank-subtracted and plotted as a function of the drug concentration. The data was analyzed by non-linear regression using the following one-component binding model that relates the fluorescence intensity observed (I_{obs}) with the apparent equilibrium dissociation constant $K_{d,MDL}$ as:

$$K_{d,MDL} = \frac{[Tub] \cdot [MDL]}{[Tub - MDL]} \quad (1)$$

$$I_{obs} = \frac{I_{free} + \left(\frac{[MDL]}{K_{d,MDL}} \cdot I_{bound}\right)}{1 + \frac{[MDL]}{K_{d,MDL}}} \quad (2)$$

Where (Tub) and (MDL) are the concentrations of free tubulin and MDL at equilibrium, I_{free} and I_{bound} are fluorescence signals of the free MDL in solution and of MDL bound to tubulin under saturating concentrations, respectively. Weights were assigned to each data point based on the reciprocal of the standard deviation of each data point (averages of three to four measurements). For comparing plots of the various tubulins, or the different drugs, the data was converted to fraction bound with the following relationship:

$$f_b = \frac{I_{obs} - I_{free}}{I_{bound} - I_{free}} \quad (3)$$

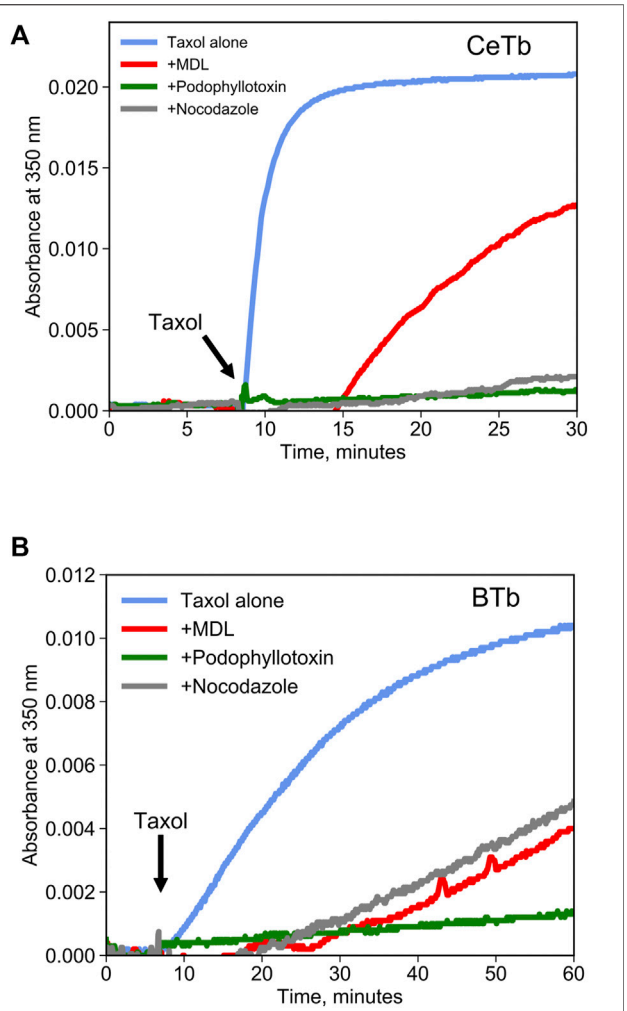

FIGURE 2 | Inhibition of tubulin polymerization by colchicine-site drugs. Tubulin from brain **(A)** or from erythrocytes **(B)** was incubated at 2 μM in polymerization buffer at 37°C, and the absorbance at 350 nm was registered for 10 min prior to starting the polymerization by the addition of taxol 2 μM (arrow). Drugs were included in polymerization buffer and used at a concentration of 20 μM.

TABLE 1 | Inhibition of tubulin taxol-induced polymerization by colchicine-site drugs.

Drug	Brain tubulin (BTb) % inhibition at 60 min	Erythrocyte tubulin (CeTb) % inhibition at 30 min
Taxol (control)	0	0
MDL	64	38
Podophyllotoxin	90	95
Nocodazole	55	90
Mebendazole	92	25

Polymerization in presence of taxol alone was considered the 100%. Tubulin was used at 2 μM, Taxol at 2 μM and drugs were used at 20 μM in polymerization buffer at 30°C.

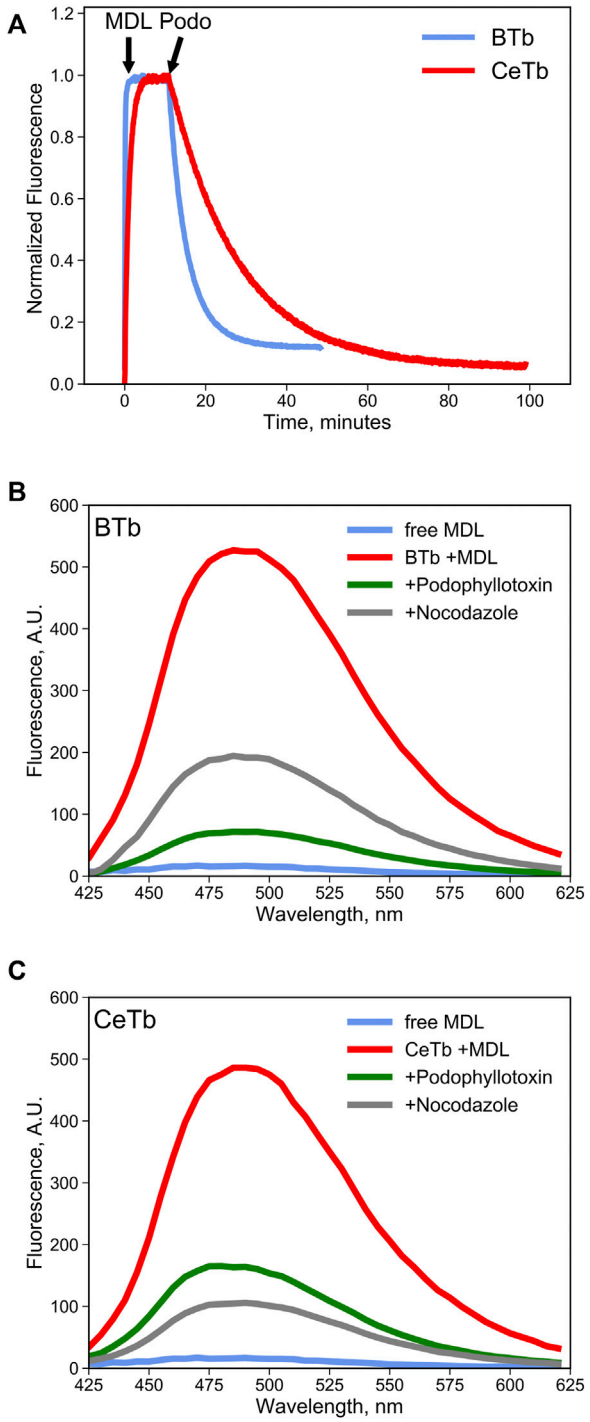

FIGURE 3 | MDL binding to tubulin and competition by colchicine-site drugs. **(A)** the fluorescence enhancement of MDL upon binding to tubulin was used to follow the kinetics of the interaction. Fluorescence was recorded at 550 nm every 5 s with excitation at 400 nm. Tubulin 1 μM was incubated in PM buffer at room temperature for at least 30 min prior to addition of the drugs at the indicated times (arrows). MDL was used at 10 μM and podophyllotoxin at 100 μM. **(B,C)** fluorescence emission spectra of free MDL in solution or bound to brain **(B)** tubulin or to erythrocyte **(C)** tubulin in PM buffer at 25°C. Colchicine-site drugs were added at 50 μM final concentration

(*Continued*)

FIGURE 3 | in PM buffer prior to addition of 10 μM MDL. The decrease in MDL fluorescence is evidence the competitive binding by the selected drugs that displaces the fluorescent molecule from the colchicine site in tubulin.

In the competition experiments, for instance with podophyllotoxin, the value of IC_{50} was determined graphically from plots of f_b vs. (podophyllotoxin) and the value of the apparent dissociation constant, $K_{d,podo}$ was calculated with the following equation (Yung-Chi and Prusoff, 1973; Craig, 1993):

$$K_{d,podo} = \frac{IC_{50}}{1 + \frac{[MDL]}{K_{d,MDL}}} \quad (4)$$

For single point competition experiments, the F/F_{max} ratios were calculated from the fluorescence intensity values recorded in the presence of the competitor drug, F, and the fluorescence intensity of MDL in the absence of competitor, F_{max}. The percentage inhibition was calculated from the F/Fmax ratios:

$$\%_{inhibition} = \left(1 - \frac{F}{F_{max}}\right) \times 100 \quad (5)$$

All of the competition titrations yielded curves consistent with simple single-site binding, and therefore we make the assumption that all of the tested compounds do as well. With this assumption, single point data (50 μM test compound) was fit with a single-site binding isotherm by non-linear regression. Then the mid-point of that curve ($IC_{50\%}$) was used to calculate the $K_{d(app)}$ using **Eq. 4**, as above. The curve-fitting procedure did not converge for % inhibition below 1%, therefore the apparent dissociation constant could not be determined in those cases (nd). For further details and examples, see **Supplementary Material**.

3 RESULTS

3.1 Interaction of a Fluorescent Probe With CeTb

Competition binding assays are often used as a method to quantify binding to a target protein. Such assays can be performed using a tritiated ligand that is known to bind to the target, but spectroscopic methods are more convenient. Colchicine is often used for competition binding studies on tubulin, but it does not bind well to CeTb so it cannot be used for the purposes of this study. Another molecule that is a candidate for a competition binding assay is known in the literature as MDL-27048 (**Figure 1**). The fluorescence of MDL-27048 (hereafter referred to as MDL) is very weak when free in solution and greatly enhanced upon binding to the colchicine site of mammalian brain tubulin (BTb) (Peyrot et al., 1992). However, it was unknown whether MDL would interact with CeTb. Colchicine-site drugs inhibit the polymerization of purified tubulin into microtubules. In assays using tubulin from mammalian brain, MDL has been found to inhibit polymerization (Peyrot et al., 1989). Therefore, we

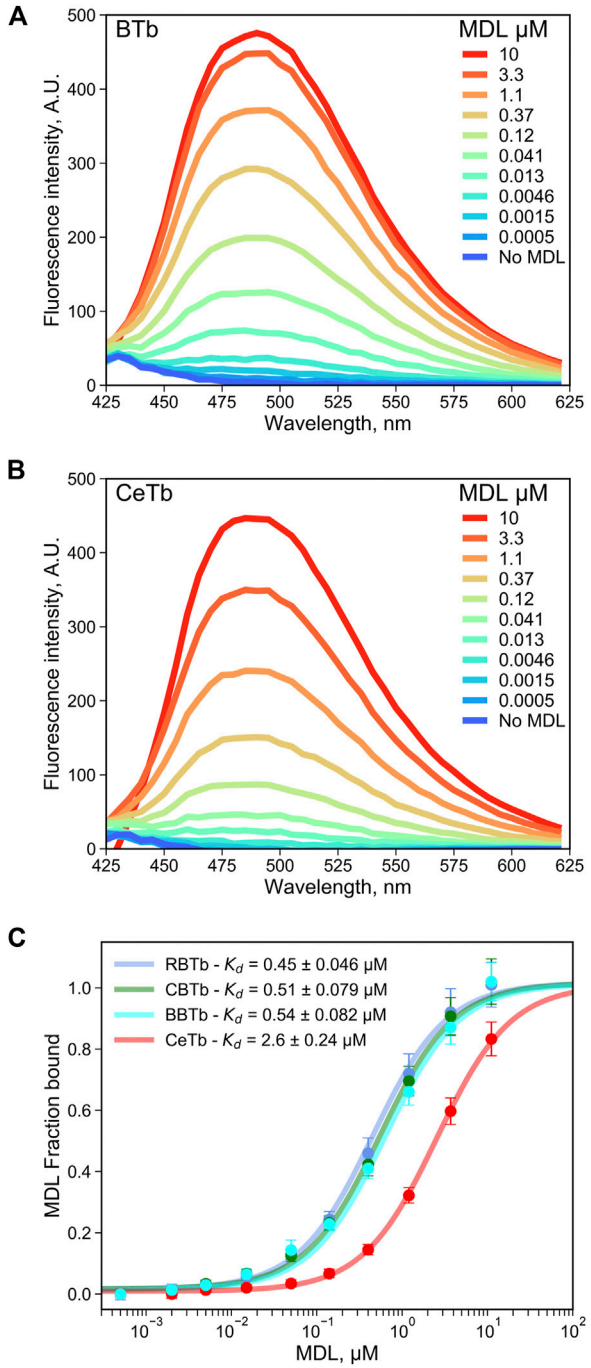

FIGURE 4 | Determination of the dissociation constant for tubulin—MDL interaction. The fluorescence enhancement of MDL upon binding to tubulin from brain **(A)** or from erythrocytes **(B)**, both at 1 μM, was monitored by recording the fluorescence emission spectra with excitation at 400 nm. **(C)** the MDL concentration-dependent change in the fluorescence intensity at 550 nm was used to determine the dissociation constant by non-linear regression using **Eq. 1**. The binding isotherms of tubulin extracted from chicken erythrocytes (CeTb) is compared with tubulin extracted from rat brain (RBTb), from chicken brain (CBTb and from cow brain (bovine, BBTb). The data points are the averages of three to four samples and the error bars are standard deviations. The best-fit K_d are shown with the standard errors of the fits.

TABLE 2 | Apparent dissociation constants for the Tubulin—MDL interaction measured by dilution experiments.

Tubulin source	$K_{d,MDL}$, μM
Chicken brain (CBTb)	0.51 ± 0.079
Rat brain (RBTb)	0.45 ± 0.046
Bovine brain (BBTb)	0.54 ± 0.082
Chicken Erythrocytes (CeTb)	2.6 ± 0.24

*Uncertainties are the standard errors of the fits from **Figure 4**.*

polymerized CeTb in the presence of MDL to look for inhibition. We found that MDL does inhibit the polymerization of CeTb (**Figure 2**; quantitation is in **Table 1**), indicating that it does interact with CeTb.

It is reasonable to suppose that MDL binds to the colchicine site on CeTb, as it does to BTb, resulting in inhibition of polymerization of both tubulins. To be useful in a competition binding assay, it must also exhibit a spectroscopic change upon binding. We therefore looked for a change in the fluorescence of MDL in the presence of tubulin, including CeTb. The emission spectrum showed a large enhancement of fluorescence upon binding to CeTb, as well as to BTb (**Figure 3**). Fluorescence intensity increases rapidly upon addition of MDL to BTb or CeTb, and is then displaced by addition of 10-fold excess of the colchicine site ligand podophyllotoxin (structure in **Figure 1**). Displacement kinetics differ between BTb and CeTb, indicating a slower off-rate for MDL from CeTb compared to BTb. Addition of the benzimidazole nocodazole also displaces MDL, confirming the usefulness of this assay for binding of diverse compounds.

This emission enhancement allowed us to determine the binding affinity of MDL for CeTb, compared to brain tubulin from chicken brain (CBTb), rat brain (RBTb), and bovine brain (BBTb) (**Figures 4A,B**). Tubulins were titrated with MDL, and the concentration dependence of the emission signal was used to determine the affinity. The resulting binding isotherms are shown in **Figure 4C** and the fitted K_d values for binding are presented in **Figure 4C** and **Table 2**. It is notable that all the brain tubulins, including CBTb, yield very similar Kd for MDL binding to the protein, while MDL binding to CeTb shows affinity ~5–fold weaker than to brain tubulins.

As a test of utility of MDL in a competition assay for ligand binding to the colchicine site, the binding of the reversible colchicine site ligand podophyllotoxin was chosen. It was shown in **Figure 2** that excess podophyllotoxin could displace MDL from both BTb and CeTb, so we used titration of tubulin-MDL with increasing concentrations of podophyllotoxin to measure displacement by loss of fluorescence intensity. The resulting data for BTb and for CeTb are shown in **Figures 5A,B**, respectively. Displacement as a function of podophyllotoxin concentration is shown in **Figure 5C**, and the derived K_d for binding of podophyllotoxin to BTb and to CeTb (calculated as described in Materials and Methods) are given in the inset to **Figure 5C** and in **Table 3**. The K_d for podophyllotoxin binding to BTb was found to be ~0.5 μM, essentially the same as the literature value of 0.55 μM found in rat brain tubulin using tritiated podophyllotoxin (Cortese et al., 1977). The K_d for CeTb,

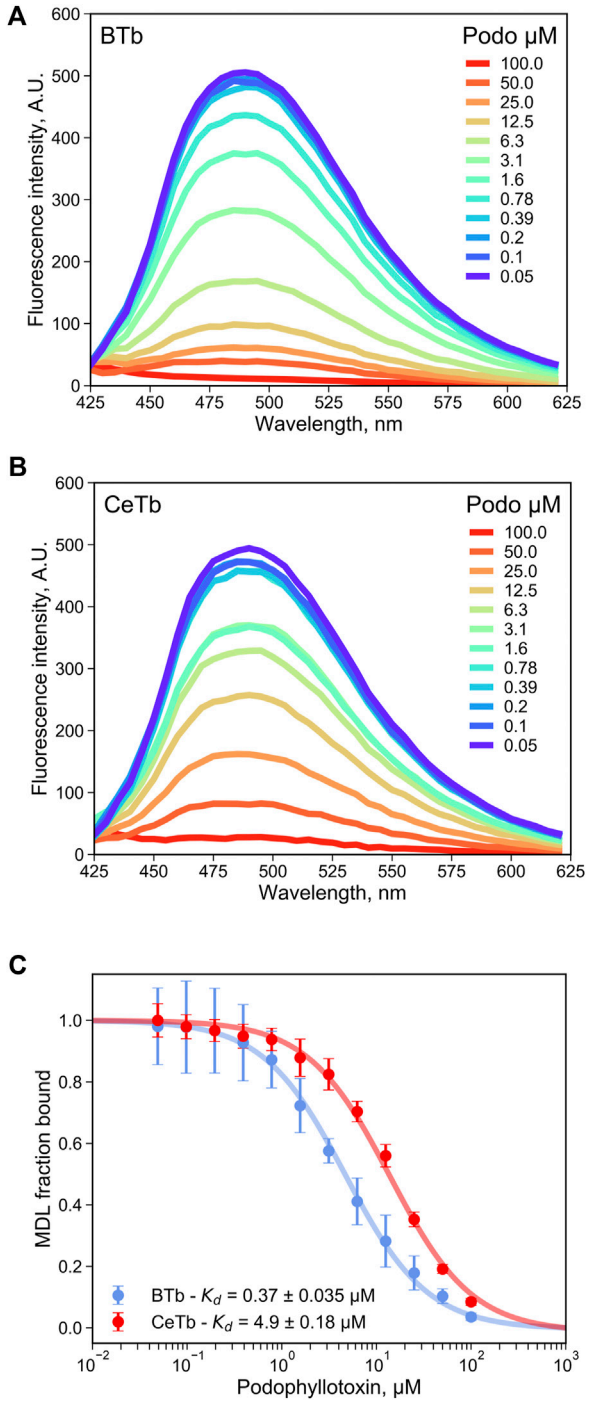

FIGURE 5 | Determination of the dissociation constant for tubulin—podophyllotoxin interaction by competition experiments. The fluorescence of tubulin-bound MDL gradually decreases upon displacement by the competitor podophyllotoxin as monitored by the fluorescence emission spectra with excitation at 400 nm, for tubulin from brain **(A)** or from erythrocytes **(B)**. **(C)** the podophyllotoxin concentration-dependent change in the fluorescence intensity at 550 nm was used to determine the apparent dissociation constant by non-linear regression using **Eq. 4**. 1 μM tubulin with 5 μM MDL was incubated in PM buffer at room temperature at the indicated podophyllotoxin concentrations. The data points are the average of three to

(*Continued*)

FIGURE 5 | four measurements and the error bars are standard deviations. The uncertainties of K_d values are the standard error of the fits.

~6 μM indicates about a 12-fold weaker binding of podophyllotoxin for CeTb compared to BTb.

A similar analysis was performed using the compound cis-Combretastatin A4 (structure in **Figure 1**), This two-ring analog of colchicine binds with considerable affinity as well as specificity (the trans-form is notably less potent) and has been the subject of much preclinical development (Cushman et al., 1991) [reviewed in (Sackett, 1993)]. Titration of CeTb- and BTb-bound MDL with combretastatin A4 yielded a K_d of 5.7 ± 0.32 μM for CeTb, while the K_d for BBTb was found to be 0.13 ± 0.011 μM (**Supplementary Figure S5**) The K_d for BBTb is similar to the literature value of 0.12 μM (Lin et al., 1989). Results are included in **Table 3**, and indicate a ~44-fold weaker binding to CeTb compared to BTb.

Since fluorescence titration and competition assays with MDL and two standard compounds yielded binding values consistent with literature values with BTb, we accept the values obtained for CeTb as well and turned our attention to other compounds using this assay. The first group of compounds we examined were the benzimidazoles. These compounds have a history as antihelmintics that target parasite tubulin over mammalian host tubulin, but are causing renewed interest as potential repurposed agents in human oncology (Son et al., 2020). Five compounds were chosen for a full competition titration against CeTb- and BTb-bound MDL. The titration curves and best fits to the data are shown in **Figure 6**, and the obtained K_d values are presented in **Table 3**. The data show that nocodazole yields a Kd of about 1 μM to BTb, similar to the published value of 2.5 μM (Head et al., 1985). Mebendazole binding to BTb is similar, and both compounds have similar Kd (within a factor of two) with either tubulin. Other compounds (albendazole, oxibendazole, carbendazim) show moderate binding affinity with CeTb, but no detectable binding to BTb.

The dissociation constants obtained for selected compounds are combined in **Table 4** for both CeTb and BTb. The last column

TABLE 3 | Dissociation constants of tubulin—benzimidazoles-, podophyllotoxin-, and combretastatin A4 - interaction measured by competition titration with MDL.

Drug	Brain tubulin (BTb)		Erythrocyte tubulin (CeTb)	
	IC_{50}, μM	K_d, μM	IC_{50}, μM	K_d, μM
Nocodazole	11 ± 1.2	1.0 ± 0.11	1.5 ± 0.11	0.51 ± 0.036
Mebendazole	14 ± 2.5	1.3 ± 0.23	6.8 ± 0.73	2.3 ± 0.25
Carbendazim	nb	nb	37 ± 5.4	13 ± 1.8
Oxibendazole	nb	nb	36 ± 5.6	12 ± 1.9
Albendazole	nb	nb	104 ± 12	35 ± 4.0
Podophyllotoxin	4.0 ± 1.0	0.37 ± 0.035	15 ± 0.53	4.9 ± 0.18
Combretastatin A4	2.6 ± 0.22	0.13 ± 0.011	20 ± 1.2	5.7 ± 0.32

*K_d was calculated with **Equation 4**.*
Uncertainties are the standard errors of the fits. nb, no binding detected.

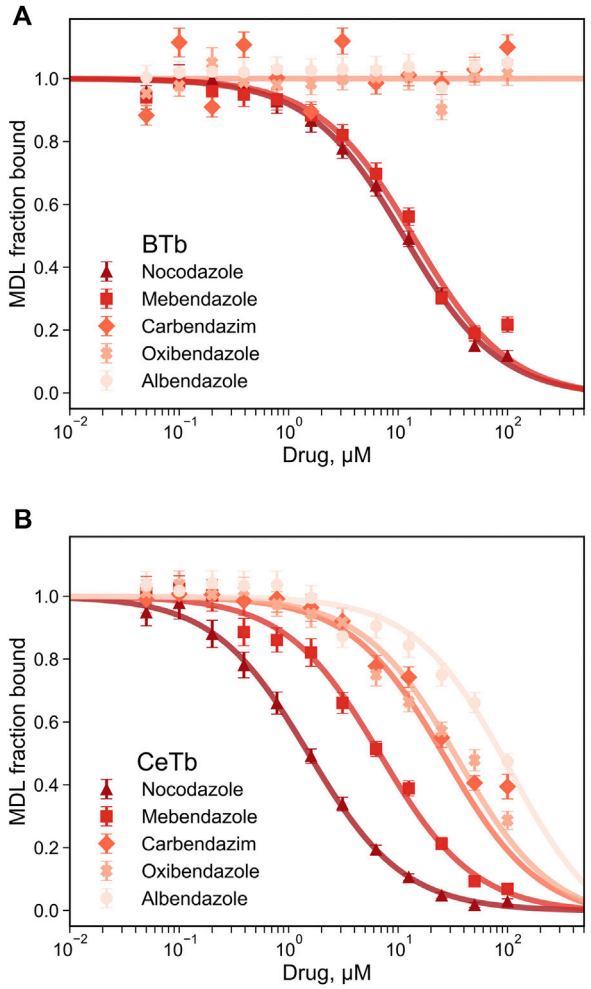

FIGURE 6 | Determination of the dissociation constant for tubulin—benzimidazoles interaction by competition experiments. The fluorescence of tubulin-bound MDL gradually decreases upon displacement by the benzimidazoles competitors. Fluorescence was monitored at 550 nm with excitation at 400 nm, for tubulin from brain **(A)** or from erythrocytes **(B)**. The reaction mixtures contained 1 μM tubulin with 5 μM MDL incubated in PM buffer at room temperature at the indicated drug concentrations. The data points are the average of three to four measurements and the error bars are standard deviations. The best-fit K_d with the standard errors of the fits are shown in **Table 3**.

shows the ratio of the drug's K_d for binding to CeTb compared to that for BTb. A ratio >1 (i.e., K_d for CeTb > K_d for BTb) indicates weaker binding to CeTb than to BTb. It is clear that the relative affinity for the two tubulins shows considerable variation, with the greatest differential in the first three "standard" colchicine site compounds found with Combretastatin A4, the strongest binding ligand for BTb, showing 44-fold lower affinity for CeTb. In the benzimidazoles, however, the range of K_d ratios is even broader, since two of the compounds do not show binding to BTb at all under these assay conditions.

3.2 Screen of Known Colchicine-Site Ligands

Next, we used this method to screen a single concentration of a series of molecules. Many colchicine-site ligands are known, so these were an excellent starting point to look for drugs that have activity in CeTb. A series of known colchicine site drugs was obtained and screened for binding to CeTb. Some compounds are structurally close to colchicine, others not so similar, including benzimidazoles. The molecules studied above, podophyllotoxin and combretastatin, were included in the screen. The results for these two drugs were consistent with the full binding curves obtained above, so we felt that valuable information about the interaction of the various drugs with CeTb (and BTb) could be obtained from a single concentration reading. For this purpose, we used a relatively high concentration of test compounds in order to probe weaker as well as stronger binding.

The results of the single-point screen are shown in **Tables 5–8**. The test compounds are divided into the following groupings: three-ring colchicine analogs, two-ring colchicine analogs, a group of diverse colchicine-site compounds which are structurally unrelated to the colchicine groups, and the benzimidazoles. Information about the compounds is given in **Supplementary Table S1** and structures in **Supplementary Figures S1–S4**.

A comment about this assay is in order. The assay measures the inhibition of MDL binding to CeTb and BTb by a single concentration of test compound. Since the two tubulins have 5-fold difference in K_d for MDL, a reduction in MDL binding by an identical fraction will imply different binding strengths in the two tubulins. Since MDL binding to CeTb is weaker than to BTb, it

TABLE 4 | Dissociation constants of selected drugs with CeTb and BTb.

Drug	Erythrocyte tubulin (CeTb) K_d, μM	Brain tubulin (BTb) K_d, μM	Ratio[a]
MDL	2.6	0.51	5
Podophyllotoxin	4.9	0.37	13
Combretastatin A4	5.7	0.13	44
Nocodazole	0.6	1.1	0.5
Mebendazole	2.6	1.4	1.9
Albendazole	35	nd[b]	nd
Oxibendazole	12	nd	nd

[a]*The last column ("Ratio") shows the K_d of the drug and CeTb divided by the K_d of the drug and BBTb.*
[b]*nd, not determined.*

TABLE 5 | MDL competitive binding inhibition by colchicine site 3-ring drugs.

#	Drug	BTb %	BTb $K_{d(app)}$, μM	CeTb %	CeTb $K_{d(app)}$, μM
1	Colchicine	58	3.2	24	54
2	Colcemid	60	3.0	28	44
3	Deacetylcolchicine (DAC)	26	13	11	138
4	Desacetamidocolchicine (DAAC)	76	1.4	38	28
5	Isocolchicine	1	502	3	565
6	Cornigerine	67	2.2	36	30
7	Steganacin	50	4.5	50	17
8	Allocolchicine	52	4.2	28	44
9	Allo methyl ketone	93	0.34	86	2.7
10	Allo ethyl ketone	92	0.39	89	2.1
11	Thiocolchicine	43	6	31	38
12	1,2-Didemethylcolchicine	11	37	6	269
13	Podophyllotoxin	90	0.73	81	5.9
14	Azatoxin	<1	nd	4	416
15	Colchiceine	11	37	10	153
16	Trimethylcolchicinic acid	22	16	24	54

nd, not determined

TABLE 6 | MDL competitive binding inhibition by colchicine site 2-ring drugs.

#	Drug	BTb %	BTb $K_{d(app)}$, μM	CeTb %	CeTb $K_{d(app)}$, μM
17	AC (MTC)	16	24	3	565
18	Combrestastatin (CS) A2	91	0.44	81	3.9
19	CS-A4 cis	92	0.39	64	9.5
20	CS-A4 trans	44	5.8	7	228
21	Dyhydro CS A4	46	5.3	10	153
22	Trimethoxy resveratrol (trans)	8	53	28	43
23	Resveratrol	2	235	4	416
24	MDL	nd	nd	nd	nd

nd, not determined

TABLE 7 | MDL competitive binding inhibition by other non-colchicine structure drugs.

#	Drug	BTb %	BTb Kd (app), μM	CeTb %	CeTb Kd (app), μM
25	Tubulazole C	31	10	10	153
26	Tubulazole T	<1	nd	12	124
27	Indanocine	57	3.4	50	16
28	T113242	44	5.8	2	872
29	T138067 (Batabulin)	36	8.0	4	415
30	ABT-751	44	5.8	12	124
31	TN16	74	1.5	34	32
32	Tivantinib	48	4.9	24	53
33	Plinabulin	<1	nd	<1	nd
34	Lexibulin	80	1.1	6	268
35	Curvulin	3	152	2	872
36	Indibulin (D248510)	7	61	10	153
37	Curvularin	<1	nd	<1	nd
38	Dehydrocurvularin	2	234	1	1865
39	Tryprostatin	<1	nd	<1	nd
40	2-methoxyestradiol (2-ME)	12	33	1	1865
41	Berberine	4	111	2	872
42	D-64131	90	0.5	73	6.2
43	Ferulenol	10	41	2	872

nd, not determined.

TABLE 8 | MDL competitive binding inhibition by benzimidazole drugs.

#	Drug	BTb %	BTb Kd (app), μM	CeTb %	CeTb Kd (app),μM
44	Nocodazole	85	0.8	96	0.68
45	Mebendazole	82	1.0	90	1.8
46	Thiabendazole	6	72	32	35
47	Carbendazim	<1	nd	58	12
48	Fenbendazole	12	33	39	26
49	Flubendazole	46	5.3	61	10
50	Albendazole	<1	nd	35	31
51	Ricobendazole	8	52	27	45
52	Oxibendazole	<1	nd	56	13
53	Benomyl	34	8.8	45	20

nd, not determined

will be more easily competed away. Thus, with fixed tubulin and MDL concentrations of 1 and 5 μM, respectively, a competitor/compound that caused a 50% reduction in MDL binding to BTb at 50 μM, would imply a Ki of ~4.5 μM, while a 50% reduction in MDL binding to CeTb by 50 μM competitor would imply a K_i of ~17 μM. Since all of the drugs analyzed here by titration (**Figures 4–6**) yielded curves that indicate simple single-site binding, we analyzed the single concentration data using a single-site binding isotherm by non-linear regression. As with the titrations, this curve was used to obtain the $IC_{50\%}$ which served to calculate an apparent K_d ($K_{d(app)}$) using **Eq. 4** (for more details see **Section 2** and **Supplementary Figure S6**).

The drugs in the colchicine series (**Table 5**) displayed weak binding to CeTb, and in general notably lower binding to CeTb than to BTb. Isocolchicine does not bind to either tubulin, demonstrating that the stereospecific requirements for binding to CeTb mimic those of BTb. Interestingly, steganacin inhibits MDL binding to CeTb to the same extent (%) as to BTb (though note that this still indicates a lower affinity/higher $K_{d(app)}$ to CeTb than to BTb). The compounds that show the strongest binding to CeTb are the same ones that bind strongest to BTb: allocolchicine methyl ketone and allocolchicine ethyl ketone. Both compounds bind to both tubulins more strongly than does the parent compound, allocolchicine, or colchicine itself. While both compounds significantly inhibited MDL binding to both tubulins, the binding to CeTb is weaker than to BTb. By comparison to podophyllotoxin, the $K_{d(app)}$ for binding of both compounds to both tubulins can be estimated to be lower by a factor of about two than that obtained by titration with podophyllotoxin. This shows that small modifications to the structure of a colchicine-site ligand can improve binding to both tubulins. Of interest here is a rational drug design study by Paré et al. (2020) who showed that some small changes to colchicine yielded a lead compound with increased affinity for βVI tubulin and increased bioactivity towards neutrophils.

Data from the two-ring colchicine analogs (**Table 6**) demonstrate the greater relative importance of the cis configuration of the two rings in CeTb compared to BTb. This can be seen by comparing combretastatin-A2 and -A4 (cis), both of which have an unsaturated bridge holding the two rings in cis, with combretastatin-A4 (trans) and dihydrocombretastatin-A4, in which the rings are locked in trans, or are freely rotating, respectively. The potency of the two cis compounds as competitors approaches that of podophyllotoxin, and is only slightly less than the two allocolchicine analogs in **Table 5**. The lack of activity of trimethoxy resveratrol (trans) is consistent with this observation.

The compounds of diverse structure in **Table 7** yielded only two compounds with significant binding to CeTb. Indanocine shows similar inhibition of MDL binding to BTb and to CeTb, comparable to steganacin in **Table 5**, consistent with a ca. 4.5-fold difference in $K_{d(app)}$. D-64131 shows the highest inhibitory potency to both tubulins of all the compounds in this table, while still showing an approximately 10-fold ratio in $K_{d(app)}$. Binding potency is similar to podophyllotoxin (for BTb) and slightly less so for CeTb. The largest differential between the tubulins appears to be with lexibulin, which is somewhat less potent than podophyllotoxin with BTb but nearly inactive with CeTb.

Benzimidazole compounds (**Table 8**) yield several patterns of comparative inhibition. Nocodazole and mebendazole are fairly potent inhibitors of MDL binding to both tubulins, comparable to podophyllotoxin. Both compounds yielded Kd (app) values within a factor of two of the Kd values obtained from titrations, with both tubulins. Three compounds show moderate inhibition of MDL binding to both tubulins, but slightly higher % inhibition to MDL-CeTb than to MDL-BTb: fenbendazole, flubendazole, and benomyl [Kd (app) values are within a factor of two for the two tubulins]. A final group of five shows no or very low inhibition of MDL binding to BTb (<10%), but moderate to significant inhibition of MDL-CeTb: thiabendazole, carbendazim, albendazole, ricobendazole, and oxibendazole. We were somewhat surprised at the lack of inhibition of MDL binding by these compounds, especially albendazole, which has shown activity in mammalian cells that has prompted discussion of repurposing this compound for cancer therapy (Nath et al., 2020; Will Castro et al., 2021). We were unable to find a published study of direct binding of albendazole or these other benzimidazoles to BTb, and therefore we checked albendazole for direct inhibitory activity against polymerization of BTb. We observed little or no inhibition of polymerization of BTb in the albendazole concentration range that we have been studying (**Supplementary Figure S7**), consistent with the lack of inhibition of MDL binding that we observed in the titration and single-point assays.

4 DISCUSSION

These findings expand our knowledge of the structure-activity relationship of the colchicine site on CeTb, and demonstrate the utility of the MDL competition assay for testing colchicine site ligands. This assay could readily be used for other compounds. It could also be used for high throughput screening of other types of tubulins for colchicine-site drugs. In the current application, this assay readily provided binding information via competition assay, due to the

significant difference in fluorescence between the tubulin-bound and free forms of MDL.

For most compounds in this study, binding to CeTb is weaker than to BTb, to an extent that varies considerably. Perhaps this is due to these compounds having been selected for interest initially due to bioactivity against cells that express the beta tubulin isotypes in brain tubulin rather than those in erythrocyte tubulin. In any case most of the compounds from all groups that we studied did show reasonable binding to CeTB, and some bind more tightly to CeTb than to BTb. Notable in this regard are the benzimidazoles, about half of which showed significant binding to CeTb but no measurable binding to BTb under the conditions of our assay.

Previous studies showed thiabendazole to be a good inhibitor of nematode tubulin while it had virtually no effect on mammalian tubulin assembly, an observation which is consistent with our data demonstrating no MDL-BTb inhibition by thiabendazole (Dawson et al., 1984). Other studies (e.g., Lubega and Prichard, 1991) showed significant differences between benzimidazoles in binding to parasite tubulin, and also noted that some compounds showed significantly lower tubulin binding than expected from their known antihelmintic potency, possibly indicating the importance of other targets in bioactivity as well as tubulin (Shrivastava et al., 2017). Given the interest in repurposing several members of this family of compounds for human cancer therapy, a systematic direct study of benzimidazole binding to mammalian tubulin combined with a parallel measure of bioactivity such as inhibition of growth of human cell lines in culture would be a valuable addition to this field.

These findings may have relevance to human cancer. Chicken βVI and human βVI have a high degree of similarity in colchicine-binding region (Sharma et al., 2010). As we show in **Supplementary Figure S8**, of the 38 amino acid residues that fall within 6 Å of the bound colchicine, only one residue is substituted in chicken βVI compared to human βVI (I236V). Sequence alignments comparing βVI from chicken and human (and rat) are presented in **Supplementary Figure S8**. This also compares these sequences with the sequence of TUBB2B, the major β-tubulin in mammalian brain tubulin. Additionally, **Supplementary Figure S8** shows the colchicine binding site of TUBB2B and indicates the residues that differ in TUBB2B and TUBB1.

βVI tubulin has long been recognized to be present in megakaryocytes and platelets (Lewis et al., 1987), as well as in other blood cells (Leandro-García et al., 2012). Thus, study of βVI tubulin may aid in the development of drugs for cancers of a variety of hematologic tissues. In particular, the activity of some of the benzimidazoles against this isotype may be informative in the effort to repurpose these widely used antiparasite drugs to use in human disease, and to enhance effectiveness of ligands at this site in treatment of inflammatory diseases.

DATA AVAILABILITY STATEMENT

The original contributions presented in the study are included in the article/**Supplementary Material**, further inquiries can be directed to the corresponding authors.

AUTHOR CONTRIBUTIONS

FM, ML, and TC designed the experiments and acquired the data. DS and SB conceived and designed the study. FM, ML, TC, DS, and SB analyzed and discussed the data. FM, ML, DS, and SB wrote the paper. All authors read and approved the final manuscript.

FUNDING

This work was supported by the intramural Research Program of the Eunice Kennedy Shriver National Institute of Child Health and Human Development (DS and FM), and by NIH Grants R15 GM093941 and R15 CA227747 (SB, ML, and TC).

SUPPLEMENTARY MATERIAL

The Supplementary Material for this article can be found online at: https://www.frontiersin.org/articles/10.3389/fcell.2022.884287/full#supplementary-material

REFERENCES

Banerjee, A., and Luduena, R. F. (1992). Kinetics of Colchicine Binding to Purified Beta-Tubulin Isotypes from Bovine Brain. *J. Biol. Chem.* 267, 13335–13339. doi:10.1016/S0021-9258(18)42215-6

Cortese, F., Bhattacharyya, B., and Wolff, J. (1977). Podophyllotoxin as a Probe for the Colchicine Binding Site of Tubulin. *J. Biol. Chem.* 252, 1134–1140. doi:10.1016/S0021-9258(17)40631-4

Craig, D. A. (1993). The Cheng-Prusoff Relationship: Something Lost in the Translation. *Elsevier Curr. Trends* 14 (3), 89–91. doi:10.1016/0165-6147(93)90070-Z

Cushman, M., Nagarathnam, D., Gopal, D., Chakraborti, A. K., Lin, C. M., and Hamel, E. (1991). Synthesis and Evaluation of Stilbene and Dihydrostilbene Derivatives as Potential Anticancer Agents that Inhibit Tubulin Polymerization. *J. Med. Chem.* 34, 2579–2588. doi:10.1021/JM00112A036

Dawson, P. J., Gutteridge, W. E., and Gull, K. (1984). A Comparison of the Interaction of Anthelmintic Benzimidazoles with Tubulin Isolated from Mammalian Tissue and the Parasitic Nematode Ascaridia Galli. *Biochem. Pharmacol.* 33, 1069–1074. doi:10.1016/0006-2952(84)90515-X

Dmitrieff, S., Alsina, A., Mathur, A., and Nédélec, F. J. (2017). Balance of Microtubule Stiffness and Cortical Tension Determines the Size of Blood Cells with Marginal Band across Species. *Proc. Natl. Acad. Sci. U.S.A.* 114, 4418–4423. doi:10.1073/pnas.1618041114

Ducki, S., Forrest, R., Hadfield, J. A., Kendall, A., Lawrence, N. J., McGown, A. T., et al. (1998). Potent Antimitotic and Cell Growth Inhibitory Properties of Substituted Chalcones. *Bioorg. Med. Chem. Lett.* 8, 1051–1056. doi:10.1016/S0960-894X(98)00162-0

Feierbach, B., Nogales, E., Downing, K. H., and Stearns, T. (1999). Alf1p, a CLIP-170 Domain-Containing Protein, Is Functionally and Physically Associated with α-Tubulin. *J. Cell Biol.* 144, 113–124. doi:10.1083/jcb.144.1.113

Hausrat, T. J., Radwitz, J., Lombino, F. L., Breiden, P., and Kneussel, M. (2021). Alpha- and Beta-tubulin Isotypes Are Differentially Expressed during Brain Development. *Dev. Neurobiol.* 81, 333–350. doi:10.1002/DNEU.22745

Head, J., Lee, L. L., Field, D. J., and Lee, J. C. (1985). Equilibrium and Rapid Kinetic Studies on Nocodazole-Tubulin Interaction. *J. Biol. Chem.* 260, 11060–11066. doi:10.1016/S0021-9258(17)39148-2

Italiano, J. E., Bergmeier, W., Tiwari, S., Falet, H., Hartwig, J. H., Hoffmeister, K. M., et al. (2003). Mechanisms and Implications of Platelet Discoid Shape. *Blood* 101, 4789–4796. doi:10.1182/blood-2002-11-3491

Leandro-García, L. J., Leskelä, S., Inglada-Pérez, L., Landa, I., De Cubas, A. A., Maliszewska, A., et al. (2012). Hematologic β-Tubulin VI Isoform Exhibits Genetic Variability that Influences Paclitaxel Toxicity. *Cancer Res.* 72, 4744–4752. doi:10.1158/0008-5472.CAN-11-2861

Lecine, P., Italiano, J. E., Kim, S.-W., Villeval, J.-L., and Shivdasani, R. A. (2000). Hematopoietic-specific β1 Tubulin Participates in a Pathway of Platelet Biogenesis Dependent on the Transcription Factor NF-E2. *Blood* 96, 1366–1373. doi:10.1182/blood.v96.4.1366.h8001366_1366_1373

Lewis, S. A., Gu, W., and Cowan, N. J. (1987). Free Intermingling of Mammalian β-tubulin Isotypes Among Functionally Distinct Microtubules. *Cell* 49, 539–548. doi:10.1016/0092-8674(87)90456-9

Lin, C. M., Ho, H. H., Pettit, G. R., and Hamel, E. (1989). Antimitotic Natural Products Combretastatin A-4 and Combretastatin A-2: Studies on the Mechanism of Their Inhibition of the Binding of Colchicine to Tubulin. *Biochemistry* 28, 6984–6991. doi:10.1021/bi00443a031

Lubega, G. W., and Prichard, R. K. (1991). Interaction of Benzimidazole Anthelmintics with *Haemonchus contortus* Tubulin: Binding Affinity and Anthelmintic Efficacy. *Exp. Parasitol.* 73, 203–213. doi:10.1016/0014-4894(91)90023-P

Montecinos-Franjola, F., Chaturvedi, S. K., Schuck, P., and Sackett, D. L. (2019). All Tubulins Are Not Alike: Heterodimer Dissociation Differs Among Different Biological Sources. *J. Biol. Chem.* 294, 10315–10324. doi:10.1074/jbc.RA119.007973

Nath, J., Paul, R., Ghosh, S. K., Paul, J., Singha, B., and Debnath, N. (2020). Drug Repurposing and Relabeling for Cancer Therapy: Emerging Benzimidazole Antihelminthics with Potent Anticancer Effects. *Life Sci.* 258, 118189. doi:10.1016/j.lfs.2020.118189

Palasca, O., Santos, A., Stolte, C., Gorodkin, J., and Jensen, L. J. (2018). TISSUES 2.0: an Integrative Web Resource on Mammalian Tissue Expression. *Database*, 2018. doi:10.1093/DATABASE/BAY003

Paré, G., Vitry, J., Marceau, F., Vaillancourt, M., Winter, P., Bachelard, H., et al. (2020). The Development of a Targeted and More Potent, Anti-inflammatory Derivative of Colchicine: Implications for Gout. *Biochem. Pharmacol.* 180, 114125. doi:10.1016/J.BCP.2020.114125

Peyrot, V., Leynadier, D., Sarrazin, M., Briand, C., Menendez, M., Laynez, J., et al. (1992). Mechanism of Binding of the New Antimitotic Drug MDL 27048 to the Colchicine Site of Tubulin: Equilibrium Studies. *Biochemistry* 31, 11125–11132. doi:10.1021/bi00160a024

Peyrot, V., Leynadier, D., Sarrazin, M., Briand, C., Rodriquez, A., Nieto, J. M., et al. (1989). Interaction of Tubulin and Cellular Microtubules with the New Antitumor Drug MDL 27048. *J. Biol. Chem.* 264, 21296–21301. doi:10.1016/S0021-9258(19)30078-X

Sackett, D. L., Knipling, L., and Wolff, J. (1991). Isolation of Microtubule Protein from Mammalian Brain Frozen for Extended Periods of Time. *Protein Expr. Purif.* 2, 390–393. doi:10.1016/1046-5928(91)90099-5

Sackett, D. L. (1993). Podophyllotoxin, Steganacin and Combretastatin: Natural Products that Bind at the Colchicine Site of Tubulin. *Pharmacol. Ther.* 59, 163–228. doi:10.1016/0163-7258(93)90044-E

Sackett, D. L. (1995). Rapid Purification of Tubulin from Tissue and Tissue Culture Cells Using Solid-phase Ion Exchange. *Anal. Biochem.* 228, 343–348. doi:10.1006/abio.1995.1361

Schwer, H. D., Lecine, P., Tiwari, S., Italiano, J. E., Hartwig, J. H., and Shivdasani, R. A. (2001). A Lineage-Restricted and Divergent β-tubulin Isoform Is Essential for the Biogenesis, Structure and Function of Blood Platelets. *Curr. Biol.* 11, 579–586. doi:10.1016/S0960-9822(01)00153-1

Sharma, S., Poliks, B., Chiauzzi, C., Ravindra, R., Blanden, A. R., and Bane, S. (2010). Characterization of the Colchicine Binding Site on Avian Tubulin Isotype βVI. *Biochemistry* 49, 2932–2942. doi:10.1021/bi100159p

Shrivastava, N., Naim, M. J., Alam, M. J., Nawaz, F., Ahmed, S., and Alam, O. (2017). Benzimidazole Scaffold as Anticancer Agent: Synthetic Approaches and Structure-Activity Relationship. *Arch. Pharm. Chem. Life Sci.* 350, e201700040. doi:10.1002/ARDP.201700040

Son, D.-S., Lee, E.-S., and Adunyah, S. E. (2020). The Antitumor Potentials of Benzimidazole Anthelmintics as Repurposing Drugs. *Immune Netw.* 20, 1–20. doi:10.4110/in.2020.20.e29

Steinmetz, M. O., and Prota, A. E. (2018). Microtubule-Targeting Agents: Strategies to Hijack the Cytoskeleton. *Trends Cell Biol.* 28, 776–792. doi:10.1016/J.TCB.2018.05.001

Stoupa, A., Adam, F., Kariyawasam, D., Strassel, C., Gawade, S., Szinnai, G., et al. (2018). TUBB 1 Mutations Cause Thyroid Dysgenesis Associated with Abnormal Platelet Physiology. *EMBO Mol. Med.* 10. doi:10.15252/emmm.201809569

Will Castro, L. S. E. P., Pieters, W., Alemdehy, M. F., Aslam, M. A., Buoninfante, O. A., Raaijmakers, J. A., et al. (2021). The Widely Used Antihelmintic Drug Albendazole Is a Potent Inducer of Loss of Heterozygosity. *Front. Pharmacol.* 12. doi:10.3389/FPHAR.2021.596535

Yung-Chi, C., and Prusoff, W. H. (1973). Relationship between the Inhibition Constant (KI) and the Concentration of Inhibitor Which Causes 50 Per Cent Inhibition (I50) of an Enzymatic Reaction. *Biochem. Pharmacol.* 22, 3099–3108. doi:10.1016/0006-2952(73)90196-2

Conflict of Interest: The authors declare that the research was conducted in the absence of any commercial or financial relationships that could be construed as a potential conflict of interest.

Publisher's Note: All claims expressed in this article are solely those of the authors and do not necessarily represent those of their affiliated organizations, or those of the publisher, the editors and the reviewers. Any product that may be evaluated in this article, or claim that may be made by its manufacturer, is not guaranteed or endorsed by the publisher.

frontiers | Frontiers in Cell and Developmental Biology

REVIEW
published: 05 July 2022
doi: 10.3389/fcell.2022.913809

Microtubules in Microorganisms: How Tubulin Isotypes Contribute to Diverse Cytoskeletal Functions

*Abesh Bera and Mohan L. Gupta Jr**

Genetics, Development, and Cell Biology, Iowa State University, Ames, IA, United States

The cellular functions of the microtubule (MT) cytoskeleton range from relatively simple to amazingly complex. Assembled from tubulin, a heterodimeric protein with α- and β-tubulin subunits, microtubules are long, hollow cylindrical filaments with inherent polarity. They are intrinsically dynamic polymers that utilize GTP binding by tubulin, and subsequent hydrolysis, to drive spontaneous assembly and disassembly. Early studies indicated that cellular MTs are composed of multiple variants, or isotypes, of α- and β-tubulins, and that these multi-isotype polymers are further diversified by a range of posttranslational modifications (PTMs) to tubulin. These findings support the multi-tubulin hypothesis whereby individual, or combinations of tubulin isotypes possess unique properties needed to support diverse MT structures and/or cellular processes. Beginning 40 years ago researchers have sought to address this hypothesis, and the role of tubulin isotypes, by exploiting experimentally accessible, genetically tractable and functionally conserved model systems. Among these systems, important insights have been gained from eukaryotic microbial models. In this review, we illustrate how using microorganisms yielded among the earliest evidence that tubulin isotypes harbor distinct properties, as well as recent insights as to how they facilitate specific cellular processes. Ongoing and future research in microorganisms will likely continue to reveal basic mechanisms for how tubulin isotypes facilitate MT functions, along with valuable perspectives on how they mediate the range of conserved and diverse processes observed across eukaryotic microbes.

Keywords: tubulin isotype, tubulin, microtubule, microorganism, cytoskeleton

OPEN ACCESS

Edited by:
Jeffrey Moore,
University of Colorado Anschutz Medical Campus, United States

Reviewed by:
Anne Straube,
University of Warwick, United Kingdom
Susan Dutcher,
Washington University in St. Louis, United States

****Correspondence:***
Mohan L. Gupta Jr
mgupta@iastate.edu

Specialty section:
This article was submitted to Cellular Biochemistry, a section of the journal Frontiers in Cell and Developmental Biology

Received: *06 April 2022*
Accepted: *15 June 2022*
Published: *05 July 2022*

Citation:
Bera A and Gupta ML (2022) Microtubules in Microorganisms: How Tubulin Isotypes Contribute to Diverse Cytoskeletal Functions. Front. Cell Dev. Biol. 10:913809. doi: 10.3389/fcell.2022.913809

INTRODUCTION

Microtubules (MTs) are essential, intrinsically dynamic cytoskeletal filaments, polymerized from the heterodimeric protein tubulin. Each heterodimer contains two closely related, GTP-binding subunits: α-tubulin and β-tubulin (**Figure 1**). Populations of MTs in eukaryotes mediate critical functions like cell division, cell migration, and intracellular cargo transport. These processes require a high degree of fidelity to ensure cell viability, genome stability and organismal health. Thus, MTs must support a diverse range of interactions and their nucleation, dynamics and stability must be tightly regulated in both space and time.

In addition to α- and β-tubulin, the protein family also includes the ubiquitous mediator of MT nucleation, γ-tubulin (Oakley et al., 2015) and the specialized δ-, ε- and ζ-tubulins that are present in a subset of eukaryotes in which they facilitate the structure and/or function of centrioles and basal bodies (Chang and Stearns, 2000; Vaughan et al., 2000; Turk et al., 2015). Some organisms harbor

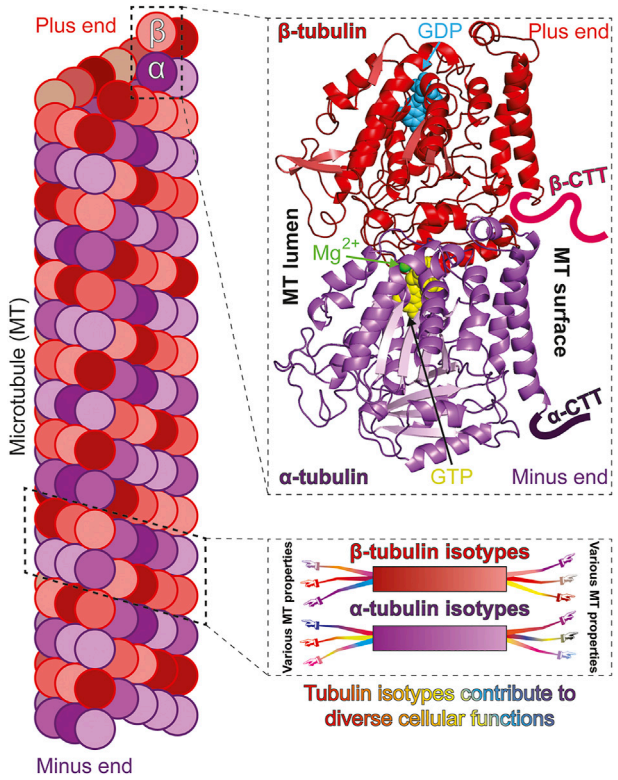

FIGURE 1 | Isotypes of α- and β-tubulin construct functionally diverse microtubules. Microtubules (MTs) polymerize from "head-to-tail" binding of tubulin, a heterodimer of α- and β-tubulin subunits (left). Both α- and β-tubulin subunits bind GTP but only the β-tubulin bound GTP is hydrolysable and exchangeable [top-right; cryo-EM structure of *S. cerevisiae* tubulin, polymerized with GTP in vitro; PDB ID: 5W3F (Howes et al., 2017)]. The carboxy terminal tails (CTTs) are normally unstructured and are only drawn representatively and not to scale. The α- and β-tubulin subunits can be encoded by multiple genes to produce variants, or isotypes (bottom-right; color gradient represents different isotypes). Tubulin isotypes can each possess common and/or unique molecular properties which expands the ability of MTs to optimally perform diverse and specialized functions (represented by arms/hands differentially extending from isotypes).

two or three variants, or isotypes, of γ-tubulin (Findeisen et al., 2014). Notably, almost all organisms utilize multiple isotypes of α- and β-tubulin to build tubulin heterodimers (Cleveland et al., 1980; Roll-Mecak, 2019). The functional role of these tubulin isotypes, however, remains largely obscure.

The β- and α-subunits of two consecutive tubulin heterodimers interact to polymerize into inherently polarized protofilaments. Lateral interactions between typically 13 protofilaments yield the hollow cylindrical structure of MTs (**Figure 1**). While both α- and β-tubulin bind GTP, nucleotide binding to α-tubulin appears mainly structural while MT assembly and disassembly is driven by the binding and subsequent hydrolysis, respectively, of GTP bound to the β-subunit (**Figure 1**) [reviewed in (Nogales, 2001)]. The transition between MT assembly and disassembly is stochastic and the phenomenon termed "dynamic instability" (Mitchison and Kirschner, 1984). The inherent polarity and dynamic instability of MTs facilitates kinesin/dynein mediated directed cargo transport (Barlan and Gelfand, 2017), MT organization (Mani et al., 2021), MT Associated Protein (MAP) interaction (Brouhard and Rice, 2018), as well as MT-dependent force generation (Forth and Kapoor, 2017).

MT behavior is controlled at multiple levels. They are regulated at the level of MT nucleation by γ-tubulin, at the level of fundamental polymer dynamics by α/β heterodimers, and at the level of macromolecular organization by a range of MT Associated Proteins (MAPs) [reviewed in (Goodson and Jonasson, 2018)]. Another layer of regulation comes from a relatively large number of posttranslational modifications (PTMs) that occur on tubulin [reviewed in (Janke and Magiera, 2020)]. A third aspect of MT regulation stems from the multiple tubulin variants, or isotypes, expressed in most cells (**Figure 1**) (Nsamba and Gupta, 2022). Relative to our understanding of how PTMs and MAPs influence MT function, which can be significant, our knowledge of how tubulin isotypes themselves contribute to the complexity of MT behaviors remains limited. Despite the contribution of PTMs and MAPs, in this review we mainly focus on the evidence that tubulin isotypes play a fundamental role in the diversity of MT functions.

Why organisms express multiple α- and β-tubulin isotypes has been a central, long-standing question. The multi-tubulin hypothesis, formulated decades ago, postulates that specific tubulin isotypes contribute unique functional properties to MTs (**Figure 1**) (Cleveland, 1987; Ludueña, 1993). The discovery that mutations in certain mammalian tubulin isotypes cause specific disorders, collectively known as tubulinopathies, lends support to this idea and emphasizes the need to elucidate the cellular roles of various isotypes (Bahi-Buisson and Maillard, 2016; Romaniello et al., 2018; Binarová and Tuszynski, 2019). Directly testing the multi-tubulin hypothesis, however, has been hampered by significant challenges. Depletion of one may lower overall tubulin levels and/or alter the relative ratios of the remaining isotypes. Excess β-tubulin relative to α-subunits can be toxic (Weinstein and Solomon, 1990), and overexpression can lead to aggregated, non-functional protein (Bhattacharya and Cabral, 2004). Thus, interpretation of cell-based experiments has often been confounded by these indirect effects. Additionally, the purification of mutant and/or single isotype tubulin was essentially restricted to yeast (Kilmartin, 1981; Davis et al., 1994; Bode et al., 2003; Drummond et al., 2011), and only recently obtained from higher eukaryotes (Minoura et al., 2013; Pamula et al., 2016; Ti et al., 2016; Vemu et al., 2017; Ayukawa et al., 2021). Thus, directly testing the role of tubulin isotypes in the multi-tubulin hypothesis has been challenging. Eukaryotic microorganisms served as pioneering model systems to investigate the function of tubulin isotypes. These organisms offer the tractability and accessibility needed to address the question. While advances in genome editing and recombinant tubulin purification have alleviated some of the constraints and challenges in more complex, higher eukaryotes, microorganisms continue to offer advantages for elucidating the fundamental mechanisms of tubulin isotypes. Microorganisms harbor conserved MT

TABLE 1 | Multiple tubulin isotypes are expressed in model microorganisms*

Model microorganism	Division/ Phylum	Tubulin isotypes/subunit				References
		alpha-tubulin genes		beta-tubulin genes		
Saccharomyces cerevisiae	Ascomycota	2	*TUB1, TUB3*	1	*TUB2*	Neff et al. (1983), Schatz et al. (1986a), Schatz et al. (1986b)
Schizosaccharomyces pombe	Ascomycota	2	*nda2, atb2*	1	*nda3*	Hiraoka et al. (1984), Toda et al. (1984)
Tetrahymena thermophilus	Ciliophora	4	*ATU1, ALT1-3*	8	*BTU1, BTU2, BLT1-6*	Callahan et al. (1984), Suprenant et al. (1985), Gaertig et al. (1993), Eisen et al. (2006)
Aspergillus nidulans	Ascomycota	2	*tubA, tubB*	2	*benA, tubC*	Sheir-Neiss et al. (1978), Morris et al. (1979), Morris et al. (1984), May et al. (1987); Doshi et al. (1991)
Fusarium graminearum	Ascomycota	2	*FgTUB4, FgTUB5*	2	*FgTUB1, FgTUB2*	Lu et al. (2000), Zhao et al. (2014)
Chlamydomonas reinhardtii	Chlorophyta	2	*tua1, tua2*	2	*tub1, tub2*	Minami et al. (1981), Silflow and Rosenbaum (1981), Brunke et al. (1982b), Youngblom et al. (1984); James et al. (1993)
Physarum polycephalum	Amoebozoa	5	*altA, altB(N), altB(E), altC, altD*	3	*betA, betB, betC*	Burland et al. (1983), Burland et al. (1984), Burland et al. (1988); Schedl et al. (1984b), Krämmer et al. (1985); Singhofer-Wowra et al. (1986), Monteiro and Cox (1987a), Monteiro and Cox (1987b), Green et al. (1987), Singhofer-Wowra and Little (1987), Solnica-Krezel et al. (1988), Werenskiold et al. (1988)
Toxoplasma gondii	Apicomplexa	3	α_1, α_2, α_3	3	β_1, β_2, β_3	Nagel and Boothroyd (1988), Hu et al. (2006), www.toxodb.org

*In ***Table 1***, gene names are presented using organism-specific syntax.*

structures, governed by homologous regulators (PTMs and MAPs), that perform functions analogous to their higher eukaryotic counterparts. They are highly tractable, allowing ease of genetic manipulation, quantification of MT-dependent processes, and in some, continuous monitoring of individual MTs during these processes. Some use relatively fewer tubulin isotypes and offer a simplified landscape (**Table 1**) (Toda et al., 1984; Schatz et al., 1986a) while many, like their higher eukaryotic counterparts, employ many isotypes despite their unicellular status (Suprenant et al., 1985; Eisen et al., 2006). Moreover, some microorganisms such as budding yeast do not utilize any or very few PTMs, further simplifying the interpretation of tubulin isotype manipulation. Indeed, the study of single isotypes, expressed at levels comparable to total tubulin isotypes in normal cells, has only been achieved using microorganisms (Nsamba et al., 2021).

Microorganisms played a critical role in the discovery of tubulin family genes and the initial characterizations of α and β tubulin isotypes. Genes encoding the tubulin family members γ (Oakley and Oakley, 1989), δ (Dutcher and Trabuco, 1998; Fromherz et al., 2004) and ε-tubulin (Goodenough and StClair, 1975; Dutcher et al., 2002) were first identified by exploiting model microorganisms. The latter two were also shown to be critical for cleavage furrow placement in *Chlamydomonas*. Moreover, beginning about 40 years ago it was recognized that most microorganisms harbor multiple isotypes of α and/or β tubulin. The tractability of model microorganisms facilitated pioneering research on tubulin isotypes. Although these early studies indicated that isotypes make distinct contributions to MT function, they also revealed relatively large redundancies among isotypes for basic MT processes. This redundancy, together with the technical limitations at that time, worked to dampened deeper exploration into tubulin isotype function in many models. In the last decade, however, a flurry of research in certain models like budding yeast, fission yeast and Tetrahymena, has yielded significant insights into the function of tubulin isotypes. The role of PTMs in regulating MT function is also becoming increasingly clear and has been reviewed recently (Wloga et al., 2017; Janke and Magiera, 2020). In this review we focus on what has been learned about the function of α- and β-tubulin isotypes using model microorganisms (**Tables 1**, **2**). We emphasize the trajectory of progress in budding yeast, as arguably the most studied system, along with what has been found in fission yeast and Tetrahymena. We summarize what is known in a range of other models to highlight the common aspects of significant redundancy coupled with unique contributions of tubulin isotypes, and the continuing opportunity to exploit these systems to learn how they facilitate the wide diversity of MT-dependent processes observed across biology. Together microorganisms hold significant potential to elucidate conserved, fundamental mechanisms by which tubulin isotypes underlie MT properties and function.

Saccharomyces cerevisiae

The initial purification of budding yeast tubulin in 1981 provided evidence, *via* 2-D gel electrophoresis, that the yeast cytoskeleton utilizes multiple tubulin isotypes (Kilmartin, 1981). Within 5 years, the full complement of one β-tubulin, *TUB2* (Neff et al., 1983), and two α-tubulin isotypes, *TUB1* and *TUB3* (Schatz et al., 1986a), was identified (**Table 1**). While the single β-tubulin is essential, the α-isotype genes are not equivalent in their ability to support viability. Cells survive disruption of *TUB3* but not *TUB1* (Schatz et al., 1986b). Northern blots with either gene as probe suggested that *TUB1* transcript was more prevalent than *TUB3*, although probe cross-hybridization prevented accurate quantification (Schatz et al.,

TABLE 2 | Microbial tubulin isotypes optimize and mediate differential organismal and cellular functions*.

Model microorganism	Tubulin isotypes possessing distinct functions		Functional significance of microbial tubulin isotypes
	alpha-tubulin genes	beta-tubulin genes	
Saccharomyces cerevisiae	*TUB1, TUB3*		***TUB1*:** Mitosis, meiosis, conjugation, benomyl hyper-resistance Schatz et al. (1986a); Schatz et al. (1986b), high MT dynamicity *in vitro* and *in vivo* Bode et al. (2003), Nsamba et al. (2021), Dyn1 mediated spindle positioning, Dyn1 pathway MAP localization Nsamba et al. (2021); ***TUB3*:** Benomyl hyper-sensitivity Nsamba et al. (2021), low MT dynamicity *in vitro* and *in vivo* Bode et al. (2003), Nsamba et al. (2021), Kar9 mediated spindle positioning, Kar9 pathway MAP localization Denarier et al. (2021); Nsamba et al. (2021).
Schizosaccharomyces pombe	*nda2, atb2*		***nda2*:** Karyogamy, nuclear positioning, duplicated centrosome migration, thiabendazole sensitivity Toda et al. (1981), Toda et al. (1983); Adachi et al. (1986), slower apparent rate constants for MT assembly, slower growth rate and lower critical concentration of MT polymerization *in vitro* Hussmann et al. (2016); ***atb2*:** spindle assembly checkpoint, heterodimer assembly Radcliffe et al. (1998), interphase MT dynamics, EB1/Mal3 localization Asakawa et al. (2006).
Tetrahymena thermophila	*ATU1,*	*BTU1, BTU2, BLT1, BLT4*	***ATU1*:** Cell viability Hai et al. (1999), ciliary and cytoplasmic MT generation Gu et al. (1995); ***BTU1*:** Cell viability Xia et al. (2000), ciliary and cytoplasmic MT generation Gu et al. (1995); ***BTU2*:** Cell viability Xia et al. (2000), ciliary MT generation Gu et al. (1995), enriched in somatic cilia and basal bodies Pucciarelli et al. (2012); ***BLT1*:** Macronuclear MT and spindle assembly, micronuclear meiotic spindle assembly during conjugation Pucciarelli et al. (2012); ***BLT4*:** Macronuclear MT and spindle assembly Pucciarelli et al. (2012).
Aspergillus nidulans	*tubA, tubB*	*benA, tubC*	***tubA*:** MT stability Gambino et al. (1984), karyokinesis, cell/nuclear morphology Doshi et al. (1991), asexual vegetative growth Oakley et al. (1987), Doshi et al. (1991), sexual development before the first meiotic division Kirk and Morris (1991); ***tubB*:** karyokinesis, cell/nuclear morphology Doshi et al. (1991); ***benA*:** MT instability Gambino et al. (1984), nuclear migration and karyogamy during vegetative growth Oakley and Morris (1980), Oakley and Morris (1981); Oakley and Rinehart (1985), benomyl hyper-sensitivity May (1989); ***tubC*:** conidiation May and Morris (1988), MT function during conidiation May et al. (1985), benomyl hyper-sensitivity May (1989).
Fusarium graminearum		*FgTUB1, FgTUB2*	***FgTUB1*:** Benzimidazole sensitive Chen et al. (2007), perithecia formation and sexual development Zhao et al. (2014), ascosporogenesis Zhao et al. (2014), Wang et al. (2019); ***FgTUB2*:** Benzimidazole resistance Chen et al. (2009), vegetative development Zhao et al. (2014), mycotoxin synthesis Wang et al. (2019).
Chlamydomonas reinhardtii *Physarum polycephalum*	*tua1, tua2* *altA, altB(N), altB(E),*	*tub1, tub2* *betA, betB, betC*	**each isoform:** differential anti-tubulin drug resistance Kato-Minoura et al. (2020). ***altA, altB(N), altB(E)*:** MT assembly in plasmodia and myxamoeba Burland et al. (1983), Roobol et al. (1984), Cunningham et al. (1993); Gerber et al. (2022), *altA* builds flagellar MTs via PTM in amoeba and flagellates Green and Dove (1984), Blindt et al. (1986), Diggins and Dove (1987), Sasse et al. (1987); ***betA*:** MT structure assembly during myxamoeba stage Burland et al. (1988), Diggins-Gilicinski et al. (1989), Gerber et al. (2022); ***betB*:** constitutively expressed in plasmodia and myxamoeba Werenskiold et al. (1988), Paul et al. (1989), benzimidazole resistance to both plasmodia and myxamoeba Burland et al. (1984); ***betC*:** anastral mitotic spindle assembly in plasmodia Burland et al. (1983), Roobol et al. (1984), Gerber et al. (2022), MT assembly in developing cells during amoeboid-plasmodial transition Solnica-Krezel et al. (1988).
Toxoplasma gondii	α_1, α_2, α_3	β_1, β_2, β_3	**α_1, β_1, β_2:** compose cortical MTs Wang et al. (2021), α_1 demonstrates dinitroaniline resistance Morrissette et al. (2004), Ma et al. (2007), Ma et al. (2010); **α_2, α_3:** potentially unique role(s) in conoid and flagellar axonemal MTs Morrissette (2015).

*In ***Table 2***, gene names are presented using organism-specific syntax.*

1986a). The idea that cells harbor more Tub1 than Tub3 subunits is consistent with the finding that although lethal, *tub1*Δ can be rescued by increased expression of *TUB3* (Schatz et al., 1986b). Yet, while *tub3*Δ cells can undergo mitosis, conjugation and meiosis, they display decreased spore viability and hypersensitivity to the microtubule destabilizer benomyl (Schatz et al., 1986b). Increased *TUB1* expression in *tub3*Δ cells rescues benomyl sensitivity, however, the sensitivity of *tub3*Δ cells made viable by additional *TUB3* was not determined (Schatz et al., 1986b). Combining the results of these studies, and the fact that *TUB1* and *TUB3* share 90% amino acid identity, but only ~73% with α-tubulins from porcine and fission yeast, it was proposed that they are functionally redundant, with the observed phenotypic effects

due to relative expression levels (Schatz et al., 1986a). Subsequent studies supported the observation of more Tub1 relative to Tub3 in soluble protein extracts and purified tubulin (Bode et al., 2003; Hanson et al., 2016; Aiken et al., 2018), but it would be 35 years before a more detailed analysis of Tub1 and Tub3 function *in vivo* was reported (Nsamba et al., 2021).

The yeast model has been exploited to investigate the regulation of cellular tubulin levels. It was initially shown that Tub1 (α-tubulin) and Tub2 (β-tubulin) polypeptide levels do not increase proportionally with gene copy number. In cells harboring extra copies of either *TUB1* or *TUB1* plus *TUB2*, expression was found to be downregulated at both the transcript and polypeptide levels, such that cells contained near normal levels of Tub1, Tub2 and Tub3 protein (Katz et al., 1990). In contrast to downregulation, budding yeast appear incapable of upregulating tubulin expression when needed. In diploid *TUB2*/*tub2*Δ hemizygous cells, Tub2 protein levels are approximately half that seen in normal *TUB2*/*TUB2* cells. Moreover, both Tub1 and Tub3 α-tubulin protein levels were concomitantly reduced by 50% (Katz et al., 1990). Similarly, total α-tubulin levels are reduced in *tub3*Δ cells (Hanson et al., 2016; Aiken et al., 2018; Denarier et al., 2021; Nsamba et al., 2021), and although *tub1*Δ cells are inviable, they are rescued by increased *TUB3* expression (Schatz et al., 1986b).

Methods to purify native (Barnes et al., 1992) and recombinant (Davis et al., 1994) yeast tubulin, including use of affinity tags (Gupta et al., 2002) and overexpression (Johnson et al., 2011) have yielded critical insights into areas of tubulin structure-function (Gupta et al., 2002; Ayaz et al., 2012), modulation of microtubule dynamics by GTP hydrolysis (Davis et al., 1994), and the dynamic properties of each isotype in reconstitution assays (Bode et al., 2003). Relative to Tub3, microtubules polymerized entirely with Tub1 display increased catastrophe frequency and depolymerization rate, leading to overall higher dynamicity. Microtubules containing a mixture of Tub1 and Tub3 α-subunits have properties intermediate to those made exclusively from Tub1 or Tub3. Thus, the benomyl sensitivity seen in *tub3*Δ cells could arise, at least in part, from the decreased stability of exclusively Tub1 microtubules. SDS-PAGE also showed that mixtures purified from wildtype cells contain ~80% Tub1 and 20% Tub3 (Bode et al., 2003). Consistent with this observation, western blots of soluble cell lysates from *tub3*Δ cells have ~70% of wildtype α-tubulin levels (Hanson et al., 2016), while those from wildtype cells show ~70% Tub1 and 30% Tub3 (Aiken et al., 2018).

With the advent of Green Fluorescent Protein, independent groups concurrently showed that GFP-Tub1 (Straight et al., 1997) and GFP-Tub3 (Carminati and Stearns, 1997) both incorporate into all microtubule structures during vegetative growth. As in other organisms, this technical advance greatly facilitated the elucidation of mechanisms controlling microtubule regulation and organization. At the tubulin molecular level, significant attention has focused on the highly variable carboxy-terminal tail (CTT). The CTT of α-tubulin is important for + TIP protein binding to microtubules and dynein-mediated nuclear movements (Badin-Larçon et al., 2004). It is also involved in membrane-bound cargo trafficking (Boscheron et al., 2016). On β-tubulin, the CTT is a critical mediator of kinesin-5 interaction (Aiken et al., 2014) and needed for accurate chromosome segregation (Fees et al., 2016). Considering these findings and the unique synthetic genetic interactions identified for either α-isotype (Nsamba et al., 2021) it is possible the CTTs of Tub1 and Tub3 possess isotype-specific properties.

Two recent studies address the function of Tub3 *in vivo*. Both examined Tub1 level in *tub3*Δ cells and found it to be between 37%–64% (Denarier et al., 2021) and ~50% (Nsamba et al., 2021) of the total α-tubulin level in wildtype cells. Consistent with these results, the *TUB1* and *TUB3* transcript levels are equivalent in wildtype cells, and *TUB1* mRNA level unchanged in *tub3*Δ cells (Nsamba et al., 2021). Quantitative imaging of mRUBY-Tub1 and mRUBY2-Tub3 also indicates that they constitute equal proportions of the α-tubulin pool (Denarier et al., 2021). At present, the discrepancy in Tub1 to Tub3 ratios between these results and previous studies remains unclear. One explanation for more Tub1 in purified mixtures and prior immunoblot analyses could be that Tub1-containing tubulin heterodimers are more successfully extracted in non-denaturing buffers and/or more tolerant of purification procedures compared to those containing Tub3. Another, more interesting possibility is that the isotypes may be independently regulated under the conditions used for the various experiments.

Cells respond differently to high overexpression of Tub1 or Tub3. Whereas expressing *TUB1* from the strong GAL1 promoter is well tolerated (Burke et al., 1989), expressing *TUB3* from the strong TEF1 promoter results in tiny colonies with sickly cells (Denarier et al., 2021). Notably, cells overexpressing *TUB3* as their sole source of α-tubulin display nearly double the typical number of microtubules in pre-anaphase spindles, emanating from significantly enlarged spindle pole bodies (Denarier et al., 2021). The increased SPB diameter is larger than would be predicated for the somewhat slower spindle assembly in these cells (Denarier et al., 2021), and thus may be a direct consequence of the increased Tub3. Additionally, localization of the negative dynein regulator, She1, to spindles containing exclusively Tub3 is increased 62% compared to spindles in wildtype cells (Denarier et al., 2021). She1 also shows increased localization, albeit slightly, to Tub3 compared to Tub1 microtubules *in vitro* (Denarier et al., 2021). Thus, the highly increased localization seen *in vivo* could be indicative of Tub3-specific mechanisms, but may also result from more microtubules present in the Tub3 spindles (Denarier et al., 2021).

During budding yeast mitosis, the spindle must be positioned across the bud neck (**Figure 2**), which is accomplished by two major and functionally redundant mechanisms (McNally, 2013). Prior to anaphase, the Kar9 mechanism links MT plus ends to myosin-dependent transport along polarized actin cables to position the spindle at the bud neck. During anaphase, the Dyn1 mechanism utilizes bud membrane-localized dynein movement along astral MTs to pull one spindle pole into the bud. Cells can tolerate the loss of either mechanism, but complete loss of both is lethal (Miller et al., 1998). While strong overexpression of *TUB3* as the sole α-tubulin makes cells significantly sick, and additional removal of Kar9 further decreases fitness, *dyn1Δ* reduces fitness comparably more than

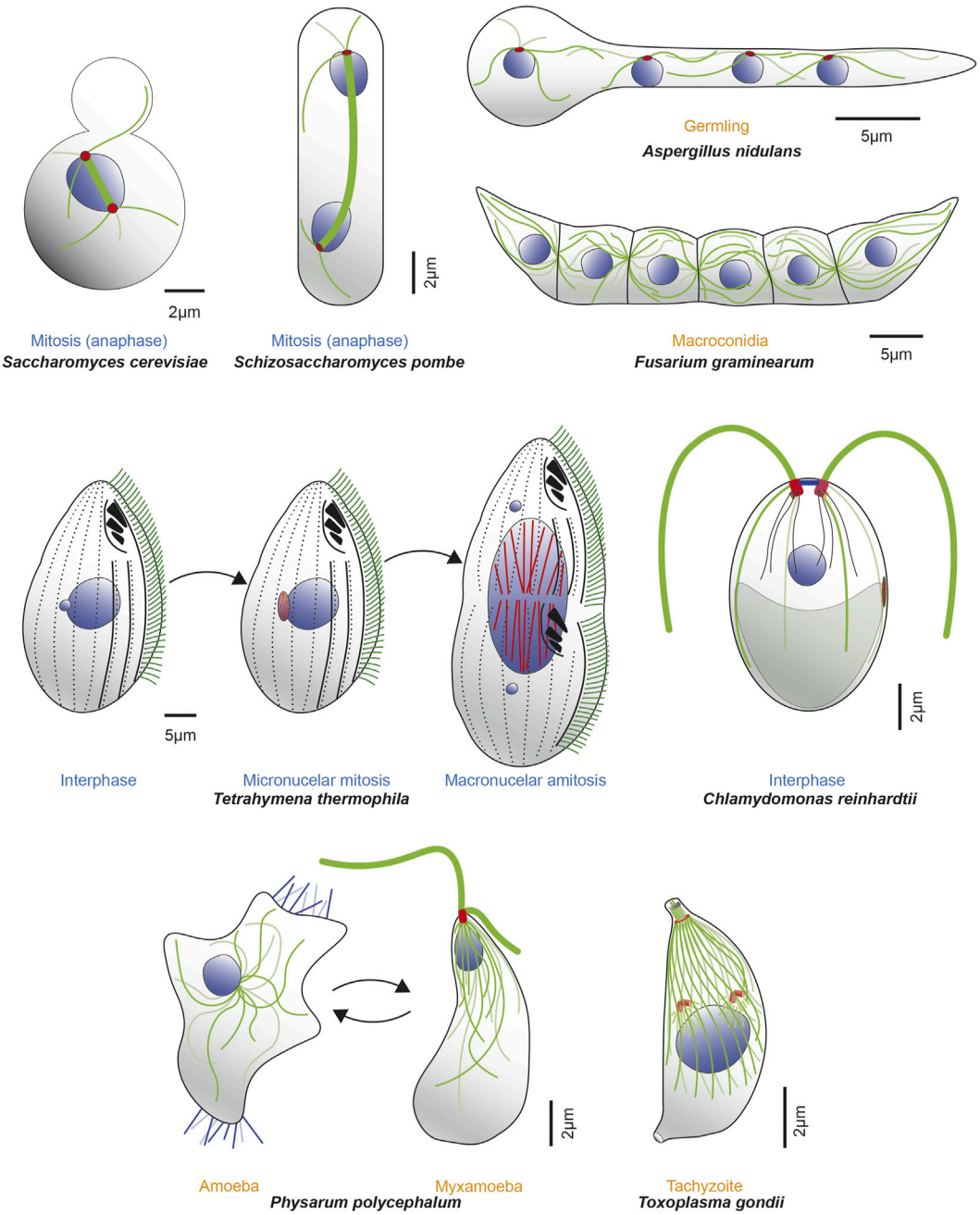

FIGURE 2 | Microorganisms express one or more α- and β-tubulin isotypes to construct various MT-organelles and to perform diverse functions with a range of complexity. Example microorganisms are represented in either different cell cycle (blue text) or life cycle (orange text) stages, along with MTs (dark and light green lines), mitotic spindle (thick green line), nuclei (blue) and corresponding MTOCs (red). Top row (from left to right, clockwise): schematics of mitotic *S. cerevisiae* in anaphase; mitotic *S. pombe* in anaphase; tetranucleate, interphase *Aspergillus nidulans* germling (germinated from conidia, an asexual, uninucleate spore produced during vegetative life cycle. Septa are not formed until third karyokinesis) and infectious *F. graminearum* multicellular macroconidia, the translucent, canoe-shaped asexual spores possessing 4–5 septa and derived from phialides, the conidium producing cells. Middle row (left): *T. thermophilus* undergoing cell division and demonstrating distinct localization of β-tubulin isotypes. Btu2 is enriched in somatic cilia (green lines on cell surface) and basal bodies (black dots beneath each cilium on cell surface; not all cilia are shown). Blt1 and Blt4 construct the spindle (red lines) in the mitotic division of the micronucleus (smaller blue circle) and also assemble MTs (red lines) during amitotic division of the macronucleus (large blue circle). Middle row (right): *C. reinhardtii* in interphase, showcasing diverse MT organelles including the two apical flagella (thick green lines projecting outward) and 4 MT rootlets (thinner green and light green lines emerging from basal bodies within the cell), which contains stable, acetylated α-tubulin. The mother (red) and daughter (dark red) basal bodies, several nucleus-basal body connectors (black lines), eyespot (brown) and chloroplast (grey object at cell posterior) are also shown. Bottom row (left): *P. polycephalum* depicted in respective amoeba and flagellate stages. The uninucleate amoeba (left) have unorganized MTs (green lines), randomly positioned nucleus (blue circle) with filopods (blue lines extending from the cytoplasm) that contributes to multidirectional movements. It reversibly transitions to the uninucleate, comma-shaped, flagellated, sexual spore myxamoeba (right). This phase demonstrates an anterior and posterior flagellum (thick green

(*Continued*)

FIGURE 2 | lines; anterior longer than posterior) that emanates from the basal body (red) as well as a flagellar cone of MTs (thinner green lines in conical arrangement, emanating from the apical basal body) that can extend to the dorsal side of the organism. The beak-shaped nucleus (blue) is positioned underneath the cone. Bottom row (right): *T. gondii* tachyzoite demonstrates a diverse array of complex MT-organelles. The spindle MTs (green lines) and the corset of 22 subpellicular MTs respectively nucleate from the centrioles (orange cylinders above the blue nucleus) and the Apical Polar Ring (APR) MTOC (orange circle at apical part of the cell). Also shown are the tubulin-based hollow cylindrical conoid (green cylinder above the APR), two preconoidal rings (grey circles) above it and two intraconoid MTs (green lines) within its circumference.

kar9Δ, suggesting the Kar9 spindle positioning mechanism may be preferentially compromised in these cells (Denarier et al., 2021). It will be interesting to learn the comparable phenotypes of cells overexpressing Tub1 as their sole source of α-tubulin.

Although *tub3*Δ cells survive with their α-tubulin coming only from the *TUB1* locus, they do not survive if the *TUB3* ORF is moved into the *TUB1* locus, under regulation of the endogenous *TUB1* regulatory elements (Nsamba et al., 2021). Conversely, while *TUB3* cannot support viability in *tub1*Δ cells, viability is restored when the *TUB1* ORF is placed in the *TUB3* locus, under regulation of the *TUB3* regulatory elements. These ORF swapping results suggest that Tub1 likely can support one or more essential processes at lower concentrations than Tub3 is able. Placing the ORF of either α-tubulin isotype into both loci created cells expressing near wildtype levels of exclusively Tub1 or Tub3. Unlike cells strongly overexpressing Tub3 (Denarier et al., 2021), both Tub1-only and Tub3-only strains expressing normal overall α-tubulin levels grow at wildtype rates (Nsamba et al., 2021). While *tub3*Δ cells are benomyl supersensitive, restoring proper α-tubulin levels with extra Tub1 produces more resistance than in wildtype cells (Schatz et al., 1986b). In contrast, Tub3-only cells expressing proper overall α-tubulin levels are highly sensitive (Nsamba et al., 2021). These opposite sensitivities suggest that, like *in vitro* (Bode et al., 2003), microtubules polymerized from either α-tubulin isotype have different functional properties in cells. Indeed, the Dyn1-mediated mechanism is more efficient on Tub1-only microtubules, while the Kar9 mechanism works better using Tub3 (Nsamba et al., 2021). Because each mechanism is optimized by a particular isotype, the microtubules containing both Tub1 and Tub3 in wildtype cells can sufficiently perform both processes. These results demonstrate that the differences in isotype properties can be leveraged to optimize the molecular mechanisms required to achieve diverse microtubule-dependent processes. Consistent with this idea, half of the ~60 synthetic genetic interactions each displayed by Tub1 or Tub3 are in common, while the other half are unique to either isotype, suggesting they differentially mediate additional functions beyond spindle positioning (Nsamba et al., 2021).

Altogether, pioneering work in budding yeast revealed a high level of redundancy between tubulin isotypes, although with some detectable influence on cellular phenotypes. Continued efforts and technical advances have more recently demonstrated that these isotype-specific properties play a significant role in differentially mediating various MT-dependent cellular processes. The budding yeast model is well positioned for further elucidation of the molecular mechanisms of tubulin isotypes.

Schizosaccharomyces pombe

Following the groundbreaking studies in budding and fission yeast that uncovered the cell-division cycle (CDC) genes as temperature sensitive mutants (Hartwell et al., 1973; Nurse, 1975), the fission yeast β-tubulin [*NDA3*; (Hiraoka et al., 1984)] and one of two α-tubulins [*NDA2*; (Toda et al., 1984)] were identified as cold sensitive nuclear division arrested mutants (**Table 1**) (Toda et al., 1983). Hybridization assays using the newly discovered *Chlamydomonas* α-tubulin cDNA (Silflow and Rosenbaum, 1981) as a probe soon revealed the second, and full complement of α-tubulins in fission yeast [*ATB2*; (Adachi et al., 1986)].

Similar to the situation in budding yeast, the α-tubulin genes in fission yeast are not equivalent in their ability to support viability. Disruption of *NDA2* renders cells inviable, while cells lacking *ATB2* continue to grow at normal rates in rich media but are hypersensitive to the microtubule destabilizer thiobendazole (Adachi et al., 1986). Like Tub3 in budding yeast, increased expression of *ATB2* can rescue cell viability in the absence of *NDA2* (Toda et al., 1984). Although *NDA2* mRNA level was observed to be significantly higher than *ATB2* transcript, at the protein level the two isotypes were observed to be equivalent (Adachi et al., 1986). Consistent with this, equivalent amounts Nda2-and Atb2-containing heterodimers are present in purified tubulin (Drummond et al., 2011). It should be noted however, that studies have also reported higher Nda2 relative to Atb2 by western blot (Radcliffe et al., 1998). Moreover, increased expression of *ATB2* mRNA induces a decrease in *NDA2* transcript level yet the inverse, increased *NDA2* expression does not cause decreased *ATB2* transcript (Adachi et al., 1986). Again, like what may occur in budding yeast, these latter two findings raise the possibility that the isotype ratio may be regulated under various culture conditions or cell cycle stages.

Despite their ability to support viability, there are indications that *NDA2* and *ATB2* are functionally distinct. Both isotypes are present at equivalent levels, at least under some conditions (Adachi et al., 1986), yet only one supports viability without increased expression (Toda et al., 1984; Adachi et al., 1986). While *ATB2* is non-essential, temperature sensitive alleles can disrupt processes including the spindle assembly checkpoint and nuclear movement (Radcliffe et al., 1998). They are also lethal in combination with cold sensitive *NDA2* alleles at permissive temperature, demonstrating *ATB2* is capable of influencing microtubule functions (Radcliffe et al., 1998). Moreover, as seen with budding yeast α-tubulin isoforms (Bode et al., 2003), Nda2 and Atb2 display distinct effects on microtubule dynamics *in vitro*. Microtubules assembled from only Nda2-containing heterodimers have slower apparent rate constants for MT assembly, slower growth rate and lower critical concentration of polymerization compared to polymers containing both Nda2 and Atb2 (Hussmann et al., 2016). Similar comparisons *in vivo* remain to be done.

The parallels observed thus far between α-tubulin isotypes in *S. cerevisiae* and *S. pombe* are striking. With the recent discoveries of how Tub1 and Tub3 differ functionally (Denarier et al., 2021; Nsamba et al., 2021), the stage is now set to investigate whether Nda2 and Atb2 differentially mediate microtubule functions as well. Like budding yeast, fission yeast is a preeminent model for the study of MAPs and regulatory factors controlling microtubule dynamics, organization, and function. Notably, how microtubules are used to support cell polarity and center the mitotic spindle in *S. pombe*, in contrast to positioning the spindle across the bud neck in *S. cerevisiae* (**Figure 2**), will likely reveal additional mechanisms by which tubulin isotypes contribute to diverse biological processes.

Tetrahymena thermophila

T. thermophila is a unicellular, ciliated, protozoan that offers multiple advantages for studying tubulin isotypes. It uses four α- and eight β-tubulin isotypes to assemble a diverse set of spatiotemporally distinct microtubule-containing structures (**Figure 2**) (Suprenant et al., 1985; Gaertig et al., 1993; Gaertig, 2000) involved in processes including ciliary motility, cell division, conjugation, cell shape maintenance and oral apparatus organization (**Table 1**) (Williams, 1975). Notably, some of these functions are absent in other common microbial systems like yeast.

The first *Tetrahymena* α-tubulin gene, *ATU1*, was found by probing digested macronuclear DNA with heterologous α-tubulin probes from chicken, *Drosophila*, and *Chlamydomonas* (Callahan et al., 1984). Within a year, seven distinct isoelectric variants of tubulin polypeptides were identified: five α and two β although it was unclear whether each represented a gene or PTM (Suprenant et al., 1985). Of the five α-tubulin variants, three are present exclusively in ciliary, and the other two exclusively in cytoplasmic microtubules. While ciliary microtubules contain both β variants, cytoplasmic microtubules possess only a single variety. Two β-tubulin genes, *BTU1* and *BTU2,* were subsequently identified but found to encode identical polypeptides (Gaertig et al., 1993). Deletion of the α-subunit, *ATU1* (Hai et al., 1999), or simultaneous loss of both β-tubulin genes (Xia et al., 2000) is lethal. The idea that a single α- and β-tubulin polypeptide generated multiple isoelectric variants and supported the diverse array of structures in *Tetrahymena* focused attention on posttranslational modifications. These efforts revealed that α-tubulin in ciliary MTs is acetylated on the highly conserved K40 (Piperno and Fuller, 1985). This PTM is non-essential in *Tetrahymena* (Gaertig et al., 1995) and initially purported to improve Kinesin-1 binding and motility (Reed et al., 2006), but later reported that this effect may be indirect (Walter et al., 2012). Similarly, glutamylation was discovered (Bré et al., 1994) and later found to be non-essential but important for assembly and function of certain organelles such as the basal body (Wloga et al., 2008) as well as force generation by ciliary dynein (Suryavanshi et al., 2010). While both α- and β-tubulins are polyglycylated, only the α-tubulin modification was found to be dispensable (Xia et al., 2000; Thazhath et al., 2002). The majority of α-tubulin isotypes also undergo detyrosination (Redeker et al., 2005). Altogether these studies demonstrate the role of PTMs in mediating distinct MT functions and support their role in the multi-tubulin hypothesis.

The importance of the C-terminal tails of α- and β-tubulins was also investigated and both were found to be essential. Interestingly, while the absence of a tail on either α- or β-tubulin is not tolerated, the tails are interchangeable in that cells grow normally with either an α-or β-tail on both subunits (Duan and Gorovsky, 2002). Moreover, a modified α-tail supports viability when paired with a β-tail lacking posttranslational modification sites but not with a deletion of the β-tail, suggesting the tails themselves have essential roles independent of PTMs (Duan and Gorovsky, 2002). During this period, it was also recognized that when cells are deciliated, transcription of the α-tubulin, *ATU1*, and both β-isotypes, *BTU1* and *BTU2*, is induced, but when cytoplasmic microtubules are perturbed only *ATU1* and *BTU1* are induced (Gu et al., 1995). These data were amongst the earliest demonstrations of tubulin gene/isotype-specific response in cells and perhaps, unsuspectingly, foretold the isotype-localization results from *Tetrahymena* that would strongly support the multi-tubulin hypothesis (Pucciarelli et al., 2012).

Our understanding of tubulin isotype function in *Tetrahymena* changed dramatically when shotgun sequencing of the 104 Mb macronuclear genome revealed three additional α-tubulin and six more β-tubulin genes, named α-like tubulin (*ALT*) and β-like tubulin (*BLT*), respectively (Eisen et al., 2006). The *ALT*'s and *BLT*'s lack the characteristic polyglutamylation and polyglycylation PTM motifs on their CTTs that otherwise serve essential roles for their canonical counterparts. The discovery of multiple α- and β-tubulin isotypes further illuminated how this single celled organism assembles and controls diverse microtubule structures. Finally, a groundbreaking study demonstrated unique utilization of specific β-isotypes (Pucciarelli et al., 2012). Using live cell imaging of GFP-tagged tubulins and biochemical fractionation assays, Btu2 was shown to be highly enriched in somatic cilia and basal bodies, while Blt1 and Blt4 appear to be absent. Moreover, the latter two, but not Btu2 are used to assemble microtubules in the macronucleus as well as mitotic spindle of the micronucleus during cell division. During conjugation, Blt1 is the only of the three isotypes to build the micronuclear meiotic spindle. *Tetrahymena* is positioned as a strong model to further elucidate the molecular mechanisms of tubulin isotypes and PTMs in governing MT functions.

Aspergillus nidulans

The filamentous ascomycote *A. nidulans* (**Figure 2**) served as an impressive pioneering model for the initial study of tubulins. Indeed, screens for sensitivity to benzimidazole, a MT destabilizer, initially uncovered *BENA* as the first known β-tubulin gene in any organism (Sheir-Neiss et al., 1978). Revertants of *ts-benA* mutants were leveraged to reveal *TUBA* (Morris et al., 1979), and two-dimensional electrophoresis using mutants of *BENA* or *TUBA* revealed the presence of at least one additional α- and β-tubulin gene (Morris et al., 1984). Its two α-tubulins, *TUBA* and *TUBB*, and two β-tubulins, *BENA* and *TUBC*, (Morris et al., 1984), were subsequently confirmed by

cloning (**Table 1**) (Sheir-Neiss et al., 1978; Morris et al., 1979, Morris et al., 1984; Gambino et al., 1984; May et al., 1987; Doshi et al., 1991).

Notably, the α- and β-tubulin isotypes display more variations than is typical within a species, with ~28 (Doshi et al., 1991) and ~18% (May et al., 1985; May et al., 1987) sequence divergence, respectively. Disruption of either the α-tubulin isotype *TUBA* or *TUBB* disrupts karyokinesis or results in abnormal cell/nucleus morphology, respectively (Doshi et al., 1991). They also operate distinctly in specific stages of the life cycle. While *TUBA* is essential during vegetative growth (Oakley et al., 1987; Doshi et al., 1991), *TUBB* is essential for development before the first meiotic division (Kirk and Morris, 1991). However, overexpression of either α-tubulin isotype largely rescues the deleterious effects from loss of the other (Kirk and Morris, 1993). Thus, although the two α-tubulins possess significant redundancy, the data suggest they harbor at least some function difference.

Disruption of either β-tubulin also produces differing phenotypes. *BENA* is essential for viability and required during vegetative growth for nuclear migration and nuclear division (Oakley and Morris, 1980, Oakley and Morris, 1981; Oakley and Rinehart, 1985). On the other hand, although *TUBC* expression specifically increases during conidiation, the process of forming and reproducing via spores without conjugation (May and Morris, 1988), and affects MT function during this process (May et al., 1985), it is not essential during any part of the life cycle (May et al., 1985; Weatherbee et al., 1985). Moreover, placing *TUBC* behind the *BENA* promoter rescues the lethality of *BENA* loss, demonstrating the two isotypes have high redundancy (May, 1989). The resulting hypersensitivity to the MT destabilizer benomyl, however, reveals that like their α-tubulin counterparts, *TUBC* and *BENA* have at least some functional difference (May, 1989). Consistent with observations in other organisms, the results reveal that tubulin isotypes in *A. nidulans* share a high level of redundancy yet suggest they also impart unique aspects to MT function.

Fusarium graminearum

F. graminearum, the anamorph of the notorious filamentous ascomycete, *Gibberella zeae*, is known for causing the economically devastating fusarium head blight (**Figure 2**) [reviewed in (Sutton, 2009; Leplat et al., 2013)]. Like *A. nidulans*, this fungus has two β-tubulin isotypes *FgTUB1* and *FgTUB2* (Lu et al., 2000) along with two α-tubulin isotypes *FgTUB4* and *FgTUB5* (**Table 1**) (Zhao et al., 2014). Following the observation that mutations in single genes result in resistance to the benzimidazole fungicides (Yuan and Zhou, 2005), both β-tubulin genes were screened for related mutations. Interestingly, despite high sequence identity with benzimidazole-resistant tubulins from other filamentous fungi, *FgTUB1* failed to display any causative mutations for resistance (Chen et al., 2007). Conversely, *FgTUB2* readily generated benzimidazole-resistant mutations (Chen et al., 2009; Liu et al., 2013). Altogether these findings indicate that the two β-tubulins in *F. graminearum* likely have distinct functional roles in the cell, or possibly different benzimidazole-binding properties, and suggest that individual tubulin isotypes can have cell context-specific interactions and/or functions that cannot be bridged by alternative isotypes.

Consistent with distinct functions, phylogenetic analysis indicates the β-tubulin isotypes in *F. graminearum* are under divergent selection pressure (Zhao et al., 2014). As a result, there are major amino acid divergences between them in the regions of GTP binding, intradimer interface, and the MT surface which could manifest as differences in properties including MT dynamicity and MAP interactions (Tassan and LeGoff, 2004; Luo et al., 2014). Loss of *FgTUB2* causes more severe growth defects than *FgTUB1*, but since only the loss of *FgTUB1* results in sterile perithecia (spore-producing fruiting body), it alone is essential for ascosporogenesis, or spores resulting from sexual reproduction (Zhao et al., 2014). It was recently found that although both β-tubulins have similar localization in all life cycle stages and overlapping functions during vegetative growth, they differ in their ability to support mycotoxin production (Wang et al., 2019). Additionally, while the transcription and translation of *FgTub1* increases in response to *FgTUB2* deletion, the opposite is not true. These data indicate that the tubulin isotypes in *F. graminearum* make distinct contributions to MT-dependent processes.

Chlamydomonas reinhardtii

C. reinhardtii, a unicellular, biflagellated, photosynthetic algae, is a proven model to study cell motility, cytoskeleton biology, and intraflagellar transport. Interestingly, despite harboring a subset of relatively complex MT structures (**Figure 2**), its pair of α-tubulin (*TUA1* and *TUA2*) and pair of β-tubulin (*TUB1* and *TUB2*) isotypes (Minami et al., 1981; Silflow and Rosenbaum, 1981; Brunke et al., 1982b) each encode identical protein products (**Table 1**) (Youngblom et al., 1984; James et al., 1993). The diversity of MT structures formed in *Chlamydomonas* from a single α- and β-tubulin polypeptide directed efforts toward PTMs. Very early in tubulin investigation the α-tubulin composition in *Chlamydomonas* was found to differ isoelectrically between axonemes and the cell body (Witman et al., 1972; Brunke et al., 1982a). The fact that *TUA1* and *TUA2* encode identical proteins, together with the finding that they are equally expressed (Witman et al., 1972; Brunke et al., 1982b; McKeithan et al., 1983), reinforced the finding that α-tubulin is differentially acetylated in the two compartments (L'Hernault and Rosenbaum, 1983, L'Hernault and Rosenbaum, 1985; McKeithan et al., 1983; Piperno and Fuller, 1985). This acetylation, which can be reversed during flagella resorption (L'Hernault and Rosenbaum, 1985), may also be important for proper photoreceptor localization (Mittelmeier et al., 2011). Within properly formed axonemes, polyglutamylation of α- and/or β-tubulin subunits regulates the function of inner-arm dyneins to control flagellar motility by modulating MT-dynein interactions (Kubo et al., 2010, Kubo et al., 2012). Together these data illustrate the importance of tubulin PTMs and MT regulators, and demonstrate that a single α- and β-tubulin isotype are capable of building a range of diverse MT structures.

Moreover, the ability to readily fractionate subcellular structures such as axonemes makes this an ideal model to

study the effects of various PTMs and MAPs on the MTs within (Orbach and Howard, 2019). Because the genes for each pair of isotypes encode identical polypeptides, screening for mutants with specific effects has been challenging. To overcome this, strains harboring single deletions of each tubulin isotype alone, as well as *tua1-tub1* and *tua2-tub1* in combination, were recently created (Kato-Minoura et al., 2020). Notably, the growth rate among the mutants is comparable, as is flagellar length and rate of growth following deflagellation. These deletion strains exhibit differing sensitivities to MT disrupting compounds and serve as more tractable platforms for uncovering tubulin mutations further altering drug sensitivity (Kato-Minoura et al., 2020). Such single isotype strains could also facilitate the investigation of PTMs and other regulatory mechanisms in the function of MT structures found in *Chlamydomonas*.

Physarum polycephalum

P. polycephalum, a myxomycete or acellular slime mold, is a protist that harbors a relatively large complement of tubulin isotypes: five α-tubulins [*ALTA*, *ALTB(N)*, *ALTB(E)*, *ALTC*, *ALTD*] (Burland et al., 1983; Schedl et al., 1984b; Krämmer et al., 1985; Singhofer-Wowra et al., 1986; Green et al., 1987; Monteiro and Cox, 1987a, Monteiro and Cox, 1987b) and three β-tubulins (*BETA*, *BETB*, *BETC*) (**Table 1**) (Burland et al., 1984; Singhofer-Wowra et al., 1986; Burland et al., 1988; Solnica-Krezel et al., 1988; Werenskiold et al., 1988). This pool of tubulin isotypes is used to support a range of MT-structures and functions in this simple protist. The isotypes are differentially expressed and incorporated into MT structures at different life cycle/ploidy phases (**Figure 2**) of this organism, namely- 1) the multinucleated, unicellular plasmodium (diploid), 2) the uninucleate, unicellular myxamoeba (haploid), 3) the motile flagellate stage (also haploid), and 4) sclerotium (a compact formation of haploid spores) (Dove and Rusch, 1980; Schedl et al., 1984b). This tubulin complement builds astral, spindle, centriole, and flagellar MTs in myxamoeba; but constructs only intranuclear, anastral mitotic spindles in the multinucleated cell stage known as coenocytic plasmodia, which lacks cytoplasmic MTs (Havercroft and Gull, 1983; Solnica-Krezel et al., 1991).

Expression of the α-tubulin isotypes is differentially regulated in various life stages of *Physarum*. Despite having only 1 MT organelle, the anastral mitotic spindle, in the coenocytic plasmodia stage, more tubulin isotypes were found to be definitively expressed in this stage [*ALTA*, *ALTB(N)*, *ALTB(E)*, *BETB*, *BETC*] than the amoeba-like myxamoeba stage (*ALTA*, *BETA*, *BETB*) (Burland et al., 1983; Roobol et al., 1984; Gerber et al., 2022). Although the α-tubulin population contains two isoelectric variants, one was found to originate via acetylation of AltA (Green and Dove, 1984; Blindt et al., 1986; Diggins and Dove, 1987; Sasse et al., 1987), leaving only one major α-isotype expressed in the myxamoeba phase (Singhofer-Wowra and Little, 1987). While *ALTB(E)* encodes one of the two major α-tubulin isoelectric variants in plasmodia, the remaining four α-tubulin genes, and particularly *ALTC* and *ALTD*, potentially encode the other isoelectric variants (Cunningham et al., 1993).The single α-tubulin expressed in myxamoeba was also found to be less prone to mutation (Singhofer-Wowra et al., 1986) than its more divergent and multiple plasmodial counterparts (Krämmer et al., 1985). This suggests that the tubulin mutational rate may be limited by the structural constraints of highly conserved MT structures like the axoneme, which is present in myxamoeba and not the plasmodial phase, but also supports the idea that utilizing multiple tubulin isotypes allows individual isotypes to more readily coevolve with specific MT-dependent processes. In plasmodia, *ALTA*, *ALTB(N)*, *ALTB(E)*, *BETB*, and *BETC* are synthesized coordinately with mitosis, but after spindle disassembly the synthesis of *BETC* is reduced significantly more than *BETB* (Schedl et al., 1984a). While all these isotypes are incorporated into the intranuclear mitotic spindle (Paul et al., 1987), it remains unknown whether the α-tubulin isotypes are functionally interchangeable or not (Green et al., 1987).

Of the three β-tubulin isotypes, *BETA* and *BETC* are exclusively expressed and incorporated into MT structures of the myxamoeba and plasmodia stages, respectively (Burland et al., 1988; Diggins-Gilicinski et al., 1989; Gerber et al., 2022). On the other hand, *BETB* is constitutively expressed during both the myxamoeba and plasmodia phases (Werenskiold et al., 1988) and incorporated into all MT structures (Paul et al., 1989). Consistent with its expression profile, mutation in *BETB* alone can adequately confer benzimidazole resistance to both plasmodia and myxamoeba (Burland et al., 1984). Interestingly, akin to tubulins in budding yeast that do not construct complex MT organelles, *Physarum* plasmodial *BETC*, which also constructs only one MT-structure, i.e., the anastral mitotic spindle, potentially has fewer functional constraints. (Solnica-Krezel et al., 1988; Solnica-Krezel et al., 1991).Indeed, *BETC* has the most divergent sequence relative to the other two β-tubulin isotypes owing to neutral drift and/or positive selection for operating in plasmodial spindles (Diggins-Gilicinski et al., 1989). This suggests the requirement to participate in multiple MT-mediated processes may select for a high level of redundancy among an organism's isotypes. Although it is absent in myxamoeba, *BETC* is still found in the astral spindles produced in developing cells during the amoeboid-to-plasmodial transition (Solnica-Krezel et al., 1988). Therefore, whether *BETC* has a specific role(s) in anastral spindles remains obscure.

Overall, the *Physarum* model offers the opportunity to explore redundancies and functional differences of tubulin isotypes in morphologically, phenotypically and genetically compartmentalized life cycle stages. Its tubulin isotypes display unique expression profiles and function in distinct, isolatable life stages. While research into *Physarum* tubulin isotypes has not progressed recently, much more remains to be explored.

Toxoplasma gondii

T. gondii is an obligate intracellular parasite capable of infecting nucleated cells and causing serious complications, including birth defects and blindness in human and animal hosts (Halonen and Weiss, 2013). Despite displaying a diverse array of MT structures (**Figure 2**) in various life cycle stages (Morrissette and Sibley, 2002; Hu et al., 2006), it was initially thought to contain just one α-tubulin and one β-tubulin gene (Nagel and Boothroyd, 1988). Relatively recently, genomic data (www.toxodb.org) revealed two

additional α- and β-tubulin isotypes, bringing the total to three each (**Table 1**) (Hu et al., 2006). Additionally, both α- and β-subunits harbor extensive PTMs (Xiao et al., 2010). Proteomic and transcriptomic data indicate that all six isoforms are expressed in tachyzoites and oocyst stages, yet α3 alone appears to have low expression in both stages (Hu et al., 2006; Xiao et al., 2010). The only isoforms detected in the cortical MT array by mass spectrometry analysis were α1, β1 and β2 (Wang et al., 2021), indicating that they potentially are the major isoforms expressed and/or enriched in this subpopulation. While the three β-tubulin isotypes have very high conservation (~97% amino acid identity), the α-tubulins are quite diverse (40%–68% identity) (Xiao et al., 2010; Wang et al., 2021), strongly implying they may fill specialized roles. Consistent with this idea, α2 specifically has four extra amino acids inserted into the H1-S2(N) loop, responsible for lateral dimer interactions. This modification may potentially impart increased flexibility to MTs containing α2 subunits (Morrissette, 2015). The CTT of α3 is extraordinarily long and less acidic than commonly seen for α-tubulins, implying it may mediate atypical interactions. Thus, α2 and α3 may potentially function in specialized structures such as conoid and flagellar axonemal MTs (Morrissette, 2015). Moreover, only mutations in α1 have demonstrated resistance to the protozoan-specific MT inhibitors dinitroanilines (Morrissette et al., 2004; Ma et al., 2007, Ma et al., 2010). These recent breakthroughs into the structural and functional differences of α-tubulin isoforms in *T. gondii* position this medically relevant parasite as a model for elucidating further mechanisms for how tubulin isotypes mediate diverse MT-based organelles.

CONCLUSION

The MT cytoskeleton is an indispensable component of eukaryotic cells. The overall structure of MTs is highly conserved, as are their main building blocks, α/β-tubulin heterodimers. Despite this high conservation, MTs accomplish a wide array of processes in diverse cellular contexts. A central question is how MTs perform such a range of tasks, often concurrently in the same cell. One common aspect in most organisms is the evolution of multiple α- and β-tubulin isotypes. How do multiple isotypes contribute to the diversity of MT functions? How is transcriptional and/or translational regulation, as well as post-translational modification of specific isotypes used to control MT behavior? How do unicellular organisms with relatively simple MT cytoskeletons benefit from multiple tubulin isotypes? These and other questions remain largely unanswered.

Microorganisms were well-represented in the vanguard of the initial discovery and characterization of tubulin isotypes. Their tractability readily allowed gene knockouts and overexpression, and facilitated subsequent analysis of cell viability and phenotypes. Some microorganisms possess only a few isotypes and a simplified repertoire of MT-dependent events, which can facilitate a mechanistic understanding of isotype contribution to the underlying processes. Others harbor several isotypes and utilize a more diverse array of MT-based structures. This allows investigation of more complex and diverse organism-specific MT arrays, such as the perithecia, or fruiting body, formation and ascosporogenesis in *Fusarium*, or highly conserved structures such as axonemes in *Tetrahymena* and *Chlamydomonas*. Moreover, distinct MT structures and dynamic behaviors are integrated into cell cycle and developmental specific stages, such as the myxamoeba-specific flagella in *Physarum*.

The early work on tubulin isotypes in microorganisms revealed two major themes. The first is that there appears to be a significant amount of redundancy among the isotypes with regard to basic MT functions. This is evident in the work described above where organisms often remain viable following loss of single isotypes. Moreover, when loss of a particular isotype is lethal, viability is often restored by increased expression of the remaining isotype(s), suggesting that at sufficiently high concentrations either isotype can adequately perform all essential functions. The second theme that emerged from work across a range of organisms is that loss of individual isotypes, while often not lethal, nearly always results in some perturbation to cellular processes and/or phenotype. Together these results demonstrate that many individual isotypes are not essential, yet most may contribute one or more unique properties that facilitate overall MT function.

The generalized finding that individual isotypes are often not required for viability demonstrated that, at least in most cases, they do not exclusively mediate specific MT functions. Phenotypes resulting from the loss or overexpression of isotypes are also difficult to separate from potential indirect effects resulting from changes in overall tubulin level and/or stoichiometries of the remaining isotypes. These aspects, together with technical challenges with direct gene replacement and obtaining recombinant tubulins, likely contributed to a relative decrease in research efforts investigating the multi-tubulin hypothesis from the tubulin isotype perspective. Work in microorgansisms also demonstrated that some species assemble a diverse array of MT structures using only a single form of α- and β-tubulin subunits. This is most evident in *Chlamydomonas* cells, which construct structures including mitotic and meiotic spindles, apical MT rootlets, basal bodies and flagella. Although *Chlamydomonas* harbors two α- and two β-tubulin genes, they each encode identical polypeptide sequences. This demonstrates that utilizing multiple tubulin isotypes is not a fundamental requirement for a wide range of MT structures and functions, and that the effects of PTMs on MTs and their regulatory proteins are also a critical part of the multi-tubulin hypothesis, or "tubulin code." Indeed, the finding that *Chlamydomonas* utilizes just one form of α- and β-tubulin heterodimer stoked research into the functions of PTMs in this and other microorganisms including *Tetrahymena*.

Continued work has shown that some isotypes do serve essential and exclusive roles in specialized structures such as axonemes in Drosophila sperm cells (Hoyle and Raff, 1990; Hutchens et al., 1997), or the highly curved ring-like MTs of the marginal band in mammalian blood platelets (Schwer et al., 2001). Moreover, recent studies using gene replacement to control for overall tubulin levels clearly show that the absence

of individual isotype can impair specific aspects of MT function (Honda et al., 2017; Nishida et al., 2021; Nsamba et al., 2021). For instance, both α-tubulin isotypes in budding yeast can support viability, yet each is required to optimize the two distinct spindle positioning mechanisms (Nsamba et al., 2021). Similarly, several neuronal specific β-tubulin isotypes in mouse are not needed for viability (Latremoliere et al., 2018; Bittermann et al., 2019) but, for instance, Tubb3 is specifically required for the timely regeneration of peripheral nervous system axons following injury (Latremoliere et al., 2018).

Overall, a central role of tubulin isotypes, which is consistent with the multi-tubulin hypothesis, is to allow MTs to more effectively perform diverse functions. In most organisms the MT cytoskeleton must concurrently support multiple processes and interactions. Thus, a high level of redundancy among isotypes is, at least in part, constrained by the need for αβ-tubulin heterodimers to maintain the ability to copolymerize and undergo dynamic instability. Their structure and function are further constrained by the requirement to at least minimally support the activities of ubiquitous and central regulators and motor proteins. Beyond these constraints, tubulin isotypes are able to coeveolve with distinct sets of regulatory proteins within organisms, and among various branches of evolution. Another key aspect that has become clear from work in microorganisms, as well as in other model systems (Nsamba and Gupta, 2022), is that α- and β-tubulin tubulin isotypes are able to significantly influence the properties and function of cellular MTs when present at substochiometric levels within the polymer. This quality is critical for understanding how mutations in a single copy of various isotypes can underlie the range of observed tubulinopathies.

Since the early investigation of tubulin and microtubule function, microbial models have provided leading insights into the role of tubulin isotypes and allowed testing of the multi-tubulin hypothesis. In a diverse range of microorganisms the groundwork has been laid that demonstrates their tubulin isotypes differentially facilitate various MT functions. Although at a slower pace, studies in microorganisms continue to yield additional details of the multifaceted role of tubulin isotypes. As advances in genomics, proteomics, and genetic manipulation expand the tractability of microbial models, they will undoubtably continue to make valuable contributions toward elucidating the role of isotypes in fundamental MT functions. Studying tubulin isotypes in a range of organisms will also reveal how they contribute to the diversity of cytoskeletal function seen across biology.

AUTHOR CONTRIBUTIONS

AB and MLG contributed equally to planning, researching, writing and revising this manuscript. AB designed and constructed the figures.

FUNDING

This work was supported by National Science Foundation grant number MCB-1846262 to M.L.G.

ACKNOWLEDGMENTS

We apologize to the researchers whose work in diverse microorganisms was omitted due to space limitations.

REFERENCES

Adachi, Y., Toda, T., Niwa, O., and Yanagida, M. (1986). Differential Expressions of Essential and Nonessential Alpha-Tubulin Genes in *Schizosaccharomyces pombe*. *Mol. Cell. Biol.* 6, 2168–2178. doi:10.1128/mcb.6.6.2168-2178.1986

Aiken, J., Moore, J. K., and Bates, E. A. (2018). TUBA1A Mutations Identified in Lissencephaly Patients Dominantly Disrupt Neuronal Migration and Impair Dynein Activity. *Hum. Mol. Genet.* 28, 1227–1243. doi:10.1093/hmg/ddy416

Aiken, J., Sept, D., Costanzo, M., Boone, C., Cooper, J. A., and Moore, J. K. (2014). Genome-wide Analysis Reveals Novel and Discrete Functions for Tubulin Carboxy-Terminal Tails. *Curr. Biol.* 24, 1295–1303. doi:10.1016/j.cub.2014.03.078

Asakawa, K., Kume, K., Kanai, M., Goshima, T., Miyahara, K., Dhut, S., et al. (2006). The V260I Mutation in Fission Yeast α-Tubulin Atb2 Affects Microtubule Dynamics and EB1-Mal3 Localization and Activates the Bub1 Branch of the Spindle Checkpoint. *MBoC* 17, 1421–1435. doi:10.1091/mbc.e05-08-0802

Ayaz, P., Ye, X., Huddleston, P., Brautigam, C. A., and Rice, L. M. (2012). A TOG: αβ-tubulin Complex Structure Reveals Conformation-Based Mechanisms for a Microtubule Polymerase. *Science* 337, 857–860. doi:10.1126/science.1221698

Ayukawa, R., Iwata, S., Imai, H., Kamimura, S., Hayashi, M., Ngo, K. X., et al. (2021). GTP-dependent Formation of Straight Tubulin Oligomers Leads to Microtubule Nucleation. *J. Cell Biol.* 220, e202007033. doi:10.1083/jcb.202007033

Badin-Larçon, A. C., Boscheron, C., Soleilhac, J. M., Piel, M., Mann, C., Denarier, E., et al. (2004). Suppression of Nuclear Oscillations in *Saccharomyces cerevisiae* Expressing Glu Tubulin. *Proc. Natl. Acad. Sci. U.S.A.* 101, 5577–5582. doi:10.1073/pnas.0307917101

Bahi-Buisson, N., and Maillard, C. (2016). "Tubulinopathies Overview," in *GeneReviews® [Internet]*. M. P. Adam, H. H. Ardinger, R. A. Pagon, et al. (Seattle (WA): University of Washington, Seattle), 1993–2022.

Barlan, K., and Gelfand, V. I. (2017). Microtubule-Based Transport and the Distribution, Tethering, and Organization of Organelles. *Cold Spring Harb. Perspect. Biol.* 9, a025817. doi:10.1101/cshperspect.a025817

Barnes, G., Louie, K. A., and Botstein, D. (1992). Yeast Proteins Associated with Microtubules *In Vitro* and *In Vivo*. *MBoC* 3, 29–47. doi:10.1091/mbc.3.1.29

Bhattacharya, R., and Cabral, F. (2004). A Ubiquitous β-tubulin Disrupts Microtubule Assembly and Inhibits Cell Proliferation. *MBoC* 15, 3123–3131. doi:10.1091/mbc.e04-01-0060

Binarová, P., and Tuszynski, J. (2019). Tubulin: Structure, Functions and Roles in Disease. *Cells* 8, 1294. doi:10.3390/cells8101294

Bittermann, E., Abdelhamed, Z., Liegel, R. P., Menke, C., Timms, A., Beier, D. R., et al. (2019). Differential Requirements of Tubulin Genes in Mammalian Forebrain Development. *Plos Genet.* 15, e1008243. doi:10.1371/journal.pgen.1008243

Blindt, A. B., Chainey, A. M., Dee, J., and Gull, K. (1986). Events in the Amoebal-Plasmodial Transition ofPhysarum Polycephalum Studied by Enrichment for Committed Cells. *Protoplasma* 132, 149–159. doi:10.1007/bf01276995

Bode, C. J., Gupta, M. L., Suprenant, K. A., and Himes, R. H. (2003). The Two α-tubulin Isotypes in Budding Yeast Have Opposing Effects on Microtubule Dynamics *In Vitro*. *EMBO Rep.* 4, 94–99. doi:10.1038/sj.embor.embor716

Boscheron, C., Caudron, F., Loeillet, S., Peloso, C., Mugnier, M., Kurzawa, L., et al. (2016). A Role for the Microtubule +end Protein Bik1 (CLIP170) and the Rho1 GTPase in Snc1 Trafficking. *J. cell Sci.* 129, 3332–3341. doi:10.1242/jcs.190330

Bré, M. H., de Néchaud, B., Wolff, A., and Fleury, A. (1994). Glutamylated Tubulin Probed in Ciliates with the Monoclonal Antibody GT335. *Cell Motil. Cytoskelet.* 27, 337–349. doi:10.1002/cm.970270406

Brouhard, G. J., and Rice, L. M. (2018). Microtubule Dynamics: an Interplay of Biochemistry and Mechanics. *Nat. Rev. Mol. Cell Biol.* 19, 451–463. doi:10.1038/s41580-018-0009-y

Brunke, K. J., Collis, P. S., and Weeks, D. P. (1982a). Post-translational Modification of Tubulin Dependent on Organelle Assembly. *Nature* 297, 516–518. doi:10.1038/297516a0

Brunke, K. J., Young, E. E., Buchbinder, B. U., and Weeks, D. P. (1982b). Coordinate Regulation of the Four Tubulin Genes of Chlamydomonas Reinhardi. *Nucl. Acids Res.* 10, 1295–1310. doi:10.1093/nar/10.4.1295

Burke, D., Gasdaska, P., and Hartwell, L. (1989). Dominant Effects of Tubulin Overexpression in *Saccharomyces cerevisiae*. *Mol. Cell Biol.* 9, 1049–1059. doi:10.1128/mcb.9.3.1049-1059.1989

Burland, T. G., Gull, K., Schedl, T., Boston, R. S., and Dove, W. F. (1983). Cell Type-dependent Expression of Tubulins in Physarum. *J. Cell Biol.* 97, 1852–1859. doi:10.1083/jcb.97.6.1852

Burland, T. G., Paul, E. C., Oetliker, M., and Dove, W. F. (1988). A Gene Encoding the Major Beta Tubulin of the Mitotic Spindle in Physarum Polycephalum Plasmodia. *Mol. Cell Biol.* 8, 1275–1281. doi:10.1128/mcb.8.3.1275-1281.1988

Burland, T. G., Schedl, T., Gull, K., and Dove, W. F. (1984). GENETIC ANALYSIS OF RESISTANCE TO BENZIMIDAZOLES IN PHYSARUM: DIFFERENTIAL EXPRESSION OF β-TUBULIN GENES. *Genetics* 108, 123–141. doi:10.1093/genetics/108.1.123

Callahan, R. C., Shalke, G., and Gorovsky, M. A. (1984). Developmental Rearrangements Associated with a Single Type of Expressed α-tubulin Gene in tetrahymena. *Cell* 36, 441–445. doi:10.1016/0092-8674(84)90237-x

Carminati, J. L., and Stearns, T. (1997). Microtubules Orient the Mitotic Spindle in Yeast through Dynein-dependent Interactions with the Cell Cortex. *J. cell Biol.* 138, 629–641. doi:10.1083/jcb.138.3.629

Chang, P., and Stearns, T. (2000). δ-Tubulin and ε-Tubulin: Two New Human Centrosomal Tubulins Reveal New Aspects of Centrosome Structure and Function. *Nat. Cell Biol.* 2, 30–35. doi:10.1038/71350

Chen, C.-J., Yu, J.-J., Bi, C.-W., Zhang, Y.-N., Xu, J.-Q., Wang, J.-X., et al. (2009). Mutations in a β-Tubulin Confer Resistance of Gibberella Zeae to Benzimidazole Fungicides. *Phytopathology* 99, 1403–1411. doi:10.1094/phyto-99-12-1403

Chen, C., Wang, J., Luo, Q., Yuan, S., and Zhou, M. (2007). Characterization and Fitness of Carbendazim-Resistant Strains ofFusarium Graminearum (Wheat Scab). *Pest. Manag. Sci.* 63, 1201–1207. doi:10.1002/ps.1449

Cleveland, D. W., Lopata, M. A., MacDonald, R. J., Cowan, N. J., Rutter, W. J., and Kirschner, M. W. (1980). Number and Evolutionary Conservation of α- and β-tubulin and Cytoplasmic β- and γ-actin Genes Using Specific Cloned cDNA Probes. *Cell* 20, 95–105. doi:10.1016/0092-8674(80)90238-x

Cleveland, D. W. (1987). The Multitubulin Hypothesis Revisited: what Have We Learned? *J. Cell Biol.* 104, 381–383. doi:10.1083/jcb.104.3.381

Cunningham, D. B., Buchschacher, G. L., Burland, T. G., Dove, W. F., Kessler, D., and Paul, E. C. A. (1993). Cloning and Characterization of the altA -tubulin Gene of Physarum. *J. General Microbiol.* 139, 137–151. doi:10.1099/00221287-139-1-137

Davis, A., Sage, C. R., Dougherty, C. A., and Farrell, K. W. (1994). Microtubule Dynamics Modulated by Guanosine Triphosphate Hydrolysis Activity of β-Tubulin. *Science* 264, 839–842. doi:10.1126/science.8171338

Denarier, E., Ecklund, K. H., Berthier, G., Favier, A., O'Toole, E. T., Gory-Fauré, S., et al. (2021). Modeling a Disease-Correlated Tubulin Mutation in Budding Yeast Reveals Insight into MAP-Mediated Dynein Function. *MBoC* 32, ar10. doi:10.1091/mbc.e21-05-0237

Diggins, M. A., and Dove, W. F. (1987). Distribution of Acetylated Alpha-Tubulin in Physarum Polycephalum. *J. Cell Biol.* 104, 303–309. doi:10.1083/jcb.104.2.303

Diggins-Gilicinski, M., Solnica-Krezel, L., Burland, T. G., Paul, E. C., and Dove, W. F. (1989). The Localization of the Divergent Beta 2-tubulin Isotype in the Microtubular Arrays of Physarum Polycephalum. *J. Cell Sci.* 94, 217–226. doi:10.1242/jcs.94.2.217

Doshi, P., Bossie, C. A., Doonan, J. H., Mays, G. S., and Morris, N. R. (1991). Two α-tubulin Genes of Aspergillus nidulans Encode Divergent Proteins. *Molec. Gen. Genet.* 225, 129–141. doi:10.1007/bf00282651

Drummond, D. R., Kain, S., Newcombe, A., Hoey, C., Katsuki, M., and Cross, R. A. (2011). Purification of Tubulin from the Fission Yeast *Schizosaccharomyces pombe*. *Methods Mol. Biol. Clift. NJ)* 777, 29–55. doi:10.1007/978-1-61779-252-6_3

Duan, J., and Gorovsky, M. A. (2002). Both Carboxy-Terminal Tails of α- and β-Tubulin Are Essential, but Either One Will Suffice. *Curr. Biol.* 12, 313–316. doi:10.1016/s0960-9822(02)00651-6

Dutcher, S. K., Morrissette, N. S., Preble, A. M., Rackley, C., and Stanga, J. (2002). ε-Tubulin Is an Essential Component of the Centriole. *MBoC* 13, 3859–3869. doi:10.1091/mbc.e02-04-0205

Dutcher, S. K., and Trabuco, E. C. (1998). TheUNI3Gene Is Required for Assembly of Basal Bodies ofChlamydomonasand Encodes δ-Tubulin, a New Member of the Tubulin Superfamily. *MBoC* 9, 1293–1308. doi:10.1091/mbc.9.6.1293

Eisen, J. A., Coyne, R. S., Wu, M., Wu, D., Thiagarajan, M., Wortman, J. R., et al. (2006). Macronuclear Genome Sequence of the Ciliate Tetrahymena Thermophila, a Model Eukaryote. *Plos Biol.* 4, e286. doi:10.1371/journal.pbio.0040286

Fees, C. P., Aiken, J., O'Toole, E. T., Giddings, T. H., and Moore, J. K. (2016). The Negatively Charged Carboxy-Terminal Tail of β-tubulin Promotes Proper Chromosome Segregation. *MBoC* 27, 1786–1796. doi:10.1091/mbc.e15-05-0300

Findeisen, P., Mühlhausen, S., Dempewolf, S., Hertzog, J., Zietlow, A., Carlomagno, T., et al. (2014). Six Subgroups and Extensive Recent Duplications Characterize the Evolution of the Eukaryotic Tubulin Protein Family. *Genome Biol. Evol.* 6, 2274–2288. doi:10.1093/gbe/evu187

Forth, S., and Kapoor, T. M. (2017). The Mechanics of Microtubule Networks in Cell Division. *J. Cell Biol.* 216, 1525–1531. doi:10.1083/jcb.201612064

Fromherz, S., Giddings, T. H., Gomez-Ospina, N., and Dutcher, S. K. (2004). Mutations in α-tubulin Promote Basal Body Maturation and Flagellar Assembly in the Absence of δ-tubulin. *J. Cell Sci.* 117, 303–314. doi:10.1242/jcs.00859

Gaertig, J., Cruz, M. A., Bowen, J., Gu, L., Pennock, D. G., and Gorovsky, M. A. (1995). Acetylation of Lysine 40 in Alpha-Tubulin Is Not Essential in Tetrahymena Thermophila. *J. Cell Biol.* 129, 1301–1310. doi:10.1083/jcb.129.5.1301

Gaertig, J. (2000). Molecular Mechanisms of Microtubular Organelle Assembly in Tetrahymena. *J. Eukaryot. Microbiol.* 47, 185–190. doi:10.1111/j.1550-7408.2000.tb00037.x

Gaertig, J., Thatcher, T. H., McGrath, K. E., Callahan, R. C., and Gorovsky, M. A. (1993). Perspectives on Tubulin Isotype Function and Evolution Based on the Observation that Tetrahymena Thermophila Microtubules Contain a Single Alpha- and Beta- Tubulin. *Cell Motil. Cytoskelet.* 25, 243–253. doi:10.1002/cm.970250305

Gambino, J., Bergen, L. G., and Morris, N. R. (1984). Effects of Mitotic and Tubulin Mutations on Microtubule Architecture in Actively Growing Protoplasts of Aspergillus nidulans. *J. Cell Biol.* 99, 830–838. doi:10.1083/jcb.99.3.830

Gartz Hanson, M., Aiken, J., Sietsema, D. V., Sept, D., Bates, E. A., Niswander, L., et al. (2016). Novel α-tubulin Mutation Disrupts Neural Development and Tubulin Proteostasis. *Dev. Biol.* 409, 406–419. doi:10.1016/j.ydbio.2015.11.022

Gerber, T., Loureiro, C., Schramma, N., Chen, S., Jain, A., Weber, A., et al. (2022). Spatial Transcriptomic and Single-Nucleus Analysis Reveals Heterogeneity in a Gigantic Single-Celled Syncytium. *Elife* 11, e69745. doi:10.7554/elife.69745

Goodenough, U. W., and StClair, H. S. (1975). BALD-2: a Mutation Affecting the Formation of Doublet and Triplet Sets of Microtubules in Chlamydomonas Reinhardtii. *J. Cell Biol.* 66, 480–491. doi:10.1083/jcb.66.3.480

Goodson, H. V., and Jonasson, E. M. (2018). Microtubules and Microtubule-Associated Proteins. *Cold Spring Harb. Perspect. Biol.* 10, a022608. doi:10.1101/cshperspect.a022608

Green, L. L., and Dove, W. F. (1984). Tubulin Proteins and RNA during the Myxamoeba-Flagellate Transformation of Physarum Polycephalum. *Mol. Cell. Biol.* 4, 1706–1711. doi:10.1128/mcb.4.9.1706-1711.1984

Green, L. L., Schroeder, M. M., Diggins, M. A., and Dove, W. F. (1987). Developmental Regulation and Identification of an Isotype Encoded by altB, an Alpha-Tubulin Locus in Physarum Polycephalum. *Mol. Cell Biol.* 7, 3337–3340. doi:10.1128/mcb.7.9.3337-3340.1987

Gu, L., Gaertig, J., Stargell, L. A., and Gorovsky, M. A. (1995). Gene-specific Signal Transduction between Microtubules and Tubulin Genes in Tetrahymena Thermophila. *Mol. Cell Biol.* 15, 5173–5179. doi:10.1128/mcb.15.9.5173

Gupta, M. L., Bode, C. J., Thrower, D. A., Pearson, C. G., Suprenant, K. A., Bloom, K. S., et al. (2002). β-Tubulin C354 Mutations that Severely Decrease

Microtubule Dynamics Do Not Prevent Nuclear Migration in Yeast. *MBoC* 13, 2919–2932. doi:10.1091/mbc.e02-01-0003

Hai, B., Gaertig, J., and Gorovsky, M. A. (1999). Chapter 28 Knockout Heterokaryons Enable Facile Mutagenic Analysis of Essential Genes in Tetrahymena. *Methods Cell Biol.* 62, 513–531. doi:10.1016/s0091-679x(08)61554-x

Halonen, S. K., and Weiss, L. M. (2013). Toxoplasmosis. *Handb. Clin. Neurol.* 114, 125–145. doi:10.1016/b978-0-444-53490-3.00008-x

Hartwell, L. H., Mortimer, R. K., Culotti, J., and Culotti, M. (1973). GENETIC CONTROL of the CELL DIVISION CYCLE IN YEAST: V. GENETIC ANALYSIS of Cdc MUTANTS. *Genetics* 74, 267–286. doi:10.1093/genetics/74.2.267

Havercroft, J. C., and Gull, K. (1983). Demonstration of Different Patterns of Microtubule Organization in Physarum Polycephalum Myxamoebae and Plasmodia Using Immunofluorescence Microscopy. *Eur. J. Cell Biol.* 32, 67–74.

Hiraoka, Y., Toda, T., and Yanagida, M. (1984). The NDA3 Gene of Fission Yeast Encodes β-tubulin: A Cold-Sensitive Nda3 Mutation Reversibly Blocks Spindle Formation and Chromosome Movement in Mitosis. *Cell* 39, 349–358. doi:10.1016/0092-8674(84)90013-8

Honda, Y., Tsuchiya, K., Sumiyoshi, E., Haruta, N., and Sugimoto, A. (2017). Tubulin Isotype Substitution Revealed that Isotype Composition Modulates Microtubule Dynamics in *C. elegans* Embryos. *J. Cell Sci.* 130, 1652–1661. doi:10.1242/jcs.200923

Howes, S. C., Geyer, E. A., LaFrance, B., Zhang, R., Kellogg, E. H., Westermann, S., et al. (2017). Structural Differences between Yeast and Mammalian Microtubules Revealed by Cryo-EM. *J. Cell Biol.* 216, 2669–2677. doi:10.1083/jcb.201612195

Hoyle, H. D., and Raff, E. C. (1990). Two Drosophila Beta Tubulin Isoforms Are Not Functionally Equivalent. *J. Cell Biol.* 111, 1009–1026. doi:10.1083/jcb.111.3.1009

Hu, K., Johnson, J., Florens, L., Fraunholz, M., Suravajjala, S., DiLullo, C., et al. (2006). Cytoskeletal Components of an Invasion Machine-The Apical Complex of Toxoplasma Gondii. *Plos Pathog.* 2, e13. doi:10.1371/journal.ppat.0020013

Hussmann, F., Drummond, D. R., Peet, D. R., Martin, D. S., and Cross, R. A. (2016). Alp7/TACC-Alp14/TOG Generates Long-Lived, Fast-Growing MTs by an Unconventional Mechanism. *Sci. Rep.* 6, 20653. doi:10.1038/srep20653

Hutchens, J. A., Hoyle, H. D., Turner, F. R., and Raff, E. C. (1997). Structurally Similar Drosophila Alpha-Tubulins Are Functionally Distinct *In Vivo*. *MBoC* 8, 481–500. doi:10.1091/mbc.8.3.481

James, S. W., Silflow, C. D., Stroom, P., and Lefebvre, P. A. (1993). A Mutation in the Alpha 1-tubulin Gene of Chlamydomonas Reinhardtii Confers Resistance to Anti-microtubule Herbicides. *J. Cell Sci.* 106, 209–218. doi:10.1242/jcs.106.1.209

Janke, C., and Magiera, M. M. (2020). The Tubulin Code and its Role in Controlling Microtubule Properties and Functions. *Nat. Rev. Mol. Cell Biol.* 21, 307–326. doi:10.1038/s41580-020-0214-3

Johnson, V., Ayaz, P., Huddleston, P., and Rice, L. M. (2011). Design, Overexpression, and Purification of Polymerization-Blocked Yeast αβ-Tubulin Mutants. *Biochemistry* 50, 8636–8644. doi:10.1021/bi2005174

Kato-Minoura, T., Ogiwara, Y., Yamano, T., Fukuzawa, H., and Kamiya, R. (2020). Chlamydomonas Reinhardtii Tubulin-Gene Disruptants for Efficient Isolation of Strains Bearing Tubulin Mutations. *Plos One* 15, e0242694. doi:10.1371/journal.pone.0242694

Katz, W., Weinstein, B., and Solomon, F. (1990). Regulation of Tubulin Levels and Microtubule Assembly in *Saccharomyces cerevisiae*: Consequences of Altered Tubulin Gene Copy Number. *Mol. Cell. Biol.* 10, 5286–5294. doi:10.1128/mcb.10.10.5286-5294.1990

Kilmartin, J. V. (1981). Purification of Yeast Tubulin by Self-Assembly *In Vitro*. *Biochemistry* 20, 3629–3633. doi:10.1021/bi00515a050

Kirk, K. E., and Morris, N. R. (1993). Either alpha-tubulin Isogene Product Is Sufficient for Microtubule Function during All Stages of Growth and Differentiation in Aspergillus nidulans. *Mol. Cell. Biol.* 13, 4465–4476. doi:10.1128/mcb.13.8.4465

Kirk, K. E., and Morris, N. R. (1991). The tubB Alpha-Tubulin Gene Is Essential for Sexual Development in Aspergillus nidulans. *Genes Dev.* 5, 2014–2023. –2023. doi:10.1101/gad.5.11.2014

Krämmer, G., Singhofer-Wowra, M., Seedorf, K., Little, M., and Schedl, T. (1985). A Plasmodial Alpha-Tubulin cDNA from Physarum Polycephalum. Nucleotide Sequence and Comparative Analysis. *J. Mol. Biol.* 183, 633–638. doi:10.1016/0022-2836(85)90176-7

Kubo, T., Yagi, T., and Kamiya, R. (2012). Tubulin Polyglutamylation Regulates Flagellar Motility by Controlling a Specific Inner-Arm Dynein that Interacts with the Dynein Regulatory Complex. *Cytoskeleton* 69, 1059–1068. doi:10.1002/cm.21075

Kubo, T., Yanagisawa, H.-a., Yagi, T., Hirono, M., and Kamiya, R. (2010). Tubulin Polyglutamylation Regulates Axonemal Motility by Modulating Activities of Inner-Arm Dyneins. *Curr. Biol.* 20, 441–445. doi:10.1016/j.cub.2009.12.058

L'Hernault, S. W., and Rosenbaum, J. L. (1985). Chlamydomonas .alpha.-tubulin Is Posttranslationally Modified by Acetylation on the .epsilon.-amino Group of a Lysine. *Biochemistry* 24, 473–478. doi:10.1021/bi00323a034

L'Hernault, S. W., and Rosenbaum, J. L. (1983). Chlamydomonas Alpha-Tubulin Is Posttranslationally Modified in the Flagella during Flagellar Assembly. *J. Cell Biol.* 97, 258–263. doi:10.1083/jcb.97.1.258

Latremoliere, A., Cheng, L., DeLisle, M., Wu, C., Chew, S., Hutchinson, E. B., et al. (2018). Neuronal-Specific TUBB3 Is Not Required for Normal Neuronal Function but Is Essential for Timely Axon Regeneration. *Cell Rep.* 24, 1865–1879. e9. doi:10.1016/j.celrep.2018.07.029

Leplat, J., Friberg, H., Abid, M., and Steinberg, C. (2013). Survival of Fusarium Graminearum, the Causal Agent of Fusarium Head Blight. A Review. *Agron. Sustain. Dev.* 33, 97–111. doi:10.1007/s13593-012-0098-5

Liu, S., Duan, Y., Ge, C., Chen, C., and Zhou, M. (2013). Functional Analysis of the β 2 -tubulin Gene of Fusarium Graminearum and the β -tubulin Gene of Botrytis Cinerea by Homologous Replacement. *Pest. Manag. Sci.* 69, 582–588. doi:10.1002/ps.3474

Lu, Y. J., Zhou, M. G., Ye, Z. Y., Hollomon, D. W., and Butters, J. A. (2000). Cloning and Characterization of β-Tubulin Gene Fragment from Carbendazim Resistance Strain of Fusarium Graminearum. *Acta Phytopathol. Sin.* 30, 30–34.

Ludueña, R. F. (1993). Are Tubulin Isotypes Functionally Significant. *MBoC* 4, 445–457. doi:10.1091/mbc.4.5.445

Luo, Y., Zhang, H., Qi, L., Zhang, S., Zhou, X., Zhang, Y., et al. (2014). Fg K In1 Kinase Localizes to the Septal Pore and Plays a Role in Hyphal Growth, Ascospore Germination, Pathogenesis, and Localization of T Ub1 Beta-tubulins in F Usarium Graminearum. *New Phytol.* 204, 943–954. doi:10.1111/nph.12953

Ma, C., Li, C., Ganesan, L., Oak, J., Tsai, S., Sept, D., et al. (2007). Mutations in α-Tubulin Confer Dinitroaniline Resistance at a Cost to Microtubule Function. *MBoC* 18, 4711–4720. doi:10.1091/mbc.e07-04-0379

Ma, C., Tran, J., Gu, F., Ochoa, R., Li, C., Sept, D., et al. (2010). Dinitroaniline Activity in Toxoplasma Gondii Expressing Wild-type or Mutant α-Tubulin. *Antimicrob. Agents Chemother.* 54, 1453–1460. doi:10.1128/aac.01150-09

Mani, N., Wijeratne, S. S., and Subramanian, R. (2021). Micron-scale Geometrical Features of Microtubules as Regulators of Microtubule Organization. *Elife* 10, e63880. doi:10.7554/elife.63880

May, G. S., Gambino, J., Weatherbee, J. A., and Morris, N. R. (1985). Identification and Functional Analysis of Beta-Tubulin Genes by Site Specific Integrative Transformation in Aspergillus nidulans. *J. Cell Biol.* 101, 712–719. doi:10.1083/jcb.101.3.712

May, G. S., and Morris, N. R. (1988). Developmental Regulation of a Conidiation Specific β-tubulin in Aspergillus nidulans. *Dev. Biol.* 128, 406–414. doi:10.1016/0012-1606(88)90302-8

May, G. S. (1989). The Highly Divergent Beta-Tubulins of Aspergillus nidulans Are Functionally Interchangeable. *J. Cell Biol.* 109, 2267–2274. doi:10.1083/jcb.109.5.2267

May, G. S., Tsang, M. L.-S., Smith, H., Fidel, S., and Morris, N. R. (1987). Aspergillus nidulans β-tubulin Genes Are Unusually Divergent. *Gene* 55, 231–243. doi:10.1016/0378-1119(87)90283-6

McKeithan, T., Lefebvre, P., Silflow, C., and Rosenbaum, J. (1983). Multiple Forms of Tubulin in Polytomella and Chlamydomonas: Evidence for a Precursor of Flagellar α-tubulin. *J. Cell Biol.* 96, 1056–1063. doi:10.1083/jcb.96.4.1056

McNally, F. J. (2013). Mechanisms of Spindle Positioning. *J. Cell Biol.* 200, 131–140. doi:10.1083/jcb.201210007

Miller, R. K., Heller, K. K., Frisèn, L., Wallack, D. L., Loayza, D., Gammie, A. E., et al. (1998). The Kinesin-Related Proteins, Kip2p and Kip3p, Function Differently in Nuclear Migration in Yeast. *MBoC* 9, 2051–2068. doi:10.1091/mbc.9.8.2051

Minami, S., Collis, P. S., Young, E. E., and Weeks, D. P. (1981). Tubulin Induction in C. Reinhardii: Requirement for Tubulin mRNA Synthesis. *Cell* 24, 89–95. doi:10.1016/0092-8674(81)90504-3

Minoura, I., Hachikubo, Y., Yamakita, Y., Takazaki, H., Ayukawa, R., Uchimura, S., et al. (2013). Overexpression, Purification, and Functional Analysis of Recombinant Human Tubulin Dimer. *FEBS Lett.* 587, 3450–3455. doi:10.1016/j.febslet.2013.08.032

Mitchison, T., and Kirschner, M. (1984). Dynamic Instability of Microtubule Growth. *Nature* 312, 237–242. doi:10.1038/312237a0

Mittelmeier, T. M., Boyd, J. S., Lamb, M. R., and Dieckmann, C. L. (2011). Asymmetric Properties of the Chlamydomonas Reinhardtii Cytoskeleton Direct Rhodopsin Photoreceptor Localization. *J. Cell Biol.* 193, 741–753. doi:10.1083/jcb.201009131

Monteiro, M. J., and Cox, R. A. (1987a). Differential Expression of an α-tubulin Gene during the Development of Physarum Polycephalum. *Febs Lett.* 217, 260–264. doi:10.1016/0014-5793(87)80674-9

Monteiro, M. J., and Cox, R. A. (1987b). Primary Structure of an α-tubulin Gene of Physarum Polycephalum. *J. Mol. Biol.* 193, 427–438. doi:10.1016/0022-2836(87)90257-9

Morris, J. A., Gambino, J., and Bergen, L. G. (1984). "Tubulins of Aspergillus Nidulans: Genetics, Biochemistry and Function," in *Molecular Biology of the Cytoskeleton*. Editors G. Borisy, D. Cleveland, and D. Murphy (New York: Cold Spring Harbor Laboratories), 211–222.

Morrissette, N. S., Mitra, A., Sept, D., and Sibley, L. D. (2004). Dinitroanilines Bind α-Tubulin to Disrupt Microtubules. *MBoC* 15, 1960–1968. doi:10.1091/mbc.e03-07-0530

Morrissette, N. S., and Sibley, L. D. (2002). Cytoskeleton of Apicomplexan Parasites. *Microbiol. Mol. Biol. Rev.* 66, 21–38. doi:10.1128/mmbr.66.1.21-38.2002

Morrissette, N. (2015). Targeting Toxoplasma Tubules: Tubulin, Microtubules, and Associated Proteins in a Human Pathogen. *Eukaryot. Cell* 14, 2–12. doi:10.1128/ec.00225-14

Nagel, S., and Boothroyd, J. (1988). The α- and β-tubulins of Toxoplasma Gondii Are Encoded by Single Copy Genes Containing Multiple Introns. *Mol. Biochem. Parasitol.* 29, 261–273. doi:10.1016/0166-6851(88)90081-3

Neff, N. F., Thomas, J. H., Grisafi, P., and Botstein, D. (1983). Isolation of the β-tubulin Gene from Yeast and Demonstration of its Essential Function *In Vivo*. *Cell* 33, 211–219. doi:10.1016/0092-8674(83)90350-1

Nishida, K., Tsuchiya, K., Obinata, H., Onodera, S., Honda, Y., Lai, Y.-C., et al. (2021). Expression Patterns and Levels of All Tubulin Isotypes Analyzed in GFP Knock-In *C. elegans* Strains. *Cell Struct. Funct.* 46, 51–64. doi:10.1247/csf.21022

Nogales, E. (2001). Structural Insights into Microtubule Function. *Annu. Rev. Biophys. Biomol. Struct.* 30, 397–420. doi:10.1146/annurev.biophys.30.1.397

Nsamba, E. T., Bera, A., Costanzo, M., Boone, C., and Gupta, M. L. (2021). Tubulin Isotypes Optimize Distinct Spindle Positioning Mechanisms during Yeast Mitosis. *J. Cell Biol.* 220, e202010155. doi:10.1083/jcb.202010155

Nsamba, E. T., and Gupta, M. L. (2022). Tubulin Isotypes - Functional Insights from Model Organisms. *J. Cell Sci.* 135, jcs259539. doi:10.1242/jcs.259539

Nurse, P. (1975). Genetic Control of Cell Size at Cell Division in Yeast. *Nature* 256, 547–551. doi:10.1038/256547a0

Oakley, B. R., and Morris, N. R. (1981). A β-tubulin Mutation in Aspergillus nidulans that Blocks Microtubule Function without Blocking Assembly. *Cell* 24, 837–845. doi:10.1016/0092-8674(81)90109-4

Oakley, B. R., and Morris, N. R. (1980). Nuclear Movement Is β-tubulin-dependent in Aspergillus nidulans. *Cell* 19, 255–262. doi:10.1016/0092-8674(80)90407-9

Oakley, B. R., Oakley, C. E., and Rinehart, J. E. (1987). Conditionally Lethal tubA α-tubulin Mutations in Aspergillus nidulans. *Mole Gen. Genet.* 208, 135–144. doi:10.1007/bf00330434

Oakley, B. R., Paolillo, V., and Zheng, Y. (2015). γ-Tubulin Complexes in Microtubule Nucleation and beyond. *MBoC* 26, 2957–2962. doi:10.1091/mbc.e14-11-1514

Oakley, B. R., and Rinehart, J. E. (1985). Mitochondria and Nuclei Move by Different Mechanisms in Aspergillus nidulans. *J. Cell Biol.* 101, 2392–2397. doi:10.1083/jcb.101.6.2392

Oakley, C. E., and Oakley, B. R. (1989). Identification of γ-tubulin, a New Member of the Tubulin Superfamily Encoded by mipA Gene of Aspergillus nidulans. *Nature* 338, 662–664. doi:10.1038/338662a0

Orbach, R., and Howard, J. (2019). The Dynamic and Structural Properties of Axonemal Tubulins Support the High Length Stability of Cilia. *Nat. Commun.* 10, 1838. doi:10.1038/s41467-019-09779-6

Pamula, M. C., Ti, S.-C., and Kapoor, T. M. (2016). The Structured Core of Human β Tubulin Confers Isotype-specific Polymerization Properties. *J. Cell Biol.* 213, 425–433. doi:10.1083/jcb.201603050

Paul, E. C. A., Burland, T. G., and Gull, K. (1989). Location of a Single -Tubulin Gene Product in Both Cytoskeletal and Mitotic-Spindle Microtubules in Physarum Polycephalum. *Microbiology* 135, 623–628. doi:10.1099/00221287-135-3-623

Paul, E. C. A., Roobol, A., Foster, K. E., and Gull, K. (1987). Patterns of Tubulin Isotype Synthesis and Usage during Mitotic Spindle Morphogenesis inPhysarum. *Cell Motil. Cytoskelet.* 7, 272–281. doi:10.1002/cm.970070309

Piperno, G., and Fuller, M. T. (1985). Monoclonal Antibodies Specific for an Acetylated Form of Alpha-Tubulin Recognize the Antigen in Cilia and Flagella from a Variety of Organisms. *J. Cell Biol.* 101, 2085–2094. doi:10.1083/jcb.101.6.2085

Pucciarelli, S., Ballarini, P., Sparvoli, D., Barchetta, S., Yu, T., Detrich, H. W., et al. (2012). Distinct Functional Roles of β-Tubulin Isotypes in Microtubule Arrays of Tetrahymena Thermophila, a Model Single-Celled Organism. *PloS one* 7, e39694. doi:10.1371/journal.pone.0039694

Radcliffe, P., Hirata, D., Childs, D., Vardy, L., and Toda, T. (1998). Identification of Novel Temperature-Sensitive Lethal Alleles in Essential β-Tubulin and Nonessential α2-Tubulin Genes as Fission Yeast Polarity Mutants. *MBoC* 9, 1757–1771. doi:10.1091/mbc.9.7.1757

Redeker, V., Levilliers, N., Vinolo, E., Rossier, J., Jaillard, D., Burnette, D., et al. (2005). Mutations of Tubulin Glycylation Sites Reveal Cross-Talk between the C Termini of α- and β-Tubulin and Affect the Ciliary Matrix in Tetrahymena. *J. Biol. Chem.* 280, 596–606. doi:10.1074/jbc.m408324200

Reed, N. A., Cai, D., Blasius, T. L., Jih, G. T., Meyhofer, E., Gaertig, J., et al. (2006). Microtubule Acetylation Promotes Kinesin-1 Binding and Transport. *Curr. Biol.* 16, 2166–2172. doi:10.1016/j.cub.2006.09.014

Roll-Mecak, A. (2019). How Cells Exploit Tubulin Diversity to Build Functional Cellular Microtubule Mosaics. *Curr. Opin. Cell Biol.* 56, 102–108. doi:10.1016/j.ceb.2018.10.009

Romaniello, R., Arrigoni, F., Fry, A. E., Bassi, M. T., Rees, M. I., Borgatti, R., et al. (2018). Tubulin Genes and Malformations of Cortical Development. *Eur. J. Med. Genet.* 61, 744–754. doi:10.1016/j.ejmg.2018.07.012

Ronald Morris, N., Lai, M. H., and Elizabeth Oakley, C. (1979). Identification of a Gene for α-tubulin in Aspergillus nidulans. *Cell* 16, 437–442. doi:10.1016/0092-8674(79)90019-9

Roobol, A., Wilcox, M., Paul, E. C., and Gull, K. (1984). Identification of Tubulin Isoforms in the Plasmodium of Physarum Polycephalum by *In Vitro* Microtubule Assembly. *Eur. J. Cell Biol.* 33, 24–28.

Sasse, R., Glyn, M. C., Birkett, C. R., and Gull, K. (1987). Acetylated Alpha-Tubulin in Physarum: Immunological Characterization of the Isotype and its Usage in Particular Microtubular Organelles. *J. Cell Biol.* 104, 41–49. doi:10.1083/jcb.104.1.41

Schatz, P. J., Pillus, L., Grisafi, P., Solomon, F., and Botstein, D. (1986a). Two Functional Alpha-Tubulin Genes of the Yeast *Saccharomyces cerevisiae* Encode Divergent Proteins. *Mol. Cell Biol.* 6, 3711–3721. doi:10.1128/mcb.6.11.3711-3721.1986

Schatz, P. J., Solomon, F., and Botstein, D. (1986b). Genetically Essential and Nonessential Alpha-Tubulin Genes Specify Functionally Interchangeable Proteins. *Mol. Cell. Biol.* 6, 3722–3733. doi:10.1128/mcb.6.11.3722

Schedl, T., Burland, T. G., Gull, K., and Dove, W. F. (1984a). Cell Cycle Regulation of Tubulin RNA Level, Tubulin Protein Synthesis, and Assembly of Microtubules in Physarum. *J. Cell Biol.* 99, 155–165. doi:10.1083/jcb.99.1.155

Schedl, T., Owens, J., Dove, W. F., and Burland, T. G. (1984b). GENETICS OF THE TUBULIN GENE FAMILIES OF PHYSARUM. *Genetics* 108, 143–164. doi:10.1093/genetics/108.1.143

Schwer, H. D., Lecine, P., Tiwari, S., Italiano, J. E., Hartwig, J. H., and Shivdasani, R. A. (2001). A Lineage-Restricted and Divergent β-tubulin Isoform Is Essential for the Biogenesis, Structure and Function of Blood Platelets. *Curr. Biol.* 11, 579–586. doi:10.1016/s0960-9822(01)00153-1

Sheir-Neiss, G., Lai, M. H., and Morris, N. R. (1978). Identification of a Gene for β-tubulin in Aspergillus Nidulans. *Cell* 15, 639–647. doi:10.1016/0092-8674(78)90032-6

Silflow, C., and Rosenbaum, J. L. (1981). Multiple α- and β-tubulin Genes in Chlamydomonas and Regulation of Tubulin mRNA Levels after Deflagellation. *Cell* 24, 81–88. doi:10.1016/0092-8674(81)90503-1

Singhofer-Wowra, M., Little, M., Clayton, L., Dawson, P., and Gull, K. (1986). Amino Acid Sequence Data of α-tubulin from Myxamoebae of Physarum Polycephalum. *J. Mol. Biol.* 192, 919–924. doi:10.1016/0022-2836(86)90037-9

Singhofer-Wowra, M., and Little, M. (1987). Isolation and Sequencing of α-tubulin Peptides from Myxamoebae of the Slime Mould Physarum Polycephalum. *Biochimica Biophysica Acta (BBA) - Protein Struct. Mol. Enzym.* 913, 51–59. doi:10.1016/0167-4838(87)90231-7

Solnica-Krezel, L., Burland, T. G., and Dove, W. F. (1991). Variable Pathways for Developmental Changes of Mitosis and Cytokinesis in Physarum Polycephalum. *J. Cell Biol.* 113, 591–604. doi:10.1083/jcb.113.3.591

Solnica-Krezel, L., Dove, W. F., and Burland, T. G. (1988). Activation of a -Tubulin Gene during Early Development of the Plasmodium in Physarum Polycephalum. *Microbiology* 134, 1323–1331. doi:10.1099/00221287-134-5-1323

Straight, A. F., Marshall, W. F., Sedat, J. W., and Murray, A. W. (1997). Mitosis in Living Budding Yeast: Anaphase A but No Metaphase Plate. *Science* 277, 574–578. doi:10.1126/science.277.5325.574

Suprenant, K. A., Hays, E., LeCluyse, E., and Dentler, W. L. (1985). Multiple Forms of Tubulin in the Cilia and Cytoplasm of Tetrahymena Thermophila. *Proc. Natl. Acad. Sci. U.S.A.* 82, 6908–6912. doi:10.1073/pnas.82.20.6908

Suryavanshi, S., Eddé, B., Fox, L. A., Guerrero, S., Hard, R., Hennessey, T., et al. (2010). Tubulin Glutamylation Regulates Ciliary Motility by Altering Inner Dynein Arm Activity. *Curr. Biol.* 20, 435–440. doi:10.1016/j.cub.2009.12.062

Sutton, J. C. (2009). Epidemiology of Wheat Head Blight and Maize Ear Rot Caused byFusarium Graminearum. *Can. J. Plant Pathology* 4, 195–209. doi:10.1080/07060668209501326

Tassan, J.-P., and Goff, X. (2004). An Overview of the KIN1/PAR-1/MARK Kinase Family. *Biol. Cell* 96, 193–199. doi:10.1016/j.biolcel.2003.10.009

Thazhath, R., Liu, C., and Gaertig, J. (2002). Polyglycylation Domain of β-tubulin Maintains Axonemal Architecture and Affects Cytokinesis in Tetrahymena. *Nat. Cell Biol.* 4, 256–259. doi:10.1038/ncb764

Ti, S.-C., Pamula, M. C., Howes, S. C., Duellberg, C., Cade, N. I., Kleiner, R. E., et al. (2016). Mutations in Human Tubulin Proximal to the Kinesin-Binding Site Alter Dynamic Instability at Microtubule Plus- and Minus-Ends. *Dev. cell* 37, 72–84. doi:10.1016/j.devcel.2016.03.003

Toda, T., Adachi, Y., Hiraoka, Y., and Yanagida, M. (1984). Identification of the Pleiotropic Cell Division Cycle Gene NDA2 as One of Two Different α-tubulin Genes in schizosaccharomyces Pombe. *Cell* 37, 233–241. doi:10.1016/0092-8674(84)90319-2

Toda, T., Umesono, K., Hirata, A., and Yanagida, M. (1983). Cold-sensitive Nuclear Division Arrest Mutants of the Fission Yeast *Schizosaccharomyces pombe*. *J. Mol. Biol.* 168, 251–270. doi:10.1016/s0022-2836(83)80017-5

Toda, T., Yamamoto, M., and Yanagida, M. (1981). Sequential Alterations in the Nuclear Chromatin Region during Mitosis of the Fission Yeast *Schizosaccharomyces pombe*: Video Fluorescence Microscopy of Synchronously Growing Wild-type and Cold-Sensitive Cdc Mutants by Using a DNA-Binding Fluorescent Probe. *J. Cell Sci.* 52, 271–287. doi:10.1242/jcs.52.1.271

Turk, E., Wills, A. A., Kwon, T., Sedzinski, J., Wallingford, J. B., and Stearns, T. (2015). Zeta-Tubulin Is a Member of a Conserved Tubulin Module and Is a Component of the Centriolar Basal Foot in Multiciliated Cells. *Curr. Biol.* 25, 2177–2183. doi:10.1016/j.cub.2015.06.063

Vaughan, S., Attwood, T., Navarro, M., Scott, V., McKean, P., and Gull, K. (2000). New Tubulins in Protozoal Parasites. *Curr. Biol.* 10, R258–R259. doi:10.1016/s0960-9822(00)00414-0

Vemu, A., Atherton, J., Spector, J. O., Moores, C. A., and Roll-Mecak, A. (2017). Tubulin Isoform Composition Tunes Microtubule Dynamics. *MBoC* 28, 3564–3572. doi:10.1091/mbc.e17-02-0124

Walter, W. J., Beránek, V., Fischermeier, E., and Diez, S. (2012). Tubulin Acetylation Alone Does Not Affect Kinesin-1 Velocity and Run Length *In Vitro*. *Plos One* 7, e42218. doi:10.1371/journal.pone.0042218

Wang, H., Chen, D., Li, C., Tian, N., Zhang, J., Xu, J.-R., et al. (2019). Stage-specific Functional Relationships between Tub1 and Tub2 Beta-Tubulins in the Wheat Scab Fungus Fusarium Graminearum. *Fungal Genet. Biol.* 132, 103251. doi:10.1016/j.fgb.2019.103251

Wang, X., Fu, Y., Beatty, W. L., Ma, M., Brown, A., Sibley, L. D., et al. (2021). Cryo-EM Structure of Cortical Microtubules from Human Parasite Toxoplasma Gondii Identifies Their Microtubule Inner Proteins. *Nat. Commun.* 12, 3065. doi:10.1038/s41467-021-23351-1

Weatherbee, J. A., May, G. S., Gambino, J., and Morris, N. R. (1985). Involvement of a Particular Species of Beta-Tubulin (Beta 3) in Conidial Development in Aspergillus nidulans. *J. Cell Biol.* 101, 706–711. doi:10.1083/jcb.101.3.706

Weinstein, B., and Solomon, F. (1990). Phenotypic Consequences of Tubulin Overproduction in *Saccharomyces cerevisiae*: Differences between Alpha-Tubulin and Beta-Tubulin. *Mol. Cell Biol.* 10, 5295–5304. doi:10.1128/mcb.10.10.5295-5304.1990

Werenskiold, A. K., Poetsch, B., and Haugli, F. (1988). Cloning and Expression of a Beta Tubulin Gene of Physarum Polycephalum. *Eur. J. Biochem.* 174, 491–495. doi:10.1111/j.1432-1033.1988.tb14125.x

W. F. Dove and H. P. Rusch (Editors) (1980). *Growth and Differentiation in Physarum Polycephalum* (New Jersey, US: Princeton University Press).

Williams, N. E. (1975). Regulation of Microtubules in Tetrahymena. *Int. Rev. Cytol.* 41, 59–86. doi:10.1016/s0074-7696(08)60966-3

Witman, G. B., Carlson, K., Berliner, J., and Rosenbaum, J. L. (1972). CHLAMYDOMONAS FLAGELLA. *J. Cell Biol.* 54, 507–539. doi:10.1083/jcb.54.3.507

Wloga, D., Joachimiak, E., and Fabczak, H. (2017). Tubulin Post-Translational Modifications and Microtubule Dynamics. *Ijms* 18, 2207. doi:10.3390/ijms18102207

Wloga, D., Rogowski, K., Sharma, N., Van Dijk, J., Janke, C., Edde´, B., et al. (2008). Glutamylation on α-Tubulin Is Not Essential but Affects the Assembly and Functions of a Subset of Microtubules in Tetrahymena Thermophila. *Eukaryot. Cell* 7, 1362–1372. doi:10.1128/ec.00084-08

Xia, L., Hai, B., Gao, Y., Burnette, D., Thazhath, R., Duan, J., et al. (2000). Polyglycylation of Tubulin Is Essential and Affects Cell Motility and Division in Tetrahymena Thermophila. *J. Cell Biol.* 149, 1097–1106. doi:10.1083/jcb.149.5.1097

Xiao, H., El Bissati, K., Verdier-Pinard, P., Burd, B., Zhang, H., Kim, K., et al. (2010). Post-translational Modifications to Toxoplasma Gondii α- and β-Tubulins Include Novel C-Terminal Methylation. *J. Proteome Res.* 9, 359–372. doi:10.1021/pr900699a

Youngblom, J., Schloss, J. A., and Silflow, C. D. (1984). The Two Beta-Tubulin Genes of Chlamydomonas Reinhardtii Code for Identical Proteins. *Mol. Cell Biol.* 4, 2686–2696. doi:10.1128/mcb.4.12.268610.1128/mcb.4.12.2686-2696.1984

Yuan, S., and Zhou, M. (2005). A Major Gene for Resistance to Carbendazim, in Field Isolates ofGibberella Zeae. *Can. J. Plant Pathology* 27, 58–63. doi:10.1080/07060660509507194

Zhao, Z., Liu, H., Luo, Y., Zhou, S., An, L., Wang, C., et al. (2014). Molecular Evolution and Functional Divergence of Tubulin Superfamily in the Fungal Tree of Life. *Sci. Rep.* 4, 6746. doi:10.1038/srep06746

Conflict of Interest: The authors declare that the research was conducted in the absence of any commercial or financial relationships that could be construed as a potential conflict of interest.

Publisher's Note: All claims expressed in this article are solely those of the authors and do not necessarily represent those of their affiliated organizations, or those of the publisher, the editors and the reviewers. Any product that may be evaluated in this article, or claim that may be made by its manufacturer, is not guaranteed or endorsed by the publisher.

frontiers | Frontiers in Cell and Developmental Biology

TYPE Review
PUBLISHED 01 September 2022
DOI 10.3389/fcell.2022.880761

OPEN ACCESS

EDITED BY
Richard Luduena,
The University of Texas Health Science Center at San Antonio, United States

REVIEWED BY
Dulal Panda,
Indian Institute of Technology Bombay, India
Anna Akhmanova,
Utrecht University, Netherlands

*CORRESPONDENCE
Vadym Sulimenko,
vadym.sulimenko@img.cas.cz
Pavel Dráber,
paveldra@img.cas.cz

SPECIALTY SECTION
This article was submitted to Cellular Biochemistry, a section of the journal Frontiers in Cell and Developmental Biology

RECEIVED 21 February 2022
ACCEPTED 03 August 2022
PUBLISHED 01 September 2022

CITATION
Sulimenko V, Dráberová E and Dráber P (2022), γ-Tubulin in microtubule nucleation and beyond.
Front. Cell Dev. Biol. 10:880761.
doi: 10.3389/fcell.2022.880761

γ-Tubulin in microtubule nucleation and beyond

Vadym Sulimenko*, Eduarda Dráberová and Pavel Dráber*

Laboratory of Biology of Cytoskeleton, Institute of Molecular Genetics of the Czech Academy of Sciences, Prague, Czechia

Microtubules composed of αβ-tubulin dimers are dynamic cytoskeletal polymers that play key roles in essential cellular processes such as cell division, organelle positioning, intracellular transport, and cell migration. γ-Tubulin is a highly conserved member of the tubulin family that is required for microtubule nucleation. γ-Tubulin, together with its associated proteins, forms the γ-tubulin ring complex (γ-TuRC), that templates microtubules. Here we review recent advances in the structure of γ-TuRC, its activation, and centrosomal recruitment. This provides new mechanistic insights into the molecular mechanism of microtubule nucleation. Accumulating data suggest that γ-tubulin also has other, less well understood functions. We discuss emerging evidence that γ-tubulin can form oligomers and filaments, has specific nuclear functions, and might be involved in centrosomal cross-talk between microtubules and microfilaments.

KEYWORDS

microtubule nucleation, αβ-tubulin dimer, γ-tubulin functions, γ-tubulin isotypes, γ-tubulin ring complexes (γ-TuRC)

Introduction

The microtubule cytoskeleton is essential for vital cellular functions such as cell division, maintenance of cell shape, organelle positioning, intracellular transport, and cell migration. Microtubules are dynamic in nature and oscillate stochastically between phases of assembly and disassembly in a process known as "dynamic instability of microtubules" (Mitchison and Kirschner, 1984). The major building components of microtubules are αβ-tubulin heterodimers that form cylinders with a diameter of ~25 nm. αβ-Tubulins are linked head-to-tail and form a polar protofilament. The lateral connection of thirteen protofilaments forms a left-handed helical microtubule wall. Polar microtubules have structurally distinct ends: a fast-growing plus end (+) that exposes β-tubulin and a slow-growing minus end (-) that exposes α-tubulin. Both subunits bind GTP, but hydrolysis occurs only at the β-subunit (Nogales and Wang, 2006). In cells, the (-)-ends of microtubules are anchored in microtubule organization centers (MTOCs), whereas the unanchored (+)-ends are very dynamic. Due to the dynamic properties, the microtubule network remodels in response to various signaling stimuli.

The low concentration of αβ-tubulin dimer in the cytosol prevents spontaneous nucleation of microtubules. Therefore, nucleation occurs from MTOCs. The centrosome, which consists of two centrioles surrounded by pericentriolar material (PCM), is the major MTOC in mammalian cells. In addition, the centrosome locally concentrates

various signaling molecules, including kinases and phosphatases, integrates various signaling pathways (Arquint et al., 2014) and is involved in actin filament organization (Farina et al., 2016; Inoue et al., 2019). Microtubules are also nucleated from other MTOCs such as the Golgi apparatus, pre-existing microtubules, nuclear envelope, chromatin, cell cortex endosomes and mitochondria as reviewed recently (Paz and Lüders, 2018; Akhmanova and Kapitein, 2022). These noncentrosomal MTOCs play important roles in the construction and regulation of the dynamic microtubule system.

γ-Tubulin (Oakley and Oakley, 1989) is a highly conserved member of the tubulin family (Ludueña, 2013), present at less than 1% the level of αβ-tubulin (Stearns et al., 1991). It combines with other proteins to form γ-tubulin complexes, which are the basic elements for nucleation of microtubules from MTOCs at various cellular sites as reviewed previously (Oakley et al., 2015; Petry and Vale, 2015; Tovey et al., 2018; Thawani and Petry, 2021).

This review focuses on recent research and emerging issues related to the γ-tubulin functions. Particular attention is paid to the structure of the γ-tubulin ring complex (γ-TuRC), the regulation of centrosomal microtubule nucleation, the ability of γ-tubulin to form oligomers, and the nuclear functions of γ-tubulin. We also discuss the role of γ-TuRC in centrosomal microfilament/microtubule cross-talk.

γ-Tubulin isotypes and posttranslational modifications

Isotypes of α- and β-tubulins, encoded by multiple genes, differ mainly in their C-terminal tails (CTTs). The differences between isotypes are often evolutionarily highly conserved, indicating their functional importance (Ludueña, 1993). Nine isotypes for each tubulin subunit have been identified in humans. Some isotypes are ubiquitous, while others are found only in specialized microtubule assemblies (Ludueña, 2013; Roll-Mecak, 2020). In contrast, in humans, there are only two γ-tubulin genes (*TUBG1* and *TUBG2*) with 94% sequence similarity, which are located in tandem at the 17th chromosome (Wise et al., 2000). The difference between human γ-tubulin-1 and γ-tubulin-2 is only ten amino acids, nine of which are located in the C-terminal domains of the molecules (aa 389–451). Nevertheless, they can be distinguished based on their electrophoretic and immunochemical properties (Ohashi et al., 2016; Dráberová et al., 2017). Both γ-tubulins are capable of nucleating microtubules (Vinopal et al., 2012). While γ-tubulin-1 is ubiquitously found, γ-tubulin-2 is mainly expressed in the brain (Wise et al., 2000; Yuba-Kubo et al., 2005). The function of γ-tubulin-2 is unclear, but based on its accumulation in neuroblastoma cells under oxidative stress and in mature neurons, it may have a prosurvive function. In mature neurons, dominant γ-tubulin-1 may ensure noncentrosomal microtubule nucleation (Dráberová et al., 2017).

The atomic structure of γ-tubulin shows a conformation similar to α- and β-tubulins (Aldaz et al., 2005; Rice et al., 2008). When the defined microtubule polarity is extended to the ends of the αβ-tubulin dimer and each tubulin monomer, the (+)-end of γ-tubulin contacts the (-)-end of α-tubulin. γ-Tubulin shares high homology with β-tubulin in the (+)-end face involved in longitudinal contacts between αβ-tubulin dimers (Inclán and Nogales, 2001). Similar to αβ-tubulin dimers, γ-tubulin binds GTP, which enhances its interaction with αβ-tubulin dimers in both budding yeast *Saccharomyces cerevisiae* (Gombos et al., 2013) and reconstituted human γ-TuRC (Wieczorek et al., 2021).

Extensive posttranslational modifications (PTMs) of α- and β-tubulin isotypes (Janke and Magiera, 2020) generate multiple charge variants of both subunits, termed tubulin isoforms, which can be separated by isoelectric focusing (Wolff et al., 1982; Linhartová et al., 1992). PTMs of γ-tubulins also generate multiple charge variants that have been distinguished using 2D-PAGE in various systems, including budding yeast (Vogel et al., 2001), nucleated erythrocytes (Linhartová et al., 2002), brains (Détraves et al., 1997; Sulimenko et al., 2002), and various cell lines (Kukharskyy et al., 2004; Dráberová et al., 2017). Of the PTMs of γ-tubulin, most data have been collected on its phosphorylation. Large-scale phosphoproteomic analysis of spindle pole bodies (SPBs) in budding yeast revealed multiple phosphorylation sites on γ-tubulin (Tub4) (Keck et al., 2011; Lin et al., 2011; Fong et al., 2018). Phosphomimetic mutations of highly conserved Tub4 sites resulted in spindle assembly defects (S360) (Keck et al., 2011; Lin et al., 2011), increased number of SPB microtubules (Y445) (Vogel et al., 2001), defects in spindle alignment (Y362) (Shulist et al., 2017), induced metaphase arrest (S74 and S100) (Lin et al., 2011), and cell cycle delay (S71) (Fong et al., 2018). Overall, these data strongly suggest that phosphorylation of γ-tubulin is important for the control of microtubule organization in the course of cell cycle in yeast. Multiple phosphorylation sites on γ-tubulin are also important for basal body assembly and stability, as shown in the ciliate *Tetrahymena thermophila* (Joachimiak et al., 2018). Phosphorylation analysis of human mitotic protein complexes revealed multiple phosphorylation sites on γ-tubulin (Hegemann et al., 2011), but the corresponding kinases are largely unknown. In mammals, the kinase BRSK1 (SADB), which controls cell cycle progression, phosphorylates γ-tubulin at S131 and S385. Phosphorylation at the S131 residue controled centrosome duplication (Alvarado-Kristensson et al., 2009), while phosphorylation at the S385 residue regulated cellular localization of γ-tubulin. Phosphomimetic S385D γ-tubulin translocated to the nucleus and influenced the execution of S phase (Eklund et al., 2014). Recently, the nonreceptor tyrosine kinase c-Abl was reported to phosphorylate γ-tubulin at Y443, the equivalent residue of Y445 in yeast γ-tubulin. Phosphorylation at the Y443 residue promoted assembly of γ-TuRC and nucleation of centrosomal microtubules (Wang et al., 2022). γ-Tubulin may also be a substrate for Cdk2 (cyclin-dependent kinase 2) at S80 (Chi et al., 2008). Additional serine and threonine phosphorylation sites (S32,

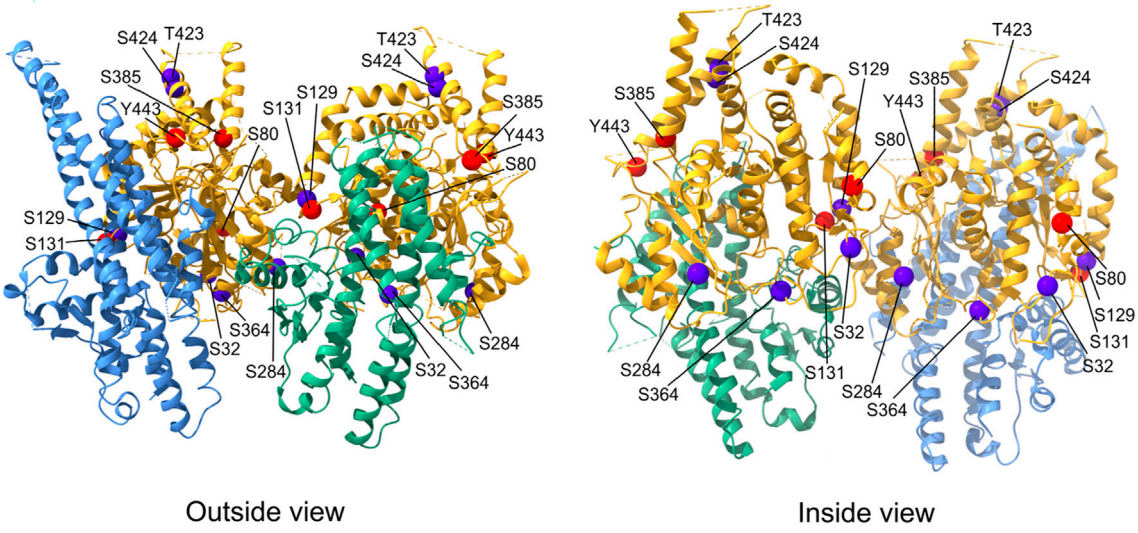

FIGURE 1
Distribution of phosphorylation sites on human γ-tubulin. Exterior and interior views of the γ-TuSC portion containing γ-tubulins (yellow) interacting with the C-terminal GRIP2 domains of GCP2 (green) and GCP3 (light blue). The position of γ-tubulin phosphorylation sites for which kinases are known are marked with red spheres, phosphorylation sites without corresponding kinases are marked with dark blue spheres. The molecular structure representation is based on native human γ-TuRC (PDB: 6v6s) and was generated using ChimeraX 1.3 software.

S129, S284, S364, T423, and S424) have been identified by mass spectrometry on human γ-tubulin (PhosphoSitePlus database), but their functional significance is unknown. The distribution of known phosphorylation sites on the human γ-tubulin molecule is shown in Figure 1.

Ubiquitination is another PTM relevant to γ-tubulin. Monoubiquitination of γ-tubulin by the BRCA1 (breast cancer type 1 susceptibility protein)/BARD1 (BRCA1-associated RING domain protein 1) E3 ligase complex results in detachment of γ-tubulin from the centrosome and inhibition of microtubule nucleation (Hsu et al., 2001; Starita et al., 2004; Sankaran et al., 2005). On the other hand, removal of ubiquitin from γ-tubulin by the deubiquitylase BAP1 (BRCA1-associated protein-1) leads to accumulation of unmodified γ-tubulin at the centrosome (Zarrizi et al., 2014). Polyubiquitination of γ-tubulin by the E3 ligases cullin 1, cullin 4A, and cullin 4B, followed by its proteosomal degradation, plays an important role in the dismantling of γ-tubulin complexes (Thirunavukarasou et al., 2015; Yin et al., 2021). Finally, acetylation of human γ-tubulin (K397, K400) was also identified by mass spectrometry (PhosphoSitePlus database), but the function is unknown.

γ-Tubulin nucleation complexes

γ-Tubulin together with its associated proteins forms complexes that are essential for microtubule nucleation. A large fraction of cytosolic γ-tubulin exists in a tetrameric complex with γ-tubulin complex protein (GCP)2 and GCP3 in stoichiometry 2:1:1, termed the γ-tubulin small complex (γ-TuSC), with a molecular weight of ~300 kDa (Oegema et al., 1999; Kollman et al., 2008). In budding yeast, where Spc97 and Spc98 are homologs of GCP2 and GCP3, respectively, the γ-TuSC represents a major structural unit of the γ-TuRC (Kollman et al., 2015). In higher eukaryotes, γ-TuSCs with additional γ-tubulins and GCP4-6 form the helical ring of γ-TuRC with a molecular weight of ~2.2-MDa. γ-TuRC provides a template that mimics the geometry of microtubules and stimulates microtubule nucleation (Moritz et al., 1995; Zheng et al., 1995; Kollman et al., 2010).

GCP2-6 each bind directly to γ-tubulin to form GCP-γ-tubulin heterodimers (called spokes). Spokes assemble into a left-handed, cone-shaped structure that controls microtubule assembly and facilitates lateral interactions between αβ-tubulin dimers (Kollman et al., 2011). Two short homologous regions are unique to GCPs: the N-terminal GRIP (γ-tubulin ring protein) 1 domain and the C-terminal GRIP2 domain. The flexible connection between these domains allows rearrangement of the γ-tubulin positions in the complex. The GRIP2 domains interact with γ-tubulins, while the GRIP1 domains form the primary interface between GCP proteins (Gunawardane et al., 2000; Kollman et al., 2011). Detailed γ-TuRC structures have recently been uncovered by four independent studies that provide mechanistic insights into how microtubules are templated from γ-TuRC (Wieczorek et al., 2020b; Consolati et al., 2020; Liu et al., 2020; Zimmermann et al., 2020). Cryo-

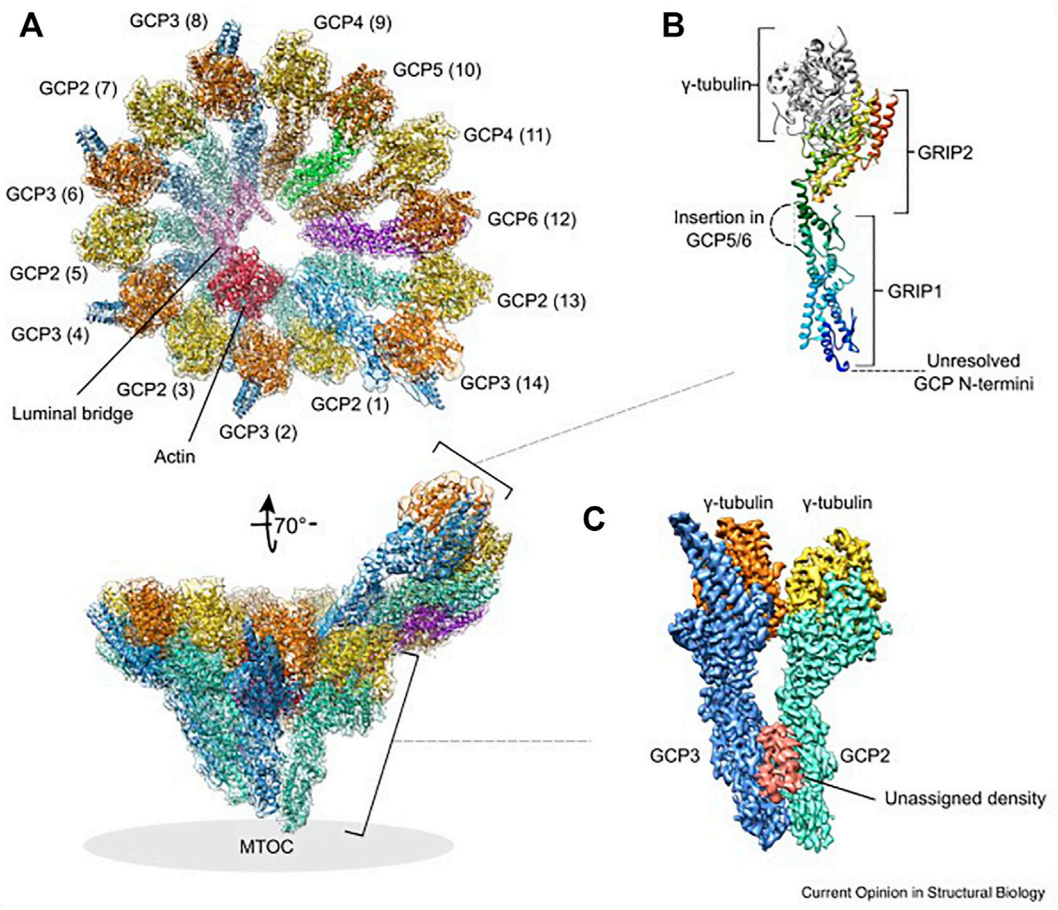

FIGURE 2
Structure and molecular architecture of human γ-TuRC. **(A)** General architecture of the left-handed γ-TuRC spiral as determined by cryo-EM single-particle analysis, resolution 3.8 Å. γ-Tubulins (yellow, orange), GCP2 (aquamarine), GCP3 (blue), GCP4 (brown), GCP5 (green), GCP6 (purple), actin (red) and the luminal bridge (pink) are shown. The spokes (GCP-γ-tubulin heterodimers) are numbered (1–14 in brackets). In the tilted view, the approximate location of the MTOC is indicated. The orientation of subcomplexes shown in panel **(B)** and **(C)** is indicated. **(B)** General architecture of a GCP-γ-tubulin spoke. The GCP N-terminal GRIP1 and C-terminal GRIP2 domains are annotated. Unresolved GCP segments are indicated by dashed lines. GCP is shown in rainbow colors from N-terminus (blue) to the C-terminus (red). **(C)** Location of the unassigned density segment (red) present on each GCP(2–3) subcomplex of the human γ-TuRC. This figure was prepared using PDB 6V6S and EMD-21074. Reprinted by permission from Current Opinion in Structural Biology (Zupa et al., 2021).

EM reconstructions showed that γ-TuRC has a width of ~30 nm and a height of ~25 nm. The 14 spokes are aligned laterally to form a short helix, and the γ-tubulins are located on the open side of the cone, in the C-terminal region of each GCP. Spoke positions 1 and 14 partially overlap. Spoke positions 1-8 are occupied by four γ-TuSCs, whereas spoke positions 9–14 contain GCP4, GCP5, GCP4, and GCP6, and a terminal γ-TuSC. All studies identified a scaffold in the complex interior, called the lumenal bridge, which surprisingly also contains actin. In addition to actin, the luminal bridge includes two small molecules of MZT1 (mitotic spindle organizing protein 1), the N-terminus of GCP6 and the N-terminus of GCP3 (Wieczorek et al., 2020a).

The assembly of γ-TuRC is modular, starting with the formation of a stable subcomplex of six spokes, consisting of GCP2-3-4-5-4-6, which then expands with the addition of four preformed GCP2-3 units (γ-TuSC), MZT1, and actin (Würtz et al., 2022). DNAseI binds directly to actin with high affinity. The *in vitro* nucleation activity of isolated endogenous γ-TuRC was markedly inhibited after treatment with DNAseI, and saturation of DNAseI with actin abolished this inhibition, suggesting a functional importance of actin in the complex (Liu et al., 2020). Actin has been shown not to be required for assembly of γ-TuRC, but to determine the geometry of the complex and ensure effective nucleation of microtubules (Würtz et al., 2022). On the outer surface of reconstituted γ-

TuRC, MZT1, and MZT2 were identified to bind to the N-terminal domains of GCPs. These MZT1/2 proteins may aid in the recruitment of γ-TuRC to the centrosome (Wieczorek et al., 2020a; Consolati et al., 2020; Würtz et al., 2022). The location of γ-tubulin molecules at the interface between γ-TuRC and αβ-tubulin dimers does not correspond exactly to the geometry of microtubules. While spokes 1–8 with four GCP2-3 units (γ-TuSC) follow microtubule symmetry and adopt a "closed conformation," spokes 9–14 are less tightly aligned and do not serve as a perfect template for microtubule nucleation. They are asymmetric in both diameter and spacing and have an "open conformation" (Wieczorek et al., 2020b; Consolati et al., 2020; Liu et al., 2020; Zimmermann et al., 2020). This could explain why the cytosolic γ-TuRC exhibits low nucleation activity (Consolati et al., 2020). The molecular architecture and structure of γ-TuRC is shown in Figure 2.

The deciphered structure of γ-TuRC supports a model of microtubule nucleation in which γ-tubulins recruit αβ-tubulin dimers and promote their lateral interactions during the early stages of microtubule assembly (Zheng et al., 1995; Keating and Borisy, 2000; Moritz et al., 2000; Wiese and Zheng, 2000). It has been shown that the association of as few as four αβ-tubulin dimers (minimal nucleus) in the rate-limiting step is sufficient for γ-TuRC-mediated nucleation (Consolati et al., 2020; Thawani et al., 2020). This process is thus more efficient than spontaneous nucleation of microtubules in solution, which requires cooperative assembly of eight αβ-tubulin dimers in the rate-limiting step (Thawani et al., 2020). It is supposed that a conformational changes leading to fully closed γ-TuRC, consistent with 13-fold microtubule symmetry, are required to increase the efficiency of γ-TuRC nucleation.

γ-TuRC activation

Although the mechanisms of γ-TuRC activation are not well understood, there is evidence that activation of γ-TuRC may occur by multiple mechanisms. Activating protein factors, phosphorylation of γ-TuRC-building and activating proteins, or conformational changes after binding of αβ-tubulin could be involved in context-specific activation.

Several candidates might play a role as γ-TuRC activating factors. CDK5RAP2 (cyclin-dependent kinase 5 regulatory subunit-associated protein 2/centrosomal protein 215/Cep215) is the best characterized mammalian activator (Fong et al., 2008). It contains an activating ~5.5-kDa domain (γ-TuNA/γ-TuRC-mediated nucleation activator 1/centrosomin motif 1/CM1) that is conserved in all eukaryotes among proteins that recruit γ-TuRCs to MTOCs (Lin et al., 2015). *In vitro* experiments with purified γ-TuRCs showed differential effects of CM1 on nucleation activity. When the CM1 domain was added to human γ-TuRC, nucleation activity increased 7.1-fold (Choi et al., 2010). However, when the CM1 domain was added to *Xenopus* γ-TuRC, the activity increased only 1.7-fold (Liu et al., 2020) or only insignificantly (Thawani et al., 2020). On the other hand, functional complexes resembling γ-TuRC were formed when the CDK5RAP2 homolog Mto 1/2 from the fission yeast *Schizosaccharomyces pombe* was added to γ-TuSC (Leong et al., 2019). It has also been shown that binding of the CM1 domain from the budding yeast Spc110 protein to γ-TuSC results in structural changes that facilitate assembly of γ-TuRC (Brilot et al., 2021). It has been suggested that the kinase NME7 (nucleoside diphosphate kinase 7), which copurifies with γ-TuRC (Wieczorek et al., 2020b; Liu et al., 2020), may also serve as an activating factor (Liu et al., 2014). However, when NME7 was added to γ-TuRC nucleation assays, the nucleation activity increased only 2.5-fold (Liu et al., 2014) or insignificantly (Thawani et al., 2020). Since the corresponding substrate of NME7 on γ-TuRC is unknown, the question remains whether NME7 can actually activate γ-TuRC. TPX2 (targeting protein for Xklp2), the multifunctional Ran-GTP-regulated factor for spindle assembly (Roostalu and Surrey, 2017; Tovey and Conduit, 2018), could also serve as an activating protein. High concentrations of human TPX2 stimulated γ-TuRC-dependend microtubule nucleation (Consolati et al., 2020). In contrast, such stimulation was not observed in *Xenopus* (Thawani et al., 2020). These differences may reflect the species-specific activity of TPX2. Recently, the well-characterized microtubule polymerase XMAP215 (*Xenopus* microtubule assembly protein 215 kDa; mammalian ch-TOG [colonic and hepatic tumor overexpressed gene protein]) was shown to interact with γ-tubulin complexes (Gunzelmann et al., 2018; Thawani et al., 2018). It also increases the nucleation activity of γ-TuRC up to 25-fold (Consolati et al., 2020; Thawani et al., 2020). It has been proposed that XMAP215 complements γ-TuRC dependent nucleation. XMAP215 first associates with the γ-TuRC and then delivers αβ-tubulin interacting with its TOG domains to the γ-TuRC and subsequently to the growing microtubule end (Thawani et al., 2020). The open question is whether the activity of XMAP-215 is synergistic or additive with γ-tubulin (King et al., 2020).

As described in the previous text, γ-tubulin has multiple phosphorylation sites, and its phosphorylation can modulate the conformational changes required for γTuRC activation. Phosphorylation of sites at the (+) end of γ-tubulin could directly regulate interactions with αβ-tubulin dimers, and the same is true for phosphorylation of sites at the lateral contacts between γ-tubulin and αβ-tubulin dimers (Kollman et al., 2015). Some of the known phosphorylation sites on the human γ-tubulin molecule are located at important interface between γ-TuSCs and may affect the formation of γ-TuRC (Figure 1).

GCPs are also phosphorylated (Hegemann et al., 2011; Santamaria et al., 2011; Fong et al., 2018; Brilot et al., 2021). Surprisingly, phosphorylation at most of the mapped sites on γ-TuSC appears to destabilize the assembled γ-TuRC. On the other

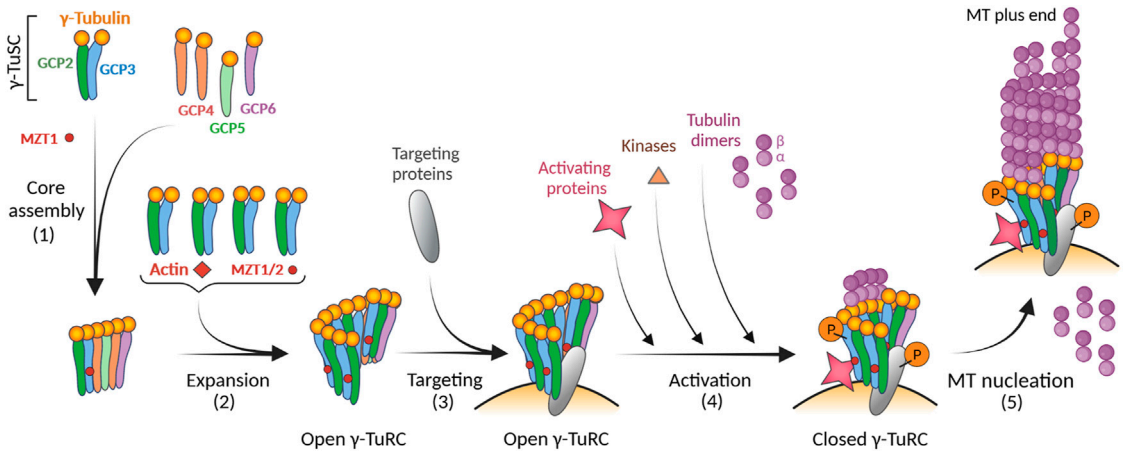

FIGURE 3
Model for the modular assembly of γ-TuRC and its activation. The first step in the formation of γ-TuRC is the core assembly of the stable subcomplex from γ-TuSC (2 molecules of γ-tubulin and one copy each of GCP2 and GCP3), GCP-γ-tubulin heterodimers (spokes; one molecule of γ-tubulin and one copy each of GCP4, GCP5 or GCP6), and MZT1 **(1)**. During the expansion phase, four additional γ-TuSC units, MZT1/2, and actin are added **(2)**. The resulting γ-TuRCs with the open conformation are concentrated onto centrosomes *via* targeting proteins (e.g., CDK5RAP2, NEDD1) **(3)**. The pitch and diameter of open γ-TuRC are incompatible with those of assembled microtubules. This suggests that the complex undergoes a conformational change through its activation to reduce its diameter before microtubule nucleation. Different modes of activation, including direct binding of activating proteins (e.g., CDK5RAP2, NME7), phosphorylation of γ-TuRC by kinases, or increased concentration of αβ-tubulins, can result in a conformational change leading to a closed γ-TuRC **(4)**. Different types of activation may occur simultaneously. Nucleation-competent γ-TuRC with a closed conformation can then effectively nucleate microtubule (MT) **(5)**. Created with BioRender.com.

hand, a stabilizing effect of phosphorylation was predicted at two sites (Brilot et al., 2021). This highlights that phosphorylation and dephosphorylation may play complex modulatory roles in the activation of γ-TuRC. In higher eukaryotes, only a few kinases are known to phosphorylate GCPs. GCP6 is phosphorylated by the kinases PLK4 (polo-like kinase 4) (Bahtz et al., 2012) and Cdk1 (cyclin-dependent kinase 1) (Oriolo et al., 2007). Phosphorylation of GCP5 by GSK3β (glycogen synthase kinase 3β) inhibits the accumulation of γ-TuRC at centrosomes (Horio and Oakley, 1994). In addition, activating factors can also be regulated by phosphorylation. It has been reported that binding of human CDK5RAP2 (Hanafusa et al., 2015) or SPD-5 (spindle-defective protein 5), a CM1 domain-containing protein from *Caenorhabditis elegans* (Ohta et al., 2021) to γ-TuRCs depends on phosphorylation. Furthermore, binding of CDK5RAP2 to γ-TuRC is regulated by autoinhibition, and phosphorylation helps to abrogate this activity (Tovey et al., 2021). The activating role of NME7 kinase can be affected by its autophosphorylation (Liu et al., 2014). TPX2 is the major cofactor for the mitotic kinase Aurora A, which is indirectly involved in the regulation of γ-TuRC-driven microtubule nucleation (Kufer et al., 2002; Meunier and Vernos, 2016; Joukov and De Nicolo, 2018). Overall, phosphorylation of building components of γ-TuRC may affect the complex stability. Further regulation of microtubule nucleation activity may occur through phosphorylation of activating proteins.

Finally, it was suggested that the driving force for achieving a fully closed γ-TuRC conformation might be the arrangement of αβ-tubulin dimers at the γ-TuRC itself. Using computational modelling, it was shown that four laterally associated tubulin dimers at the γ-TuRC create a transition state that closes the γ-TuRC (Thawani et al., 2020). Interestingly, *Caenorhabditis* mitotic centrosomes concentrate soluble αβ-tubulin more than 10-fold compared to the cytoplasm (Baumgart et al., 2019). Thus, the concentration of αβ-tubulin dimers could also modulate the γ-TuRC nucleation activity. An open question is whether, in cells expressing different isotypes of α- and β-tubulins, some tubulin isotypes might be better substrates for microtubule nucleation driven by γ-TuRC (Ti et al., 2018). The model for the modular assembly and activation of γ-TuRC is shown in Figure 3.

γ-TuRC recruitment to centrosome

In addition to activating proteins, there are other proteins, referred to here as targeting/anchoring proteins, that are involved in the regulation of γ-TuRC-driven microtubule nucleation. They are not essential for the assembly of γ-TuRC, but they help in the recruitment and tethering of the complex to MTOCs. Below, we provide an overview of regulatory proteins important for centrosomal microtubule nucleation in mammalian cells. For

TABLE 1 Building components of γ-TuRC and major regulatory proteins of centrosomal microtubule nucleation in mammalian interphase cells.

γ-TuRC	γ-tubulin, GCP2, GCP3, GCP4, GCP5, GCP6, Actin, MZT1, MZT2
Activating	CDK5RAP2, NME7, chTOG/XMAP215,TPX2
Targeting/Anchoring	CDK5RAP2, NEDD1, AKAP9, Cep192, Ninein, Pericentrin
	Dynein complex, FSD1, MSD1-WDR8, Augmin complex

a detailed discussion of noncentrosomal microtubule nucleation, we refer reader to recent reviews (Valenzuela et al., 2020; Wilkes and Moore, 2020; Akhmanova and Kapitein, 2022).

Targeting/anchoring of γ-TuRCs to interphase centrosomes is mediated by CDK5RAP2 *via* its CM2 domain (centrosomin motif 2) (Wang et al., 2010) and by NEDD1 (neural precursor cell expressed developmentally down-regulated protein 1/GCP-WD) (Haren et al., 2006; Lüders et al., 2006). Ninein anchors γ-TuRCs to subdistal appendages of the mother centriole (Bouckson-Castaing et al., 1996; Delgehyr et al., 2005). This process may involve dynein complex, which can be activated by ninein (Redwine et al., 2017). γ-TuRC may also be bound to the central region of the mother centriole *via* the centrosomal protein FSD1 (Tu et al., 2018) or to the proximal/PCM region *via* the protein complex MSD1-WDR8 (Hori et al., 2015). Augmin (HAUS) complex interacts with γ-TuRC and is required for branching microtubule nucleation (Goshima et al., 2008). Recently, augmin-γ-TuRC was identified in the lumen of the centriole, and it was shown that γ-TuRCs are recruited to the luminal region by the interaction of augmin with the centriole inner scaffold protein POC5 (Schweizer et al., 2021). Cep192 (centrosomal protein 192), which is implicated in the recruitment of γ-TuRC to centrosome (Gomez-Ferreria et al., 2007; O'Rourke et al., 2014), anchors γ-TuRC both to PCM and to the outer sides of centrioles (Schweizer et al., 2021). Additional proteins such as AKAP9 (A-kinase anchoring protein 9; AKAP450) (Takahashi et al., 2002; Ong et al., 2018), and pericentrin (Kendrin) (Zimmerman et al., 2004; Lawo et al., 2012) are also important for centrosomal localization of the complex, but since they are incorporated into PCM, they may also indirectly modulate γ-TuRC binding. Spatially and temporally distinct subpopulations of γ-TuRCs in centrosomes may be involved in different functions. In addition to canonical microtubule nucleation, γ-TuRC participates in centriole biogenesis and stabilization, and in microtubule anchoring (Schweizer and Lüders, 2021; Vineethakumari and Lüders, 2022). The structural elements of γ-TuRC and the major regulatory proteins of centrosomal microtubule nucleation in mammalian interphase cells are summarized in Table 1.

Phosphorylation of targeting/anchoring proteins affects recruitment of γ-TuRCs to centrosomes. NEDD1 is phosphorylated at multiple sites (Gomez-Ferreria et al., 2012), and sequential phosphorylation of NEDD1 by Cdk1 (cyclin-dependent kinase 1) and Plk1 (polo-like kinase 1) is essential for centrosomal targeting of γ-TuRC (Zhang et al., 2009). Phosphorylation of NEED1 by Cdk1 is required for its interaction with Plk1 and allows binding of γ-TuRC to pre-existing microtubules *via* the multiprotein augmin complex (Haren et al., 2009; Johmura et al., 2011). The kinase Aurora A phosphorylates NEDD1, which is a prerequisite for nucleation of microtubules from chromatin (Pinyol et al., 2013; Scrofani et al., 2015). Moreover, phosphorylation of NEDD1 by PLK4 promotes its interaction with SAS-6, the central component of the centriolar cartwheel (Chi et al., 2021), which associates with γ-TuRC during initiation of centriole duplication (Gupta et al., 2020). Phosphorylation of pericentrin by Plk1 (Santamaria et al., 2011) supports the accumulation of NEDD1 and CEP192 at the centrosome (Lee and Rhee, 2011). Phosphorylation of proteins participating in the recruitment of γ-TuRC to centrosomes therefore plays an important role in centriole biogenesis and microtubule nucleation.

Besides targeting/anchoring proteins, several modulatory proteins, not covered in this review, are also critical for regulating microtubule nucleation from centrosomes (Sulimenko et al., 2017). These proteins likely affect microtubule nucleation more indirectly. As an example, TACC3 (transforming acidic coiled-coil containing protein 3) stabilizes γ-TuRC during its assembly from γ-TuSC (Singh et al., 2014; Rajeev et al., 2019). On the other hand the putative tumor suppressor cyclin-dependent kinase five regulatory subunit-associated protein 3 (CDK5RAP3; C53) (Wang et al., 2007), which exerts multiple functions in cell cycle regulation, DNA damage response, cell invasion, and ER homeostasis (Sheng et al., 2021), interacts with γ-TuRC and acts as a negative regulator of microtubule nucleation. Displacement of C53 from the centrosome by exposure of cells to ER stress stimulates microtubule nucleation (Klebanovych et al., 2022). Intriquingly, some GTPase-activating proteins (GAPs) for ARF small GTPases (Sztul et al., 2019) may also be involved in regulating centrosomal microtubule nucleation. GAP ELMOD2, which acts with the GTPase ARL2, associates with centrosomes, and its deletion suppresses γ-TuRC recruitment and microtubule nucleation (Turn et al., 2020). Similarly, GAP GIT1, which acts with the GTPase Arf6 and functions as signalling adaptor protein, also associates with centrosomes

(Zhao et al., 2005). Depletion of GIT1 suppresses centrosomal γ-tubulin accumulation and microtubule nucleation (Sulimenko et al., 2015; Černohorská et al., 2016). This suggests that signalling pathways other than those involving kinases and phosphatases may be involved in the regulation of γ-TuRC-dependent microtubule nucleation.

Interestingly, interactions between γ-tubulin and proteins essential for nonmuscle actin assembly, such as the Arp2/3 complex and its activator WASH, have been reported in different systems (Schaerer-Brodbeck and Riezman, 2003; Monfregola et al., 2010). Arp 2/3 requires profilin 1 for actin assembly, which sequesters actin, accelerates actin nucleotide exchange, and can dock to free actin filament (+)-ends as profilin-actin. Profilin 1 plays a key role in coordinating the different sub-arrangemeents in dynamic actin cytoarchitecture (Henty-Ridilla and Goode, 2015). Profilin 1 associates with γ-TuRC and its deletion enhances centrosomal microtubule nucleation in interphase cells (Nejedlá et al., 2021). As centrosomes have been proposed to nucleate actin polymerization (Farina et al., 2019; Inoue et al., 2019), it is possible that loss of profilin 1 results in less polymerization-ready actin (profilin-actin) and fewer actin filaments around centrosomes. The reduced steric hindrance could lead to increased *de novo* microtubule nucleation, as has been proposed for mitotic centrosomes (Plessner et al., 2019). Alternatively, deletion of profilin 1 would make more actin accessible for association with γ-TuRCs, which in turn would increase functional complexes formation and microtubule nucleation. The activity of γ-TuRC may therefore play an important role in centrosomal microfilament/microtubule cross-talk (Karlsson and Dráber, 2021).

γ-Tubulin oligomers and filaments

Several studies using purified cellular or recombinant γ-tubulins have shown that γ-tubulin is capable of forming filamentous structures *in vitro*. The results of high-resolution microscopy suggest that such structures may also be present in cells, as documented below.

Acentrosomal plant cells contain large amounts of γ-tubulin compared to animal cells, and plant γ-tubulin forms heterogeneous complexes of high molecular weight (Dryková et al., 2003). Immunopurification of γ-tubulin with an anti-peptide antibody to γ-tubulin was performed from *Arabidopsis thaliana* cells. Analysis of the purified γ-tubulin with negative staining and transmission electron microscopy (TEM) revealed helically entangled double filaments together with filament bundles. Atomic force microscopy (AFM) showed that the most common width of the double-stranded filaments is 8.5 nm, which corresponds to the width inferred from TEM analysis (~6 × 9 nm in a cross-section). When overexpressed GFP-labeled γ-tubulin was purified from *Arabidopsis* cells with anti-GFP antibody and acid elution, immunofluorescence microscopy revealed fibrillar structures. When purification was performed at a low SDS concentration that interfered with the interactions between γ-tubulin and GCPs, short γ-tubulin filaments were also detected. This suggests that *Arabidopsis* γ-tubulin is capable of forming filaments *in vitro* in the absence of GCPs (Chumová et al., 2018). Such formation of γ-tubulin filaments was not restricted to plant cells. When overexpressed RFP-labeled γ-tubulin from human osteosarcoma cells U2OS was purified using anti-RFP antibody and acid elution, immunofluorescence microscopy revealed filaments. In the absence of GCPs, filaments were also formed, but they were shorter. TEM confirmed the double-stranded character of the filaments (Chumová et al., 2018). Oligomerization of γ-tubulin has been previously reported in microtubule proteins isolated from porcine brain by two temperature-dependent cycles of polymerization and depolymerization (MTP-2). MTP-2 preparations electrophoretically separated under nondenaturing conditions generated "ladders" of multiple oligomers containing α-tubulin and γ-tubulin (Sulimenko et al., 2002). After isolation of γ-tubulin from MTP-2 with an anti-peptide antibody to γ-tubulin and immunizing peptide elution, γ-tubulin oligomers were detected in samples lacking αβ-tubulin dimers. Moreover, purified γ-tubulin from brain lacking both GCPs and αβ-tubulin dimers was capable of forming oligomers (Chumová et al., 2018).

Formation of γ-tubulin oligomers *in vitro* was also observed in the case of isolated recombinant proteins. TEM analysis of purified His_6-labeled human γ-tubulin expressed in *E. coli* revealed a meshwork of γ-tubulin filaments termed γ-strings (Rosselló et al., 2018). Purified recombinant human γ-tubulin expressed in *E. coli* formed conformationally distinct aggregates, including long thin fibers ~6.7 nm wide, in the presence of ATP and chaperonin CCT of type II (Pouchucq et al., 2018). Interestingly, purified Tev-StrepII-His6-labeled human γ-tubulin produced in Sf9 insect cells by a baculovirus expression system self-assembled into filaments with variable width at high γ-tubulin concentration (1–2 μM) (Thawani et al., 2020). 3D reconstructions of negatively stained electron micrographs of thin width γ-tubulin filaments revealed four linear arrays of interacting γ-tubulins. When the crystal structure of human γ-tubulin (PDB: 1Z5W) (Aldaz et al., 2005) was docked to the reconstituted filaments, a lateral arrangement of γ-tubulin in a linear array was revealed with a repeat unit of approximately 54 Å (Thawani et al., 2020). This closely matched the lateral repeats but not the longitudinal repeats (40 Å) of αβ-tubulin in microtubule lattice (PDB: 6DPU) (Zhang et al., 2018). Arrays of γ-tubulin were also generated from purified myc-His_6-tagged human γ-tubulin expressed in Sf9 cells at concentrations of 0.25 μM and above. Helical reconstruction of negative-stain electron micrographs of the γ-tubulin arrays revealed a fivefold symmetry with a hollow center and a diameter of ~15 nm. Docking of the crystal structure

of γ-tubulin to 3D reconstruction of electron micrographs disclosed a lateral arrangement of γ-tubulins along the long axis with their (+) ends facing outward enabling interaction with αβ-tubulin. The γ-tubulin arrays promoted formation of microtubules and nucleation capacity correlated with array formation (King et al., 2020). Short templating γ-tubulin oligomers might enhance the rate of spontaneous αβ-tubulin assembly by eliminating kinetic barrier to lateral αβ-tubulin growth (Rice et al., 2021). Overall, the results of the *in vitro* experiments demonstrate the intrinsic capability of γ-tubulin to form oligomers and filaments.

γ-Tubulin arrays were detected *in vivo* in interphase cells. Association of γ-tubulin along pre-existing microtubules has been observed in higher plants (Liu et al., 1993) or fission yeasts (Sawin et al., 2004). In S2 cells of *Drosophila melanogaster*, γ-tubulin localized along interphase microtubules in the form of γ-TuRC, and it was proposed that the γ-TuRC could regulate microtubule dynamics by limiting catastrophes (Bouissou et al., 2009). γ-Tubulin was found on microtubules forming a marginal band in erythroid cells of the chicken embryo (Linhartová et al., 2002), and in cultured mammalian cell lines in interphase, where it sporadically coated microtubules in limited regions (Hubert et al., 2011). In contrast, tubular γ-tubulin structures that were not associated with microtubules were found in the fraction of cells overexpressing tagged γ-tubulin, suggesting that γ-tubulin retains the potential to assemble into macromolecular assemblies *in vivo* (Shu and Joshi, 1995). Interestingly, superresolution microscopy in *Arabidopsis* cells revealed short γ-tubulin filaments outside the microtubules. They accumulated both at the mitotic spindle poles and at the outer membrane of the nuclear envelope. It has been suggested that γ-tubulin may form a dynamic 3D structure of more or less densely packed, laterally connected filaments (Chumová et al., 2018). Such fibrillar structures were distinct from the dynamic polar fibers termed γ-tubules that have been detected in mammalian tissue culture cell lines and reportedly to be formed in a GTP-dependent manner from γ-TuRCs and pericentrin (Lindström and Alvarado-Kristensson, 2018). However, pericentrin is not present in the *Arabidopsis* genome. The role of fibrillar γ-tubulin assemblies is currently unclear. It has been proposed that they have sequestration and scaffolding functions (Chumová et al., 2021). They may also participate in mechanotransduction processes, as they are associated with the multiprotein complex LINC (linker of nucleoskeleton and cytoskeleton) (Rosselló et al., 2018; Chumová et al., 2019; Corvaisier and Alvarado-Kristensson, 2020). Interestingly, γ-tubulin has been detected in inner membranes and matrix of isolated mitochondria (Dráberová et al., 2017), and it has been suggested that γ-tubulin filaments (γ-strings) may represent mitochondrial structural components (Lindström et al., 2018). As described in the following section, γ-tubulin can also be found in cell nuclei. It has been proposed that γ-tubulin filaments may also play a structural role in nuclei (Corvaisier et al., 2021). Further studies are however needed to verify the presence of fibrillar γ-tubulin assemblies in different model systems, determine their composition, structure and decipher their cellular function(s).

γ-Tubulin nuclear functions

Contrary to the persistent view that γ-tubulin is a typical cytosolic protein, γ-tubulin has been localized in the nuclei of both plant (Binarová et al., 2000) and animal cells (Lesca et al., 2005; Höög et al., 2011). In addition, specific nuclear localization signal (NLS) in the γ-tubulin molecule was deciphered (Höög et al., 2011). Proteomic analysis suggested that γ-tubulin might be also in nucleoli (Andersen et al., 2002). A significant increase in γ-tubulin protein level observed in glioblastoma cell lines (Katsetos et al., 2009) contributed to the unequivocal confirmation of nucleolar γ-tubulin (Hořejší et al., 2012). Surprisingly, GCP2 and GCP3 were also found in nucleoli, although no NLSs were identified in these molecules. This suggests that both proteins might enter the nucleus by hitchhiking on γ-tubulin (Dráberová et al., 2015).

There is evidence that γ-tubulin has nuclear-specific functions. It has been reported that BRSK1-mediated phosphorylation of γ-tubulin at S385 leads to transient nuclear accumulation of γ-tubulin in S phase of cell cycle (Eklund et al., 2014). Nuclear γ-tubulin attenuates the activity of E2F transcription factors, important regulators of cell cycle progression, in both animals (Höög et al., 2011) and plants (Kállai et al., 2020). It was found that γ-tubulin and DP1 (E2F heterodimerization protein) compete for the same binding site on E2F and that the tumor suppressor retinoblastoma protein 1 (RB1) and γ-tubulin regulate each other's expression. Interestingly, a proapoptotic effect was observed in cancer cells with nonfunctional RB1 signaling after depletion of γ-tubulin protein levels (Ehlén et al., 2012). The E2Fs-γ-tubulin interactions may participate in coordinating genome duplication with spindle assembly in both animal cells containing centrosomes and in acentrosomal plant cells in which microtubules are nucleated from dispersed sites (Binarová et al., 2006; Pastuglia et al., 2006). In addition, E2Fa and RBR1 (*Arabidopsis* homolog of RB1) form foci in plant cells in response to double-strand breaks that seem to allow recruitment of the repair protein Rad51 (Biedermann et al., 2017; Horvath et al., 2017). In mammalian cells, Rad51 interacts with γ-tubulin in response to DNA damage (Lesca et al., 2005). These results suggest that E2Fs-γ-tubulin complexes may promote DNA repair or control the expression of genes related to DNA repair (Raynaud and Nisa, 2020).

γ-Tubulin colocalizes in nucleoli with a putative tumor suppressor C53, and it has been shown that C53 inhibits G_2/M checkpoint activation by DNA damage. Overexpression of γ-

tubulin counteracts this C53 action (Hořejší et al., 2012). Besides, γ-tubulin may be involved in DNA damage repair processes as it associates not only with Rad51 (Lesca et al., 2005) but also with BRCA1 (Hubert et al., 2011), and ATR (Zhang et al., 2007). Proliferating cell nuclear antigen (PCNA) is a coordinator of DNA replication and repair (Stoimenov and Helleday, 2009). It has been reported that γ-tubulin binds PCNA and aids in its recruitment to chromatin in mammalian cells. A positive correlation between γ-tubulin and PCNA expression was found in all examined tumor types (Corvaisier et al., 2021). Finally, γ-tubulin is capable to modulate the anaphase-promoting complex/cyclosome (APC/C), which is a large protein complex with multiple subunits that is important for cell cycle regulation. There is strong evidence that in *Aspergillus nidulans* γ-tubulin plays an important role in regulating APC/C during interphase (Nayak et al., 2010) by inactivation of the APC/C activator CdhA (*A. nidulans* homolog of Cdh1) at the G1-to-S transition (Edgerton-Morgan and Oakley, 2012). Deciphering the molecular mechanisms underlying the various nucleus-specific functions of γ-tubulin remains the major challenge for future studies.

Concluding remarks

Recent structural studies of γ-TuRCs have been very informative, but molecular mechanisms how factors involved in promoting the transition from the open to the closed state of γ-TuRCs needs to be thoroughly characterized. Many proteins (targeting, activating, anchoring, modulating) that interact with γ-TuRCs are required to nucleate microtubule at right place and time. However, the upstream signaling pathways ensuring that these regulatory proteins act in concert and initiate microtubule nucleation according to the cell's requirements are largely unknown. It is becoming increasingly clear that kinases and phosphatases are important for microtubule regulation. Therefore, functional characterization of phosphorylation sites in γ-TuRCs and interacting proteins is required. Another important issue to be resolved is the analysis of γ-TuRC subpopulations that differ in composition or PTMs. Future studies are also needed to determine whether different γ-TuRCs can independently nucleate cell type-specific noncentrosomal microtubules. A detailed understanding of the molecular mechanisms of microtubule nucleation should provide new insights into the importance of γ-TuRC dysregulation in cancer cell behaviour and in neurological diseases and could lead to the development of highly specific γ-tubulin drugs (Dráber and Dráberová, 2021).

In recent years, the functions of γ-tubulin independent of microtubule nucleation have received more attention. High-resolution cryo-electron microscopy will be essential for deciphering the structure of recently reported γ-tubulin fibers and their high-level assemblies in a cellular context. Understanding the role of γ-tubulin isotypes under different stress conditions, in cell cycle checkpoints and in DNA repair will be important to elucidate their roles in carcinogenesis.

Finally, it has become increasingly evident that microtubules and microfilaments frequently cooperate. Recent work suggests that both microtubules and actin filaments are nucleated from centrosomes and that actin and its associated proteins control microtubule nucleation. Sophisticated *in vitro* reconstitution experiments should shed light on the role of proteins regulating microtubule nucleation in the cross-talk between microtubules and microfilaments.

Author contributions

VS, ED, and PD wrote the manuscript. All authors approved the submitted version.

Funding

This work was supported by grant 21-30281S from the Czech Science Foundation, grants LTAUSA19118 and LX22NPO5102 from the Ministry of Education, Youth and Sports of the Czech Republic, and institutional research support (RVO 68378050).

Acknowledgments

We thank Tetyana Sulimenko for preparation of figures. This article relies on a wealth of data from different laboratories. We have cited the appropriate original publications wherever possible, and we apologize to all researchers whose work on γ-tubulin was not included in this article.

Conflict of interest

The authors declare that the research was conducted in the absence of any commercial or financial relationships that could be construed as a potential conflict of interest.

Publisher's note

References

Akhmanova, A., and Kapitein, L. C. (2022). Mechanisms of microtubule organization in differentiated animal cells. *Nat. Rev. Mol. Cell Biol.* 23, 541–558. doi:10.1038/s41580-022-00473-y

Aldaz, H., Rice, L. M., Stearns, T., and Agard, D. A. (2005). Insights into microtubule nucleation from the crystal structure of human γ-tubulin. *Nature* 435, 523–527. doi:10.1038/nature03586

Alvarado-Kristensson, M., Rodriguez, M. J., Silio, V., Valpuesta, J. M., and Carrera, A. C. (2009). SADB phosphorylation of γ-tubulin regulates centrosome duplication. *Nat. Cell Biol.* 11, 1081–1092. doi:10.1038/ncb1921

Andersen, J. S., Lyon, C. E., Fox, A. H., Leung, A. K. L., Lam, Y. W., Steen, H., et al. (2002). Directed proteomic analysis of the human nucleolus. *Curr. Biol.* 12, 1–11. doi:10.1016/s0960-9822(01)00650-9

Arquint, C., Gabryjonczyk, A. M., and Nigg, E. A. (2014). Centrosomes as signalling centres. *Philos. Trans. R. Soc. Lond. B Biol. Sci.* 369, e20130464. doi:10.1098/rstb.2013.0464

Bahtz, R., Seidler, J., Arnold, M., Haselmann-Weiss, U., Antony, C., Lehmann, W. D., et al. (2012). GCP6 is a substrate of Plk4 and required for centriole duplication. *J. Cell Sci.* 125, 486–496. doi:10.1242/jcs.093930

Baumgart, J., Kirchner, M., Redemann, S., Bond, A., Woodruff, J., Verbavatz, J. M., et al. (2019). Soluble tubulin is significantly enriched at mitotic centrosomes. *J. Cell Biol.* 218, 3977–3985. doi:10.1083/jcb.201902069

Biedermann, S., Harashima, H., Chen, P., Heese, M., Bouyer, D., Sofroni, K., et al. (2017). The retinoblastoma homolog RBR1 mediates localization of the repair protein RAD51 to DNA lesions in *Arabidopsis*. *EMBO J.* 36, 1279–1297. doi:10.15252/embj.201694571

Binarová, P., Cenklová, V., Hause, B., Kubátová, E., Lysák, M., Doležel, J., et al. (2000). Nuclear γ-tubulin during acentriolar plant mitosis. *Plant Cell* 12, 433–442. doi:10.1105/tpc.12.3.433

Binarová, P., Cenklová, V., Procházková, J., Doskočilová, A., Volc, J., Vrlík, M., et al. (2006). γ-Tubulin is essential for acentrosomal microtubule nucleation and coordination of late mitotic events in *Arabidopsis*. *Plant Cell* 18, 1199–1212. doi:10.1105/tpc.105.038364

Bouckson-Castaing, V., Moudjou, M., Ferguson, D. J., Mucklow, S., Belkaid, Y., Milon, G., et al. (1996). Molecular characterisation of ninein, a new coiled-coil protein of the centrosome. *J. Cell Sci.* 109, 179–190. doi:10.1242/jcs.109.1.179

Bouissou, A., Verollet, C., Sousa, A., Sampaio, P., Wright, M., Sunkel, C. E., et al. (2009). γ-Tubulin ring complexes regulate microtubule plus end dynamics. *J. Cell Biol.* 187, 327–334. doi:10.1083/jcb.200905060

Brilot, A. F., Lyon, A. S., Zelter, A., Viswanath, S., Maxwell, A., MacCoss, M. J., et al. (2021). CM1-driven assembly and activation of yeast γ-tubulin small complex underlies microtubule nucleation. *eLife* 10, e65168. doi:10.7554/eLife.65168

Černohorská, M., Sulimenko, V., Hájková, Z., Sulimenko, T., Sládková, V., Vinopal, S., et al. (2016). GIT1/βPIX signaling proteins and PAK1 kinase regulate microtubule nucleation. *Biochim. Biophys. Acta* 1863, 1282–1297. doi:10.1016/j.bbamcr.2016.03.016

Chi, W., Wang, G., Xin, G., Jiang, Q., and Zhang, C. (2021). PLK4-phosphorylated NEDD1 facilitates cartwheel assembly and centriole biogenesis initiations. *J. Cell Biol.* 220, e202002151. doi:10.1083/jcb.202002151

Chi, Y., Welcker, M., Hizli, A. A., Posakony, J. J., Aebersold, R., and Clurman, B. E. (2008). Identification of CDK2 substrates in human cell lysates. *Genome Biol.* 9, R149. doi:10.1186/gb-2008-9-10-r149

Choi, Y. K., Liu, P., Sze, S. K., Dai, C., and Qi, R. Z. (2010). CDK5RAP2 stimulates microtubule nucleation by the γ-tubulin ring complex. *J. Cell Biol.* 191, 1089–1095. doi:10.1083/jcb.201007030

Chumová, J., Kourová, H., Trögelová, L., Daniel, G., and Binarová, P. (2021). γ-Tubulin complexes and fibrillar arrays: two conserved high molecular forms with many cellular functions. *Cells* 10, e776. doi:10.3390/cells10040776

Chumová, J., Kourová, H., Trögelová, L., Halada, P., and Binarová, P. (2019). Microtubular and nuclear functions of γ-tubulin: Are they LINCed? *Cells* 8, e259. doi:10.3390/cells8030259

Chumová, J., Trögelová, L., Kourová, H., Volc, J., Sulimenko, V., Halada, P., et al. (2018). γ-Tubulin has a conserved intrinsic property of self-polymerization into double stranded filaments and fibrillar networks. *Biochim. Biophys. Acta. Mol. Cell Res.* 1865, 734–748. doi:10.1016/j.bbamcr.2018.02.009

Consolati, T., Locke, J., Roostalu, J., Chen, Z. A., Gannon, J., Asthana, J., et al. (2020). Microtubule nucleation properties of single human γTuRCs explained by their cryo-EM structure. *Dev. Cell* 53, 603–617. doi:10.1016/j.devcel.2020.04.019

Corvaisier, M., and Alvarado-Kristensson, M. (2020). Non-canonical functions of the γ-tubulin meshwork in the regulation of the nuclear architecture. *Cancers (Basel)* 12, e3102. doi:10.3390/cancers12113102

Corvaisier, M., Zhou, J., Malycheva, D., Cornella, N., Chioureas, D., Gustafsson, N. M. S., et al. (2021). The γ-tubulin meshwork assists in the recruitment of PCNA to chromatin in mammalian cells. *Commun. Biol.* 4, e767. doi:10.1038/s42003-021-02280-1

Delgehyr, N., Sillibourne, J., and Bornens, M. (2005). Microtubule nucleation and anchoring at the centrosome are independent processes linked by ninein function. *J. Cell Sci.* 118, 1565–1575. doi:10.1242/jcs.02302

Détraves, C., Mazarguil, H., Lajoie-Mazenc, I., Julian, M., Raynaud-Messina, B., and Wright, M. (1997). Protein complexes containing γ-tubulin are present in mammalian brain microtubule protein preparations. *Cell Motil. Cytoskelet.* 36, 179–189. doi:10.1002/(SICI)1097-0169(1997)36:2<179:AID-CM7>3.0.CO;2-4

Dráber, P., and Dráberová, E. (2021). Dysregulation of microtubule nucleating proteins in cancer cells. *Cancers (Basel)* 13, e5638. doi:10.3390/cancers13225638

Dráberová, E., D'Agostino, L., Caracciolo, V., Sládková, V., Sulimenko, T., Sulimenko, V., et al. (2015). Overexpression and nucleolar localization of γ-tubulin small complex proteins GCP2 and GCP3 in glioblastoma. *J. Neuropathol. Exp. Neurol.* 74, 723–742. doi:10.1097/NEN.0000000000000212

Dráberová, E., Sulimenko, V., Vinopal, S., Sulimenko, T., Sládková, V., D'Agostino, L., et al. (2017). Differential expression of human γ-tubulin isotypes during neuronal development and oxidative stress points to a γ-tubulin-2 prosurvival function. *FASEB J.* 31, 1828–1846. doi:10.1096/fj.201600846RR

Dryková, D., Sulimenko, V., Cenklová, V., Volc, J., Dráber, P., and Binarová, P. (2003). Plant γ-tubulin interacts with αβ-tubulin dimers and forms membrane-associated complexes. *Plant Cell* 15, 465–480. doi:10.1105/tpc.007005

Edgerton-Morgan, H., and Oakley, B. R. (2012). γ-Tubulin plays a key role in inactivating APC/C^{Cdh1} at the G_1-S boundary. *J. Cell Biol.* 198, 785–791. doi:10.1083/jcb.201203115

Ehlén, Å., Rosselló, C. A., von Stedingk, K., Höög, G., Nilsson, E., Pettersson, H. M., et al. (2012). Tumors with nonfunctional retinoblastoma protein are killed by reduced γ-tubulin levels. *J. Biol. Chem.* 287, 17241–17247. doi:10.1074/jbc.M112.357038

Eklund, G., Lang, S., Glindre, J., Ehlén, A., and Alvarado-Kristensson, M. (2014). The nuclear localization of γ-tubulin is regulated by SadB-mediated phosphorylation. *J. Biol. Chem.* 289, 21360–21373. doi:10.1074/jbc.M114.562389

Farina, F., Gaillard, J., Guerin, C., Coute, Y., Sillibourne, J., Blanchoin, L., et al. (2016). The centrosome is an actin-organizing centre. *Nat. Cell Biol.* 18, 65–75. doi:10.1038/ncb3285

Farina, F., Ramkumar, N., Brown, L., Samandar Eweis, D., Anstatt, J., Waring, T., et al. (2019). Local actin nucleation tunes centrosomal microtubule nucleation during passage through mitosis. *EMBO J.* 38, e99843. doi:10.15252/embj.201899843

Fong, K. K., Zelter, A., Graczyk, B., Hoyt, J. M., Riffle, M., Johnson, R., et al. (2018). Novel phosphorylation states of the yeast spindle pole body. *Biol. Open* 7, bio033647. doi:10.1242/bio.033647

Fong, K. W., Choi, Y. K., Rattner, J. B., and Qi, R. Z. (2008). CDK5RAP2 is a pericentriolar protein that functions in centrosomal attachment of the γ-tubulin ring complex. *Mol. Biol. Cell* 19, 115–125. doi:10.1091/mbc.e07-04-0371

Gombos, L., Neuner, A., Berynskyy, M., Fava, L. L., Wade, R. C., Sachse, C., et al. (2013). GTP regulates the microtubule nucleation activity of γ-tubulin. *Nat. Cell Biol.* 15, 1317–1327. doi:10.1038/ncb2863

Gomez-Ferreria, M. A., Bashkurov, M., Helbig, A. O., Larsen, B., Pawson, T., Gingras, A. C., et al. (2012). Novel NEDD1 phosphorylation sites regulate γ-tubulin binding and mitotic spindle assembly. *J. Cell Sci.* 125, 3745–3751. doi:10.1242/jcs.105130

Gomez-Ferreria, M. A., Rath, U., Buster, D. W., Chanda, S. K., Caldwell, J. S., Rines, D. R., et al. (2007). Human Cep192 is required for mitotic centrosome and spindle assembly. *Curr. Biol.* 17, 1960–1966. doi:10.1016/j.cub.2007.10.019

Goshima, G., Mayer, M., Zhang, N., Stuurman, N., and Vale, R. D. (2008). Augmin: a protein complex required for centrosome-independent microtubule generation within the spindle. *J. Cell Biol.* 181, 421–429. doi:10.1083/jcb.200711053

Gunawardane, R. N., Martin, O. C., Cao, K., Zhang, L., Dej, K., Iwamatsu, A., et al. (2000). Characterization and reconstitution of *Drosophila* γ-tubulin ring complex subunits. *J. Cell Biol.* 151, 1513–1524. doi:10.1083/jcb.151.7.1513

Gunzelmann, J., Ruthnick, D., Lin, T. C., Zhang, W., Neuner, A., Jakle, U., et al. (2018). The microtubule polymerase Stu2 promotes oligomerization of the γ-TuSC for cytoplasmic microtubule nucleation. *eLife* 7, e39932. doi:10.7554/eLife.39932

Gupta, H., Rajeev, R., Sasmal, R., Radhakrishnan, R. M., Anand, U., Chandran, H., et al. (2020). SAS-6 Association with γ-tubulin ring complex is required for centriole duplication in human cells. *Curr. Biol.* 30, 2395–2403. doi:10.1016/j.cub.2020.04.036

Hanafusa, H., Kedashiro, S., Tezuka, M., Funatsu, M., Usami, S., Toyoshima, F., et al. (2015). PLK1-dependent activation of LRRK1 regulates spindle orientation by phosphorylating CDK5RAP2. *Nat. Cell Biol.* 17, 1024–1035. doi:10.1038/ncb3204

Haren, L., Remy, M. H., Bazin, I., Callebaut, I., Wright, M., and Merdes, A. (2006). NEDD1-dependent recruitment of the γ-tubulin ring complex to the centrosome is necessary for centriole duplication and spindle assembly. *J. Cell Biol.* 172, 505–515. doi:10.1083/jcb.200510028

Haren, L., Stearns, T., and Lüders, J. (2009). Plk1-dependent recruitment of γ-tubulin complexes to mitotic centrosomes involves multiple PCM components. *PLoS One* 4, e5976. doi:10.1371/journal.pone.0005976

Hegemann, B., Hutchins, J. R., Hudecz, O., Novatchkova, M., Rameseder, J., Sykora, M. M., et al. (2011). Systematic phosphorylation analysis of human mitotic protein complexes. *Sci. Signal.* 4, rs12. doi:10.1126/scisignal.2001993

Henty-Ridilla, J. L., and Goode, B. L. (2015). Global resource distribution: allocation of actin building blocks by profilin. *Dev. Cell* 32, 5–6. doi:10.1016/j.devcel.2014.12.022

Höög, G., Zarrizi, R., von Stedingk, K., Jonsson, K., and Alvarado-Kristensson, M. (2011). Nuclear localization of γ-tubulin affects E2F transcriptional activity and S-phase progression. *FASEB J.* 25, 3815–3827. doi:10.1096/fj.11-187484

Hořejší, B., Vinopal, S., Sládková, V., Dráberová, E., Sulimenko, V., Sulimenko, T., et al. (2012). Nuclear γ-tubulin associates with nucleoli and interacts with tumor suppressor protein C53. *J. Cell. Physiol.* 227, 367–382. doi:10.1002/jcp.22772

Hori, A., Morand, A., Ikebe, C., Frith, D., Snijders, A. P., and Toda, T. (2015). The conserved Wdr8-hMsd1/SSX2IP complex localises to the centrosome and ensures proper spindle length and orientation. *Biochem. Biophys. Res. Commun.* 468, 39–45. doi:10.1016/j.bbrc.2015.10.169

Horio, T., and Oakley, B. R. (1994). Human γ-tubulin functions in fission yeast. *J. Cell Biol.* 126, 1465–1473. doi:10.1083/jcb.126.6.1465

Horvath, B. M., Kourova, H., Nagy, S., Nemeth, E., Magyar, Z., Papdi, C., et al. (2017). *Arabidopsis* RETINOBLASTOMA RELATED directly regulates DNA damage responses through functions beyond cell cycle control. *EMBO J.* 36, 1261–1278. doi:10.15252/embj.201694561

Hsu, L. C., Doan, T. P., and White, R. L. (2001). Identification of a γ-tubulin-binding domain in BRCA1. *Cancer Res.* 61, 7713–7718. PMID: 11691781.

Hubert, T., Vandekerckhove, J., and Gettemans, J. (2011). Cdk1 and BRCA1 target γ-tubulin to microtubule domains. *Biochem. Biophys. Res. Commun.* 414, 240–245. doi:10.1016/j.bbrc.2011.09.064

Inclán, Y. F., and Nogales, E. (2001). Structural models for the self-assembly and microtubule interactions of δ-delta- and ε-tubulin. *J. Cell Sci.* 114, 413–422. doi:10.1242/jcs.114.2.413

Inoue, D., Obino, D., Pineau, J., Farina, F., Gaillard, J., Guerin, C., et al. (2019). Actin filaments regulate microtubule growth at the centrosome. *EMBO J.* 38, e99630. doi:10.15252/embj.201899630

Janke, C., and Magiera, M. M. (2020). The tubulin code and its role in controlling microtubule properties and functions. *Nat. Rev. Mol. Cell Biol.* 21, 307–326. doi:10.1038/s41580-020-0214-3

Joachimiak, E., Jerka-Dziadosz, M., Krzemien-Ojak, L., Waclawek, E., Jedynak, K., Urbanska, P., et al. (2018). Multiple phosphorylation sites on γ-tubulin are essential and contribute to the biogenesis of basal bodies in *Tetrahymena*. *J. Cell. Physiol.* 233, 8648–8665. doi:10.1002/jcp.26742

Johmura, Y., Soung, N. K., Park, J. E., Yu, L. R., Zhou, M., Bang, J. K., et al. (2011). Regulation of microtubule-based microtubule nucleation by mammalian polo-like kinase 1. *Proc. Natl. Acad. Sci. U. S. A.* 108, 11446–11451. doi:10.1073/pnas.1106223108

Joukov, V., and De Nicolo, A. (2018). Aurora-PLK1 cascades as key signaling modules in the regulation of mitosis. *Sci. Signal.* 11, eaar4195. doi:10.1126/scisignal.aar4195

Kállai, B. M., Kourová, H., Chumová, J., Papdi, C., Trögelová, L., Kofroňová, O., et al. (2020). γ-Tubulin interacts with E2F transcription factors to regulate proliferation and endocycling in Arabidopsis. *J. Exp. Bot.* 71, 1265–1277. doi:10.1093/jxb/erz498

Karlsson, R., and Dráber, P. (2021). Profilin-A master coordinator of actin and microtubule organization in mammalian cells. *J. Cell. Physiol.* 236, 7256–7265. doi:10.1002/jcp.30379

Katsetos, C. D., Dráberová, E., Legido, A., and Dráber, P. (2009). Tubulin targets in the pathobiology and therapy of glioblastoma multiforme. II. γ-Tubulin. *J. Cell. Physiol.* 221, 514–520. doi:10.1002/jcp.21884

Keating, T. J., and Borisy, G. G. (2000). Immunostructural evidence for the template mechanism of microtubule nucleation. *Nat. Cell Biol.* 2, 352–357. doi:10.1038/35014045

Keck, J. M., Jones, M. H., Wong, C. C., Binkley, J., Chen, D., Jaspersen, S. L., et al. (2011). A cell cycle phosphoproteome of the yeast centrosome. *Science* 332, 1557–1561. doi:10.1126/science.1205193

King, B. R., Moritz, M., Kim, H., Agard, D. A., Asbury, C. L., and Davis, T. N. (2020). XMAP215 and γ-tubulin additively promote microtubule nucleation in purified solutions. *Mol. Biol. Cell* 31, 2187–2194. doi:10.1091/mbc.E20-02-0160

Klebanovych, A., Vinopal, S., Dráberová, E., Sládková, V., Sulimenko, T., Sulimenko, V., et al. (2022). C53 interacting with UFM1-protein ligase 1 regulates microtubule nucleation in response to ER stress. *Cells* 11, e555. doi:10.3390/cells11030555

Kollman, J. M., Greenberg, C. H., Li, S., Moritz, M., Zelter, A., Fong, K. K., et al. (2015). Ring closure activates yeast γTuRC for species-specific microtubule nucleation. *Nat. Struct. Mol. Biol.* 22, 132–137. doi:10.1038/nsmb.2953

Kollman, J. M., Merdes, A., Mourey, L., and Agard, D. A. (2011). Microtubule nucleation by γ-tubulin complexes. *Nat. Rev. Mol. Cell Biol.* 12, 709–721. doi:10.1038/nrm3209

Kollman, J. M., Polka, J. K., Zelter, A., Davis, T. N., and Agard, D. A. (2010). Microtubule nucleating γ-TuSC assembles structures with 13-fold microtubule-like symmetry. *Nature* 466, 879–882. doi:10.1038/nature09207

Kollman, J. M., Zelter, A., Muller, E. G., Fox, B., Rice, L. M., Davis, T. N., et al. (2008). The structure of the γ-tubulin small complex: Implications of its architecture and flexibility for microtubule nucleation. *Mol. Biol. Cell* 19, 207–215. doi:10.1091/mbc.e07-09-0879

Kufer, T. A., Sillje, H. H., Korner, R., Gruss, O. J., Meraldi, P., and Nigg, E. A. (2002). Human TPX2 is required for targeting Aurora-A kinase to the spindle. *J. Cell Biol.* 158, 617–623. doi:10.1083/jcb.200204155

Kukharskyy, V., Sulimenko, V., Macurek, L., Sulimenko, T., Dráberová, E., and Dráber, P. (2004). Complexes of γ-tubulin with non-receptor protein tyrosine kinases Src and Fyn in differentiating P19 embryonal carcinoma cells. *Exp. Cell Res.* 298, 218–228. doi:10.1016/j.yexcr.2004.04.016

Lawo, S., Hasegan, M., Gupta, G. D., and Pelletier, L. (2012). Subdiffraction imaging of centrosomes reveals higher-order organizational features of pericentriolar material. *Nat. Cell Biol.* 14, 1148–1158. doi:10.1038/ncb2591

Lee, K., and Rhee, K. (2011). PLK1 phosphorylation of pericentrin initiates centrosome maturation at the onset of mitosis. *J. Cell Biol.* 195, 1093–1101. doi:10.1083/jcb.201106093

Leong, S. L., Lynch, E. M., Zou, J., Tay, Y. D., Borek, W. E., Tuijtel, M. W., et al. (2019). Reconstitution of microtubule nucleation *in vitro* reveals novel roles for Mzt1. *Curr. Biol.* 29, 2199–2207. doi:10.1016/j.cub.2019.05.058

Lesca, C., Germanier, M., Raynaud-Messina, B., Pichereaux, C., Etievant, C., Emond, S., et al. (2005). DNA damage induce γ-tubulin-RAD51 nuclear complexes in mammalian cells. *Oncogene* 24, 5165–5172. doi:10.1038/sj.onc.1208723

Lin, T. C., Gombos, L., Neuner, A., Sebastian, D., Olsen, J. V., Hrle, A., et al. (2011). Phosphorylation of the yeast γ-tubulin Tub4 regulates microtubule function. *PLoS ONE* 6, e19700. doi:10.1371/journal.pone.0019700

Lin, T. C., Neuner, A., and Schiebel, E. (2015). Targeting of γ-tubulin complexes to microtubule organizing centers: conservation and divergence. *Trends Cell Biol.* 25, 296–307. doi:10.1016/j.tcb.2014.12.002

Lindström, L., and Alvarado-Kristensson, M. (2018). Characterization of γ-tubulin filaments in mammalian cells. *Biochim. Biophys. Acta. Mol. Cell Res.* 1865, 158–171. doi:10.1016/j.bbamcr.2017.10.008

Lindström, L., Li, T., Malycheva, D., Kancharla, A., Nilsson, H., Vishnu, N., et al. (2018). The GTPase domain of γ-tubulin is required for normal mitochondrial function and spatial organization. *Commun. Biol.* 1, 37. doi:10.1038/s42003-018-0037-3

Linhartová, I., Dráber, P., Dráberová, E., and Viklický, V. (1992). Immunological discrimination of β-tubulin isoforms in developing mouse brain. Posttranslational modification of non-class III β-tubulins. *Biochem. J.* 288, 919–924. doi:10.1042/bj2880919

Linhartová, I., Novotná, B., Sulimenko, V., Dráberová, E., and Dráber, P. (2002). γ-tubulin in chicken erythrocytes: changes in localization during cell differentiation and characterization of cytoplasmic complexes. *Dev. Dyn.* 223, 229–240. doi:10.1002/dvdy.10047

Liu, B., Marc, J., Joshi, H. C., and Palevitz, B. A. (1993). A γ-tubulin-related protein associated with the microtubule arrays of higher plants in a cell cycle-dependent manner. *J. Cell Sci.* 104, 1217–1228. doi:10.1242/jcs.104.4.1217

Liu, P., Choi, Y. K., and Qi, R. Z. (2014). NME7 is a functional component of the γ-tubulin ring complex. *Mol. Biol. Cell* 25, 2017–2025. doi:10.1091/mbc.E13-06-0339

Liu, P., Zupa, E., Neuner, A., Böhler, A., Loerke, J., Flemming, D., et al. (2020). Insights into the assembly and activation of the microtubule nucleator γ-TuRC. *Nature* 578, 467–471. doi:10.1038/s41586-019-1896-6

Lüders, J., Patel, U. K., and Stearns, T. (2006). GCP-WD is a γ-tubulin targeting factor required for centrosomal and chromatin mediated microtubule nucleation. *Nat. Cell Biol.* 8, 137–147. doi:10.1038/ncb1349

Ludueña, R. F. (1993). Are tubulin isotypes functionally significant? *Mol. Biol. Cell* 4, 445–457. doi:10.1091/mbc.4.5.445

Ludueña, R. F. (2013). A hypothesis on the origin and evolution of tubulin. *Int. Rev. Cell Mol. Biol.* 302, 41–185. doi:10.1016/B978-0-12-407699-0.00002-9

Meunier, S., and Vernos, I. (2016). Acentrosomal microtubule assembly in mitosis: the where, when, and how. *Trends Cell Biol.* 26, 80–87. doi:10.1016/j.tcb.2015.09.001

Mitchison, T., and Kirschner, M. (1984). Dynamic instability of microtubule growth. *Nature* 312, 237–242. doi:10.1038/312237a0

Monfregola, J., Napolitano, G., D'Urso, M., Lappalainen, P., and Ursini, M. V. (2010). Functional characterization of Wiskott-Aldrich syndrome protein and scar homolog (WASH), a bi-modular nucleation-promoting factor able to interact with biogenesis of lysosome-related organelle subunit 2 (BLOS2) and γ-tubulin. *J. Biol. Chem.* 285, 16951–16957. doi:10.1074/jbc.M109.078501

Moritz, M., Braunfeld, M. B., Guenebaut, V., Heuser, J., and Agard, D. A. (2000). Structure of the γ-tubulin ring complex: a template for microtubule nucleation. *Nat. Cell Biol.* 2, 365–370. doi:10.1038/35014058

Moritz, M., Braunfeld, M. B., Sedat, J. W., Alberts, B., and Agard, D. A. (1995). Microtubule nucleation by γ-tubulin-containing rings in the centrosome. *Nature* 378, 638–640. doi:10.1038/378638a0

Nayak, T., Edgerton-Morgan, H., Horio, T., Xiong, Y., De Souza, C. P., Osmani, S. A., et al. (2010). γ-tubulin regulates the anaphase-promoting complex/cyclosome during interphase. *J. Cell Biol.* 190, 317–330. doi:10.1083/jcb.201002105

Nejedlá, M., Klebanovych, A., Sulimenko, V., Sulimenko, T., Dráberová, E., Dráber, P., et al. (2021). The actin regulator profilin 1 is functionally associated with the mammalian centrosome. *Life Sci. Alliance* 4, e202000655. doi:10.26508/lsa.202000655

Nogales, E., and Wang, H. W. (2006). Structural mechanisms underlying nucleotide-dependent self-assembly of tubulin and its relatives. *Curr. Opin. Struct. Biol.* 16, 221–229. doi:10.1016/j.sbi.2006.03.005

O'Rourke, B. P., Gomez-Ferreria, M. A., Berk, R. H., Hackl, A. M., Nicholas, M. P., O'Rourke, S. C., et al. (2014). Cep192 controls the balance of centrosome and non-centrosomal microtubules during interphase. *PLoS One* 9, e101001. doi:10.1371/journal.pone.0101001

Oakley, B. R., Paolillo, V., and Zheng, Y. (2015). γ-Tubulin complexes in microtubule nucleation and beyond. *Mol. Biol. Cell* 26, 2957–2962. doi:10.1091/mbc.E14-11-1514

Oakley, C. E., and Oakley, B. R. (1989). Identification of γ-tubulin, a new member of the tubulin superfamily encoded by mipA gene of *Aspergillus nidulans*. *Nature* 338, 662–664. doi:10.1038/338662a0

Oegema, K., Wiese, C., Martin, O. C., Milligan, R. A., Iwamatsu, A., Mitchison, T. J., et al. (1999). Characterization of two related *Drosophila* γ-tubulin complexes that differ in their ability to nucleate microtubules. *J. Cell Biol.* 144, 721–733. doi:10.1083/jcb.144.4.721

Ohashi, T., Yamamoto, T., Yamanashi, Y., and Ohsugi, M. (2016). Human TUBG2 gene is expressed as two splice variant mRNA and involved in cell growth. *FEBS Lett.* 590, 1053–1063. doi:10.1002/1873-3468.12163

Ohta, M., Zhao, Z., Wu, D., Wang, S., Harrison, J. L., Gomez-Cavazos, J. S., et al. (2021). Polo-like kinase 1 independently controls microtubule-nucleating capacity and size of the centrosome. *J. Cell Biol.* 220, e202009083. doi:10.1083/jcb.202009083

Ong, S. T., Chalasani, M. L. S., Fazil, M., Prasannan, P., Kizhakeyil, A., Wright, G. D., et al. (2018). Centrosome- and Golgi-localized protein kinase N-associated protein serves as a docking platform for protein kinase A signaling and microtubule nucleation in migrating T-cells. *Front. Immunol.* 9, e397. doi:10.3389/fimmu.2018.00397

Oriolo, A. S., Wald, F. A., Canessa, G., and Salas, P. J. (2007). GCP6 binds to intermediate filaments: a novel function of keratins in the organization of microtubules in epithelial cells. *Mol. Biol. Cell* 18, 781–794. doi:10.1091/mbc.e06-03-0201

Pastuglia, M., Azimzadeh, J., Goussot, M., Camilleri, C., Belcram, K., Evrard, J. L., et al. (2006). γ-Tubulin is essential for microtubule organization and development in *Arabidopsis*. *Plant Cell* 18, 1412–1425. doi:10.1105/tpc.105.039644

Paz, J., and Lüders, J. (2018). Microtubule-organizing centers: towards a minimal parts list. *Trends Cell Biol.* 28, 176–187. doi:10.1016/j.tcb.2017.10.005

Petry, S., and Vale, R. D. (2015). Microtubule nucleation at the centrosome and beyond. *Nat. Cell Biol.* 17, 1089–1093. doi:10.1038/ncb3220

Pinyol, R., Scrofani, J., and Vernos, I. (2013). The role of NEDD1 phosphorylation by Aurora A in chromosomal microtubule nucleation and spindle function. *Curr. Biol.* 23, 143–149. doi:10.1016/j.cub.2012.11.046

Plessner, M., Knerr, J., and Grosse, R. (2019). Centrosomal Actin Assembly is required for proper mitotic spindle formation and chromosome congression. *iScience* 15, 274–281. doi:10.1016/j.isci.2019.04.022

Pouchucq, L., Lobos-Ruiz, P., Araya, G., Valpuesta, J. M., and Monasterio, O. (2018). The chaperonin CCT promotes the formation of fibrillar aggregates of γ-tubulin. *Biochim. Biophys. Acta. Proteins Proteom.* 1866, 519–526. doi:10.1016/j.bbapap.2018.01.007

Rajeev, R., Singh, P., Asmita, A., Anand, U., and Manna, T. K. (2019). Aurora A site specific TACC3 phosphorylation regulates astral microtubule assembly by stabilizing γ-tubulin ring complex. *BMC Mol. Cell Biol.* 20, 58. doi:10.1186/s12860-019-0242-z

Raynaud, C., and Nisa, M. (2020). A conserved role for γ-tubulin as a regulator of E2F transcription factors. *J. Exp. Bot.* 71, 1199–1202. doi:10.1093/jxb/erz557

Redwine, W. B., DeSantis, M. E., Hollyer, I., Htet, Z. M., Tran, P. T., Swanson, S. K., et al. (2017). The human cytoplasmic dynein interactome reveals novel activators of motility. *eLife* 6, e28257. doi:10.7554/eLife.28257

Rice, L. M., Montabana, E. A., and Agard, D. A. (2008). The lattice as allosteric effector: structural studies of αβ- and γ-tubulin clarify the role of GTP in microtubule assembly. *Proc. Natl. Acad. Sci. U. S. A.* 105, 5378–5383. doi:10.1073/pnas.0801155105

Rice, L. M., Moritz, M., and Agard, D. A. (2021). Microtubules form by progressively faster tubulin accretion, not by nucleation-elongation. *J. Cell Biol.* 220, e202012079. doi:10.1083/jcb.202012079

Roll-Mecak, A. (2020). The tubulin code in microtubule dynamics and information encoding. *Dev. Cell* 54, 7–20. doi:10.1016/j.devcel.2020.06.008

Roostalu, J., and Surrey, T. (2017). Microtubule nucleation: beyond the template. *Nat. Rev. Mol. Cell Biol.* 18, 702–710. doi:10.1038/nrm.2017.75

Rosselló, C. A., Lindström, L., Eklund, G., Corvaisier, M., and Alvarado-Kristensson, M. A. (2018). γ-Tubulin-γ-tubulin interactions as the basis for the formation of a meshwork. *Int. J. Mol. Sci.* 19, 3245. doi:10.3390/ijms19103245

Sankaran, S., Starita, L. M., Groen, A. C., Ko, M. J., and Parvin, J. D. (2005). Centrosomal microtubule nucleation activity is inhibited by BRCA1-dependent ubiquitination. *Mol. Cell. Biol.* 25, 8656–8668. doi:10.1128/MCB.25.19.8656-8668.2005

Santamaria, A., Wang, B., Elowe, S., Malik, R., Zhang, F., Bauer, M., et al. (2011). The Plk1-dependent phosphoproteome of the early mitotic spindle. *Mol. Cell. Proteomics* 10, M110.004457. doi:10.1074/mcp.M110.004457

Sawin, K. E., Lourenco, P. C., and Snaith, H. A. (2004). Microtubule nucleation at non-spindle pole body microtubule-organizing centers requires fission yeast centrosomin-related protein mod20p. *Curr. Biol.* 14, 763–775. doi:10.1016/j.cub.2004.03.042

Schaerer-Brodbeck, C., and Riezman, H. (2003). Genetic and biochemical interactions between the Arp2/3 complex, Cmd1p, casein kinase II, and Tub4p in yeast. *FEMS Yeast Res.* 4, 37–49. doi:10.1016/S1567-1356(03)00110-7

Schweizer, N., Haren, L., Dutto, I., Viais, R., Lacasa, C., Merdes, A., et al. (2021). Sub-centrosomal mapping identifies augmin-γTuRC as part of a centriole-stabilizing scaffold. *Nat. Commun.* 12, e6042. doi:10.1038/s41467-021-26252-5

Schweizer, N., and Lüders, J. (2021). From tip to toe - dressing centrioles in γTuRC. *J. Cell Sci.* 134, jcs258397. doi:10.1242/jcs.258397

Scrofani, J., Sardon, T., Meunier, S., and Vernos, I. (2015). Microtubule nucleation in mitosis by a RanGTP-dependent protein complex. *Curr. Biol.* 25, 131–140. doi:10.1016/j.cub.2014.11.025

Sheng, L., Li, J., Rao, S., Yang, Z., and Huang, Y. (2021). Cyclin-dependent kinase 5 regulatory subunit associated protein 3: Potential functions and implications for development and disease. *Front. Oncol.* 11, 760429. doi:10.3389/fonc.2021.760429

Shu, H. B., and Joshi, H. C. (1995). γ-tubulin can both nucleate microtubule assembly and self-assemble into novel tubular structures in mammalian cells. *J. Cell Biol.* 130, 1137–1147. doi:10.1083/jcb.130.5.1137

Shulist, K., Yen, E., Kaitna, S., Leary, A., Decterov, A., Gupta, D., et al. (2017). Interrogation of γ-tubulin alleles using high-resolution fitness measurements reveals a distinct cytoplasmic function in spindle alignment. *Sci. Rep.* 7, 11398. doi:10.1038/s41598-017-11789-7

Singh, P., Thomas, G. E., Gireesh, K. K., and Manna, T. K. (2014). TACC3 protein regulates microtubule nucleation by affecting γ-tubulin ring complexes. *J. Biol. Chem.* 289, 31719–31735. doi:10.1074/jbc.M114.575100

Starita, L. M., Machida, Y., Sankaran, S., Elias, J. E., Griffin, K., Schlegel, B. P., et al. (2004). BRCA1-dependent ubiquitination of γ-tubulin regulates centrosome number. *Mol. Cell. Biol.* 24, 8457–8466. doi:10.1128/MCB.24.19.8457-8466.2004

Stearns, T., Evans, L., and Kirschner, M. (1991). γ-tubulin is a highly conserved component of the centrosome. *Cell* 65, 825–836. doi:10.1016/0092-8674(91)90390-k

Stoimenov, I., and Helleday, T. (2009). PCNA on the crossroad of cancer. *Biochem. Soc. Trans.* 37, 605–613. doi:10.1042/BST0370605

Sulimenko, V., Hájková, Z., Černohorská, M., Sulimenko, T., Sládková, V., Dráberová, L., et al. (2015). Microtubule nucleation in mouse bone marrow-derived mast cells is regulated by the concerted action of GIT1/βPIX proteins and calcium. *J. Immunol.* 194, 4099–4111. doi:10.4049/jimmunol.1402459

Sulimenko, V., Hájková, Z., Klebanovych, A., and Dráber, P. (2017). Regulation of microtubule nucleation mediated by γ-tubulin complexes. *Protoplasma* 254, 1187–1199. doi:10.1007/s00709-016-1070-z

Sulimenko, V., Sulimenko, T., Poznanovic, S., Nechiporuk-Zloy, V., Böhm, J. K., Macůrek, L., et al. (2002). Association of brain γ-tubulins with αβ-tubulin dimers. *Biochem. J.* 365, 889–895. doi:10.1042/BJ20020175

Sztul, E., Chen, P. W., Casanova, J. E., Cherfils, J., Dacks, J. B., Lambright, D. G., et al. (2019). ARF GTPases and their GEFs and GAPs: concepts and challenges. *Mol. Biol. Cell* 30, 1249–1271. doi:10.1091/mbc.E18-12-0820

Takahashi, M., Yamagiwa, A., Nishimura, T., Mukai, H., and Ono, Y. (2002). Centrosomal proteins CG-NAP and kendrin provide microtubule nucleation sites by anchoring γ-tubulin ring complex. *Mol. Biol. Cell* 13, 3235–3245. doi:10.1091/mbc.e02-02-0112

Thawani, A., Kadzik, R. S., and Petry, S. (2018). XMAP215 is a microtubule nucleation factor that functions synergistically with the γ-tubulin ring complex. *Nat. Cell Biol.* 20, 575–585. doi:10.1038/s41556-018-0091-6

Thawani, A., and Petry, S. (2021). Molecular insight into how γ-TuRC makes microtubules. *J. Cell Sci.* 134, jcs245464. doi:10.1242/jcs.245464

Thawani, A., Rale, M. J., Coudray, N., Bhabha, G., Stone, H. A., Shaevitz, J. W., et al. (2020). The transition state and regulation of γ-TuRC-mediated microtubule nucleation revealed by single molecule microscopy. *eLife* 9, e54253. doi:10.7554/eLife.54253

Thirunavukarasou, A., Govindarajalu, G., Singh, P., Bandi, V., Muthu, K., and Baluchamy, S. (2015). Cullin 4A and 4B ubiquitin ligases interact with γ-tubulin and induce its polyubiquitination. *Mol. Cell. Biochem.* 401, 219–228. doi:10.1007/s11010-014-2309-7

Ti, S. C., Alushin, G. M., and Kapoor, T. M. (2018). Human β-tubulin isotypes can regulate microtubule protofilament number and stability. *Dev. Cell* 47, 175–190. doi:10.1016/j.devcel.2018.08.014

Tovey, C. A., and Conduit, P. T. (2018). Microtubule nucleation by γ-tubulin complexes and beyond. *Essays Biochem.* 62, 765–780. doi:10.1042/EBC20180028

Tovey, C. A., Tsuji, C., Egerton, A., Bernard, F., Guichet, A., de la Roche, M., et al. (2021). Autoinhibition of Cnn binding to γ-TuRCs prevents ectopic microtubule nucleation and cell division defects. *J. Cell Biol.* 220, e202010020. doi:10.1083/jcb.202010020

Tovey, C. A., Tubman, C. E., Hamrud, E., Zhu, Z., Dyas, A. E., Butterfield, A. N., et al. (2018). γ-TuRC heterogeneity revealed by analysis of Mozart1. *Curr. Biol.* 28, 2314–2323. doi:10.1016/j.cub.2018.05.044

Tu, H. Q., Qin, X. H., Liu, Z. B., Song, Z. Q., Hu, H. B., Zhang, Y. C., et al. (2018). Microtubule asters anchored by FSD1 control axoneme assembly and ciliogenesis. *Nat. Commun.* 9, e5277. doi:10.1038/s41467-018-07664-2

Turn, R. E., East, M. P., Prekeris, R., and Kahn, R. A. (2020). The ARF GAP ELMOD2 acts with different GTPases to regulate centrosomal microtubule nucleation and cytokinesis. *Mol. Biol. Cell* 31, 2070–2091. doi:10.1091/mbc.E20-01-0012

Valenzuela, A., Meservey, L., Nguyen, H., and Fu, M. M. (2020). Golgi outposts nucleate microtubules in cells with specialized shapes. *Trends Cell Biol.* 30, 792–804. doi:10.1016/j.tcb.2020.07.004

Vineethakumari, C., and Lüders, J. (2022). Microtubule anchoring: attaching dynamic polymers to cellular structures. *Front. Cell Dev. Biol.* 10, e867870. doi:10.3389/fcell.2022.867870

Vinopal, S., Černohorská, M., Sulimenko, V., Sulimenko, T., Vosecká, V., Flemr, M., et al. (2012). γ-Tubulin 2 nucleates microtubules and is downregulated in mouse early embryogenesis. *PLoS ONE* 7, e29919. doi:10.1371/journal.pone.0029919

Vogel, J., Drapkin, B., Oomen, J., Beach, D., Bloom, K., and Snyder, M. (2001). Phosphorylation of γ-tubulin regulates microtubule organization in budding yeast. *Dev. Cell* 1, 621–631. doi:10.1016/s1534-5807(01)00073-9

Wang, G. F., Dong, Q., Bai, Y., Gu, J., Tao, Q., Yue, J., et al. (2022). c-Abl kinase-mediated phosphorylation of γ-tubulin promotes γ-tubulin ring complexes assembly and microtubule nucleation. *J. Biol. Chem.* 298, e101778. doi:10.1016/j.jbc.2022.101778

Wang, J., An, H., Mayo, M. W., Baldwin, A. S., and Yarbrough, W. G. (2007). LZAP, a putative tumor suppressor, selectively inhibits NF-κB. *Cancer Cell* 12, 239–251. doi:10.1016/j.ccr.2007.07.002

Wang, Z., Wu, T., Shi, L., Zhang, L., Zheng, W., Qu, J. Y., et al. (2010). Conserved motif of CDK5RAP2 mediates its localization to centrosomes and the Golgi complex. *J. Biol. Chem.* 285, 22658–22665. doi:10.1074/jbc.M110.105965

Wieczorek, M., Huang, T. L., Urnavicius, L., Hsia, K. C., and Kapoor, T. M. (2020a). MZT proteins form multi-faceted structural modules in the γ-tubulin ring complex. *Cell Rep.* 31, e107791. doi:10.1016/j.celrep.2020.107791

Wieczorek, M., Urnavicius, L., Ti, S. C., Molloy, K. R., Chait, B. T., and Kapoor, T. M. (2020b). Asymmetric molecular architecture of the human γ-tubulin ring complex. *Cell* 180, 165–175. doi:10.1016/j.cell.2019.12.007

Wieczorek, M., Ti, S. C., Urnavicius, L., Molloy, K. R., Aher, A., Chait, B. T., et al. (2021). Biochemical reconstitutions reveal principles of human γ-TuRC assembly and function. *J. Cell Biol.* 220, e202009146. doi:10.1083/jcb.202009146

Wiese, C., and Zheng, Y. (2000). A new function for the γ-tubulin ring complex as a microtubule minus-end cap. *Nat. Cell Biol.* 2, 358–364. doi:10.1038/35014051

Wilkes, O. R., and Moore, A. W. (2020). Distinct microtubule organizing center mechanisms combine to generate neuron polarity and arbor complexity. *Front. Cell. Neurosci.* 14, e594199. doi:10.3389/fncel.2020.594199

Wise, D. O., Krahe, R., and Oakley, B. R. (2000). The γ-tubulin gene family in humans. *Genomics* 67, 164–170. doi:10.1006/geno.2000.6247

Wolff, A., Denoulet, P., and Jeantet, C. (1982). High level of tubulin microheterogeneity in the mouse brain. *Neurosci. Lett.* 31, 323–328. doi:10.1016/0304-3940(82)90041-6

Würtz, M., Zupa, E., Atorino, E. S., Neuner, A., Böhler, A., Rahadian, A. S., et al. (2022). Modular assembly of the principal microtubule nucleator γ-TuRC. *Nat. Commun.* 13, e473. doi:10.1038/s41467-022-28079-0

Yin, C., Lui, E. S. W., Jiang, T., and Qi, R. Z. (2021). Proteolysis of γ-tubulin small complex proteins is mediated by the ubiquitin-proteasome system. *FEBS Lett.* 595, 1987–1996. doi:10.1002/1873-3468.14146

Yuba-Kubo, A., Kubo, A., Hata, M., and Tsukita, S. (2005). Gene knockout analysis of two γ-tubulin isoforms in mice. *Dev. Biol.* 282, 361–373. doi:10.1016/j.ydbio.2005.03.031

Zarrizi, R., Menard, J. A., Belting, M., and Massoumi, R. (2014). Deubiquitination of γ-tubulin by BAP1 prevents chromosome instability in breast cancer cells. *Cancer Res.* 74, 6499–6508. doi:10.1158/0008-5472.CAN-14-0221

Zhang, R., LaFrance, B., and Nogales, E. (2018). Separating the effects of nucleotide and EB binding on microtubule structure. *Proc. Natl. Acad. Sci. U. S. A.* 115, E6191–E6200. doi:10.1073/pnas.1802637115

Zhang, S., Hernmerich, P., and Grosse, F. (2007). Centrosomal localization of DNA damage checkpoint proteins. *J. Cell. Biochem.* 101, 451–465. doi:10.1002/jcb.21195

Zhang, X., Chen, Q., Feng, J., Hou, J., Yang, F., Liu, J., et al. (2009). Sequential phosphorylation of Nedd1 by Cdk1 and Plk1 is required for targeting of the γTuRC to the centrosome. *J. Cell Sci.* 122, 2240–2251. doi:10.1242/jcs.042747

Zhao, Z. S., Lim, J. P., Ng, Y. W., Lim, L., and Manser, E. (2005). The GIT-associated kinase PAK targets to the centrosome and regulates Aurora-A. *Mol. Cell* 20, 237–249. doi:10.1016/j.molcel.2005.08.035

Zheng, Y., Alberts, B., and Mitchison, T. (1995). Nucleation of microtubule assembly by a γ-tubulin-containing ring complex. *Nature* 378, 578–583. doi:10.1038/378578a0

Zimmerman, W. C., Sillibourne, J., Rosa, J., and Doxsey, S. J. (2004). Mitosis-specific anchoring of γ-tubulin complexes by pericentrin controls spindle organization and mitotic entry. *Mol. Biol. Cell* 15, 3642–3657. doi:10.1091/mbc.e03-11-0796

Zimmermann, F., Serna, M., Ezquerra, A., Fernandez-Leiro, R., Llorca, O., and Lüders, J. (2020). Assembly of the asymmetric human γ-tubulin ring complex by RUVBL1-RUVBL2 AAA ATPase. *Sci. Adv.* 6, eabe0894. doi:10.1126/sciadv.abe0894

Zupa, E., Liu, P., Würtz, M., Schiebel, E., and Pfeffer, S. (2021). The structure of the γ-TuRC: a 25-years-old molecular puzzle. *Curr. Opin. Struct. Biol.* 66, 15–21. doi:10.1016/j.sbi.2020.08.008

frontiers | Frontiers in Cell and Developmental Biology

TYPE Review
PUBLISHED 15 February 2023
DOI 10.3389/fcell.2023.1136699

OPEN ACCESS

EDITED BY
Jack Adam Tuszynski,
University of Alberta, Canada

REVIEWED BY
Francesca Bartolini,
Columbia University, United States
Torben Johann Hausrat,
University of Hamburg, Germany

*CORRESPONDENCE
David A. Keays,
keays@bio.lmu.de

SPECIALTY SECTION
This article was submitted to Cellular Biochemistry, a section of the journal Frontiers in Cell and Developmental Biology

RECEIVED 03 January 2023
ACCEPTED 02 February 2023
PUBLISHED 15 February 2023

CITATION
Cushion TD, Leca I and Keays DA (2023), MAPping tubulin mutations.
Front. Cell Dev. Biol. 11:1136699.
doi: 10.3389/fcell.2023.1136699

MAPping tubulin mutations

Thomas D. Cushion[1,2], Ines Leca[2] and David A. Keays[1,2,3]*

[1]Department of Physiology, Development and Neuroscience, University of Cambridge, Cambridge, United Kingdom, [2]Research Institute of Molecular Pathology (IMP), Vienna Biocenter (VBC), Vienna, Austria, [3]Division of Neurobiology, Department Biology II, Ludwig-Maximilians-University Munich, Munich, Germany

Microtubules are filamentous structures that play a critical role in a diverse array of cellular functions including, mitosis, nuclear translocation, trafficking of organelles and cell shape. They are composed of α/β-tubulin heterodimers which are encoded by a large multigene family that has been implicated in an umbrella of disease states collectively known as the tubulinopathies. *De novo* mutations in different tubulin genes are known to cause lissencephaly, microcephaly, polymicrogyria, motor neuron disease, and female infertility. The diverse clinical features associated with these maladies have been attributed to the expression pattern of individual tubulin genes, as well as their distinct Functional repertoire. Recent studies, however, have highlighted the impact of tubulin mutations on microtubule-associated proteins (MAPs). MAPs can be classified according to their effect on microtubules and include polymer stabilizers (e.g., tau, MAP2, doublecortin), destabilizers (e.g., spastin, katanin), plus-end binding proteins (e.g., EB1-3, XMAP215, CLASPs) and motor proteins (e.g., dyneins, kinesins). In this review we analyse mutation-specific disease mechanisms that influence MAP binding and their phenotypic consequences, and discuss methods by which we can exploit genetic variation to identify novel MAPs.

KEYWORDS

microtubules, tubulinopathies, dynein, kinesin, disease, microtubule-associated protein

Introduction

Microtubules

Microtubules are large polymers formed by repeats of α- and β-tubulin heterodimers. Tubulin heterodimers fold *via* a highly conserved and complex pathway involving chaperones, chaperonins and other co-factors (Lewis et al., 1997). Once folded, the α- and β-subunits bind a molecule of guanosine triphosphate (GTP) each, at two conserved structural motifs: the non-exchangeable site and the exchangeable site (Nogales et al., 1998; Lowe et al., 2001). Heterodimers assemble longitudinally into protofilaments, arranged uniformly with β-tubulin exposed at the growing tip, with 13 protofilaments associating laterally to form a hollow, cylindrical structure (Nogales, 2001). Microtubules cycle between periods of steady growth (polymerisation) and rapid collapse (de-polymerisation or "catastrophe"), by the addition or loss of tubulin heterodimers (Mitchison and Kirschner, 1984). This behaviour is utilised by every mammalian cell to perform a range of functions, including the control of cell morphology, cell motility, intracellular transport, and cell division. To accurately perform such a wide repertoire of tasks, microtubules are subject to regulation on multiple levels. Whilst they are often depicted as homogenous chains of α/β-tubulin heterodimers, microtubules can be constituted by a variety of similar yet subtly distinct α- and β-tubulin isotypes, each compatible with the structure of the

microtubule polymer lattice. These tubulin isotypes are encoded for by different tubulin genes distributed across the human genome: eight α- and nine β-tubulins (Breuss and Keays, 2014).

Each of these tubulin isotypes has a unique expression pattern (Leandro-García et al., 2010). For instance, TUBB3 is predominantly found in post-mitotic neurons, TUBA8 in muscles and the testes (Braun et al., 2010), TUBB1 in haemopoietic cells (Leandro-García et al., 2010), and TUBB8 in oocytes (Feng et al., 2016). The consequence of this variation in expression is that microtubules in different cell types consist of a different blend of tubulin heterodimers. This is relevant because it confers different properties on those microtubules, enables different microtubule-associated proteins to bind, and it results in different disease states when they are mutated. While tubulin isotypes share a high degree of sequence homology, they exhibit notable divergence in the unstructured carboxy-terminal tail (CTT) which extends outwards and away from the microtubule wall and into the cell cytoplasm (Nogales et al., 1998). These CTTs are predicted to play an important role in many respects of microtubule biology. Importantly, they are site of multiple reversible post-translational modifications including de-tyrosination, glutamylation and glycylation (Janke and Bulinski, 2011). Despite emerging evidence that CTTs might play an unexpected role modulating microtubule polymerisation dynamics (Parker et al., 2018; Chen et al., 2021), it is their relative accessibility at the polymer exterior that are thought to be critical to the function of another key regulator of microtubule behaviour, the wide range of microtubule-associated proteins (MAPs).

microtubule-associated proteins

Microtubule-associated proteins were originally defined as those proteins that purified with microtubules from brain extracts (Sloboda et al., 1975). With the passage of time and the development of various methods, this criterion has been refined. In addition to co-sedimenting with microtubules, MAPs should co-localize with microtubules by immunofluorescence in cultured cells and their staining pattern should become dispersed upon addition of depolymerizing drugs (Huber et al., 1985; Bodakuntla et al., 2019). MAPs can be further categorized based on their function and/or localization on microtubules (Tortosa et al., 2016; Tortosa et al., 2017; Goodson and Jonasson, 2018; Bodakuntla et al., 2019). Motor proteins (e.g., dyneins, kinesins) are MAPs responsible for generating cellular forces and for intracellular transport. Some MAPs contribute to microtubule nucleation (e.g., doublecortin) while others promote catastrophe by depolymerization or severing (e.g., spastin, katanin). "+TIP" binding proteins (e.g., EB1-3, XMAP215, CLASPs) and minus-end binding proteins (e.g., CAMSAP1-3) bind to the plus- and minus-ends of microtubules respectively, whilst structural MAPs bind along the lateral-wall (lattice) of microtubules, acting as cross-linkers with intermediate filaments and the actin cytoskeleton (e.g., MACF1, MACF2) (Hendershott and Vale, 2014; Tortosa et al., 2016). Some authors also consider tubulin-modifying enzymes as MAPs, since they necessarily interact with microtubules to deposit specific PTMs (Kapitein and Hoogenraad, 2015; Tortosa et al., 2016), as well as several metabolic enzymes that have been shown to bind microtubules (Walsh et al., 1989; Lloyd and Hardin, 1999). In addition, there are MAPs that are recruited to the microtubules indirectly, *via* other proteins that bind to microtubules. Examples include the phosphatase, PP1, recruited to microtubule polymers by tau, and a group of kinases, MAST1-4, that preferentially colocalize with microtubules in the presence of other MAPs (Walden and Cowan, 1993; Liao et al., 1998; Tripathy et al., 2018). For a comprehensive overview of MAP subtypes and functions, we recommend the following review (Bodakuntla et al., 2019).

With this plethora of functions, it is not surprising that each family of MAPs adopts a unique structural conformation and interacts with microtubules differently (Amos and Schlieper, 2005; Bodakuntla et al., 2019). There is no consensus amino acid sequence or 3D structure for the microtubule-binding domain of different MAP families. In fact, some of the domains reported assume distinct forms; either helical coiled-coils or hairpins, or more globular domains like the CAP-Gly and calponin-homology domain found in end-binding MAPs (Amos and Schlieper, 2005). These observations highlight the potential for several MAPs to decorate microtubules simultaneously. For example, doublecortin (DCX) which is a neuronal MAP, is known to bind adjacent protofilaments, providing a contact point between protofilaments (Bechstedt and Brouhard, 2012). On the other hand, tau, one of the first MAPs to be identified, binds to the microtubule surface, longitudinally along protofilaments (Amos and Schlieper, 2005). Moreover, it has been demonstrated that specific tubulin PTMs affect the interaction with several MAPs, such as the regulation of Tau binding through polyglutamylation of tubulin CTTs (Boucher et al., 1994; Gadadhar et al., 2017; Bodakuntla et al., 2019; Hausrat et al., 2022).

The tubulinopathies

Mutations in multiple tubulin genes have been associated with human disease. Known collectively as the 'tubulinopathies', this disease spectrum encompasses numerous neurodevelopmental disorders including, microcephaly, lissencephaly, and polymicrogyria, reflecting the large number of tubulin genes expressed during embryonic brain formation (e.g., *TUBA1A*, *TUBB2A*, *TUBB2B*, *TUBB3*, *TUBB5*) (Keays et al., 2007; Jaglin et al., 2009; Poirier et al., 2010; Breuss et al., 2012; Cushion et al., 2014; Romaniello et al., 2018). In addition to cortical malformations, the tubulinopathies also include disorders of ocular motor function (associated with variants in *TUBB3*, *TUBB2B* & *TUBA1A*), whispering dysphonia (*TUBB4A*), amyotrophic lateral sclerosis (*TUBA4A*), female meiotic infertility (*TUBB8*), Leber congenital amaurosis with hearing loss (*TUBB4B*), and macrothrombocytopaenia (*TUBB1*) (Kunishima et al., 2009; Bahi-Buisson et al., 2014; Smith et al., 2014; Feng et al., 2016; Luscan et al., 2017; Strassel et al., 2019; Jurgens et al., 2021; Kimmerlin et al., 2022). Irrespective of the clinical attributes of the disease the tubulinopathies are predominantly due to *de novo* heterozygous, missense mutations and are predicted to act in a gain-of-function manner in most instances (Figure 1) (Romaniello et al., 2018; Leca et al., 2020). The different diseases that result from tubulin mutations is thought to reflect the expression pattern of a given isoform and the functional repertoire of that protein.

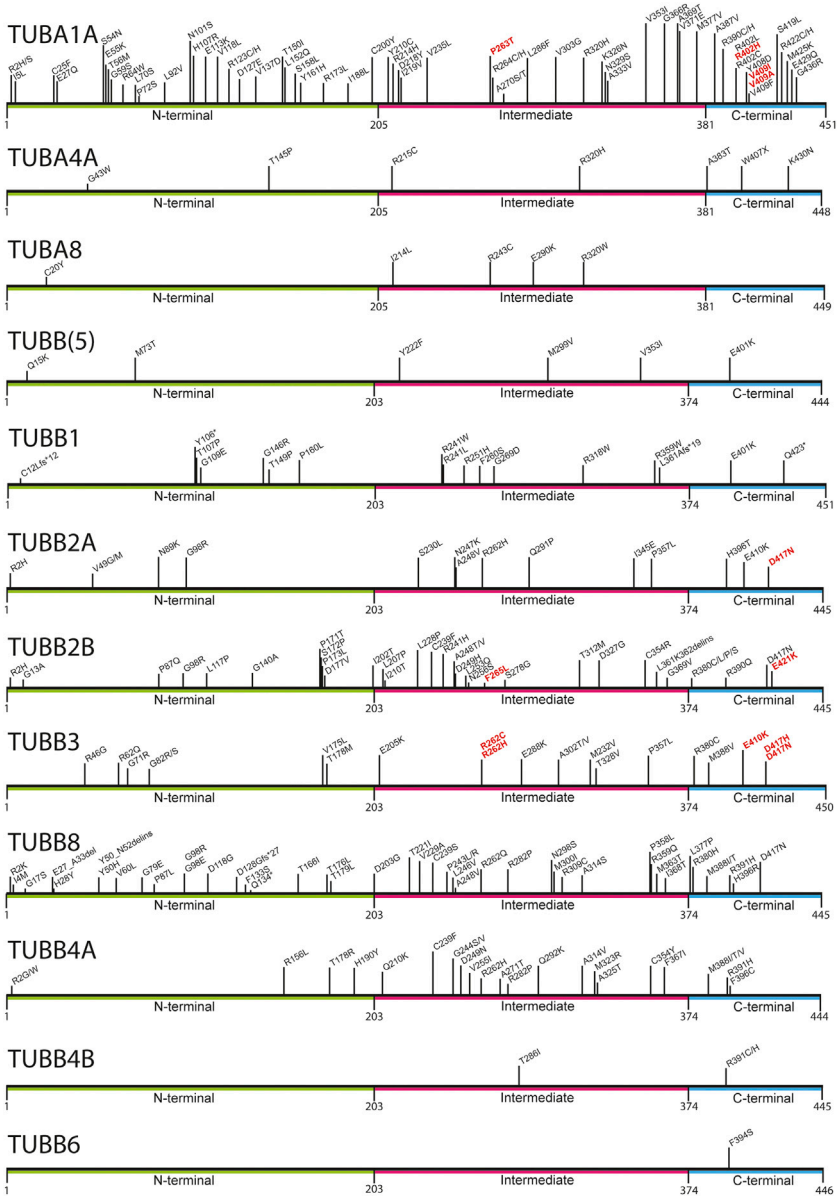

FIGURE 1
Mapping of pathogenic tubulin mutations across tubulin isotypes. Tubulin proteins can be divided into three regions: the N-terminal (green), Intermediate (pink), and C-terminal (blue) domains. The latter constitutes the major MAP-binding region of tubulin. Variants shown to affect MAP interaction are highlighted in red.

Nevertheless, mutations in different tubulin genes can result in strikingly similar phenotypes. For instance, a E421K mutation in TUBB2B and a R262C mutation in TUBB3 both cause ocular motor dysfunction, whereas individuals with a T312M variant in TUBB2B and a R46G mutation in TUBB3 both present with multifocal polymicrogyria (Jaglin et al., 2009; Tischfield et al., 2010; Cederquist et al., 2012; Bahi-Buisson et al., 2014). This raises the prospect that a critical determinant that predicts a disease outcome is the actual amino acid mutated, and the molecular pathway disrupted.

Mechanistic studies have explored how tubulin mutations can influence microtubule biology. Some variants have been shown to perturb the chaperone-mediated folding of heterodimers (e.g., TUBA1A L397P) (Tian et al., 2010), while others have no detectable influence on folding whatsoever (e.g., R402H in TUBA1A), generating heterodimers that integrate into microtubules with ease. The latter are of particular interest because recent studies have highlighted that they can alter the interaction between microtubule polymers with MAPs (Figure 2). In this review, we focus on the tubulin gene variants that have been shown to modify binding of MAPs including kinesin, dynein, XMAP215, CLASP and EB1 (Table 1), how these might affect microtubule function, and the extent to which they determine the disease state.

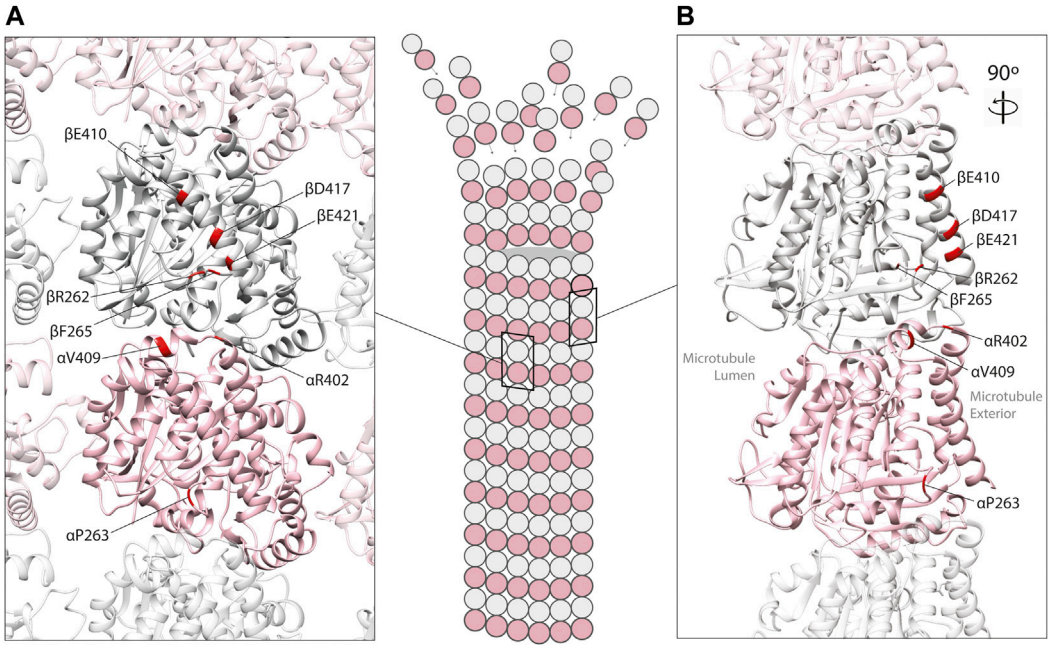

FIGURE 2
In silico homology model of an α/β-tubulin heterodimer **(A)** facing the exterior surface of a microtubule polymer and **(B)** a rotated side view of an individual microtubule protofilament (PDB 2XRP) (Fourniol et al., 2010). α-tubulin is represented by a pink ribbon, β-tubulin in silver. Unstructured, tubulin carboxy-terminal tails are not shown. Mutated residues shown to effect MAP binding are mapped onto α- and β-tubulin subunits (red).

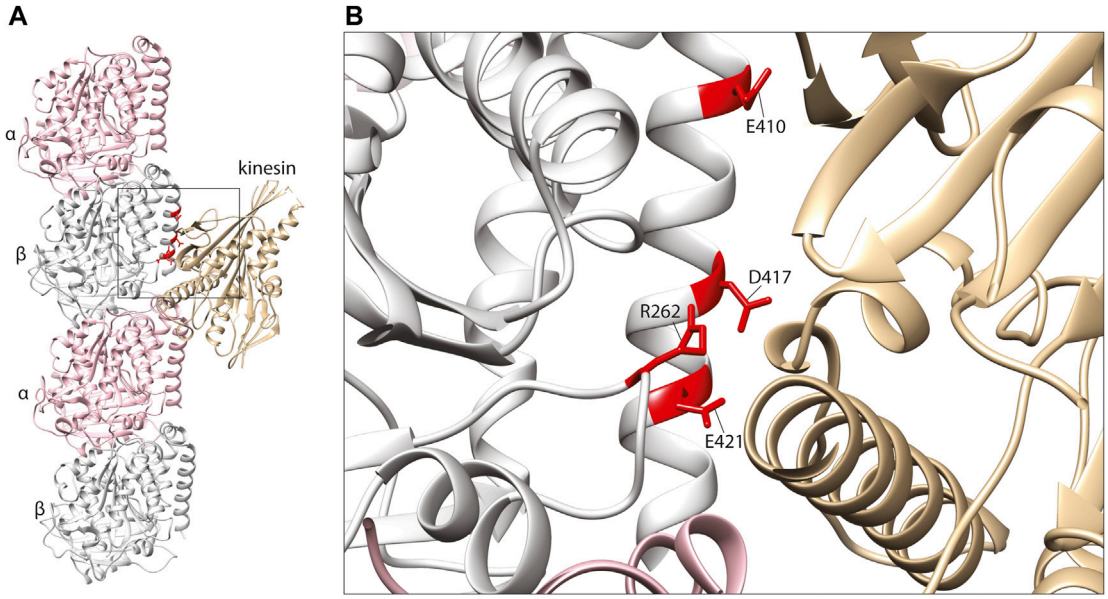

FIGURE 3
(A) *In silico* homology model of a microtubule protofilament with bound kinesin. α-tubulins are represented by a pink ribbon, β-tubulins in silver and kinesin in gold (PDB 6ZPI) (Atherton et al., 2020). **(B)** A detailed view of the predicted kinesin-interacting domain of β-tubulin. Mutated residues shown to effect kinesin binding and/or processivity shown in red.

Motor proteins: Kinesins

Kinesins are one of two major microtubule-associated molecular motors. There are at least 45 mammalian "KIF" genes that can be broadly categorised into two main types: 1) motile kinesins which use ATP chemical energy to shuttle intracellular cargo along microtubule 'tracks' (usually towards polymer plus-ends); and 2) non-motile kinesins that de-polymerise microtubules (Dagenbach

TABLE 1 Tubulin gene variants shown to affect MAP interaction. H = alpha-helix; B = beta-strand; CFEOM3 = Congenital Fibrosis of the extraocular muscle; CFEOM3 = Congenital Fibrosis of the extraocular muscle type 3; MCD = Malformations of cortical development.

Kinesin				
Variant	*Isotype*	*Subunit Position*	*Patient Phenotype*	*References*
R262C	TUBB3	H8-B7 Loop	Eye movement disorder (CFEOM3)	Tischfield et al. (2010)
R262H	TUBB3	H8-B7 Loop	Eye movement disorder (CFEOM3)	Tischfield et al., 2010, Ti et al. (2016)
E410K	TUBB3	H11-H12 Loop	Eye movement disorder (CFEOM3)	Tischfield et al. (2010)
D417N	TUBB3	H12	Eye movement disorder (CFEOM3)	Tischfield et al. (2010)
D417H	TUBB3	H12	Eye movement disorder (CFEOM3)	Tischfield et al. (2010), Ti et al. (2016)
E421K	TUBB2B	H12	MCD (polymicrogyria) and eye movement disorder (CFEOM)	Cederquist et al. (2012)
Dynein				
R402H	TUBA1A	H11-H12 Loop	MCD (Lissencephaly)	Aiken et al. (2019), Leca et al. (2020)
Bim1 (EB1)				
F265L	TUBB2B	B7	MCD (Polymicrogyria)	Denarier et al. (2019)
XMAP215				
V409I	TUBA1A	H11-H12 Loop	MCD (Pachygyria)	Hoff et al. (2022)
V409A	TUBA1A	H11-H12 Loop	MCD (Agyria)	Hoff et al. (2022)
CLASP1 & CLASP2				
P263T	TUBA1A	H8-B7 Loop	MCD (Lissencephaly)	Yu et al. (2016)
R402H	TUBA1A	H11-H12 Loop	MCD (Lissencephaly)	Yu et al. (2016)

and Endow, 2004). Motile kinesins (e.g., KIF1A, KIF1Bβ, KIF5A and KIF21A) are particularly important for neuronal function and survival, as essential proteins within axons and synaptic termini must be transported considerable distances from the cell body (Hirokawa et al., 2009). They are also crucial for mitotic division, facilitating efficient chromosomal congression and segregation during cell division (Wordeman, 2010).

The key sites of interaction between tubulins and kinesins were initially discovered using alanine mutation scanning, identifying positively charged amino acids on the motor protein corresponding to three negatively charged residues on the β-tubulin subunit: E410, D417, and E421 (Woehlke et al., 1997; Uchimura et al., 2006) (Figure 3). These three amino acids are conserved throughout β-tubulins, and pathogenic mutants affecting these positions have since been identified in TUBB2A, TUBB2B, TUBB3, and TUBB8 (Tischfield et al., 2010; Cederquist et al., 2012; Feng et al., 2016; Sferra et al., 2018). The effects of TUBB3 mutants on kinesin function have been examined comprehensively. TUBB3 is a neuron-specific tubulin isotype (Cleveland, 1987; Joshi and Cleveland, 1989), and *TUBB3* mutations typically cause structural brain malformations and/or congenital fibrosis of the extraocular muscle 3 (CFEOM3), an axon guidance disorder affecting the muscles that control the eye (Poirier et al., 2010; Tischfield et al., 2010). In order to model the disease mechanisms of TUBB3-related CFEOM3, Tischfield and others generated and characterised a TUBB3 R262C mouse mutant (Tischfield et al., 2010). Consistent with patients carrying this variant, the mouse mutant exhibited axon guidance defects (including in the oculomotor nerve), but otherwise normal brain architecture. The authors hypothesised that kinesin dysfunction may be implicated in the pathology of CFEOM3, as mutations in *KIF21A* had been shown to cause similar oculomotor defects (Yamada et al., 2003). Despite not binding directly with kinesin, the R262 residue is predicted to form a H-bond with D417 (Figure 3B) (Tischfield et al., 2010). Co-immunoprecipitation of brain lysates revealed a reduction of microtubule-bound KIF21 in R262C mutant mice compared to wild-type littermates, suggesting that loss of the R262-D417 H-bond alters the tertiary structure of β-tubulin at the kinesin-interacting interface. To test their hypothesis on a wider range of TUBB3 variants, the authors turned to a budding yeast system to assess kinesin processivity. Using this model, they assessed the accumulation of yeast kinesins, Kip3p & Kip2p, at the growing tip of microtubules (Carvalho et al., 2004; Gupta et al., 2006). Compared to wild-type controls, yeast expressing TUBB3 R262C, R262H, E410K, D417H & D417N showed a significant reduction of kinesin at microtubule plus ends, further implicating the motor protein in the disease state (Tischfield et al., 2010).

Building upon these findings, Hirokawa and others investigated fourteen β-tubulin mutations associated with either CFEOM3 or brain malformations using overexpression in dissociated mouse neurons (Niwa et al., 2013). Tracking known kinesin cargos, VAMP2, RAB3, and mitochondria, they observed diminished axonal transport in the presence of the TUBB3 mutants E410K and D417H (Nangaku et al., 1994; Tanaka et al., 1998; Niwa et al., 2008; Song et al., 2009; Niwa et al., 2013). Microtubule co-sedimentation confirmed a reduction in kinesin binding with these two variants, with significantly increased levels of kinesin (but not dynein) detected in the cytoplasmic fraction (Niwa et al.,

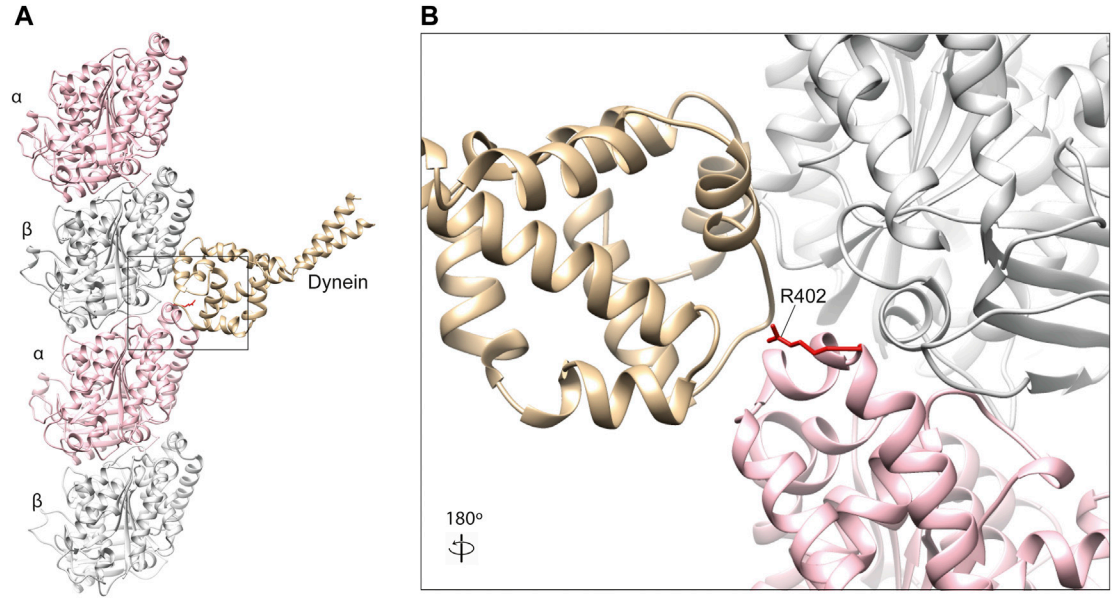

FIGURE 4
(A) *In silico* homology model of a microtubule protofilament with bound dynein. α-tubulins are represented by a pink ribbon, β-tubulins in silver and dynein microtubule-binding domain in gold (PDB 3J1T) (Redwine et al., 2012). **(B)** A detailed view of the dynein-interacting domain. The R402 residue of α-tubulin (red) is a hot-spot for pathogenic variants in TUBA1A, which have been shown to affect dynein interaction and processivity (Aiken et al., 2019; Leca et al., 2020).

2013). Importantly, variants associated with only mild CFEOM3 or cortical malformations exhibited normal kinesin function in these assays, supporting a potential phenotype-specific disease pathway. Consistent with a gain-of-function mechanism, the authors showed that mutant subunits only perturb kinesin function when incorporated into microtubules (Niwa et al., 2013). Furthermore, such effects were not restricted to TUBB3, as axonal transport defects were also observed for equivalent substitutions in TUBB2B and TUBB5 (Niwa et al., 2013). This observation was corroborated by reduced kinesin binding and processivity due to two further gene variants, TUBB2A D417N and TUBB2B E421K, associated with progressive neuropathy and CFEOM, respectively (Cederquist et al., 2012; Sferra et al., 2018). These phenotypes are distinct from the cortical brain malformations which are commonly associated with genetic changes in *TUBB2A* and *TUBB2B* (Romaniello et al., 2018). Taken together, these data highlight the existence of mutation specific disease mechanisms that diminish kinesin interaction and intracellular trafficking necessary to generate, guide and maintain healthy and functional neuronal processes.

Motor proteins: Dynein

The second major family of microtubule-bound motor proteins are the dyneins. In a similar fashion to kinesins, dyneins shuttle along microtubule 'tracks' using energy generated through ATP hydrolysis. They are large complexes composed of two identical heavy chains which include the microtubule binding domain and a number of intermediate and light chains (Vallee et al., 2004). They are responsible for transport of intracellular cargo towards microtubule minus ends and are involved in both cell division and cell migration (Vale, 2003).

Key dynein-binding tubulin residues were first probed for using a mutant alanine screen (Uchimura et al., 2015). This highlighted two α-tubulin residues of particularly importance, R402 (Figure 4) and E415, located within the H11–H12 loop and alpha-helix 12 of the α-tubulin subunit respectively (Nogales et al., 1998; Uchimura et al., 2015). These amino acids are predicted to form salt bridges with one another stabilising the α-tubulin C-terminal hairpin structure important for MAP binding, as well as forming salt bridges directly with dynein (Lowe et al., 2001; Aiken et al., 2019). Despite this, binding between microtubules and the motor protein was still observed even after substituting these residues to alanine (Uchimura et al., 2015). Directional movement was completely ablated however, suggesting R402 and E415 function primarily as structural signals for ATPase activation (Uchimura et al., 2015).

To our knowledge, pathogenic α-tubulin mutants affecting E415 have not been reported. R402, on the other hand, is a known hot-spot for human mutations in *TUBA1A*, with substitutions of this residue constituting almost a third of all reported variants in the gene (Bahi-Buisson et al., 2014). Individuals with R402 C/H/L substitutions commonly present with lissencephaly, a severe cerebral cortex malformation caused by defective neuronal migration during brain development (Moon and Wynshaw-Boris, 2013). Consistent with this observation mutations in dynein heavy chain (DYNC1H1) also cause cortical malformations (Vissers et al., 2010; Poirier et al., 2013), as do variants affecting dynein regulators LIS1 and NDEL1 (Yamada et al., 2008).

Using a yeast as a model system, Aiken and others investigated the consequences of two TUBA1A arginine 402 variants (R402C and R402H) on dynein function (Aiken et al., 2019). They generated analogous mutants in *Saccharomyces cerevisiae*, substituting the equivalent arginine (R403) in the major yeast α-tubulin, Tub1. They confirmed that both mutants form functional tubulin heterodimers which incorporate into endogenous microtubules, supporting a gain-of-function mechanism (Aiken et al., 2019). Unlike the multiple specialised roles of dynein in neurons, dynein's solitary task in yeast is to translocate the nucleus and mitotic spindle across the plane of cytokinesis (Aiken et al., 2019). Aiken and others analysed hydroxyurea-induced S-phase arrest to isolate spindle sliding events, providing a clear and robust readout to assess mutant effects on dynein function. They reported a reduction in frequency and distance of sliding events for both R403C&H mutants compared to wild type. Importantly, they confirmed dynein recruitment to microtubule plus-ends (a prerequisite for retrograde locomotion) was normal and that kinesin function was undisturbed, suggesting these mutants directly affect dynein interaction and processivity (Aiken et al., 2019).

These conclusions have been further supported by an independent study in our lab which generated a conditional *Tuba1a* R402H mutant mouse (Leca et al., 2020). Expression of the R402H mutation in both the developing cortex and hippocampus resulted in a severe defect in neuronal migration, consistent with the patient phenotype. To gain insight into the underlying molecular mechanisms we performed microtubule co-sedimentation on brain lysates and undertook quantitative mass spectrometry. Comparison of the "microtubule proteome" identified 286 proteins that were significantly altered in R402H animals, seven of which were known MAPs (Leca et al., 2020). Western blot analysis of these seven proteins confirmed that five were present at lower levels in brain lysates R402H mutants (VAPA, VAPAB, REEP1, EZRIN, and PRNP). Only dynein intermediate chain (DYNC1I1) was expressed at endogenous levels but associated less with microtubules. To assess dynein processivity in the presence of this variant, cortical neurons were cultured from mutant and wild-type mice and live cell tracking of dynein-mediated lysosomal transport performed. This highlighted a significant reduction in lysosomal run length, suggesting that dynein processivity towards the cell soma was compromised in mutant animals (Leca et al., 2020). Consistent with dynein dysfunction, we showed a defect in nucleus-centrosome coupling in R402H animals indicative of impaired dynein-mediated nucleokinesis and migration (Leca et al., 2020). Intriguingly, we did not observe any difference in the levels of sedimented dynein heavy chain (DYNC1H1) which binds directly to microtubules, in contrast to the intermediate chain (DYNC1I1) which serves as a bridge between the heavy chain and cargo adaptor (Carter et al., 2008; Schroeder et al., 2014). Moreover, given the large number of proteins dysregulated in R402H animals, it is apparent that a single point mutation can have pleiotropic effects, potentially on multiple uncharacterised MAPs.

Microtubule plus-end MAPs (and TAPs)

Microtubule plus-end MAPs or "+TIPs" collectively describe a diverse subset of proteins which, as their name may suggest, localize at the growing tips of microtubule polymers (Perez et al., 1999; Mimori-Kiyosue et al., 2000; Jiang et al., 2012). Certain plus-end MAPs, such as the end-binding protein family (EB1, EB3) are known to recruit and form complex networks with other + TIPs at this region of the microtubule polymer, whereas others bind to the microtubule end directly (Honnappa et al., 2005; Slep et al., 2005; Honnappa et al., 2009; Al-Bassam et al., 2010; Kumar et al., 2017). Plus-end MAPs generally regulate one or more of the basic parameters underlying microtubule dynamics: rate of polymerisation, rate of de-polymerisation, the frequency of catastrophe and/or the frequency of rescue (Straube, 2011). Examples include microtubule polymerases (e.g., XMAP215s) that catalyse and accelerate microtubule growth, and Cytoplasmic Linker-Associated Proteins (CLASPs) that stem microtubule depolymerisation events and potentiate re-growth (Gard and Kirschner, 1987; Al-Bassam and Chang, 2011; Moriwaki and Goshima, 2016). Evidence suggests that tubulin mutations can affect the correct localisation and function of these specialised MAPs, further highlighting their critical role in microtubule biology.

Plus-end MAPs: XMAP215 family microtubule polymerases

This family is named after the XMAP215 microtubule polymerase identified in *Xenopus laevis* but also comprises human Colonic and Hepatic Tumour Overexpressed Gene (ch-TOG), Minispindles (*D. melanogaster*), and Stu2 (*S. cerevisiae*) (Gard and Kirschner, 1987; Wang and Huffaker, 1997; Charrasse et al., 1998; Cullen et al., 1999). As with many plus end-binding proteins, the XMAP215s are composed of arrayed tubulin-binding Tumour Overexpressed Gene (TOG) motifs, containing 250 amino acid residue repeats (Akhmanova et al., 2001; Cassimeris et al., 2001; Leano et al., 2013). Two of these, TOG1 and TOG2, are structurally conserved and present in all family members but, in higher eukaryotes, five TOG domains are separated by unstructured linkers of 60–100 residues (Figure 5A) (Currie et al., 2011; Widlund et al., 2011). The TOG1 and TOG2 domains of yeast Stu2 and their association with tubulin have been examined in detail (Ayaz et al., 2012). TOG1 and TOG2 are predicted to bind tubulins at a 1:1 ratio, but with a particular affinity for curved heterodimer conformations. This propensity for curved tubulin localises these polymerases to the growing tip as, here, recently incorporated tubulins initially assume an expanded and flayed configuration before integrating into the microtubule lattice (Ayaz et al., 2014).

Microtubule polymerisation is highly dependent on local concentrations of un-polymerised "free" tubulin surrounding the growing tip (Desai and Mitchison, 1997; Howard and Hyman, 2009). Through their tubulin-binding TOG domains, XMAP215s enrich local concentrations of free tubulin near microtubule plus-end (Figure 5B). TOG domains are thought to work in a coordinated fashion to catalyse polymerisation, as they can discriminate between conformational states of tubulin dimers (Ayaz et al., 2012). Initially, TOG1 recognises and captures naturally curved free heterodimers, subsequently recruiting them into a growing microtubule. Upon integration into the microtubule, heterodimers assume a slightly straighter configuration, after which they can no longer bind TOG1 but are "handed-off" to TOG2. When fully embedded into the microtubule lattice formation, the conformation of tubulin

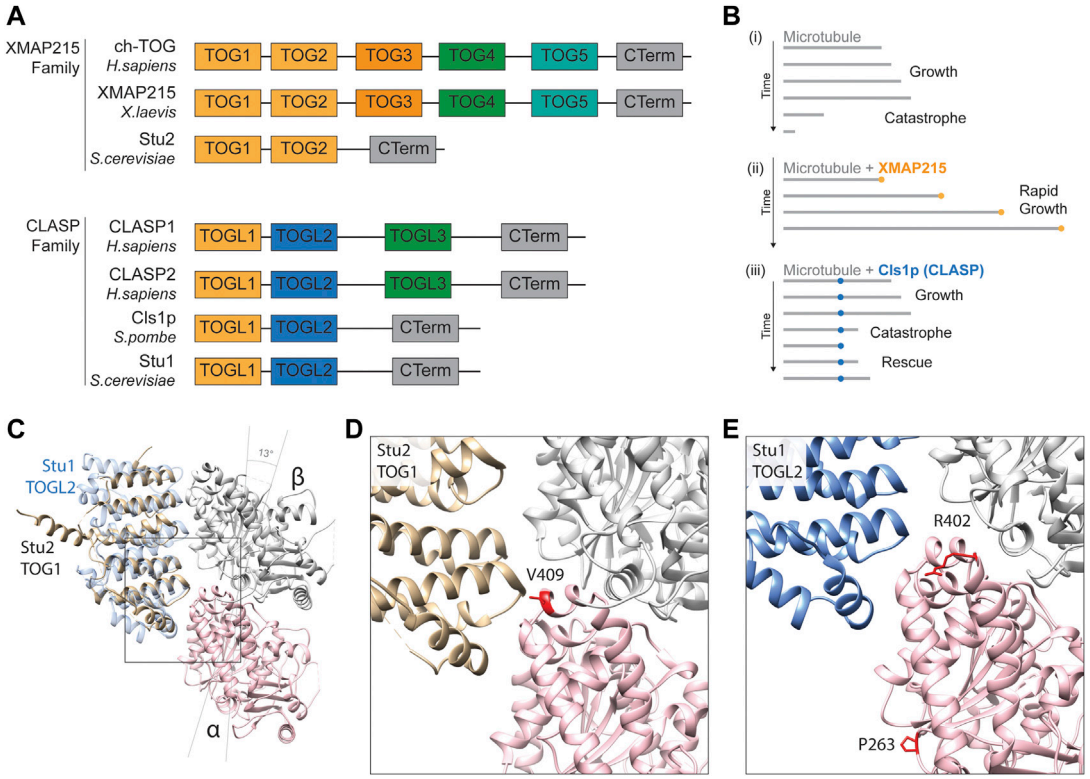

FIGURE 5
(A) Schematic alignment and positional conservation of TOG domains in XMAP215 family microtubule polymerases and CLASPs [adapted from (Al-Bassam and Chang, 2011; Byrnes and Slep, 2017)]. **(B)** Schematic depiction of dynamic behaviour of (i) pure microtubules (grey lines), (ii) accelerated microtubule polymerisation in the presence of XMAP215 family polymerases (gold), and (iii) microtubule rescue mediated by fission yeast CLASP, Cls1p (blue), adapted from (Al-Bassam and Chang, 2011). **(C)** Homology model depiction of a unpolymerised tubulin heterodimer complexed with TOG1 domain of *S. cerevisiae* microtubule polymerase Stu2 (gold) (PDB 4FFB) and docked TOGL2 domain of Stu1 (*S. cerevisiae* CLASP; blue) (PDB 6COK) (Ayaz et al., 2012; Majumdar et al., 2018). α-tubulins are represented by a pink ribbon, β-tubulins in silver. Both TOGs bind preferentially to curved tubulin heterodimers, hence α- and β-tubulin subunits are tilted 13 to form this complex (Ayaz et al., 2012). **(D)** A detailed view of the predicted TOG1 binding interface of tubulin heterodimers. The α-tubulin residue valine 409 (410 in yeast) (red) is directly involved in TOG1 binding, with substitutions affecting its binding and localisation to microtubule plus-ends (Hoff et al., 2022). **(E)** Detailed view of the predicted TOGL2 binding interface of tubulin heterodimers. Mutating α-tubulin proline 263 and arginine 402 (P264 and R402 in yeast) have been shown to reduce binding affinity with human CLASPs 1 & 2 (Yu et al., 2016).

becomes too straight for TOG2, which in turn releases the polymerised heterodimer (Ayaz et al., 2012). It has since been shown that TOGs 1-3 preferentially bind curved heterodimers, whilst TOG 4 and 5 are structurally distinct and bind microtubule-incorporated subunits (Byrnes and Slep, 2017).

A key residue at the heart of the TOG1/2-tubulin interface is valine 409 of α-tubulin, located within the H11-H12 loop (Figures 5C, D) (Nogales et al., 1998; Ayaz et al., 2012). Two pathogenic variants in TUBA1A have been reported at this residue, V409I and V409A, identified in individuals with pachygyria and agyria (mild and severe lissencephaly) respectively (Bahi-Buisson et al., 2014; Fallet-Bianco et al., 2014). Given the position of the residue, Hoff and others sought to investigate whether this mutation altered XMAP215 interaction (Hoff et al., 2022). Mutating the equivalent valine (V410) in yeast α-tubulin Tub1 to isoleucine or alanine they showed that both V409I and V409A mutants diminished the levels of Stu2/XMAP215 at the microtubule tip through a reduction in Stu2 TOG1 binding affinity (Hoff et al., 2022). Surprisingly they showed that this caused an increase in microtubule polymerisation rates, concurrent with a reduction in the frequency of catastrophes (Hoff et al., 2022). The effects on polymerisation speeds were echoed when overexpressing these mutants in mouse primary neurons and, in both models, the effects were more prominent with the valine to alanine mutant, concomitant with the more severe phenotype in the individual carrying the TUBA1A p.V409A mutation (Hoff et al., 2022). In order to reconcile the somewhat contradictory decrease in TOG binding of α-tubulin mutants with faster polymerisation rates, Hoff and others proposed a model by which the V410I&A mutants result in straighter heterodimers that weaken the binding potential of Stu2 TOG domains but, simultaneously, favour efficient microtubule incorporation and subsequent growth (Hoff et al., 2022). Whilst this hypothesis remains to be tested it provides an important reminder that multiple aspects of microtubule function can be perturbed simultaneously by individual tubulin amino acid substitutions.

Plus-end MAPs: CLASPs

The CLASPs are MAPs that counteract microtubule catastrophe by stabilising de-polymerisation and potentiating 'rescue' (Al-

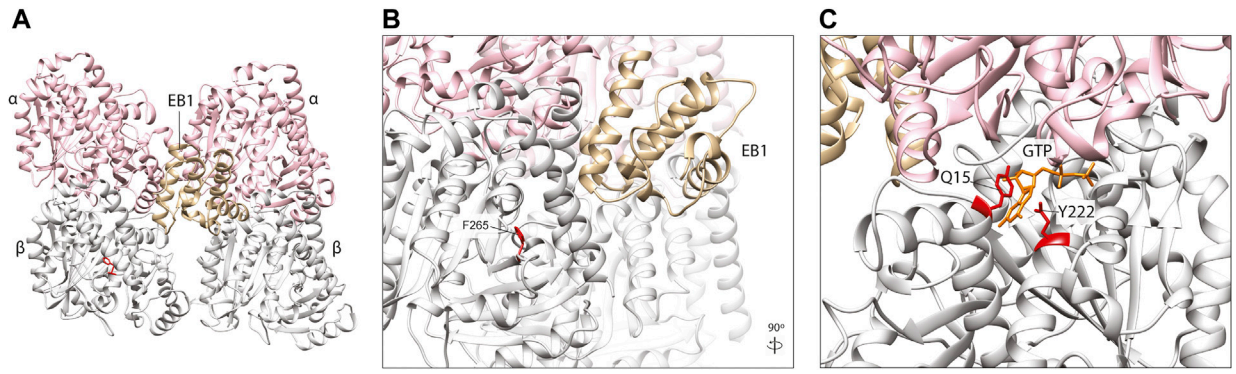

FIGURE 6
(A) *In silico* homology model of a microtubule protofilament with bound Calponin Homology domain of *S. pombe* EB1 homologue, Mal3 (labelled EB1). α-tubulins are represented by a pink ribbon, β-tubulins in silver and EB1 in gold (PDB 4ABO) (Maurer et al., 2012). **(B)** A detailed view of the EB1-tubulin interface. The F265 residue (red), associated with neurodevelopmental disease and shown to affect EB1 binding in yeast (Jaglin et al., 2009; Denarier et al., 2019), is not predicted to interact directly with this plus-end MAP, suggesting it may act *via* allosteric reconfiguration. **(C)** TUBB5 Q15 and Y222 (red) are located within the β-tubulin GTP (orange)-binding site and variants affecting these residues might to affect nucleotide interaction and/or hydrolysis which, in turn, could influence EB2 binding.

Bassam et al., 2010). This family includes human CLASP1 and CLASP2, Stu1 into yeast (*S. cerevisiae*) and Cls1p (or Peg1) in fission yeast (*S. pombe*) (Yin et al., 2002; Grallert et al., 2006; Sousa et al., 2007). Whilst CLASPs are known to associate with microtubule plus-end through EB1-mediated recruitment (Honnappa et al., 2009), they are also able to bind the microtubule polymer lattice directly through two serine/arginine-rich C-terminal domains (Wittmann and Waterman-Storer, 2005; Al-Bassam et al., 2010). Whilst the C-terminal domain attaches to the microtubule lattice, two parallel N-terminal TOG-like (TOGL) domains (related structurally to those found in XMAP215 polymerases) work in tandem to lasso free tubulin heterodimers in the surrounding cytoplasm (Al-Bassam et al., 2010). Through these TOG-like motifs, CLASPs function as a molecular safety net during microtubule catastrophe (Figure 5B), restoring local concentrations of free tubulin dimers to offset rapid rates of disassembly and initiate microtubule rescue.

Recently, tubulin gene mutations have been shown to affect CLASP recognition and/or binding (Yu et al., 2016). To identify novel Tubulin-Associated Proteins (TAPs), Yu and others developed a dual tubulin expression construct system to introduce equimolar levels of *TUBB3* and biotinylated *TUBA1A* into HEK293T cells (Yu et al., 2016). Complementing this with quantitative mass spectrometry, they could identify TAPs pulled down with transgenic tubulin through streptavidin-mediated purification. Among the most abundant proteins in the "Tubulome" were CLASP1 & CLASP2 (Yu et al., 2016), confirming a strong affinity of CLASP TOG-like domains for free tubulin (Al-Bassam et al., 2010). The authors built upon their initial dataset by introducing two tubulin variants associated with human cortical malformations into this expression vector: TUBA1A P263T and R402H (Poirier et al., 2007; Yu et al., 2016). When expressing these mutant constructs in this system, the authors detected notable reductions in the pull-down efficiency of both CLASP1 & CLASP2, as well as the Golgi-associated protein GCC185, a known interactor of CLASP (Efimov et al., 2007; Yu et al., 2016). Interestingly, whilst arginine 402 is near the predicted interface between CLASP TOG-like regions and tubulin (Figures 5C, E), proline 263 looks unlikely to contribute directly to CLASP binding. The TUBA1A P263T variant might therefore affect CLASP binding indirectly through allosteric changes to the tubulin heterodimer.

Plus-end MAPs: EBs

The End-Binding proteins (EB1-3) are an evolutionarily conserved family of plus-end MAPs. They localise to the microtubule tip through an N-terminal Calponin Homology (CH) domain, which binds most efficiently to the newest, stable portion of the microtubule (Hayashi and Ikura, 2003; Maurer et al., 2011). The CH domains bind four tubulin subunits simultaneously, bridging two adjacent protofilaments and at an interdimer interface (between different heterodimers) (Maurer et al., 2012) (Figure 6A). Rather than providing direct structural support, EBs predominantly recruit other plus-end MAPs to this region and are therefore key players in co-ordinating MAP-mediated control of microtubule dynamics (Slep et al., 2005).

A TUBB2B F265L mutation that causes multifocal polymicrogyria (Jaglin et al., 2009), has been shown to disrupt binding of the yeast homologue of EB1 known as Bim1 (Denarier et al., 2019). Denarier and others introduced the F265L mutation into Tub2 in yeast, and demonstrated that it incorporates into microtubules (Denarier et al., 2019), despite previous evidence that it compromises protein folding and heterodimerisation efficiency (Jaglin et al., 2009). This resulted in a viable yeast strain with microtubules that were smaller but more stable, with a reduced frequency of microtubule catastrophe events, increased pause duration and increased resistance to the depolymerising drug Benomyl (Denarier et al., 2019). This was attributed to perturbation of microtubule association with Bim1, the yeast homologue of EB1 which showed a marked reduction in plus end binding in the case of the F265L mutant. Surprisingly, F265 which is located

within a beta-sheet (B7) of the β-tubulin subunit (Nogales et al., 1998), does not lie at the key point-of-contact between EB1 and microtubules (Maurer et al., 2012; Howes et al., 2017). This residue sits within the β-tubulin 'intermediate domain', and its side chain is angled towards the core of the subunit (Figures 6A, B) where it is potentially involved in maintaining the structural integrity of the globular protein. EB binding, however, is thought to be sensitive to subtle structural changes within the microtubule lattice, closely linked to the nucleotide state of heterodimers at the polymer tip (Maurer et al., 2012). Accordingly, the authors hypothesised that the F265L variant affects EB1/Bim1 interaction indirectly, through conformational changes to the β-tubulin and/or adjacent subunits, which modify the CH binding pocket at the microtubule exterior (Denarier et al., 2019).

Whilst all EB family proteins (EB1-3) bind microtubule-tips through conserved CH domains, they are each thought to bind to spatially distinct sites with preference for different tubulin nucleotide states (Roth et al., 2018). EB2 is arguably the outlier in this protein family; it is the most diverse in terms of amino acid sequence divergence, it does not promote microtubule growth, it does not dimerise, and it associates along the microtubule lattice during mitosis (Juwana et al., 1999; Li et al., 2022). Four EB2-specific microtubule binding residues within the CH domain are thought to contribute to its unique polymer-binding behaviour (Roth et al., 2018). A mutation in one of these residues, R143C, plus two others within the microtubule-binding CH domain (N68S and Y87C) are known to cause Circumferential Skin Creases Kunze Type, a congenital disorder characterised by excessive skin folds, intellectual disability, and dysmorphic features (Isrie et al., 2015). All three variants increase EB2 co-sedimentation with microtubules *in vitro* (Isrie et al., 2015). Intriguingly, two TUBB5 variants, Q15K and Y222C, are also associated with this distinctive condition (Isrie et al., 2015). Given the strong phenotypic overlap between these TUBB5 and EB2 variants, they could act through a common molecular mechanism. Whilst the pathogenic TUBB5 residues are located outside the CH-binding motif, they are proximal to each other within the core of the β-tubulin subunit (Figure 6C). Significantly, they are located within the 'exchangeable' GTP binding site, with Q15 known to bind directly to the nucleotide (Lowe et al., 2001). TUBB5 Q15K and Y222C may therefore distort the highly conserved GTP binding motif and/or rate of GTP hydrolysis which could disrupt the nucleotide state-dependent binding of EB2 at microtubule plus-ends (Figure 6C).

Concluding remarks

To support the diversification of life from simple microbes to complex multicellular organisms, the dynamic behaviour of microtubules has been harnessed to execute a growing assortment of specialised intracellular tasks. To unlock the full potential of these cytoskeletal polymers, complex families of MAPs have co-evolved alongside increasingly diverse tubulin isotypes to finely choreograph distinct populations of microtubule polymers to enable changes in cell morphology, cell migration, intracellular transport, and mitotic division. Mutations in the tubulin genes can have serious consequences for human health, with an ever-expanding array of disease states associated with *de novo* missense mutations. Our challenge is to understand how these mutations cause disease, and to exploit this understanding to develop personalised medicines in the future. This review has focused on a series of emerging studies that have asked how tubulin mutations influence MAP binding, specifically, *KIF21A*, the dynein complex, XMAP215, CLASP1/2, and EB1/2. This analysis has highlighted the importance of mutation specific mechanisms, which perturb a particular pathway and consequentially result in a disease with defined attributes. While some mutations influence MAP binding in a predictable way given their physical proximity, it is evident that tubulin variants can have allosteric effects on microtubule structure thereby influencing MAP binding in unexpected ways. This is perhaps one reason, why the phenotypic prediction of tubulin mutations has proved to be so difficult (Attard et al., 2022).

It is clear that much remains to be discovered. At least 180 tubulin variants have been described in the literature to date, but only twelve (four α- and eight β-tubulin) have been explicitly shown to affect MAP interaction and/or function. This reflects the laborious nature of mechanistic studies in microtubule biology, prompting many investigators to use yeast as a model system. While efficient and robust, yeast cannot replicate the cocktail of MAPs that are present in the mammalian brain, nor the diversity of tubulin isotypes and PTMs. On the other hand it is not feasible or practical to generate conditional mouse models for each tubulin variant. An alternative way forward is to exploit technological developments in stem cell biology and 3D tissue-specific organoid cultures. It is now possible to generate and characterise cerebral organoids from iPSC lines generated from patients with tubulin mutations, alongside CRISPR-repaired isogenic controls. Coupled with advanced quantitative proteomic methods, investigators can interrogate the effect of tubulin mutations on the microtubule proteome in a human system with greater ease (Leca et al., 2020; Rafiei and Schriemer, 2022). This would permit the identification of novel MAPs relevant to disease states, as it likely there are numerous uncharacterised MAPs that have yet to be identified that influence microtubule behaviour in unexpected ways (Jijumon et al., 2022). In the future these cellular systems may provide a powerful and patient-specific platform to screen for personalised therapeutic interventions.

Author contributions

TC was the lead author, with contributions from DK and IL. DK reviewed and revised the manuscript with TC.

Acknowledgments

We wish to thank members of the DK lab past and present for the stimulating discussions and support.

Conflict of interest

The authors declare that the research was conducted in the absence of any commercial or financial relationships that could be construed as a potential conflict of interest.

Publisher's note

References

Aiken, J., Moore, J. K., and Bates, E. A. (2019). TUBA1A mutations identified in lissencephaly patients dominantly disrupt neuronal migration and impair dynein activity. *Hum. Mol. Genet.* 28 (8), 1227–1243. doi:10.1093/hmg/ddy416

Akhmanova, A., Hoogenraad, C. C., Drabek, K., Stepanova, T., Dortland, B., Verkerk, T., et al. (2001). Clasps are CLIP-115 and -170 associating proteins involved in the regional regulation of microtubule dynamics in motile fibroblasts. *Cell* 104 (6), 923–935. doi:10.1016/s0092-8674(01)00288-4

Al-Bassam, J., and Chang, F. (2011). Regulation of microtubule dynamics by TOG-domain proteins XMAP215/Dis1 and CLASP. *Trends Cell Biol.* 21 (10), 604–614. doi:10.1016/j.tcb.2011.06.007

Al-Bassam, J., Kim, H., Brouhard, G., van Oijen, A., Harrison, S. C., and Chang, F. (2010). CLASP promotes microtubule rescue by recruiting tubulin dimers to the microtubule. *Dev. Cell* 19 (2), 245–258. doi:10.1016/j.devcel.2010.07.016

Amos, L. A., and Schlieper, D. (2005). Microtubules and maps. *Adv. Protein Chem.* 71, 257–298. doi:10.1016/S0065-3233(04)71007-4

Atherton, J., Hummel, J. J., Olieric, N., Locke, J., Pena, A., Rosenfeld, S. S., et al. (2020). The mechanism of kinesin inhibition by kinesin-binding protein. *Elife* 9, e61481. doi:10.7554/eLife.61481

Attard, T. J., Welburn, J. P. I., and Marsh, J. A. (2022). Understanding molecular mechanisms and predicting phenotypic effects of pathogenic tubulin mutations. *PLoS Comput. Biol.* 18 (10), e1010611. doi:10.1371/journal.pcbi.1010611

Ayaz, P., Munyoki, S., Geyer, E. A., Piedra, F. A., Vu, E. S., Bromberg, R., et al. (2014). A tethered delivery mechanism explains the catalytic action of a microtubule polymerase. *Elife* 3, e03069. doi:10.7554/eLife.03069

Ayaz, P., Ye, X., Huddleston, P., Brautigam, C. A., and Rice, L. M. (2012). A TOG:αβ-tubulin complex structure reveals conformation-based mechanisms for a microtubule polymerase. *Science* 337 (6096), 857–860. doi:10.1126/science.1221698

Bahi-Buisson, N., Poirier, K., Fourniol, F., Saillour, Y., Valence, S., Lebrun, N., et al. (2014). The wide spectrum of tubulinopathies: What are the key features for the diagnosis? *Brain* 137 (6), 1676–1700. doi:10.1093/brain/awu082

Bechstedt, S., and Brouhard, G. J. (2012). Doublecortin recognizes the 13-protofilament microtubule cooperatively and tracks microtubule ends. *Dev. Cell* 23 (1), 181–192. doi:10.1016/j.devcel.2012.05.006

Bodakuntla, S., Jijumon, A. S., Villablanca, C., Gonzalez-Billault, C., and Janke, C. (2019). Microtubule-associated proteins: Structuring the cytoskeleton. *Trends Cell Biol.* 29 (10), 804–819. doi:10.1016/j.tcb.2019.07.004

Boucher, D., Larcher, J. C., Gros, F., and Denoulet, P. (1994). Polyglutamylation of tubulin as a progressive regulator of *in vitro* interactions between the microtubule-associated protein Tau and tubulin. *Biochemistry* 33 (41), 12471–12477. doi:10.1021/bi00207a014

Braun, A., Breuss, M., Salzer, M. C., Flint, J., Cowan, N. J., and Keays, D. A. (2010). Tuba8 is expressed at low levels in the developing mouse and human brain. *Am. J. Hum. Genet.* 86 (5), 819–822. doi:10.1016/j.ajhg.2010.03.019

Breuss, M., Heng, J. I., Poirier, K., Tian, G., Jaglin, X. H., Qu, Z., et al. (2012). Mutations in the β-tubulin gene TUBB5 cause microcephaly with structural brain abnormalities. *Cell Rep.* 2 (6), 1554–1562. doi:10.1016/j.celrep.2012.11.017

Breuss, M., and Keays, D. A. (2014). Microtubules and neurodevelopmental disease: The movers and the makers. *Adv. Exp. Med. Biol.* 800, 75–96. doi:10.1007/978-94-007-7687-6_5

Byrnes, A. E., and Slep, K. C. (2017). TOG-tubulin binding specificity promotes microtubule dynamics and mitotic spindle formation. *J. Cell Biol.* 216 (6), 1641–1657. doi:10.1083/jcb.201610090

Carter, A. P., Garbarino, J. E., Wilson-Kubalek, E. M., Shipley, W. E., Cho, C., Milligan, R. A., et al. (2008). Structure and functional role of dynein's microtubule-binding domain. *Science* 322 (5908), 1691–1695. doi:10.1126/science.1164424

Carvalho, P., Gupta, M. L., Jr., Hoyt, M. A., and Pellman, D. (2004). Cell cycle control of kinesin-mediated transport of Bik1 (CLIP-170) regulates microtubule stability and dynein activation. *Dev. Cell* 6 (6), 815–829. doi:10.1016/j.devcel.2004.05.001

Cassimeris, L., Gard, D., Tran, P. T., and Erickson, H. P. (2001). XMAP215 is a long thin molecule that does not increase microtubule stiffness. *J. Cell Sci.* 114 (16), 3025–3033. doi:10.1242/jcs.114.16.3025

Cederquist, G. Y., Luchniak, A., Tischfield, M. A., Peeva, M., Song, Y., Menezes, M. P., et al. (2012). An inherited TUBB2B mutation alters a kinesin-binding site and causes polymicrogyria, CFEOM and axon dysinnervation. *Hum. Mol. Genet.* 21 (26), 5484–5499. doi:10.1093/hmg/dds393

Charrasse, S., Schroeder, M., Gauthier-Rouviere, C., Ango, F., Cassimeris, L., Gard, D. L., et al. (1998). The TOGp protein is a new human microtubule-associated protein homologous to the Xenopus XMAP215. *J. Cell Sci.* 111 (10), 1371–1383. doi:10.1242/jcs.111.10.1371

Chen, J., Kholina, E., Szyk, A., Fedorov, V. A., Kovalenko, I., Gudimchuk, N., et al. (2021). α-tubulin tail modifications regulate microtubule stability through selective effector recruitment, not changes in intrinsic polymer dynamics. *Dev. Cell* 56 (14), 2016–2028. doi:10.1016/j.devcel.2021.05.005

Cleveland, D. W. (1987). The multitubulin hypothesis revisited: What have we learned? *J. Cell Biol.* 104 (3), 381–383. doi:10.1083/jcb.104.3.381

Cullen, C. F., Deak, P., Glover, D. M., and Ohkura, H. (1999). Mini spindles: A gene encoding a conserved microtubule-associated protein required for the integrity of the mitotic spindle in Drosophila. *J. Cell Biol.* 146 (5), 1005–1018. doi:10.1083/jcb.146.5.1005

Currie, J. D., Stewman, S., Schimizzi, G., Slep, K. C., Ma, A., and Rogers, S. L. (2011). The microtubule lattice and plus-end association of Drosophila Mini spindles is spatially regulated to fine-tune microtubule dynamics. *Mol. Biol. Cell* 22 (22), 4343–4361. doi:10.1091/mbc.E11-06-0520

Cushion, T. D., Paciorkowski, A. R., Pilz, D. T., Mullins, J. G., Seltzer, L. E., Marion, R. W., et al. (2014). De novo mutations in the beta-tubulin gene TUBB2A cause simplified gyral patterning and infantile-onset epilepsy. *Am. J. Hum. Genet.* 94 (4), 634–641. doi:10.1016/j.ajhg.2014.03.009

Dagenbach, E. M., and Endow, S. A. (2004). A new kinesin tree. *J. Cell Sci.* 117 (1), 3–7. doi:10.1242/jcs.00875

Denarier, E., Brousse, C., Sissoko, A., Andrieux, A., and Boscheron, C. (2019). A neurodevelopmental TUBB2B beta-tubulin mutation impairs Bim1 (yeast EB1)-dependent spindle positioning. *Biol. Open* 8 (1), bio038620. doi:10.1242/bio.038620

Desai, A., and Mitchison, T. J. (1997). Microtubule polymerization dynamics. *Annu. Rev. Cell Dev. Biol.* 13, 83–117. doi:10.1146/annurev.cellbio.13.1.83

Efimov, A., Kharitonov, A., Efimova, N., Loncarek, J., Miller, P. M., Andreyeva, N., et al. (2007). Asymmetric CLASP-dependent nucleation of noncentrosomal microtubules at the trans-Golgi network. *Dev. Cell* 12 (6), 917–930. doi:10.1016/j.devcel.2007.04.002

Fallet-Bianco, C., Laquerriere, A., Poirier, K., Razavi, F., Guimiot, F., Dias, P., et al. (2014). Mutations in tubulin genes are frequent causes of various foetal malformations of cortical development including microlissencephaly. *Acta Neuropathol. Commun.* 2, 69. doi:10.1186/2051-5960-2-69

Feng, R., Sang, Q., Kuang, Y., Sun, X., Yan, Z., Zhang, S., et al. (2016). Mutations in TUBB8 and human oocyte meiotic arrest. *N. Engl. J. Med.* 374 (3), 223–232. doi:10.1056/NEJMoa1510791

Fourniol, F. J., Sindelar, C. V., Amigues, B., Clare, D. K., Thomas, G., Perderiset, M., et al. (2010). Template-free 13-protofilament microtubule-MAP assembly visualized at 8 A resolution. *J. Cell Biol.* 191 (3), 463–470. doi:10.1083/jcb.201007081

Gadadhar, S., Bodakuntla, S., Natarajan, K., and Janke, C. (2017). The tubulin code at a glance. *J. Cell Sci.* 130 (8), 1347–1353. doi:10.1242/jcs.199471

Gard, D. L., and Kirschner, M. W. (1987). A microtubule-associated protein from Xenopus eggs that specifically promotes assembly at the plus-end. *J. Cell Biol.* 105 (5), 2203–2215. doi:10.1083/jcb.105.5.2203

Goodson, H. V., and Jonasson, E. M. (2018). Microtubules and microtubule-associated proteins. *Cold Spring Harb. Perspect. Biol.* 10 (6), a022608. doi:10.1101/cshperspect.a022608

Grallert, A., Beuter, C., Craven, R. A., Bagley, S., Wilks, D., Fleig, U., et al. (2006). *S. pombe* CLASP needs dynein, not EB1 or CLIP170, to induce microtubule instability and slows polymerization rates at cell tips in a dynein-dependent manner. *Genes Dev.* 20 (17), 2421–2436. doi:10.1101/gad.381306

Gupta, M. L., Jr., Carvalho, P., Roof, D. M., and Pellman, D. (2006). Plus end-specific depolymerase activity of Kip3, a kinesin-8 protein, explains its role in positioning the yeast mitotic spindle. *Nat. Cell Biol.* 8 (9), 913–923. doi:10.1038/ncb1457

Hausrat, T. J., Janiesch, P. C., Breiden, P., Lutz, D., Hoffmeister-Ullerich, S., Hermans-Borgmeyer, I., et al. (2022). Disruption of tubulin-alpha4a polyglutamylation prevents aggregation of hyper-phosphorylated tau and microglia activation in mice. *Nat. Commun.* 13 (1), 4192. doi:10.1038/s41467-022-31776-5

Hayashi, I., and Ikura, M. (2003). Crystal structure of the amino-terminal microtubule-binding domain of end-binding protein 1 (EB1). *J. Biol. Chem.* 278 (38), 36430–36434. doi:10.1074/jbc.M305773200

Hendershott, M. C., and Vale, R. D. (2014). Regulation of microtubule minus-end dynamics by CAMSAPs and Patronin. *Proc. Natl. Acad. Sci. U. S. A.* 111 (16), 5860–5865. doi:10.1073/pnas.1404133111

Hirokawa, N., Noda, Y., Tanaka, Y., and Niwa, S. (2009). Kinesin superfamily motor proteins and intracellular transport. *Nat. Rev. Mol. Cell Biol.* 10 (10), 682–696. doi:10.1038/nrm2774

Hoff, K. J., Aiken, J. E., Gutierrez, M. A., Franco, S. J., and Moore, J. K. (2022). TUBA1A tubulinopathy mutants disrupt neuron morphogenesis and override XMAP215/Stu2 regulation of microtubule dynamics. *Elife* 11, e76189. doi:10.7554/eLife.76189

Honnappa, S., Gouveia, S. M., Weisbrich, A., Damberger, F. F., Bhavesh, N. S., Jawhari, H., et al. (2009). An EB1-binding motif acts as a microtubule tip localization signal. *Cell* 138 (2), 366–376. doi:10.1016/j.cell.2009.04.065

Honnappa, S., John, C. M., Kostrewa, D., Winkler, F. K., and Steinmetz, M. O. (2005). Structural insights into the EB1-APC interaction. *EMBO J.* 24 (2), 261–269. doi:10.1038/sj.emboj.7600529

Howard, J., and Hyman, A. A. (2009). Growth, fluctuation and switching at microtubule plus ends. *Nat. Rev. Mol. Cell Biol.* 10 (8), 569–574. doi:10.1038/nrm2713

Howes, S. C., Geyer, E. A., LaFrance, B., Zhang, R., Kellogg, E. H., Westermann, S., et al. (2017). Structural differences between yeast and mammalian microtubules revealed by cryo-EM. *J. Cell Biol.* 216 (9), 2669–2677. doi:10.1083/jcb.201612195

Huber, G., Alaimo-Beuret, D., and Matus, A. (1985). MAP3: Characterization of a novel microtubule-associated protein. *J. Cell Biol.* 100 (2), 496–507. doi:10.1083/jcb.100.2.496

Isrie, M., Breuss, M., Tian, G., Hansen, A. H., Cristofoli, F., Morandell, J., et al. (2015). Mutations in either TUBB or MAPRE2 cause circumferential skin Creases Kunze type. *Am. J. Hum. Genet.* 97 (6), 790–800. doi:10.1016/j.ajhg.2015.10.014

Jaglin, X. H., Poirier, K., Saillour, Y., Buhler, E., Tian, G., Bahi-Buisson, N., et al. (2009). Mutations in the beta-tubulin gene TUBB2B result in asymmetrical polymicrogyria. *Nat. Genet.* 41 (6), 746–752. doi:10.1038/ng.380

Janke, C., and Bulinski, J. C. (2011). Post-translational regulation of the microtubule cytoskeleton: Mechanisms and functions. *Nat. Rev. Mol. Cell Biol.* 12 (12), 773–786. doi:10.1038/nrm3227

Jiang, K., Toedt, G., Montenegro Gouveia, S., Davey, N. E., Hua, S., van der Vaart, B., et al. (2012). A Proteome-wide screen for mammalian SxIP motif-containing microtubule plus-end tracking proteins. *Curr. Biol.* 22 (19), 1800–1807. doi:10.1016/j.cub.2012.07.047

Jijumon, A. S., Bodakuntla, S., Genova, M., Bangera, M., Sackett, V., Besse, L., et al. (2022). Lysate-based pipeline to characterize microtubule-associated proteins uncovers unique microtubule behaviours. *Nat. Cell Biol.* 24 (2), 253–267. doi:10.1038/s41556-021-00825-4

Joshi, H. C., and Cleveland, D. W. (1989). Differential utilization of beta-tubulin isotypes in differentiating neurites. *J. Cell Biol.* 109 (2), 663–673. doi:10.1083/jcb.109.2.663

Jurgens, J. A., Barry, B. J., Lemire, G., Chan, W. M., Whitman, M. C., Shaaban, S., et al. (2021). Novel variants in TUBA1A cause congenital fibrosis of the extraocular muscles with or without malformations of cortical brain development. *Eur. J. Hum. Genet.* 29 (5), 816–826. doi:10.1038/s41431-020-00804-7

Juwana, J. P., Henderikx, P., Mischo, A., Wadle, A., Fadle, N., Gerlach, K., et al. (1999). EB/RP gene family encodes tubulin binding proteins. *Int. J. Cancer* 81 (2), 275–284. doi:10.1002/(sici)1097-0215(19990412)81:2<275::aid-ijc18>3.0.co;2-z

Kapitein, L. C., and Hoogenraad, C. C. (2015). Building the neuronal microtubule cytoskeleton. *Neuron* 87 (3), 492–506. doi:10.1016/j.neuron.2015.05.046

Keays, D. A., Tian, G., Poirier, K., Huang, G. J., Siebold, C., Cleak, J., et al. (2007). Mutations in alpha-tubulin cause abnormal neuronal migration in mice and lissencephaly in humans. *Cell* 128 (1), 45–57. doi:10.1016/j.cell.2006.12.017

Kimmerlin, Q., Dupuis, A., Bodakuntla, S., Weber, C., Heim, V., Henriot, V., et al. (2022). Mutations in the most divergent α-tubulin isotype, α8-tubulin, cause defective platelet biogenesis. *J. Thromb. Haemost.* 20 (2), 461–469. doi:10.1111/jth.15573

Kumar, A., Manatschal, C., Rai, A., Grigoriev, I., Degen, M. S., Jaussi, R., et al. (2017). Short linear sequence motif LxxPTPh targets diverse proteins to growing microtubule ends. *Structure* 25 (6), 924–932. doi:10.1016/j.str.2017.04.010

Kunishima, S., Kobayashi, R., Itoh, T. J., Hamaguchi, M., and Saito, H. (2009). Mutation of the beta1-tubulin gene associated with congenital macrothrombocytopenia affecting microtubule assembly. *Blood* 113 (2), 458–461. doi:10.1182/blood-2008-06-162610

Leandro-García, L. J., Leskelä, S., Landa, I., Montero-Conde, C., López-Jiménez, E., Letón, R., et al. (2010). Tumoral and tissue-specific expression of the major human beta-tubulin isotypes. *Cytoskelet. Hob.* 67 (4), 214–223. doi:10.1002/cm.20436

Leano, J. B., Rogers, S. L., and Slep, K. C. (2013). A cryptic TOG domain with a distinct architecture underlies CLASP-dependent bipolar spindle formation. *Structure* 21 (6), 939–950. doi:10.1016/j.str.2013.04.018

Leca, I., Phillips, A. W., Hofer, I., Landler, L., Ushakova, L., Cushion, T. D., et al. (2020). A proteomic survey of microtubule-associated proteins in a R402H TUBA1A mutant mouse. *PLoS Genet.* 16 (11), e1009104. doi:10.1371/journal.pgen.1009104

Lewis, S. A., Tian, G., and Cowan, N. J. (1997). The alpha- and beta-tubulin folding pathways. *Trends Cell Biol.* 7 (12), 479–484. doi:10.1016/S0962-8924(97)01168-9

Li, Y. Y., Lei, W. L., Zhang, C. F., Sun, S. M., Zhao, B. W., Xu, K., et al. (2022). MAPRE2 regulates the first meiotic progression in mouse oocytes. *Exp. Cell Res.* 416 (1), 113135. doi:10.1016/j.yexcr.2022.113135

Liao, H., Li, Y., Brautigan, D. L., and Gundersen, G. G. (1998). Protein phosphatase 1 is targeted to microtubules by the microtubule-associated protein Tau. *J. Biol. Chem.* 273 (34), 21901–21908. doi:10.1074/jbc.273.34.21901

Lloyd, P. G., and Hardin, C. D. (1999). Role of microtubules in the regulation of metabolism in isolated cerebral microvessels. *Am. J. Physiol.* 277 (6), C1250–C1262. doi:10.1152/ajpcell.1999.277.6.C1250

Lowe, J., Li, H., Downing, K. H., and Nogales, E. (2001). Refined structure of alpha beta-tubulin at 3.5 A resolution. *J. Mol. Biol.* 313 (5), 1045–1057. doi:10.1006/jmbi.2001.5077

Luscan, R., Mechaussier, S., Paul, A., Tian, G., Gerard, X., Defoort-Dellhemmes, S., et al. (2017). Mutations in TUBB4B cause a distinctive sensorineural disease. *Am. J. Hum. Genet.* 101 (6), 1006–1012. doi:10.1016/j.ajhg.2017.10.010

Majumdar, S., Kim, T., Chen, Z., Munyoki, S., Tso, S. C., Brautigam, C. A., et al. (2018). An isolated CLASP TOG domain suppresses microtubule catastrophe and promotes rescue. *Mol. Biol. Cell* 29 (11), 1359–1375. doi:10.1091/mbc.E17-12-0748

Maurer, S. P., Bieling, P., Cope, J., Hoenger, A., and Surrey, T. (2011). GTPgammaS microtubules mimic the growing microtubule end structure recognized by end-binding proteins (EBs). *Proc. Natl. Acad. Sci. U. S. A.* 108 (10), 3988–3993. doi:10.1073/pnas.1014758108

Maurer, S. P., Fourniol, F. J., Bohner, G., Moores, C. A., and Surrey, T. (2012). EBs recognize a nucleotide-dependent structural cap at growing microtubule ends. *Cell* 149 (2), 371–382. doi:10.1016/j.cell.2012.02.049

Mimori-Kiyosue, Y., Shiina, N., and Tsukita, S. (2000). The dynamic behavior of the APC-binding protein EB1 on the distal ends of microtubules. *Curr. Biol.* 10 (14), 865–868. doi:10.1016/s0960-9822(00)00600-x

Mitchison, T., and Kirschner, M. (1984). Dynamic instability of microtubule growth. *Nature* 312 (5991), 237–242. doi:10.1038/312237a0

Moon, H. M., and Wynshaw-Boris, A. (2013). Cytoskeleton in action: Lissencephaly, a neuronal migration disorder. *Wiley Interdiscip. Rev. Dev. Biol.* 2 (2), 229–245. doi:10.1002/wdev.67

Moriwaki, T., and Goshima, G. (2016). Five factors can reconstitute all three phases of microtubule polymerization dynamics. *J. Cell Biol.* 215 (3), 357–368. doi:10.1083/jcb.201604118

Nangaku, M., Sato-Yoshitake, R., Okada, Y., Noda, Y., Takemura, R., Yamazaki, H., et al. (1994). KIF1B, a novel microtubule plus end-directed monomeric motor protein for transport of mitochondria. *Cell* 79 (7), 1209–1220. doi:10.1016/0092-8674(94)90012-4

Niwa, S., Takahashi, H., and Hirokawa, N. (2013). β-Tubulin mutations that cause severe neuropathies disrupt axonal transport. *EMBO J.* 32 (10), 1352–1364. doi:10.1038/emboj.2013.59

Niwa, S., Tanaka, Y., and Hirokawa, N. (2008). KIF1Bbeta- and KIF1A-mediated axonal transport of presynaptic regulator Rab3 occurs in a GTP-dependent manner through DENN/MADD. *Nat. Cell Biol.* 10 (11), 1269–1279. doi:10.1038/ncb1785

Nogales, E. (2001). Structural insight into microtubule function. *Annu. Rev. Biophys. Biomol. Struct.* 30, 397–420. doi:10.1146/annurev.biophys.30.1.397

Nogales, E., Wolf, S. G., and Downing, K. H. (1998). Structure of the alpha beta tubulin dimer by electron crystallography. *Nature* 391 (6663), 199–203. doi:10.1038/34465

Parker, A. L., Teo, W. S., Pandzic, E., Vicente, J. J., McCarroll, J. A., Wordeman, L., et al. (2018). β-tubulin carboxy-terminal tails exhibit isotype-specific effects on microtubule dynamics in human gene-edited cells. *Life Sci. Alliance* 1 (2), e201800059. doi:10.26508/lsa.201800059

Perez, F., Diamantopoulos, G. S., Stalder, R., and Kreis, T. E. (1999). CLIP-170 highlights growing microtubule ends *in vivo*. *Cell* 96 (4), 517–527. doi:10.1016/s0092-8674(00)80656-x

Poirier, K., Keays, D. A., Francis, F., Saillour, Y., Bahi, N., Manouvrier, S., et al. (2007). Large spectrum of lissencephaly and pachygyria phenotypes resulting from de novo missense mutations in tubulin alpha 1A (TUBA1A). *Hum. Mutat.* 28 (11), 1055–1064. doi:10.1002/humu.20572

Poirier, K., Lebrun, N., Broix, L., Tian, G., Saillour, Y., Boscheron, C., et al. (2013). Mutations in TUBG1, DYNC1H1, KIF5C and KIF2A cause malformations of cortical development and microcephaly. *Nat. Genet.* 45 (6), 639–647. doi:10.1038/ng.2613

Poirier, K., Saillour, Y., Bahi-Buisson, N., Jaglin, X. H., Fallet-Bianco, C., Nabbout, R., et al. (2010). Mutations in the neuronal ß-tubulin subunit TUBB3 result in malformation of cortical development and neuronal migration defects. *Hum. Mol. Genet.* 19 (22), 4462–4473. doi:10.1093/hmg/ddq377

Rafiei, A., and Schriemer, D. C. (2022). A crosslinking mass spectrometry protocol for the structural analysis of microtubule-associated proteins. *Methods Mol. Biol.* 2456, 211–222. doi:10.1007/978-1-0716-2124-0_14

Redwine, W. B., Hernandez-Lopez, R., Zou, S., Huang, J., Reck-Peterson, S. L., and Leschziner, A. E. (2012). Structural basis for microtubule binding and release by dynein. *Science* 337 (6101), 1532–1536. doi:10.1126/science.1224151

Romaniello, R., Arrigoni, F., Fry, A. E., Bassi, M. T., Rees, M. I., Borgatti, R., et al. (2018). Tubulin genes and malformations of cortical development. *Eur. J. Med. Genet.* 61, 744–754. doi:10.1016/j.ejmg.2018.07.012

Roth, D., Fitton, B. P., Chmel, N. P., Wasiluk, N., and Straube, A. (2018). Spatial positioning of EB family proteins at microtubule tips involves distinct nucleotide-dependent binding properties. *J. Cell Sci.* 132 (4), jcs219550. doi:10.1242/jcs.219550

Schroeder, C. M., Ostrem, J. M., Hertz, N. T., and Vale, R. D. (2014). A Ras-like domain in the light intermediate chain bridges the dynein motor to a cargo-binding region. *Elife* 3, e03351. doi:10.7554/eLife.03351

Sferra, A., Fattori, F., Rizza, T., Flex, E., Bellacchio, E., Bruselles, A., et al. (2018). Defective kinesin binding of TUBB2A causes progressive spastic ataxia syndrome resembling sacsinopathy. *Hum. Mol. Genet.* 27 (11), 1892–1904. doi:10.1093/hmg/ddy096

Slep, K. C., Rogers, S. L., Elliott, S. L., Ohkura, H., Kolodziej, P. A., and Vale, R. D. (2005). Structural determinants for EB1-mediated recruitment of APC and spectraplakins to the microtubule plus end. *J. Cell Biol.* 168 (4), 587–598. doi:10.1083/jcb.200410114

Sloboda, R. D., Rudolph, S. A., Rosenbaum, J. L., and Greengard, P. (1975). Cyclic AMP-dependent endogenous phosphorylation of a microtubule-associated protein. *Proc. Natl. Acad. Sci. U. S. A.* 72 (1), 177–181. doi:10.1073/pnas.72.1.177

Smith, B. N., Ticozzi, N., Fallini, C., Gkazi, A. S., Topp, S., Kenna, K. P., et al. (2014). Exome-wide rare variant analysis identifies TUBA4A mutations associated with familial ALS. *Neuron* 84 (2), 324–331. doi:10.1016/j.neuron.2014.09.027

Song, A. H., Wang, D., Chen, G., Li, Y., Luo, J., Duan, S., et al. (2009). A selective filter for cytoplasmic transport at the axon initial segment. *Cell* 136 (6), 1148–1160. doi:10.1016/j.cell.2009.01.016

Sousa, A., Reis, R., Sampaio, P., and Sunkel, C. E. (2007). The Drosophila CLASP homologue, Mast/Orbit regulates the dynamic behaviour of interphase microtubules by promoting the pause state. *Cell Motil. Cytoskelet.* 64 (8), 605–620. doi:10.1002/cm.20208

Strassel, C., Magiera, M. M., Dupuis, A., Batzenschlager, M., Hovasse, A., Pleines, I., et al. (2019). An essential role for α4A-tubulin in platelet biogenesis. *Life Sci. Alliance* 2 (1), e201900309. doi:10.26508/lsa.201900309

Straube, A. (2011). How to measure microtubule dynamics? *Methods Mol. Biol.* 777, 1–14. doi:10.1007/978-1-61779-252-6_1

Tanaka, Y., Kanai, Y., Okada, Y., Nonaka, S., Takeda, S., Harada, A., et al. (1998). Targeted disruption of mouse conventional kinesin heavy chain, kif5B, results in abnormal perinuclear clustering of mitochondria. *Cell* 93 (7), 1147–1158. doi:10.1016/s0092-8674(00)81459-2

Tian, G., Jaglin, X. H., Keays, D. A., Francis, F., Chelly, J., and Cowan, N. J. (2010). Disease-associated mutations in TUBA1A result in a spectrum of defects in the tubulin folding and heterodimer assembly pathway. *Hum. Mol. Genet.* 19 (18), 3599–3613. doi:10.1093/hmg/ddq276

Tischfield, M. A., Baris, H. N., Wu, C., Rudolph, G., Van Maldergem, L., He, W., et al. (2010). Human TUBB3 mutations perturb microtubule dynamics, kinesin interactions, and axon guidance. *Cell* 140 (1), 74–87. doi:10.1016/j.cell.2009.12.011

Tortosa, E., Adolfs, Y., Fukata, M., Pasterkamp, R. J., Kapitein, L. C., and Hoogenraad, C. C. (2017). Dynamic palmitoylation targets MAP6 to the axon to promote microtubule stabilization during neuronal polarization. *Neuron* 94 (4), 809–825. doi:10.1016/j.neuron.2017.04.042

Tortosa, E., Kapitein, L. C., and Hoogenraad, C. C. (2016). "Microtubule organization and microtubule-associated proteins (MAPs)," in *Dendrites* (Berlin, Germany: Springer), 31–75.

Tripathy, R., Leca, I., van Dijk, T., Weiss, J., van Bon, B. W., Sergaki, M. C., et al. (2018). Mutations in MAST1 cause mega-corpus-callosum syndrome with cerebellar hypoplasia and cortical malformations. *Neuron* 100 (6), 1354–1368. doi:10.1016/j.neuron.2018.10.044

Uchimura, S., Fujii, T., Takazaki, H., Ayukawa, R., Nishikawa, Y., Minoura, I., et al. (2015). A flipped ion pair at the dynein-microtubule interface is critical for dynein motility and ATPase activation. *J. Cell Biol.* 208 (2), 211–222. doi:10.1083/jcb.201407039

Uchimura, S., Oguchi, Y., Katsuki, M., Usui, T., Osada, H., Nikawa, J., et al. (2006). Identification of a strong binding site for kinesin on the microtubule using mutant analysis of tubulin. *EMBO J.* 25 (24), 5932–5941. doi:10.1038/sj.emboj.7601442

Vale, R. D. (2003). The molecular motor toolbox for intracellular transport. *Cell* 112 (4), 467–480. doi:10.1016/s0092-8674(03)00111-9

Vallee, R. B., Williams, J. C., Varma, D., and Barnhart, L. E. (2004). Dynein: An ancient motor protein involved in multiple modes of transport. *J. Neurobiol.* 58 (2), 189–200. doi:10.1002/neu.10314

Vissers, L. E., de Ligt, J., Gilissen, C., Janssen, I., Steehouwer, M., de Vries, P., et al. (2010). A de novo paradigm for mental retardation. *Nat. Genet.* 42 (12), 1109–1112. doi:10.1038/ng.712

Walden, P. D., and Cowan, N. J. (1993). A novel 205-kilodalton testis-specific serine/threonine protein kinase associated with microtubules of the spermatid manchette. *Mol. Cell Biol.* 13 (12), 7625–7635. doi:10.1128/mcb.13.12.7625

Walsh, J. L., Keith, T. J., and Knull, H. R. (1989). Glycolytic enzyme interactions with tubulin and microtubules. *Biochim. Biophys. Acta* 999 (1), 64–70. doi:10.1016/0167-4838(89)90031-9

Wang, P. J., and Huffaker, T. C. (1997). Stu2p: A microtubule-binding protein that is an essential component of the yeast spindle pole body. *J. Cell Biol.* 139 (5), 1271–1280. doi:10.1083/jcb.139.5.1271

Widlund, P. O., Stear, J. H., Pozniakovsky, A., Zanic, M., Reber, S., Brouhard, G. J., et al. (2011). XMAP215 polymerase activity is built by combining multiple tubulin-binding TOG domains and a basic lattice-binding region. *Proc. Natl. Acad. Sci. U. S. A.* 108 (7), 2741–2746. doi:10.1073/pnas.1016498108

Wittmann, T., and Waterman-Storer, C. M. (2005). Spatial regulation of CLASP affinity for microtubules by Rac1 and GSK3beta in migrating epithelial cells. *J. Cell Biol.* 169 (6), 929–939. doi:10.1083/jcb.200412114

Woehlke, G., Ruby, A. K., Hart, C. L., Ly, B., Hom-Booher, N., and Vale, R. D. (1997). Microtubule interaction site of the kinesin motor. *Cell* 90 (2), 207–216. doi:10.1016/s0092-8674(00)80329-3

Wordeman, L. (2010). How kinesin motor proteins drive mitotic spindle function: Lessons from molecular assays. *Semin. Cell Dev. Biol.* 21 (3), 260–268. doi:10.1016/j.semcdb.2010.01.018

Yamada, K., Andrews, C., Chan, W. M., McKeown, C. A., Magli, A., de Berardinis, T., et al. (2003). Heterozygous mutations of the kinesin KIF21A in congenital fibrosis of the extraocular muscles type 1 (CFEOM1). *Nat. Genet.* 35 (4), 318–321. doi:10.1038/ng1261

Yamada, M., Toba, S., Yoshida, Y., Haratani, K., Mori, D., Yano, Y., et al. (2008). LIS1 and NDEL1 coordinate the plus-end-directed transport of cytoplasmic dynein. *EMBO J.* 27 (19), 2471–2483. doi:10.1038/emboj.2008.182

Yin, H., You, L., Pasqualone, D., Kopski, K. M., and Huffaker, T. C. (2002). Stu1p is physically associated with beta-tubulin and is required for structural integrity of the mitotic spindle. *Mol. Biol. Cell* 13 (6), 1881–1892. doi:10.1091/mbc.01-09-0458

Yu, N., Signorile, L., Basu, S., Ottema, S., Lebbink, J. H. G., Leslie, K., et al. (2016). Isolation of functional tubulin dimers and of tubulin-associated proteins from mammalian cells. *Curr. Biol.* 26 (13), 1728–1736. doi:10.1016/j.cub.2016.04.069

Frontiers in
Cell and Developmental Biology

Explores the fundamental biological processes of life, covering intracellular and extracellular dynamics.

The world's most cited developmental biology journal, advancing our understanding of the fundamental processes of life. It explores a wide spectrum of cell and developmental biology, covering intracellular and extracellular dynamics.

Discover the latest Research Topics

See more →

Frontiers

Avenue du Tribunal-Fédéral 34
1005 Lausanne, Switzerland
frontiersin.org

Contact us

+41 (0)21 510 17 00
frontiersin.org/about/contact